REGULATORY MECHANISMS OF LEAF SENESCENCE UNDER ENVIRONMENTAL STRESSES

EDITED BY: Yasuhito Sakuraba, Stefan Hortensteiner, Nam-Chon Paek, Jinjie Li and Soyon Park

PUBLISHED IN: Frontiers in Plant Science

frontiers Research Topics

frontiers

ISSN 1664-8714
ISBN 978-2-88966-076-6
DOI 10.3389/978-2-88966-076-6

About Frontiers

Frontiers is more than just an open-access publisher of scholarly articles: it is a pioneering approach to the world of academia, radically improving the way scholarly research is managed. The grand vision of Frontiers is a world where all people have an equal opportunity to seek, share and generate knowledge. Frontiers provides immediate and permanent online open access to all its publications, but this alone is not enough to realize our grand goals.

Frontiers Journal Series

The Frontiers Journal Series is a multi-tier and interdisciplinary set of open-access, online journals, promising a paradigm shift from the current review, selection and dissemination processes in academic publishing. All Frontiers journals are driven by researchers for researchers; therefore, they constitute a service to the scholarly community. At the same time, the Frontiers Journal Series operates on a revolutionary invention, the tiered publishing system, initially addressing specific communities of scholars, and gradually climbing up to broader public understanding, thus serving the interests of the lay society, too.

Dedication to Quality

Each Frontiers article is a landmark of the highest quality, thanks to genuinely collaborative interactions between authors and review editors, who include some of the world's best academicians. Research must be certified by peers before entering a stream of knowledge that may eventually reach the public - and shape society; therefore, Frontiers only applies the most rigorous and unbiased reviews.
Frontiers revolutionizes research publishing by freely delivering the most outstanding research, evaluated with no bias from both the academic and social point of view. By applying the most advanced information technologies, Frontiers is catapulting scholarly publishing into a new generation.

What are Frontiers Research Topics?

Frontiers Research Topics are very popular trademarks of the Frontiers Journals Series: they are collections of at least ten articles, all centered on a particular subject. With their unique mix of varied contributions from Original Research to Review Articles, Frontiers Research Topics unify the most influential researchers, the latest key findings and historical advances in a hot research area! Find out more on how to host your own Frontiers Research Topic or contribute to one as an author by contacting the Frontiers Editorial Office: researchtopics@frontiersin.org

REGULATORY MECHANISMS OF LEAF SENESCENCE UNDER ENVIRONMENTAL STRESSES

Topic Editors:
Yasuhito Sakuraba, The University of Tokyo, Japan
Stefan Hortensteiner, University of Zurich, Switzerland
Nam-Chon Paek, Seoul National University, South Korea
Jinjie Li, China Agricultural University, China
Soyon Park, Virginia Tech, United States

Citation: Sakuraba, Y., Hortensteiner, S., Paek, N.-C., Li, J., Park, S., eds. (2020). Regulatory Mechanisms of Leaf Senescence Under Environmental Stresses. Lausanne: Frontiers Media SA. doi: 10.3389/978-2-88966-076-6

Table of Contents

frontiers in Plant Science

EDITORIAL
published: 19 August 2020
doi: 10.3389/fpls.2020.01293

Editorial: Regulatory Mechanisms of Leaf Senescence Under Environmental Stresses

Yasuhito Sakuraba[1]*, *Jinjie Li*[2], *Soyon Park*[3] and *Nam-Chon Paek*[4]

[1] Biotechnology Research Center, The University of Tokyo, Tokyo, Japan, [2] Key Lab of Crop Heterosis and Utilization of Ministry of Education, China Agricultural University, Beijing, China, [3] Division of Plant Science, University of Missouri, Columbia, MO, United States, [4] Department of Plant Science, Seoul National University, Seoul, South Korea

Keywords: leaf senescence, stay green, environmental stress, phytohormones, transcription factors

Editorial on the Research Topic

Regulatory Mechanisms of Leaf Senescence Under Environmental Stress

Leaf senescence defines the final stage of the leaf developmental program and is characterized by extensive destabilization of intracellular organelles and decomposition of macromolecules in order to relocate nutrients to the actively developing organs. Over the last two decades, a number of genes associated with leaf senescence have been identified, thus significantly enhancing our understanding of the regulatory mechanisms underlying this phenomenon (Woo et al., 2019; Sakuraba et al., 2020). However, given the complexity of leaf senescence, many molecular mechanisms and associated factors involved in this process might still be unknown.

The purpose of this Research Topic is to identify the genes or regulatory mechanisms associated with environmental stress-induced leaf senescence or the regulatory mechanisms underlying environmental stress responses that are potentially important for the regulation of leaf senescence. In this Research Topic, a total of 10 research articles have been accepted for publication; these articles focus on a wide range of plant species, including the model plant *Arabidopsis thaliana* and various crops such as rice (*Oryza sativa*), tobacco (*Nicotiana tabacum*), and cotton (*Gossypium hirsutum*).

Light deprivation is one of the many environmental stresses that induce leaf senescence. In *Arabidopsis*, dark-induced leaf senescence requires phytochrome-interacting transcription factors (TFs), PIF4 and PIF5 (Sakuraba et al., 2014), as well as phytohormones such as abscisic acid (ABA) and ethylene. In this Research Topic, Ueda et al. investigated the relationship between ethylene, ABA, and PIFs in dark-induced leaf senescence in *Arabidopsis*. The *pif4 pif5* double mutant exhibited delayed yellowing during dark-induced leaf senescence. However, they showed that during ABA-induced leaf senescence under light, the *pif4 pif5* double mutant did not show decreased sensitivity to ABA, suggesting that PIF4 and PIF5 act upstream of ABA signaling. On the other hand, the triple mutant of *pif4 pif5* and ethylene-insensitive *ein2* exhibited a stronger delayed senescence phenotype than the *ein2* single mutant and *pif4 pif5* double mutant, suggesting that EIN2-mediated ethylene signaling and PIF4/PIF5 independently regulate dark-induced leaf senescence.

NAC and WRKY TFs are considered to play important roles in the regulation of leaf senescence. In this Research Topic, Doll et al. reported that *Arabidopsis* WRKY25 acts as a negative regulator of hydrogen peroxide (H_2O_2)-mediated promotion of leaf senescence. WRKY25 binds to and enhances the activity of the promoter of the *WRKY53* gene, which encodes a key TF that

OPEN ACCESS

Edited by:
Paula Casati,
Centro de Estudios Fotosintéticos y Bioquímicos (CEFOBI), Argentina

Reviewed by:
Kazuo Nakashima,
Japan International Research Center for Agricultural Sciences (JIRCAS), Japan

***Correspondence:**
Yasuhito Sakuraba
usakurab@mail.ecc.u-tokyo.ac.jp

Specialty section:
This article was submitted to Plant Abiotic Stress, a section of the journal Frontiers in Plant Science

Received: *08 July 2020*
Accepted: *07 August 2020*
Published: *19 August 2020*

Citation:
Sakuraba Y, Li J, Park S and Paek N-C (2020) Editorial: Regulatory Mechanisms of Leaf Senescence Under Environmental Stresses. Front. Plant Sci. 11:1293. doi: 10.3389/fpls.2020.01293

promotes leaf senescence; however, WRKY25 directly represses the activity of its own gene promoter. Additionally, Doll et al. showed that MEKK1, a component of the mitogen-activated protein kinase (MAPK) signaling pathway, enhances the ability of WRKY25 to activate the *WRKY53* promoter. Thus, WRKY25 and WRKY53 form a highly complex and robust regulatory network to regulate H_2O_2-mediated promotion of leaf senescence. On the other hand, Gu et al. reported that in cotton (*Gossypium hirsutum*), GhWRKY91 acts as a negative regulator of leaf senescence. Constitutive expression of *GhWRKY91* in *Arabidopsis* delayed leaf yellowing during natural leaf senescence and under dehydration stress. Furthermore, they demonstrated that GhWRKY91 activates the promoter of *GhWRKY17*, which is involved in ABA signaling and reactive oxygen species (ROS) production.

Compared with NAC and WRKY TFs, roles of other TFs in the regulation of leaf senescence remain unclear. Zhang et al. reported that DEAR4, a DREB/CBF family TF, acts as a positive regulator of leaf senescence in *Arabidopsis*. Transgenic *Arabidopsis* plants overexpressing *DEAR4* exhibited accelerated leaf yellowing during natural and dark-induced senescence. In addition, they also showed that *DEAR4* overexpressing plants were more sensitive to high salinity and drought stresses than wild-type plants, and DEAR4 increased the sensitivity to these environmental stresses probably by enhancing ROS production. On the other hand, Lim et al. identified a novel senescence-associated AP2/ERF family TF in rice, ETHYLENE RESPONSE FACTOR 101 (OsERF101). OsERF101 directly activates the transcription of genes encoding OsNAP and OsMYC2 TFs, both of which activate genes associated with chlorophyll degradation and jasmonate (JA) signaling.

A balance between carbon (C) and nitrogen (N) availability is one of the key determinants affecting the progression of leaf senescence. *Arabidopsis* plants grown under N-deficient conditions with elevated CO_2 levels exhibited precocious leaf senescence (Aoyama et al., 2014). Li et al. identified several key components of the C/N-nutrient response including a leucine-rich repeat receptor-like kinase with extracellular malectin-like domain (LMK1) using phosphoproteomics approaches. Further analyses revealed that LMK1 exhibits cell death induction activity in plant leaves. Thus, LMK1 potentially acts as a key regulator of the progression of C/N imbalance-induced leaf senescence.

Cytokinin (CK) negatively regulates leaf senescence and enhances tolerance to environmental stresses, such as drought and high salinity. In tobacco, constitutive expression of *ISOPENTENYL TRANSFERASE* (*IPT*), which encodes a key CK biosynthetic enzyme, delayed leaf senescence but also caused negative growth phenotypes, such as dwarfism and root growth inhibition (Smart et al., 1991). In this Research Topic, Avni et al. reported that transgenic tobacco plants overexpressing the *IPT* gene under the control of the stress-inducible promoter of the *Arabidopsis METALLOTHIONEIN* gene were tolerant to dehydration and high salinity stresses and showed normal growth and metabolic maintenance. Thus, environmental stress-specific induction of CK biosynthesis is a useful approach for developing plants with improved biomass and yield under environmental stress conditions, and this approach can be applied to various crop species.

The phytohormone ABA is closely associated with the drought stress response. In this Research Topic, three studies identified proteins involved in the ABA-dependent drought stress response in *Arabidopsis*. Baek et al. reported the role of *Arabidopsis* PR5 receptor-like kinase 2 (AtPR5K2) in the drought stress response. They showed that AtPR5K2 physically interacts with and phosphorylates Type 2C protein phosphatases, ABA-INSENSITIVE 1 (ABI1) and ABI2, which regulate the initiation of ABA signaling. Baek et al. investigated the role of *Arabidopsis* RPD3-type HISTONE DEACETYLASE 9 (HDA9) in the ABA-dependent drought stress response. HDA9 physically interacts with ABA-INSENSITIVE 4 (ABI4), a key ABA signaling TF, and the results of chromatin immunoprecipitation and quantitative PCR (ChIP-qPCR) indicated that the HDA9–ABI4 complex directly represses the expression of *CYP707A1* and *CYP707A2* genes, which encode ABA catabolic enzymes. On the other hand, a previous study showed that the HDA9–POWERDRESS (PWR) complex participates in the regulation of leaf senescence, flowering time, and floral dormancy. Khan et al. showed that both HDA9 and PWR interact with ABI4, probably forming the PWR–HDA9–ABI4 complex, and repress the expression of genes associated with ABA metabolism and signaling.

In conclusion, we believe that studies included within the Research Topic "Regulatory Mechanisms of Leaf Senescence Under Environmental Stress" improve our understanding of the molecular mechanisms of environmental stress-induced leaf senescence. We sincerely appreciate all scientists who kindly allowed us to publish their work in this Research Topic.

AUTHOR CONTRIBUTIONS

All authors listed have made substantial, direct, and intellectual contribution to the work and approved it for publication.

FUNDING

YS is supported by a grant from JSPS KAKENHI (grant no. 17H05024).

ACKNOWLEDGMENTS

We thank Dr. Stefan Hörtensteiner for his support as a guest editor of this Research Topic "Regulatory Mechanisms of Leaf Senescence under Environmental Stresses."

REFERENCES

Aoyama, S., Reyes, T. H., Guglielminetti, L., Lu, Y., Morita, Y., Sato, T., et al. (2014). Ubiquitin ligase ATL31 functions in leaf senescence in response to the balance between atmospheric CO_2 and nitrogen availability in Arabidopsis. *Plant Cell Physiol.* 55, 293–305. doi: 10.1093/pcp/pcu002

Sakuraba, Y., Jeong, J., Kang, M. Y., Kim, J., Paek, N. C., and Choi, G. (2014). Phytochrome-interacting transcription factors PIF4 and PIF5 induce leaf senescence in *Arabidopsis*. *Nat. Commun.* 5, 4636. doi: 10.1038/ncomms5636

Sakuraba, Y., Kim, D., Han, S. H., Kim, S. H., Piao, W., Yanagisawa, S., et al. (2020). Multilayered regulation of membrane-bound ONAC054 is essential for abscisic acid-induced leaf senescence in rice. *Plant Cell* 32, 630–649. doi: 10.1105/tpc.19.00569

Smart, C. M., Scofield, S. R., Bevan, M. W., and Dyer, T. A. (1991). Delayed leaf senescence in tabacco plants transformed with Tmr, a gene for cytokinin production in Agrobacterium. *Plant Cell* 3, 647–656. doi: 10.1104/tpc.3.7.647

Woo, H. R., Kim, H. J., Lim, P. O., and Nam, H. G. (2019). Leaf Senescence: System and Dynamics Aspects. *Annu. Rev. Plant Biol.* 70, 347–376. doi: 10.1146/annurev-arplant-050718-095859

Conflict of Interest: The authors declare that the research was conducted in the absence of any commercial or financial relationship that could be constructed as a potential conflict of interest.

frontiers in Plant Science

ORIGINAL RESEARCH
published: 11 October 2019
doi: 10.3389/fpls.2019.01146

AtPR5K2, a PR5-Like Receptor Kinase, Modulates Plant Responses to Drought Stress by Phosphorylating Protein Phosphatase 2Cs

Dongwon Baek[1†], Min Chul Kim[1,2†], Dhinesh Kumar[1,3†], Bokyung Park[4], Mi Sun Cheong[1,2], Wonkyun Choi[5], Hyeong Cheol Park[5], Hyun Jin Chun[2], Hee Jin Park[6,7], Sang Yeol Lee[1], Ray A. Bressan[8], Jae-Yean Kim[1] and Dae-Jin Yun[6]**

[1] Division of Applied Life Science (BK21plus program), Plant Molecular Biology and Biotechnology Research Center, Gyeongsang National University, Jinju, South Korea, [2] Institute of Agriculture & Life Science, Gyeongsang National University, Jinju, South Korea, [3] Donald Danforth Plant Science Center, St Louis, MO, United States, [4] Gyeongsangnam-do Agricultural Research and Extension Services, Jinju, South Korea, [5] Division of Ecological Conservation, Bureau of Ecological Research, National Institute of Ecology (NIE), Seocheon, South Korea, [6] Department of Biomedical Science and Engineering, Konkuk University, Seoul, South Korea, [7] Institute of Glocal Disease Control, Konkuk University, Seoul, South Korea, [8] Department of Horticulture and Landscape Architecture, Purdue University, West Lafayette, IN, United States

Cell surface receptors perceive signals from the environment and transfer them to the interior of the cell. The *Arabidopsis thaliana* PR5 receptor-like kinase (AtPR5K) subfamily consists of three members with extracellular domains that share sequence similarity with the PR5 proteins. In this study, we characterized the role of AtPR5K2 in plant drought-stress signaling. *AtPR5K2* is predominantly expressed in leaves and localized to the plasma membrane. The *atpr5k2-1* mutant showed tolerance to dehydration stress, while *AtPR5K2*-overexpressing plants was hypersensitive to drought. Bimolecular fluorescence complementation assays showed that AtPR5K2 physically interacted with the type 2C protein phosphatases ABA-insensitive 1 (ABI1) and ABI2 and the SNF1-related protein kinase 2 (SnRK2.6) proteins, all of which are involved in the initiation of abscisic acid (ABA) signaling; however, these interactions were inhibited by treatments of exogenous ABA. Moreover, AtPR5K2 was found to phosphorylate ABI1 and ABI2, but not SnRK2.6. Taken together, these results suggest that AtPR5K2 participates in ABA-dependent drought-stress signaling through the phosphorylation of ABI1 and ABI2.

Keywords: drought stress, abscisic acid, receptor-like kinase, ABI1, ABI2, SnRK2.6, phosphorylation, *Arabidopsis thaliana*

OPEN ACCESS

Edited by:
Nam-Chon Paek, Seoul National University, South Korea

Reviewed by:
Jing Bo Jin, Chinese Academy of Sciences, China
Miguel A Botella, University of Málaga, Spain

***Correspondence:**
Jae-Yean Kim
kimjy@gnu.ac.kr
Dae-Jin Yun
djyun@konkuk.ac.kr

†These authors have contributed equally to this work

Specialty section:
This article was submitted to Plant Abiotic Stress, a section of the journal Frontiers in Plant Science

Received: *09 May 2019*
Accepted: *22 August 2019*
Published: *11 October 2019*

Citation:
Baek D, Kim MC, Kumar D, Park B, Cheong MS, Choi W, Park HC, Chun HJ, Park HJ, Lee SY, Bressan RA, Kim J-Y and Yun D-J (2019) AtPR5K2, a PR5-Like Receptor Kinase, Modulates Plant Responses to Drought Stress by Phosphorylating Protein Phosphatase 2Cs. Front. Plant Sci. 10:1146. doi: 10.3389/fpls.2019.01146

INTRODUCTION

Plant receptors perceive signals from external stimuli and transmit this information to the interior of the cell (McCarty and Chory, 2000). These receptors are typically composed of three major domains: an external ligand-binding domain for detecting the signal, a transmembrane domain for anchoring to the cell membrane, and an intracellular domain for transmitting the signal inside the cell to generate a signaling cascade (Hohmann et al., 2017). To sense and transmit the vast numbers of signals arising from environmental stimuli, plants have functionally evolved a large family of membrane receptor kinases and receptor-like kinases (RLKs) (Shiu and Bleecker, 2001; Hohmann et al., 2017).

In the *Arabidopsis thaliana* genome, the RLKs are represented by 610 proteins divided into 44 subfamilies and at least 16 types, which have unique extracellular domain structures and functions (Shiu and Bleecker, 2001). Plant RLKs have different functions according to the types of motifs in their extracellular domains (Shiu and Bleecker, 2001); for example, the extracellular domains of leucine-rich repeat RLKs (LRR-RLKs) play important roles in the protein–protein interactions required for various signal transduction pathways in plant growth and development (Kobe and Deisenhofer, 1994; Torii et al., 1996; Clark et al., 1997; Yokoyama et al., 1998; Schoof et al., 2000; Mandel et al., 2016). The S-receptor kinases (SRKs) that possess a membrane-spanning serine/threonine kinase motif are involved in the determination of pollen-derived S-haplotype specificity for self-incompatibility (Hatakeyama et al., 2001; Takayama and Isogai, 2003). The lectin RLKs interact with extracellular carbohydrates such as glucose, mannose, fructose, chitobiose, and other sugars, and play roles in plant developmental processes and the signaling responses to plant hormones during various abiotic and biotic stresses (Loris et al., 2003; Vaid et al., 2012; Yang et al., 2016). The CRINKLY4 (CR4) family of RLKs contain a tumor necrosis factor receptor motif and are required for vegetative growth, floral organ development, aleurone formation in seeds, and sex determination (Becraft et al., 1996; Jin et al., 2000; Kang et al., 2002; Tian et al., 2007; Nikonorova et al., 2015), while the wall-associated kinase family of RLKs possess epidermal growth factor-like domains and are essential regulators of cell expansion, immunity resistance, and heavy metal tolerance in *Arabidopsis* (Verica and He, 2002; Verica et al., 2003; Hou et al., 2005; Wang et al., 2012). The pathogenesis-related 5 (PR5) RLKs (PR5Ks) are activated by several hormones and pathogenic infections (Thomma et al., 1998; Clarke et al., 2000; Durrant and Dong, 2004; van Loon et al., 2006).

Osmotin has been classified into the PR5 family with thaumatin-like domain (Abdin et al., 2011). Osmotin has been identified as the predominant protein (24 kDa protein) from osmotically adapted tobacco cells (Singh et al., 1985; Singh et al., 1987; Yun et al., 1997). In addition, osmotin is synthesized in root in response to exogenous abscisic acid (ABA) and accumulated in the presence of NaCl (Singh et al., 1987). The osmotin and osmotin-like proteins (OLPs), having antifungal activity, are basic isoform of the thaumatin-like proteins (TLPs) and share highly similar amino acid sequences (Yun et al., 1997; Shiu and Bleecker, 2001; Abdin et al., 2011; Misra et al., 2016). In addition to their common thaumatin-like domain, the OLPs and TLPs contain two additional domains to function, protein kinase-like domains and bifunctional inhibitor/lipid-transfer/seed storage 2S albumin domains (Liu J et al., 2010; Abdin et al., 2011). These proteins have been implicated in a wide range of cellular processes, including enzyme activation, the assembly of macromolecules, the cellular localization of proteins, and protein degradation (Liu J et al., 2010; Abdin et al., 2011). Moreover, the expression of OLP and TLP genes is induced by various environmental stresses, such as pathogens, salt, ABA, drought, cold, and wounding, suggesting that they may also function in stress signaling (Singh et al., 1989; Yun et al., 1998; van Loon et al., 2006; Misra et al., 2016). An *in silico* analysis of the structural features of these proteins suggested that they bind to specific receptors (Misra et al., 2016); however, the nature of their binding partners and the molecular and phenotypic consequences of such interactions remain unknown.

The phytohormone ABA is associated with diverse processes in plant growth and development, including seed maturation, seed dormancy, stomatal closure, and seedling growth (Finkelstein et al., 2002). ABA also plays major roles in plant-adaptive mechanisms to abiotic stresses such as cold, drought, and salinity, principally by regulating stomatal closure (Zhu, 2002; Raghavendra et al., 2010; Roychoudhury et al., 2013). The protein phosphatase type 2C (PP2C) proteins, including ABA-insensitive 1 (ABI1), ABI2, AtPP2CA/ABA hypersensitive germination 3 (AHG3), AHG1, hypersensitive to ABA 1 (HAB1), and HAB2, serve as negative regulators of ABA signaling (Kuhn et al., 2006; Saez et al., 2006; Yoshida et al., 2006b; Fujii et al., 2009a; Nishimura et al., 2009; Nishimura et al., 2010). In the absence of ABA, the activated PP2Cs bind to the SNF1-related protein kinase 2s (SnRK2s) and dephosphorylate their serine residues, preventing them from phosphorylating their targets in the ABA signaling pathway (Yoshida et al., 2006a; Fujii and Zhu, 2009b). ABA signals are detected by the pyrabactin resistance (PYR)/PYR1-like (PYL)/regulatory component of ABA receptor (RCAR) proteins, key ABA receptors that activate ABA signaling by binding both the ABA molecule and the PP2C proteins to inhibit the phosphatase activity of the PP2Cs (Fujii et al., 2009a; Park et al., 2009; Nishimura et al., 2010; Gonzalez-Guzman et al., 2012; Lee et al., 2013). This releases the SnRK2s from the PP2Cs–SnRK2s complex, which enables them to be activated by autophosphorylation and/or phosphorylation by other kinases (Melcher et al., 2009; Yin et al., 2009). The activated SnRK2s phosphorylate and activate several transcription factors involved in ABA signal transduction, such as the ABRE binding factor (ABF) transcription factors (Umezawa et al., 2009b; Xie et al., 2012). The core components, including the PYLs, PP2Cs, and SnRK2s, form a signaling complex known as the "ABA signalosome" or "ABA core signaling module" (Umezawa et al., 2009a and Umezawa et al., 2009b); however, the detailed regulation of the ABA signalosome in RLK-mediated signaling requires further studies.

In plant expressed sequence tag databases, 3 PR5Ks from among 27 proteins in the PR5 family included thaumatin domain in N-terminal region (Liu J et al., 2010). Here, we characterized the roles of the three *Arabidopsis* PR5-like receptor kinases (AtPR5Ks) in ABA-dependent drought-stress response. The *atpr5k2-1* mutant was found to be hypersensitive to drought stress but resistant to exogenous ABA stress. We revealed that AtPR5K2 acts as a negative regulator of ABA signaling during drought stress. AtPR5K2 phosphorylates ABI1 and ABI2 and functions most probably by modulating the phosphatase activity of PP2Cs of the ABA signalosome components.

MATERIALS AND METHODS

In silico Analysis

The amino acid sequence analysis programs on TAIR (https://www.arabidopsis.org/) were used to search for homologous genes. Multiple sequence alignments of proteins were carried out

using ClustalW (http://www.genome.jp/tools/clustalw) and the Plant Protein Phosphorylation DataBase (http://www.p3db.org).

Plant Materials and Growth Conditions

The *A. thaliana* wild type (WT) used in this study was Col-0 ecotype, and all mutant and gene-overexpressing transgenic plants had a Col-0 background. The *pr5k1-1* (Salk_142707), *pr5k2-1* (GK_321B01), and *pr5k3-1* (GABI_254G07) mutants were obtained from the *Arabidopsis* Biological Resource Center (*pr5k1-1*) and the GABI collection (*pr5k2-1* and *pr5k3-1*). Homozygous mutants were identified using a genomic PCR analysis with a T-DNA left border primer (LBb1.3) and two pairs of *PR5K*-specific primers. The sequences of experimental primers used for genotyping the various mutants are described in **Supplemental Table 1**.

Arabidopsis seeds were sterilized for 5 min with a 70% ethanol and 2% sodium hypochlorite solution (Yakuri pure chemicals, Kyoto, Japan) and then washed five times with sterilized water. After stratification for 3 days at 4°C in the dark, the seeds were plated on 1/2-strength Murashige and Skoog (MS) plates (pH 5.7) containing 0.6% agar and 1.5% sucrose, and grown in a growth chamber with 16-h light/8-h dark photoperiod at 23°C.

Physiological Assays

To test drought sensitivity, 3-week-old plants grown in soil with sufficient water were not watered for 11 or 13 days. After rewatering, the recovery of the drought-treated plants was monitored. The drought experiments were repeated four times using at least 12 plants for each line in each experiment. To measure the transpirational water loss, leaves were detached from 4-week-old plants grown in soil and placed on Petri dishes. Their fresh weights were measured periodically at the indicated times and the percentage of water loss. The water loss assays were repeated three times using at least 15 plants for each line in each experiment.

To measure the percentage of cotyledon greening, the seeds of all experimental plants were harvested at the same time and grown on 1/2-strength MS plates (pH 5.7) containing 0.6% agar and 1.5% sucrose, without or with different concentrations of ABA (Sigma-Aldrich, St. Louis, MO, USA) and other abiotic stresses such as NaCl, mannitol, KCl, and LiCl. Cotyledon greening was determined after their expansion. The percentage of cotyledon greening was obtained from three biological replications using at least 48 seedlings for each line in each replication.

Generation of *PR5K2*-Overexpressing Transgenic Plants

To generate the *PR5K2*-overexpressing transgenic plants, the full length of *PR5K2* complementary DNA (cDNA) was amplified from WT using PCR and cloned into *pMDC83* gateway vector (Thermo Fisher Scientific, MA, USA), which contained a hygromycin resistance gene and a *GFP* fusion sequence. *Arabidopsis* plants were transformed using *Agrobacterium tumefaciens*-mediated methods (Clough and Bent, 1998). The *PR5K2*-overexpressing transgenic plants were selected on 1/2 MS medium containing 30 μg/l of hygromycin (Merck, NJ, USA), and their *PR5K2* expression levels were analyzed using reverse transcription PCR (RT-PCR) using gene-specific primers listed in **Supplemental Table 1**.

Quantitative RT-PCR Analysis

Total RNA was extracted and purified from different *Arabidopsis* tissues using the RNeasy Plant Mini Kit (Qiagen, Hilden, Germany), according to the manufacturer's instructions, and treated with DNaseI (Sigma-Aldrich, St. Louis, MO, USA) to remove any genomic DNA contaminants. For the RT-PCR and quantitative RT-PCR (qRT-PCR) analyses, 2 μg total RNA was used for cDNA synthesis using SuperScript III (Thermo Fisher Scientific, MA, USA), in accordance with the manufacturer's protocol. The qRT-PCR analysis was performed using a SYBR Green Supermix kit (Bio-Rad Laboratories, Hercules, CA, USA), and the relative gene expression levels were automatically calculated using the CFX384 real-time PCR detection system (Bio-Rad Laboratories, Hercules, CA, USA). The qRT-PCR was performed using the following conditions: 95°C for 10 min, followed by 50 cycles of 95°C for 10 s, 60°C for 30 s, and 72°C for 30 s. The expression of *TUBULIN2* was used as the endogenous control. The qRT-PCR experiments were performed in three independent replicates. The gene-specific primers used are listed in **Supplemental Table 1**.

Transient Assays to Determine the Subcellular Localization of PR5K2

The full-length *PR5K2* cDNA was cloned into the *Xba*I and *Bam*HI sites of a superfolder green fluorescent protein (sGFP) vector plasmid containing the sGFP to create a chimeric GFP-fusion construct under the control of the CaMV *35S* promoter. To investigate the subcellular localization of PR5K2, *PR5K2-sGFP* was introduced into *Arabidopsis* protoplasts using a polyethylene glycol-mediated transformation (Baek et al., 2013). To confirm the localization of PR5K2 in the plasma membrane, the *pMDC83* vector containing *PR5K2-GFP* was transformed into *A. tumefaciens* (GV3101 strain). The transformed cells were infiltrated into the leaves of 3-week-old tobacco (*Nicotiana benthamiana*) plants. The *PR5K2-GFP*-infiltrated leaves were plasmolyzed by cutting them into small pieces and soaking them in an enzyme solution including osmoticum (mannitol and $MgSO_4$) and a protectant ($CaCl_2$) for 1 h. The fluorescent signals were detected using GFP filter (excitation, 488 nm; emission, 510 nm) and RFP filter (excitation, 543 nm; emission, 581 nm) on a confocal laser-scanning microscope (Olympus FV1000; Olympus, Tokyo, Japan). The wavelength range of bright field was in 30 nm for GFP and 100 nm for RFP. The confocal lasers were used argon for GFP and Green HeNe for RFP.

Kinase Assays

The sequences of the PR5K2 kinase domain (wPR5K2KD) and the mutagenized PR5K2 kinase domain (mPR5K2KD) were amplified from full-length *PR5K2* using PCR and sequence-specific primers. The mPR5K2KD kinase domain was generated using site-directed mutagenesis methods that converted the lysine residue of the kinase domain to alanine. The *wPR5K2KD* and *mPR5K2KD* sequences were cloned into the *Eco*RI and *Sal*I sites of the *pGEX5X-1* vector, which provided the GST expression. The GST-fused recombinant proteins were expressed in *Escherichia coli* (BL21 strain) and purified using glutathione sepharose 4B (GE Healthcare, Chicago, IL, USA), according to the manufacturer's

instructions. GST proteins were used as a control. For the *in vitro* autophosphorylation assays, 2 μg of the recombinant protein was incubated at 30°C for 30 min in a kinase buffer containing 20 mM 4-(2-hydroxyethyl)-1-piperazineethanesulfonic acid (pH 7.5), 20 mM $MgCl_2$, 2 mM $MnCl_2$, and 1 μCi of [γ-32P] ATP (3,000 Ci/mmol). After separating the reaction products on a 10% polyacrylaminde gel using sodium dodecyl sulfate polyacrylamide gel electrophoresis (SDS-PAGE), the phosphorylated proteins were detected using autoradiography.

The in-gel kinase assays were performed using a 10% polyacrylaminde SDS-PAGE gel embedded with 0.1 mg/ml either ABI1 or ABI2 as a kinase substrate, as previously described (Liu X et al., 2010) and with minor modifications. The mutagenized ABI1 and ABI2 proteins were generated using site-directed mutagenesis methods that converted the serine residue of their kinase domains to alanine. After electrophoresis with GST, wPR5K2KD, or mPR5K2KD, the gels were washed three times with washing buffer containing 25 mM Tris–HCl (pH 7.5), 0.5 mM dithiothreitol (DTT), 0.1 mM Na_3VO_4, 5 mM NaF, 5% dried nonfat milk, and 0.1% Triton X-100. After removing the SDS, the gels were incubated at room temperature for 30 min in a reaction buffer containing 25 mM Tris–HCl (pH 7.5), 2 mM EGTA, 12 mM $MgCl_2$, 1 mM DTT, and 0.1 mM Na_3VO_4. The reaction samples were combined with 250 nM ATP and 50 μCi of [γ-^{32}P] ATP (3,000 Ci/mmol) in the same reaction buffer, then incubated at room temperature for 1.5 h. ABI1 and ABI2 phosphorylation were visualized using autoradiography.

Bimolecular Fluorescence Complementation Assays in Tobacco Leaves

Bimolecular fluorescence complementation (BiFC) assays were performed using *Agrobacterium*-infiltrated methods (Tian et al., 2011). The full-length sequences of *PR5K2*, *ABI1*, *ABI2*, *SnRK2.6*, and *PYR1* were cloned into the binary gateway vectors *pDEST-^{GW}VYNE* or *pDEST-^{GW}VYCE* (Gehl et al., 2009). The N-terminal fragment (YFP^{VN}; 1–173 a.a. of eYFP) of Venus eYFP was fused to PR5K2, while the C-terminal fragment (YFP^{VC}; 156–239 a.a. of eYFP) was fused to the putative interaction partners used in the BiFC assay. The leaves of 4-week-old *N. benthamiana* plants were coinfiltrated with *A. tumefaciens* (OD_{600} = 0.5) carrying *pDEST-^{GW}VYNE-PR5K2* (*PR5K2^{VN}*) and either *pDEST-^{GW}VYCE-ABI1* (*ABI1^{VC}*), *pDEST-^{GW}VYCE-ABI2* (*ABI2^{VC}*), *pDEST-^{GW}VYCE-SnRK2.6* (*SnRK2.6^{VC}*), or *pDEST-^{GW}VYCE-PYR1* (*PYR1^{VC}*), together with the *p19* plasmid, in infiltration buffer (10 mM MES, 10 mM $MgCl_2$, and 100 μM acetosyringone). After 2 days of incubation, the fluorescence signals were detected using a GFP filter (excitation, 488 nm; emission, 510 nm) on a confocal laser-scanning microscope (Olympus FV1000; Olympus, Tokyo, Japan).

Co-Immunoprecipitation Assays

The full length of *ABI1* and *ABI2* cDNA was amplified from the WT using PCR and cloned into the *pEarleyGate 301* gateway vector (Thermo Fisher Scientific, Waltham, MA, USA), which contained a *Basta* resistance gene and a *HA* fusion sequence. The total proteins from equal amounts of *N. benthamiana* leaves expressing both *PR5K2-GFP* and *ABI1-HA* or *ABI2-HA* proteins were extracted in extraction buffer consisting of 100 mM Tris–HCl (pH 7.5), 150 mM NaCl, 1% NP-40, 1 mM ethylenediaminetetraacetic acid, 3 mM DTT, 2 mM Na_2VO_3, 2 mM NaF, 50 mM MG132, and protease inhibitor cocktail (Roche, Basel, Switzerland). α-GFP cross-linked to protein A agarose (Thermo Fisher Scientific, Waltham, MA, USA) was added to the total protein extract and incubated for 1 h at 4°C. After electrophoresis, immunoblotting was carried out using rat α-HA antibodies (Roche, Basel, Switzerland) and rabbit α-GFP antibodies (Abcam, Cambridge, UK). The antigen protein was detected using chemiluminescence with the enhanced-chemiluminescence-detecting reagent (GE Healthcare, Chicago, IL, USA) and ChemiDoc™ System (Bio-Rad Laboratories, Hercules, CA, USA).

RESULTS

Identification of the AtPR5K2 Receptor Kinase Involved in Drought-Stress Signaling

The PR5Ks, which exist in both monocots and dicots, are composed of a signal peptide, and a transmembrane domain, an extracellular thaumatin-like domain, and an intracellular Ser/Thr kinase domain (Shiu and Bleecker, 2001; Liu J et al., 2010; Abdin et al., 2011; **Supplementary Figure 1A**). There are three *Arabidopsis PR5K* genes: *AtPR5K1* (*At5g38280*), *AtPR5K2* (*At4g18250*), and *AtPR5K3* (*At1g70250*). The amino acid sequence of AtPR5K1 has a 55.0% similarity to AtPR5K2 and a 56.2% similarity to AtPR5K3, while the amino acid sequence of AtPR5K2 has a 50.6% similarity to AtPR5K3 (**Supplementary Figure 1B**). We analyzed expression of *PR5Ks* genes by *Arabidopsis* eFP Browser at BAR website (http://bar.utoronto.ca/efp/cgi-bin/efpWeb.cgi). Expression patterns of *PR5K1*, *PR5K2*, and *PR5K3* genes in developmental tissues were very different from each other (**Supplementary Figure 2**). To understand the biological function of the AtPR5Ks, we identified homozygous T-DNA insertion knockout mutants of the three *AtPR5K* genes, *atpr5k1-1*, *atpr5k2-1*, and *atpr5k3-1*, using genomic PCR and RT-PCR analyses (**Supplementary Figure 3**). These three *atpr5k* mutants did not show any significant phenotypic differences to the WT plants under normal growth conditions (**Figure 1A** and **Supplementary Figure 4A**).

We then tested the potential involvement of the *PR5K*s with the plant responses to various abiotic stresses, including drought stress. To test their drought tolerance, water was withheld from 3-week-old WT and *atpr5k* mutant plants for 11 days, after which they were rewatered. After 1 day of rewatering, a drought tolerance phenotype could be observed in the *atpr5k2-1* mutant plants (~81.25% survival rate) in comparison with the WT plants (~54.17% survival rate) (**Figure 1A**); however, the drought responses of the *atpr5k1-1* and *atpr5k3-1* mutants were similar to the WT plants. This suggests that *AtPR5K2* plays a role in drought-stress signaling (**Supplementary Figure 4**). In additions, the messenger RNA expression of *RD29B* in *atpr5k2-1* mutant was higher than that in WT plants under drought stress condition (**Supplementary Figure 5**). To further confirm the role of *AtPR5K2* in stress signaling, we generated AtPR5K2-overexpressing (AtPR5K2-OX) plants by introducing the full-length *AtPR5K2* cDNA into the WT plant. Two independent AtPR5K2-OX lines (#1 and #2) with different levels of *AtPR5K2* expression were selected (**Supplementary Figure 6**).

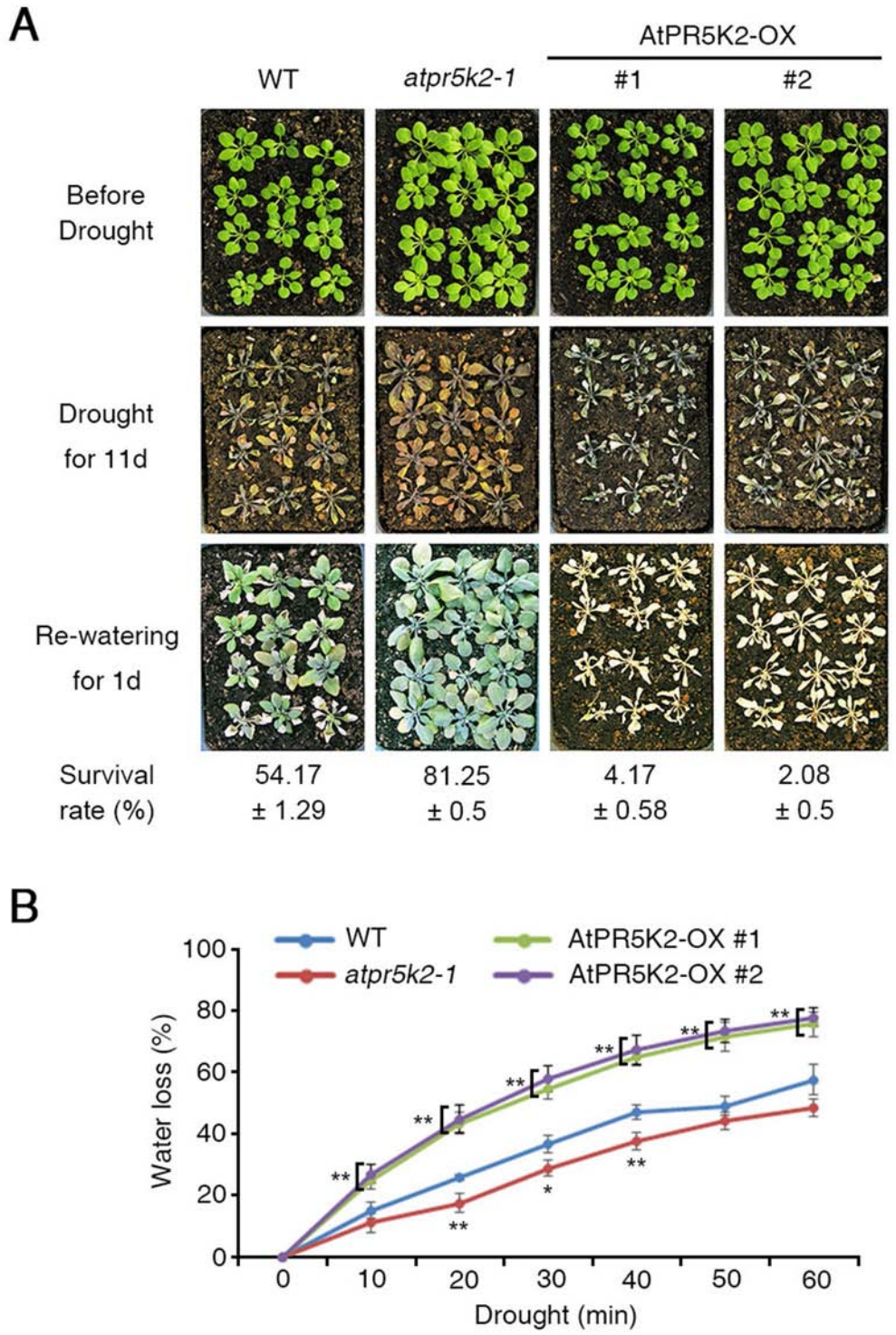

FIGURE 1 | The phenotypes of the *atpr5k2-1* mutant and AtPR5K2-overexpressing (AtPR5K2-OX) plants in response to drought stress. **(A)** Wild type (WT), *atpr5k2-1*, and AtPR5K2-overexpressing plants (AtPR5K2-OX #1 and #2) were grown in soil with sufficient water for 3 weeks (upper row). Water was then withheld from the plants for 11 days (middle), after which the plants were rewatered for 1 day (bottom). The survival rates of the WT, *atpr5k2-1*, and AtPR5K2-OX #1 and #2 lines under drought conditions were assessed in four replicates (n = 48). **(B)** Transpirational water loss was measured in detached leaves of 4-week-old WT, *atpr5k2-1*, and AtPR5K2-OX #1 and #2 plants. The fresh weights were measured at the indicated time points, and water loss was normalized relative to a percentage of their initial fresh weight. Error bars indicate the standard deviation from three independent experiments. Asterisks represent significant differences from the WT (*$0.01 < p \leq 0.01$, Student's t test).

When subjected to 11 days of drought stress and 1 day of rewatering, the AtPR5K2-OX plants exhibited a hypersensitivity to drought response (approximately 2.08–4.17% survival rate) than the WT plants (**Figure 1A**).

We further examined the transpirational water loss of the WT, *atpr5k2-1*, and AtPR5K2-OX plants by measuring the changes in the fresh weights of detached leaves from 4-week-old plants over time. Water was lost more slowly from the *atpr5k2-1* plants than from the WT, but more rapidly from the AtPR5K2-OX plants (**Figure 1B**). In addition, in the absence of ABA, stomatal opening in WT, *atpr5k2-1*, and AtPR5K2-OX plants were not different. However, in the presence of ABA, stomatal aperture in *atpr5k2-1* mutant was more significantly decreased than that in WT. The stomatal aperture of AtPR5K2-OX plants was comparable to that of WT (**Supplementary Figure 7**). We also tested the potential involvement of AtPR5K2 in the responses to other abiotic stresses; however, both the *atpr5k2-1* mutant and the AtPR5K2-OX plants did not show any obvious phenotypic differences to WT in response to the NaCl, KCl, LiCl, and mannitol stresses (**Supplementary Figure 8**). These results suggest that *AtPR5K2* plays a role in the regulation of plant responses to drought stress specifically.

AtPR5K2 Plays a Negative Role in ABA Signaling

Water deficiency in plants has huge influences on plant growth and productivity (Bartels and Sunkar, 2005). Under water-deficient conditions, the initial plant response is to regulate the accumulation of ABA (Bartels and Sunkar, 2005). To determine whether AtPR5K2 is involved in ABA signaling, we examined the phenotypes of the *atpr5k2-1* mutant and AtPR5K2-OX plants when treated with exogenous ABA. When placed on a medium containing 0.75 μM ABA, the germination of the AtPR5K2-OX seeds was significantly enhanced compared with the WT, although the germination of the *atpr5k2-1* seeds was not affected (**Figure 2A**). After germination in the presence of 0.5 μM ABA, the *atpr5k2-1* mutants showed slower (~2.7-fold) cotyledon greening than the WT; however, the cotyledon greening of the AtPR5K2-OX plants was ~1.56-fold faster than that of the WT (**Figure 2B**). The results indicated that AtPR5K2 functions as a negative regulator of ABA signaling during seed germination.

Functional Characterization of AtPR5K2

To study the molecular functions of AtPR5K2, we used qRT-PCR to analyze the expression pattern of *AtPR5K2* in various *Arabidopsis* tissues, including the rosette leaves, roots, stems, cauline leaves, flowers, and siliques. We found that *AtPR5K2* is highly expressed in the rosette and cauline leaves (**Figure 3A**). Furthermore, the messenger RNA level of *AtPR5K2* was dramatically induced in response to drought stress (**Supplementary Figure 9**). To examine the subcellular localization of the AtPR5K2 protein, the full-length *AtPR5K2* cDNA was fused with GFP and expressed under the control of CaMV *35S* promoter. Aquaporin fused with red fluorescent protein was used as a plasma-membrane marker. *35S:AtPR5K2-GFP* and *35S:Aquaporin-RFP* were transiently coexpressed in *Arabidopsis* protoplasts, and the GFP signal was

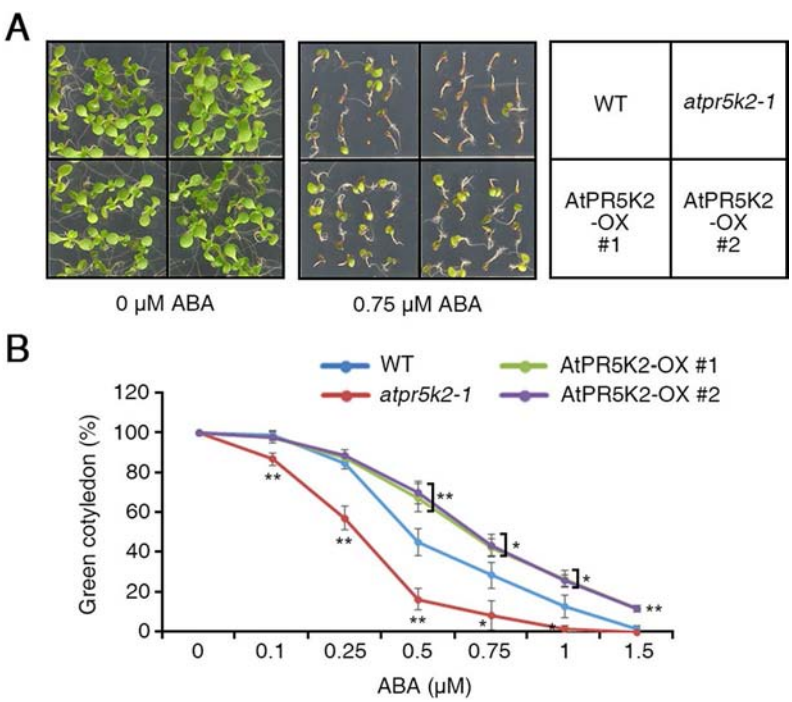

FIGURE 2 | The phenotypes of the *atpr5k2-1* mutant and AtPR5K2-overexpressing (AtPR5K2-OX) plants in response to ABA stress. **(A)** WT, *atpr5k2-1*, and AtPR5K2-OX #1 and #2 plants were germinated on 1/2 Murashige and Skoog (MS) with and without 0.75 μM abscisic acid (ABA) for 5 days. The ABA sensitivity analysis was performed in triplicate by using at least 50 seeds from each line in each experiment. **(B)** The cotyledon greening of WT, *atpr5k2-1*, and AtPR5K2-OX #1 and #2 seedlings germinated on 1/2 MS containing different concentrations of ABA for 5 days. Cotyledon greening was determined as a percentage of the seeds plated ($n = 50$). Error bars indicate the standard deviation from three independent experiments. Asterisks represent significant differences from the WT (*$0.01 < p \leq 0.01$, Student's *t* test).

observed to overlap with the plasma-membrane signal, suggesting that the protein is localized to the plasma membrane (**Figure 3B**). To confirm its plasma membrane localization, we induced plasmolysis in tobacco epidermal cells expressing *AtPR5K2-GFP*. The GFP fluorescence was still observed at clear separation of the plant protoplast from the cell wall organizing Hechtian strands, which was interrelated cell wall and plasma membrane after plasmolysis (**Figure 3C**). These data indicated that AtPR5K2 was localized to the plasma membrane.

One of the AtPR5Ks, AtPR5K1, was previously been shown to have autocatalytic kinase activity *in vitro* (Wang et al., 1996). To determine whether AtPR5K2 has autophosphorylation activity, we fused the protein kinase domain-encoding sequence of *AtPR5K2* (wPR5K2KD) with *GST* and expressed it in *E. coli*. The purified recombinant wPR5K2KD proteins were reacted with radioactive [γ-^{32}P] ATP and separated using SDS-PAGE. A phosphorylated band was detected on the resulting gel at the position approximating a molecular weight of 65 kDa, which corresponded to the molecular weight of the recombinant wPR5K2KD protein (**Figure 3D**). To impede the kinase activity of AtPR5K2, we substituted the lysine residue (amino acid position 352) in the kinase domain with arginine. This lysine residue is known to be important for ATP binding in many kinases (Carrera et al., 1993). The kinase activity of the mPR5K2KD protein was significantly reduced compared with that of wPR5K2KD (**Figure 3D**), indicating that AtPR5K2 has a functional kinase activity.

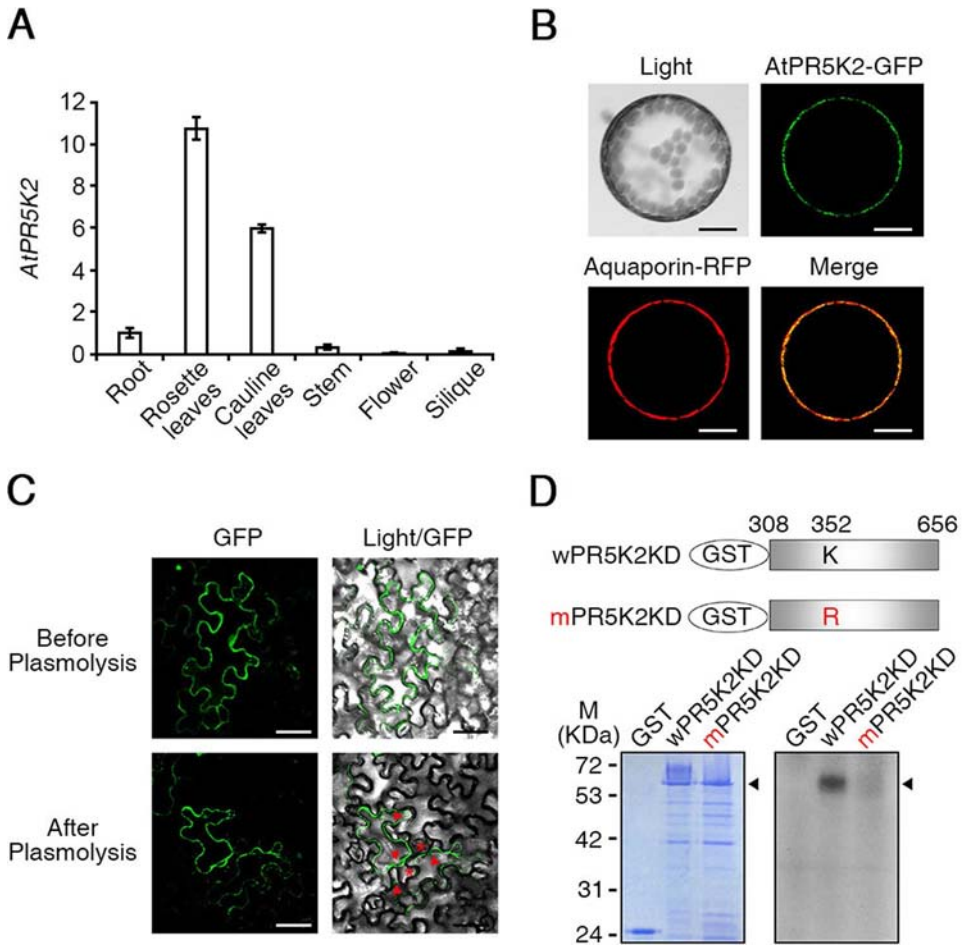

FIGURE 3 | Expression patterns and subcellular localization of AtPR5K2. **(A)** The expression of *AtPR5K2* in various tissues of *Arabidopsis thaliana*. Total RNA was extracted from the roots, rosette leaves, cauline leaves, stems, flowers, and siliques of the wild-type plants. The transcript levels of *AtPR5K2* were measured using quantitative reverse transcription PCR (qRT-PCR) and calculated relative to the expression of the endogenous control gene, *TUBULIN2*. Error bars represent the ± SD from three independent experiments. **(B)** Subcellular localization of AtPR5K2 in *Arabidopsis* protoplasts. *35S:AtPR5K2-GFP* and *Aquaporin-RFP* were coexpressed in *Arabidopsis* protoplasts, which were analyzed using confocal fluorescence microscopy and photographed after 24 h of incubation at 22°C. Aquaporin-RFP is a plasma-membrane marker. Scale bars represent 10 μm. **(C)** Subcellular localization of AtPR5K2 in the epidermal cells of tobacco (*Nicotiana benthamiana*) leave expressing *35S:AtPR5K2-GFP* before and after plasmolysis. The epidermal cells were analyzed using confocal fluorescence microscopy and photographed after 48 h of incubation at 25°C. Scale bars represent 20 μm. Red asterisk indicates that AtPR5K2-GFP signal remains in the Hechtian strands. Red arrowheads point to the retracted plasma membrane. **(D)** *In vitro* kinase assays of AtPR5K2. The upper panel indicates the schematic structure of the GST-fused AtPR5K2 kinase domain (wPR5K2KD) and the GST-fused mutagenized AtPR5K2 kinase domain (mPR5K2KD). Each kinase domain was individually expressed in *Escherichia coli*, and 2 μg purified proteins was incubated in kinase assay buffer. Radioactive-labeled products were separated on sodium dodecyl sulfate polyacrylamide gel electrophoresis (SDS-PAGE) gels and detected using radioactivity (bottom right). After electrophoresis, the purified products were stained with Coomassie brilliant blue (bottom left).

AtPR5K2 Interacts With Protein Phosphatase 2C and SnRK2.6 in the ABA Signaling Pathway

The core components of the ABA signalosome, including the PYR/PYL/RCAR ABA receptors, PP2Cs, and SnRK2s, play a major role in the ABA signal transduction and plant adaptive responses to environmental stresses (Ma et al., 2009; Melcher et al., 2009). The PP2Cs, ABI1 and ABI2, act as negative regulators of ABA signaling (Kuhn et al., 2006; Saez et al., 2006), while SnRK2.6/OST1 acts as a positive regulator of ABA-dependent stomatal closure (Yoshida et al., 2006a; Kulik et al., 2011). To test whether AtPR5K2 is involved in ABA signalosome-mediated signaling, we tested the *in vivo* interaction between AtPR5K2 and the PP2Cs using BiFC assays. The full-length *AtPR5K2* cDNA sequence was fused to the N-terminal fragment of the Venus protein (AtPR5K2^{VN}), while ABI1 or ABI2 was fused to the C-terminal fragment of Venus (ABI1^{VC} or ABI2^{VC}, respectively). Fluorescence signals were detected in the plasma membrane of the tobacco epidermal cells when AtPR5K2^{VN} was coexpressed with ABI1^{VC} or ABI2^{VC} (**Figure 4A**), while no fluorescence signals were detected when these constructs were coexpressed with the empty YFP^{VC} or YFP^{VN} vectors (**Supplementary Figure 10**). To further confirm the interaction of AtPR5K2 with ABI1 or ABI2, we conducted *in vivo* coimmunoprecipitation assays in tobacco leaves. The full-length AtPR5K2 sequence was fused to GFP (AtPR5K2-GFP), while ABI1 and ABI2 were individually fused to the HA tag protein (ABI1-HA or ABI2-HA). The total proteins of tobacco leave coinfiltrated AtPR5K2-GFP and ABI1-HA or ABI2-HA were immunoprecipitated with an α-GFP antibody, and the eluted precipitates were detected using an α-HA antibody, revealing that AtPR5K2 interacts with ABI1 and ABI2 *in vivo* (**Figure 4B**).

The physical interaction of the PP2Cs with the PYLs or SnRK2s was previously identified during ABA signaling (Yoshida et al., 2006a; Park et al., 2009; Nishimura et al., 2010). To test interaction between AtPR5K2 and SnRK2.6 or PYL1, we performed BiFC assays using SnRK2.6 or PYL1 fused to the C-terminal fragment of Venus (SnRK2.6^{VC} and PYL1^{VC}, respectively). Fluorescence signals were detected in the plasma membrane of the epidermal cells coexpressing *AtPR5K2^{VN}* and *SnRK2.6^{VC}* (**Figure 4C**); however, no interaction was detected between AtPR5K2^{VN} and PYL1^{VC} (**Figure 4D**). Taken together, these results suggest that AtPR5K2 plays an important role in the regulation of ABA core signaling by interacting with the PP2Cs and SnRK2.6.

ABA Affects the Interactions of AtPR5K2 With the PP2Cs and SnRK2.6

In the absence of ABA, the PP2Cs inhibit the autophosphorylation and activation of SnRK2.6 in ABA core signaling, while intracellular ABA enhances the *in vivo* interaction between the PP2Cs and PYL receptors (Nishimura et al., 2010). Thus, in the presence of ABA, the inhibitory effect of the PP2Cs on SnRK2.6 is removed, activating SnRK2.6 to phosphorylate ion channels or AREB/ABF transcription factors to stimulate the ABA response (Yoshida et al., 2006a; Yoshida et al., 2010). To investigate whether elevated cellular ABA levels affect the interaction of AtPR5K2 with the PP2Cs or SnRK2.6, we performed the BiFC assays in the presence and absence of exogenous ABA, by coexpressing AtPR5K2^{VN} with ABI1^{VC}, ABI2^{VC}, or SnRK2.6^{VC} in tobacco cells. The fluorescence signals in the tobacco leaves coexpressing AtPR5K2^{VN}/ABI1^{VC}, AtPR5K2^{VN}/ABI2^{VC}, and AtPR5K2^{VN}/SnRK2.6^{VC} were weaker in the presence of 10 μM exogenous ABA conditions than in the absence of ABA (**Figure 5**), suggesting that elevated ABA levels disrupt the interaction of AtPR5K2 with ABI1, ABI2, and SnRK2.6.

AtPR5K2 Phosphorylates the PP2Cs ABI1 and ABI2

To investigate whether AtPR5K2 could specifically phosphorylate ABI1, ABI2, or SnRK2.6, we performed in-gel kinase assays to test the phosphorylation of ABI1-GST, ABI2-GST, and SnRK2.6-GST by AtPR5K2. The kinase domain of PR5K2 (wPR5K2KD) phosphorylated ABI1 and ABI2 (**Figure 6**); however, no phosphorylation was detected when SnRK2.6 or GST were used as substrates (**Figure 6** and **Supplementary Figure 11**). In addition, the phosphorylation of ABI1 and ABI2 was strongly attenuated by the mutation of the PR5K kinase domain (mPR5K2KD; **Figure 6**).

To further confirm that ABI1 and ABI2 function as substrates for AtPR5K2, we investigated the putative phosphorylation site of ABI1 and ABI2 by analyzing the amino acid sequences the of PP2Cs using the Plant Protein Phosphorylation DataBase (http://www.p3db.org). The putative phosphorylation sites in ABI1 (Ser-314) and ABI2 (Ser-304) were substituted with alanine (ABI1^{S314A} and ABI2^{S304A}, respectively; Han et al., 2018). We performed in-gel kinase assays using ABI1^{S314A} and ABI2^{S304A} as substrates for the AtPR5K2 kinase domain (**Figure 6**), revealing that their phosphorylation by wPR5K2KD was greatly attenuated in comparison with the WT ABI1 and ABI2 proteins (**Figure 6**). These results suggested that AtPR5K2 phosphorylates the ABI1 and ABI2 phosphatases to modulate their activities during ABA core signaling.

DISCUSSION

AtPR5K2 Negatively Regulates ABA Signaling

Several RLKs are known to function in abiotic stress signaling (Osakabe et al., 2005; Bai et al., 2009; Tanaka et al., 2012; Kumar et al., 2017). Some RLKs are involved in ABA signaling; however, the mechanisms by which they interact with the ABA core signaling pathway were not previously understood. *AtRPK1* expression is rapidly induced by various abiotic stresses, such as ABA, drought, salinity, and cold, indicating that RPK1 mediates abiotic stress responses (Hong et al., 1997), while proline-rich extensin-like receptor kinase 4, an ABA- and Ca^{2+}-activated protein kinase, was functionally characterized in the initial stages of ABA signaling (Bai et al., 2009). A cysteine-rich repeat RLK36negatively regulates ABA and osmotic stress signaling by interacting with receptor-like cytosolic kinase 1 (Tanaka et al., 2012). BRI1-associated receptor kinase 1 interacts with SnRK2.6 to induce stomatal closure in response to ABA, in contrast with the function of ABI1 during the ABA responses (Shang et al., 2016). Receptor dead kinase 1 is a positive regulator of ABA-dependent abiotic-stress signaling (Kumar et al., 2017). In the present study, we characterized the role of AtPR5K2 in ABA-dependent drought-stress signaling. It was

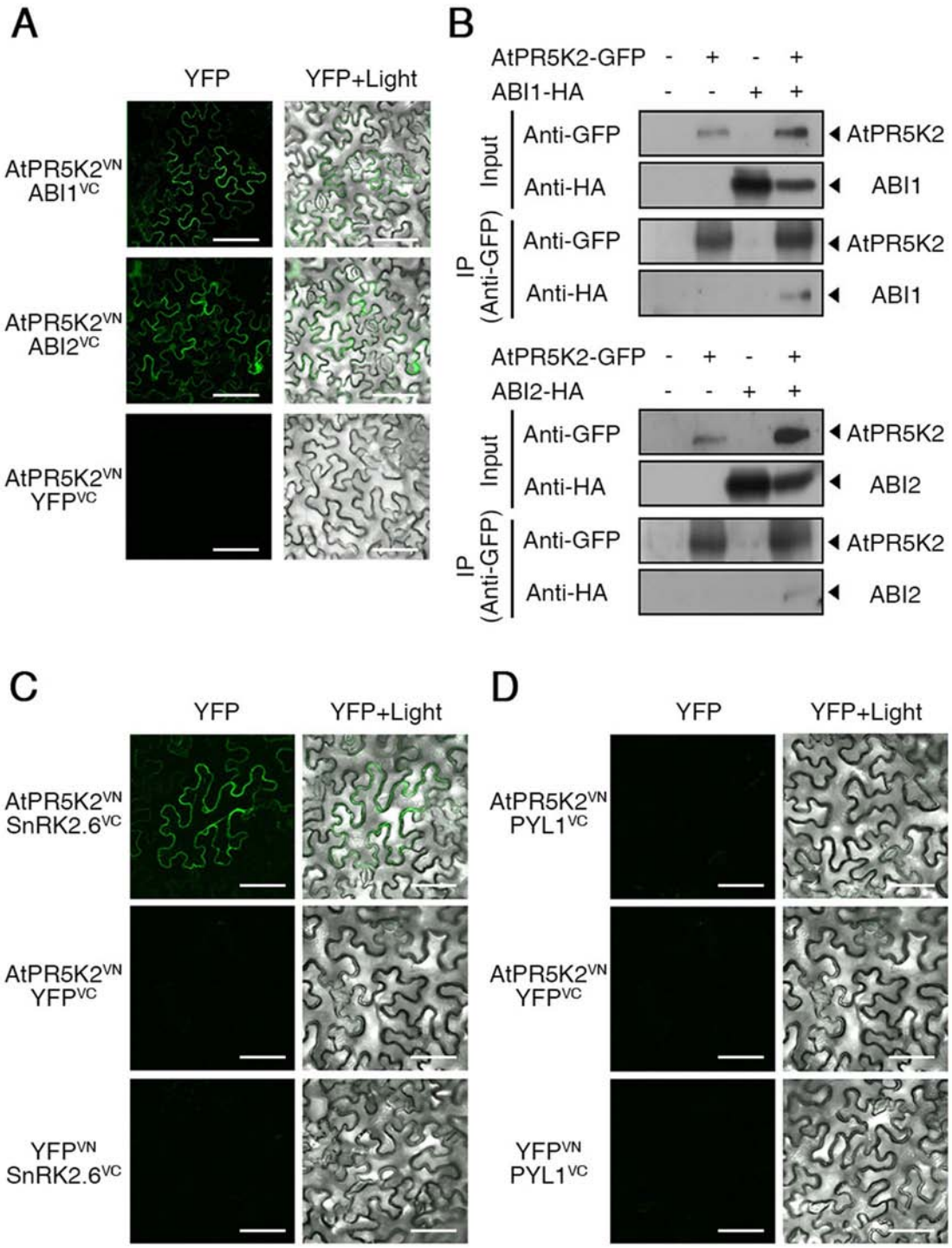

FIGURE 4 | AtPR5K2 interaction with ABI1, ABI2, and SnRK2.6 *in vivo* and *in vitro*. **(A)** Bimolecular fluorescence complementation (BiFC) analysis of AtPR5K2 and PP2Cs coexpressed in tobacco (*Nicotiana benthamiana*) leaves. VN and VC indicate the N- and C-terminal regions of Venus (eYFP), respectively. The epidermal cells were analyzed using confocal fluorescence microscopy and photographed after 48 h of incubation at 25°C. Scale bars represent 100 μm. **(B)** AtPR5K2 forms a complex with the PP2Cs. Each combination of *35S:AtPR5K2-GFP*, *35S:ABI1-HA*, and *35S:ABI2*-HA were transiently expressed in tobacco plants. The proteins were immunoprecipitated with an alpha-green fluorescent protein (α-GFP) antibody and resolved with SDS-PAGE. The immunoblots were probed with an α-GFP antibody to detect AtPR5K2 or an α-HA antibody to detect ABI1 and ABI2. The minus (–) indicated empty vectors (*35S:GFP* or *35S:HA*, respectively) as negative controls. (C and D) BiFC analysis of AtPR5K2 and SnRK2.6 **(C)** or PYL1 **(D)** coexpressed in tobacco leaves. The epidermal cells were analyzed using confocal fluorescence microscopy and photographed after 48 h of incubation at 25°C. Scale bars represent 100 μm.

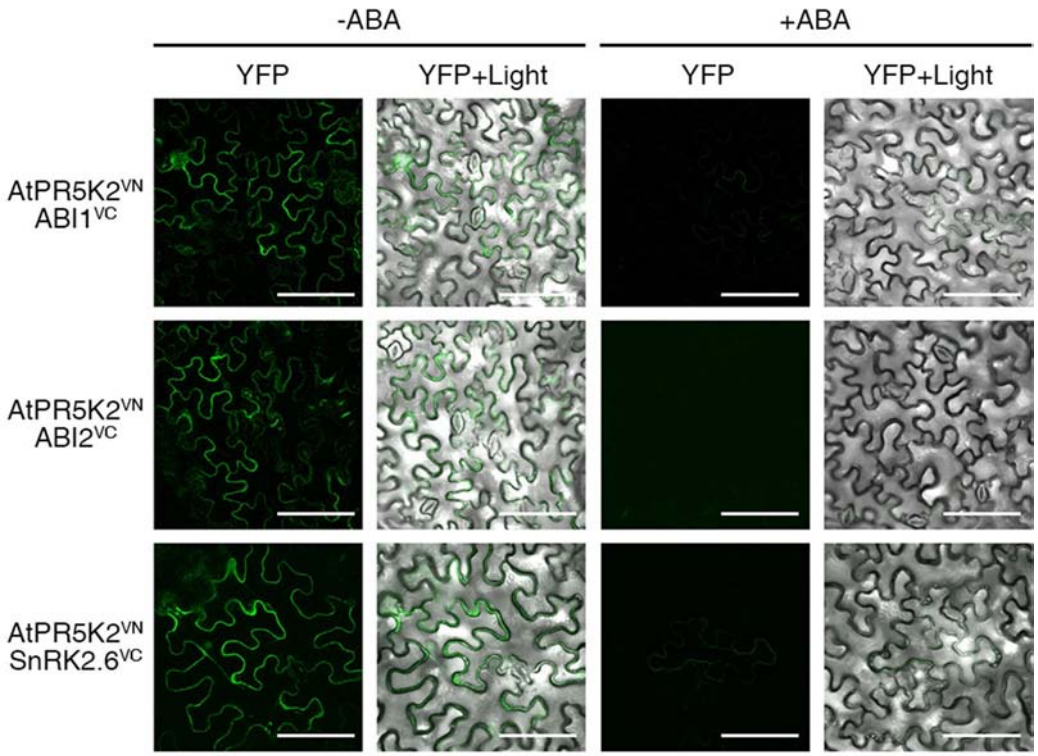

FIGURE 5 | Influence of the AtPR5K2 complex on ABA stress signaling. BiFC analysis of AtPR5K2 and ABI1, ABI2, or SnRK2.6 transiently coexpressed in tobacco (*Nicotiana benthamiana*) leaves in the presence of absence of 10 μM exogenous ABA. VN and VC indicate the N- and C-terminal regions of Venus (eYFP), respectively. The epidermal cells were analyzed using confocal fluorescence microscopy and photographed after 48 h of incubation at 25°C in the presence or absence of ABA. Scale bars represent 100 μm

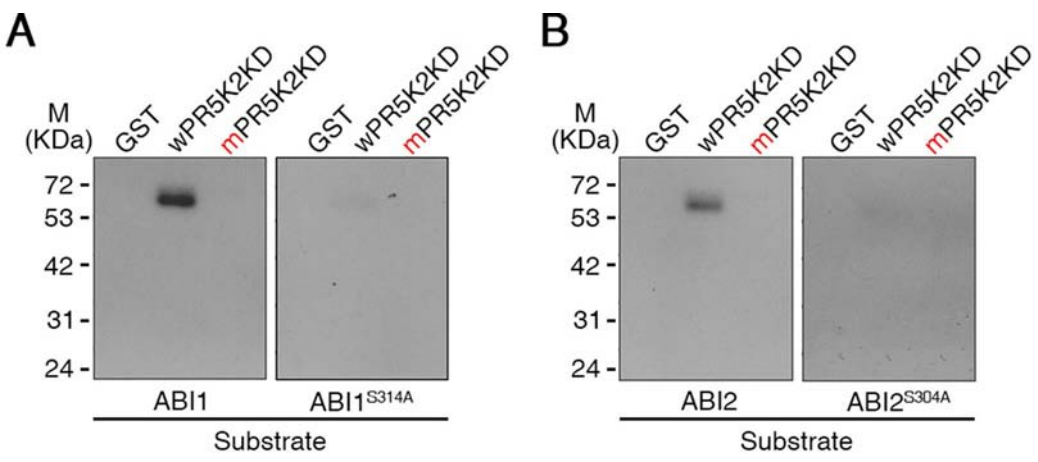

FIGURE 6 | In-gel kinase assay of AtPR5K2. The recombinant fusion protein of the AtPR5K2 kinase domain (wPR5K2KD) or the mutagenized AtPR5K2 kinase domain (mPR5K2KD) was denatured and separated on an SDS gel. An in-gel kinase assay was performed using recombinant ABI1 (**A**; left), ABI1^{S314A} (**A**; right), ABI2 (**B**; left), or ABI2^{S304A} (**B**; right) as an embedded substrate. The GST tag served as a negative control.

found to interact with ABI1 and ABI2 on the plasma membrane (**Figure 4**) and phosphorylate them *in vitro* (**Figures 3** and **6**). ABI1 and ABI2 are typical PP2C proteins and key negative regulators of the ABA core signaling pathway (Cutler et al., 2010; Raghavendra et al., 2010). In addition, the AtPR5K2-OX plants underwent significantly higher levels of cotyledon greening than the WT when treated with ABA (**Figure 2**). These findings suggested that AtPR5K2 could act as a negative regulator of ABA signaling that modulates the functions of the PP2Cs.

Age-dependent leaf senescence is associated with various environmental stresses and changes of various plant hormones, such as ABA (Lim et al., 2007). It is recently reported that drought

tolerance is enhanced when drought-induced leaf senescence is delayed in plants (Rivero et al., 2007). *Arabidopsis* RPK1, receptor protein kinase 1, mediates ABA-induced and age-dependent leaf senescence (Lee et al., 2011). The ABA receptor PYL9 improved ability of drought resistance as well as ABA-induced leaf senescence (Zhao et al., 2016). These results suggest the crosstalk between ABA-dependent drought stress signaling and leaf senescence. Based on these observations, it would be possible that AtPR5K2 may play a role in cross-talk between ABA-dependent drought stress signaling and leaf senescence. We intend to test the role of AtPR5K2 in drought- and ABA-mediated leaf senescence in the future study.

AtPR5K2 Directly Phosphorylates the PP2Cs But Not SnRK2.6 in the ABA Signalosome

Although AtPR5K1 was previously reported to have kinase activity (Wang et al., 1996), the function of the closely related AtPR5K2 protein was not previously known. AtPR5K2 comprises a thaumatin-like domain, a transmembrane domain, and a Ser/Thr kinase domain, the latter of which showed high similarity with that of AtPR5K1 (**Supplementary Figure 1**). Like AtPR5K1, AtPR5K2 has an efficient kinase activity which requires the lysine residue in its kinase domain (**Figure 3D**).

We investigated several major components of the ABA core signaling pathway as potential target substrates for AtPR5K2. ABI1, ABI2, and SnRK2.6 were previously known to be activated by phosphorylation during the ABA response (Kulik et al., 2011; Ma et al., 2009; Umezawa et al., 2009b; Ng et al., 2011); however, the mechanisms of this phosphorylation remained unclear. We showed that AtPR5K2 phosphorylated ABI1 and ABI2 *in vitro* (**Figure 6**), but did not use SnRK2.6 as a substrate (**Supplementary Figure 11**). In addition, we identified the putative phosphorylation sites of ABI1 (Ser-314) and ABI2 (Ser-304) used by AtPR5K2 (**Figure 6**). To our knowledge, AtPR5K2 is the first plant novel receptor kinase known to phosphorylate ABI1 and ABI2.

Proposed Working Model of AtPR5K2 in ABA Core Signaling

The ABA-mediated signal transduction pathway has been extensively studied, and many of its regulators have been elucidated (Finkelstein et al., 2002; Cutler et al., 2010; Raghavendra et al., 2010). Here, we added a new key component, AtPR5K2, to the ABA core signaling pathway (**Figure 7**). In the absence of ABA, AtPR5K2 interacts with the PP2Cs and SnRK2.6, but not with PYL1 ABA receptor. Active AtPR5K2 phosphorylates PP2C phosphatases, such as ABI1 and ABI2, which inhibit the activity of SnRK2.6, a positive regulator of ABA signaling, *via* dephosphorylation. This means that, in the absence of ABA, AtPR5K interrupts the ABA signal transduction and the expression of the ABA-dependent genes. Under stress conditions, such as drought, increased intracellular ABA dissociates the PP2Cs and SnRK2.6 from AtPR5K2 (**Figure 5** and **Figure 7**). The released PP2Cs directly bind to both ABA and the PYL receptors and become inactivated. Subsequently, the SnRK2.6 kinase is activated by autophosphorylation and phosphorylates the ABRE/ABF transcription factors to induce the expression of ABA-dependent genes, which enhances plant tolerance to various abiotic stresses (**Figure 7**).

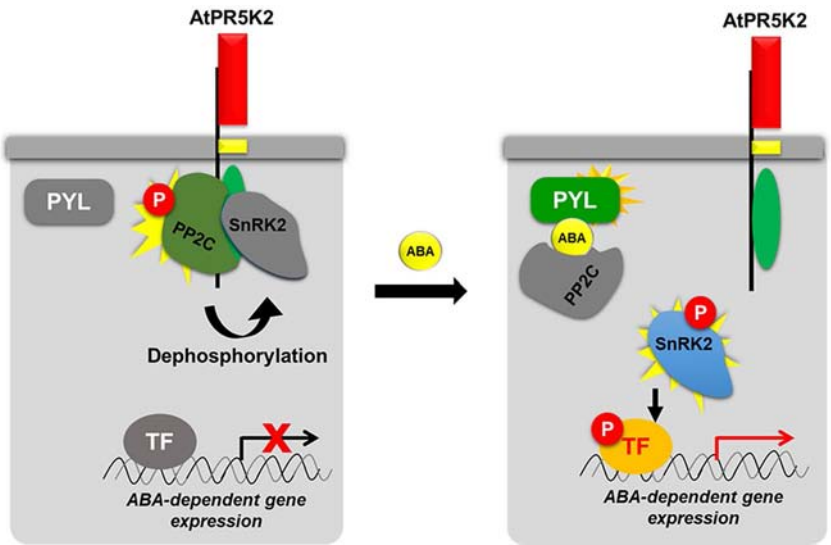

FIGURE 7 | Proposed working model of AtPR5K2 in ABA core signaling. AtPR5K2 is single transmembrane protein with an N-terminal thaumatin-like domain (red box), a single transmembrane domain (yellow box), and a C-terminal Ser/Thr kinase domain (green oval). In the absence of ABA, the phosphatase activity of the PP2Cs is enhanced by AtPR5K2-dependent phosphorylation. The activated PP2Cs dephosphorylate the SnRK2s, decreasing their activity. Thus, the ABA-dependent gene expression regulated by SnRK2 is attenuated. In the presence of ABA, the protein–protein interaction affinities among AtPR5K2, PP2Cs, and SnRK2s are weakened. This means that the PP2Cs and SnRK2 are released from AtPR5K2, freeing SnRK2.6 to autophosphorylate itself and phosphorylate the transcription factors regulating ABA-dependent gene expression. In the case of the PP2Cs and SnRK2.6, a vivid coloration indicates an active status, while the gray color indicates an inactive status. The red circle containing the letter "P" indicates phosphorylation.

CONCLUSION

We identified and characterized the role of AtPR5K2, a PR5-like receptor kinase, in ABA core signaling during plant responses to drought stress. The AtPR5K2-OX plants were hypersensitive to drought stress and tolerant of exogenous ABA, suggesting that AtPR5K2 mediates ABA-dependent drought-stress signaling. Our molecular and biochemical results suggest that, under normal growth conditions, AtPR5K2 probably deactivates ABA core signaling and ABA-dependent gene expression by modulating the phosphorylation status of the PP2Cs and SnRK2.6, a major factor in stomatal closure. In response to abiotic stresses, however, AtPR5K2 turns on the ABA core signaling cascade and ABA-dependent gene expression by releasing the PP2Cs and freeing SnRK2.6 to promote ABA signaling. Our results demonstrate that AtPR5K2 plays an important role as a key negative regulator of ABA core signaling by phosphorylating the PP2C phosphatases, such as ABI1 and ABI2.

DATA AVAILABILITY STATEMENT

All datasets for this study are included in the manuscript and the **Supplementary Files**.

AUTHOR CONTRIBUTIONS

DB, MK, J-YK, and D-JY designed the experiments. DB and DK performed most of the experiments, and MK, J-YK, and D-JY wrote the manuscript. HC, SL, and RB discussed and commented on the results and manuscripts. BP, MC, WC, HCP, and HJP performed some of the experiments. D-JY, J-YK, MK, and DB provided funding for research work.

FUNDING

This work was supported by the Next Generation BioGreen21 Program [SSAC, grant number PJ01318201 (to D-JY) and PJ01318202 (to MCK)], the Rural Development Administration Republic of Korea, and the Basic Science Research Program through the National Research Foundation of Korea (NRF) funded by the Ministry of Education [2015R1A6A1A03031413 (to MCK), NRF-2017R1A4A1015515 (to J-YK), 2016R1D1A1B01011803 (to DB), and Global Resea rch Laboratory 2017K1A1A2013146 (to D-JY)].

SUPPLEMENTARY MATERIAL

The Supplementary Material for this article can be found online at: https://www.frontiersin.org/articles/10.3389/fpls.2019.01146/full#supplementary-material

REFERENCES

Abdin, M. Z., Kiran, U., and Alam, A. (2011). Analysis of osmotin, a PR protein as metabolic modulator in plants. *Bioinformation* 5 (8), 336–340. doi: 10.6026/97320630005336

Baek, D., Kim, M. C., Chun, H. J., Kang, S., Park, H. C., Shin, G., et al. (2013). Regulation of miR399f transcription by AtMYB2 affects phosphate starvation responses in *Arabidopsis*. *Plant Physiol.* 161 (1), 362–373. doi: 10.1104/pp.112.205922

Bai, L., Zhang, G., Zhou, Y., Zhang, Z., Wang, W., Du, Y., et al. (2009). Plasma membrane-associated proline-rich extensin-like receptor kinase 4, a novel regulator of Ca signalling, is required for abscisic acid responses in *Arabidopsis thaliana*. *Plant J.* 60 (2), 314–327. doi: 10.1111/j.1365-313X.2009.03956.x

Bartels, D., and Sunkar, R. (2005). Drought and Salt Tolerance. *Plants. Crit. Rev. Plant Sci.* 24 (1), 23–58.

Becraft, P. W., Stinard, P. S., and McCarty, D. R. (1996). CRINKLY4: a TNFR-like receptor kinase involved in maize epidermal differentiation. *Science* 273 (5280), 1406–1409. doi: 10.1126/science.273.5280.1406

Carrera, A. C., Alexandrov, K., and Roberts, T. M. (1993). The conserved lysine of the catalytic domain of protein kinases is actively involved in the phosphotransfer reaction and not required for anchoring ATP. *Proc. Natl. Acad. Sci. U.S.A.* 90 (2), 442–446. doi: 10.1073/pnas.90.2.442

Clark, S. E., Williams, R. W., and Meyerowitz, E. M. (1997). The CLAVATA1 gene encodes a putative receptor kinase that controls shoot and floral meristem size in *Arabidopsis*. *Cell* 89 (4), 575–585. doi: 10.1016/S0092-8674(00)80239-1

Clarke, J. D., Volko, S. M., Ledford, H., Ausubel, F. M., and Dong, X. (2000). Roles of salicylic acid, jasmonic acid, and ethylene in CPR-induced resistance in *Arabidopsis*. *Plant Cell* 12 (11), 2175–2190. doi: 10.1105/tpc.12.11.2175

Clough, S. J., and Bent, A. F. (1998). Floral dip: a simplified method for *Agrobacterium*-mediated transformation of *Arabidopsis thaliana*. *Plant J.* 16 (6), 735–743. doi: 10.1046/j.1365-313x.1998.00343.x

Cutler, S. R., Rodriguez, P. L., Finkelstein, R. R., and Abrams, S. R. (2010). Abscisic acid: emergence of a core signaling network. *Annu. Rev. Plant Biol.* 61, 651–679. doi: 10.1146/annurev-arplant-042809-112122

Durrant, W. E., and Dong, X. (2004). Systemic acquired resistance. *Annu. Rev. Phytopathol.* 42, 185–209. doi: 10.1146/annurev.phyto.42.040803.140421

Finkelstein, R. R., Gampala, S. S., and Rock, C. D. (2002). Abscisic acid signaling in seeds and seedlings. *Plant Cell* 14 (Suppl), S15–S45. doi: 10.1105/tpc.010441

Fujii, H., and Zhu, J. K. (2009b). Arabidopsis mutant deficient in 3 abscisic acid-activated protein kinases reveals critical roles in growth, reproduction, and stress. *Proc. Natl. Acad. Sci. U.S.A.* 106 (20), 8380–8385. doi: 10.1073/pnas.0903144106

Fujii, H., Chinnusamy, V., Rodrigues, A., Rubio, S., Antoni, R., Park, S. Y., et al. (2009a). In vitro reconstitution of an abscisic acid signalling pathway. *Nature* 462 (7273), 660–664. doi: 10.1038/nature08599

Gehl, C., Waadt, R., Kudla, J., Mendel, R. R., and Hänsch, R. (2009). New GATEWAY vectors for high throughput analyses of protein–protein interactions by bimolecular fluorescence complementation. *Mol. Plant* 2 (5), 1051–1058. doi: 10.1093/mp/ssp040

Gonzalez-Guzman, M., Pizzio, G. A., Antoni, R., Vera-Sirera, F., Merilo, E., Bassel, G. W., et al. (2012). *Arabidopsis* PYR/PYL/RCAR receptors play a major role in quantitative regulation of stomatal aperture and transcriptional response to abscisic acid. *Plant Cell* 24 (6), 2483–2496. doi: 10.1105/tpc.112.098574

Han, T., Zhan, W., Gan, M., Liu, F., Yu, B., Chin, Y. E., et al. (2018). Phosphorylation of glutaminase by PKCε is essential for its enzymatic activity and critically contributes to tumorigenesis. *Cell Res.* 28 (6), 655–669. doi: 10.1038/s41422-018-0021-y

Hatakeyama, K., Takasaki, T., Suzuki, G., Nishio, T., Watanabe, M., Isogai, A., et al. (2001). The S receptor kinase gene determines dominance relationships in stigma expression of self-incompatibility in Brassica. *Plant J.* 26 (1), 69–76. doi: 10.1046/j.1365-313x.2001.01009.x

Hohmann, U., Lau, K., and Hothorn, M. (2017). The structural basis of ligand perception and signal activation by receptor kinases. *Annu. Rev. Plant Biol.* 68, 109–137. doi: 10.1146/annurev-arplant-042916-040957

Hong, S. W., Jon, J. H., Kwak, J. M., and Nam, H. G. (1997). Identification of a receptor-like protein kinase gene rapidly induced by abscisic acid, dehydration, high salt, and cold treatments in *Arabidopsis thaliana*. *Plant Physiol.* 113 (4), 1203–1212. doi: 10.1104/pp.113.4.1203

Hou, X., Tong, H., Selby, J., Dewitt, J., Peng, X., and He, Z. H. (2005). Involvement of a cell wall-associated kinase, WAKL4, in Arabidopsis mineral responses. *Plant Physiol.* 139 (4), 1704–1716. doi: 10.1104/pp.105.066910

Jin, P., Guo, T., and Becraft, P. W. (2000). The maize CR4 receptor-like kinase mediates a growth factor-like differentiation response. *Genesis* 27, 104–116. doi: 10.1002/1526-968X(200007)27:3<104::AID-GENE30>3.0.CO;2-I

Kang, S.-G., Lee, H. J., and Suh, S.-G. (2002). The maize Crinkly4 gene is expressed spatially in vegetative and floral organs. *J. Plant Biol.* 45, 219–224. doi: 10.1007/BF03030363

Kobe, B., and Deisenhofer, J. (1994). The leucine-rich repeat: a versatile binding motif. *Trends Biochem. Sci.* 19 (10), 415–421. doi: 10.1016/0968-0004(94)90090-6

Kuhn, J. M., Boisson-Dernier, A., Dizon, M. B., Maktabi, M. H., and Schroeder, J. I. (2006). The protein phosphatase AtPP2CA negatively regulates abscisic acid signal transduction in *Arabidopsis*, and effects of abh1 on AtPP2CA mRNA. *Plant Physiol.* 140 (1), 127–139. doi: 10.1104/pp.105.070318

Kulik, A., Wawer, I., Krzywińska, E., Bucholc, M., and Dobrowolska, G. (2011). SnRK2 protein kinases--key regulators of plant response to abiotic stresses. *OMICS*. 15 (12), 859–872. doi: 10.1089/omi.2011.0091

Kumar, D., Kumar, R., Baek, D., Hyun, T. K., Chung, W. S., Yun, D. J., et al. (2017). *Arabidopsis thaliana* receptor dead kinase1 functions as a positive regulator in plant responses to ABA. *Mol. Plant* 10 (2), 223–243. doi: 10.1016/j.molp.2016.11.011

Lee, I. C., Hong, S. W., Whang, S. S., Lim, P. O., Nam, H. G., and Koo, J. C. (2011). Age-dependent action of an ABA-inducible receptor kinase, RPK1, as a positive regulator of senescence in *Arabidopsis* leaves. *Plant Cell Physiol.* 52 (4), 651–662. doi: 10.1093/pcp/pcr026

Lee, S. C., Lim, C. W., Lan, W., He, K., and Luan, S. (2013). ABA signaling in guard cells entails a dynamic protein-protein interaction relay from the PYL-RCAR family receptors to ion channels. *Mol. Plant* 6 (2), 528–538. doi: 10.1093/mp/sss078

Lim, P. O., Kim, H. J., and Nam, H. G. (2007). Leaf senescence. *Annu. Rev. Plant Biol.* 58, 115–136. doi: 10.1146/annurev.arplant.57.032905.105316

Liu, J. J., Sturrock, R., and Ekramoddoullah, A. K. (2010). The superfamily of thaumatin-like proteins: its origin, evolution, and expression towards biological function. *Plant Cell Rep.* 29 (5), 419–436. doi: 10.1007/s00299-010-0826-8

Liu, X. M., Kim, K. E., Kim, K. C., Nguyen, X. C., Han, H. J., Jung, M. S., et al. (2010). Cadmium activates *Arabidopsis* MPK3 and MPK6 *via* accumulation of reactive oxygen species. *Phytochemistry* 71 (5–6), 614–618. doi: 10.1016/j.phytochem.2010.01.005

Loris, R., Imberty, A., Beeckmans, S., Van Driessche, E., Read, J. S., Bouckaert, J., et al. (2003). Crystal structure of *Pterocarpus angolensis* lectin in complex with glucose, sucrose, and turanose. *J. Biol. Chem.* 278 (18), 16297–16303. doi: 10.1074/jbc.M211148200

Ma, Y., Szostkiewicz, I., Korte, A., Moes, D., Yang, Y., Christmann, A., et al. (2009). Regulators of PP2C phosphatase activity function as abscisic acid sensors. *Science* 324 (5930), 1064–1068. doi: 10.1126/science.1172408

Mandel, T., Candela, H., Landau, U., Asis, L., Zelinger, E., Carles, C. C., et al. (2016). Differential regulation of meristem size, morphology and organization by the ERECTA, CLAVATA and class III HD-ZIP pathways. *Development* 143 (9), 1612–1622. doi: 10.1242/dev.129973

McCarty, D. R., and Chory, J. (2000). Conservation and innovation in plant signaling pathways. *Cell* 103 (2), 201–209. doi: 10.1016/S0092-8674(00)00113-6

Melcher, K., Ng, L. M., Zhou, X. E., Soon, F. F., Xu, Y., Suino-Powell, K. M., et al. (2009). A gate–latch–lock mechanism for hormone signalling by abscisic acid receptors. *Nature* 462 (7273), 602–608. doi: 10.1038/nature08613

Misra, R. C., Sandeep, Kamthan, M., Kumar, S., and Ghosh, S. (2016). A thaumatin-like protein of *Ocimum basilicum* confers tolerance to fungal pathogen and abiotic stress in transgenic *Arabidopsis*. *Sci. Rep.* 6, 25340. doi: 10.1038/srep25340

Ng, L. M., Soon, F. F., Zhou, X. E., West, G. M., Kovach, A., Suino-Powell, K. M., et al. (2011). Structural basis for basal activity and autoactivation of abscisic acid (ABA) signaling SnRK2 kinases. *Proc. Natl. Acad. Sci. U.S.A.* 108 (52), 21259–21264. doi: 10.1073/pnas.1118651109

Nikonorova, N., Vu, L. D., Czyzewicz, N., Gevaert, K., and De Smet, I. (2015). A phylogenetic approach to study the origin and evolution of the CRINKLY4 family. *Front. Plant Sci.* 6, 880. doi: 10.3389/fpls.2015.00880

Nishimura, N., Hitomi, K., Arvai, A. S., Rambo, R. P., Hitomi, C., Cutler, S. R., et al. (2009). Structural mechanism of abscisic acid binding and signaling by dimeric PYR1. *Science* 326 (5958), 1373–1379. doi: 10.1126/science.1181829

Nishimura, N., Sarkeshik, A., Nito, K., Park, S. Y., Wang, A., Carvalho, P. C., et al. (2010). PYR/PYL/RCAR family members are major in-vivo ABI1 protein phosphatase 2C-interacting proteins in *Arabidopsis*. *Plant J.* 61 (2), 290–299. doi: 10.1111/j.1365-313X.2009.04054.x

Osakabe, Y., Maruyama, K., Seki, M., Satou, M., Shinozaki, K., and Yamaguchi-Shinozaki, K. (2005). Leucine-rich repeat receptor-like kinase1 is a key membrane-bound regulator of abscisic acid early signaling in *Arabidopsis*. *Plant Cell* 17 (4), 1105–1119. doi: 10.1105/tpc.104.027474

Park, S. Y., Fung, P., Nishimura, N., Jensen, D. R., Fujii, H., Zhao, Y., et al. (2009). Abscisic acid inhibits type 2C protein phosphatases *via the* PYR/PYL family of START proteins. *Science* 324 (5930), 1068–1071. doi: 10.1126/science.1173041

Raghavendra, A. S., Gonugunta, V. K., Christmann, A., and Grill, E. (2010). ABA perception and signalling. *Trends Plant Sci.* 15 (7), 395–401. doi: 10.1016/j.tplants.2010.04.006

Rivero, R. M., Kojima, M., Gepstein, A., Sakakibara, H., Mittler, R., Gepstein, S., et al. (2007). Delayed leaf senescence induces extreme drought tolerance in a flowering plant. *Proc. Natl. Acad. Sci. U.S.A.* 104 (49), 19631–19636. doi: 10.1073/pnas.0709453104

Roychoudhury, A., Paul, S., and Basu, S. (2013). Cross-talk between abscisic acid-dependent and abscisic acid-independent pathways during abiotic stress. *Plant Cell Rep.* 32 (7), 985–1006. doi: 10.1007/s00299-013-1414-5

Saez, A., Robert, N., Maktabi, M. H., Schroeder, J. I., Serrano, R., and Rodriguez, P. L. (2006). Enhancement of abscisic acid sensitivity and reduction of water consumption in *Arabidopsis* by combined inactivation of the protein phosphatases type 2C ABI1 and HAB1. *Plant Physiol.* 141 (4), 1389–1399. doi: 10.1104/pp.106.081018

Schoof, H., Lenhard, M., Haecker, A., Mayer, K. F., Jürgens, G., and Laux, T. (2000). The stem cell population of Arabidopsis shoot meristems in maintained by a regulatory loop between the CLAVATA and WUSCHEL genes. *Cell* 100 (6), 635–644. doi: 10.1016/S0092-8674(00)80700-X

Shang, Y., Dai, C., Lee, M. M., Kwak, J. M., and Nam, K. H. (2016). BRI1-associated receptor kinase 1 regulates guard cell ABA signaling mediated by open stomata 1 in *Arabidopsis*. *Mol. Plant* 9 (3), 447–460. doi: 10.1016/j.molp.2015.12.014

Shiu, S. H., and Bleecker, A. B. (2001). Receptor-like kinases from *Arabidopsis* form a monophyletic gene family related to animal receptor kinases. *Proc. Natl. Acad. Sci. U.S.A.* 98, 10763–10768. doi: 10.1073/pnas.181141598

Singh, N. K., Handa, A. K., Hasegawa, P. M., and Bressan, R. A. (1985). Proteins associated with adaptation of cultured tobacco cells to NaCl. *Plant Physiol.* 79, 126–137. doi: 10.1104/pp.79.1.126

Singh, N. K., LaRosa, P. C., Handa, A. K., Hasegawa, P. M., and Bressan, R. A. (1987). Hormonal regulation of protein synthesis associated with salt tolerance in plant cells. *Proc. Natl. Acad. Sci. U.S.A.* 84, 739–743. doi: 10.1073/pnas.84.3.739

Singh, N. K., Nelson, D. E., Kuhn, D., Hasegawa, P. M., and Bressan, R. A. (1989). Molecular cloning of osmotin and regulation of its expression by ABA and adaptation to low water potential. *Plant Physiol.* 90 (3), 1096–1101. doi: 10.1104/pp.90.3.1096

Takayama, S., and Isogai, A. (2003). Molecular mechanism of self-recognition in *Brassica* self-incompatibility. *J. Exp. Bot.* 54 (380), 149–156. doi: 10.1093/jxb/erg007

Tanaka, H., Osakabe, Y., Katsura, S., Mizuno, S., Maruyama, K., Kusakabe, K., et al. (2012). Abiotic stress-inducible receptor-like kinases negatively control ABA signaling in *Arabidopsis*. *Plant J.* 70 (4), 599–613. doi: 10.1111/j.1365-313X.2012.04901.x

Thomma, B. P., Eggermont, K., Penninckx, I. A., Mauch-Mani, B., Vogelsang, R., Cammue, B. P., et al. (1998). Separate jasmonate-dependent and salicylate-dependent defense-response pathways in *Arabidopsis* are essential for resistance to distinct microbial pathogens. *Proc. Natl. Acad. Sci. U.S.A.* 95 (25), 15107–15111. doi: 10.1073/pnas.95.25.15107

Tian, G., Lu, Q., Zhang, L., Kohalmi, S. E., and Cui, Y. (2011). Detection of protein interactions in plant using a gateway compatible bimolecular fluorescence complementation (BiFC) system. *J. Vis. Exp.* (55), e3473. doi: 10.3791/3473

Tian, Q., Olsen, L., Sun, B., Lid, S. E., Brown, R. C., Lemmon, B. E., et al. (2007). Subcellular localization and functional domain studies of DEFECTIVE

KERNEL1 in maize and Arabidopsis suggest a model for aleurone cell fate specification involving CRINKLY4 and SUPERNUMERARY ALEURONE LAYER1. *Plant Cell* 19, 3127–3145. doi: 10.1105/tpc.106.048868

Torii, K. U., Mitsukawa, N., Oosumi, T., Matsuura, Y., Yokoyama, R., Whittier, R. F., et al. (1996). The *Arabidopsis* ERECTA gene encodes a putative receptor protein kinase with extracellular leucine-rich repeats. *Plant Cell* 8 (4), 735–746. doi: 10.1105/tpc.8.4.735

Umezawa, T., Nakashima, K., Miyakawa, T., Kuromori, T., Tanokura, M., Shinozaki, K., et al. (2009b). Molecular basis of the core regulatory network in ABA responses: sensing, signaling and transport. *Plant Cell Physiol.* 51 (11), 1821–1839. doi: 10.1093/pcp/pcq156

Umezawa, T., Sugiyama, N., Mizoguchi, M., Hayashi, S., Myouga, F., Yamaguchi-Shinozaki, K., et al. (2009a). Type 2C protein phosphatases directly regulate abscisic acid-activated protein kinases in *Arabidopsis*. *Proc. Natl. Acad. Sci. U.S.A.* 106 (41), 17588–17593. doi: 10.1073/pnas.0907095106

Vaid, N., Pandey, P. K., and Tuteja, N. (2012). Genome-wide analysis of lectin receptor-like kinase family from *Arabidopsis* and rice. *Plant Mol. Biol.* 80, 365–388. doi: 10.1007/s11103-012-9952-8

van Loon, L. C., Rep, M., and Pieterse, C. M. (2006). Significance of inducible defense-related proteins in infected plants. *Annu. Rev. Phytopathol.* 44, 135–162. doi: 10.1146/annurev.phyto.44.070505.143425

Verica, J. A., and He, Z. H. (2002). The cell wall-associated kinase (WAK) and WAK-like kinase gene family. *Plant Physiol.* 129 (2), 455–459. doi: 10.1104/pp.011028

Verica, J. A., Chae, L., Tong, H., Ingmire, P., and He, Z. H. (2003). Tissue-specific and developmentally regulated expression of a cluster of tandemly arrayed cell wall-associated kinase-like kinase genes in *Arabidopsis*. *Plant Physiol.* 133 (4), 1732–1746. doi: 10.1104/pp.103.028530

Wang, N., Huang, H. J., Ren, S. T., Li, J. J., Sun, Y., Sun, D. Y., et al. (2012). The rice wall-associated receptor-like kinase gene OsDEES1 plays a role in female gametophyte development. *Plant Physiol.* 160 (2), 696–707. doi: 10.1104/pp.112.203943

Wang, X., Zafian, P., Choudhary, M., and Lawton, M. (1996). The PR5K receptor protein kinase from *Arabidopsis thaliana* is structurally related to a family of plant defense proteins. *Proc. Natl. Acad. Sci. U.S.A.* 93 (6), 2598–2602. doi: 10.1073/pnas.93.6.2598

Xie, T., Ren, R., Zhang, Y. Y., Pang, Y., Yan, C., Gong, X., et al. (2012). Molecular mechanism for inhibition of a critical component in the *Arabidopsis thaliana* abscisic acid signal transduction pathways, SnRK2.6, by protein phosphatase ABI1. *J. Biol. Chem.* 287 (1), 794–802. doi: 10.1074/jbc.M111.313106

Yang, Y., Labbé, J., Muchero, W., Yang, X., Jawdy, S. S., Kennedy, M., et al. (2016). Genome-wide analysis of lectin receptor-like kinases in *Populus*. *BMC Genomics* 17, 699. doi: 10.1186/s12864-016-3026-2

Yin, P., Fan, H., Hao, Q., Yuan, X., Wu, D., Pang, Y., et al. (2009). Structural insights into the mechanism of abscisic acid signaling by PYL proteins. *Nat. Struct. Mol. Biol.* 16 (12), 1230–1236. doi: 10.1038/nsmb.1730

Yokoyama, R., Takahashi, T., Kato, A., Torii, K. U., and Komeda, Y. (1998). The *Arabidopsis* ERECTA gene is expressed in the shoot apical meristem and organ primordia. *Plant J.* 15 (3), 301–310. doi: 10.1046/j.1365-313X.1998.00203.x

Yoshida, R., Umezawa, T., Mizoguchi, T., Takahashi, S., Takahashi, F., and Shinozaki, K. (2006a). The regulatory domain of SRK2E/OST1/SnRK2.6 interacts with ABI1 and integrates abscisic acid (ABA) and osmotic stress signals controlling stomatal closure in *Arabidopsis*. *J. Biol. Chem.* 281 (8), 5310–5318. doi: 10.1074/jbc.M50982020

Yoshida, T., Fujita, Y., Sayama, H., Kidokoro, S., Maruyama, K., Mizoi, J., et al. (2010). AREB1, AREB2, and ABF3 are master transcription factors that cooperatively regulate ABRE-dependent ABA signaling involved in drought stress tolerance and require ABA for full activation. *Plant J.* 61 (4), 672–685. doi: 10.1111/j.1365-313X.2009.04092.x

Yoshida, T., Nishimura, N., Kitahata, N., Kuromori, T., Ito, T., Asami, T., et al. (2006b). ABA-hypersensitive germination3 encodes a protein phosphatase 2C (AtPP2CA) that strongly regulates abscisic acid signaling during germination among *Arabidopsis* protein phosphatase 2Cs. *Plant Physiol.* 140 (1), 115–126. doi: 10.1104/pp.105.070128

Yun, D. J., Ibeas, J. I., Lee, H., Coca, M. A., Narasimhan, M. L., Uesono, Y., et al. (1998). Osmotin, a plant antifungal protein, subverts signal transduction to enhance fungal cell susceptibility. *Mol. Cell* 1 (6), 807–817. doi: 10.1016/S1097-2765(00)80080-5

Yun, D. J., Zhao, Y., Pardo, J. M., Narasimhan, M. L., Damsz, B., Lee, H., et al. (1997). Stress proteins on the yeast cell surface determine resistance to osmotin, a plant antifungal protein. *Proc. Natl. Acad. Sci. U.S.A.* 94 (13), 7082–7087. doi: 10.1073/pnas.94.13.7082

Zhao, Y., Chan, Z., Gao, J., Xing, L., Cao, M., Yu, C., et al. (2016). ABA receptor PYL9 promotes drought resistance and leaf senescence. *Proc. Natl. Acad. Sci. U.S.A.* 113 (7), 1949–1954. doi: 10.1073/pnas.1522840113

Zhu, J.-K. (2002). Salt and drought stress signal transduction in plants. *Annu Rev Plant Biol.* 53, 247–273.

Conflict of Interest: The authors declare that the research was conducted in the absence of any commercial or financial relationships that could be construed as a potential conflict of interest.

frontiers in Plant Science

ORIGINAL RESEARCH
published: 29 October 2019
doi: 10.3389/fpls.2019.01352

The Cotton GhWRKY91 Transcription Factor Mediates Leaf Senescence and Responses to Drought Stress in Transgenic *Arabidopsis thaliana*

Lijiao Gu, Qiang Ma, Chi Zhang, Congcong Wang, Hengling Wei, Hantao Wang and Shuxun Yu**

State Key Laboratory of Cotton Biology, Institute of Cotton Research of CAAS, Anyang, China

WRKY transcription factors (TFs) play essential roles in the plant response to leaf senescence and abiotic stress. However, the WRKY TFs involved in leaf senescence and stress tolerance in cotton (*Gossypium hirsutum* L.) are still largely unknown. In this study, a WRKY gene, *GhWRKY91*, was isolated and thoroughly characterized. Transcriptional activity assays showed that GhWRKY91 could activate transcription in yeast. The expression pattern of *GhWRKY91* during leaf senescence, and in response to abscisic acid (ABA) and drought stress was evaluated. β-Glucuronidase (GUS) activity driven by the *GhWRKY91* promoter in transgenic *Arabidopsis* was reduced upon exposure to ABA and drought treatments. Constitutive expression of *GhWRKY91* in *Arabidopsis* delayed natural leaf senescence. *GhWRKY91* transgenic plants exhibited increased drought tolerance and presented delayed drought-induced leaf senescence, as accompanied by reinforced expression of stress-related genes and attenuated expression of senescence-associated genes (SAGs). Yeast one-hybrid (Y1H) assays and electrophoretic mobility shift assays (EMSAs) revealed that GhWRKY91 directly targets *GhWRKY17*, a gene associated with ABA signals and reactive oxygen species (ROS) production. A transient dual-luciferase reporter assay demonstrated that GhWRKY91 activated the expression of *GhWRKY17*. Our results suggest that GhWRKY91 might negatively regulate natural and stress-induced leaf senescence and provide a foundation for further functional studies on leaf senescence and the stress response in cotton.

Keywords: GhWRKY91, leaf senescence, abscisic acid, drought, *GhWRKY17*, cotton

OPEN ACCESS

Edited by:
Yasuhito Sakuraba, The University of Tokyo, Japan

Reviewed by:
Himanshu Tak, Bhabha Atomic Research Centre (BARC), India
Zhong Qi Fan, Fujian Agriculture and Forestry University, China

****Correspondence:***
Hantao Wang
w.wanghantao@163.com
Shuxun Yu
Ysx195311@163.com

Specialty section:
This article was submitted to Plant Abiotic Stress, a section of the journal Frontiers in Plant Science

Received: *08 April 2019*
Accepted: *01 October 2019*
Published: *29 October 2019*

Citation:
Gu L, Ma Q, Zhang C, Wang C, Wei H, Wang H and Yu S (2019) The Cotton GhWRKY91 Transcription Factor Mediates Leaf Senescence and Responses to Drought Stress in Transgenic Arabidopsis thaliana. Front. Plant Sci. 10:1352. doi: 10.3389/fpls.2019.01352

INTRODUCTION

The WRKY gene family is a large family of plant-specific transcription factors (TFs) that play important roles in various processes, such as stem elongation (Zhang et al., 2011), pathogen resistance (Pan and Jiang, 2014), leaf senescence (Xie et al., 2014), panicle development (Xiang et al., 2017), trichome and seed coat development (Johnson et al., 2002), pollen development (Guan et al., 2014), fruit ripening (Jiang et al., 2017), and biotic and abiotic stress responses (Pan and Jiang,

Abbreviations: ABA, abscisic acid; EMSA, electrophoretic mobility shift assay; GUS, β-glucuronidase; qRT-PCR, quantitative real-time PCR; ROS, reactive oxygen species; SAGs, senescence-associated genes; TFs, transcription factors; and WT, wild-type.

2014). WRKY TFs have one or two conserved WRKY domains that consist of approximately 60 amino acids, with a WRKYGQK sequence in the N-terminal region and a C2H2 or C2HC zinc finger motif in the C-terminal region. WRKY TFs can be divided into three groups [I, II (IIa-e), and III] on the basis of their structure and evolutionary history (Eulgem et al., 2000; Rushton et al., 2010). WRKY TFs can interact with W-box cis-elements [TTGAC(C/T)] in the promoter regions of downstream genes to regulate the expression of those genes, thus leading to improved plant adaptation to environmental changes (Fan et al., 2017).

In agricultural production, leaf senescence leads to a decline in photosynthesis, which greatly limits the yield potential of crops. As the final stage of plant development, leaf senescence causes changes in plant cell structure, physiological and biochemical parameters, hormone levels, and gene expression (Lim et al., 2007). Genes expression significantly increases during leaf senescence include those that encode TFs such NACs (NAM, ATAF1/2 and CUC2) and WRKYs (Balazadeh et al., 2008; Guo et al., 2010; Lin et al., 2015; Wu et al., 2016). For example, an aging upregulated NAC TF, GhNAP, delays leaf senescence in RNA interference (RNAi) cotton plants *via* abscisic acid (ABA)-mediated pathways (Fan et al., 2015). A growing number of WRKY TFs are considered senescence regulators in plants (Kim et al., 2017). In *Arabidopsis*, AtWRKY6 (Robatzek and Somssich, 2002; Zhang et al., 2018), AtWRKY22 (Zhou et al., 2011), AtWRKY45 (Chen et al., 2017), AtWRKY53 (Miao et al., 2004), and AtWRKY75 (Guo et al., 2017a) act as positive regulators during natural leaf senescence, whereas AtWRKY18 (Potschin et al., 2014), AtWRKY54 (Besseau et al., 2012), AtWRKY57 (Jiang et al., 2014), and AtWRKY70 (Ulker et al., 2007) function as negative regulators. Furthermore, AtWRKY22 has been shown to promote and delay leaf senescence in overexpression plants and in T-DNA insertion mutants under dark conditions, respectively (Zhou et al., 2011). *Atwrky57* mutants exhibit a jasmonic acid (JA)-induced early leaf senescence phenotype in which auxin functions as an antagonist (Jiang et al., 2014). In rice, OsWRKY23 has been shown to be involved in dark-induced leaf senescence in transgenic *Arabidopsis* plants (Jing et al., 2009). WRKY TFs are also involved in vegetative and fruit senescence, including BrWRKY65 in Chinese flowering cabbage (Fan et al., 2017) and LcWRKY1 in litchi (Jiang et al., 2017). Two cotton WRKY TFs, GhWRKY27 (Gu et al., 2019) and GhWRKY42 (Gu et al., 2018b), were recently identified to promote leaf senescence in transgenic *Arabidopsis* plants, suggesting that WRKY TFs have important roles during leaf senescence in cotton.

Drought or water shortage is one of the main environmental factors that reduces crop yields (Cominelli and Tonelli, 2010). Due to global warming and water shortages, water for crop irrigation is becoming increasingly limited and the development of drought-resistant crop species is particularly important (White et al., 2004). The mechanism of drought resistance in plants is very complex and is usually regulated by multiple genes, including those that encode WRKY TFs (Reynolds and Tuberosa, 2008; Pinto et al., 2010; Dou et al., 2014). Previous reports have shown that overexpression of wheat (*Triticum aestivum* L.) TaWRKY10 confers drought tolerance to transgenic tobacco plants by mediating osmotic balance, the production of reactive oxygen species (ROS), and the expression of stress-responsive genes (Wang et al., 2013). TaWRKY44 positively regulates drought stress in transgenic tobacco plants by scavenging ROS that have accumulated *via* cellular antioxidant systems or stress-related gene expression (Wang et al., 2015). ABA is an important plant hormone that participates in a variety of signal transduction pathways, especially those involved in plant resistance to adverse environmental stimuli such as drought, salt, and low temperature (Cutler et al., 2010). Adverse environmental conditions can cause the rapid accumulation of ABA, thus leading to stomatal closure and reduced water loss, which together constitute the main factor that leads to drought tolerance in plants (Cominelli and Tonelli, 2010; Krasensky and Jonak, 2012). Overexpression of GhWRKY27a reduces the drought tolerance of transgenic tobacco plants, and this effect is associated with enhanced stomatal opening and attenuated expression of ABA- and drought-associated genes (Yan et al., 2015). The constitutive expression of GhWRKY41 in tobacco improves salt and drought tolerance by enhancing stomatal closure in an ABA-dependent manner (Chu et al., 2015). Together, the results of these studies suggest that WRKY TFs play important roles in the drought stress response mediated by ABA signalling.

Plant growth and crop productivity are severely influenced by external environmental factors (such as biotic stress, abiotic stress, and signalling molecules) and internal growth factors (Gustafson, 1946). Leaf senescence, an internal factor, is a common phenomenon during plant development (Lim et al., 2007). In agricultural production, some early-maturing cotton varieties tend to age prematurely, which severely affects their fibre yield and quality (Yu et al., 2005). We previously performed a genome-wide analysis of the WRKY gene family and found that WRKY TFs in cotton were differentially expressed during different stages of leaf senescence and under various stresses (Lin et al., 2015). These findings provide a basis for further exploring the involvement of WRKY TFs in leaf senescence- and stress-associated regulatory pathways in cotton.

The objective of our study was to examine the functional role of the GhWRKY91 TF in the regulation of leaf senescence and the drought stress response. Therefore, we isolated and characterized the *GhWRKY91* gene and analyzed its expression pattern. Our results showed that GhWRKY91 is involved in delayed natural and drought-induced leaf senescence, and increases drought tolerance in transgenic *Arabidopsis* plants. Furthermore, GhWRKY91 activates expression of its target gene *GhWRKY17*. Our findings reveal important functions of GhWRKY91 in leaf senescence and the response to drought stress, and provide a theoretical basis for developing cotton materials that present non-premature senescence and are stress tolerant.

MATERIALS AND METHODS

Plant Materials and Growth Conditions

The cotton varieties CCRI10 (prematurely senescent), CCRI74 (prematurely senescent), and Liao4086 (non-prematurely senescent) were used in this study. Different tissues were sampled from the CCRI10 variety. To examine the functional role of

GhWRKY91 during leaf senescence, the expression profile of *GhWRKY91* was detected in 15-, 25-, 35-, 45-, 55-, and 65-day-old CCRI36 cotton leaves using transcriptome data (Lin et al., 2015). The data were normalized using the transcripts per million clean tags (TPM) algorithm (Lakhotia et al., 2014). The expression pattern of *GhWRKY91* was also measured in the top four leaves of the CCRI10 and Liao4086 varieties; the leaves were marked at the flowering stage and collected after one week at five notable development phases (7, 14, 21, 28, and 35 days). In addition, the expression patterns were measured in CCRI74 cotton leaves, which included newly flattened to nearly completely senescent leaves at five different development stages (stages 1–5) (Gu et al., 2018a).

With respect to ABA and drought treatments, CCRI10 seeds were germinated in soil in a greenhouse at 25 ± 1°C under a 16 h light/8 h dark photoperiod. Ten-day-old seedlings were treated with 200 μM ABA and 20% (w/v) polyethylene glycol 6000 (PEG6000) according to Gu et al. (2018b). The cotyledon samples were harvested at 0, 2, 4, 6, 8 and 12 h. Each sample contained three biological replicates.

The *Arabidopsis thaliana* Columbia ecotype (Col-0) was used as the wild type (WT). Transgenic plants expressing 35S::*GhWRKY91* or *ProGhWRKY91*::GUS were obtained using WT background plants. The seeds were surface sterilized and germinated on 1/2 Murashige and Skoog (1/2MS) (Murashige and Skoog, 1962) agar media in a growth chamber at 22°C under a 16 h light/8 h dark photoperiod. Two-week-old seedlings were then transplanted into soil in a greenhouse at 22 ± 1°C under a 16 h light/8 h dark photoperiod.

Gene Cloning and Sequence Analysis

The full-length cDNA, genomic DNA, and promoter fragments of *GhWRKY91* were amplified from the cDNA and DNA products of CCRI10 cotton leaves. The PCR products were inserted into a clone vector, and the recombinant constructs were transferred into the DH5α strain for sequencing. The intron-exon structure was generated using GSDS 2.0 (http://gsds.cbi.pku.edu.cn/). The cis-elements were predicted using PlantCARE (http://bioinformatics.psb.ugent.be/webtools/plantcare/html). A multiple sequence alignment was carried out using DNAMAN software. Phylogenetic analyses were performed using the MEGA 7 program and the neighbour-joining method. All primers used in this study are listed in **Supplementary Table 1**.

DNA, RNA Extraction, and Quantitative Real-Time PCR (qRT-PCR)

Genomic DNA was extracted *via* the cetyl-trimethylammonium bromide (CTAB) method as described previously (Porebski et al., 1997). Total RNA was isolated using an RNAprep Pure Plant Kit (DP441) (Tiangen, Beijing, China). The RNA was used as a template for cDNA synthesis *via* a PrimeScript™ RT Reagent Kit with gDNA Eraser (Perfect Real Time) (RR047A) (TaKaRa, Dalian, China). qRT-PCR was performed using SYBR® Premix Ex Taq™ (Tli RNaseH Plus) (RR420A) (TaKaRa, Dalian, China) and an ABI 7500 Real-Time PCR System (Applied Biosystems, Foster City, CA, USA). The thermocycler programme consisted of pre-denaturation at 95°C for 30 s followed by 40 cycles at 95°C for 5 s and then 60°C for 34 s. Each sample was analyzed based on three technical replicates and the data were calculated in accordance with the $2^{-\Delta\Delta Ct}$ formula (Livak and Schmittgen, 2001). *Gossypium hirsutum Actin* (*GhActin*) and *Arabidopsis thaliana UBQ10* (*AtUBQ10*) were used as reference genes.

Transcription Activation Assays

The *GhWRKY91* gene was cloned and inserted into the *Eco*RI and *Bam*HI sites of pGBKT7 to create pGBKT7-GhWRKY91 plasmids. The pGBKT7-GhWRKY91 and pGADT7 plasmids were co-transformed into Y2HGold cells. The transformed products were cultured and detected on SD-Trp-Leu (DDO), SD-Trp-Leu-His-Ade (QDO), and QDO/X-a-Gal (QDO/X) medium. The detailed protocol followed that of the Matchmaker™ Gold Yeast Two-Hybrid System (Clontech).

Vector Construction and Genetic Transformation of *Arabidopsis thaliana*

The *GhWRKY91* gene was inserted into the *Bam*HI and *Sac*I sites of the binary vector pBI121 to generate 35S::*GhWRKY91* plasmids. To measure the promoter activity of *GhWRKY91*, a 2009 bp promoter fragment was inserted into the *Hin*dIII and *Bam*HI sites of the pBI121 vector to generate *ProGhWRKY91*::GUS plasmids. The 35S::*GhWRKY91* and *ProGhWRKY91*::GUS recombinant plasmids were subsequently introduced into *Agrobacterium tumefaciens* strain LBA4404. The LBA4404 cells harboring the fusion constructs were transformed into WT plants *via* the floral dip method (Clough and Bent, 1998). The positive plants were selected on 1/2MS medium containing kanamycin (100 mg/L), and further confirmed *via* PCR and qRT-PCR. T_3 generation plants were used for phenotypic observation of leaf senescence and stress treatments.

Analysis of Transgenic *Arabidopsis* Plants Under Normal, ABA, and Drought Conditions

To observe the phenotypes of transgenic plants under normal conditions, the seeds of the WT and three independent 35S::*GhWRKY91* lines (OE91-12, OE91-13, and OE91-20) were surface sterilized and germinated on 1/2MS agar medium. After two weeks, the seedlings were transplanted to soil, and the natural growth phenotype was observed. The rosette leaves from 50-day-old plants were sampled for qRT-PCR detection of senescence-associated genes (SAGs).

To investigate the ABA and drought tolerance of plants, each pot was divided into four sections on average. WT, OE91-12, OE91-13, and OE91-20 seedlings (8 seedlings per line) were planted in each section of the same pot to maintain the same growth conditions until the seedlings were three weeks old. Afterward, the seedlings were sprayed with 50 μM ABA and irrigated with 15% (w/v) PEG6000 (to mimic drought). Untreated seedlings were used as controls. Because of the different concentration sensitivities of different species to stress treatments, the treatment concentration of *Arabidopsis* was different from that of the cotton. The rosette leaves were collected

and used to analyze the expression of SAGs, and ABA- and stress-related genes. In addition, the plants were subjected to a water shortage treatment. Irrigation was withheld for four-week-old WT, OE91-12, OE91-13, and OE91-20 plants for approximately 2 weeks. The plants were imaged after their main stems were cut and removed. Three replicates were included per treatment.

β-Glucuronidase (GUS) Histochemical Staining

To investigate the promoter activity in different tissues, 8-day-old seedlings, stems, leaves, flower buds, flowers, and fruit pods from *ProGhWRKY91*::GUS plants were used for GUS staining. For the stress treatments, two-week-old *ProGhWRKY91*::GUS seedlings were treated in 1/2MS liquid medium that was supplemented with or without 100 μM ABA and 200 mM mannitol. Due to the difference in experiment purposes, the stress concentration was different from that of overexpression lines. GUS staining was performed as described previously (Jefferson et al., 1987). The treated samples were immersed in GUS histochemical staining buffers [0.1 mM $NaPO_4$ (pH 7.0), 10 mM EDTA-Na_2 (pH 8.0), 0.1% Triton X-100, 1 mM $K_3Fe(CN)_6$, and 2 mM X-Gluc], and subsequently incubated at 37°C overnight. After staining, the samples were decolorized in 75% ethanol until the color of the negative control turned white. GUS activity was estimated based on the presence of blue. In addition, the GUS staining assay is representative of the results in two independent transgenic lines.

Yeast One Hybrid (Y1H) Assays

The *GhWRKY91* gene was cloned into pGADT7 vector at the *Eco*RI and *Bam*HI sites to create pGADT7-GhWRKY91 prey plasmids. Three copies of specific fragments from the promoter regions of *GhWRKY3*, *GhWRKY17*, *GhWRKY25*, *GhWRKY27a*, *GhWRKY68*, *ASCORBATE PEROXIDASE 1* (*GhAPX1*), and *RESPONSIVE TO DESICCATION 22* (*GhRD22*) were cloned into a pHIS2 vector to generate bait carriers (**Supplementary Table 2**). The pGADT7-GhWRKY91 construct and each bait carrier were subsequently co-transformed into Y187 yeast cells. The transformed yeast cells were grown and detected on DDO and SD-Trp-Leu-His (TDO) medium that were supplemented with 200 mM 3-amino-1,2,4-triazole (3-AT) (TDO + 200 mM 3-AT) to evaluate protein-DNA interactions based on growth ability.

Electrophoretic Mobility Shift Assays (EMSAs)

The *GhWRKY91* gene was cloned into pGEX-4T-1 to produce pGEX-4T-1-GhWRKY91 constructs, which were fused to a glutathione S-transferase (GST) tag at the N-terminus. The pGEX-4T-1-GhWRKY91 constructs were transformed into the *E. coli* strain Arctic-Express™, after which, the cells containing the fusion plasmids were induced by 0.5 mM isopropyl-β-D-thiogalactoside (IPTG) at 20°C for 4 h at 220 r/min. The fusion proteins were purified with a GST Fusion Protein Purification Kit (GenScript) and digested to remove any GST tags. Any biotin end-labelled probes containing a W-box originated from the promoter regions of *GhWRKY17*, *GhWRKY27a*, *GhWRKY68*, and *GhAPX1*. Unlabelled probes were used as cold competitors. We performed the EMSAs using a LightShift® Chemiluminescent EMSA Kit (Thermo Scientific, Waltham, MA, USA).

Dual-Luciferase Reporter Assay

The *GhWRKY91* gene was cloned into the pGreenII 62-SK effecter vector, and the *GhWRKY17* promoter was cloned into pGreenII0800-LUC reporter vector. The recombinant plasmids were transformed into the GV3101 (pSoup-p19) strain. The culture was incubated to an OD600 value of 0.8 and adjusted to an OD600 value of 0.6 with the infiltration buffer (10 mM $MgCl_2$, 10 mM MES, and 100 μM acetosyringone). After resting at room temperature for 3 h, the suspensions of effecter and reporter were mixed in a 9:1 ratio and co-infiltrated into tobacco leaves according to the method by Hellens et al. (Hellens et al., 2005). Three days later, the LUC and REN values were obtained using a Dual-Luciferase® Reporter Assay System (Promega, USA) on a GloMax 20/20 Luminometer (Promega, USA). The trans-activation of the GhWRKY91 TF to *GhWRKY17* promoter was indicated by the LUC/REN ratio. At least six independent repeats were performed.

RESULTS

Cloning and Sequence Analysis of GhWRKY91

The genomic DNA and full-length cDNA sequences of *GhWRKY91* (GenBank accession number: KF669793) were amplified from the cotton variety CCRI10. The *GhWRKY91* gene contained three exons and two introns, and the genomic DNA sequence was interrupted by two introns of 105 and 97 bp at the 'GG' and 'GT' sites (**Figure 1A**). The open reading frame of *GhWRKY91* was 822 bp in length and encoded 273 amino acid residues. The estimated molecular mass of the GhWRKY91 protein was 29.82 kDa, and the isoelectric point was 5.13. A comparison of the protein sequences of GhWRKY91 with its related proteins from different species demonstrated that GhWRKY91 was 98.53% homologous to GhWRKY65 (Gh_D10G0329.1), 50.71% homologous to AtWRKY65 (AT1G29280.1), 39.16% homologous to AtWRKY69 (AT3G58710.1), and 33.54% homologous to OsWRKY65 (XP_015647591.1). A multiple sequence alignment revealed that the GhWRKY91 protein includes one WRKY domain that comprises approximately 60 amino acids with a highly conserved amino acid sequence (WRKYGQK) and a C2H2 putative zinc finger motif, indicating that GhWRKY91 belongs to the group II family (**Figure 1B**). According to the phylogenetic tree, group II members could be divided into five subgroups (IIa-IIe), and GhWRKY91 was closely related to group IIe members (**Figure 1C**).

Transcriptional Activity of GhWRKY91

A transcriptional activation assay was performed *in vitro* to demonstrate whether GhWRKY91 has transcription activation activity in yeast cells. The plasmids of the experimental group (pGADT7+pGBKT7-GhWRKY91), positive group, and negative

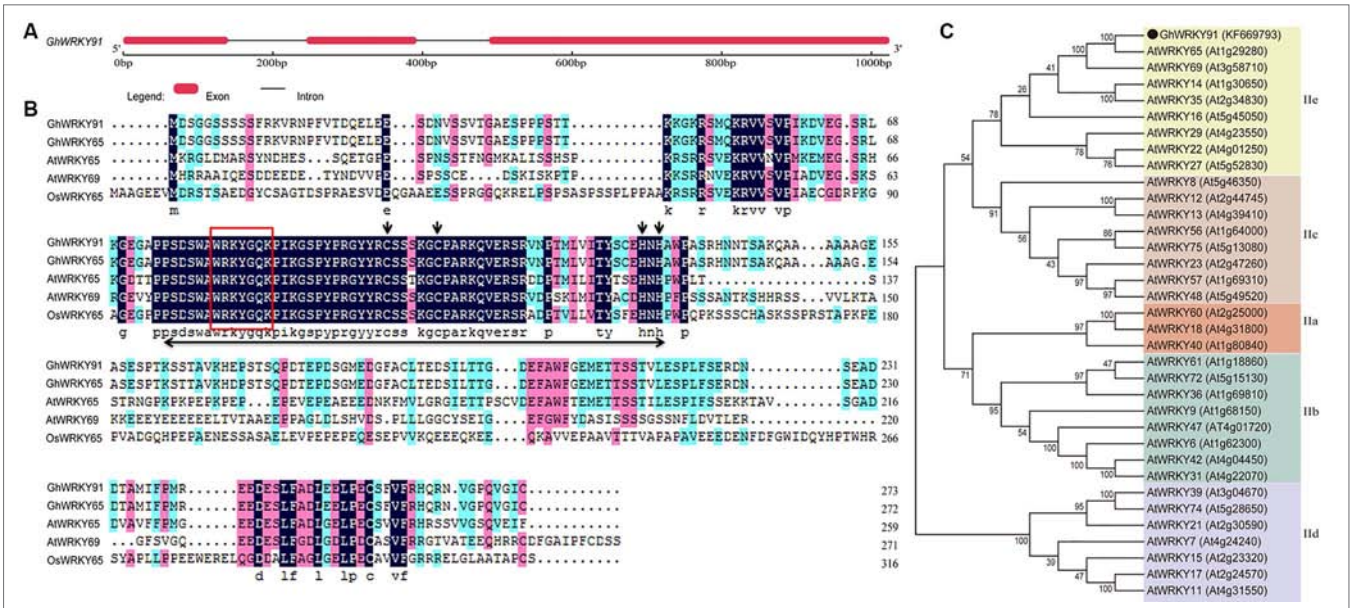

FIGURE 1 | Sequence and phylogenetic analyses of GhWRKY91. **(A)** Exon-intron structure of the *GhWRKY91* gene. The thick red line represents an exon, and the black line represents an intron. **(B)** Sequence alignment of the GhWRKY91 protein with the closely related proteins GhWRKY65 (Gh_D10G0329.1), AtWRKY65 (AT1G29280.1), AtWRKY69 (AT3G58710.1), and OsWRKY65 (XP_015647591.1). The WRKY domain is indicated by a double-headed arrow. The highly conserved core sequence WRKYGQK in the WRKY domain is represented by a red box. The C and H residues in the zinc finger motif are indicated by downward arrows. **(C)** Phylogenetic relationship of the GhWRKY91 protein with other group II WRKY proteins from *Arabidopsis*. GhWRKY91 is indicated by the black dot. The abbreviations before the gene names are as follows: Gh, *Gossypium hirsutum*; At, *Arabidopsis thaliana*; and Os, *Oryza sativa*.

group were transformed into Y2HGold yeast cells and assayed on DDO, QDO, and QDO/X agar medium. The results showed that all transformation products can grow normally on DDO medium (**Figure 2**). The experimental group and positive group grew well on QDO medium and turned blue on QDO/X medium, whereas the negative group could not; indicating that GhWRKY91 could autonomously activate the reporter genes in the absence of a prey protein (**Figure 2**).

Expression Patterns of *GhWRKY91* During Leaf Senescence and Under Stress Treatments

The transcriptome data (Lin et al., 2015) showed that *GhWRKY91* transcripts increased as the CCRI36 cotton leaves aged and was highly expressed in senescent leaves (**Figure 3A**). In addition, the expression of *GhWRKY91* increased gradually with leaf senescence and was more prevalent in the premature-senescence cotton variety CCRI10 than in the non-premature-senescence variety Liao4086 (**Figure 3B**). With respect to ABA stress, ABA treatment repressed the expression of *GhWRKY91* in a time series of 2–12 h (**Figure 3C**). With respect to the drought treatment, the *GhWRKY91* transcripts accumulated immediately and peaked at 2 h after the initial treatment, followed by a decrease in accumulation throughout the remaining 4–12 h (**Figure 3D**).

GhWRKY91 Promoter Analysis

The cis-elements in the *GhWRKY91* promoter were predicted using PlantCARE. The results revealed that stress response-, light response-, and development-related elements were present in this region (**Supplementary Table 3**). The stress responsive elements included ABA (ABRE, ACGTG), low temperature (LTR, CCGAAA), and anaerobic (ARE, AAACCA) associated elements (**Supplementary Table 3**).

In eight-day-old seedlings, GUS staining was observed mainly in the cotyledons, hypocotyls, and upper parts of the roots (**Supplementary Figure 1A**). At the vegetative stage, GUS staining was found in the stems and leaves, especially at the edge of the leaves (**Supplementary Figure 1B**, **C**). However, during the generative growth phase, GUS activity was almost undetectable in the flower, buds, and fruit pods (**Supplementary Figure 1D**–**F**).

GUS activity was strongly expressed in cotyledons but weakly expressed in rosette leaves in the control (**Figure 4A**). After the ABA and mannitol treatments, the GUS signal was weak in the cotyledons and rosette leaves compared with the control seedlings (**Figures 4B**, **C**). Similarly, GUS staining was inconspicuous in the roots treated with ABA and drought compared with the control (**Figures 4D**–**F**).

Overexpression of *GhWRKY91* Delayed Leaf Senescence in Transgenic *Arabidopsis* Plants

To evaluate the influence of the *GhWRKY91* gene on plants, we overexpressed *GhWRKY91* in *Arabidopsis* plants. The transgenic lines (OE91-12, OE91-13 and OE91-20) containing T-DNA with 35S::*GhWRKY91* were generated (**Figure 5A**) and confirmed by PCR (**Supplementary Figure 2A**) and qRT-PCR (**Figure 5B**).

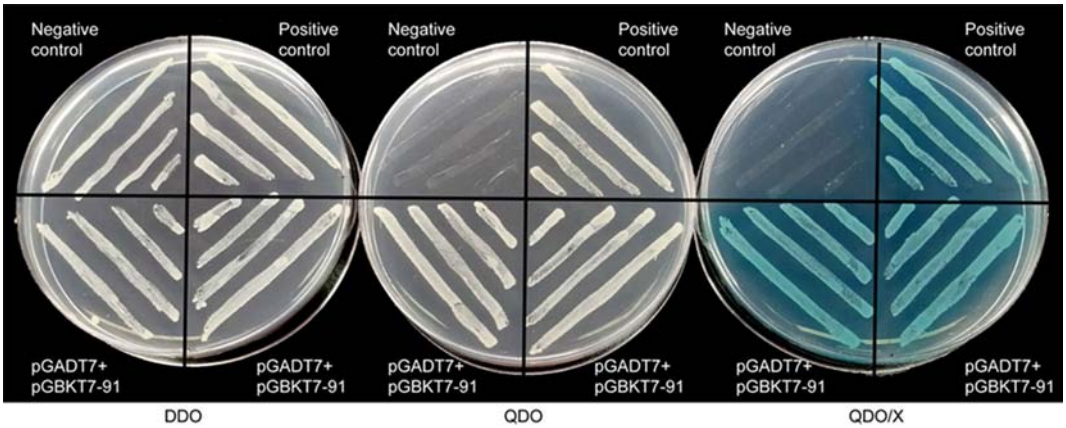

FIGURE 2 | Transcriptional activity of GhWRKY91 in Y2HGold yeast cells. Yeast cells were assayed on DDO (SD-Trp-Leu), QDO (SD-Trp-Leu-His-Ade) and QDO/X (SD-Trp-Leu-His-Ade/X-a-Gal) medium. The combination of the pGADT7-large T and pGBKT7-p53 plasmids was used as a positive control. The combination of the pGADT7-large T and pGBKT7-laminC plasmids was used as a negative control.

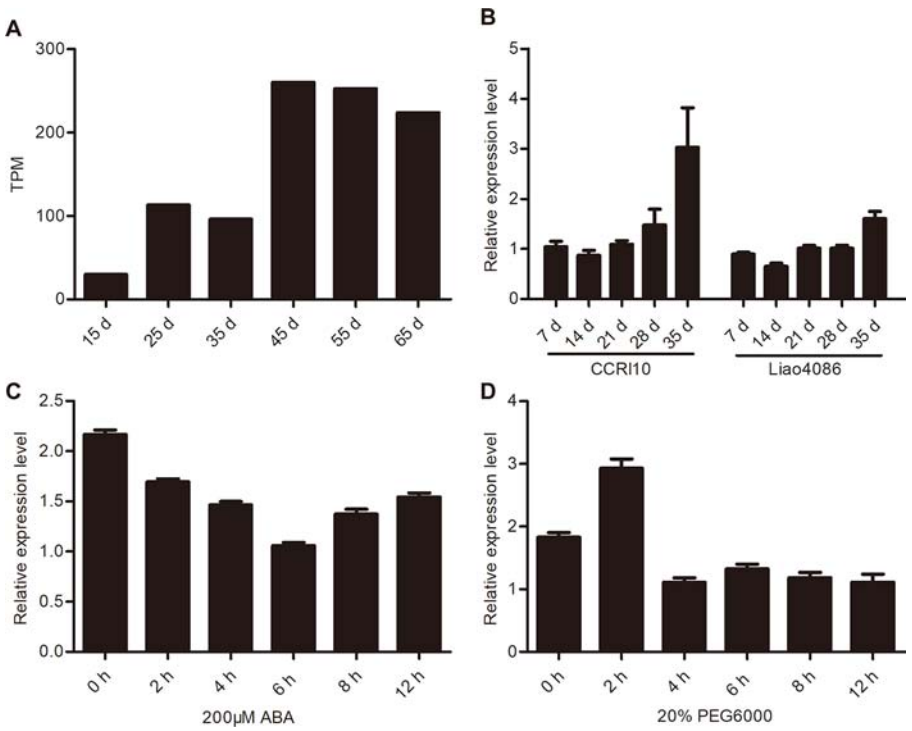

FIGURE 3 | Expression patterns of *GhWRKY91* during leaf senescence and under stress treatments. **(A)** Expression profiles of *GhWRKY91* in 15-, 25-, 35-, 45-, 55-, and 65-day-old CCRI36 cotton leaves using the transcriptome data (Lin et al., 2015). TPM, transcripts per million clean tags. **(B)** Transcript levels of *GhWRKY91* at different stages of leaf senescence in CCRI10 and Liao4086 varieties. **(C–D)** Transcript levels of *GhWRKY91* under ABA and PEG6000 treatments. *GhActin* served as the reference gene. The data are the means ± standard errors (SEs) of three biological replicates.

The 21-day-old transgenic plants were relatively smaller in size than the WT plants (**Supplementary Figure 2B**). The 35-day-old transgenic *Arabidopsis* plants exhibited delayed flowering and leaf senescence compared with the WT plants (**Supplementary Figure 2B**). When the plants were 50 days old, the WT plants became severely senescent and yellow, while the transgenic plants were still green with only a small amount of yellowing (**Figure 5C**). In addition, we assessed the transcript levels of SAGs that are up-regulated factors during leaf senescence in the 50-day-old plants. The results showed that the transcript levels of SAGs *AtNAP/ANAC029* (AT1G69490), *AtSAG12* (AT5G45890), *AtSAG13* (AT2G29350), *AtORE1/ANAC092* (AT5G39610), *AtWRKY6* (AT1G62300), *STAY-GREEN1* (*AtSGR1*) (AT4G22920), and *PHEOPHYTIN PHEOPHORBIDE*

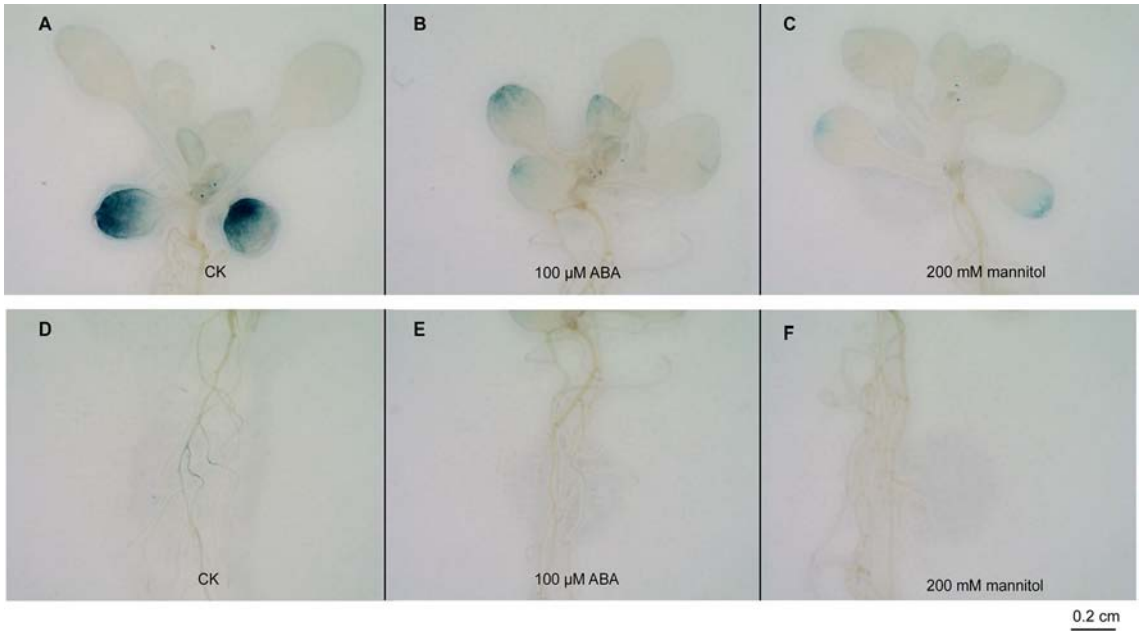

FIGURE 4 | Histochemical GUS assays in *ProGhWRKY91*::GUS transgenic *Arabidopsis* plants. **(A–C)** GUS staining of the leaves under control, ABA, and mannitol treatments. **(D–F)** GUS staining of the roots under control, ABA, and mannitol treatments. Bar = 0.2 cm.

HYDROLASE (*AtPPH*) (AT5G13800) were significantly lower in the transgenic plants than in the WT plants (**Figure 5D–J**). However, there was no difference in the transcript levels of *NON-YELLOW COLORING 1* (*AtNYC1*) (AT4G13250) between the WT and transgenic plants (**Figure 5K**).

Overexpression of *GhWRKY91* Improved Drought Tolerance in Transgenic *Arabidopsis* Plants

Four-week-old plants in pots were used for the water deficit treatment. After water was withheld for two weeks, the WT plants showed definitive wilting and yellowing, while the transgenic plants were still very green (**Figure 6A**). Three-week-old plants were subjected to a 15% PEG6000 treatment, and after one week, the WT plants displayed a greater extent of yellow leaves than the transgenic plants (**Figure 6B**).

The expression levels of stress-inducible genes (*DELTA-1-PYRROLINE-5-CARBOXYLATE SYNTHETASE* (*AtP5CS*), AT2G39800; *AtP5CS1*, AT2G39800; *AtRD29A*, AT5G52310; and *COLD-REGULATED 15A* (*AtCOR15A*), AT2G42540) and SAGs (*AtSAG12*; *AtSAG13*) were examined in the presence and absence of 15% PEG6000. Generally, the expression levels of *AtP5CS*, *AtP5CS1*, *AtRD29A,* and *AtCOR15A* were similar or higher in the transgenic plants than in the WT plants under normal conditions but were significantly elevated in the transgenic plants compared with the WT plants in response to the PEG6000 treatment (**Figures 6C–F**). The expression levels of *AtSAG12* and *AtSAG13* were markedly lower in the transgenic plants than the WT plants under normal conditions. However, although the expression levels of the two genes were elevated in the presence of 15% PEG6000, they were still significantly lower in the transgenic plants than in the WT plants (**Figures 6G**, **H**).

GhWRKY91 Bound Directly to the Promoter of *GhWRKY17 and* Trans-Activated *GhWRKY17* Expression

Previous studies showed that *GhWRKY3* (Guo et al., 2011), *GhWRKY17* (Yan et al., 2014), *GhWRKY25* (Liu et al., 2016), *GhWRKY27a* (Yan et al., 2015), and *GhWRKY68* (Jia et al., 2015) were involved in the regulation of salt, drought, and ABA responses through mediating ROS production and ABA signalling. The *APX* gene encodes an ROS-scavenging enzyme that catalyses the reduction of hydrogen peroxide (Ozyigit et al., 2016), and RD22 is involved in drought tolerance (Harshavardhan et al., 2014). To identify the regulatory mechanism of GhWRKY91, we predicted the W-boxes in the promoters of these genes and found that W-boxes were present in their promoters, indicating the potential roles of these genes as targets. In the Y1H system, the transformation product containing GhWRKY91 and the special fragment in the promoter region of *GhWRKY17* grew well on TDO + 200 mM 3-AT selective medium, whereas the others did not grow or only displayed defective spots (**Figure 7A**).

For the EMSA assays, the probes and sequence locations in the region upstream of the ATG initiation site of the genes (*GhWRKY17*, *GhWRKY27a*, *GhWRKY68,* and *GhAPX1*) are presented in **Figure 7B**. The lanes containing only biotin-labelled probes were used as negative controls (**Figure 7C**; lanes 1, 4, 6, and 8). None of the probes from the *GhWRKY27a*, *GhWRKY68,* or *GhAPX1* genes were bound by the GhWRKY91 protein to produce delayed bands (**Figure 7C**; lanes 5, 7, 9). However, the

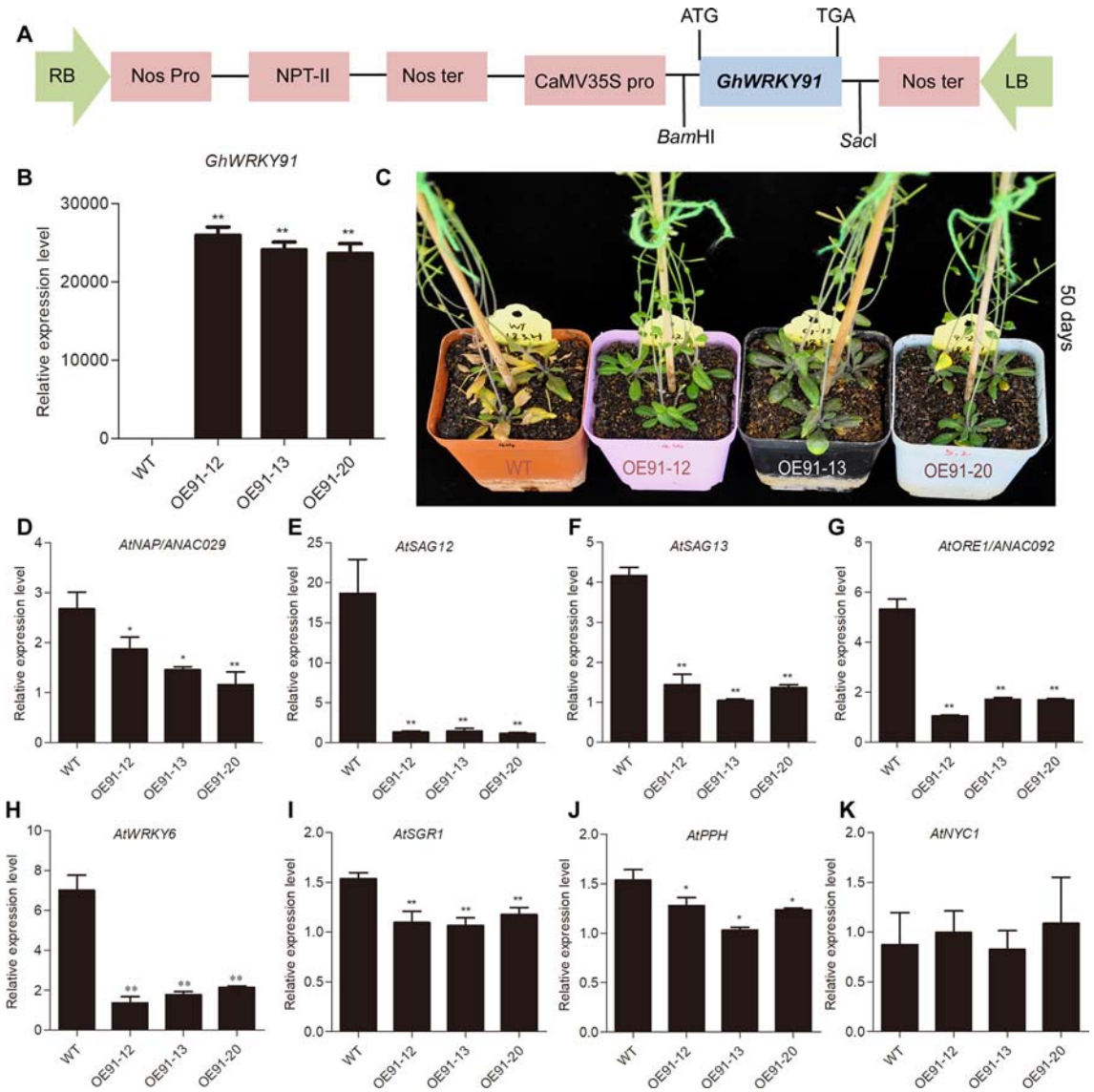

FIGURE 5 | Overexpression of *GhWRKY91* in *Arabidopsis* plants delayed leaf senescence. **(A)** The T-DNA construction diagram used for *Arabidopsis* transformation. **(B)** Transcript levels of *GhWRKY91* in WT and transgenic plants. **(C)** Phenotypic characteristics of WT and transgenic plants grown for 50 days. The seeds of WT and transgenic lines were germinated on 1/2MS agar media in a growth chamber at 22°C under a 16 h light/8 h dark photoperiod. Two-week-old seedlings were then transplanted into soil in a greenhouse at 22 ± 1°C under a 16 h light/8 h dark photoperiod, and the natural senescence phenotype was observed in 50-day-old plants. **(D–K)** Transcript levels of SAGs in the rosette leaves of WT and transgenic plants grown for 50 days. *AtUBQ10* served as the reference gene. The data are the means ± SEs of three biological replicates. **P < 0.01 and *P < 0.05.

labelled probes of *GhWRKY17* could be recognized and bound by the GhWRKY91 protein, thus causing a mobility shift (**Figure 7C**; lane 2). The unlabelled probes of *GhWRKY17* were overdosed as cold competitors; in these cases, most of the labelled wild probes bound by the GhWRKY91 protein were competitively replaced by unlabelled wild probes, resulting in the disappearance of the bands (**Figure 7C**; lane 3), indicating that GhWRKY91 could bind to the promoter of *GhWRKY17*.

To elucidate the relationship of GhWRKY91 in the regulation of *GhWRKY17* expression, a transient dual-luciferase assay was conducted in tobacco. The control data (pGreenII 62-SK empty vector pus the *GhWRKY17* promoter) were set to 1, and the experimental group data were the ratio to the control group. As a result, as shown in **Figure 7D**, the LUC/REN ratio was extremely significantly increased in the experimental group and 4.61 times that of the control group.

DISCUSSION

Growing evidence has shown that WRKY TFs are widely involved in plant development, leaf senescence and various

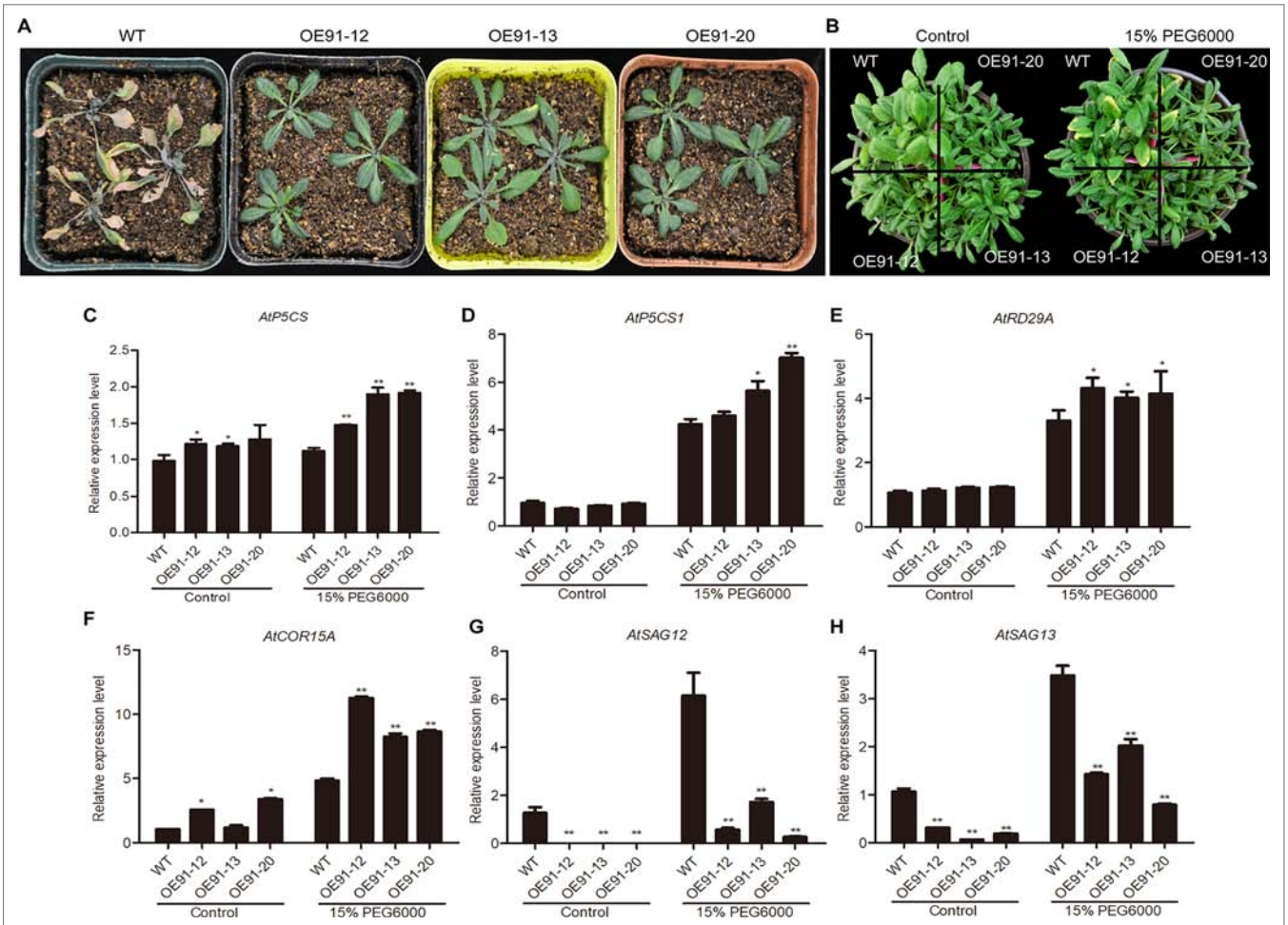

FIGURE 6 | Overexpression of *GhWRKY91* in *Arabidopsis* plants improved drought tolerance. **(A)** Phenotypic characteristics of six-week-old WT and transgenic plants under water deficit conditions. Four-week-old WT and transgenic plants grown in soil were subjected to a water shortage treatment for approximately two weeks. **(B)** Phenotypic characteristics of four-week-old WT and transgenic plants under the control and PEG6000 treatments. Three-week-old WT and transgenic plants grown in soil were irrigated with 15% PEG6000 for one week. Plants grown under normal growth conditions severed as controls. All the plants were grown in a greenhouse at 22 ± 1°C under a 16 h light/8 h dark approximately. **(C–F)** Expression levels of the stress-related genes *AtP5CS*, *AtP5CS1*, *AtRD29A,* and *AtCOR15A* in four-week-old WT and transgenic plants. **(G–H)** Expression levels of the SAGs *AtSAG12* and *AtSAG13* in the WT and transgenic plants. *AtUBQ10* was used as the reference control. The data are the means ± SEs of three biological replicates. ** $P < 0.01$ and * $P < 0.05$.

abiotic/biotic stress responses (Lim et al., 2007; Yu et al., 2012; Xiao et al., 2013; Pan and Jiang, 2014). However, the function roles of WRKY TFs remain to be explored in cotton plants. In the present study, we isolated the WRKY TF GhWRKY91 from cotton and characterized its functional roles. A sequence analysis revealed that the GhWRKY91 protein has one WRKY domain with a C2H2 zinc finger motif, indicating that GhWRKY91 is a group II member according to the criteria of Eulgem et al. (2000). A phylogenetic analysis revealed that GhWRKY91 clustered with group IIe WRKY TFs from *Arabidopsis*, which were further classified into the group IIe subfamily.

Some of WRKY TFs were shown to be important senescence regulators in plants (Lim et al., 2007; Besseau et al., 2012). To characterize the functional role of GhWRKY91 in leaf senescence, we examined the transcripts of *GhWRKY91* at different stages of leaf senescence in cotton. We observed that the expression of *GhWRKY91* increased as leaf senescence progressed and was highly expressed in senescent leaves, implying that *GhWRKY91* may serve as a senescence-related gene in cotton. In addition, the expression level of *GhWRKY91* was higher in the premature-senescence variety CCRI10 than in the non-premature-senescence variety Liao4086. Previous studies have shown that *GhNAC79* (Guo et al., 2017b) and *GhNAC12* (Zhao et al., 2016) are highly expressed in premature-senescence varieties, and that *Arabidopsis* plants transformed with these genes positively regulate age-triggered leaf senescence, which prompted us to explore the relationship between GhWRKY91 and leaf senescence in transgenic materials further.

Previous studies shown that the senescence characteristics of *Arabidopsis* plants can be further verified by the expression of SAGs (Kim et al., 2013; Chen et al., 2017). In our study, the senescence-positive SAGs including *AtNAP/ANAC029* (Guo

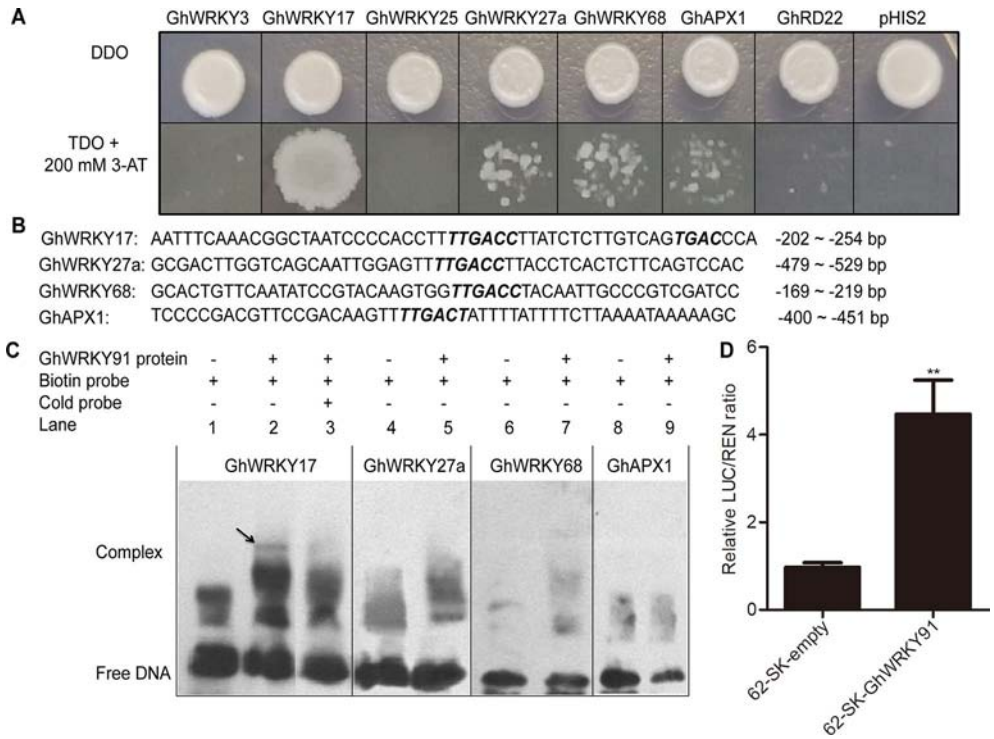

FIGURE 7 | GhWRKY91 directly targets the promoter of *GhWRKY17* and trans-activates *GhWRKY17* expression. **(A)** Interaction between GhWRKY91 and the promoters of candidate target genes *GhWRKY3*, *GhWRKY17*, *GhWRKY25*, *GhWRKY27a*, *GhWRKY68*, *GhAPX1,* and *GhRD22* in Y1H system. The combination of pGADT7-GhWRKY91 and pHIS2 plasmids was used as a negative control. **(B)** Probe sequences of *GhWRKY17*, *GhWRKY27a*, *GhWRKY68,* and *GhAPX1* for the EMSA assays. **(C)** Binding of GhWRKY91 to the W-boxes in the promoters of *GhWRKY17*, *GhWRKY27a*, *GhWRKY68,* and *GhAPX1* in EMSA assays. '–' indicates absence, while '+' indicates presence. **(D)** GhWRKY91 trans-activates *GhWRKY17* promoter in transient dual-luciferase reporter system. The LUC/REN ratio of the combination of pGreenII-62-SK empty vector and *GhWRKY17* promoter was set as 1. The data are the means ± SEs of six biological replicates. **P < 0.01.

and Gan, 2006), *AtWRKY6* (Robatzek and Somssich, 2002), and *AtORE1/ANAC092* (Kim et al., 2009) and the chlorophyll degradation-related genes *AtSGR1* (Sakuraba et al., 2014b) and *AtPPH* (Schelbert et al., 2009), *AtSAG12* (James et al., 2018), and *AtSAG13* (Chen et al., 2017) were investigated. Transgenic *Arabidopsis* plants overexpressing *GhWRKY91* display a delayed-leaf senescence phenotype that corresponded with the reduced expression of these SAGs, suggesting that *GhWRKY91* might negatively regulate leaf senescence. In addition, among these genes, AtWRKY6 interacts with the gibberellin (GA) signalling component/DELLA protein RGA to repress the transcriptional activation of AtWRKY6 on downstream SAGs in dark-induced leaf senescence in *Arabidopsis* (Robatzek and Somssich, 2002; Zhang et al., 2018). *AtORE1/ANAC092* is regulated by ethylene signalling (Kim et al., 2009), ABA signalling (Sakuraba et al., 2014a), and the circadian rhythm (Kim et al., 2018), and it directly regulates a number of genes related to SAGs (Woo et al., 2019). These studies suggest that *GhWRKY91* might affect hormone-related signalling pathways during leaf senescence. Moreover, differential SAG expression detected in the different transgenic lines may be due to independent transformation events and positional effects of the T-DNA insertions (Negi et al., 2015). *AtNYC1* encodes a chlorophyll b reductase that is involved in the degradation of chlorophyll b and LHCII (light harvesting complex II) (Horie et al., 2009). However, the expression of *AtNYC1* did not differ between WT and transgenic lines, indicating the complexity of the regulatory mechanism of leaf senescence. In addition, some studies have linked ABA and drought to plant leaf senescence (Woo et al., 2019). For example, the SNAC-A (A subfamily of stress-responsive NAC) septuple (*anac055anac019anac072anac002anac081anac102anac032*) mutant exhibits delayed ABA-induced leaf senescence in *Arabidopsis* (Takasaki et al., 2015). In barley, WHIRLY1 knockdown lines exhibit delayed drought-induced leaf senescence (Janack et al., 2016). However, leaf senescence associated with WRKY TFs under ABA and drought stress conditions is largely unknown in cotton. Here, *GhWRKY91* was found to delay ABA- and drought-induced leaf senescence in transgenic *Arabidopsis* plants (**Supplementary Figure 3** and **Figure 6**). Taken together, our results suggest that GhWRKY91 might serve as a negative regulator during natural leaf senescence and during ABA- and drought-induced leaf senescence, thus expanding the functional roles of WRKY TFs during leaf senescence in cotton. Our results also showed that the maximum expression of *GhWRKY91* occurred in the roots and not in the leaves, indicating that this gene may have other functions yet to be discovered.

The expression of *GhWRKY91* was downregulated by ABA and drought treatment in cotton and verified by GUS activity in

transgenic *Arabidopsis* plants containing the *GhWRKY91* promoter, indicating that *GhWRKY91* expression might be suppressed by ABA and drought. To further study the relationship of ABA and drought stress with *GhWRKY91*, *GhWRKY91*-overexpressing plants were subjected to ABA and drought treatments and the transgenic plants exhibited delayed ABA-induced leaf senescence and improved drought tolerance. To gain further insight into the mechanism of *GhWRKY91* in the ABA response, the transcripts of positive senescence regulators (*AtWRKY53*, *AtSAG13,* and *AtPPH*) and ABA-responsive genes (*HYPERSENSITIVE TO ABA1* (*AtHAB1*), *ABA INSENSITIVE 1* (*AtABI1*), *ABA-RESPONSIVE ELEMENT BINDING PROTEIN 1* (*AtAREB1/ABF2),* and *AtAREB2/ABF4*) were investigated. After ABA treatment, the expression levels of *AtWRKY53*, *AtSAG13,* and *AtPPH* were significantly lower in transgenic plants than in WT (**Supplementary Figure 3B–D**), indicating that *GhWRKY91* could delay ABA-induced leaf senescence. Exogenous ABA application can alter the expression of ABA-responsive genes (Himmelbach et al., 2003). *AtHAB1* and *AtABI1* are members of the protein phosphatase 2C (PP2C) family and involved in the negative regulation of ABA signalling (Merlot et al., 2001; Saez et al., 2004). AREB/ABFs, which are positive regulators in the ABA signalling pathway, bind to ABA-responsive elements in the promoter of ABA-inducible genes (Leite et al., 2014). The transcript levels of negative regulators *AtHAB1* and *AtABI1* were significantly higher in transgenic plants than WT (**Supplementary Figures 3E**, **F**). However, the expression levels of positive regulators *AtAREB1/ABF2* and *AtAREB2/ABF4* were also higher in transgenic plants than in WT (**Supplementary Figure 3G–H**), suggesting a contradictory mechanism in delayed leaf senescence. In our study, overexpression of *GhWRKY91* in *Arabidopsis* caused marginal stunting (**Supplementary Figure 2B**). In our study, the transcript levels of *AtAREB1*/*ABF2* and *AtAREB2*/*ABF4* were upregulated in transgenic plants. Previous studies showed that the overexpression of the *Arabidopsis AtAREB1*/*ABF2* or *AtAREB2*/*ABF4* genes in potato plants caused short and stunted growth (Garcia et al., 2014). Therefore, high expression of *AtAREB1/ABF2* and *AtAREB2/ABF4* may be associated with stunting in transgenic plants, thus leading to delayed leaf senescence. Moreover, the ABA responsive *cis*-element ABRE (ACGTG) was presented in the promoter region of *GhWRKY91*, suggesting the probable role of *GhWRKY91* in plant development by ABA signalling.

To explore the mechanism of *GhWRKY91* in drought tolerance, the stress-related genes *AtP5CS*, *AtP5CS1*, *AtRD29A,* and *AtCOR15A* were identified. Plants invoke various resistance mechanisms to manage various environmental stresses (Ashraf and Foolad, 2007; Shi et al., 2014). P5CS is a key enzyme involved in the synthesis of proline (Hu et al., 1992; Ashraf and Foolad, 2007), which can stabilize metabolic processes in protoplast colloids and prevent dehydration of cells (Hu et al., 1992; Ashraf and Foolad, 2007). Increased enzymatic activity of P5CS leads to increased biosynthesis of proline, thus improving plant resistance to stress (Yamchi et al., 2007). *RD29A*, which encodes a hydrophilic protein, is strongly induced by ABA, drought, and salt stress (Msanne et al., 2011). In addition, DRE and ABRE motifs are present in the promoter of *RD29A*, suggesting important roles for *RD29A* during drought and the ABA response (Yamaguchi-Shinozaki and Shinozaki, 1993). The *COR15A* gene is considered a marker for drought stress and participates in stress responses *via* an ABA-dependent signalling pathway (Meng et al., 2015). In our study, *GhWRKY91*-overexpressing plants exhibited improved drought tolerance, and the expression levels of stress-related genes were significantly higher in the transgenic plants, indicating that *GhWRKY91* may positively regulate drought tolerance *via* ABA signalling pathways and some small molecules.

WRKY TFs can specifically bind to W-box [TTGAC(C/T)] elements in the promoters of target genes to activate or inhibit their expression (Rushton et al., 2010). WRKY genes usually contain W-box cis-elements that can combine with other WRKY TFs or the gene itself (Skibbe et al., 2008; van Verk et al., 2011). Previous reports showed that ectopic overexpression of *GhWRKY17* increases transgenic tobacco plant sensitivity to ABA, drought, and salt stress by participating in the ABA signalling pathway and affecting the antioxidant enzyme system (Yan et al., 2014). Our results showed that W-box elements are indeed present in the *GhWRKY17* promoter. In addition, *GhWRKY17* was targeted directly by GhWRKY91, suggesting that GhWRKY91 may regulate the transcriptional expression of *GhWRKY17*. The dual-luciferase reporter assay demonstrated that GhWRKY91 activates the expression of *GhWRKY17*. Thus, GhWRKY91 may be involved in the ABA regulatory network and

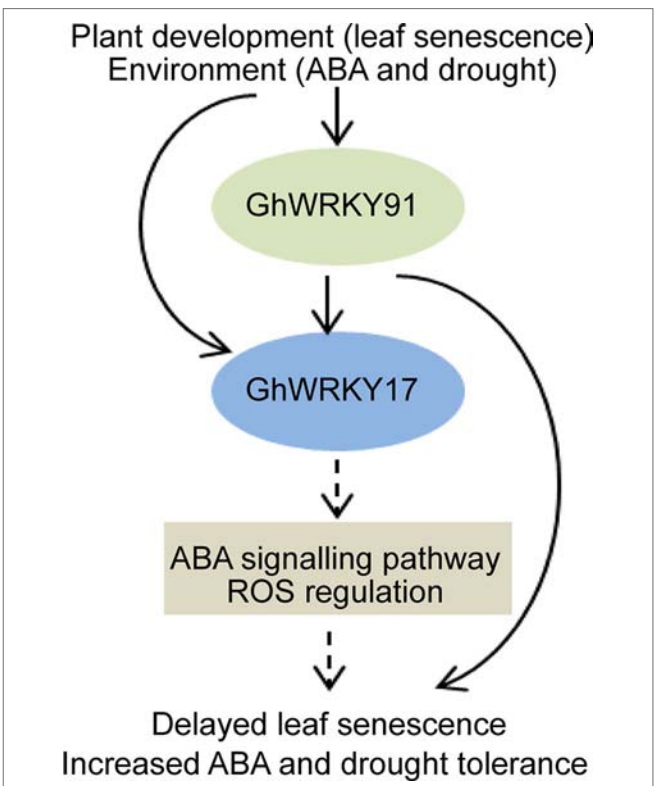

FIGURE 8 | Proposed model for the regulatory mechanism of GhWRKY91. The expression of *GhWRKY91* and *GhWRKY17* is influenced by leaf senescence, ABA, and drought stresses. GhWRKY91 actives the expression of *GhWRKY17*, which is associated with ABA signalling pathways and ROS production. The solid arrows indicate results that have been experimentally determined, whereas dashed arrows indicate speculated effects supported by the literature.

may mediate the intracellular ROS balance *via* transcriptional activation of *GhWRKY17* expression. Expression analysis revealed that the *GhWRKY17* transcripts were downregulated by leaf senescence (**Supplementary Figure 4**), but induced in response to ABA and drought treatments (Yan et al., 2014). The expression of *GhWRKY91* was upregulated by leaf senescence and downregulated by ABA and drought. We found that *GhWRKY91* and *GhWRKY17* presented opposite expression trends under leaf senescence, ABA and drought stress. Therefore, we speculated that there may be some genes that inhibit *GhWRKY17* expression activated by GhWRKY91. However, additional experiments are needed to validate this hypothesis.

In summary, we assumed that GhWRKY91, which contributes to delayed natural leaf senescence and stress-induced (ABA and drought) leaf senescence in transgenic *Arabidopsis* plants, activates the expression of *GhWRKY17*, a gene associated with ABA signalling pathways and ROS production (**Figure 8**). However, the complex regulatory mechanisms underlying these phenomena remain to be clarified in further studies. Our results provide valuable information for helping understand the relationships among WRKY TFs and increase our understanding of the molecular mechanisms of GhWRKY91 during leaf senescence and stress responses in cotton. In addition, these findings provided a theoretical basis for cultivating cotton varieties with non-premature senescence and stress resistance.

DATA AVAILABILITY STATEMENT

All datasets for this study are included in the article/ **Supplementary Material**.

AUTHOR CONTRIBUTIONS

SY and HTW designed the research program. HTW, LG, and HLW analyzed the data. QM, CZ, and CW revised the language and collected the data. LG performed the experiment and wrote the manuscript. All authors have read and approved the final manuscript.

FUNDING

This work was supported by the China Agriculture Research System (grant number CARS-15-06).

SUPPLEMENTARY MATERIAL

The Supplementary Material for this article can be found online at: https://www.frontiersin.org/articles/10.3389/fpls.2019.01352/full#supplementary-material

REFERENCES

Ashraf, M., and Foolad, M. R. (2007). Roles of glycine betaine and proline in improving plant abiotic stress resistance. *Environ. Exp. Bot.* 59 (2), 206–216. doi: 10.1016/j.envexpbot.2005.12.006

Balazadeh, S., Riano-Pachon, D. M., and Mueller-Roeber, B. (2008). Transcription factors regulating leaf senescence in *Arabidopsis thaliana*. *Plant Biol (Stuttg)* 10 Suppl 1, 63–75. doi: 10.1111/j.1438-8677.2008.00088.x

Besseau, S., Li, J., and Palva, E. T. (2012). WRKY54 and WRKY70 co-operate as negative regulators of leaf senescence in *Arabidopsis thaliana*. *J. Exp. Bot.* 63 (7), 2667–2679. doi: 10.1093/jxb/err450

Chen, L., Xiang, S., Chen, Y., Li, D., and Yu, D. (2017). Arabidopsis WRKY45 interacts with the DELLA protein RGL1 to positively regulate age-triggered leaf senescence. *Mol. Plant.* 10 (9), 1174–1189. doi: 10.1016/j.molp.2017.07.008

Chu, X. Q., Wang, C., Chen, X. B., Lu, W. J., Li, H., Wang, X. L., et al. (2015). The cotton WRKY gene GhWRKY41 positively regulates salt and drought stress tolerance in transgenic nicotiana benthamiana. *PloS One* 10 (11), e0143022. doi: 10.1371/journal.pone.0143022

Clough, S. J., and Bent, A. F. (1998). Floral dip: a simplified method for Agrobacterium-mediated transformation of *Arabidopsis thaliana*. *Plant J.* 16 (6), 735–743. doi: 10.1046/j.1365-313x.1998.00343.x

Cominelli, E., and Tonelli, C. (2010). Transgenic crops coping with water scarcity. *New Biotechnol.* 27 (5), 473–477. doi: 10.1016/j.nbt.2010.08.005

Cutler, S. R., Rodriguez, P. L., Finkelstein, R. R., and Abrams, S. R. (2010). Abscisic acid: emergence of a core signaling network. *Ann. Rev. Plant Biol.* 61, 651–679. doi: 10.1146/annurev-arplant-042809-112122

Dou, L., Zhang, X., Pang, C., Song, M., Wei, H., Fan, S., et al. (2014). Genome-wide analysis of the WRKY gene family in cotton. *Mol. Genet. Genomics* 289 (6), 1103–1121. doi: 10.1007/s00438-014-0872-y

Eulgem, T., Rushton, P. J., Robatzek, S., and Somssich, I. E. (2000). The WRKY superfamily of plant transcription factors. *Trends In Plant Sci.* 5 (5), 199–206. doi: 10.1016/S1360-1385(00)01600-9

Fan, K., Bibi, N., Gan, S., Li, F., Yuan, S., Ni, M., et al. (2015). A novel NAP member GhNAP is involved in leaf senescence in *Gossypium hirsutum*. *J. Exp. Bot.* 15 (66), 4669–4682. doi: 10.1093/jxb/erv240

Fan, Z. Q., Tan, X. L., Shan, W., Kuang, J. F., Lu, W. J., and Chen, J. Y. (2017). BrWRKY65, a WRKY transcription factor, is involved in regulating three leaf senescence-associated genes in chinese flowering cabbage. *Int. J. Mol. Sci.* 18 (6), 1228. doi: 10.3390/Ijms18061228

Garcia, M. N. M., Stritzler, M., and Capiati, D. A. (2014). Heterologous expression of *Arabidopsis* ABF4 gene in potato enhances tuberization through ABA-GA crosstalk regulation. *Planta* 239 (3), 615–631. doi: 10.1007/s00425-013-2001-2

Gu, L., Dou, L., Guo, Y., Wang, H., Li, L., Wang, C., et al. (2019). The WRKY transcription factor GhWRKY27 coordinates the senescence regulatory pathway in upland cotton (*Gossypium hirsutum* L.). *BMC Plant Biol.* 19 (1), 116. doi: 10.1186/s12870-019-1688-z

Gu, L., Li, L., Wei, H., Wang, H., Su, J., Guo, Y., et al. (2018a). Identification of the group IIa WRKY subfamily and the functional analysis of GhWRKY17 in upland cotton (*Gossypium hirsutum* L.). *PLoS One* 13 (1), e0191681. doi: 10.1371/journal.pone.0191681

Gu, L., Wei, H., Wang, H., Su, J., and Yu, S. (2018b). Characterization and functional analysis of GhWRKY42, a group IId WRKY gene, in upland cotton (*Gossypium hirsutum* L.). *BMC Genet.* 19 (1), 48. doi: 10.1186/s12863-018-0653-4

Guan, Y., Meng, X., Khanna, R., LaMontagne, E., Liu, Y., and Zhang, S. (2014). Phosphorylation of a WRKY transcription factor by MAPKs is required for pollen development and function in *Arabidopsis*. *PLoS Genet* 10 (5), e1004384. doi: 10.1371/journal.pgen.1004384

Guo, P. R., Li, Z. H., Huang, P. X., Li, B. S., Fang, S., Chu, J. F., et al. (2017a). A tripartite amplification loop involving the transcription factor WRKY75, salicylic acid, and reactive oxygen species accelerates leaf senescence. *Plant Cell* 29 (11), 2854–2870. doi: 10.1105/tpc.17.00438

Guo, R., Yu, F., Gao, Z., An, H., Cao, X., and Guo, X. (2011). GhWRKY3, a novel cotton (*Gossypium hirsutum* L.) WRKY gene, is involved in diverse stress responses. *Mol. Biol. Rep.* 38 (1), 49–58. doi: 10.1007/s11033-010-0076-4

Guo, Y., Cai, Z., and Gan, S. (2010). Transcriptome of *Arabidopsis* leaf senescence. *Plant Cell and Environ.* 27 (5), 521–549. doi: 10.1111/j.1365-3040.2003.01158.x

Guo, Y., and Gan, S. (2006). AtNAP, a NAC family transcription factor, has an important role in leaf senescence. *Plant J* 46 (4), 601–612. doi: 10.1111/j.1365-313X.2006.02723.x

Guo, Y., Pang, C., Jia, X., Ma, Q., Dou, L., Zhao, F., et al. (2017b). An NAM domain gene, GhNAC79, improves resistance to drought stress in upland cotton. *Front Plant Sci.* 8, 1657. doi: 10.3389/fpls.2017.01657

Gustafson, F. G. (1946). Influence of external and internal factors on growth hormone in green plants. *Plant Physiol* 21 (1), 49–62. doi: 10.1104/pp.21.1.49

Harshavardhan, V. T., Van Son, L., Seiler, C., Junker, A., Weigelt-Fischer, K., Klukas, C., et al. (2014). AtRD22 and AtUSPL1, members of the plant-specific BURP domain family involved in *Arabidopsis thaliana* drought tolerance. *PLoS One* 9 (10), e110065. doi: 10.1371/journal.pone.0110065

Hellens, R. P., Allan, A. C., Friel, E. N., Bolitho, K., Grafton, K., Templeton, M. D., et al. (2005). Transient expression vectors for functional genomics, quantification of promoter activity and RNA silencing in plants. *Plant Methods* 1, 13. doi: 10.1186/1746-4811-1-13

Himmelbach, A., Yang, Y., and Grill, E. (2003). Relay and control of abscisic acid signaling. *Cur.r Opin Plant Biol* 6 (5), 470–479. doi: 10.1016/S1369-5266(03)00090-6

Horie, Y., Ito, H., Kusaba, M., Tanaka, R., and Tanaka, A. (2009). Participation of chlorophyll b reductase in the initial step of the degradation of light-harvesting chlorophyll a/b-protein complexes in *Arabidopsis*. *J Biol Chem.* 284 (26), 17449–17456. doi: 10.1074/jbc.M109.008912

Hu, C. A., Delauney, A. J., and Verma, D. P. (1992). A bifunctional enzyme (delta 1-pyrroline-5-carboxylate synthetase) catalyzes the first two steps in proline biosynthesis in plants. *Proc Natl Acad Sci U S A* 89 (19), 9354–9358. doi: 10.1073/pnas.89.19.9354

James, M., Poret, M., Masclaux-Daubresse, C., Marmagne, A., Coquet, L., Jouenne, T., et al. (2018). SAG12, a major cysteine protease involved in nitrogen allocation during senescence for seed production in *arabidopsis thaliana*. *Plant Cell Physiol.* 59 (10), 2052–2063. doi: 10.1093/pcp/pcy125

Janack, B., Sosoi, P., Krupinska, K., and Humbeck, K. (2016). Knockdown of WHIRLY1 affects drought stress-induced leaf senescence and histone modifications of the senescence-associated gene HvS40. *Plants (Basel)* 5 (3), 37. doi: 10.3390/plants5030037

Jefferson, R. A., Kavanagh, T. A., and Bevan, M. W. (1987). GUS fusions: beta-glucuronidase as a sensitive and versatile gene fusion marker in higher plants. *The EMBO j.* 13 (6), 3901–3907. doi: 10.1089/dna.1987.6.583

Jia, H., Wang, C., Wang, F., Liu, S., Li, G., and Guo, X. (2015). GhWRKY68 reduces resistance to salt and drought in transgenic Nicotiana benthamiana. *PLoS One* 10 (3), e0120646. doi: 10.1371/journal.pone.0120646

Jiang, G. X., Yan, H. L., Wu, F. W., Zhang, D. D., Zeng, W., Qu, H. X., et al. (2017). Litchi fruit LcNAC1 is a target of LcMYC2 and regulator of fruit senescence through its interaction with LcWRKY1. *Plant Cell Physiol.* 58 (6), 1075–1089. doi: 10.1093/pcp/pcx054

Jiang, Y. J., Liang, G., Yang, S. Z., and Yu, D. Q. (2014). Arabidopsis WRKY57 functions as a node of convergence for jasmonic acid- and auxin-mediated signaling in jasmonic acid-induced leaf senescence. *Plant Cell* 26 (1), 230–245. doi: 10.1105/tpc.113.117838

Jing, S. J., Zhou, X., Song, Y., and Yu, D. Q. (2009). Heterologous expression of OsWRKY23 gene enhances pathogen defense and dark-induced leaf senescence in *Arabidopsis*. *Plant Growth Reg.* 58 (2), 181–190. doi: 10.1007/s10725-009-9366-z

Johnson, C. S., Kolevski, B., and Smyth, D. R. (2002). TRANSPARENT TESTA GLABRA2, a trichome and seed coat development gene of *Arabidopsis*, encodes a WRKY transcription factor. *Plant Cell* 14 (6), 1359–1375. doi: 10.1105/tpc.001404

Kim, H., Kim, H. J., Vu, Q. T., Jung, S., McClung, C. R., Hong, S., et al. (2018). Circadian control of ORE1 by PRR9 positively regulates leaf senescence in *Arabidopsis*. *Proc. Acad. Sci. U.S. A.* 115 (33), 8448–8453. doi: 10.1073/pnas.1722407115

Kim, J., Kim, J. H., Lyu, J. I., Woo, H. R., and Lim, P. O. (2017). New insights into the regulation of leaf senescence in *Arabidopsis*. *J. Exp. Bot.* 69 (4), 787–799. doi: 10.1093/jxb/erx287

Kim, J. H., Woo, H. R., Kim, J., Lim, P. O., Lee, I. C., Choi, S. H., et al. (2009). Trifurcate feed-forward regulation of age-dependent cell death involving miR164 in *Arabidopsis*. *Sci.* 323 (5917), 1053–1057. doi: 10.1126/science.1166386

Kim, Y. S., Sakuraba, Y., Han, S. H., Yoo, S. C., and Paek, N. C. (2013). Mutation of the *Arabidopsis* NAC016 transcription factor delays leaf senescence. *Plant Cell Physiol.* 54 (10), 1660–1672. doi: 10.1093/pcp/pct113

Krasensky, J., and Jonak, C. (2012). Drought, salt, and temperature stress-induced metabolic rearrangements and regulatory networks. *J. Exp. Bot.* 63 (4), 1593–1608. doi: 10.1093/jxb/err460

Lakhotia, N., Joshi, G., Bhardwaj, A. R., Katiyar-Agarwal, S., Agarwal, M., Jagannath, A., et al. (2014). Identification and characterization of miRNAome in root, stem, leaf and tuber developmental stages of potato (Solanum tuberosum L.) by high-throughput sequencing. *BMC Plant Biol.* 14, 6. doi: 10.1186/1471-2229-14-6

Leite, J. P., Barbosa, E. G. G., Marin, S. R. R., Marinho, J. P., Carvalho, J. F. C., Pagliarini, R. F., et al. (2014). Overexpression of the activated form of the AtAREB1 gene (AtAREB1 Delta QT) improves soybean responses to water deficit. *Genet. Mol. Res.* 13 (3), 6272–6286. doi: 10.4238/2014.August.15.10

Lim, P. O., Kim, H. J., and Nam, H. G. (2007). Leaf senescence. *Annu. Rev. Plant Biol.* 58, 115–136. doi: 10.1146/annurev.arplant.57.032905.105316

Lin, M., Pang, C., Fan, S., Song, M., Wei, H., and Yu, S. (2015). Global analysis of the *Gossypium hirsutum* L. Transcriptome during leaf senescence by RNA-Seq. *BMC Plant Biol.* 15, 43. doi: 10.1186/s12870-015-0433-5

Liu, X., Song, Y., Xing, F., Wang, N., Wen, F., and Zhu, C. (2016). GhWRKY25, a group I WRKY gene from cotton, confers differential tolerance to abiotic and biotic stresses in transgenic Nicotiana benthamiana. *Methods* 253 (5), 1265–1281. doi: 10.1007/s00709-015-0885-3

Livak, K. J., and Schmittgen, T. D. (2001). Analysis of relative gene expression data using real-time quantitative PCR and the 2(T)(-Delta Delta C) method. *Methods* 25 (4), 402–408. doi: 10.1006/meth.2001

Meng, L. S., Wang, Z. B., Yao, S. Q., and Liu, A. (2015). The ARF2-ANT-COR15A gene cascade regulates ABA-signaling-mediated resistance of large seeds to drought in *Arabidopsis*. *J. Cell Sci.* 128 (21), 3922–3932. doi: 10.1242/jcs.171207

Merlot, S., Gosti, F., Guerrier, D., Vavasseur, A., and Giraudat, J. (2001). The ABI1 and ABI2 protein phosphatases 2C act in a negative feedback regulatory loop of the abscisic acid signalling pathway. *Plant J* 25 (3), 295–303. doi: 10.1046/j.1365-313x.2001.00965.x

Miao, Y., Laun, T., Zimmermann, P., and Zentgraf, U. (2004). Targets of the WRKY53 transcription factor and its role during leaf senescence in *Arabidopsis*. *Plant Mol.Biol.* 55 (6), 853–867. doi: 10.1007/s11103-005-2142-1

Msanne, J., Lin, J. S., Stone, J. M., and Awada, T. (2011). Characterization of abiotic stress-responsive *Arabidopsis thaliana* RD29A and RD29B genes and evaluation of transgenes. *Planta* 234 (1), 97–107. doi: 10.1007/s00425-011-1387-y

Murashige, T., and Skoog, F. (1962). A revised medium for rapid growth and bio assays with tobacco tissue cultures. *Physiol Plant* 15, 473–497. doi: 10.1111/j.1399-3054.1962.tb08052.x

Negi, S., Tak, H., and Ganapathi, T. R. (2015). Expression analysis of MusaNAC68 transcription factor and its functional analysis by overexpression in transgenic banana plants. *Plant Cell Tissue Organ Culture* 125 (1), 1–12. doi: 10.1007/s11240-015-0929-6

Ozyigit, I. I., Filiz, E., Vatansever, R., Kurtoglu, K. Y., Koc, I., Ozturk, M. X., et al. (2016). Identification and comparative analysis of H2O2-scavenging Enzymes (ascorbate peroxidase and glutathione peroxidase) in selected plants employing bioinformatics approaches. *Front. Plant Sci.* 7, 301. doi: 10.3389/Fpls.2016.00301

Pan, L. J., and Jiang, L. (2014). Identification and expression of the WRKY transcription factors of Carica papaya in response to abiotic and biotic stresses. *Mol. Biol. Rep.* 41 (3), 1215–1225. doi: 10.1007/s11033-013-2966-8

Pinto, R. S., Reynolds, M. P., Mathews, K. L., McIntyre, C. L., Olivares-Villegas, J. J., and Chapman, S. C. (2010). Heat and drought adaptive QTL in a wheat population designed to minimize confounding agronomic effects. *Theor. App. Genet.* 121 (6), 1001–1021. doi: 10.1007/s00122-010-1351-4

Porebski, S., Bailey, L. G., and Baum, B. R. (1997). Modification of a CTAB DNA extraction protocol for plants containing high polysaccharide and polyphenol components. *Plant Mol. Biol. Rep.* 15 (1), 8–15. doi: 10.1007/BF02772108

Potschin, M., Schlienger, S., Bieker, S., and Zentgraf, U. (2014). Senescence networking: WRKY18 is an upstream regulator, a downstream target gene, and a protein interaction partner of WRKY53. *J. Plant Growth Regul.* 33 (1), 106–118. doi: 10.1007/s00344-013-9380-2

Reynolds, M., and Tuberosa, R. (2008). Translational research impacting on crop productivity in drought-prone environments. *Curr. Opin.Plant Biol.* 11 (2), 171–179. doi: 10.1016/j.pbi.2008.02.005

Robatzek, S., and Somssich, I. E. (2002). Targets of AtWRKY6 regulation during plant senescence and pathogen defense. *Genes Dev.* 16 (9), 1139–1149. doi: 10.1101/gad.222702

Rushton, P. J., Somssich, I. E., Ringler, P., and Shen, Q. J. (2010). WRKY transcription factors. *Trends Plant Sci* 15 (5), 247–258. doi: 10.1016/j.tplants.2010.02.006

Saez, A., Apostolova, N., Gonzalez-Guzman, M., Gonzalez-Garcia, M. P., Nicolas, C., Lorenzo, O., et al. (2004). Gain-of-function and loss-of-function phenotypes of the protein phosphatase 2C HAB1 reveal its role as a negative regulator of abscisic acid signalling. *Plant J* 37 (3), 354–369. doi: 10.1046/j.1365-313X.2003.01966.x

Sakuraba, Y., Jeong, J., Kang, M. Y., Kim, J., Paek, N. C., and Choi, G. (2014a). Phytochrome-interacting transcription factors PIF4 and PIF5 induce leaf senescence in *Arabidopsis*. *Nat. Commun.* 5, 4636. doi: 10.1038/ncomms5636

Sakuraba, Y., Park, S. Y., Kim, Y. S., Wang, S. H., Yoo, S. C., Hortensteiner, S., et al. (2014b). Arabidopsis STAY-GREEN2 is a negative regulator of chlorophyll degradation during leaf senescence. *Mol. Plant.* 7 (8), 1288–1302. doi: 10.1093/mp/ssu045

Schelbert, S., Aubry, S., Burla, B., Agne, B., Kessler, F., Krupinska, K., et al. (2009). Pheophytin pheophorbide hydrolase (Pheophytinase) is involved in chlorophyll breakdown during leaf senescence in arabidopsis. *Plant Cell* 21 (3), 767–785. doi: 10.1105/tpc.108.064089

Shi, W. N., Hao, L. L., Li, J., Liu, D. D., Guo, X. Q., and Li, H. (2014). The Gossypium hirsutum WRKY gene GhWRKY39-1 promotes pathogen infection defense responses and mediates salt stress tolerance in transgenic Nicotiana benthamiana. *Plant Cell R.* 33 (3), 483–498. doi: 10.1007/s00299-013-1548-5

Skibbe, M., Qu, N., Galis, I., and Baldwin, I. T. (2008). Induced plant defenses in the natural environment: Nicotiana attenuata WRKY3 and WRKY6 coordinate responses to herbivory. *Plant Cell* 20 (7), 1984–2000. doi: 10.1105/tpc.108.058594

Takasaki, H., Maruyama, K., Takahashi, F., Fujita, M., Yoshida, T., Nakashima, K., et al. (2015). SNAC-As, stress-responsive NAC transcription factors, mediate ABA-inducible leaf senescence. *Plant J.* 84 (6), 1114–1123. doi: 10.1111/tpj.13067

Ulker, B., Mukhtar, M. S., and Somssich, I. E. (2007). The WRKY70 transcription factor of *Arabidopsis* influences both the plant senescence and defense signaling pathways. *Planta* 226 (1), 125–137. doi: 10.1007/s00425-006-0474-y

van Verk, M. C., Bol, J. F., and Linthorst, H. J. (2011). WRKY transcription factors involved in activation of SA biosynthesis genes. *BMC Plant Biol.* 11, 89. doi: 10.1186/1471-2229-11-89

Wang, C., Deng, P. Y., Chen, L. L., Wang, X. T., Ma, H., Hu, W., et al. (2013). A Wheat WRKY transcription factor TaWRKY10 confers tolerance to multiple abiotic stresses in transgenic tobacco. *Plos One* 8 (6), e65120. doi: 10.1371/journal.pone.0065120

Wang, X. T., Zeng, J., Li, Y., Rong, X. L., Sun, J. T., Sun, T., et al. (2015). Expression of TaWRKY44, a wheat WRKY gene, in transgenic tobacco confers multiple abiotic stress tolerances. *Front. Plant Sci.* 6, 615. doi: 10.3389/fpls.2015.00615

White, J. W., McMaster, G. S., and Edmeades, G. O. (2004). Physiology, genomics and crop response to global change. *Field Crops Res.* 90 (1), 1–3. doi: 10.1016/j.fcr.2004.07.001

Woo, H. R., Kim, H. J., Lim, P. O., and Nam, H. G. (2019). Leaf senescence: systems and dynamics aspects. *Annu. Rev. Plant Biol.* 70, 347–376. doi: 10.1146/annurev-arplant-050718-095859

Wu, X. Y., Hu, W. J., Luo, H., Xia, Y., Zhao, Y., Wang, L. D., et al. (2016). Transcriptome profiling of developmental leaf senescence in sorghum (Sorghum bicolor). *Plant. Mol. Biol.* 92 (4-5), 555–580. doi: 10.1007/s11103-016-0532-1

Xiang, J. S., Tang, S., Zhi, H., Jia, G. Q., Wang, H. J., and Diao, X. M. (2017). Loose Panicle1 encoding a novel WRKY transcription factor, regulates panicle development, stem elongation, and seed size in foxtail millet [Setaria italica (L.) P. Beauv.]. *Plos One* 12 (6), e0178730. doi: 10.1371/journal.pone.0178730

Xiao, J., Cheng, H., Li, X., Xiao, J., Xu, C., and Wang, S. (2013). Rice WRKY13 regulates cross talk between abiotic and biotic stress signaling pathways by selective binding to different cis-elements. *Plant Physiol* 163 (4), 1868–1882. doi: 10.1104/pp.113.226019

Xie, Y., Huhn, K., Brandt, R., Potschin, M., Bieker, S., Straub, D., et al. (2014). REVOLUTA and WRKY53 connect early and late leaf development in *Arabidopsis*. *Dev.* 141 (24), 4772–4783. doi: 10.1242/dev.117689

Yamaguchi-Shinozaki, K., and Shinozaki, K. (1993). Arabidopsis DNA encoding two desiccation-responsive rd29 genes. *Plant Physiol* 101 (3), 1119–1120. doi: 10.1104/pp.101.3.1119

Yamchi, A., Jazii, F. R., Mousavi, A., and Karkhane, A. A. (2007). Proline accumulation in transgenic tobacco as a result of expression of *Arabidopsis* Delta(1)-pyrroline-5-carboxylate synthetase (P5CS) during osmotic stress. *J. Plant Biochem. Biotechnol.* 16 (1), 9–15. doi: 10.1007/Bf03321922

Yan, H., Jia, H., Chen, X., Hao, L., An, H., and Guo, X. (2014). The cotton WRKY transcription factor GhWRKY17 functions in drought and salt stress in transgenic Nicotiana benthamiana through ABA signaling and the modulation of reactive oxygen species production. *Plant Cell Physiol.* 55 (12), 2060–2076. doi: 10.1093/pcp/pcu133

Yan, Y., Jia, H., Wang, F., Wang, C., Liu, S., and Guo, X. (2015). Overexpression of GhWRKY27a reduces tolerance to drought stress and resistance to Rhizoctonia solani infection in transgenic Nicotiana benthamiana. *Front Physiol.* 6, 265. doi: 10.3389/fphys.2015.00265

Yu, F., Huaxia, Y., Lu, W., Wu, C., Cao, X., and Guo, X. (2012). GhWRKY15, a member of the WRKY transcription factor family identified from cotton (*Gossypium hirsutum* L.), is involved in disease resistance and plant development. *BMC Plant Biol.* 12, 144. doi: 10.1186/1471-2229-12-144

Yu, S. X., Song, M. Z., Fan, S. L., Wang, W., and Yuan, R. H. (2005). Biochemical genetics of short-season cotton cultivars that express early maturity without senescence. *J. Integ. Plant. Biol.* 47 (3), 334–342. doi: 10.1111/j.1744-7909.2005.00029.x

Zhang, C. Q., Xu, Y., Lu, Y., Yu, H. X., Gu, M. H., and Liu, Q. Q. (2011). The WRKY transcription factor OsWRKY78 regulates stem elongation and seed development in rice. *Planta* 234 (3), 541–554. doi: 10.1007/s00425-011-1423-y

Zhang, Y., Liu, Z., Wang, X., Wang, J., Fan, K., Li, Z., et al. (2018). DELLA proteins negatively regulate dark-induced senescence and chlorophyll degradation in *Arabidopsis* through interaction with the transcription factor WRKY6. *Plant Cell Rep.* 37 (7), 981–992. doi: 10.1007/s00299-018-2282-9

Zhao, F., Ma, J., Li, L., Fan, S., Guo, Y., Song, M., et al. (2016). GhNAC12, a neutral candidate gene, leads to early aging in cotton (*Gossypium hirsutum* L). *Gene.* 576 (1 Pt 2), 268–274. doi: 10.1016/j.gene.2015.10.042

Zhou, X., Jiang, Y. J., and Yu, D. Q. (2011). WRKY22 transcription factor mediates dark-induced leaf senescence in *Arabidopsis*. *Mol. And Cells* 31 (4), 303–313. doi: 10.1007/s10059-011-0047-1

Conflict of Interest: The authors declare that the research was conducted in the absence of any commercial or financial relationships that could be construed as a potential conflict of interest.

frontiers in Plant Science

ORIGINAL RESEARCH
published: 23 January 2020
doi: 10.3389/fpls.2019.01734

Arabidopsis thaliana WRKY25 Transcription Factor Mediates Oxidative Stress Tolerance and Regulates Senescence in a Redox-Dependent Manner

Jasmin Doll[†], *Maren Muth*[†], *Lena Riester*, *Sabrina Nebel*, *Justine Bresson*, *Hsin-Chieh Lee and Ulrike Zentgraf*[*]

Center for Plant Molecular Biology (ZMBP), University of Tuebingen, Tuebingen, Germany

OPEN ACCESS

Edited by:
Yasuhito Sakuraba,
The University of Tokyo, Japan

Reviewed by:
Klaus Humbeck,
Martin Luther University of Halle-Wittenberg, Germany
Raquel Lia Chan,
CONICET Santa Fe, Argentina

***Correspondence:**
Ulrike Zentgraf
ulrike.zentgraf@zmbp.uni-tuebingen.de

[†]*These authors share first authorship*

Specialty section:
This article was submitted to Plant Abiotic Stress, a section of the journal Frontiers in Plant Science

Received: *20 August 2019*
Accepted: *10 December 2019*
Published: *23 January 2020*

Citation:
Doll J, Muth M, Riester L, Nebel S, Bresson J, Lee H-C and Zentgraf U (2020) Arabidopsis thaliana WRKY25 Transcription Factor Mediates Oxidative Stress Tolerance and Regulates Senescence in a Redox-Dependent Manner. Front. Plant Sci. 10:1734. doi: 10.3389/fpls.2019.01734

Senescence is the last developmental step in plant life and is accompanied by a massive change in gene expression implying a strong participation of transcriptional regulators. In the past decade, the WRKY53 transcription factor was disclosed to be a central node of a complex regulatory network of leaf senescence and to underlie a tight multi-layer control of expression, activity and protein stability. Here, we identify WRKY25 as a redox-sensitive up-stream regulatory factor of *WRKY53* expression. Under non-oxidizing conditions, WRKY25 binds to a specific W-box in the *WRKY53* promoter and acts as a positive regulator of *WRKY53* expression in a transient expression system using Arabidopsis protoplasts, whereas oxidizing conditions dampened the action of WRKY25. However, overexpression of *WRKY25* did not accelerate senescence but increased lifespan of Arabidopsis plants, whereas the knock-out of the gene resulted in the opposite phenotype, indicating a more complex regulatory function of WRKY25 within the WRKY subnetwork of senescence regulation. In addition, overexpression of WRKY25 mediated higher tolerance to oxidative stress and the intracellular H_2O_2 level is lower in *WRKY25* overexpressing plants and higher in *wrky25* mutants compared to wildtype plants suggesting that WRKY25 is also involved in controlling intracellular redox conditions. Consistently, *WRKY25* overexpressers had higher and *wrky* mutants lower H_2O_2 scavenging capacity. Like already shown for WRKY53, MEKK1 positively influenced the activation potential of WRKY25 on the *WRKY53* promoter. Taken together, WRKY53, WRKY25, MEKK1 and H_2O_2 interplay with each other in a complex network. As H_2O_2 signaling molecule participates in many stress responses, WRKK25 acts most likely as integrators of environmental signals into senescence regulation.

Keywords: Arabidopsis, transcription factor network, WRKY factors, oxidative stress tolerance, redox-dependent DNA-binding, leaf senescence

INTRODUCTION

Senescence is the last step during plant development and is genetically programmed to maximize the remobilization of nutrients out of the senescing tissue into developing parts of the plants before organs finally die. Before anthesis, sequential leaf senescence leads to the reallocation of mineral, nitrogen and carbon sources from older leaves to newly developing non-reproductive organs. After anthesis, monocarpic leaf senescence is launched and governs the nutrient repartitioning to the now developing reproductive organs and, therefore, has a critical impact on yield quality and quantity. Induction and progression of leaf senescence is mainly achieved by switching-on genes involved in degradation and mobilization of macromolecules and turning-off genes related to photosynthesis. A temporal transcript profiling, using microarrays with high-resolution covering 22 time points of a defined leaf of *Arabidopsis thaliana* during onset and progression of leaf senescence, revealed a distinct chronology of events (Breeze et al., 2011). Remarkably, the first processes to be activated are autophagy and transport followed by reactions to reactive oxygen species (ROS) and subsequently to abscisic acid (ABA) and jasmonic acid (JA). This clearly indicates that ROS, ABA and JA are important early signals in leaf senescence. In consistence, intracellular hydrogen peroxide contents increase during bolting and flowering of Arabidopsis plants when monocarpic senescence is induced (Zimmermann et al., 2006) while decreasing hydrogen peroxide levels lead to a delay of the onset of leaf senescence (Bieker et al., 2012).

These massive changes in the transcriptome suggest a central role for transcriptional regulators. The two transcription factor families of WRKY and NAM-, ATAF-, and CUC-like (NAC) factors, which largely expanded in the plant kingdom, are overrepresented in the senescence transcriptome of Arabidopsis (Guo et al., 2004) and appear to be ideal candidates for regulatory functions. Several members of both families play important roles in senescence, not only in Arabidopsis but also in other plant species (Miao et al., 2004; Uauy et al., 2006; Ülker et al., 2007; Kim et al., 2009; Breeze et al., 2011; Yang et al., 2011; Besseau et al., 2012; Wu et al., 2012; Gregersen et al., 2013).

The WRKY transcription factor family of *A. thaliana* consists of 75 members, subdivided into three different groups according to their protein motifs and domains (Eulgem et al., 2000; Rushton et al., 2010). Many WKRY factors are activated after pathogen attack but also in response to abiotic stress (for review see Birkenbihl et al., 2017; Jiang et al., 2017). Moreover, members of all three groups are involved in senescence regulation and many of these react to ROS, SA and JA signals indicating a cross-talk between stress responses and senescence. Besides this cross-talk to stress responses, the *WRKY53* upstream regulator REVOLUTA mediates a redox-related communication between early leaf patterning and senescence as REVOLUTA is involved in both processes (Xie et al., 2014; Kim et al., 2017).

Interestingly, almost all members of the WRKY family contain one or more W-boxes (the consensus binding motif TTGACC/T of all WRKY factors) in their promoters, pointing to a WRKY transcriptional network (Dong et al., 2003; Llorca et al., 2014). Even though all WRKYs bind to these consensus sequences, there appears to be a selectivity of specific factors for specific boxes most likely due to the surrounding sequences (Rushton et al., 2010; Brand et al., 2013; Potschin et al., 2014). However, besides regulating transcription of each other, WRKY factors are also able to form heterodimers, leading to a change in DNA-binding specificity (Xu et al., 2006). In addition, many other proteins interact physically with WRKY proteins influencing their activity and stability (for review see Chi et al., 2013). One central node in the WRKY network regulating early senescence is WRKY53. WRKY53 underlies a tight regulation governed by multi-layer mechanisms to control expression, activity and protein stability. When leaf senescence is induced, the *WRKY53* gene locus is activated by the histone modifications H3K4me2 and H3K4me3 (Ay et al., 2009; Brusslan et al., 2012), whereas DNA methylation remains unchanged and overall very low (Zentgraf et al., 2010). At least 12, most likely even more, proteins are able to bind to the promoter of *WRKY53* (GATA4, AD-Protein, WRKY53 itself, several other WRKYs, MEKK1, REVOLUTA, WHIRLY1) and influence the expression of *WRKY53* (Miao et al., 2004; Miao et al., 2007; Miao et al., 2008; Potschin et al., 2014; Xie et al., 2014; Ren et al., 2017, unpublished results). All these factors are involved in senescence regulation but it is still unclear whether they all bind at exactly the same time, whether they compete with each other, or whether they form higher order complexes. Except for the WRKYs that bind to the W-boxes in the *WRKY53* promoter, all other proteins have different binding motifs so that in principle a simultaneous interaction would be possible. The *WRKY53* promoter contains at least three W-boxes, which show preferential binding activities for different WRKY factors but competition would be also a mean of regulation. Moreover, WRKYs can also form heterodimers, which makes the situation even more complicated. However, all these aspects need further investigations. For MEKK1, it has already been shown that it can interact with WRKY53 and AD-Protein on the protein level (Miao et al., 2007; Miao et al., 2008). Whether WRKY53 or other WRKYs compete with AD-protein for MEKK1 interaction or whether they form higher order complexes is currently analyzed in more detail. These findings have been compiled in a model (Zentgraf et al., 2010) und smaller subnetworks have already schematically drawn for some candidates like WRKY18, REVOLUTA or WHIRLY1 (Potschin et al., 2014; Xie et al., 2014; Ren et al., 2017).

Moreover, the WRKY53 protein also directly interacts with a histone deacetylase 9 (HDA9) to recruit POWERDRESS and HDA9 to W-box containing promoter regions to remove H3 acetylation marks and thereby suppress the expression of key negative senescence regulators (Chen et al., 2016). This clearly suggests that WRKY53 itself is also involved in changing epigenetic marks of senescence regulators in a feedback loop. Phosphorylation by the MAP kinase kinase kinase MEKK1 or the interaction with the epithiospecifier ESP/ESR directly influences the DNA-binding activity of WRKY53 (Miao et al., 2007; Miao and Zentgraf, 2007). On top of that, the E3 ubiquitin

ligase UPL5 tightly controls the protein amount of WRKY53 (Miao and Zentgraf, 2010). The complexity of the WRKY network is illustrated by the fact that one and the same WRKY factor, namely WRKY18, acts as upstream regulator, downstream target and protein interaction partner of WRKY53 (Potschin et al., 2014).

In order to unravel the molecular mechanisms of the senescence-regulating WRKY network in more detail, we screened the W-boxes of the *WRKY53* promoter for DNA-protein interactions with other leaf senescence-associated WRKY proteins and tested their impact on *WRKY53* expression using a transient expression system in Arabidopsis protoplasts. Here we used WRKYs which are expressed in leaves during onset and progression of senescence and which belong to the three different subgroups of the WRKY family, namely WRKY18 (group IIa), WRKY25 (group I) and WRKY53 itself (group III). Out of the 15 WKRYs analyzed by an ELISA-based DNA-protein interaction assay and reporter gene expression assays, WRKY18 had a very strong binding affinity to all W-boxes of the *WRKY53* promoter but a very low selectivity. Moreover, WRKY18 was characterized to be the strongest negative regulator of *WRKY53* expression (Potschin et al., 2014). Besides WRKY18, WRKY25 was one of the strongest interaction partners of the *WRKY53* promoter but in this case turned out to be a strong positive regulator of *WRKY53* expression. Therefore, we wanted to analyze the interplay between WRKY53 and WRKY25 in more detail. Here we could show that DNA-binding as well as transcriptional activation potential of WRKY25 is dependent on the redox conditions. Intracellular hydrogen peroxide concentrations are altered in plants with altered *WRKY25* expression and the *WRKY25* overexpressing plants are more tolerant against oxidative stress. WRKY25 appears to foster the activation of the H_2O_2-mediated expression of the transcription factors *WRKY18* but dampens the H_2O_2-response of *WRKY53*, *ZAT12*, and *ANAC092* in mature leaves. However, contradicting its positive effect on *WRKY53* expression and the senescence phenotype of the *WRKY53* overexpressing plants, *WRKY25* overexpressing plants exhibited a delayed senescence phenotype, whereas *wrky25* mutant plants showed slightly accelerated senescence. This clearly points to a more complex regulatory network. Moreover, the influence of MEKK1 as modulator of WRKY53 activity on the action of WRKY25 was tested.

RESULTS

WRKY25 Binds Directly to the Promoter of *WRKY53 in* a Redox-Sensitive Manner

Out of the 15 WKRYs analyzed by an ELISA-based DNA-protein interaction assay, WRKY18 (group IIa) and WRKY25 (group I) had a very strong binding affinity. In contrast to WRKY18, which strongly binds to all W-boxes in the *WRKY53* promoter (Potschin et al., 2014), WRKY25 also had a strong binding activity but selectively bound to W-box1, to a much lesser extend to W-box2 and 3, the TGAC cluster and an artificial 3× W-box (**Figures 1A, B**). Binding was completely abolished when W-box1 was mutated or an unrelated G-box motive was coupled to the ELISA plates. All binding reactions increased with protein concentrations and no binding could be detected with crude extracts of *E. coli* cells expressing no recombinant protein. Both proteins were present approximately to the same extent in *E. coli* crude extracts (**Figure S1**). As many WRKY factors signal back to their own promoters in positive or negative feedback loops, we also tested whether WRKY25 can bind to the W-boxes in its own promoter. Here, WRKY25 was able to bind to W-box1 and 4, whereas W-box2 and 3 exhibited lower binding affinities. *Vice versa*, WRKY53 also bound preferentially to W-box 1 of the *WRKY25* promoter but to W-box2 of its own promoter, as already shown before (**Figure 1C**, Potschin et al., 2014). This indicates that according to DNA-binding, there is a cross-regulation between both genes and both genes are regulated by feedback mechanisms.

We already know for a long time that *WRKY53* expression can be induced by H_2O_2 treatment (Miao et al., 2004; Xie et al., 2014). As the WRKY25 protein contains two potentially redox-sensitive zinc-finger DNA-binding domains, it is an excellent candidate for direct redox regulation (Arrigo, 1999). Therefore, we wanted to test whether the WRKY25 DNA-binding reaction is sensitive to reducing or oxidizing agents and analyzed the ability of WRKY25 to bind to W-box1 of the *WRKY53* promoter and W-box1 of the *WRKY25* promoter under different redox conditions. Whereas reducing conditions (DTT addition) clearly and significantly increased DNA-binding ability to both W-boxes, oxidizing conditions (H_2O_2 addition) significantly reduced the binding activity in comparison to standard binding conditions (**Figure 2**). In order to test whether this redox-dependent binding can be driven back and forth when redox conditions change, we added increasing amounts of H_2O_2 to the DTT pre-treated binding reactions and *vice versa*. Both redox-related changes in DNA-binding activity of WRKY25 were reversible indicating that WRKY25 can directly adapt its DNA-binding activity to the redox status of the cell. However, not all WRKYs show this redox-sensitivity, e.g. WRKY18 appears to be insensitive, whereas WRKY53 DNA-binding seems to be diminished under oxidizing and reducing conditions, but this reduction was not statistically significant (**Figure S2**).

WRKY25 Acts as Positive Regulator of *WRKY53* Expression Under Non-Oxidizing Conditions

To investigate, how WRKY25 affects the expression of *WRKY53* and *vice versa*, we performed a transient co-transformation of *WRKY53* or *WRKY25* promoter:*GUS* constructs with 35S:*WRKY25* and 35S:*WRKY53* effector constructs, respectively, using an Arabidopsis protoplast system (**Figure 3A**). The protoplast system was used to confirm the identified DNA-Protein interactions of the *in vitro* assay also *in vivo*. However, it is clear that the protoplast system is still an artificial system not taking into account development cues, but it can provide inside into the possible basic regulatory mechanisms. Using this *in vivo* system, the WRKY25 effector significantly up-regulated promoter *WRKY53*-driven *GUS* expression. In contrast, it

down-regulated *GUS* expression driven by its own promoter pointing to a negative feedback regulation. The WRKY53 effector slightly activated reporter gene expression driven by its own promoter as already described before (Potschin et al., 2014). Surprisingly, WRKY53 had only low effects (1.4-fold) on reporter gene expression driven by the promoter of *WRKY25* (**Figure 3A**), even though WRKY53 is able to bind strongly to the W-boxes of this promoter (**Figure 1C**) indicating that strong binding does not necessarily mean that gene expression is highly affected. If both effector constructs were co-expressed, additive effects were detected leaving the question open whether or not heterodimers are formed.

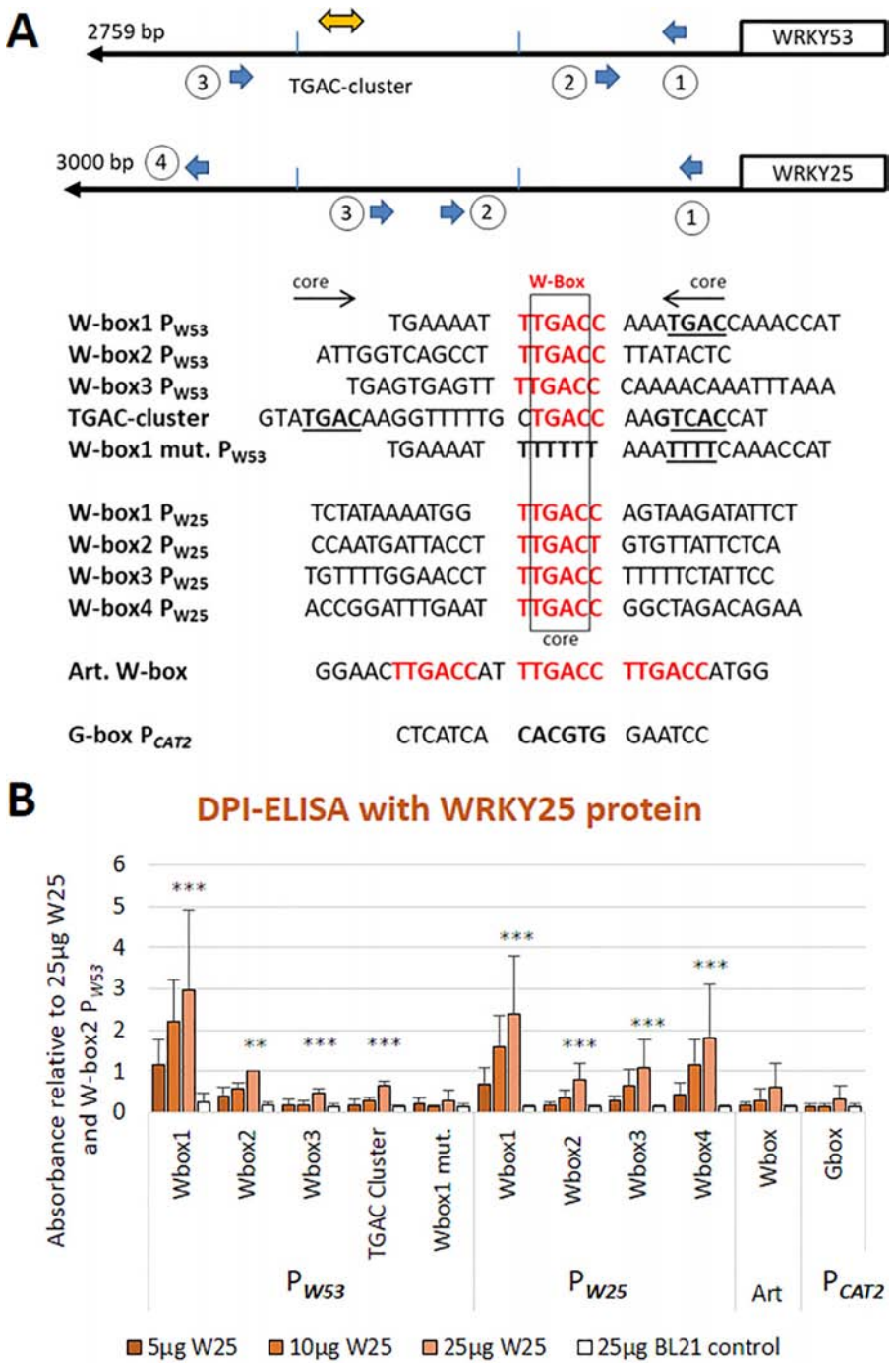

FIGURE 1 | Continued

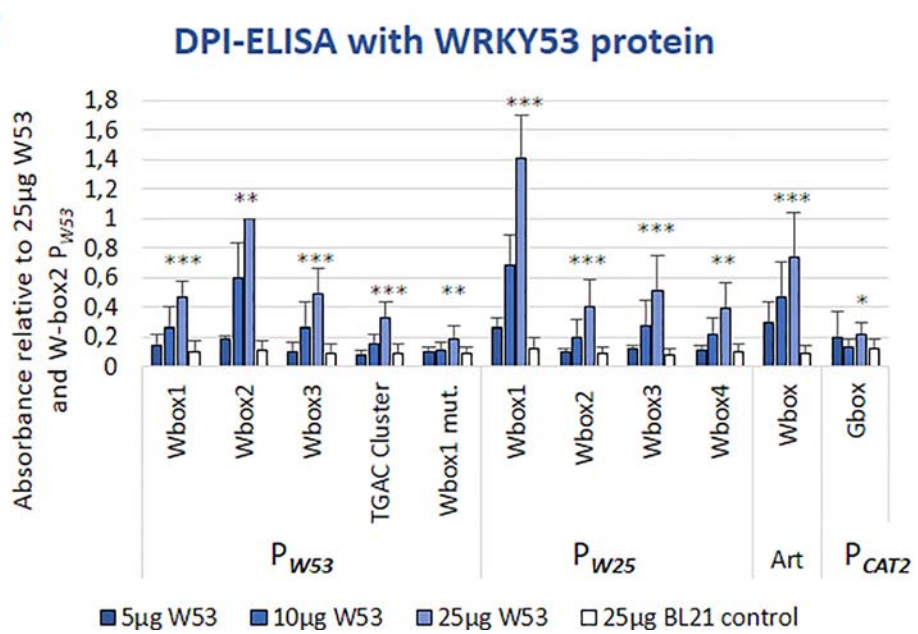

FIGURE 1 | WRKY25 is able to bind directly to the *WRKY53* promoter. **(A)** Schematic drawing of positions and sequences of the W-boxes in the *WRKY53* and *WRKY25* promoters used for DPI-ELISAs; perfect W-box motifs are highlighted in red; the TGAC core sequence is indicated in bold and underlined; the direction of the motif is indicated by the arrows. An artificial sequence containing three perfect W-boxes was used as a positive control (Art. W-box), a G-box of the *CATALASE2* promoter was used as a negative control. **(B)** DPI-ELISA with different amounts of crude extracts of *E. coli* BL21 cells expressing WRKY25 proteins and different biotinylated DNA fragments. **(C)** DPI-ELISA with different amounts of crude extracts of *E. coli* BL21 cells expressing WRKY53 proteins and different biotinylated DNA fragments. Absorbance values are indicated relative to values of 25 µg WRKY25 or WRKY53 to W-box2 P_{W53}, respectively, (mean values ± SD, n = 3-4). Kruskal–Wallis-test was performed for statistically significant differences of all values compared to 25 µg BL21 control (*$P \leq 0.05$, **$P \leq 0.01$, ***$P \leq 0.001$).

As DNA-binding of WRKY25 was redox-sensitive, we wanted to find out, whether also target gene expression is affected by the redox conditions. Since we wanted to change the redox conditions within a physiological range, we did not treat protoplasts directly with high amounts of H_2O_2. Instead, we developed a transient expression system using Arabidopsis protoplast in the presence of 3-Amino-Triazol (3′-AT), which inhibits catalase function, and would therefore provoke physiological changes in intracellular H_2O_2 levels. Inhibition of catalase activity was almost complete and leads to increasing concentrations of H_2O_2 in the cells, but had no effect on the GUS activity measurement (**Figure S3**). Using this assay, WKRY25 effector proteins were significantly less efficient under oxidizing conditions, most likely due to lower DNA-binding affinity. WRKY53 effector proteins appeared also to be less efficient, but the effect was only significant for the WRKY25 promoter, not for its own. The effects were still significant when a combination of both effectors constructs was used (**Figure 3B**).

MEKK1 Increases the Effect of WRKY25 Proteins on Promoter of *WRKY53* Driven Gene Expression

As expression of *WRKY53* is enhanced by a direct binding of MEKK1 to the promoter region of *WRKY53* and a protein–protein interaction between WRKY53 and MEKK1 leads to phosphorylation of WRKY53 (Miao et al., 2007), we tested whether WRKY25 activity can also be enhanced by adding a 35S:*MEKK1* construct as additional effector in a protoplast co-transformation assay. Indeed, the presence of the MEKK1 protein significantly increased *WRKY53* promoter-driven reporter gene expression by WRKY25 to approximately the same extent as MEKK1 presence exhibits on WRKY53 activity itself (**Figure 3C**). Thus, MEKK1 interplay with WRKY factors is not restricted to WRKY53, but appears to be a more general phenomenon. First evidence for a direct protein-protein interaction between several WRKY factors and MEKK1 was obtained in a Yeast-Split-Ubiquitin system, in which many, but not all tested WRKYs could interact with MEKK1 (data not shown). WRKY18, which acted as a repressor on promoter *WRKY53*-driven reporter gene expression (Potschin et al., 2014), even changed its activity in the presence of MEKK1 from a repressor to an activator (**Figure S4A**). Moreover, we tested the role of MEKK1 in senescence regulation. As *MEKK1* knock-out plants die before they develop the first true leaves, we used an estradiol-inducible $amiRNA_{MEKK1}$ line to knock-down MEKK1 by treatment with 3 µM ß-estradiol or mock every 7 days starting on day 25 after germination. In this system, knock-down of MEKK1 can be controlled by GFP expression, which is under the control of the same amiRNA (Li et al., 2013). Here we could show that conditional knock-down of *MEKK1* in plants exhibit an accelerated senescence phenotype (**Figures S4B–D**). Taken together, MEKK1 appears to act as negative regulator of senescence at least in part by modulating the activity of different WRKY factors. However, whether the interaction with WRKY25

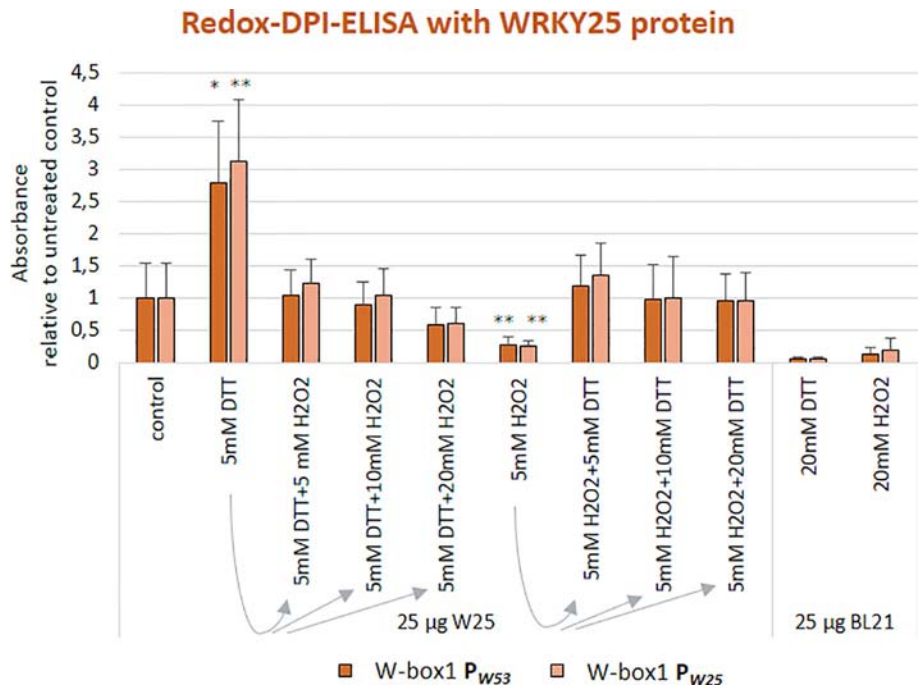

FIGURE 2 | WRKY25 binding to the *WRKY53* promoter is redox-dependent. Redox-DPI-ELISA with 25 µg of crude extracts of *E. coli* BL21 cells expressing WRKY25 proteins and the 5'biotinylated annealed oligonucleotides W-box1 P_{W53} and W-box1 P_{W25}. Protein extracts were reduced or oxidized by addition of either DTT or H_2O_2 to examine a redox-dependent binding of WRKY25. A fraction of the DTT-reduced proteins was re-oxidized by addition of increasing H_2O_2 concentrations to prove the reversibility of the redox effect. The same procedure was applied to the H_2O_2-oxidized proteins using increasing amounts of DTT. Absorbance values are indicated relative to control without treatment (mean values ± SD, n = 4). Kruskal–Wallis-test was performed for statistically significant differences of all values compared to control (*$P \leq 0.05$, **$P \leq 0.01$).

or WRKY18 is direct as it is for WRKY53, or is mediated by the classical MAPK pathway, still has to be elucidated.

WRKY25 Is Involved in Senescence Regulation

To evaluate the participation of WRKY25 in senescence regulation, we analyzed plants with a T-DNA insertion in the *WRKY25* gene lacking a functional WRKY25 protein and *WRKY25* overexpressing plants. A T-DNA insertion in the last of five exons of *WRKY25* (SAIL_529_B11) was confirmed by PCR and expression of *WRKY25* was analyzed by qRT-PCR (**Figure S5B**). Moreover, for overexpression of *WRKY25,* we first transformed plants using a 35S:*WRKY25* construct. However, qRT-PCR revealed that *WRKY25* was not overexpressed; in contrast, the endogenous gene expression was severely silenced throughout plant development (**Figure S5A**) so that we used this line as knock-down line (35S:*WRKY25si*) to confirm the results of the *wrky25* mutant plants. In a second attempt, we used the *UBIQITIN10* promoter for more moderate overexpression and we created two independent plant lines overexpressing *WRKY25* to different extents with different transgene expression levels (**Figure S5B**). In addition, double-knock-out mutants were created by crossing the single mutant lines *wrky25* (SAIL_529_B11) and *wrky53* (SALK_034157; Miao et al., 2004) with each other. F2 progenies were screened for homozygous double-knock-out plants. In order to compare leaves of the same position within the rosette for senescence symptoms, leaves were color-coded during development (Bresson et al., 2018). Altered *WRKY25* expression had almost no effect on the speed of the general development of the plants (**Figure S6**). Bolts appeared at approximately week 5 in all lines, first flowers at approximately week 6 and first siliques also developed synchronously. However, leaf size slightly increased in the overexpression lines whereas leaves of the *wrky25* mutant, the *wrky25/wrky53* double-knock-out plants and the *WRKY25* silenced line were slightly smaller. To evaluate senescence in detail, we sorted the rosette leaves of all lines by the color code according to their age to compare the respective leaves with each other. A typical example of rosette leaves of 8-week-old plants is shown in **Figure 4A**. However, as there are always differences between individual plants of one line, a statistical analysis of at least six plants was done by grouping the leaves into four categories by an automated colorimetric assay (ACA; Bresson et al., 2018) according to their leaf color (green; green/yellow; fully yellow and brown/dry) from weeks 5 to 8 (**Figure 4B**). The photosynthetic status of the plants was analyzed using a Pulse-Amplitude-Modulation (PAM) method (**Figure 4C**). Amongst the chlorophyll fluorescence imaging parameters, the Fv/Fm ratio is reflecting the maximal quantum yield of PSII photochemistry. Moreover, the expression of the senescence marker genes *CHLOROPHYLL A/B BINDING*

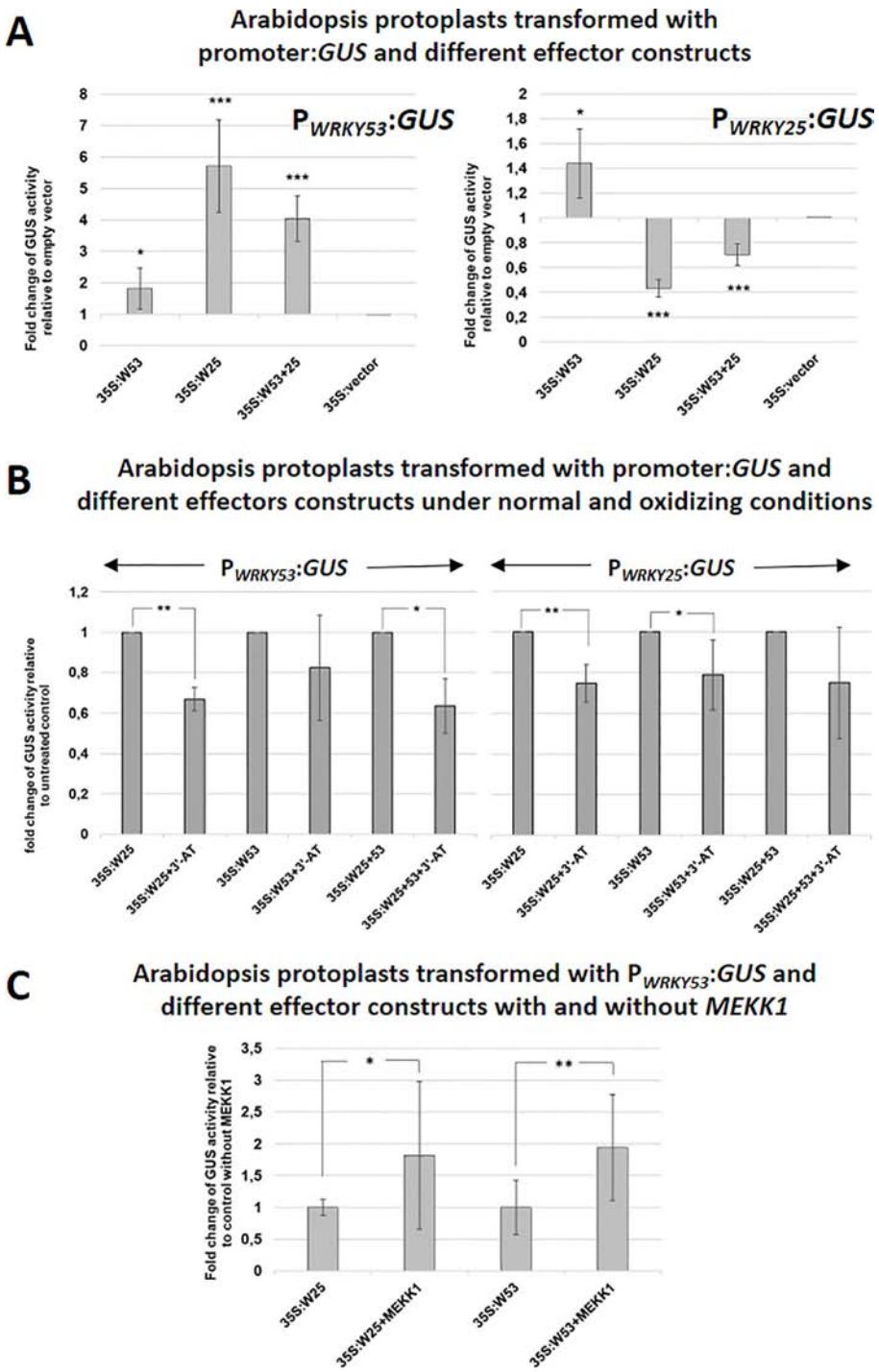

FIGURE 3 | WRKY25 positively regulates *WRKY53* under non-oxidizing conditions. **(A)** Arabidopsis protoplasts were transiently transformed with 5 µg of effector-, 5 µg of reporter-plasmid DNA and 0.1 µg of a luciferase construct for normalization. A 2.8-kbp-fragment of the *WRKY53* promoter and a 3.0-kbp-sequence of the *WRKY25* promoter fused to the *GUS* gene were used as reporter constructs. 35S:*WRKY25* and 35S:*WRKY53* constructs were used as effector plasmids. GUS activity was measured on the next day. The values are presented relative to the empty vector control (mean values ± SD, n = 6 independent transfromations). One sample t-test was performed, (*$P \leq 0.05$, **$P \leq 0.01$, ***$P \leq 0.001$) **(B)** GUS assays were performed with protoplasts, which were simultaneously incubated overnight with 10 mM 3'-AT to inhibit catalase activities leading to higher H_2O_2 level. The values are presented relative to the untreated control transformations (mean values ± SD, n = 3–7 independent transformations). One sample t-test was performed, (*$P \leq 0.05$, **$P \leq 0.01$). **(C)** Co-transformation assays with 35S:*MEKK1* were performed. The values are presented relative to transformation without MEKK1 (mean values ± SD, n = 4–5 independent transformations). Kruskal–Wallis-test was performed, (*$P \leq 0.05$, **$P \leq 0.01$).

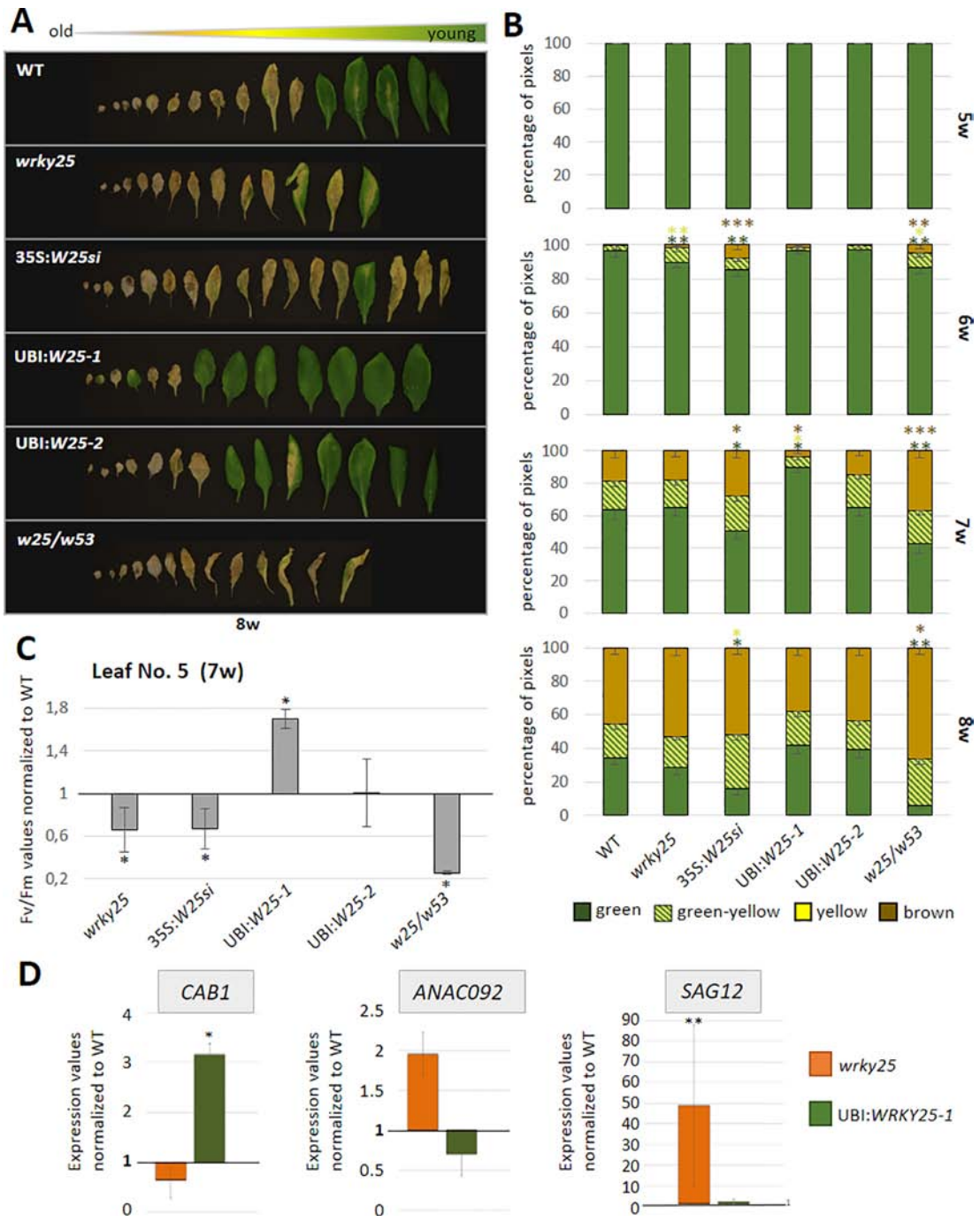

FIGURE 4 | Senescence phenotypes of *WRKY25* transgenic and mutant lines. **(A)** Col-0 wildtype (WT), *wrky25* mutant (*wrky25*), *WRKY25* overexpressing (UBI:*W25-1* and UBI:*W25-2*), *WRKY25* silenced (35S:*W25si*) and *wrky25-wrky53* double-knock-out (*w25/w53*) plants were analyzed over development. A photograph of rosette leaves of 8-week-old plants sorted according to their age is shown. **(B)** Quantitative evaluation of leaf senescence by categorizing individual leaves of at least six plants into four groups according to their color: green, green leaves starting to get yellow (green-yellow), completely yellow leaves (yellow) and dead and/or brown leaves (brown/dry). The percentage of each group with respect to total leaf numbers are presented (mean values ± SE, n = 6). **(C)** Fv/Fm values were measured with PAM for leaves of position 5 of 7-week-old plants (mean values ± SE, n = 6). One sample t-test was performed for statistical differences of all values compared to Col-0 (*$P \leq 0.05$) **(D)** Expression of the senescence associated marker genes *ANAC092*, *CAB1, SAG12* were analyzed by qRT-PCR and normalized to the expression of the *ACTIN2* gene. *SAG12* in 6-week and *ANAC092* and *CAB1* in 7-week-old plants. Shown are *wrky25* and UBI:*W25-1* plants normalized to Col-0 (mean values ± SE, n = 3). Kruskal–Wallis-test was performed for statistically significant differences (*$P \leq 0.05$, **$P \leq 0.01$, ***$P \leq 0.001$).

PROTEIN 1 (*CAB1*) being downregulated, the NAC transcription factor *ANAC092*, and *SENESCENCE-ASSOCIATED GENE 12* (*SAG12)* being upregulated were analyzed by qRT-PCR (**Figure 4D**). In comparison to Col-0 wildtype plants, *WRKY25* overexpressing plants showed significantly delayed visible senescence symptoms, which was in consistence with a delay in the decrease of the Fv/Fm ratio measured in leaf No. 5 and leaf No. 10 (**Figure 4C**, **Figure S7**). Furthermore, a higher expression of *CAB1* in 7-week-old plants as well as a lower expression of *ANAC092* and *SAG12* in 6-week-old plants of *WRKY25* overexpressing line compared to wildtype confirmed a delayed senescence phenotype. In contrast, senescence and loss of photosynthetic activity was accelerated in the *wrky25* mutant plants and the 35S:*WRKY25si* line (**Figures 4A–C**). Higher up-regulation of *ANAC092* and *SAG12* expression in 6-week-old plants and lower *CAB1* expression in 7-week-old plants in *wrky25* mutant line clearly indicate an accelerated senescence phenotype (**Figure 4D**). Remarkably, the expression of *WRKY53* was lower in the *WRKY25* overexpressing as well as in the *wrky25* mutant lines in comparison to WT (**Figure 5**), suggesting a more complex regulation of WRKY53 expression during development. Moreover, the expression of two tested WRKY genes (*WRKY18* and *WRKY40*) was antagonistic in *WRKY25* overexpressing and mutant plants, but only at week 5; at later stages also these two WRKY genes were down-regulated in both lines. We have chosen WRKY40 as it is also expressed in senescent leaf tissue. WRKY40 was also shown to regulate *WRKY53* expression in a negative way, but to a lesser extent. Moreover, it is the closest relative of WRKY18 also belonging to group IIa so that we can see whether regulatory processes are group specific which appears to be the case. This clearly indicates that no simple regulatory circuits are in place between these WRKY proteins and genes. WRKY25 as well as WRKY53 and WRKY18 appear to be part of a WRKY subnetwork, which is embedded in the overall complex senescence regulatory network. Interfering on the expression of one WRKY gene can lead to an imbalance in the subnetwork, which might explain that mutant and overexpressing plants showed the same effects on the expression of specific WRKYs. Taken together, WRKY25 appears to be part of the WRKY subnetwork and a redox-sensitive negative regulator of senescence.

WRKY25 Mediates Tolerance Against Oxidative Stress

As WRKY25 action appears to be redox-sensitive, we wanted to analyze whether WRKY25 is also involved in the response to oxidative stress or plays a role in the signaling of H_2O_2 *in planta*. Therefore, we germinated seeds of WT, *wrky25* mutant, *wrky53* mutant, 35S:*WRKY25si*, the *WRKY25* overexpressing lines as well as the double mutant *wrky25/wrky53* on plates containing 10 mM H_2O_2 (**Figure 6A**). After 7 to 10 days, the percentages of green seedlings per total seedling numbers were counted. The experiment was repeated six times and the outcome of these series were summarized in a heat map showing the tolerance against H_2O_2 (**Figure 6B**). The germination rate on the control plates without H_2O_2 was almost 100% for all plant lines used. The 35S:*WRKY25si* and the *WRKY25* overexpressing lines *(*UBI:*W25-1* and UBI:*W25-2*) germinated much better on H_2O_2 plates in comparison to WT as well as the *wrky53* single mutant. In contrast, the *wrky25* as well as the *wrky25/wrky53* mutant seeds germinated significantly worse compared to WT. Therefore, WRKY25 seems to mediate a higher tolerance against H_2O_2. Even though gene silencing was clearly shown from the late seedling stage until the end of leaf development (**Figure S5**), the *wrky25* mutant and the 35S:*WRKY25si* knock-down line behave different in this experiment. This behavior can only be explained by the assumption that during very early stages of germination, the 35S:*WRKY25* line overexpressed the transgene but gene silencing was not yet established at this very early time points. This could indeed be confirmed by expression analyses of *WRKY25* in the 35S:*WRKY25si* line using qRT-PCR in very early germination states (4 and 7 day old seedlings, **Figure S5A**).

In order to test whether this tolerance is due to higher antioxidative capacities in these lines, we measured intracellular H_2O_2 contents of leaf No. 8 in 8-week-old plants of these lines (**Figure 6C**). Less intracellular H_2O_2 was measured in the overexpressing lines, while more H_2O_2 appears to be present in the mutants and the silenced line in comparison to WT (**Figure 6C**). Moreover, the H_2O_2 scavenging capacity of leaf discs of the different lines was tested by incubating these discs for 2 h in H_2O_2 solution and measure the remaining H_2O_2 using peroxide strips (**Figure 6D**). As expected, the antioxidative capacity of the *WRKY25* overexpressing lines was slightly higher, whereas scavenging in the mutant and silencing lines was lower. Taken together, WRKY25 does not only mediate a higher tolerance against oxidative stress but is also involved in the regulation of intracellular H_2O_2 levels, at least in later developmental stages. This might also contribute to the negative effect of WRKY25 on senescence since H_2O_2 acts as signaling molecule to induce senescence and, most likely, also participates in membrane deterioration and lipid peroxidation processes in later stages (Chia et al., 1981). The conclusions on the role of WRKY25 in senescence-related redox signal transduction is further supported by a dark-induced senescence experiment including *wrky25*, *catalase2* (*cat2*) and *wrky25/cat2* double-knock-out plants (**Figure S8**). As expected, *cat2* and *wrky25* had lower H_2O_2 scavenging capacity than wildtype plants resulting in a higher H_2O_2 content in the mutant lines (**Figures S8B, C**). Remarkably, *wrky25/cat2* double mutants showed an additive effect indicating that higher H_2O_2 content in *wrky25* mutant plants is not due to lower catalase activity. This was also visualized by the CAT-activity staining of a native PAGE, in which CAT2 activity of wildtype and *wrky25* mutant plants appear to be very similar (**Figure S8A**). Moreover, dark-induced senescence was more pronounced in *wrky25* or *cat2* mutant compared to wildtype leaves and was enhanced in the *wrky25/cat2* double mutant, correlating with their intracellular H_2O_2 contents (**Figures S8B, D**).

WRKY25 Enhances *WRKY53* Response to Oxidizing Conditions

Because *WRKY53* is strongly up-regulated after treatment with H_2O_2 in Arabidopsis (Miao et al., 2004; Xie et al., 2014), WRKY25 DNA-binding is redox-sensitive (**Figure 2A**) and its positive effect on *WRKY53* expression is diminished under

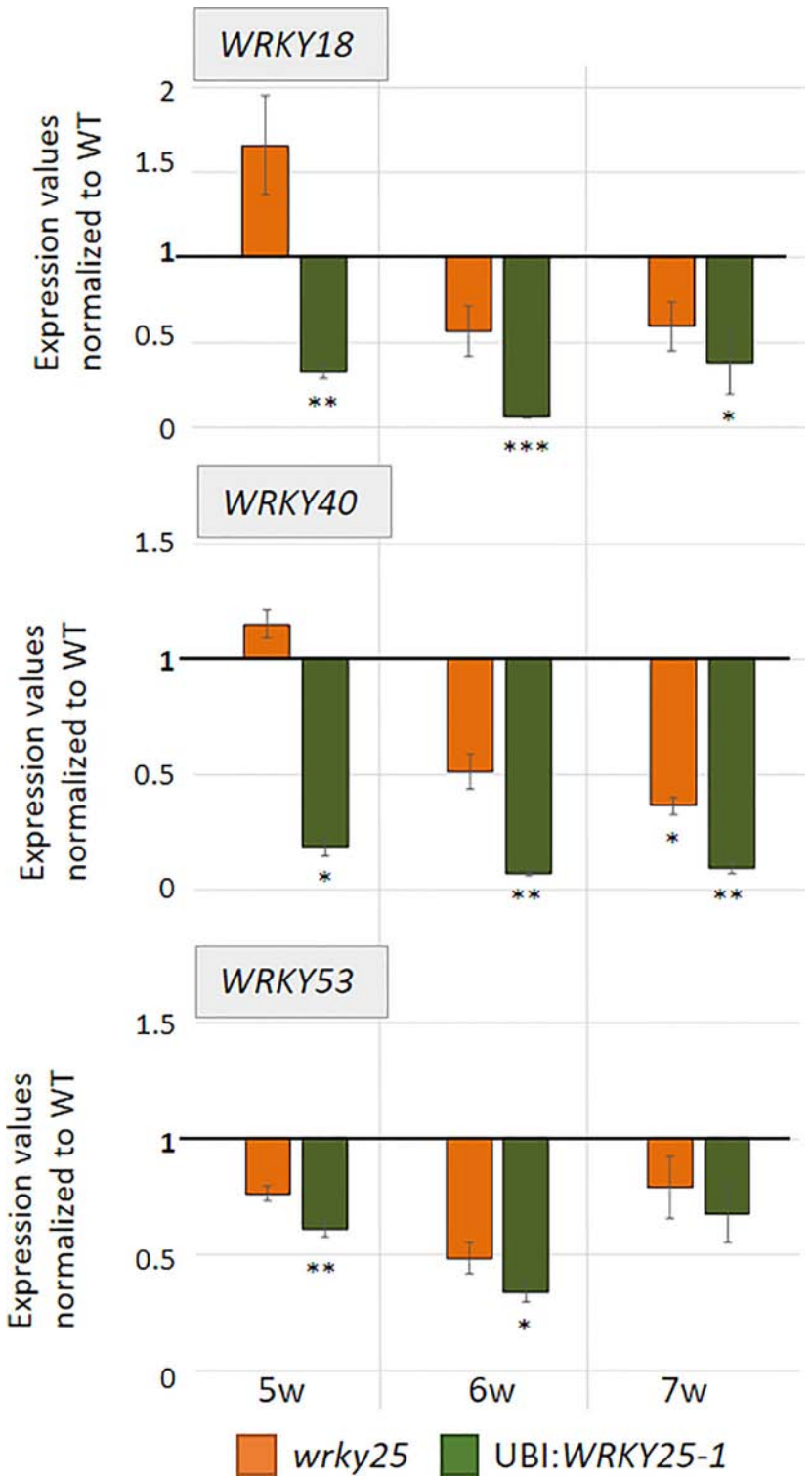

FIGURE 5 | WRKY genes expression analyses. Expression of different WRKY genes (*WRKY53*, *WRKY18*, *WRKY40*) were analyzed in Col-0 (WT), *wrky25* mutant and *WRKY25* overexpression line (UBI : *WRKY25-1)* by qRT-PCR and normalized to the expression of the *ACTIN2* gene. Three pools were analyzed; one pool consists of leaf No. 6 and 7 of two different plants. In week 7, only two pools of the *35S:W25si* plant line and of the *wrky25* line were analyzed but here with six technical replicates. Expression values were normalized to Col-0 and Col-0 was set to 1 (mean values, n = 3, ± SE). Kruskal–Wallis-test was performed for statistically significant differences of all value compared to Col-0 (*$P \leq 0.05$, **$P \leq 0.01$, ***$P \leq 0.001$).

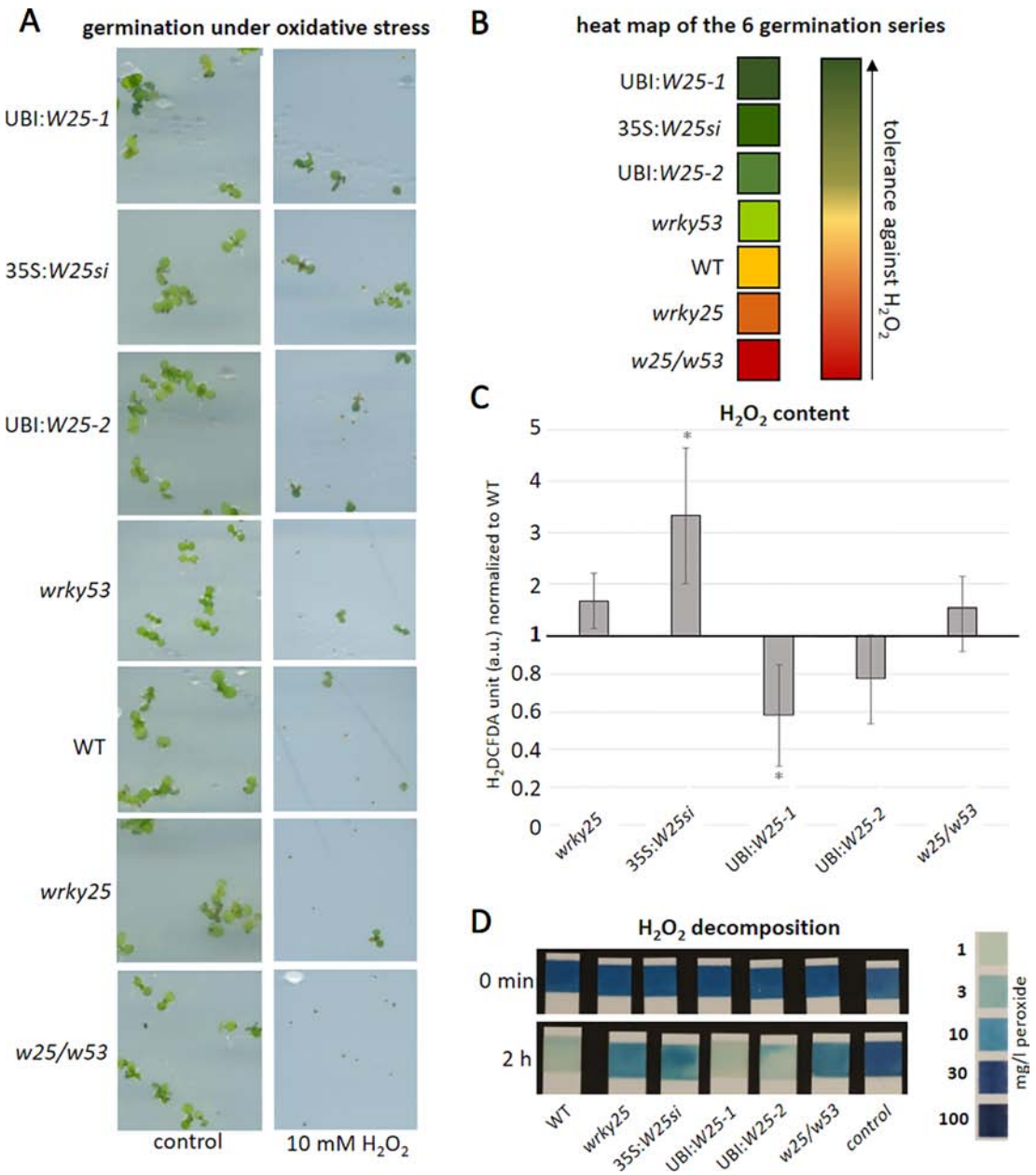

FIGURE 6 | WRKY25 mediates H_2O_2 tolerance. **(A–B)** Col-0 (WT), *wrky25* mutant, *wrky53* mutant, *WRKY25* overexpressing (*UBI:W25-1; UBI:W25-2*) and *WRKY25* silenced (*35S:W25si*) as well as the double-knock-out plants (*w25/w53*) were sown on ½ MS plates with and without 10 mM H_2O_2. A minimum of 30 seeds were put onto the plates and the experiment repeated 6 times (n = 6) **(A)** shows a representative sector of the plates with and without H_2O_2 in media. **(B)** summarizes the six independent experiments in a heat map. Dark green means the most tolerant against H_2O_2, dark red the most sensitive towards H_2O_2. **(C)** H_2O_2 content was measured over plant development using H_2DCFDA fluorescence; leaves No. 8 of 8-week-old plants are shown. Fluorescence is indicated in arbitrary units (a.u.), normalized to leaf weight and expressed relative to WT (± SE, n = 4). One Sample t-test was performed for statistical differences of all values compared to WT (*$P \leq 0.1$) **(D)** Leaf discs of leaf No. 5 of 6-week-old plants were incubated in a 30 mg/l H_2O_2 solution. As control H_2O_2 solution without leaf discs was measured. At timepoint 0 min and 2 h the decomposition of H_2O_2 was determined using commercially available peroxide sticks, color scale for H_2O_2 content is provided on the right.

oxidizing conditions (**Figure 3B**), we wanted to find out, whether WRKY25 is required for the induction of *WRKY53* expression after H_2O_2 treatment. Therefore, leaves of *wrky25* and *wrky53* single as well as double mutants and WT plants were detached and incubated in 10 mM H_2O_2. The expression of *WRKY53* and several other H_2O_2-responsive genes (*WRKY25*, *ANAC092, WRKY18* and *ZAT12*) was determined after 0 min, 30 min, 1 h and 3 h using qRT-PCR (**Figure 7**). All tested genes were responsive to H_2O_2 in wildtype. *WRKY53* expression increased most prominently in 7-week-old plants after 1 h of H_2O_2

treatment. This response is clearly dampened in *wrky25* mutant leaves. In contrast, the *WRKY25* mRNA level highly increased in leaves of young 5-week-old wildtype plants 1 h after H_2O_2 treatment and responsiveness becomes lower with age. Again, this response is diminished in *wrky53* mutant leaves in all tested developmental stages indicating that WRKY25 is involved in H_2O_2 response of *WRKY53* and *vice versa*. *ANAC092* responded most prominent also in 7-week-old leaves, similar to *WRKY53*. This response is also suppressed in the *wrky25* and in the *wrky53* leaves, and even more in the double mutant suggesting that both factors are involved in the H_2O_2 responsiveness of *ANAC092*. The same held true for *ZAT12* expression, here a higher basal expression could be observed in 7-week-old leaves of *wrky53* so that the H_2O_2 treatment did not lead to a further induction. In contrast, induction of *WRKY18* expression by H_2O_2 was much more pronounced in 5-week-old *wrky25*, *wrky53* and the double mutant compared to wildtype leaves, whereas the response was attenuated in older stages in all mutant lines. This supports the idea of a variable function of WRKY53 and WRKY25 on the *WRKY18* promoter: in early developmental stages, they act as repressors, in later stages as activators. Taken together, WRKY25 as well as WRKY53 are involved in H_2O_2 induction of variable genes including each other and, depending on the developmental stage of the plants; they can have opposing effects on the same gene promoters, again indicating a very complex regulatory interaction.

DISCUSSION

ROS, especially hydrogen peroxide, act as signaling molecules during senescence and/or stress responses. However, how this signal is perceived and transmitted into senescence onset and progression or stress response activation is still far from being understood. One of the central features of senescence is a massive change in the transcriptome, in which photosynthesis related genes are shut down and genes related to degradation and remobilization processes are turned on. Therefore, transcription factors would be ideal candidates to take up ROS signals directly. Indeed, for some transcription factors of different families such as class I TCP factors (Viola et al., 2013), HSF8 (Giesgut et al., 2015) or the bZIP factor GBF1 (Shaikhali et al., 2012), a redox-sensitive action has already been disclosed. Moreover, the plant specific protein GIP1 enhances DNA-binding activity of GBF3 and reduces DNA-binding activity of other members of the G-group bZIP factors in Arabidopsis, namely bZIP16, bZIP68, and GBF1, under non-reducing conditions through direct physical interaction. Whereas reduced GIP1 predominantly exists in a monomeric form and is involved in formation of DNA–protein complexes of G-group bZIPs, oxidized GIP1 is released from these complexes and instead performs chaperone function (Shaikhali, 2015). Due to space limitation, not all examples can be mentioned here, but taken together redox conditions can influence gene expression through the action of transcription factors in several ways: changing DNA-binding activity or activation potential or intracellular localization or interaction with specific partners or proteolytic degradation or a combination of those. He et al. (2018) just recently reviewed this topic very nicely. Here, we could show that WRKY25 DNA-binding activity is redox-sensitive, and that these redox-sensitive changes in activity are reversible as a function of the redox conditions (**Figure 2**). Not all WRKY factors show these features, as e.g. WRKY18 DNA-binding activity appears not to be redox-sensitive at all and WRKY53 DNA-binding activity was only very slightly influenced by changes in the redox environment (**Figure S2**). Redox sensitivity often relies on the alteration of the redox state of certain Cys residues. In WRKY25 belonging to the group I WRKY factors, two DNA-binding domains including $CX_{4-5}CX_{22-23}HXH$ zinc fingers are present. Moreover, an additional Cys can be found very closely to the N terminus, which cannot be detected in WRKY53 or WRKY18 proteins and could therefore be involved in redox sensitivity. Whereas WRKY53 has no other Cys besides the Cys of the zinc finger, WRKY18 has three additional Cys residues but is not redox sensitive at all (**Figure S9**). Hence, we speculate that either the two zinc fingers are necessary to confer redox sensitivity or an additional Cys has to be at a certain position within the protein to contribute to redox sensitivity. However, this will be subject of further investigations. Currently, we are mutating the additional Cys in WRKY25 to see whether this residue is involved or responsible for the redox sensitivity of WRKY25. Moreover, we will include an additional Cys at the N terminus of WRKY18 to see whether we can render WRKY18 redox sensitive. In contrast to WRKY18, which strongly binds to all W-boxes of the *WRKY53* promoter (Potschin et al., 2014), WRKY25 binds selectively to a specific W-box in the promoter of *WRKY53* and can positively influence its expression (**Figures 1** and **3**). Under oxidizing conditions, activation of *WRKY53* expression by WRKY25 is dampened (**Figure 3**). Even though binding and transactivation is lower under oxidizing conditions, WRKY25 is still involved in the response of the WRKY53 promoter to oxidizing conditions *in planta*, as H_2O_2 response of *WRKY53* was much lower in the *wrky25* mutants compared to WT plants, especially in later stages (**Figure 7**). At the first glance, this appears to be a contradiction, but as WRKY25 is also involved in down-regulation of H_2O_2 contents and negatively regulates its own expression, two negative feedback loops are at work. This indicates that WRKY25 function might be to prevent an overshooting of the reaction to H_2O_2. In addition, not only *WRKY53* response to oxidative stress appears to be attenuated by WRKY25 but also *ZAT12* and *ANAC092* response. In contrast, *WRKY18* reaction appears to be enhanced, but only in young plants (**Figure 7**). As already mentioned before, *WRKY25* expression is induced by H_2O_2, whereas WRKY25 at the same time reduces intracellular H_2O_2 contents, especially in later stages of senescence, as lower or higher H_2O_2 levels were measured in *WRKY25* overexpressing plants and *wrky25* mutant or knock-down lines, respectively (**Figures 6** and **7**). High H_2O_2 contents in later stages of senescence are most likely involved in membrane deterioration and lipid peroxidation processes as part of the senescence degradation processes

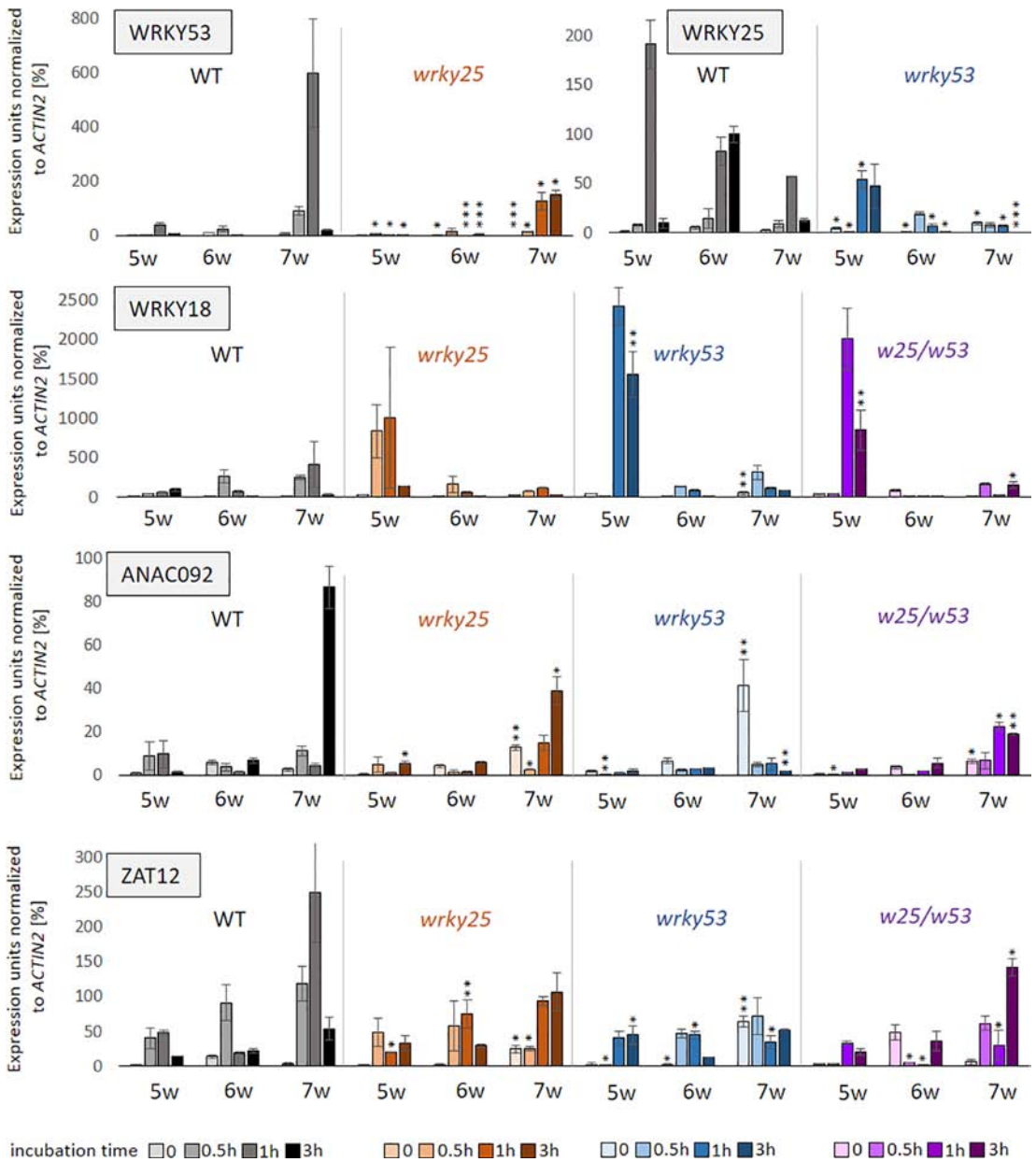

FIGURE 7 | Influence of oxidizing conditions on gene expression. Leaves of position 10 were harvested of six plants of Col-0 (WT), *wrky25* (orange) and *wrky53* (blue) single and double (purple) mutant plants, respectively. Leaves of 5, 6 and 7 week-old-plants were incubated in 10 mM H_2O_2 for 0–3 h. After incubation, three leaves were pooled and expression of *WRKY18*, *WRKY25*, *WRKY53*, *ZAT12* and *ANAC092* was determined by qRT-PCR in these two pools. Expression values normalized to *ACTIN2* expression are presented (mean values ± SD, n = 2, one biological replicate consists already of a pool of three plants for each timepoint). Kruskal–Wallis-test was performed for statistically significant differences of all values at each timepoint compared to Col-0 (*$P \leq 0.05$, **$P \leq 0.01$, ***$P \leq 0.001$).

(Chia et al., 1981). This is in line with the senescence acceleration or delay of the *WRKY25* overexpressing plants and *wrky25* mutant or knock-down lines, respectively (**Figure 4**, **Figure S8**).

A simple gene for gene relationship between *WRKY25* and *WRKY53* would suggest opposite phenotypes. As *WRKY53* has been characterized as positive regulator of leaf senescence (Miao et al., 2004), overexpression of *WRKY25* should lead to increased *WRKY53* levels and to the same senescence phenotype as *WRKY53* overexpression. *Vice versa*, knock-down or mutation of *WRKY25* should exhibit the same phenotype as knock-down or mutation of *WRKY53*. However, the senescence phenotype of *WRKY25* overexpressing plants and *wrky25* mutant or knock-down lines was found to be exactly opposite to the expected phenotype of a positive *WRKY53* regulator. This can be explained by the fact that WRKY25 and WRKY53 are not acting in a simple signal transduction pathway but in a

complex regulatory network between many members of the WRKY transcription factor family showing multilayer feedback regulations. In the same line of evidence, WRKY18 was characterized to be a negative up-stream regulator as well as a down-stream target and a protein interaction partner of WRKY53 (Potschin et al., 2014). Here, we could show that WRKY25 is also a redox sensitive up-stream regulator and down-stream target gene of WRKY53 (**Figures 3** and **7**). Moreover, WRKY25 appears to be involved in the H_2O_2 response of WRKY18 and WRKY53 expression but in opposite directions and at different times (**Figure 7**). In addition, MEKK1 action brings in a further layer of complexity. Co-expression of MEKK1 led to a reversal of WRKY18 action on *WRKY53* expression, since a 35S:*MEKK1* construct as co-effector to 35S:*WRKY18* reversed the repressor function of WRKY18 on the *WRKY53* promoter to an activator (**Figure S4A**). In contrast, the activator function of WRKY25 on the expression of the *WRKY53* promoter is enhanced approx. 2-fold by the addition of 35S:*MEKK1* as co-effector construct (**Figure 3C**). Whether this is due to a direct phosphorylation of WRKY25 by MEKK1, taking the same short cut as already shown for WRKY53 (Miao et al., 2007), or through classical MAPK signal transduction will be subject of further investigations. Noteworthy, WRKY25 and WRKY33 interact with many VQ proteins (Cheng et al., 2012), one of which is MKS1 (MAP KINASE SUBSTRATE 1), a substrate of MAPK4 (Andreasson et al., 2005). For WRKY33 it was shown that it exists in nuclear complexes with MPK4 and MKS1. Upon activation of MPK4 *via* MEKK1 and MKK1/2 signaling, MKS1 is phosphorylated by MPK4 and WRKY33 is released from MPK4 interaction and activates its downstream genes such as *PAD3* encoding an enzyme required for antimicrobial camalexin production (Qiu et al., 2008). Moreover, WRKY25 negatively regulates SA-mediated defense responses against *Pseudomonas syringae* (Zheng et al., 2007) and MPK4 is a repressor of SA-dependent defense responses (Petersen et al., 2000). Furthermore, MEKK1 kinase activity and protein stability is regulated by H_2O_2 in a proteasome-dependent manner and *mekk1* heterozygous mutants were compromised in ROS-induced MPK4 activation. Like WRKY25, MEKK1 regulates accumulation of intracellular H_2O_2 and alters expression of genes related to ROS signaling and homeostasis such as *ZAT12* (Nakagami et al., 2006). Like *WRKY25* and *WRKY53*, *MEKK1* expression is up-regulated by H_2O_2 treatment and mRNA levels start to increase with onset of senescence in parallel to *WRKY53* (Miao et al., 2007). Therefore, the influence of MEKK1 on the transactivation activity of WRKY25 provides another link to redox signaling. Moreover, we could show by conditional knock-down of *MEKK1* in plants that MEKK1 is part of the complex senescence regulation (**Figure S4**).

Expression of *WRKY25* is not only induced by oxidative stress but also during heat or salt stress. Moreover, *WRKY25* overexpressing plants were not only more tolerant to oxidative stress (**Figure 6**) but also to salt stress (Jiang and Deyholos, 2009) as well as to high temperatures (Li et al., 2011). During heat stress, WRKY25, WRKY26, and WRKY33 were positively cross-regulated, which confirms the complexity of the WRKY network (Li et al., 2011). Remarkably, ROS levels increase during salt and heat stress pointing to the possibility that *WRKY25* induction under salt and heat stress is mediated by oxidizing conditions. Many WRKY factors including WRKY25 and WRKY53 are up-regulated more than 5-fold in various plant lines with altered intracellular levels of specific ROS (Gadjev et al., 2006). In the same line of evidence, expression of *WRKY18*, *WRKY25* and *WRKY53* was also increased in *cat1,2,3* triple mutant plants (Su et al., 2018). Moreover, not only *WRKY25* gene expression and its DNA-binding activity are altered by higher ROS levels but WRKY25 is also involved in the regulation of the intracellular H_2O_2 content, especially in later stages of development (**Figure 6**) creating a feedback loop.

A further level of complexity is installed by epigenetic control of the WRKY gene expression. JMJ27, a jumonji-family demethylases, removes repressive H3K9me2 and H3K9me1 marks and thereby activates transcription. ChIP analysis revealed that the chromatin at the *WRKY25* promoter was hyper-methylated in *jmj27* mutants indicating that JMJ27 regulates *WRKY25* expression at least in part by directly controlling methylation levels of H3K9 histones (Dutta et al., 2017). *WRKY53* expression is also regulated by epigenetic changes in histone methylation (Ay et al., 2009). Moreover, the WRKY53 protein was detected in a complex with histone deacetylase 9 (HDA9) and POWERDRESS to recruit this complex to W-box containing promoter regions of key negative senescence regulators to remove H3 acetylation marks (Chen et al., 2016). Therefore, WRKY53 expression is regulated by epigenetic changes on its own promoter but the WRKY53 protein is also involved in changing epigenetic marks on other promoters.

We have summarized our data in a model, which describes a small subnetwork between WRKY18, WRKY25 and WRK53 and the role of H_2O_2 in this subnetwork at the onset of senescence (**Figure 8**). Several feedback loops are installed to control an overshooting of the system and to supply a high plasticity, which is needed to constantly integrate all kinds of incoming intracellular and environmental signals. The complex interactions within this subnetwork of just three WRKY factors illustrates the high complexity of the whole WRKY network, which is not only regulated by H_2O_2 as signaling molecule but also highly controlled by salicylic and jasmonic acid. Moreover, the WRKY network is just a subsection of the higher order regulatory network of leaf senescence. Nevertheless, understanding the regulation of single components or subnetworks will in the long run help to decipher the different mechanisms acting in the whole network and contribute to modeling approaches.

MATERIALS AND METHODS

Protein Expression and Extraction for DPI-ELISA

For protein expression of WRKY25 and WRKY53 in the *E. coli* strain BL21-SI, the coding sequences of *WRKY25* (1,182 bp) and

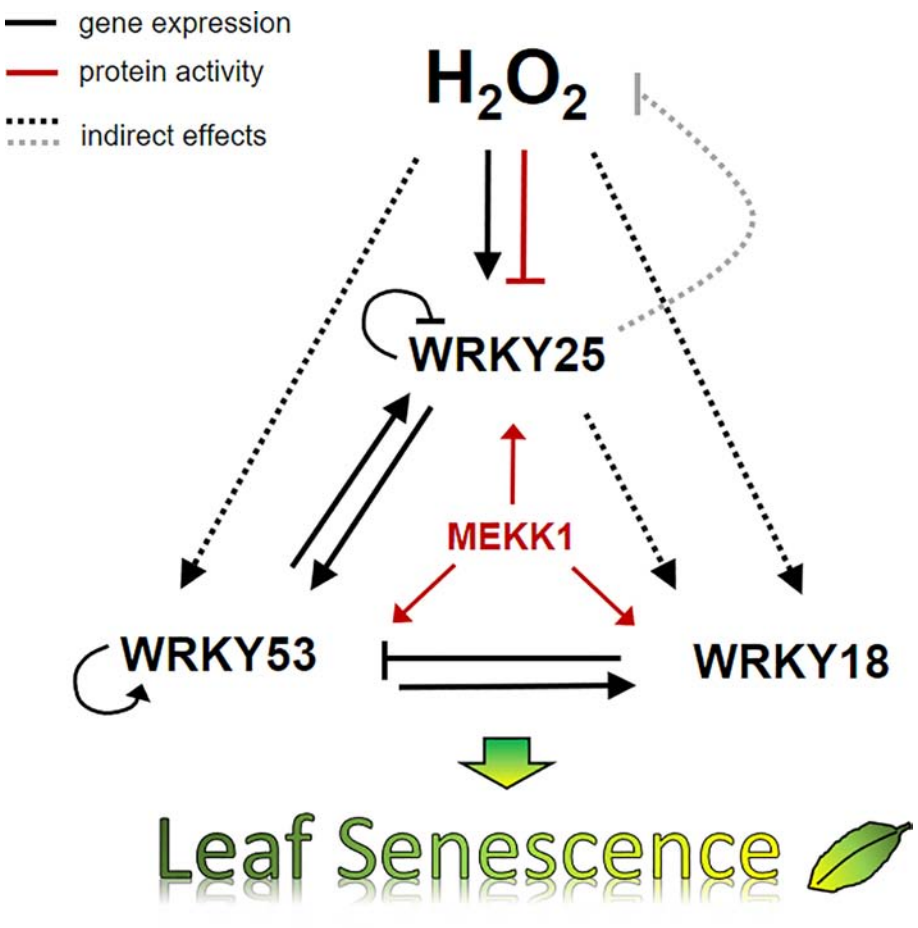

FIGURE 8 | Model of H_2O_2 and the WRKY18-53-25 subnetwork. A model summarizing the impact of H_2O_2 and WRKY25 on senescence in 7 week-old plants is presented. Solid lines show direct interactions whereas dotted lines show interaction, which may be direct or indirect. Black arrows describe the effects on gene expression, red arrows effects on protein activity, and the grey line effects on the intracellular hydrogen peroxide level. The expression of all three WRKY genes of the small WRKY53-25-18 subnetwork are controlled by hydrogen peroxide contents and hydrogen peroxide has a direct negative effect on the binding activity of WRKY25 to DNA. All three genes are under feedback control of their own gene products. In addition, MEKK1 increases the activity of all three WRKY factors. Moreover, WRKY25 can form heterodimers with WRKY53 and the heterodimer has a lower transactivation activity compared to the WRKY25 homodimer. This interplay determines in the end whether leaf senescence is accelerated or delayed.

WRKY53 (975 bp) were cloned into the vector pETG-10A to be coupled with an N-terminal fused 6×His-tag. The *E. coli* cells were grown in 10 ml selective medium overnight. One hundred milliliter LB-medium were inoculated with 3 ml of this pre-culture and, after shaking for 1.5 h at 37°C, a final concentration of 1 mM IPTG was added for induction of protein expression. After 1 h of shaking at 18°C, cells were harvested (2,500 g, 20 min, 4°C) and suspended in protein extraction buffer (4 mM Hepes pH 7.5, 100 mM KCl, 8% (v/v) glycerol, 1× complete proteinase inhibitor (*Roche*) without EDTA). Proteins were extracted by sonication to keep native conditions. The protein concentrations of the crude extracts were detected by Bradford assays (Bradford, 1976; *Bio-Rad*).

DPI-ELISA

The ELISA-based DNA–protein interaction assay was performed as described by Potschin et al. (2014). In brief, the 5' biotinylated double-stranded oligonucleotides were added to streptavidin-coated ELISA plates (*Thermo Scientific*). After blocking the plate with blocking solution *(Roche, blocking reagent for ELISA)*, crude extracts were diluted with protein dilution buffer (4 mM Hepes pH 7.5, 100 mM KCl, 8% (v/v) glycerol) and increasing protein concentrations (5, 10, 25 µg) were added to the DNA bound to the plates. The plates were incubated 1 h with mild shaking so that the biotinylated DNA–protein complexes were formed. Subsequently, wells were washed at least twice (*Qiagen blocking buffer*, *Anti-His-HRP conjugate kit*) and incubated for another hour with Anti His-HRP conjugate antibodies (*Qiagen*) diluted 1:1,500. After washing several times, positive interactions were detected by a peroxidase reaction with ortho-phenylenediamine (OPD-tablets, *Thermo Scientific*). The yellow color was measured using a plate-reader (*TECAN*, Safire XFluor4). For Redox-DPI-ELISAs, 25 µg of the protein crude extracts were used. Reduction or oxidation of the protein extracts was performed by adding

either DTT or H_2O_2 (final concentration 5 mM). In order to show reversibility of the redox effects, a fraction of the DTT-reduced proteins was oxidized again by addition of increasing amounts of H_2O_2 (final concentration 5, 10 and 20 mM). Similarly, the oxidized proteins were reduced again by adding increasing amounts of DTT. After these redox-treatments, a DPI-ELISA was performed as described above. To conserve the redox-state of the proteins bound to the biotinylated DNA, the same DTT or H_2O_2 concentrations were added to the washing buffer and the antibody solution. The antibody reaction was not altered by these treatments.

Protoplast Preparation and Transformation

Protoplasts derived from a cell culture of *A. thaliana* var. Columbia 0 were prepared following a standard protocol (for details see http://www.zmbp.uni-tuebingen.de/c-facilit/plant-transformation.html). These protoplasts were then treated with PEG1500 and transiently transformed with different constructs following the protocol published in Mehlhorn et al. (2018). Effector and reporter constructs were co-transfected with a luciferase construct for GUS reporter assays (for details see *GUS Reporter Assay*).

GUS Reporter Assay

Arabidopsis protoplasts were transformed using 5 µg of effector and 5 µg of reporter plasmid DNA. As an internal transformation control, a luciferase construct (pBT8-35SLUCm3) was co-transfected. After incubation overnight in the dark, GUS activity assays were performed with the protoplast as described by Jefferson et al. (1987). To correct for transformation efficiency, GUS activity was normalized to luciferase fluorescence. As effector constructs, the coding sequences of *WRKY25* (1182 bp), *WRKY53* (975 bp) and *MEKK1* (1827 bp) cloned into the vector pJAN33 were used. As reporter construct, a 3,000-bp-fragment upstream of the *WRKY25* start codon and a 2,759-bp-sequence upstream of the start codon of *WRKY53* was cloned into the binary vector pBGWFS7.0. The 3'-AT (3-Amino-1,2,4-triazole) GUS assays were performed as described above except that 10 mM 3'-AT or the same volume of water was added before overnight incubation.

Plant Material and Cultivation

All experiments were performed with *A. thaliana* Ecotype Columbia 0 (Col-0). Plants were grown on standard soil under long day conditions (16 h of light) with only moderate light intensity (60–100 µmol s^{-1} m^{-2}) in a climatic chamber at 20°C (day) and 18°C (night). Bolts and flowers developed within approx. 4–5 weeks. Individual leaf positions within the rosettes were coded with different colored threads, so that individual leaves could be analyzed according to their age even at very late stages of development (Hinderhofer and Zentgraf, 2001; Bresson et al., 2018). Numbering started with No. 1 for the first true leaf without taking the cotelydones into account. Plant material was harvested always at the same time to avoid circadian effects. The Nottingham Arabidopsis Stock Centre (NASC) kindly provided the T-DNA insertion line of *WRKY25* (SAIL_529_B11; previously characterized in Jiang and Deyholos, 2009), of *WRKY53* (SALK_034157, previously characterized in Miao et al., 2004), and *CAT2* (SALK_057998, previously described in Queval et al., 2007). Using PCR, homozygous plants were characterized with different combinations of gene specific and T-DNA left border primers. Double-knock-out mutants (*wrky25/wrky53*) were generated by crossing *wrky25* and *wrky53* mutants. F2 progenies were selected for homozygous double-knock-out plants by PCR. Dr. Changle Ma, Shangdong Normal University, China (Su et al., 2018), kindly provided seeds of the homozygous *wrky25/cat2* double-knock-out plants. The *WRKY25* overexpressing plants were transformed by floral dip of Col-0 wildtype plants into *Agrobacterium tumefaciens* cultures in two different attempts. First, a 35S:*WRKY25* construct was transformed leading to plants in which the transgene induced gene silencing (plant line 35S:*W25si*; pB7RWG2) and, therefore, was used as a *knock-down* line. Second, a *UBQ10:WRKY25* construct was transformed (plant line UBI:*W25-1* and UBI:*W25-2*; pUBN-GFP-Dest) and overexpression was confirmed by qRT-PCR. For the germination experiments, seeds of different plant lines were sterilized by sodium hypochlorite and plated on ½ MS-plates (1 L: 2.15 g MS micro and macro elements (Duchefa), 15 g sucrose, pH 5.7–5.8, 8 g agar).

Senescence Phenotyping

For the evaluation of leaf senescence phenotypes, rosette leaves were aligned according to the age of the leaves with the help of a color code and a variety of parameters indicating the state of senescence were measured (Bresson et al., 2018). Leaves of six plants per timepoint were analyzed. At position 5 and 10, Fv/Fm values were determined using the Imaging-Pulse-Amplitude-Modulation (PAM) method, indicating the activity of the photosystem II (PSII) (Chlorophyll fluorometer Maxi version; ver. 2-46i, Walz GmbH, Effeltrich, Germany). Leaves were photographed according to their age and by an automated colorimetric assay (ACA) pixelwise grouped into four categories: green leaves (green), leaves starting to get yellow (green-yellow), completely yellow leaves (yellow) and brown and/or dead leaves (brown/dead). (ACA; Bresson et al., 2018; http://www.zmbp.uni-tuebingen.de/gen-genetics/research-groups/zentgraf/resources.html)

In addition, RNA was extracted from leaves No. 6 and 7 and qRT-PCR analyses were performed for the senescence-associated marker genes *ANAC092* (At5g39610) encoding a NAC-domain transcription factor, *CAB1* (At1g29930) encoding a subunit of light-harvesting complex II, *SAG12* (At5g45890) encoding a cysteine protease and different WRKY genes (*WRKY53* (At4g23810), *WRKY18* (At4g31800), *WRKY40* (At1g80840)). Expression was normalized to *ACTIN2* (At3g18780).

Quantitative RT-PCR

Total RNA was extracted with the RNeasy Plant Mini Kit (*Qiagen*). Subsequent cDNA synthesis was performed with RevertAid Reverse Transcriptase (*Thermo Scientific*. For the qRT-PCR, KAPA SYBR® Fast Biorad iCycler (*KAPA Biosystems*) master mix was used following the manufacturer´s protocol. Expression of analyzed genes was normalized to

ACTIN2. In order to keep the results comparable to former results, we only used *ACTIN2* as reference gene since *ACTIN2* has been proven to be very stably expressed all over leaf development (Panchuck et al., 2005). Relative quantification to *ACTIN2* was calculated with the ΔΔCT-method according to Pfaffl (2001). Primers and Atg numbers are indicated in **Table S1**.

H_2O_2 Measurement and Treatments

For oxidative stress treatment during germination, 10 mM H_2O_2 was added to the 1/2 MS agar (1 L: 2.15 g MS micro and macro elements (*Duchefa*), 15 g sucrose, pH 5.7–5.8, 8 g agar) and seeds were spread on plates with and without H_2O_2. After 3 days in darkness, the plates were incubated in light in the climate chambers and the number of green seedlings was counted after 7–10 days. This experiment was repeated six times, plates were photographed, green seedlings counted and summarized according to their tolerance against H_2O_2 in a heat map.

For intracellular H_2O_2 measurement, carboxy-H_2DCFDA (2',7'-Dichlordihydrofluorescein-diacetat) was chosen, which is able to passively diffuse across cellular membranes as non-polar dye. After deacetylation by an intracellular esterase, the molecule gets polar and is trapped inside the cells. The deacetylated carboxy-H_2DCFDA can then be oxidized by H_2O_2 and converted to the highly fluorescent di-chlorofluorescein (DCF). Therefore, only intracellular H_2O_2 is measured. Leaves of position 8 of 4- to 8-week-old plants were harvested and incubated for exactly 45 min in carboxy-H_2DCFDA working-solution (200 µg in 40 ml MS-Medium pH 5.7–5.8). Subsequently, the leaves were rinsed with water and frozen in liquid nitrogen. After homogenization in 500 µl 40 mM Tris pH 7.0, the samples were centrifuged at 4°C for 15 min. Fluorescence of the supernatant was measured in a *Berthold* TriStar LB941 plate reader (480 nm excitation, 525 nm emission).

For testing the response to H_2O_2 treatment, leaves of position 8 of 5, 6 and 7-week-old plants were incubated for 0, 30 min, 1 h and 3 h in 10 mM H_2O_2 including 0.1% Tween. After incubation time, leaves were washed in water and immediately frozen in liquid nitrogen. Gene expression was determined by qRT-PCR.

The decomposition of H_2O_2 was examined using commercially available peroxide strips (Dosatest peroxide test strips 100, VWR Chemicals). Therefore, leaf discs were excelled of leaves of position 5 of 6- and 7-week-old plants and were incubated into a 30 mg/l H_2O_2 solution. Strips were submerged for 1 s into the solution immediately after placing the leaf disc into the solution (timepoint 0 min) and again after 2 h. The amount of peroxide can be read out by the given control color scale. The weaker the blue color the less peroxide is present in the solution.

DATA AVAILABILITY STATEMENT

All datasets generated for this study are included in the article/ **Supplementary Material**.

AUTHOR CONTRIBUTIONS

Conceptualization was done by UZ, MM and JD. Methodology was developed by MM and JD. Experiments were performed by JD, MM, LR, SN and H-CL. Data and formal analysis was done by JD, JB and LR. The original draft was written by UZ. Reviewing and editing was done by JD, LR, MM and UZ. Funding acquisition: UZ. Supervision: UZ.

FUNDING

This work was financially supported by the Deutsche Forschungsgemeinschaft (DFG), Collaborative Research Centre 1101 (SFB1101, TP B06). The Alexander v. Humboldt Foundation supported JB.

ACKNOWLEDGMENTS

We are grateful for the excellent technical assistance of Gesine Seibold. We thank the NASC for supplying seeds of the *WRKY25* (SAIL_529_B11) and *WRKY53* (SALK_034157) T-DNA insertion lines and Dr. Ma, Shandong Normal University, China for seeds of the homozygous *wrky25/cat2* double mutant.

SUPPLEMENTARY MATERIAL

The Supplementary Material for this article can be found online at: https://www.frontiersin.org/articles/10.3389/fpls.2019.01734/full#supplementary-material

REFERENCES

Andreasson, E., Jenkins, T., Brodersen, P., Thorgrimsen, S., Petersen, N. H., Zhu, S., et al. (2005). The MAP kinase substrate MKS1 is a regulator of plant defense responses. *EMBO J.* 24, 2579–2589. doi: 10.1038/sj.emboj.7600737

Arrigo, A. P. (1999). Gene expression and the thiol redox state. *Free Radical Biol. Med.* 27, 936–944. doi: 10.1016/s0891-5849(99)00175-6

Ay, N., Irmler, K., Fischer, A., Uhlemann, R., Reuter, G., and Humbeck, K. (2009). Epigenetic programming *via* histone methylation at *WRKY53* controls leaf senescence in *Arabidopsis thaliana*. *Plant J.* 58 (2), 333–346. doi: 10.1111/j.1365-313X.2008.03782.x

Besseau, S., Li, J., and Palva, E. T. (2012). WRKY54 and WRKY70 co-operate as negative regulators of leaf senescence in Arabidopsis thaliana. *J. Exp. Bot.* 63 (7), 2667–2679. doi: 10.1093/jxb/err450

Bieker, S., Riester, L., Stahl, M., Franzaring, J., and Zentgraf, U. (2012). Senescence-specific alteration of hydrogen peroxide levels in *Arabidopsis thaliana* and oilseed rape spring variety *Brassica napus* L. cv. Mozart. *J. Integr. Plant Biol.* 54, 540–554. doi: 10.1111/j.1744-7909.2012.01147.x

Birkenbihl, R. P., Liu, S., and Somssich, I. E. (2017). Transcriptional events defining plant immune responses. *Curr. Opin. Plant Biol.* 38, 1–9. doi: 10.1016/j.pbi.2017.04.004

Bradford, M. M. (1976). A rapid and sensitive method for the quantitation of microgram quantities of protein utilizing the principle of protein-

dye binding. *Anal. Biochem.* 72, 248–254. doi: 10.1016/0003-2697(76)90527-3

Brand, L. H., Fischer, N. M., Harter, K., Kohlbacher, O., and Wanke, D. (2013). Elucidating the evolutionary conserved DNA-binding specificities of WRKY transcription factors by molecular dynamics and *in vitro* binding assays. *Nucleic Acids Res.* 41, 9764–9778. doi: 10.1093/nar/gkt732

Breeze, E., Harrison, E., McHattie, S., Hughes, L., Hickman, R., Hill, C., et al. (2011). High-resolution temporal profiling of transcripts during Arabidopsis leaf senescence reveals a distinct chronology of processes and regulation. *Plant Cell* 23, 873–894. doi: 10.1105/tpc.111.083345

Bresson, J., Bieker, S., Riester, L., Doll, J., and Zentgraf, U. (2018). A guideline for leaf senescence analyses: from quantification to physiological and molecular investigations. *J. Exp. Bot.* 69, 769–786. doi: 10.1093/jxb/erx246

Brusslan, J. A., Rus Alvarez-Canterbury, A. M., Nair, N. U., Rice, J. C., Hitchler, M. J., and Pellegrini, M. (2012). Genome-wide evaluation of histone methylation changes associated with leaf senescence in Arabidopsis. *PloS One* 7, e33151. doi: 10.1371/journal.pone.0033151

Chen, X., Lu, L., Mayer, K. S., Scalf, M., Qian, S., Lomax, A., et al. (2016). POWERDRESS interacts with HISTONE DEACETYLASE 9 to promote aging in Arabidopsis. *Elife* 5, e17214. doi: 10.7554/eLife.17214

Cheng, Y., Zhou, Y., Yang, Y., Chi, Y. J., Zhou, J., Chen, J. Y., et al. (2012). Structural and functional analysis of VQ motif-containing proteins in Arabidopsis as interacting proteins of WRKY transcription factors. *Plant Physiol.* 159, 810–825. doi: 10.1104/pp.112.196816

Chi, Y., Yang, Y., Zhou, Y., Zhou, J., Fan, B., Yu, J. Q., et al. (2013). Protein-Protein Interactions in the Regulation of WRKY Transcription Factors. *Mol. Plant* 6, 287–300. doi: 10.1093/mp/sst026

Chia, L. S., Thompson, J. E., and Dumbroff, E. B. (1981). Simulation of the effects of leaf senescence on membranes by treatment with paraquat. *Plant Physiol.* 67 (3), 415–420. doi: 10.1104/pp.67.3.415

Dong, J., Chen, C., and Chen, Z. (2003). Expression profiles of the Arabidopsis WRKY gene superfamily during plant defense response. *Plant Mol. Biol.* 51, 21–37. doi: 10.1023/a:1020780022549

Dutta, A., Choudhary, P., Caruana, J., and Raina, R. (2017). JMJ27, an Arabidopsis H3K9 histone demethylase, modulates defense against Pseudomonas syringae and flowering time. *Plant J.* 91, 1015–1028. doi: 10.1111/tpj.13623

Eulgem, T., Rushton, P. J., Robatzek, S., and Somssich, I. E. (2000). The WRKY superfamily of plant transcription factors. *Trends Plant Sci.* 5, 199–206. doi: 10.1016/S1360-1385(00)01600-9

Gadjev, I., Vanderauwera, S., Gechev, T. S., Laloi, C., Minkov, I. N., Shulaev, V., et al. (2006). Transcriptomic footprints disclose specificity of reactive oxygen species signaling in Arabidopsis. *Plant Physiol.* 141, 436–445. doi: 10.1104/pp.106.078717

Giesguth, M., Sahm, A., Simon, S., and Dietz, K. J. (2015). Redox-dependent translocation of the heat shock transcription factor AtHSFA8 from the cytosol to the nucleus in Arabidopsis thaliana. *FEBS Lett.* 589, 718–725. doi: 10.1016/j.febslet.2015.01.039

Gregersen, P. L., Culetic, A., Boschian, L., and Krupinska, K. (2013). Plant senescence and crop productivity. *Plant Mol. Biol.* 82, 603–622. doi: 10.1007/s11103-013-0013-8

Guo, Y., Cai, Z., and Gan, S. (2004). Transcriptome of Arabidopsis leaf senescence. *Plant Cell Environ.* 27, 521–549. doi: 10.1111/j.1365-3040.2003.01158.x

He, H., Van Breusegem, F., and Mhamdi, A. (2018). Redox-dependent control of nuclear transcription in plants. *J. Exp. Bot.* 69, 3359–3372. doi: 10.1093/jxb/ery130

Hinderhofer, K., and Zentgraf, U. (2001). Identification of a transcription factor specifically expressed at the onset of leaf senescence. *Planta* 213, 469–473. doi: 10.1007/s004250000512

Jefferson, R. A., Kavanagh, T. A., and Bevan, M. W. (1987). GUS fusions: ß-glucuronidase as a sensitive and versatile gene fusion marker in higher plants. *EMBO J.* 6, 3901–3907. doi: 10.1002/j.1460-2075.1987.tb02730.x

Jiang, Y., and Deyholos, M. K. (2009). Functional characterization of Arabidopsis NaCl-inducible WRKY25 and WRKY33 transcription factors in abiotic stresses. *Plant Mol. Biol.* 69, 91–105. doi: 10.1007/s11103-008-9408-3

Jiang, J., Ma, S., Ye, N., Jiang, M., Cao, J., and Zhang, J. (2017). WRKY transcription factors in plant responses to stresses. *J. Integr. Plant Biol.* 59, 86–101. doi: 10.1111/jipb.12513

Kim, J. H., Woo, H. R., Kim, J., Lim, P. O., Lee, I. C., Choi, S. H., et al. (2009). Trifurcate feed-forward regulation of age-dependent cell death involving miR164 in Arabidopsis. *Science* 323 (5917), 1053–1057. doi: 10.1126/science.1166386

Kim, J., Kim, J. H., Lyu, J. I., Woo, H. R., and Lim, P. O. (2017). New insights into the regulation of leaf senescence in Arabidopsis. *J. Exp. Bot.* 69, 787–799. doi: 10.1093/jxb/erx287

Li, S., Fu, Q., Chen, L., Huang, W., and Yu, D. (2011). *Arabidopsis thaliana* WRKY25, WRKY26, and WRKY33 coordinate induction of plant thermotolerance. *Planta* 233, 1237–1252. doi: 10.1007/s00425-011-1375-2

Li, J. F., Chung, H. S., Niu, Y., Bush, J., McCormack, M., and Sheen, J. (2013). Comprehensive protein-based artificial microRNA screens for effective gene silencing in plants. *Plant Cell* 2, 1507–1522. doi: 10.1105/tpc.113.112235

Llorca, M. C., Potschin, M., and Zentgraf, U. (2014). bZIPs and WRKYs: two large transcription factor families executing two different functional strategies. *Front. Plant Sci.* 5, 169. doi: 10.3389/fpls.2014.00169

Mehlhorn, D. G., Wallmeroth, N., Berendzen, K. W., and Grefen, C. (2018). "2in1 vectors improve *in planta* BiFC and FRET analyses," in *The Plant Endoplasmic Reticulum. Methods in Molecular Biology*, vol. 1691 . Eds. C. Hawes and V. Kriechbaumer (New York, NY: Humana Press). doi: 10.1007/978-1-4939-7389-7

Miao, Y., and Zentgraf, U. (2007). The antagonist function of Arabidopsis WRKY53 and ESR/ESP in leaf senescence is modulated by the jasmonic and salicylic acid equilibrium. *Plant Cell* 19, 819–830. doi: 10.1105/tpc.106.042705

Miao, Y., and Zentgraf, U. (2010). A HECT E3 ubiquitin ligase negatively regulates Arabidopsis leaf senescence through degradation of the transcription factor WRKY53. *Plant J.* 63, 179–188. doi: 10.1111/j.1365-313X.2010.04233.x

Miao, Y., Laun, T., Zimmermann, P., and Zentgraf, U. (2004). Targets of the WRKY53 transcription factor and its role during leaf senescence in Arabidopsis. *Plant Mol. Biol.* 55, 853–867. doi: 10.1007/s11103-004-2142-6

Miao, Y., Laun, T. M., Smykowski, A., and Zentgraf, U. (2007). Arabidopsis MEKK1 can take a short cut: it can directly interact with senescence-related WRKY53 transcription factor on the protein level and can bind to its promoter. *Plant Mol. Biol.* 65, 63–76. doi: 10.1007/s11103-007-9198-z

Miao, Y., Smykowski, A., and Zentgraf, U. (2008). A novel upstream regulator of WRKY53 transcription during leaf senescence in Arabidopsis thaliana. *Plant Biol.* 101, 110–120. doi: 10.1111/j.1438-8677.2008.00083.x

Nakagami, H., Soukupová, H., Schikora, A., Zárský, V., and Hirt, H. (2006). A Mitogen-activated protein kinase kinase kinase mediates reactive oxygen species homeostasis in Arabidopsis. *J. Biol. Chem.* 281, 38697–38704. doi: 10.1074/jbc.M605293200

Panchuck, I. I., Zentgraf, U., and Volkov, R. A. (2005). Expression of the Apx gene family during leaf senescence of Arabidopsis thaliana. *Planta* 222, 926–932. doi: 10.1007/s00425-005-0028-8

Petersen, M., Brodersen, P., Naested, H., Andreasson, E., Lindhart, U., Johansen, B., et al. (2000). Arabidopsis map kinase 4 negatively regulates systemic acquired resistance. *Cell* 103, 1111–1120. doi: 10.1016/s0092-8674(00)00213-0

Pfaffl, M. W. (2001). A new mathematical model for relative quantification in real-time RT-PCR. *Nucleic Acids Res.* 29, e45. doi: 10.1093/nar/29.9.e45

Potschin, M., Schlienger, S., Bieker, S., and Zentgraf, U. (2014). Senescence Networking: WRKY18 is an upstream regulator, a downstream target gene, and a protein interaction partner of WRKY53. *J. Plant Growth Reg.* 33, 106–118. doi: 10.1007/s00344-013-9380-2

Qiu, J. L., Fiil, B. K., Petersen, K., Nielsen, H. B., Botanga, C. J., Thorgrimsen, S., et al. (2008). Arabidopsis MAP kinase 4 regulates gene expression through transcription factor release in the nucleus. *EMBO J.* 27, 2214–2221. doi: 10.1038/emboj.2008.147

Queval, G., Issakidis-Bourguet, E., Hoeberichts, F. A., Vandorpe, M., Gakière, B., Vanacker, H., et al. (2007). Conditional oxidative stress responses in the Arabidopsis photorespiratory mutant cat2 demonstrate that redox state is a key modulator of daylength-dependent gene expression, and define photoperiod as a crucial factor in the regulation of H_2O_2-induced cell death. *Plant J.* 52, 640–657. doi: 10.1111/j.1365-313X.2007.03263.x

Ren, Y., Li, Y., Jiang, Y., Wu, B., and Miao, Y. (2017). Phosphorylation of WHIRLY1 by CIPK14 Shifts Its Localization and Dual Functions in Arabidopsis. *Mol. Plant* 10, 749–763. doi: 10.1016/j.molp.2017.03.011

Rushton, P. J., Somssich, I. E., Ringler, P., and Shen, Q. J. (2010). WRKY transcription factors. *Trends Plant Sci.* 15, 247–258. doi: 10.1016/j.tplants.2010.02.006

Shaikhali, J., Norén, L., de Dios Barajas-López, J., Srivastava, V., König, J., Sauer, U. H., et al. (2012). Redox-mediated mechanisms regulate DNA binding activity of the G-group of basic region leucine zipper (bZIP) transcription factors in Arabidopsis. *J. Biol. Chem.* 287, 27510–27525. doi: 10.1074/jbc.M112.361394

Shaikhali, J. (2015). GIP1 protein is a novel cofactor that regulates DNA-binding affinity of redox-regulated members of bZIP transcription factors involved in the early stages of Arabidopsis development. *Protoplasma* 252, 867–883. doi: 10.1007/s00709-014-0726-9

Su, T., Wang, P., Li, H., Zhao, Y., Lu, Y., Dai, P., et al. (2018). The Arabidopsis catalase triple mutant reveals important roles of catalases and peroxisome-derived signaling in plant development. *J. Integr. Plant Biol.* 60, 591–607. doi: 10.1111/jipb.12649

Uauy, C., Distelfeld, A., Fahima, T., Blechl, A., and Dubcovsky, J. (2006). A NAC Gene regulating senescence improves grain protein, zinc, and iron content in wheat. *Science* 314, 1298–1301. doi: 10.1126/science.1133649

Ülker, B., Shahid Mukhtar, M., and Somssich, I. E. (2007). The WRKY70 transcription factor of Arabidopsis influences both the plant senescence and defense signaling pathways. *Planta* 226, 125–137. doi: 10.1007/s00425-006-0474-y

Viola, I. L., Güttlein, L. N., and Gonzalez, D. H. (2013). Redox modulation of plant developmental regulators from the class I TCP transcription factor family. *Plant Physiol.* 162, 1434–1447. doi: 10.1104/pp.113.216416

Wu, A., Allu, A. D., Garapati, P., Siddiqui, H., Dortay, H., Zanor, M. I., et al. (2012). JUNGBRUNNEN1, a reactive oxygen species-responsive NAC transcription factor, regulates longevity in Arabidopsis. *Plant Cell* 24, 482–506. doi: 10.1105/tpc.111.090894

Xie, Y., Huhn, K., Brandt, R., Potschin, M., Bieker, S., Straub, D., et al. (2014). REVOLUTA and WRKY53 connect early and late leaf development in Arabidopsis. *Development* 141, 4772–4783. doi: 10.1242/dev.117689

Xu, X., Chen, C., Fan, B., and Chen, Z. (2006). Physical and functional interactions between pathogen-induced Arabidopsis WRKY18, WRKY40, and WRKY60 transcription factors. *Plant Cell* 18, 1310–1326. doi: 10.1105/tpc.105.037523

Yang, S. D., Seo, P. J., Yoon, H. K., and Park, C. M. (2011). The Arabidopsis NAC transcription factor VNI2 integrates abscisic acid signals into leaf senescence *via the* COR/RD genes. *Plant Cell* 23, 2155–2168. doi: 10.1105/tpc.111.084913

Zentgraf, U., Laun, T., and Miao, Y. (2010). The complex regulation of WRKY53 during leaf senescence of *Arabidopsis thaliana*. *Eur. J. Cell Biol.* 89, 133–137. doi: 10.1016/j.ejcb.2009.10.014

Zheng, Z., Mosher, S. L., Fan, B., Klessig, D. F., and Chen, Z. (2007). Functional analysis of Arabidopsis WRKY25 transcription factor in plant defense against *Pseudomonas syringae*. *BMC Plant Biol.* 7, 2. doi: 10.1186/1471-2229-7-2

Zimmermann, P., Heinlein, C., Orendi, G., and Zentgraf, U. (2006). Senescence specific regulation of catalases in Arabidopsis thaliana (L.) Heynh. *Plant Cell Environ.* 29, 1049–1060. doi: 10.1111/j.1365-3040.2005.01459.x

Conflict of Interest: The authors declare that the research was conducted in the absence of any commercial or financial relationships that could be construed as a potential conflict of interest.

frontiers in Plant Science

ORIGINAL RESEARCH
published: 25 February 2020
doi: 10.3389/fpls.2020.00143

Histone Deacetylase HDA9 With ABI4 Contributes to Abscisic Acid Homeostasis in Drought Stress Response

Dongwon Baek[1†], *Gilok Shin*[2†], *Min Chul Kim*[1,3†], *Mingzhe Shen*[1], *Sang Yeol Lee*[1] *and Dae-Jin Yun*[2*]

[1] Division of Applied Life Science (BK21plus program), Plant Molecular Biology and Biotechnology Research Center, Gyeongsang National University, Jinju, South Korea, [2] Department of Biomedical Science and Engineering, Konkuk University, Seoul, South Korea, [3] Institute of Agriculture & Life Science, Gyeongsang National University, Jinju, South Korea

OPEN ACCESS

Edited by:
Nam-Chon Paek,
Seoul National University,
South Korea

Reviewed by:
Jianhua Zhu,
University of Maryland,
United States
Abel Rosado,
University of British Columbia,
Canada

***Correspondence:**
Dae-Jin Yun
djyun@konkuk.ac.kr

[†]These authors have contributed equally to this work

Specialty section:
This article was submitted to Plant Abiotic Stress, a section of the journal Frontiers in Plant Science

Received: 22 October 2019
Accepted: 30 January 2020
Published: 25 February 2020

Citation:
Baek D, Shin G, Kim MC, Shen M, Lee SY and Yun D-J (2020) Histone Deacetylase HDA9 With ABI4 Contributes to Abscisic Acid Homeostasis in Drought Stress Response. Front. Plant Sci. 11:143. doi: 10.3389/fpls.2020.00143

Drought stress, a major environmental factor, significantly affects plant growth and reproduction. Plants have evolved complex molecular mechanisms to tolerate drought stress. In this study, we investigated the function of the *Arabidopsis thaliana* RPD3-type HISTONE DEACETYLASE 9 (HDA9) in response to drought stress. The loss-of-function mutants *hda9-1* and *hda9-2* were insensitive to abscisic acid (ABA) and sensitive to drought stress. The ABA content in the *hda9-1* mutant was reduced in wild type (WT) plant. Most histone deacetylases in animals and plants form complexes with other chromatin-remodeling components, such as transcription factors. In this study, we found that HDA9 interacts with the ABA INSENSITIVE 4 (ABI4) transcription factor using a yeast two-hybrid assay and coimmunoprecipitation. The expression of *CYP707A1* and *CYP707A2*, which encode (+)-ABA 8′-hydroxylases, key enzymes in ABA catabolic pathways, was highly induced in *hda9-1*, *hda9-2*, *abi4*, and *hda9-1 abi4* mutants upon drought stress. Chromatin immunoprecipitation and quantitative PCR showed that the HDA9 and ABI4 complex repressed the expression of *CYP707A1* and *CYP707A2* by directly binding to their promoters in response to drought stress. Taken together, these data suggest that HDA9 and ABI4 form a repressive complex to regulate the expression of *CYP707A1* and *CYP707A2* in response to drought stress in *Arabidopsis*.

Keywords: drought stress, abscisic acid, histone deacetylase, HDA9, ABI4, 8′-hydroxylase, *Arabidopsis thaliana*

INTRODUCTION

Drought stress causes serious damage to plant growth, survival, and productivity (Zhu, 2001). Plants have evolved a variety of complex signaling mechanisms to sense and acclimate to drought stress (Bohnert and Sheveleva, 1998). Accumulation of the phytohormone, abscisic acid (ABA), helps to protect plants from drought stress by controlling seed maturation and dormancy during seed development and seedling growth (Finkelstein and Lynch, 2000; Lopez-Molina et al., 2001). ABA

also plays a major role in regulating physiological processes in the drought stress signaling pathway, primarily by controlling stomatal aperture and modulating the expression of many ABA-responsive genes that function in drought tolerance (Yamaguchi-Shinozaki and Shinozaki, 2006; Cutler et al., 2010; Raghavendra et al., 2010).

The levels of endogenous ABA are regulated by the balance of ABA biosynthesis and catabolism (Xiong and Zhu, 2003; Nambara and Marion-Poll, 2005). When plants are exposed to drought stress or exogenous ABA, most of the major enzymes of the ABA biosynthesis pathway, including a zeaxanthin epoxidase (ZEP/AtABA1), 9-*cis*-epoxycarotenoid dioxygenase3 (NCED3), molybdenum cofactor (moco/AtABA3), and *Arabidopsis* aldehyde oxidase3 (AAO3), are activated, with the exception of short-chain dehydrogenase/reductase (SDR/AtABA2) (Xiong and Zhu, 2003; Dong et al., 2015). In ABA catabolism, endogenous ABA is converted from the active to the inactive form through degradation to generate phaseic acid (PA) by ABA 8′-hydrolases, a key enzyme in ABA catabolic pathways (Kushiro et al., 2004; Dong et al., 2015). During seed imbibition, reduction of ABA levels is associated with increasing levels of PA in plants (Jacobsen et al., 2002; Kushiro et al., 2004). The ABA 8′-hydroxylase family includes four members, CYP707A1 to CYP707A4, which increase in abundance during seed dormancy and germination (Jacobsen et al., 2002; Kushiro et al., 2004). CYP707A1 and CYP707A2 cause a sharp reduction in ABA levels during seed maturation and germination (Jacobsen et al., 2002; Okamoto et al., 2006). However, CYP707A4 diurnally regulates ABA levels through conjugation/deconjugation (Pan et al., 2009). In plants, large amounts of ABA are converted into the ABA-glucose ester, the inactive glucose conjugate form, and are transported to the vacuoles by the β-glucosidase AtBG1 (Lee et al., 2006).

ABA signaling pathways for seed maturation and dormancy are controlled by ABA-responsive transcription factors that regulate gene expression (Finkelstein et al., 2002). The representative transcription factors (*e.g.*, ABA INSENSITIVE 3 (ABI3), ABI4, and ABI5) are associated with regulating sensitivity to ABA (Finkelstein et al., 2002; Shu et al., 2016). In addition, ABI3, ABI4, and ABI5 have distinct roles in ABA-dependent seed maturation and dormancy (Shu et al., 2016). ABI3 is a negative regulator of seed germination in both the ABA and gibberellic acid signaling pathways (Yuan and Wysocka-Diller, 2006). Although ABI5 interacts with ABI3, ABI5 is epistatic to ABI3 (Lopez-Molina et al., 2002). ABI5 affects the ubiquitin ligase activity of KEEP ON GOING (KEG) following germination (Stone et al., 2006). ABI4, which is specifically expressed in the embryo, plays a unique and important role in the catabolism of embryonic lipids during seed germination (Penfield et al., 2006).

Epigenetic modifications are important regulatory mechanisms of gene transcription and play essential roles in plant development and stress responses (Yuan et al., 2013). The reversible process of histone acetylation and deacetylation by histone acetyltransferases (HATs) and histone deacetylases (HDACs) has been implicated in genome expression, chromatin structural organization, and gene function (Wang et al., 2014; Verdin and Ott, 2015). The HDAC family in *Arabidopsis* is made up of 18 members and is categorized into three groups: twelve REDUCED POTASSIUM DEPENDENCY PROTEIN 3 (RPD3/HDA1), four HISTONE DEACETYLASE 2 (HD2), and two SILENT INFORMATION REGULATOR PROTEIN 2 (SIR2) (Pandey et al., 2002; Hollender and Liu, 2008). HDACs in the RPD3/HDA1 group have multiple functions, including plant development, DNA methylation, and pathogen defense signaling (Aufsatz et al., 2002; Zhou et al., 2005; Liu et al., 2013; Cigliano et al., 2013; Ryu et al., 2014). HD2 HDACs are plant-specific and are involved in developmental processes and stress responses (Zhou et al., 2004; Sridha and Wu, 2006; Luo et al., 2012a). HDACs in the SIR2 group are associated with energy metabolism in the mitochondria and the transition of leaf tissue to callus (König et al., 2014; Lee et al., 2016).

The RPD3 group is further classified into three classes based on sequence similarity and phylogenetic analysis, with four HDACs belonging to class I (HDA19, HDA6, HDA7, and HDA9), three to class II (HDA5, HDA15, and HDA18), and one to class III (HDA2). HDA8, HDA14, HDA10, and HDA17 of the RPD3 group are unclassified members (Pandey et al., 2002; Hollender and Liu, 2008). Recent studies have suggested that the HDACs in class I are involved in abiotic stress signaling, responding to salt, ABA, and drought stress (Song et al., 2005; Sridha and Wu, 2006; Chen and Wu, 2010; Luo et al., 2012a; Ryu et al., 2014). HDA6 and HDA19 play an important role in modulating seed germination during salt stress responses and in response to ABA, as well as abiotic stress-induced gene expression in *Arabidopsis* (Chen and Wu, 2010; Luo et al., 2012b; Ryu et al., 2014). Furthermore, HDA19 acts as a transcriptional repressor through the formation of a protein complex with AtERF7 and AtSin3 (Song et al., 2005). In contrast to the *hda19* and *hda6* mutants, the HDA9 mutants, *hda9-1* and *hda9-2*, were insensitive to salt stress and ABA during seedling root growth and seed germination (Zheng et al., 2016). Moreover, HDA9 forms a complex with PWR and transcription factor WRKY53, and PWR plays an important role as a regulator for HDA9 nuclear accumulation (Chen et al., 2016). Several class I HDACs function as positive regulators of stress responses; however, a few others negatively regulate plant stress responses by repressing the expression of stress-responsive genes (Zheng et al., 2016).

Although the function of HDA9 in salt and drought stress responses can be explained by its negative effects on the expression of stress-responsive genes, the mechanism by which it affects other aspects of stress signaling pathways remains unknown. Here, we show that HDA9 acts in association with an ABA-related transcription factor to repress gene expression through histone deacetylation. HDA9 interacts with ABI4 *in vivo*, and the HDA9–ABI4 complex acts together on *AtCYP707A1* and *AtCYP707A2* in the regulation of drought stress. Furthermore, the HDA9-ABI4 complex regulates the levels of endogenous ABA during drought stress. These findings revealed that the HDA9–ABI4 complex regulates histone deacetylation to control a wide variety of biological processes during drought stress responses.

MATERIALS AND METHODS

Plant Materials and Growth Conditions

The wild type (WT) *Arabidopsis thaliana* used in this study was Col-0 ecotype, and all mutants were on the Col-0 background. Seeds were grown on 1/2 Murashige and Skoog (MS) media with 1.5% (w/v) sucrose, pH 5.7 under a long-day photoperiod (16 h light/8 h dark) at 23°C. The *hda9-1* (SALK_007123) mutant was obtained from NASC (http://arabidopsis.info/), and *hda9-2* (Gk_305G03) mutant from ABRC (http://www.arabidopsis.org/) (van Zanten et al., 2014). Dr. Nho kindly provided two seeds of *hda9-1*/HDA9 complementation plant (#7 and #11 lines) with a C-terminal HA tag (Kang et al., 2015).

We generated the *hda9-1abi4* double mutant by crossing the homozygous *hda9-1* and *abi4* (CS8104; Zhang et al., 2013) single mutant and then self-pollinated the F1 generation. To select the compatible lines of F2 (10 lines) and homozygous F3 (5 lines) generation, we performed PCR genotyping analysis and DNA sequencing (**Supplemental Table S2**).

Physiological Assay

For ABA germination assays, seeds were grown on 1/2 MS medium containing 1.5% sucrose with various concentrations of ABA (Sigma, St. Louis, MO, USA). Successful germination in the presence of ABA was determined by the presence of green cotyledons 5 d after sowing. Four experimental repeats were carried out, each one containing at least 32 seeds. For drought tests, one-week-old seedlings grown on MS medium were transferred to the soil. Transferred seedlings were adapted to the soil for one week under identical conditions followed by withholding water for 11 d. After rewatering for 1 d, recovery of WT, mutants and transgenic plants was monitored. Three experimental repeats were carried out each one containing at least 36 plants. For water loss assays, one-week-old seedlings grown on MS medium were transferred to the soil. After growing for two weeks, plant shoots were cut and placed in petri dishes. The dishes were maintained in the growth chamber and the loss of fresh weight was determined at the indicated times. The experiments were performed with three independent replicates with eight plants per replicate.

Stomatal Aperture Bioassays

Developmentally similar leaves were detached from 10-day-old seedlings and floated on stomatal opening buffer (5 mM MES, 5 mM KCl, 50 μM $CaCl_2$, pH 5.6) under light for 2 h and then treated with 5 μM ABA for 2 h. After ABA treatment, the leaves were fragmented using a scalpel, and the epidermal fragments were quickly mounted for visualization in a scanning electron microscope (JSM-6380LV; JEOL, Akishima, Japan). The stomatal aperture was determined from measurements of 50 to 80 stomata per treatment. Each experiment was repeated four times.

Yeast Two-Hybrid Assay

For yeast two-hybrid experiments, *pDONR™/Zeo-HDA9* and *pDONR™/Zeo-ABI4* were fused in the yeast two-hybrid destination vector *pDEST22* (harboring activation domain) and *pDEST32* (harboring DNA binding domain) to generate construct vector, *pDEST22-HDA9* and *pDEST32-ABI4*, respectively. These plasmids were transformed into the *Saccharomyces cerevisiae* (*YRG2*). Protein–protein interactions were determined by the growth of yeast colonies on SD/-Trp-Leu (Sc-TL) or SD/-Trp-Leu-His (Sc-TLH; Takara Bio, Kusatsu, Japan) agar media containing 3-amino-1,2,4-triazole (3-AT; 25 mM). Empty vector was used as a negative control.

Protein Extraction and CoImmunoprecipitation Assay

Total protein was extracted from three-week-old *Nicotiana benthamiana* leaves and the extraction buffer contained 100 mM Tris-Cl, pH 7.5, 150 mM NaCl, 0.5% NP-40, 1 mM EDTA, 3 mM DTT and protease inhibitors (1 mM PMSF, 5 μg ml^{-1} leupeptin, 1 μg ml^{-} aprotinin, 1 μg/ml pepstatin, 5 μg/ml antipain, 5 μg/ml chymostatin, 2 mM Na_2VO_3, 2 mM NaF, and 50 mM MG132) (Park et al., 2018). For coimmunoprecipitation assays of *N. benthamiana*, leaves were coinfiltrated with *Agrobacterium tumefaciens* (*GV3101*) cell expressing the indicated plasmid combination using *35S:HDA9-3xHA* and *35S:ABI4-GFP*. Total protein reacted for immunoprecipitation using rabbit anti-GFP polyclonal (Abcam, Cambridge, MA, USA) and protein A agarose (Invitrogen, Carlsbad, CA, USA). For immunoblotting, membranes were incubated with the appropriate anti-HA (Roche, Indianapolis, IN, USA), and detected using ECL-detection reagent (GE Healthcare, Little Chalfont, Buckinghamshire, UK). For the coimmunoprecipitation assays three independent replicates were carried out.

RNA Isolation and Quantitative PCR Analyses

Total RNA was extracted from plants (harvest timing is described in each experiment) with the RNeasy Plant Mini Kit (Qiagen, Hilden, Germany) and treated with DNase (Sigma, St. Louis, MO, USA). 2 μg RNAs were used for the synthesis of the first-strand cDNA using the Thermoscript™ RT-PCR System (Invitrogen, Carlsbad, CA, USA). Quantitative PCR was performed using SYBR Green PCR Master Mix kit (SYBR Green Supermix; Bio-Rad, Hercules, CA, USA) according to instructions with the CFX96 real-time PCR detection system (Bio-Rad, Hercules, CA, USA). The expression of *TUBULIN8* was used as the endogenous control. The qRT-PCR experiments were performed in three independent replicates. The sequences of primers used in qRT-PCR are listed in **Supplemental Table S2**.

Quantitative Determination of Abscisic Acid

Endogenous ABA was extracted from 10-day-old plants with/without dehydration stress and analyzed using Phytodetek ABA test Kit (Agdia Incorporated, IN, USA) according to the manufacturer's instruction. Three biological repeats and three technical repeats were performed and measured for each sample.

Chromatin Immunoprecipitation Assay

The ChIP assays were performed as previously described (Saleh et al., 2008). Nuclei from two-week-old *hda9-1HDA9-HA* plants were extracted with CelLytic™ PN Isolation/extraction Kit

(Sigma, St. Louis, MO, USA) and sonicated (Bioruptor, Tokyo, Japan). Immunoprecipitations were carried out using an anti-HA antibody (Roche, Indianapolis, IN, USA) with salmon sperm DNA/protein A agarose (Upstate, New York, USA) beads. Treatment with antirat IgG was used as a negative control to detect background levels in each ChIP experiment. The immunoprecipitated DNA was quantified by qRT-PCR analysis. The expression of *TUBULIN4* was used as the internal control. The ChIP experiments were performed in three independent replicates. The specific primer sequences are provided in **Supplemental Table S2**.

RESULTS

HDA9 Mediates in Seed Germination and Stomatal Closure by ABA

To investigate functional characterization of HDA9, two independent mutants, *hda9-1* (SALK_007123) and *hda9-2* (CS370750), were obtained from the *Arabidopsis* Biological Resource Center (**Supplementary Figure S1**). The *hda9*-1 and *hda9-2* mutants have T-DNA insertions in the first intron and fifth exon of HDA9, respectively (**Supplementary Figure S1A**). The presence of the T-DNA at the expected location in the *hda9* mutants was verified by genome diagnostic PCR (**Supplementary Figure S1B**). Quantitative reverse transcription PCR (qRT-PCR) analyses indicated that *hda9-1* and *hda9-2* were RNA null mutants (**Supplementary Figure S1C**). Although HDA9 is involved in seed dormancy and germination, the ABA sensitivity of *hda9* mutant is similar compared to that of WT (van Zanten et al., 2014). ABA enhances seed dormancy and inhibits germination and root growth by regulating the balance of endogenous phytohormones (Finkelstein et al., 2008). To investigate the function of HDA9 in ABA signaling, we examined the physiological responses of the *hda9* mutants (*hda9-1* and *hda9-2*), and *HDA9 promoter:HDA9-HA* in the *hda9-1* mutant (#11 line; *hda9-1*/HDA9) complemented transgenic plants in response to ABA. Compared to the WT plants, seed germination of the *hda9* mutants was significantly enhanced when exposed to exogenous ABA. However, the *hda9-1*/HDA9 plant showed a similar phenotype to the WT plants (**Figure 1A**). The percentage of fully opened green cotyledons in WT, *hda9* mutants, and *hda9-1*/HDA9 were similar in the absence of ABA (**Figure 1B**). However, in the presence of 0.5 μM ABA, the percentage of green cotyledons in the *hda9* mutants were approximately 70–80%, compared to 35–40% for the WT and the *hda9-1*/HDA9 seedlings (**Figure 1B**).

Upon sensing abiotic stress, plants increase their endogenous ABA content to induce stomatal closure (Vishwakarma et al., 2017). To investigate whether HDA9 influences ABA-mediated changes in the stomata, stomatal closure responses were determined in the WT, *hda9* mutants, and *hda9-1*/HDA9 plants under exogenous ABA treatment. The guard cell sizes, stomatal density, and stomatal apertures were similar in the

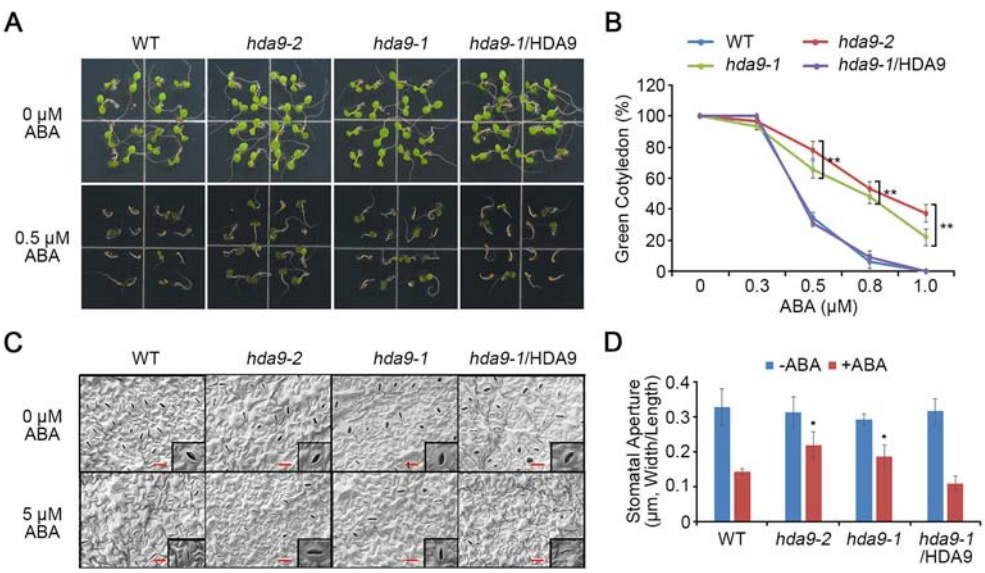

FIGURE 1 | *hda9* mutants are insensitive to ABA. **(A)** Seeds of WT, *hda9-1*, *hda9-2*, and *hda9-1*/HDA9 were germinated on MS media supplemented with and without 5 μM ABA. Photographs were taken 5 d after sowing. **(B)** Quantification of germination rate of WT, *hda9-1*, *hda9-2*, and *hda9-1*/HDA9 on different concentrations of ABA. The values indicated means ± SE of n = 4 biological replicates of at least 32 seeds for each experiment. Asterisks represent significant differences from the WT (*, 0.01 < *p*-value ≤ 0.05; **, *p*-value < 0.01; Student's *t*-test). **(C)** ABA-induced stomata closure. Leaves of 10-d-old seedling of WT, *hda9-1*, *hda9-2*, and *hda9-1*/HDA9 were floated in stomatal opening solution for 2 h and then incubated in the 5 μM ABA for 2 h in the light. Stomata on the abaxial surface were observed using scanning electron microscopy. **(D)** Measurement of stomatal aperture (the ratio of width to length) after ABA treatment. The values indicated means ± SE of n = 4 biological replicates of 50 to 80 stomata for each experiment. Asterisks represent significant differences from the WT (*, 0.01 < p-value ≤ 0.05; Student's *t*-test).

leaves of the WT, *hda9* mutants, and *hda9-1*/HDA9 plants at the same developmental stage (**Figures 1C, D**). However, the stomata closing in *hda9* mutants was delayed in response to ABA compared to those in WT and the *hda9-1*/HDA9 plants (**Figures 1C, D**). Therefore, these results suggested that HDA9 plays a critical role in regulating ABA-dependent stomatal closure and ABA sensitivity during seed germination.

HDA9 Regulates ABA-Dependent Hypersensitivity to Drought Stress

Stress phytohormone ABA quickly accumulates in plant tissues that are exposed to drought stress (Xu et al., 2013). Increased endogenous ABA leads to stomatal closure to minimize water loss through transpiration (Blatt, 2000). As ABA-induced stomata closing was partially suppressed in *hda9* mutants, we compared the drought tolerance of the WT, the *hda9* mutants, and *hda9-1*/HDA9 plants by counting the number of plants that survived following water deficit (**Figure 2**). Three-week-old WT, *hda9* mutants, and *hda9-1*/HDA9 plants were deprived of water for 11 d. One day after rewatering, approximately 30% of the WT and *hda9-1*/HDA9 plants survived, whereas only 5% of the *hda9* mutants survived (**Figure 2A**). In addition, the *hda9* mutants showed wilted and purple tint leaves (**Figure 2A**). The water loss in the *hda9* mutant leaves was approximately 25% more rapid than in the WT plants as measured by the progressive water loss from detached leaves (**Figure 2B**). Also, the transcriptional expression of *HDA9* was weakly induced under drought stress condition (**Supplemental Figure S2**). These results demonstrated that HDA9 plays a positive role in plant responses to drought stress.

HDA9 Interacts With the ABI4 Transcription Factor *In Vivo*

HDACs are known to interact with DNA-binding proteins to modulate gene transcription in abiotic stress responses (Song et al., 2005; Song and Galbraith, 2006). ABI3, ABI4, and ABI5 are important regulatory transcription factors during seed dormancy, germination, and development (Lopez-Molina et al., 2001; Nambara and Marion-Poll, 2005; Shu et al., 2013). To identify the mode of HDA9 function during seed germination, we tested its interaction with several known ABA-mediated transcription factors, including ABI3, ABI4, and ABI5, using the yeast two-hybrid system. Full-length cDNAs of ABI3, ABI4, and ABI5 were fused to the GAL4 activation domain and HDA9 was used as bait. The empty vectors were used as a negative control. The yeast two-hybrid assay showed that HDA9 interacts with ABI4 but not with ABI5 (**Figure 3A** and **Supplementary Figure S3**). However, HDA9 did not interact with other transcription factors, which were related in ABA responses, such as ABF1, ABF2, and ABF3 (**Supplementary Figure S3**). Also, it is not clear whether HDA9 interacts with ABI3 and/or ABF4 because of auto-activation activities of ABI3 and ABF4 in the yeast two-hybrid system using *pDEST22* and *pDEST32* vector (**Supplementary Figure S3**). To confirm the interaction of HDA9 with ABI4, we performed coimmunoprecipitation assays by using the C-terminal HA-tagged HDA9 (HDA9-HA) and the N-terminal GFP-tagged ABI4 (GFP-ABI4). Briefly, we transiently coexpressed HDA9-HA and GFP-ABI4 in *N. benthamiana* leaves using agro-infiltration. We used anti-GFP antibodies to immunoprecipitate GFP-ABI4 and performed western blots with anti-HA antibodies for analysis of the

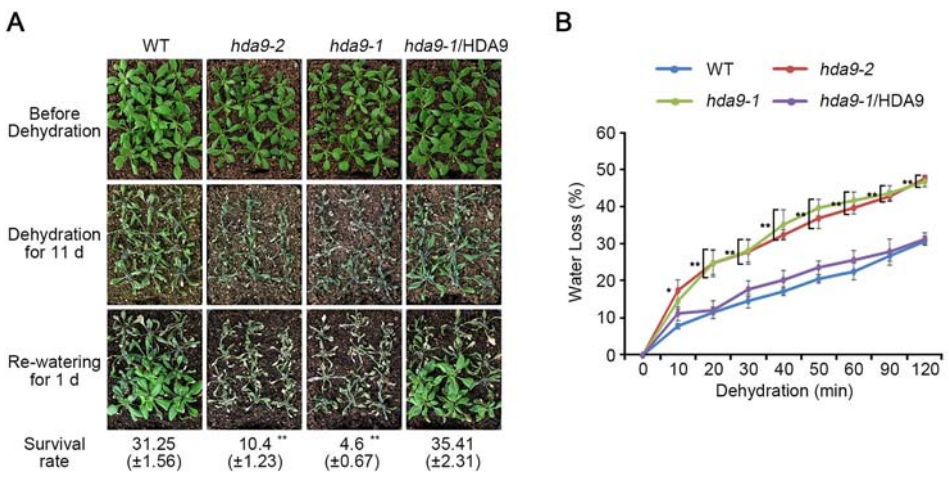

FIGURE 2 | *hda9* mutants are sensitive to dehydration. **(A)** One-week-old plants were transferred to soil and grown for an additional one week. Photographs of plants before and after stress treatment. Water was withheld from two-week-old plants for 11 d, and then plants were rewatered for 1 d before the photograph was taken. Quantitation of the survival rate of WT, *hda9-1*, *hda9-2* and *hda9-1*/HDA9 plants. The values of survival rate indicated means ± SE of n = 3 biological replicates of at least 36 plants for each experiment. **(B)** Water loss assay. Water loss is presented as the percentage of weight loss versus initial fresh weight from three-week-old WT, *hda9-1*, *hda9-2* and *hda9-1*/HDA9 plants. Water loss was calculated from the results of three independent experiments. The values of survival rate indicated means ± SE of n = 3 biological replicates of at least 8 plants for each experiment. Asterisks represent significant differences from the WT (*, 0.01 < *p*-value ≤ 0.05; **, *p*-value < 0.01; Student's *t*-test).

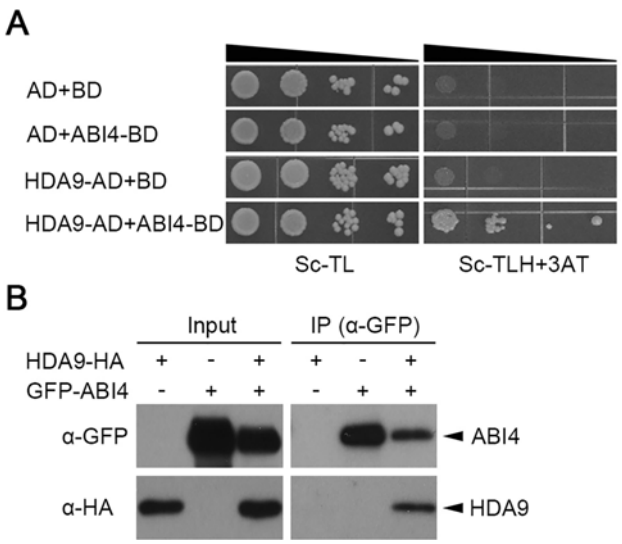

FIGURE 3 | HDA9 interacts with ABI4 *in vivo*. **(A)** Interaction between HDA9 and ABI4 by yeast two hybrid assay. BD, *pDEST32* is the bait plasmid; AD, *pDEST22* the prey plasmid. The cotransformed yeast strains were plated on the control SD-TL and selective medium SD-TLH plus 25 mM 3-AT. The combinations with empty plasmid were used as negative controls. **(B)** Coimmunoprecipitation assay between HDA9 and ABI4 proteins. Protein extracts obtained from tobacco leaves infiltrated with *Agrobacterium* harboring *35S::HDA9-HA* and *35S::ABI4-GFP* were analyzed using anti-GFP and anti-HA antibodies. Input levels of epitope tagged proteins in crude protein extracts were analyzed by immunoblotting. Immunoprecipitated epitope GFP-tagged proteins were probed with anti-HA antibodies to detect coimmunoprecipitation of ABI4-GFP with HDA9-HA.

HDA9 immunocomplexes (**Figure 3B**). These results indicate that HDA9 binds specifically to ABI4 transcription factor *in vivo*.

HDA9 Alters the Expression of ABA Catabolism-Related Genes in Drought Stress Response

ABI4, an AP2/ERF transcription factor, acts both as a positive and a negative regulator in ABA signal transduction during seed dormancy and germination (Finkelstein and Rock, 2002). To investigate the regulatory functions of HDA9 in drought stress response, we tested the transcript levels of six genes, *Lhcb1.2*, *AOX1a*, *CYP707A1*, *CYP707A2*, *ACS4*, and *ACS8*, which were negatively regulated by ABI4, in the WT, *hda9-1* mutant, and the *hda9-1*/HDA9 plants under drought stress conditions (Koussevitzky et al., 2007; Giraud et al., 2009; Shu et al., 2013; Dong et al., 2016; **Supplementary Table S1**). The transcripts of *CYP707A1* and *CYP707A2* were significantly up-regulated in the *hda9-1* and *hda9-2* mutants compared to those in the WT under drought stress conditions, whereas the *hda9-1*/HDA9 plant showed a similar expression patterns of *CYP707A1* and *CYP707A2* to the WT (**Figure 4**). However, the transcripts of *Lhcb1.2*, *AOX1a*, *ACS4,* and *ACS8* were not affected by drought stress in the WT, *hda9-1* mutant, and *hda9-1*/HDA9 plants (**Supplemental Figure S4**). In addition, because *CYP707A1* and *CYP707A2* played important roles in ABA catabolism, we measured ABA content in the WT, *hda9-1* mutant, and *hda9-1*/HDA9 plants under drought stress conditions. The ABA content in the *hda9-1* mutant seedlings was approximately 1.5-fold lower than that in the WT and *hda9-1*/HDA9 seedlings (**Figure 5**), and the ABA content in seeds of *hda9* mutant was lower than that in seeds of WT (**Supplemental Figure S5**). These results confirmed that HDA9 negatively regulated transcriptional expression of ABA catabolism-related genes for maintaining ABA level in drought stress response.

HDA9 Associated With *CYP707A1* and *CYP707A2* Promoters

ABI4 directly binds to the *CACCG* motif to activate the transcription of target genes, and to the *CCAC* element to repress the target genes (Finkelstein and Rock, 2002; Bossi et al., 2009). ABI4 represses the expression of *CYP707A1* and *CYP707A2* by directly binding to the *CCAC* elements in their promoter regions (Shu et al., 2013). To examine whether HDA9 binds to the promoter regions of *CYP707A1* and *CYP707A2*, we performed chromatin immunoprecipitation (ChIP) assays using fragments A1-1 to A1-3 and A2-1 to A2-2 of the *CYP707A1* and the *CYP707A2* promoter, respectively, both of which contained several CCAC motifs (Shu et al., 2013; **Figure 6**). ChIP

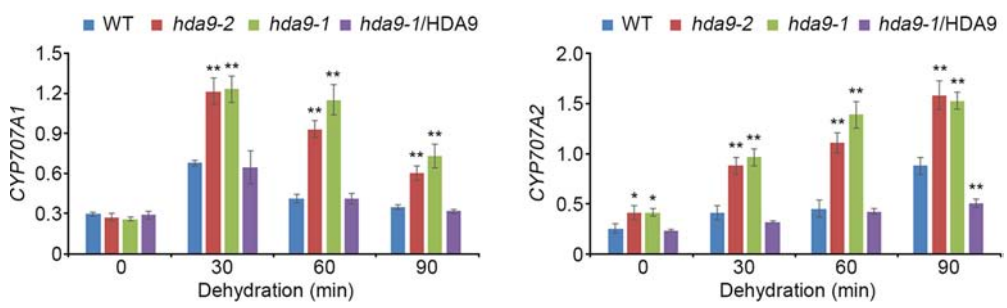

FIGURE 4 | HDA9 regulates *CYP707A1* and *CYP707A2* expression to dehydration. Quantitative RT-PCR analyses of *CYP707A1* and *CYP707A2* in WT, *hda9-1*, *hda9-2* and *hda9-1*/HDA9 after dehydration stress treatment. Total RNA was extracted from 10-d-old seedlings treated with dehydration stress for indicated times. Expression of *TUBULIN8* was used for normalization. Bars represent mean ± SD of three biological replicates with three technical replicates each. Asterisks represent significant differences from the WT (*, 0.01 < *p*-value ≤ 0.05; **, *p*-value < 0.01; Student's *t*-test).

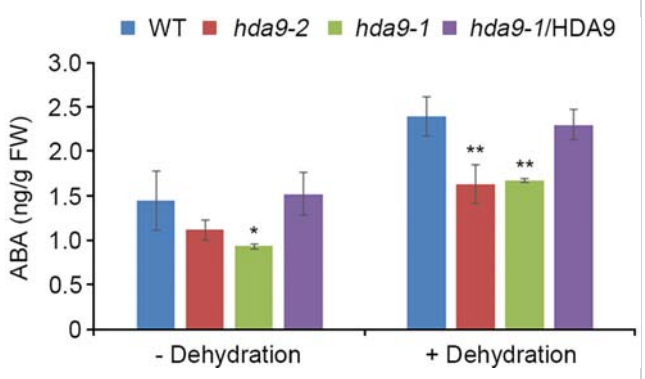

FIGURE 5 | HDA9 regulates intracellular ABA levels under dehydration stress. ABA content in detached 10-d-old WT, *hda9-1*, *hda9-2*, and *hda9-1*/HDA9 plants during a 1-h dehydration. ABA content was measured from 20 whole seedlings of each genotype. Error bars represent the SD from four independent experiments. Asterisks represent significant differences from the WT (*, *p*-value ≤ 0.05, **, *p*-value ≤ 0.01, Student's *t*-test).

experiments were conducted using the *hda9-1*/HDA9 (*HDA9 promoter:HDA9-HA* in the *hda9-1* mutant) complementation plant with an anti-HA antibody under drought stress conditions. ChIP-qPCR using the chromatin-immunoprecipitated DNA showed that three amplicons of the *CYP707A1* promoter under drought stress conditions were more strongly enriched than under normal conditions (**Figure 6A**). However, in the *CYP707A2* promoter, only the A2-1 amplicon was strongly enriched during drought stress (**Figure 6B**). We found that HDA9 associates with the *CCAC* motifs in the promoters of *CYP707A1* and *CYP707A2*. These results indicated that HDA9, together with ABI4, played an important role in ABA catabolism-mediated drought stress response by negatively regulating transcription of *CYP707A1* and *CYP707A2*.

Both HDA9 and ABI4 Act in ABA-Dependent Drought Stress Response

We found that ABA-dependent signal transduction regulated by the HDA9-ABI4 complex is essential for the ABA-mediated plant responses to drought stress. To confirm the genetic interaction between HDA9 and ABI4, we generated an *hda9-1abi4* double mutant by crossing an *hda9-1* and an *abi4* single mutant. To investigate the hypersensitivity of the *hda9-1abi4* double mutant to drought stress, we tested the phenotypes of WT, *hda9-1*, *abi4* single mutants, and the *hda9-1abi4* double mutant under drought stress conditions. When exposed to drought stress, the survival rates of the *hda9-1* and *hda9-1abi4* mutants were approximately 14.58 and 9.72%, respectively, while that of WT was approximately 43.06% (**Figure 7A**). However, drought sensitivity of *abi4* single mutant was similar with that of WT (**Figure 7**). In response to drought stress, leaf chlorosis in the *hda9-1abi4* double mutant appeared faster than in the *hda9-1* mutant (**Figure 7A**). In addition, water loss in the *hda9-1* (approximately 12.39 to 20.87%) and *hda9-1abi4* (approximately 12.21 to 23.31%) mutants was faster than in the WT and *abi4* mutant (**Figure 7B**). Water loss in the *hda9-1abi4* double mutant increased by approximately 1.51 to 4.98% than that of *hda9-1* single mutant (**Figure 7B**). Moreover, the *hda9-1* and *hda9-1abi4* mutants had more significant effects on drought-induced leaf senescence than the *abi4* mutant (**Figure 7A** and **Supplemental Figure S6**). These results suggested that

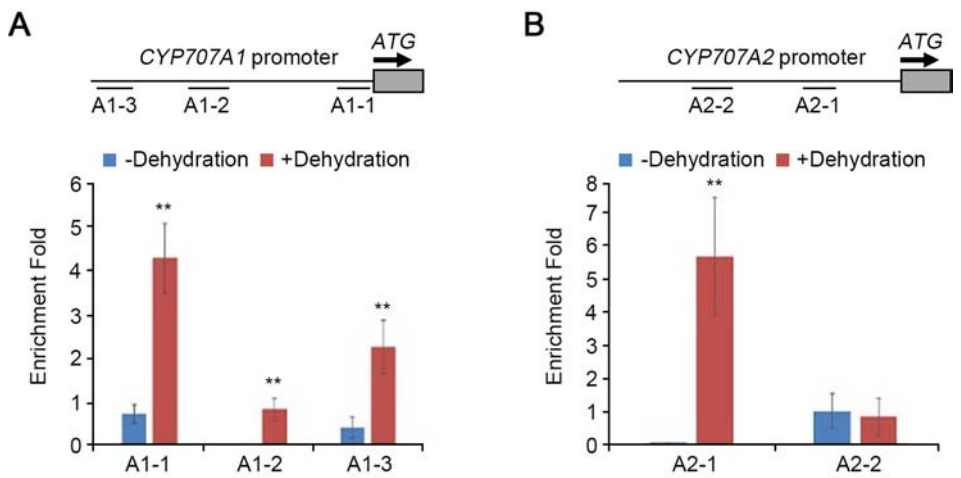

FIGURE 6 | HDA9 is associated with the promoters of *CYP707A1* and *CYP707A2* in dehydration response. The ChIP assays of the *CYP707A1* and *CYP707A2* chromatin regions associated with HDA9. The ChIP assays were performed on nuclear proteins extracted from two-week-old seedling *hda9-1*/HDA9 (with HA tag) plants with/without dehydration stress. Chromatin complex was immunoprecipitated with anti-HA antibody. Samples were quantified by real-time qPCR using specific primers for the amplicons on the different regions of the *CYP707A1* and *CYP707A2* promoter. Schematic drawing of the *CYP707A1* (at the top of **A**) and *CYP707A2* (at the top pf **B)** locus and locations of the ChIP assay amplicons (A1-1 to A1-3, A2-1 and A2-2). *TUBULIN4* expression was assessed as the internal control. The ChIP results were presented as fold enrichment of nontarget DNA. Bars represent mean ± SD of four biological replicates with three technical replicates each. Asterisks represent significant differences from the WT (**, p-value < 0.01; Student's *t*-test).

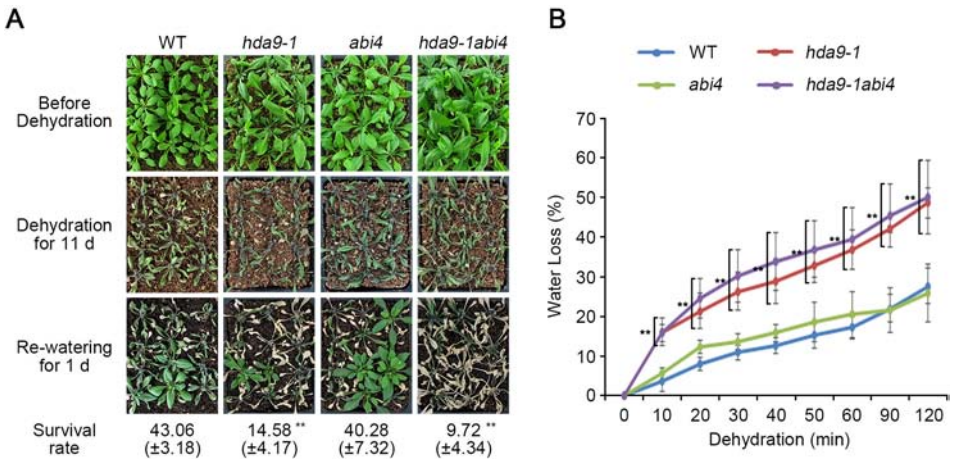

FIGURE 7 | The *hda9-1abi4* double mutants are sensitive to dehydration. **(A)** One-week-old plants were transferred to soil and grown for an additional one week. Photographs of plants were taken before and after dehydration treatment. Water was withheld from two-week-old plants for 13 d, and then plants were rewatered for 1 d before the photograph was taken. Quantitation of the survival rate of WT, *hda9-1*, *abi4*, and *hda9-1abi4* plants. The values of survival rate indicated means ± SE of n = 3 biological replicates of at least 36 plants for each experiment. **(B)** Water loss assay. Water loss is presented as the percentage of weight loss versus initial fresh weight from three-week-old WT, *hda9-1*, *abi4*, and *hda9-1abi4* plants. Water loss was calculated from the results of three independent experiments. The values of survival rate indicated means ± SE of n = 3 biological replicates of at least eight plants for each experiment. Asterisks represent significant differences from the WT (**, *p*-value < 0.01; Student's *t*-test).

HDA9 and ABI4 function together to mediate plant tolerance to drought stress.

To investigate the transcripts patterns of *CYP707A1* and *CYP707A2* in the *hda9-1abi4* double mutant under drought stress conditions, we performed qRT-PCR assays in WT, *hda9-1*, *abi4* single mutants, and the *hda9-1abi4* double mutant. The transcription of *CYP707A1* and *CYP707A2* was significantly up-regulated in *hda9-1* and *hda9-1abi4* double mutants compared to that in the WT (**Figure 8**). Their expression was also induced in *abi4* mutant even though the induction level is lower than that in *hda9-1* and *hda9-1abi4* double mutants. However, the transcript levels of *Lhcb1.2*, *AOX1a*, *ACS4*, and *ACS8* were not affected in the *hda9-1abi4* plants by drought stress (**Supplemental Figure S7**). These results demonstrated that HDA9 act as a key component in the ABA-dependent drought stress response.

DISCUSSION

Members of the RPD3/HDA1 family of HDACs act as crucial components for negative regulation of gene expression in diverse developmental processes and environmental stress signaling (Tian and Chen, 2001; Tian et al., 2003; Zhou et al., 2005; Long et al., 2006; Chen and Wu, 2010). *Arabidopsis* HDA6 and HDA19 are well known for their roles in abiotic stress signaling *via* the formation of repressive complexes. HDA6 associates with HD2C and regulates the expression of abiotic stress-responsive genes, including *ABI1*, *ABI2*, and *ERF4*, through histone modifications (Luo et al., 2012b). The repressive complexes of HDA19 with ERF3, ERF4, ERF7, SIN3, and SAP18, are core chromatin remodeling complexes in abiotic stress responses, acting by mediating histone deacetylation (Song et al., 2005; Song and Galbraith, 2006). Compared with HDA6 and HDA19, less was known about how HDA9 acts in signal transduction during abiotic stress responses. Based on our results, we propose a model for the mechanism by which HDA9 modulates ABA-dependent drought stress signaling in plants (**Figure 9**). In WT plants, the expression of ABA catabolism-related genes (*CYP707As*; *e.g.*, *CYP707A1* and *CYP707A2*), changed ABA from an active to an inactive form, 8′-hydroxyl ABA, to regulate ABA homeostasis during seed germination and plant growth. However, in plants exposed to drought stress, HDA9 together with ABI4, directly represses the expression of *CYP707As*, which improved drought tolerance through the maintenance of ABA levels in the plant. Moreover, ABA levels by ABA catabolism-related genes are enough to efficiently activate drought stress-responsive gene expression, although ABA levels rapidly increased through ABA biosynthesis under drought stress. Therefore, the HDA9–ABI4 complex most likely affects a subset of the early stages of ABA-dependent signal transduction in drought stress tolerance.

Physiological Action of HDA9 in ABA-Dependent Drought Stress Responses

Histone modifications, such as histone acetylation and deacetylation, play crucial roles in a wide range of developmental processes in plants by regulating gene expression (He et al., 2003). In particular, class I members of the RPD3/HDA1 superfamily include well-characterized HDACs, such as HDA6 and HDA19 (Hollender and Liu, 2008; Liu et al., 2014). Recent studies reported that *hda9* mutants exhibited various developmental abnormalities, including early flowering, small seedlings, slightly bulged silique tips, and reduced seed dormancy (Kim et al., 2013; van Zanten et al., 2014;

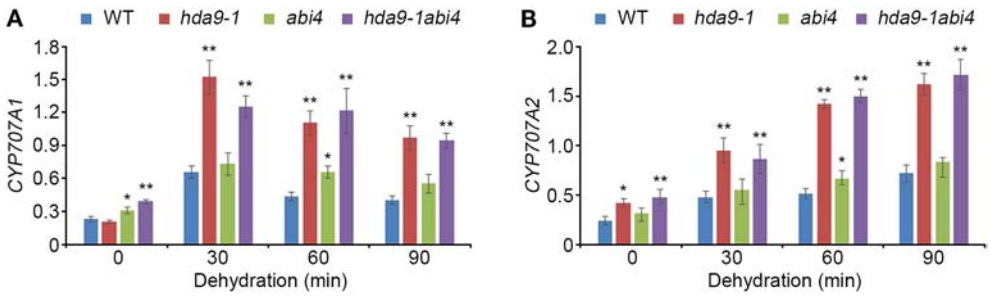

FIGURE 8 | HDA9 and ABI4 regulate *CYP707A1* and *CYP707A2* expression to dehydration. **(A, B)** Quantitative RT-PCR analyses of *CYP707A1* **(A)** and *CYP707A2* **(B)** in WT, *hda9-1*, *abi4*, and *hda9-1abi4* after dehydration stress treatment. Total RNA was extracted from 10-d-old seedlings treated with dehydration stress for indicated times. Expression of *TUBULIN8* was used for normalization. Bars represent mean ± SD of three biological replicates with three technical replicates each. Asterisks represent significant differences from the WT (*, 0.01 < *p*-value ≤ 0.05; **, *p*-value < 0.01; Student's *t*-test).

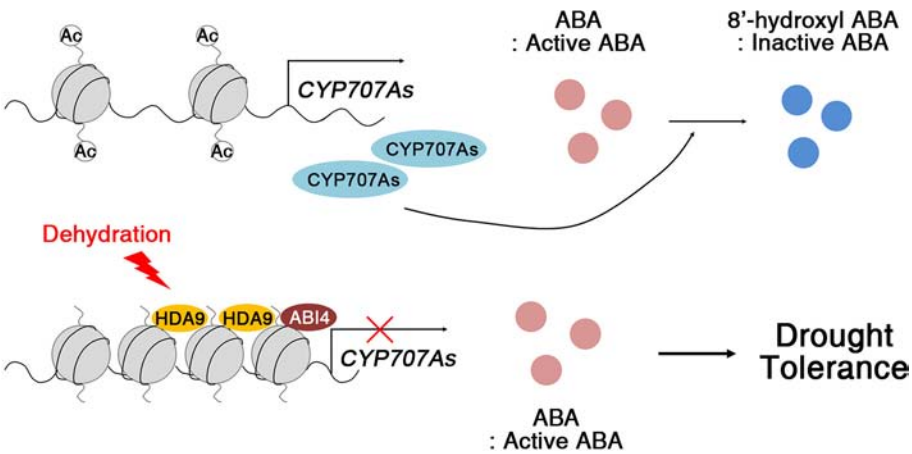

FIGURE 9 | Proposed working model of HDA9 function in drought stress response. In the absence of dehydration stress, *CYP707s* are expressed and regulate ABA hydroxylation. Drought stress triggers HDA9 and ABI4 binding to promoters of *CYP707A1* and *CYP707A2* to repress expression of *CYP707s*. ABA accumulates in the plant and activates dehydration tolerance.

Kang et al., 2015; Kim et al., 2016). The *hda9* mutant showed significant insensitivity to ABA in seed germination (**Figures 1A, B**). Consistently, it was previously reported that the seed germination of the *hda9-1* mutant was slightly enhanced compared to that of WT under 0.1 μM ABA conditions (van Zanten et al., 2014). We found that HDA9 regulated stomatal closure in the presence of exogenous ABA (**Figures 1C, D**). Moreover, the *hda9* mutants were hypersensitive to drought stress (**Figure 3**). These facts suggested that HDA9 plays an indispensable role in drought stress signal transduction by the histone modifications that determine the rate and sensitivity of downstream processes.

Drought stress promoted premature leaf senescence by phytohormone regulatory factors, particularly ABA homeostasis mechanisms (Asad et al., 2019). ABA acts as an important regulator in age-dependent physiological processes from seed germination to leaf senescence (Nambara and Marion-Poll, 2005; Wang et al., 2016; Liao et al., 2018). ABA homeostasis mechanism in ABA-mediated leaf senescence initiates from ABA biosynthesis and catabolism, ABA transport, and ABA signaling receptors (Asad et al., 2019). Then, the mechanisms of ABA-dependent leaf senescence occurred following chloroplast degradation, decline of photosynthesis, reactive oxygen species (ROS) generation, and accumulation of secondary messenger Ca^{2+} (Asad et al., 2019). We showed that leaf senescence in the *hda9-1* and *hda9-1abi4* mutants quickly progressed due to chloroplast degradation and reduced photosynthesis during drought stress (**Figure 7A** and **Supplemental Figure S6**). This suggests that HDA9 may participate in modulating leaf senescence in response to drought stress.

HDA9–ABI4 Complex Regulates Transcriptional Cascades in ABA-Dependent Signal Transduction

ABA responses in plants were mediated by numerous diverse transcription factors, indicating that transcriptional cascades are essential in ABA signal transduction and likely involved formation of a complex with ABA-dependent *cis*-regulatory element, such as ABA response element (ABRE) and ABRE-coupling element (ABRE-CE) (Busk and Pagès, 1998; Mitsuda and Ohme-Takagi, 2009; Hubbard et al., 2010; Baldoni et al., 2015). The most common transcription factors in ABA-dependent signal transduction were ABI3, ABI4, and ABI5, which regulated ABA levels during seed dormancy and germination (Söderman et al., 2000; Nakamura et al., 2001). We showed that HDA9 physically interacts with ABI4 but does not associate with other major transcription factors in ABA responses (**Figure 3** and **Supplementary Figure S3**). ABI4 transcription factor mediates phytohormone homeostasis during seed germination by regulating ABA catabolism-related and gibberellic acid (GA) biosynthesis-related gene expressions (Shu et al., 2013). In addition, the ABI4 loss-of-function mutant (*abi4-101*) exhibits highly tolerant phenotypes to several abiotic stress, such as ABA, salt, mannitol and sugar stress (Daszkowska-Golec et al., 2013). We showed that transcriptional expression of *CYP707A1* and *CYP707A2* in the *hda9-1*, *hda9-2*, and *hda9-1abi4* mutants were significantly increased compared to that in the WT under drought stress (**Figures 4** and **8**). In addition, the ABA level in the *hda9* mutant was decreased under both non-stress and drought stress conditions (**Figure 5**). Therefore, our results demonstrated that the effect of ABA in increasing the expression of *CYP707A1* and *CYP707A2* was largely impaired in the *hda9* mutants, indicating that HDA9 is a transcriptional regulator required for the proper expression of ABA catabolism-related genes in an ABA signaling pathway.

CONCLUSION

We characterized the function of HDA9, a RPD3-type HISTONE DEACETYLASE 9, in ABA-dependent drought stress response. The *hda9* mutants were tolerant during seed germination and stomata irregularity to exogenous ABA. The *hda9-1* mutants and *hda9-1abi4* double mutant were hypersensitive to drought stress, suggesting that HDA9 negatively regulates ABA catabolism-related genes, *CYP707A1* and *CYP707A2*. Our results demonstrate that HDA9 acts as an important negative regulator in transcriptional regulation of ABA catabolism-related genes, such as *CYP707A1* and *CYP707A2* in plant response to drought stress.

DATA AVAILABILITY STATEMENT

All datasets generated for this study are included in the article/ **Supplementary Material**.

AUTHOR CONTRIBUTIONS

DB, MK, and D-JY designed the experiments. DB and GS performed most of the experiments, and MK and D-JY wrote the manuscript. SL discussed and commented on the results and manuscripts. MS performed some of the experiments. D-JY, MK, and DB provided funding for research work.

FUNDING

This work was supported by the Next Generation BioGreen21 Program [SSAC, grant number PJ01318201 (to D-JY) and PJ01318202 (to MK)], the Rural Development Administration Republic of Korea, and the Basic Science Research Program through the National Research Foundation of Korea (NRF) funded by the Ministry of Education [2015R1A6A1A03031413 (to MK), 2016R1D1A1B01011803 (to DB) and Global Research Laboratory 2017K1A1A2013146 (to D-JY)].

ACKNOWLEDGMENTS

We thank Professor Yoo-Sun Noh (Seoul National University) for providing the seed of the *hda9-1*/HDA9 complementation plant.

SUPPLEMENTARY MATERIAL

The Supplementary Material for this article can be found online at: https://www.frontiersin.org/articles/10.3389/fpls.2020.00143/full#supplementary-material

REFERENCES

Asad, M. A. U., Zakari, S. A., Zhao, Q., Zhou, L., Ye, Y., and Cheng, F. (2019). Abiotic stresses intervene with aba signaling to induce destructive metabolic pathways leading to death: premature leaf senescence in plants. *Int. J. Mol. Sci.* 20 (2), E256. doi: 10.3390/ijms20020256

Aufsatz, W., Mette, M. F., van der Winden, J., Matzke, M., and Matzke, A. J. (2002). HDA6, a putative histone deacetylase needed to enhance DNA methylation induced by double-stranded RNA. *EMBO J.* 21 (24), 6832–6841. doi: 10.1093/emboj/cdf663

Baldoni, E., Genga, A., and Cominelli, E. (2015). Plant MYB transcription factors: their role in drought response mechanisms. *Int. J. Mol. Sci.* 16 (7), 15811–15851. doi: 10.3390/ijms160715811

Blatt, M. R. (2000). Cellular signaling and volume control in stomatal movements in plants. *Ann. Rev. Cell Dev. Biol.* 16, 221–241. doi: 10.1146/annurev.cellbio.16.1.221

Bohnert, H. J., and Sheveleva, E. (1998). Plant stress adaptations-making metabolism move. *Curr. Opin. Plant Biol.* 1 (3), 267–274. doi: 10.1016/S1369-5266(98)80115-5

Bossi, F., Cordoba, E., Dupré, P., Mendoza, M. S., Román, C. S., and León, P. (2009). The Arabidopsis ABA-INSENSITIVE (ABI) 4 factor acts as a central transcription activator of the expression of its own gene, and for the induction of ABI5 and SBE2.2 genes during sugar signaling. *Plant J.* 59 (3), 359–374.

Busk, P. K., and Pagès, M. (1998). Regulation of abscisic acid-induced transcription. *Plant Mol. Biol.* 37 (3), 425–435. doi: 10.1023/A:1006058700720

Chen, L. T., and Wu, K. (2010). Role of histone deacetylases HDA6 and HDA19 in ABA and abiotic stress response. *Plant Signal Behav.* 5 (10), 1318–1320. doi: 10.4161/psb.5.10.13168

Chen, X., Lu, L., Mayer, K. S., Scalf, M., Qian, S., Lomax, A., et al. (2016). POWERDRESS interacts with histone deacetylase 9 to promote aging in arabidopsis. *Elife* 5, e17214. doi: 10.7554/eLife.17214

Cigliano, R. A., Cremona, G., Paparo, R., Termolino, P., Perrella, G., Gutzat, R., et al. (2013). Histone deacetylase AtHDA7 is required for female gametophyte and embryo development in Arabidopsis. *Plant Physiol.* 163 (1), 431–440. doi: 10.1104/pp.113.221713

Cutler, S. R., Rodriguez, P. L., Finkelstein, R. R., and Abrams, S. R. (2010). Abscisic acid: emergence of a core signaling network. *Annu. Rev. Plant Biol.* 61, 651–679. doi: 10.1146/annurev-arplant-042809-112122

Daszkowska-Golec, A., Wojnar, W., Rosikiewicz, M., Szarejko, I., Maluszynski, M., Szweykowska-Kulinska, Z., et al. (2013). Arabidopsis suppressor mutant of abh1 shows a new face of the already known players: ABH1 (CBP80) and ABI4-in response to ABA and abiotic stresses during seed germination. *Plant Mol. Biol.* 81 (1-2), 189–209.

Dong, T., Park, Y., and Hwang, I. (2015). Abscisic acid: biosynthesis, inactivation, homoeostasis and signalling. *Essays Biochem.* 58, 29–48. doi: 10.1042/bse0580029

Dong, Z., Yu, Y., Li, S., Wang, J., Tang, S., and Huang, R. (2016). Abscisic acid antagonizes ethylene production through the ABI4-mediated transcriptional repression of ACS4 and ACS8 in Arabidopsis. *Mol. Plant* 9 (1), 126–135. doi: 10.1016/j.molp.2015.09.007

Finkelstein, R. R., and Lynch, T. J. (2000). Abscisic acid inhibition of radicle emergence but not seedling growth is suppressed by sugars. *Plant Physiol.* 122 (4), 1179–1186. doi: 10.1104/pp.122.4.1179

Finkelstein, R. R., and Rock, C. D. (2002). Abscisic acid biosynthesis and response. *Arabidopsis Book.* 1, e0058. doi: 10.1199/tab.0058

Finkelstein, R. R., Gampala, S. S., and Rock, C. D. (2002). Abscisic acid signaling in seeds and seedlings. *Plant Cell.* Suppl, S15–S45. doi: 10.1105/tpc.010441

Finkelstein, R., Reeves, W., Ariizumi, T., and Steber, C. (2008). Molecular aspects of seed dormancy. *Annu. Rev. Plant Biol.* 59, 387–415. doi: 10.1146/annurev.arplant.59.032607.092740

Giraud, E., Van Aken, O., Ho, L. H., and Whelan, J. (2009). The transcription factor abi4 is a regulator of mitochondrial retrograde expression of alternative oxidase1a. *Plant Physiol.* 150 (3), 1286–1296. doi: 10.1104/pp.109.139782

He, Y., Michaels, S. D., and Amasino, R. M. (2003). Regulation of flowering time by histone acetylation in Arabidopsis. *Science* 302 (5651), 1751–1754. doi: 10.1126/science.1091109

Hollender, C., and Liu, Z. (2008). Histone deacetylase genes in Arabidopsis development. *J. Integr. Plant Biol.* 50 (7), 875–885. doi: 10.1111/j.1744-7909.2008.00704.x

Hubbard, K. E., Nishimura, N., Hitomi, K., Getzoff, E. D., and Schroeder, J. I. (2010). Early abscisic acid signal transduction mechanisms: newly discovered components and newly emerging questions. *Genes Dev.* 24 (16), 1695–1708. doi: 10.1101/gad.1953910

Jacobsen, J. V., Pearce, D. W., Poole, A. T., Pharis, R. P., and Mander, L. N. (2002). Abscisic acid, phaseic acid and gibberellin contents associated with dormancy and germination in barley. *Physiol. Plant* 115 (3), 428–441. doi: 10.1034/j.1399-3054.2002.1150313.x

König, A. C., Hartl, M., Pham, P. A., Laxa, M., Boersema, P. J., Orwat, A., et al. (2014). The Arabidopsis class II sirtuin is a lysine deacetylase and interacts with mitochondrial energy metabolism. *Plant Physiol.* 164 (3), 1401–1414. doi: 10.1104/pp.113.232496

Kang, M. J., Jin, H. S., Noh, Y. S., and Noh, B. (2015). Repression of flowering under a noninductive photoperiod by the HDA9- AGL19-FT module in Arabidopsis. *New Phytol.* 206 (1), 281–294. doi: 10.1111/nph.13161

Kim, W., Latrasse, D., Servet, C., and Zhou, D. X. (2013). Arabidopsis histone deacetylase HDA9 regulates flowering time through repression of AGL19. *Biochem. Biophys. Res. Commun.* 432 (2), 394–398. doi: 10.1016/j.bbrc.2012.11.102

Kim, Y. J., Wang, R., Gao, L., Li, D., Xu, C., Mang, H., et al. (2016). POWERDRESS and HDA9 interact and promote histone H3 deacetylation at specific genomic sites in Arabidopsis. *Proc. Natl. Acad. Sci. U.S.A.* 113 (51), 14858–14863. doi: 10.1073/pnas.1618618114

Koussevitzky, S., Nott, A., Mockler, T. C., Hong, F., Sachetto-Martins, G., Surpin, M., et al. (2007). Signals from chloroplasts converge to regulate nuclear gene expression. *Science* 316 (5825), 715–719. doi: 10.1126/science.1140516

Kushiro, T., Okamoto, M., Nakabayashi, K., Yamagishi, K., Kitamura, S., Asami, T., et al. (2004). The Arabidopsis cytochrome P450 CYP707A encodes ABA 8'-hydroxylases: key enzymes in ABA catabolism. *EMBO J.* 23 (7), 1647–1656. doi: 10.1038/sj.emboj.7600121

Lee, K. H., Piao, H. L., Kim, H. Y., Choi, S. M., Jiang, F., Hartung, W., et al. (2006). Activation of glucosidase *via* stress-induced polymerization rapidly increases active pools of abscisic acid. *Cell* 126 (6), 1109–1120. doi: 10.1016/j.cell.2006.07.034

Lee, K., Park, O. S., Jung, S. J., and Seo, P. J. (2016). Histone deacetylation-mediated cellular dedifferentiation in Arabidopsis. *J. Plant Physiol.* 191, 95–100. doi: 10.1016/j.jplph.2015.12.006

Liao, Y., Bai, Q., Xu, P., Wu, T., Guo, D., Peng, Y., et al. (2018). Mutation in rice abscisic Acid2 results in cell death, enhanced disease-resistance, altered seed dormancy and development. *Front. Plant Sci.* 9, 405. doi: 10.3389/fpls.2018.00405

Liu, C., Li, L. C., Chen, W., Chen, X., Xu, Z. H., and Bai, S. N. (2013). HDA18 affects cell fate in Arabidopsis root epidermis *via* histone acetylation at four kinase genes. *Plant Cell.* 25 (1), 257–269. doi: 10.1105/tpc.112.107045

Liu, X., Yang, S., Zhao, M., Luo, M., Yu, C. W., Chen, C. Y., et al. (2014). Transcriptional repression by histone deacetylases in plants. *Mol. Plant* 7 (5), 764–772. doi: 10.1093/mp/ssu033

Long, J. A., Ohno, C., Smith, Z. R., and Meyerowitz, E. M. (2006). TOPLESS regulates apical embryonic fate in Arabidopsis. *Science* 312 (5779), 1520–1523. doi: 10.1126/science.1123841

Lopez-Molina, L., Mongrand, S., and Chua, N. H. (2001). A postgermination developmental arrest checkpoint is mediated by abscisic acid and requires the ABI5 transcription factor in Arabidopsis. *Proc. Natl. Acad. Sci. U. S. A.* 98 (8), 4782–4787. doi: 10.1073/pnas.081594298

Lopez-Molina, L., Mongrand, S., McLachlin, D., Chait, B., and Chua, N. H. (2002). ABI5 acts downstream of ABI3 to execute an ABA-dependent growth arrest during germination. *Plant J.* 32 (3), 317–328. doi: 10.1046/j.1365-313X.2002.01430.x

Luo, M., Liu, X., Singh, P., Cui, Y., Zimmerli, L., and Wu, K. (2012a). Chromatin modifications and remodeling in plant abiotic stress responses. *Biochim. Biophys. Acta* 1819 (2), 129–136. doi: 10.1016/j.bbagrm.2011.06.008

Luo, M., Wang, Y. Y., Liu, X., Yang, S., Lu, Q., Cui, Y., et al. (2012b). HD2C interacts with HDA6 and is involved in ABA and salt stress response in Arabidopsis. *J. Exp. Bot.* 63 (8), 3297–3306. doi: 10.1093/jxb/ers059

Mitsuda, N., and Ohme-Takagi, M. (2009). Functional analysis of transcription factors in Arabidopsis. *Plant Cell Physiol.* 50 (7), 1232–1248. doi: 10.1093/pcp/pcp075

Nakamura, S., Lynch, T. J., and Finkelstein, R. R. (2001). Physical interactions between ABA response loci of Arabidopsis. *Plant J.* 26 (6), 627–635. doi: 10.1046/j.1365-313x.2001.01069.x

Nambara, E., and Marion-Poll, A. (2005). Abscisic acid biosynthesis and catabolism. *Annu. Rev. Plant Biol.* 56, 165–185. doi: 10.1146/annurev.arplant.56.032604.144046

Okamoto, M., Kuwahara, A., Seo, M., Kushiro, T., Asami, T., Hirai, N., et al. (2006). CYP707A1 and CYP707A2, which encode abscisic acid 8'-hydroxylases, are indispensable for proper control of seed dormancy and germination in Arabidopsis. *Plant Physiol.* 141 (1), 97–107. doi: 10.1104/pp.106.079475

Pan, Y., Michael, T. P., Hudson, M. E., Kay, S. A., Chory, J., and Schuler, M. A. (2009). Cytochrome P450 monooxygenases as reporters for circadian-regulated pathways. *Plant Physiol.* 150 (2), 858–878. doi: 10.1104/pp.108.130757

Pandey, R., Müller, A., Napoli, C. A., Selinger, D. A., Pikaard, C. S., Richards, E. J., et al. (2002). Analysis of histone acetyltransferase and histone deacetylase families of Arabidopsis thaliana suggests functional diversification of chromatin modification among multicellular eukaryotes. *Nucleic Acids Res.* 30 (23), 5036–5055. doi: 10.1093/nar/gkf660

Park, J., Lim, C. J., Khan, I. U., Jan, M., Khan, H. A., Park, H. J., et al. (2018). Identification and molecular characterization of HOS15-interacting proteins in Arabidopsis thaliana. *J. Plant Biol.* 61, 336–345. doi: 10.1007/s12374-018-0313-2

Penfield, S., Li, Y., Gilday, A. D., Graham, S., and Graham, I. A. (2006). Arabidopsis ABA INSENSITIVE4 regulates lipid mobilization in the embryo and reveals repression of seed germination by the endosperm. *Plant Cell.* 18 (8), 1887–1899. doi: 10.1105/tpc.106.041277

Raghavendra, A. S., Gonugunta, V. K., Christmann, A., and Grill, E. (2010). ABA perception and signalling. *Trends Plant Sci.* 15 (7), 395–401. doi: 10.1016/j.tplants.2010.04.006

Ryu, H., Cho, H., Bae, W., and Hwang, I. (2014). Control of early seedling development by BES1/TPL/HDA19-mediated epigenetic regulation of ABI3. *Nat. Commun.* 5, 4138. doi: 10.1038/ncomms5138

Söderman, E. M., Brocard, I. M., Lynch, T. J., and Finkelstein, R. R. (2000). Regulation and function of the Arabidopsis ABA-insensitive4 gene in seed and abscisic acid response signaling networks. *Plant Physiol.* 124 (4), 1752–1765. doi: 10.1104/pp.124.4.1752

Saleh, A., Alvarez-Venegas, R., and Avramova, Z. (2008). An efficient chromatin immunoprecipitation (ChIP) protocol for studying histone modifications in Arabidopsis plants. *Nat. Protoc.* 3 (6), 1018–1025. doi: 10.1038/nprot.2008.66

Shu, K., Zhang, H., Wang, S., Chen, M., Wu, Y., Tang, S., et al. (2013). ABI4 regulates primary seed dormancy by regulating the biogenesis of abscisic acid and gibberellins in Arabidopsis. *PloS Genet.* 9 (6), e1003577. doi: 10.1371/journal.pgen.1003577

Shu, K., Liu, X. D., Xie, Q., and He, Z. H. (2016). Two faces of one seed: hormonal regulation of dormancy and germination. *Mol. Plant* 9 (1), 34–45. doi: 10.1016/j.molp.2015.08.010

Song, C. P., and Galbraith, D. W. (2006). AtSAP18, an orthologue of human SAP18, is involved in the regulation of salt stress and mediates transcriptional repression in Arabidopsis. *Plant Mol. Biol.* 60 (2), 241–257. doi: 10.1007/s11103-005-3880-9

Song, C. P., Agarwal, M., Ohta, M., Guo, Y., Halfter, U., Wang, P., et al. (2005). Role of an Arabidopsis AP2/EREBP-type transcriptional repressor in abscisic acid and drought stress responses. *Plant Cell.* 17 (8), 2384–2396. doi: 10.1105/tpc.105.033043

Sridha, S., and Wu, K. (2006). Identification of AtHD2C as a novel regulator of abscisic acid responses in Arabidopsis. *Plant J.* 46 (1), 124–133. doi: 10.1111/j.1365-313X.2006.02678.x

Stone, S. L., Williams, L. A., Farmer, L. M., Vierstra, R. D., and Callis, J. (2006). Keep on going, a ring e3 ligase essential for arabidopsis growth and development, is involved in abscisic acid signaling. *Plant Cell* 18 (12), 3415–3428. doi: 10.1105/tpc.106.046532

Tian, L., and Chen, Z. J. (2001). Blocking histone deacetylation in Arabidopsis induces pleiotropic effects on plant gene regulation and development. *Proc. Natl. Acad. Sci. U.S.A.* 98 (1), 200–205. doi: 10.1073/pnas.98.1.200

Tian, L., Wang, J., Fong, M. P., Chen, M., Cao, H., Gelvin, S. B., et al. (2003). Genetic control of developmental changes induced by disruption of Arabidopsis histone deacetylase 1 (AtHD1) expression. *Genetics* 165 (1), 399–409.

van Zanten, M., Zöll, C., Wang, Z., Philipp, C., Carles, A., Li, Y., et al. (2014). Histone deacetylase 9 represses seedling traits in Arabidopsis thaliana dry seeds. *Plant J.* 80 (3), 475–488. doi: 10.1111/tpj.12646

Verdin, E., and Ott, M. (2015). 50 years of protein acetylation: from gene regulation to epigenetics, metabolism and beyond. *Nat. Rev. Mol. Cell Biol.* 16 (4), 258–264. doi: 10.1038/nrm3931

Vishwakarma, K., Upadhyay, N., Kumar, N., Yadav, G., Singh, J., Mishra, R. K., et al. (2017). Abscisic acid signaling and abiotic stress tolerance in plants: a review on current knowledge and future prospects. *Front. Plant Sci.* 8, 161. doi: 10.3389/fpls.2017.00161

Wang, Z., Cao, H., Chen, F., and Liu, Y. (2014). The roles of histone acetylation in seed performance and plant development. *Plant Physiol. Biochem.* 84, 125–133. doi: 10.1016/j.plaphy.2014.09.010

Wang, F., Liu, J., Chen, M., Zhou, L., Li, Z., Zhao, Q., et al. (2016). Involvement of abscisic acid in psii photodamage and d1 protein turnover for light-induced premature senescence of rice flag leaves. *PloS One* 11 (8), e0161203. doi: 10.1371/journal.pone.0161203

Xiong, L., and Zhu, J. K. (2003). Regulation of abscisic acid biosynthesis. *Plant Physiol.* 133 (1), 29–36. doi: 10.1104/pp.103.025395

Xu, W., Jia, L., Shi, W., Liang, J., Zhou, F., Li, Q., et al. (2013). Abscisic acid accumulation modulates auxin transport in the root tip to enhance proton secretion for maintaining root growth under moderate water stress. *New Phytol.* 197 (1), 139–150. doi: 10.1111/nph.12004

Yamaguchi-Shinozaki, K., and Shinozaki, K. (2006). Transcriptional regulatory networks in cellular responses and tolerance to dehydration and cold stresses. *Annu. Rev. Plant Biol.* 57, 781–803. doi: 10.1146/annurev.arplant.57.032905.105444

Yuan, K., and Wysocka-Diller, J. (2006). Phytohormone signaling pathways interact with sugars during seed germination and seedling development. *J. Exp. Bot.* 57 (12), 3359–3367. doi: 10.1093/jxb/erl096

Yuan, L., Liu, X., Luo, M., Yang, S., and Wu, K. (2013). Involvement of histone modifications in plant abiotic stress responses. *J. Integr. Plant Biol.* 55 (10), 892–901. doi: 10.1111/jipb.12060

Zhang, Z. W., Feng, L. Y., Cheng, J., Tang, H., Xu, F., Zhu, F., et al. (2013). The roles of two transcription factors, ABI4 and CBFA, in ABA and plastid signalling and stress responses. *Plant Mol. Biol.* 83 (4-5), 445–458. doi: 10.1007/s11103-013-0102-8

Zheng, Y., Ding, Y., Sun, X., Xie, S., Wang, D., Liu, X., et al. (2016). Histone deacetylase HDA9 negatively regulates salt and drought stress responsiveness in Arabidopsis. *J. Exp. Bot.* 67 (6), 1703–1713. doi: 10.1093/jxb/erv562

Zhou, C., Labbe, H., Sridha, S., Wang, L., Tian, L., Latoszek-Green, M., et al. (2004). Expression and function of HD2-type histone deacetylases in Arabidopsis development. *Plant J.* 38 (5), 715–724. doi: 10.1111/j.1365-313X.2004.02083.x

Zhou, C., Zhang, L., Duan, J., Miki, B., and Wu, K. (2005). HISTONE DEACETYLASE19 is involved in jasmonic acid and ethylene signaling of pathogen response in Arabidopsis. *Plant Cell.* 17 (4), 1196–1204. doi: 10.1105/tpc.104.028514

Zhu, J. K. (2001). Cell signaling under salt, water and cold stresses. *Curr. Opin. Plant Biol.* 4 (5), 401–406. doi: 10.1016/S1369-5266(00)00192-8

Conflict of Interest: The authors declare that the research was conducted in the absence of any commercial or financial relationships that could be construed as a potential conflict of interest.

frontiers in Plant Science

ORIGINAL RESEARCH
published: 31 March 2020
doi: 10.3389/fpls.2020.00367

DEAR4, a Member of DREB/CBF Family, Positively Regulates Leaf Senescence and Response to Multiple Stressors in *Arabidopsis thaliana*

*Zenglin Zhang, Wei Li, Xiaoming Gao, Mengmeng Xu and Yongfeng Guo**

Tobacco Research Institute, Chinese Academy of Agricultural Sciences, Qingdao, China

Leaf senescence is a programmed developmental process regulated by various endogenous and exogenous factors. Here we report the characterization of the senescence-regulating role of *DEAR4* (AT4G36900) from the DREB1/CBF (dehydration-responsive element binding protein 1/C-repeat binding factor) family in Arabidopsis. The expression of *DEAR4* is associated with leaf senescence and can be induced by ABA, JA, darkness, drought and salt stress. Transgenic plants over-expressing *DEAR4* showed a dramatically enhanced leaf senescence phenotype under normal and dark conditions while the *dear4* knock-down mutant displayed delayed senescence. *DEAR4* over-expressing plants showed decreased seed germination rate under ABA and salt stress conditions as well as decreased drought tolerance, indicating that DEAR4 was involved in both senescence and stress response processes. Furthermore, we found that DEAR4 protein displayed transcriptional repressor activities in yeast cells. DEAR4 could directly repress the expression of a subset of *COLD-REGULATED* (*COR*) and *RESPONSIVE TO DEHYDRATION* (*RD*) genes which have been shown to be involved in leaf longevity and stress response. Also we found that DERA4 could induce the production of Reactive oxygen species (ROS), the common signal of senescence and stress responses, which gives us the clue that DEAR4 may play an integrative role in senescence and stress response via regulating ROS production.

Keywords: *DEAR4*, leaf senescence, stress, ROS, COR, RD, *Arabidopsis thaliana*

OPEN ACCESS

Edited by:
Jinjie Li,
China Agricultural University, China

Reviewed by:
Hong Zhai,
China Agricultural University, China
Kazuo Nakashima,
Japan International Research Center for Agricultural Sciences, Japan

****Correspondence:***
Yongfeng Guo
guoyongfeng@caas.cn

Specialty section:
This article was submitted to Plant Abiotic Stress, a section of the journal Frontiers in Plant Science

Received: *04 November 2019*
Accepted: *13 March 2020*
Published: *31 March 2020*

Citation:
Zhang Z, Li W, Gao X, Xu M and Guo Y (2020) DEAR4, a Member of DREB/CBF Family, Positively Regulates Leaf Senescence and Response to Multiple Stressors in Arabidopsis thaliana. Front. Plant Sci. 11:367. doi: 10.3389/fpls.2020.00367

INTRODUCTION

Senescence is the last stage of leaf development which is influenced by intrinsic and environmental factors including age, nutrients, hormones, darkness, osmotic stress, extreme temperature and pathogens (Lim et al., 2007; Guo and Gan, 2014). Most of the major plant hormones have been reported to affect leaf senescence process: abscisic acid (ABA), ethylene (ETH), jasmonic acid (JA), salicylic acid (SA) and strigolactones function in promoting senescence, while cytokinins (CK), gibberellic acid (GA) and auxin inhibit senescence (Jibran et al., 2013; Li et al., 2013; Penfold and Buchan-Wollaston, 2014; Mostofa et al., 2018). During the process of leaf senescence, cellular

metabolism and structure undergo significant changes, resulting in leaf yellowing. Meanwhile, degradation of macromolecules in senescing leaves functions to remobilize nutrients to support young vegetative organs and reproductive growth. As a mechanism of evolutional fitness, unfavorable environmental conditions can induce precocious senescence leading to reduced yield and quality of crop plants (Wu et al., 2012; Gregersen et al., 2013; Zhang and Zhou, 2013; Yolcu et al., 2017). Senescence execution requires differential expression of a large number of genes a subset of which is called senescence-associated genes (*SAGs*). A number of *SAGs* have been identified to play a regulatory role in leaf senescence. These include genes encoding transcription factors of WRKY, NAC, DREB, MYB, and bZIP family (Woo et al., 2001; Yang et al., 2011; Lee et al., 2012; Vainonen et al., 2012).

Dark-induced senescence (DIS) has been widely used as a model system in leaf senescence study (Liebsch and Keech, 2016). Differential expression of a large number of transcription factor genes during dark-induced leaf senescence have been reported (Song, 2014; Song et al., 2014; Yasuhito et al., 2014) and some of them have been studied for their function in regulating senescence. *AtWRKY22* is induced by darkness, but suppressed by light. Further study reveals that *AtWRKY22* over-expressing plants displayed accelerated senescence, whereas *AtWRKY22* loss-of-function plants showed a delay of senescence under dark condition (Zhou et al., 2011b). *RD26* loss-of-function plants displayed significantly delayed senescence under normal or dark-induced conditions with a higher chlorophyll level detected. By contrast, over-expression of *RD26* led to early leaf senescence (Takasaki et al., 2015; Kamranfar et al., 2018). Over-expression of *CBF2* and *CBF3*, two members of the DREB family in Arabidopsis, significantly delayed the onset of leaf senescence and also delayed leaf senescence induced by hormones and darkness (Sharabi-Schwager et al., 2010a,b). Phytochromes regulate light responses by promoting the degradation of PIFs (Phytochrome-interacting factors). PIF3, 4, and 5 play an important role in natural and dark induced senescence (Yasuhito et al., 2014). Mutations of the *PIFs* genes resulted in a significant delay of natural and dark induced senescence, whereas over-expression of these genes accelerated senescence. Further study revealed that PIF4 can bind the promoter of *NYE1*, the chlorophyll degradation regulatory gene, and *GLK2*, the chloroplast activity maintainer gene, resulting in induction and repression of their expression, respectively (Song et al., 2014; Shi et al., 2017a).

Jasmonic acid is involved in multiple processes including root inhibition, trichome initiation, anthocyanin accumulation, leaf senescence and biotic and abiotic stress responses (Balbi and Devoto, 2008; Wu et al., 2008; Hu et al., 2017; Song et al., 2017; Ono et al., 2019). JA signaling can be initiated by perception of jasmonoyl-L-isoleucine (JA-Ile), which binds to its receptor COI1 (CORONATINE INSENSITIVE1), an F-box domain-containing protein (Balbi and Devoto, 2008; Shan et al., 2011). It has been reported that endogenous JA content increases during leaf senescence and JA biosynthetic genes such as *LOX1*, *LOX3*, and *LOX4* are up-regulated during leaf senescence (Wasternack, 2007; Seltmann and Berger, 2013). Attached or detached leaves displayed precocious senescence under exogenous application of MeJA (Shan et al., 2011; Hu et al., 2017). Further study revealed that MYC2, 3, and 4 redundantly bind to the *SAG29* promoter and activate its expression, leading to activation of JA-induced leaf senescence (Zhu et al., 2015). In contrast, the bHLH family members including bHLH03, bHLH13, bHLH14, and bHLH17 attenuate MYC2/MYC3/MYC4-activated JA-induced leaf senescence by binding to the promoter of *SAG29* and repress its expression. It has been suggested that the activators and repressors mediated in JA-induced leaf senescence can enhance the plant survival rate in various environmental conditions (Qi et al., 2015). In addition, the NAC transcriptional factors *ANAC019*, *ANAC055*, and *RD26* are also direct targets of MYC2 in mediating JA-induced leaf senescence (Zhu et al., 2015). The JA signaling proteins JAZ4 and JAZ8 interact with transcription factor WRKY57 to negatively regulate leaf senescence induced by JA (Jiang et al., 2014). Additionally, the expression of *JAZ7* was significantly increased during darkness. *jaz7* mutant exhibited precocious senescence induced by darkness, suggesting that *JAZ7* plays a negative role in dark-induced leaf senescence (Yu et al., 2016). The Evening Complex (EC), a core component of the circadian oscillator, comprising EARLY FLOWERING3 (ELF3), EARLY FLOWERING4 (ELF4) and LUX ARRHYTHMO (LUX), plays essential roles in the plant circadian clock and negatively regulates leaf senescence in Arabidopsis. It has been reported that EC represses the expression of *MYC2* by directly binding to its promoter. *myc2myc3myc4* triple mutants abrogate the accelerated leaf senescence induced by JA in EC mutants (Zhang et al., 2018; Thines et al., 2019). Additionally, JA can positively regulate the ICE-CBF signal to enhance cold stress tolerance in Arabidopsis. Interestingly, endogenous JA content was increased under cold stress conditions. Exogenous application of MeJA enhanced cold stress tolerance. Further study revealed that JAZ1 and JAZ4 play negative roles in the ICE-CBF pathway (Hu et al., 2013, 2017).

As sessile organisms, plants have developed sophisticated mechanisms that are activated and integrated by the expression of thousands of genes to cope with variety of environmental stresses (Yeung et al., 2018; Asad et al., 2019). Many transcriptional factors were found to play key roles in stress response and tolerance. As the largest transcription factor family in Arabidopsis, the AP2/ERF family contains 147 members functionally categorized into the development-associated AP2 and RAV subgroups and the stress response-associated DREB and ERF subgroups (Liu et al., 1998; Sakuma et al., 2002). The DREB/CBF proteins are known to directly regulate target genes in response to various stresses including high salinity, drought and cold stress by directly binding the conserved DRE (Dehydration responsive element)/CRT(C-repeat) *cis*-acting regulatory elements which contains the core sequence CCGAC (Sakuma et al., 2002; Sun et al., 2008). DREB homologs have been identified in a variety of plants species including rice (Dubouzet et al., 2003), cotton (Huang and Liu, 2006; Ma et al., 2014) and soybean (Mizoi et al., 2013). In Arabidopsis, there was 57 DREB transcription factors classified into six groups termed A-1 to A-6 based on the similarities of the AP2/ERF domain (Sazegari et al., 2015). DREB1 including CBF1, CBF2, and CBF3 belongs to

the A-1 clade that play an important role in cold stress response and dark induced senescence process (Xu et al., 2010; Wang et al., 2018). Over-expression of *CBF1* or *CBF3* can also confer plant more capacity of freezing tolerance (Novillo et al., 2004; Zhou et al., 2011a). DREB2 proteins belong to the A-2 clade which is involved in regulation of drought and heat response. Over-expression of *DREB2A* improved survival rate under drought or heat stress (Schramm et al., 2008). In the A-6 clade, *RAP2.4* was induced by salt stress. Over-expression of *RAP2.4* can enhance drought tolerance in Arabidopsis. Moreover, RAP2.4A is involved in regulating expression of several chloroplast-targeted antioxidant genes. The expression of *RAP2.4B* was increased under heat stress conditions. Plants over-expressing *RAP2.4B* or *RAP2.4* were hypersensitive to exogenous ABA at germination. Over-expression of *Rap2.4f* (*At4g28140*) caused precocious senescence according to the detection of increasing chlorophyll degradation and up-regulation of many *SAGs* (Lin et al., 2008; Xu et al., 2010; Rae et al., 2011).

There are six *DEAR* genes named *DEAR1* to *DEAR6* within the Arabidopsis genome that contain sequences with homology to the DREB domain and EAR motif. Plants over-expressing *DEAR1* displayed phenotypes of cell death, increased resistance to pathogen infection and reduced freezing tolerance. Additionally, DEAR1 suppressed the expression of *DREB1/CBF* family genes induced by cold treatment, which resulted in reduced freezing tolerance (Wang et al., 2008; Tsutsui et al., 2009). *DEAR4* was identified as a regulator of cell death in the hypocotyls-root transition zone using the inducible over-expression strategy (Coego et al., 2014). In this study, we characterize the function of DEAR4, a member of DREB/CBF family, in leaf senescence and stress response. The expression of *DEAR4* was strongly induced by developmental stage, darkness and multiple stresses. Phenotype analysis revealed that DEAR4 was involved in the senescence process induced by age and darkness. Further study revealed that over-expression of *DEAR4* led to reduce expression of *COR* and *RD* genes which are involved in senescence and stress regulation. Our findings suggest that DEAR4 is a transcriptional repressor and plays a role in regulating leaf senescence and stress response by repressing the expression of *COR* and *RD* genes.

MATERIALS AND METHODS

Plant Materials, Growth Conditions

Arabidopsis seeds were surface-sterilized by 75% (v/v) ethanol followed by 3 washes with water. Then the seeds were sown on 0.5× Murashige and Skoog medium (MS) and kept at 4°C for 3 day. One-week-old seedlings were transferred into soil. Plants were grown in growth chambers at 22°C under continuously light. The mutant *dear4* (*Salk_010653c*), *dear4-1*(*Salk_045347*) and *DEAR4* inducible over-expression lines *DEAR4-ind-1*(*cs2102284*) and *DEAR4-ind-2*(*cs2102286*) used in this study were obtained from the Arabidopsis Biological Resource Center (ABRC).

Detached Leaf Phenotype Investigation

For natural leaf senescence evaluation, the fifth and sixth rosette leaves of 4-week-old plants were detached for measurements of chlorophyll content and ion leakage rate. In the hormone induced leaf senescence assay, the fifth and sixth rosette leaves of 4-week-old plants were detached and floated on 3 mL of treatment buffer (0.5× MS, 3 mM MES, PH: 5.8) supplemented with 50 μM MeJA. Petri dishes were sealed with parafilm tape, wrapped with double-layer aluminum foil. In the dark induced senescence assay, the fully expanded fifth and sixth rosette leaves were detached from 4-week-old plants grown in soil. Then, detached leaves were placed in petri dishes containing two layers of filter paper soaked in 10 mL of treatment buffer (0.5× MS, 3 mM MES adjust PH to 5.8). Then the petri dishes were wrapped in aluminum foil for 5 days. Three biological replicates were performed.

Chlorophyll Content, Ion Leakage Measurement

For chlorophyll content measurement, detached leaf was weighted and soaked in 96% (v/v) ethanol (3–4 mg of tissue in 1 mL of ethanol) overnight at room temperature in the dark condition. Total chlorophyll content was determined by measuring the absorbance at 646.6 and 663.6 nm as described (Zhang and Guo, 2018). For ion leakage measurement, detached leaves were washed three times with deionized water followed by immersion in deionized water, then gentle shaking for 1–2 h at room temperature. Total conductivity was measured as initial readings data, then samples were boiled and cooled down to room temperature and measured again with a bench-top conductivity meter (CON500, CLEAN Instruments) to get the final total conductivity. Total electrolyte leakage is determined by the following formula: Ions leakage (%) = initial / final conductivity *100 (Zhang and Guo, 2018). Three biological replicates were performed.

Hormone and Stress Treatments for Gene Expression Analysis

The fifth leaf was detached from 4-week-old plants grown in continuously light condition, then transferred into 0.5× MS liquid culture containing the plant hormones ABA (1 μM), SA (20 μM), IAA (20 μM), MeJA (20 μM), ACC (20 μM) or GR24 (5 μM), incubated for 6 and 8 h, respectively. In environmental condition treatments, the leaves were transferred into 0.5× MS liquid culture containing NaCl (100 mM), mannitol (200 mM) or transferred to 4°C from room temperature for 12 and 24 h.

qRT-PCR

Total RNA was isolated from frozen leaf samples using trizol according to instructions of the manufacturer. The RNA was treated with RNase-free DNaseI to release the genomic DNA. First-strand cDNAs were generated from total RNA by reverse transcription using an AMV reverse transcriptase first-strand cDNA synthesis kit (Life Sciences, Promega). Next, cDNA samples were used for the following qRT-PCR. Triplicate quantitative assays and three biological replicates were performed using the SYBR Green Master

mix using an ABI 7500 sequence detection system (Applied Biosystems). The relative quantitation method ($^{\Delta\Delta}$CT) was used to evaluate quantitative variation among replicates. *Actin2* were applied as internal controls to normalize all data. The primers used in this study are as follows: Q_*SAG12*_F:5′-TCCAATTCTATTCGTCTGGTGTGT-3′; Q_*SAG12*_R: 5′-CCACTTTCTCCCCATTTTGTTC-3′; Q_*SEN4*_F: 5′-GACTC TTCTCGTGGCGGCGT-3′;Q_*SEN4*_R 5′-CCCACGGCCATTC CCCAAGC-3′ Q_*ACT2*_F: 5′-TGTGCCAATCTACGAGGGTT T-3′; Q_*ACT2*_R: 5′-TTTCCCGCTCTGCTGTTGT-3′; Q_*RBC S3B*_F: 5′-AGTAATGGCTTCCTCTATGC-3′; Q_*RBCS3B*_R: 5′-GTGATGTCCTTGTTGGTCTTG-3′; Q_*DEAR4*_F:5′-GAGG TCCTTCTGCTCGGCTT-3′; Q_*DEAR4*_R:5′-CCGCCGACAT ATCTCCACCA-3′.

Stress Response Assays

For seed germination assays in different stress conditions, seeds of *DEAR4* over-expression and Col-0 were surface-sterilized and incubated in 70% (v/v) ethanol for 5 min, and then washed five times quickly with water. Then, seeds were distributed on 0.5× MS solid media supplemented with 0 mM, 50 mM, 80 mM NaCl or 0.5 μM, 0.7 μM ABA. Seeds were stratified at 4°C for 3 days then transferred to 22°C under continuously light condition. Germination was monitored every 24 h as percentage of seeds with radicles completely penetrating the seed coat, for up to 5 days. Representative graphs are shown indicating germination up to 5 days. For drought adaption measurement assay, seeds of *DEAR4* over-expression and Col-0 were sowed into soil and normally watered for 4 weeks. Then, phenotypes were observed after an additional 10 days without watering. When the Col-0 plants showed lethal phenotypes, watering was resumed, and phenotypes were observed again after an additional 5 days. The survival rate was measured based on three replicates.

Inducible Expression of *DEAR4*

A total of 3-week-old plants grown in pots were sprayed with 10 μM β-estradiol (EST) once a day for 2 days and incubated for 6 additional days. Phenotype analysis and chlorophyll content measurement were carried out as above described. Three biological replicates were performed.

Determination of H_2O_2 Accumulation

For NBT staining, the 5th leaves of 4-week old plants were detached, then, soaked in the NBT staining buffer (0.5 mg/mL NBT in 10 mM potassium phosphate buffer, pH 7.6) overnight. Leaf chlorophyll was removed in the fixative solution (ethanol: acetic acid: glycerol, 3:1:1) and then kept in the ethanol: glycerol (4:1) solution at 4°C until photographed. Endogenous hydrogen peroxide content was measured following the instructions of the manufacturer (Nanjing Jiangcheng Company, China). Three biological replicates were performed.

Dual-Luciferase (LUC) Assay

In the dual-LUC reporter assay, *CaMV35S:DEAR4* was used as the effector construct. The reporter construct pGreenII 0800-LUC harboring the firefly LUC driven by promoters of *COR15a*, *COR15b*, *RD29a* or *RD29b* which contains the *DRE/CRT* element with the length of 481 bp, 361bp, 415 bp, and 429 bp, respectively. *Renilla LUC* gene driven by the *CaMV35S* promoter was used as an internal control. The reporter construct was co-transformed with the helper plasmid p19 into Agrobacterium GV3101. The Agrobacterium culture harboring the reporter construct was either incubated alone or as a mixture with the Agrobacterium culture containing the effector construct, and infiltrated manually into the leaves of *Nicotiana benthamiana*, then the plants were moved into darkness for 3 days. Firefly and Renilla luciferase activities were measured using the Dual Luciferase Reporter Assay System (Promega) according to the instruction of the manufacturer. The Firefly/Renilla luciferase ratio indicates transcriptional activity. Three biological replicates were performed.

proDEAR4::*GUS* Construct and GUS Activity Detection

Firstly, we cloned the 1.4 kb promoter of *DEAR4* using primers: pro*DEAR4*-EcoRF:5′-CCGGAATTCattaccgcctcttccct att-3′ and pro*DEAR4*-NcoIR:5′-CATGCCATGGagtggttttc tccggagatttc-3′, then the empty construct pcambia3301 was digested by restriction enzymes Hind III and Nco I, forming the *proDEAR4*::*GUS* construct after ligation reaction using T4 ligase (NEB No. M0202). According to the method described by Jefferson et al. (1987), leaves at different developmental stages were detached, then immersed in the histochemical staining buffer (1 mM 5-bromo-4-chloro-3-indolyl-b-glucuronic acid (Gluc) solution in 100 mM sodium phosphate, pH 7.0, 10 mM EDTA, 0.5 mM potassium ferricyanide, 0.5 mM potassium ferricyanide and 0.1%Triton X-100), and then incubated at 37°C for 12 h. The leaves were destained in 70% ethanol before photographed.

Transcriptional Repression Assay in Yeast Cells

To detect the transcriptional repression activity of DEAR4, yeast one-hybrid assay was employed in this study. The DEAR4-BD, shDEAR4 (without EAR domain)-BD, DEAR4-BD-VP16, shDEAR4-BD-VP16 constructs were transformed into the yeast strain Y190. To measure the strength of the X-Gal activity, liquid assay was carried out using CPRG as substrate. Three biological replicates were performed.

Plasmid Construction and Transformation of Arabidopsis

To generate the *DEAR4* over-expression constructs, the full length of *DEAR4* CDS was amplified by nest PCR method using primers (First round primers: DEAR4-BP-F: 5′-TACAAAAAAGCAGGCTTCATGGAGACGGCGACTGAAGT GG-3′; DEAR4-BP-R:5′-GTACAAGAAAGCTGGGTCATCGT CATCTGAAGTTTCCGG-3′; second round primers: attB-F:5′-GTGGGGACAAGTTTGTACAAAAAAGCAGGCTTC-3′; attB-R:5′-GTGGGGACCACTTTGTACAAGAAAGCTGGGTC-3′). According to the instructions of the invitrogen gateway kit (kit No.11789 (BP Clonase); No.117910 (LR Clonase), the

PCR products were cloned into pDnor-207 vector using the BP enzyme. Subsequently, according to Earley et al. (2006), *DEAR4* CDS was sub-cloned into pEarleyGate202 using the LR enzyme to form the *35S*::*DEAR4* construct. Then the constructs was transformed into *Agrobacterium tumefaciens* strain GV3101. The binary constructs were transformed into Arabidopsis plants via the floral dip method (Clough and Bent, 1998). Transgenic plants were selected by glyphosate resistance.

RESULTS

The Expression Pattern of *DEAR4*

To identify new genes regulated by both senescence and light, the GENEVESTIGATOR database[1] was screened and *DEAR4* was found to be highly expressed in senescing plant tissues, meanwhile induced by dark conditions. To confirm the *in silico* data, we performed qRT-PCR to measure the expression of *DEAR4*. The results showed that expression levels of *DEAR4* increased significantly from young leaf to late senescence stage (**Figure 1A**). In Arabidopsis, senescence proceeds from the tip toward the base of a leaf. When approximately 30% of the leaf area was yellow, the sixth leaves from 4-week-old Arabidopsis plants were detached and dissected into three parts including basal, middle and tip parts (**Figure 1B**). The expression of *DEAR4* in these three parts was determined by qRT-PCR and the results showed that expression of *DEAR4* exhibited higher in the tip but lower in the base region of these senescing leaves (**Figure 1B**).

To further examine the expression pattern of *DEAR4*, we generated *proDEAR4*::*GUS* transgenic plants that harbor the 1.4 kb long *DEAR4* promoter driving the *GUS* coding sequence. Analyses of the transgenic plants revealed that strong GUS activity was detected mainly in senescent leaf tissues, which is consistent with the qRT-PCR results (**Figures 1C,D**). These data indicated that expression of *DEAR4* is associated with natural leaf senescence.

The expression changes of *DEAR4* after exogenous phytohormones application were also studied. *DEAR4* expression was significantly up-regulated to 8 folds higher 6 h after ABA treatments and to 4 folds higher at 6 h after MeJA treatments. But no significant differences in expression of *DEAR4* were observed after SA, ACC or IAA treatment (**Figure 1E**).

To obtain insight into whether *DEAR4* was also involved in stress response, the expression pattern of *DEAR4* was examined in response to environmental stimuli. As shown in **Figure 1F**, the transcript levels of *DEAR4* increased significantly in response to NaCl, darkness and drought treatments.

DEAR4 Is Involved in Age-Dependent Leaf Senescence

To investigate the function of DEAR4, we obtained two *DEAR4* T-DNA insertion mutant lines from ABRC named *dear4* (*SALK_010653c*) and *dear4-1* (*Salk_045347*). The T-DNA insertion in the *dear4* mutant is located at the 5′UTR region of *DEAR4* (**Supplementary Figure 1A**) and the qRT-PCR results showed that the transcript of *DEAR4* was significantly reduced in the *dear4* mutant (**Supplementary Figure 1B**). Plants of *dear4* displayed a delayed senescence phenotype assessed by comparing the degree of leaf yellowing with Col-0 (**Figure 2A**). In 6-week-old plants, most leaves of Col-0 turned yellow with drying, yet *dear4* mutant leaves retained their integrity and displayed only partial yellowing (**Figures 2A,B**). Consistent with the visual phenotype, the chlorophyll content of Col-0 leaves decline faster in comparison with the counterpart of *dear4* mutant plants (**Figure 2C** upper). Leaf senescence often involves reduction of plasma membrane integrity, as indicated by membrane ion leakage. The delayed senescence symptoms of *dear4* can also be evidenced by lower membrane ion leakage of the leaves compared with Col-0 (**Figure 2C** lower). As seen in **Supplementary Figure 2**, *dear4-1* displayed a similar phenotype with *dear4* in delaying leaf senescence. These results demonstrated that *DEAR4* plays a potential role in promoting leaf senescence.

Over-Expression of *DEAR4* Leads to Precocious Senescence

To further explore the biological function of DEAR4, we generate multiple independent *DEAR4* over-expression transgenic lines harboring the *DEAR4* CDS under control of the *CaMV 35S* promoter (*35S*::*DEAR4*). qRT-PCR analysis showed that *DEAR4* transcript levels in *DEAR4-OE-3* and *DEAR4-OE-5* were 8 to 10 folds higher than that of Col-0 (**Supplementary Figure 3A**). Phenotypic analysis showed that *DEAR4* over-expressing lines displayed precocious leaf senescence judged by the progression of leaf yellowing (**Figures 3A,B**). Consistent with the visible phenotype, the reduction in chlorophyll contents of leaves from the *DEAR4* over-expression lines were greater than in Col-0 (**Figure 3D**). The precocious senescence of *DEAR4* over-expression plants were supported by higher membrane ion leakage of the leaves compared with Col-0 (**Figure 3E**). These results demonstrated that *DEAR4* plays an important role in promoting leaf senescence. In addition, we stained the fully expanded rosette leaves of different genotype plants via Trypan blue staining to assess dead cell rates. As shown in **Figure 3C**, the staining of dead cells in *DEAR4* over-expression lines was higher than that in Col-0. We further examined the expression of senescence marker genes. As showed in **Supplementary Figure 4**, compare with Col-0, the expression levels of *SAG12*, *SEN4* were dramatically up-regulated in *DEAR4* over-expression lines but lower in *dear4* mutant, whereas the expression levels of photosynthetic gene such as *RBCS* were clearly down-regulated in *DEAR4* over-expression lines but up-regulated in the *dear4* mutant.

To further confirm the *DEAR4* gain-of-function phenotype, we investigated the phenotypes of *DEAR4* inducible over-expression lines which express *DEAR4* under the control of a β-estradiol (EST) inducible promoter (*DEAR4-ind-1* and *DEAR4-ind-2*). The expression of *DEAR4* was detected by qRT-PCR (**Supplementary Figure 3B**). The phenotype analysis revealed that the *DEAR4-ind* lines displayed precocious senescence after treatment with 10 μM EST compared with Col-0 (**Figure 3F**). A decline in chlorophyll content was observed in leaves of

[1]https://www.genevestigator.com/gv/index.jsp

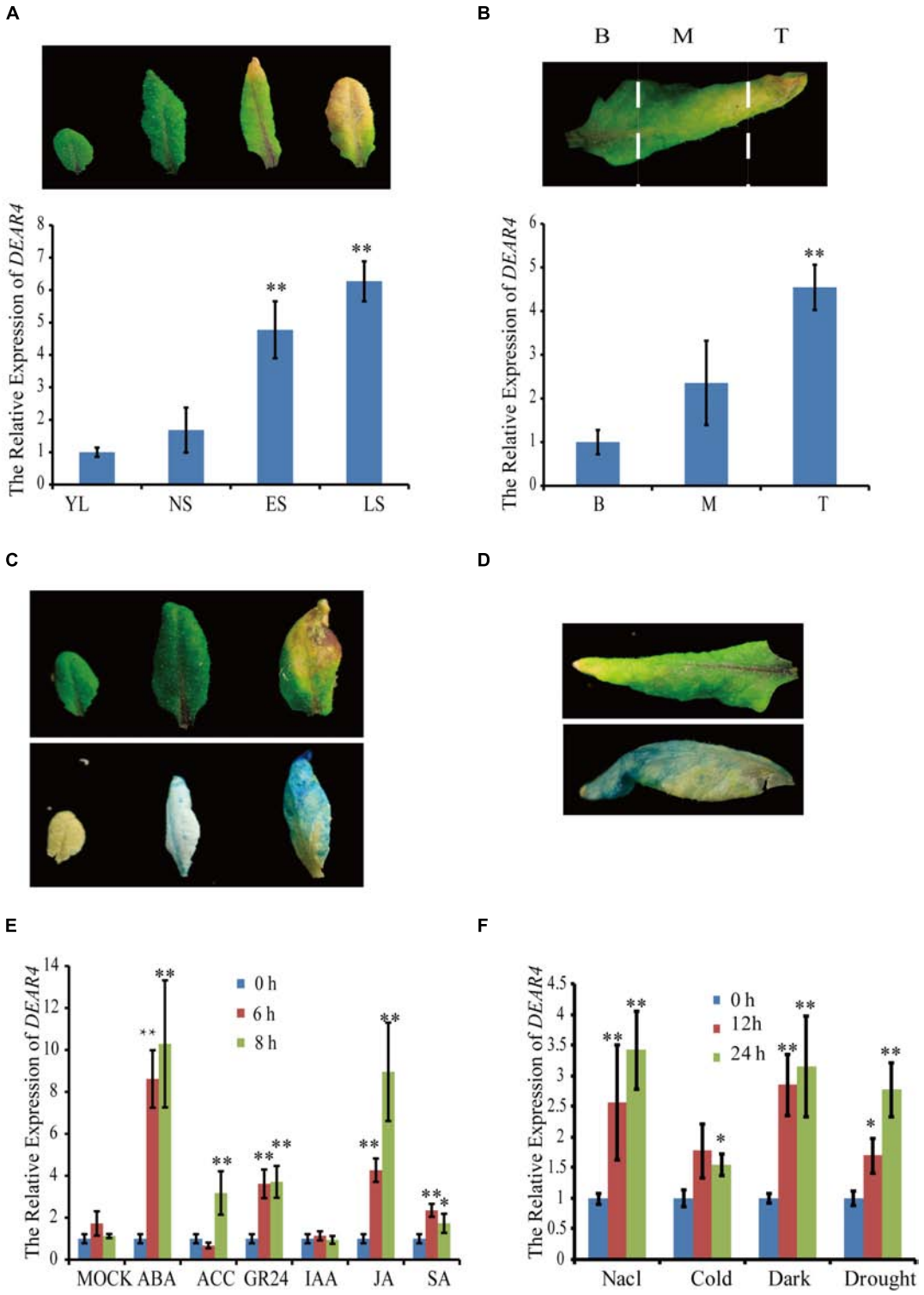

FIGURE 1 | The expression pattern of *DEAR4*. **(A)** The expression pattern of *DEAR4* at different developmental stages. YL, young leaves of 2-week old seedlings; NS, fully expanded mature leaves without senescence symptoms; ES, early senescent leaves, with <25% leaf area yellowing; LS, late senescent leaves, with >60% leaf area yellowing. **(B)** The *DEAR4* expression pattern in different parts of a senescing leaf; B, Base; M, Middle; T, Tip. **(C)** *GUS* expression detection in different stage rosette leaf of *proDEAR4*::*GUS* transgenic plants. Top Leaf, before GUS staining; bottom leaf, after GUS staining. **(D)** GUS staining results in different parts of a senescing leaf. **(E)** Effects of plant hormones on *DEAR4* expression. **(F)** Effects of different stress conditions on *DEAR4* expression. The bars are standard deviations (SD) of three biological replicates. The one and double asterisks indicate significant difference to control at the levels of $0.01 < P < 0.05$ and $P < 0.01$ using student's *t*-test, respectively.

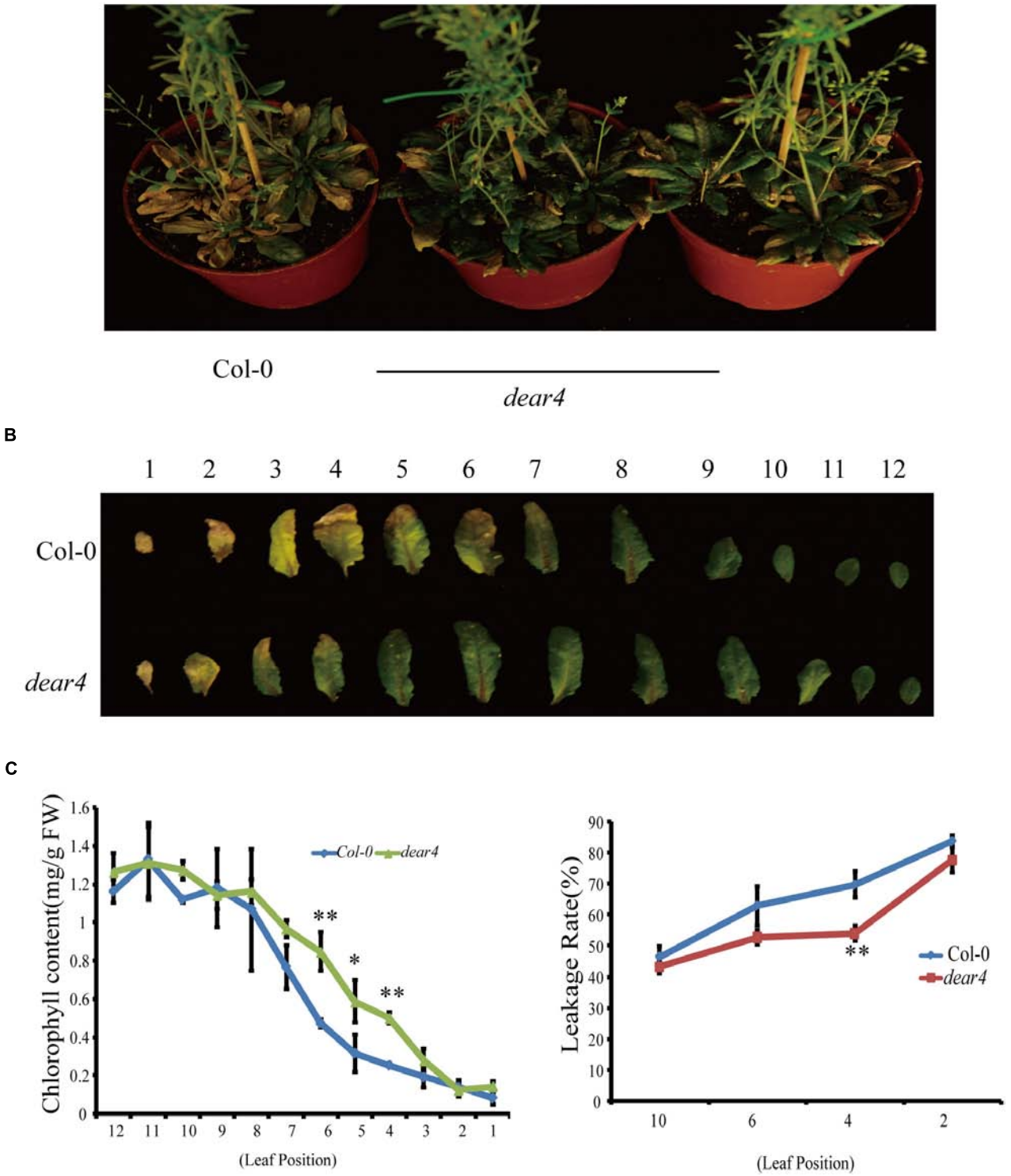

FIGURE 2 | A *DEAR4* T-DNA insertion delays leaf senescence process. **(A)** Leaf phenotype of 6-week-old Col-0 and *dear4* mutant plants. **(B)** Senescence symptoms of detached leaves of Col-0 and *dear4* plants. **(C)** Total chlorophyll content (1th–12th leaf) and ion leakage rate (the leaf position as indicated) in different genotype plants as indicated. The bars are standard deviations (SD) of three biological replicates. The one and double asterisks indicate significant difference to control at the levels of $0.01 < P < 0.05$ and $P < 0.01$ using student's *t*-test, respectively.

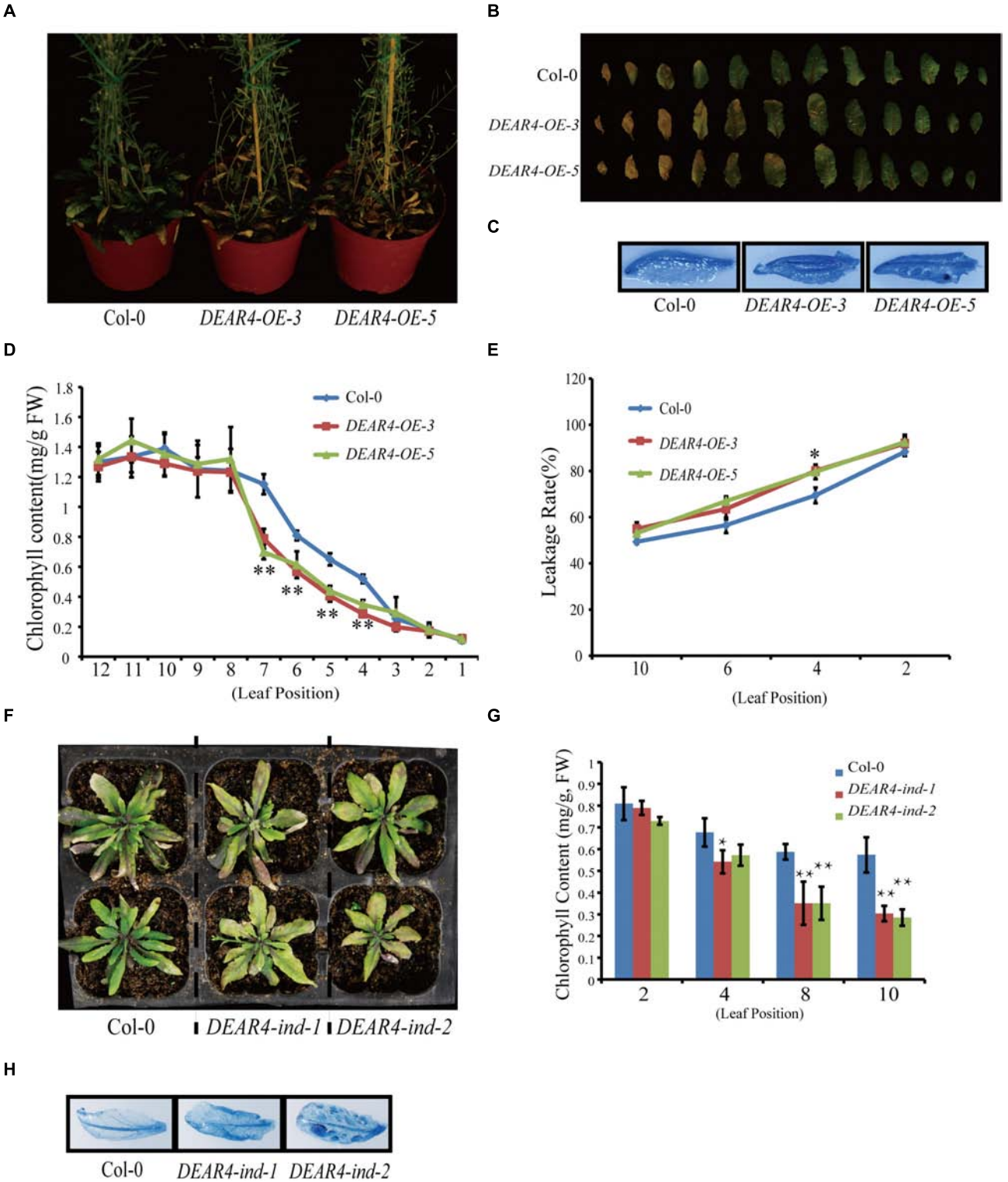

FIGURE 3 | Over-expression of *DEAR4* accelerates leaf senescence. **(A)** The phenotypes of *DEAR4* over-expression lines. **(B)** Detached leaf phenotypes of Col-0, *DEAR4-OE-3,* and *DEAR4-OE-5* described in **(A)**. **(C)** Trypan blue staining of the sixth leaf of 6-week-old Col-0 and *DEAR4* over-expression lines. **(D)** Total chlorophyll content of 1th–12th leaf from 6-week-old Col-0 and *DEAR4* over-expression lines. **(E)** Leakage rate of Col-0 and *DEAR4* over-expression lines. **(F)** Inducible over-expression of *DEAR4* causes precocious senescence. **(G)** Chlorophyll content of different genotype plants that were treated with EST. **(H)** Trypan blue staining of different plants as indicated. The bars are standard deviations (SD) of three biological replicates. The one and double asterisks indicate significant difference to control at the levels of $0.01 < P < 0.05$ and $P < 0.01$ using student's *t*-test, respectively.

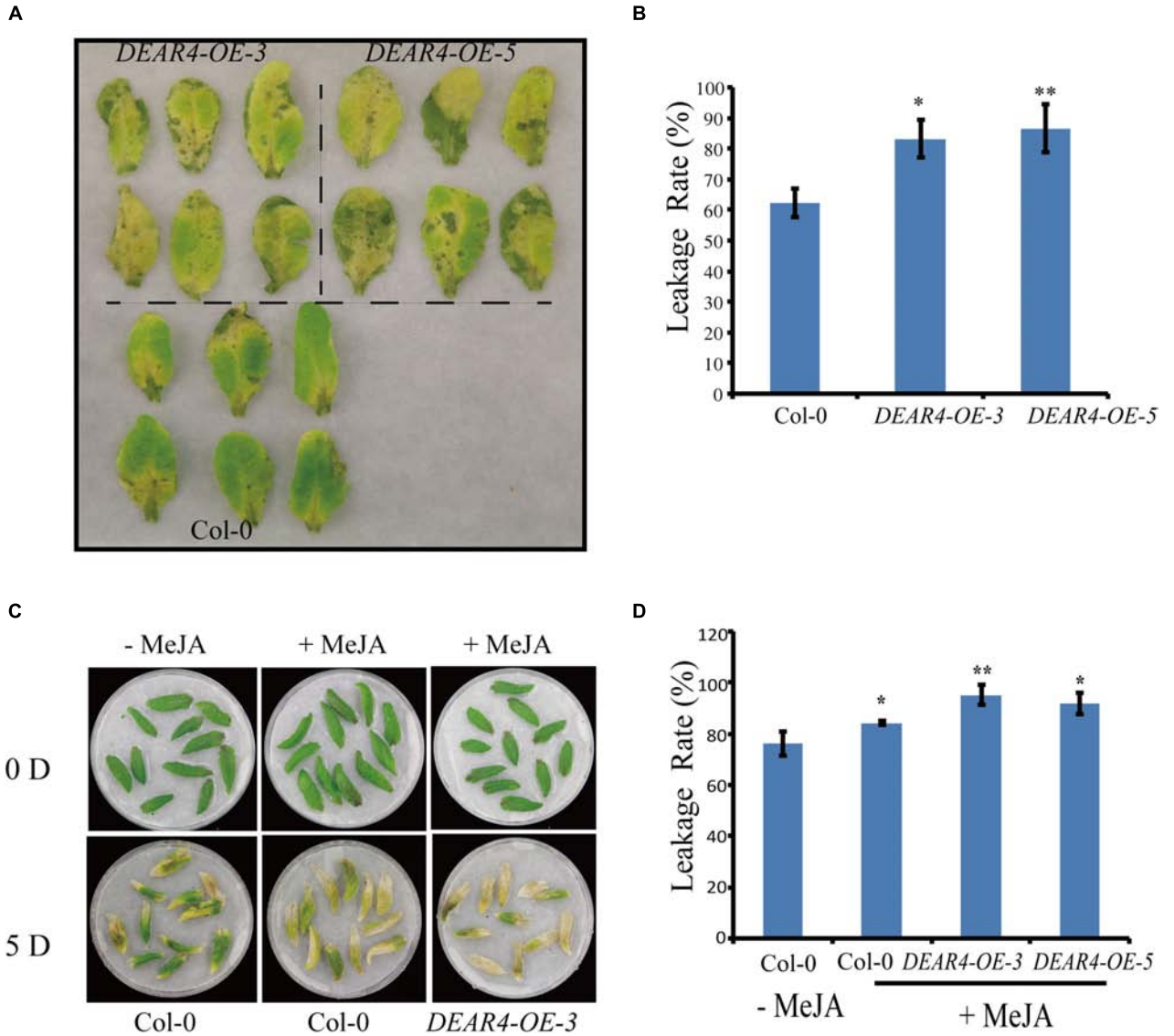

FIGURE 4 | Precocious senescence phenotypes of *DEAR4* over-expression lines in dark conditions. **(A)** Phenotypes of detached leaves in response to dark condition. **(B)** Ion leakage rate in Col-0, *DEAR4-OE-3,* and *DEAR4-OE-5*. **(C,D)** *DEAR4* over-expression plants showed enhanced sensitivity to JA. The bars are standard deviations (SD) of three biological replicates. The one and double asterisks indicate significant difference to control at the levels of $0.01 < P < 0.05$ and $P < 0.01$ using student's *t*-test, respectively.

DEAR4 inducible lines treated with EST (**Figure 3G**). Moreover, treatment with EST displayed significantly higher cell death ratio in *DEAR4* inducible gain-of-function leaves than that of control as revealed by trypan blue staining (**Figure 3H**). Taken together, these results indicated that DEAR4 functions in accelerating leaf senescence.

DEAR4 Is Involved in Senescence Induced by Darkness and JA

Given that *DEAR4* was increased at the transcriptional level under dark condition, we investigated the phenotypes of *DEAR4* over-expression plants during dark treatment. Detached leaves of Col-0 and *DEAR4* over-expression plants were covered with aluminum foil. Five days after treatment leaves from the two *DEAR4* over-expression lines exhibited an accelerated yellowing phenotype compared with those from Col-0 (**Figure 4A**). Consistent with the visible phenotype, *DEAR4* over-expression plants exhibited higher ion leakage rate compared with Col-0 (**Figure 4B**).

Since expression of *DEAR4* could be enhanced by JA treatments (**Figure 1E**), we sought to explore the relationship between DEAR4 and JA under dark condition. Detached leaves from 4-week-old plants of different genotypes were incubated with MeJA. After 5 days's MeJA treatment, *DEAR4* over-expression leaves displayed serious yellowing compared with

Col-0 (**Figure 4C**). Consistent with the visible precocious senescence, the results of ion leakage rate measurement showed that conductivity in *DEAR4* over-expression lines was higher compared with Col-0 after MeJA treatments (**Figure 4D**). The two independent overexpression lines displayed the similar phenotype.

DEAR4 Functions in Response to Drought, NaCl and ABA

Based on the expression data, *DEAR4* expression can be induced by NaCl and ABA (**Figures 1C,D**). Seeds from *DEAR4* over-expression lines and Col-0 were sowed on 0.5× MS plates supplied with different concentrations of NaCl or ABA and the percentages of seed germination were calculated based on the number of seeds showing the radicle emergence. The results showed that the percentage of germination between the Col-0 and *DEAR4* over-expression seeds were similar under normal condition. However, in the 50 mM NaCl treatment, the radicle emerged in 71.9 and 93.2% of *DEAR4-OE-3* and Col-0 seeds, respectively. Whereas, only 40.6 and 59.9% germination rates were observed in *DEAR4* over-expression and Col-0 seeds in the 80 mM NaCl treatment. In the 0.5 μM ABA treatment, 62% of the Col-0 seeds germinated, while this rate was reduced to 53% for *DEAR4* over-expression seeds (**Figures 5A,B**), the two independent overexpression lines displayed the similar results. In the drought treatment, plants of the *DEAR4-OE-3*, *DEAR4-OE-5* lines and Col-0 were grown in soil for 4 weeks under normal condition. Then, drought stress was applied by withholding watering. Survival rates of plants from different genotypes were calculated after15 days of drought stress treatment. Plants of Col-0 exhibited the survival rates of over 34.37%, which was significantly higher than *DEAR4-OE-3* and *DEAR4-OE-5* transgenic plants with the survival rates of 25 and 21.87%, respectively (**Figures 5C,D**). Taken together, these results demonstrated that *DEAR4* conferred plant more sensitive to drought and salt stress.

DEAR4 Regulates ROS Production

Reactive oxygen species are considered signaling molecules during leaf senescence and stress responses. To further understand the role of DEAR4 in leaf senescence and stress response, we employed NBT staining to visualize the levels of ROS. The fifth leaf from 4-week-old plants of different genotypes including *DEAR4* over-expression and Col-0 were detached and analyzed. As shown in **Figure 6A**, compared with Col-0, leaves of *DEAR4-OE-3* and *DEAR4-OE-5* were densely stained with dark blue and brown color by NBT staining, suggesting that DEAR4 enhanced ROS production. To further confirm the staining results, quantitative measurement was carried out to determine the endogenous H_2O_2 levels in plants of different genotypes. The results revealed that *DEAR4* over-expression plants accumulated significantly more H_2O_2 compared with Col-0 (**Figure 6B**).

DEAR4 Is a Transcriptional Repressor

The Arabidopsis DEAR4 protein contains homology to the DREB1/CBF domain and the EAR motif. EAR motifs commonly played as transcriptional repression roles in plants (Yang et al., 2018). Thus, we supposed that DEAR4 has the potential of functioning as a transcriptional repressor. To verify this point, we carried out yeast one-hybrid assay. The full-length or truncated *DEAR4* (shDEAR4, without EAR domain, 1-181aa) cDNA was fused to VP16, the activation domain of a potent viral transcriptional activator. The DEAR4 (or shDEAR4)-VP16 component group was then fused downstream of the GAL4 DNA-binding domain (GAL4-BD) in the pGBT9 vector to generate the BD-DEAR4 (or shDEAR4)-VP16 construct (**Figure 7A**). As a positive control, yeast strain Y190 carrying the reporter genes *LacZ* transformed with pGBT9-VP16 showed strong blue reaction (**Figure 7B**). Similar to pGBT9-VP16, Y190 transformed with pGBT9-shDEAR4-VP16 also displayed strong blue reaction. However, Yeast strain harboring pGBT9 empty vector displayed white reaction, similar to yeast transformed with DEAR4 fused with or without VP16 (**Figure 7B**). These results suggest that the full length DEAR4 protein plays transcriptional repression role which is dependent on the functional EAR domain.

We also carried out liquid assay using CPRG as substrate to quantify the x-gal activities from the above described yeast one-hybrid assays. Consistent with the results from blue-white reactions, the reporter gene activity in the yeast transformed with pGBT9, BD-DEAR4, BD-DEAR4-VP16, and BD-VP16 was 5.57 ± 0.68, 4.24 ± 0.67, 6.29 ± 0.37, and 79.13 ± 13.28, respectively. However, once the EAR domain was deleted, the reporter gene activity in yeast transformed with BD-shDEAR4-VP16 was up to 88.82 ± 6.44 (**Figure 7C**). Taken together, BD-VP16 protein was able to induce *lacZ* expression but DEAR4 protein repressed this process. However, DEAR4 protein with EAR domain deleted lost its transcriptional repression ability.

DEAR4 Directly Repress the Expression of *COR* and *RD29*

DEAR4 protein contains homology to the DREB1/CBF domain which binds to the DRE/CRT element containing an A/GCCGAC motif within gene promoters to regulate transcription. To further understand the molecular mechanisms underlying DEAR4's role in leaf senescence and stress responses, we investigated whether DEAR4 could regulate some downstream genes in the DRE/CRT-mediated signaling pathway. There are two putative DRE/CRT elements (−444 to −438 bp, −267 to −261 bp) upstream of the translation start site on the *COR15a* promoter and one DRE/CRT element at −266 to −260 bp from the translation start site on the promoter of *COR15b*. Meanwhile, we identified four putative DRE/CRT elements (−353 to −347 bp, −303 to −297 bp, −246 to −240 bp, −209 to −203 bp) upstream of the translation start site on the *RD29a* promoter and one DRE/CRT element (−321 to −315 bp from the translation start site) on the promoter of *RD29b*. The expression of the *COR* and *RD* genes were significantly decreased in the *DEAR4* over-expression transgenic plants (**Figure 8A**), two independent overexpression lines displayed the similar results, suggesting that DEAR4 is required for reduction of the *COR* and *RD* gene expression in leaf senescence regulation.

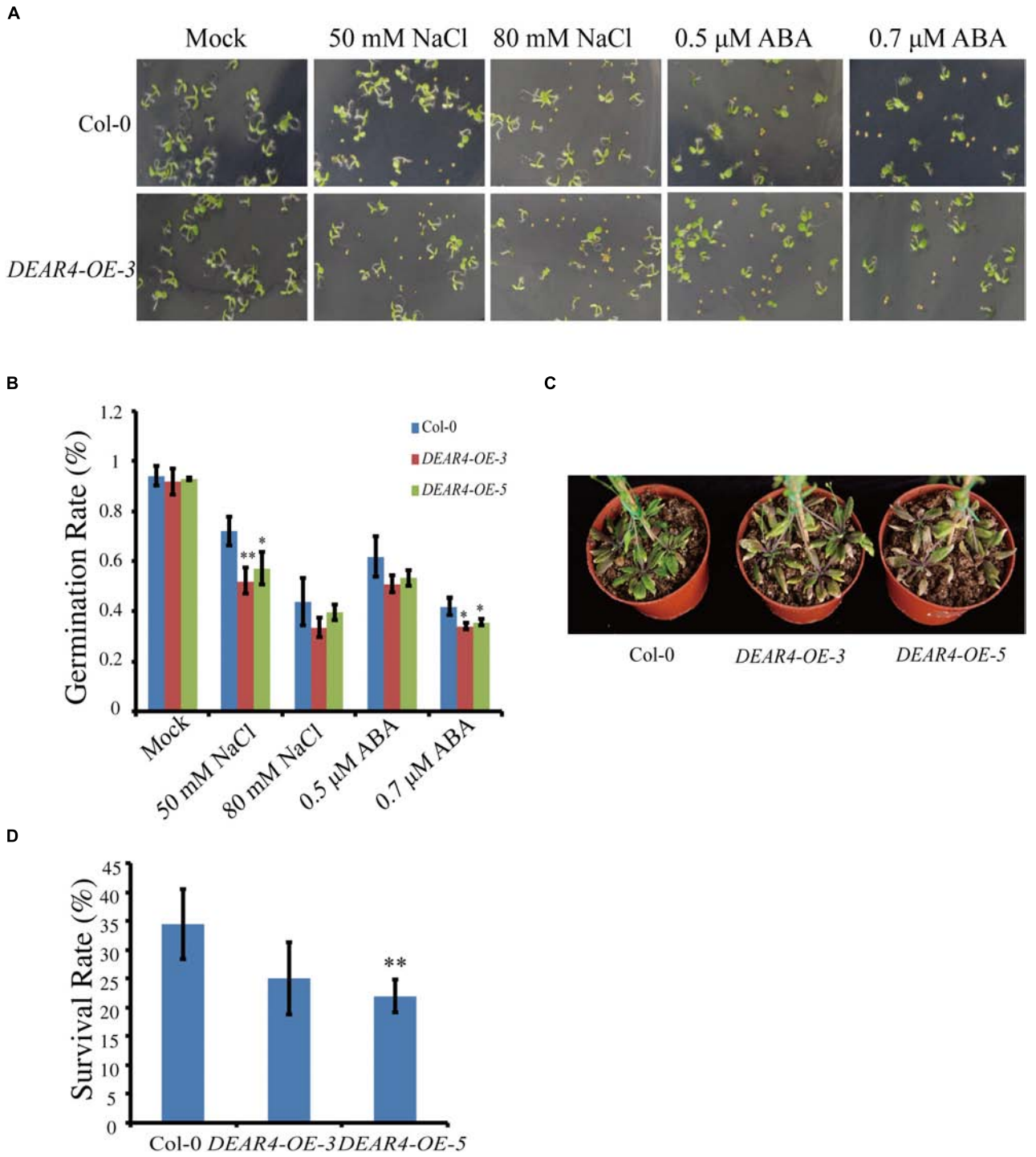

FIGURE 5 | Responses of *DEAR4* over-expression plants to NaCl, ABA and drought. **(A,B)** The effect of different concentrations of NaCl and ABA on germination of Col-0 and *DEAR4* over-expression plants. **(C,D)** *DEAR4* over-expression plants were sensitive to drought treatment. The bars are standard deviations (SD) of three biological replicates. The one and double asterisks indicate significant difference to control at the levels of $0.01 < P < 0.05$ and $P < 0.01$ using student's *t*-test, respectively.

Next, we tested whether DEAR4 directly regulates the *COR* and *RD* genes. We employed the dual luciferase strategy to investigate the direct regulation of *COR* and *RD* genes by DEAR4 in *Nicotiana benthamiana* leaves. Agrobacterium harboring the firefly luciferase-encoding gene driven by the promoter of *COR* (or *RD*) was co-transformed with or without *35S::DEAR4*. As

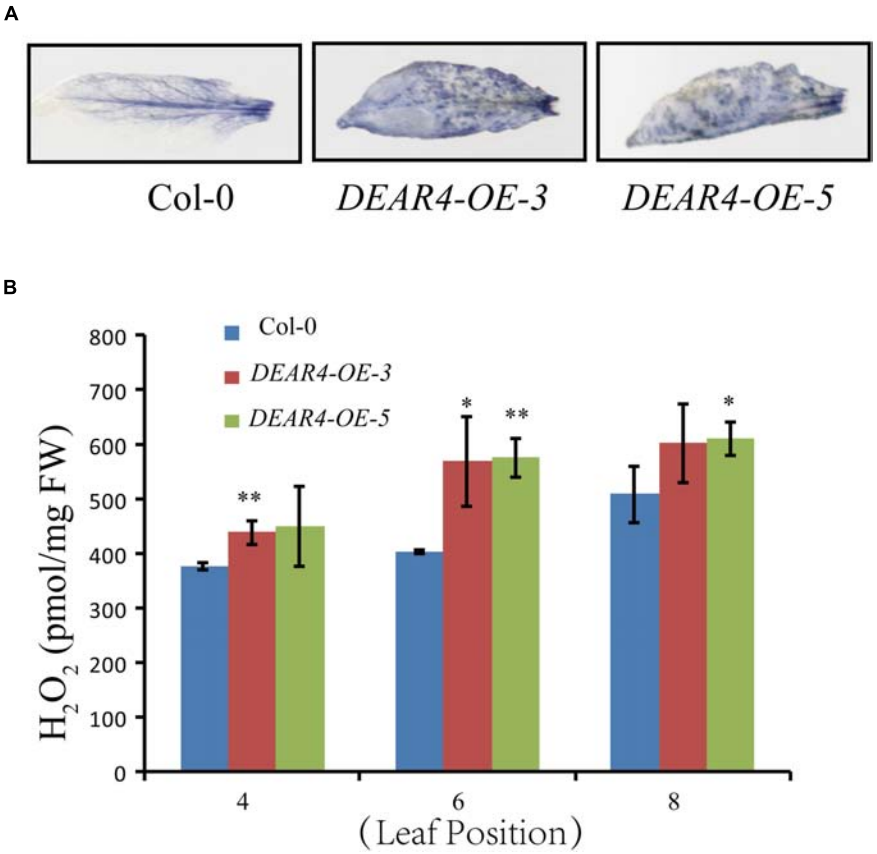

FIGURE 6 | DEAR4 promotes ROS production. **(A)** NBT staining. The 5th leaves of 4-week-old plants were used in NBT staining. **(B)** Measurement of temporal accumulation of H_2O_2 in detached leaves of plants with different genotypes. The one and double asterisk indicate significant difference to control at the levels of $0.01 < P < 0.05$ and $P < 0.01$ using student's *t*-test, respectively. The bars are standard deviations (SD) of three biological replicates.

an internal control, the *renilla luciferase* gene was driven by the *35S* promoter (**Figure 8B**). The ratio of Firefly/Renilla luciferase activities indicates the transcriptional activity of *COR* or *RD* genes. The results showed that the Firefly/Renilla luciferase ratio was significantly lower in leaves co-transformed with *DEAR4* compared to that without *DEAR4*, indicating that DEAR4 repress the expression of *COR* and *RD* genes directly (**Figure 8C**).

DISCUSSION

As the final phase of leaf development, senescence is crucial for plant survival and environmental adaptation. So far, thousands of genes and many signaling pathways have been studied for leaf senescence regulation. Among them, transcription factors are highly effective in engineering stress tolerant plants (Bengoa et al., 2019; Woo et al., 2019). A large number of transcriptional factor genes including *NAC*, *WRKY*, *MYB,* and *AP2/EREBP* were up- or down-regulated during natural and dark-induced senescence (Zhang and Zhou, 2013). Additionally, transcript profiling studies suggested that many of the genes were affected by senescence and environmental stresses at the same time (Yoshida, 2003; Sharabi-Schwager et al., 2010a; Chen et al., 2017). As the largest transcription factor family in Arabidopsis, the AP2/ERF proteins have roles in the regulation of developmental processes, hormonal signal transduction, and biotic and abiotic stress responses (Smirnoff and Bryant, 1999; Yang et al., 2019b). As one of the AP2/ERF subfamilies, members of the DREB protein family have been extensively studied over the years due to their crucial roles in regulation of abiotic- and biotic-stress responses. It's well known that DREB protein recognized the dehydration responsive element (DRE)/C-repeat with a core sequence of A/GCCGAC to regulate gene expression (Smirnoff and Bryant, 1999; Sharoni et al., 2011; Kudo et al., 2017). More and more evidence suggested that the DREB proteins play multiple roles during plant development. The *CBF* genes including *CBF1*, *−2*, *−3*, also known as *DREB1b*, *DREB1c*, and *DREB1a*, respectively, have been identified as key regulators of cold response and drought response (Liu et al., 2004; Novillo et al., 2004). In addition, *CBF* genes also play important roles in dark induced senescence (Gilmour et al., 2000; Solanke and Sharma, 2008; Zhou et al., 2011a). Here, we investigated the function of DEAR4, which contains the DREB domain but is different from the typical DREB proteins, with an EAR motif at the C terminus. Consistent with *in silico* data in publically available databases (GENEVESTIGATOR), we found

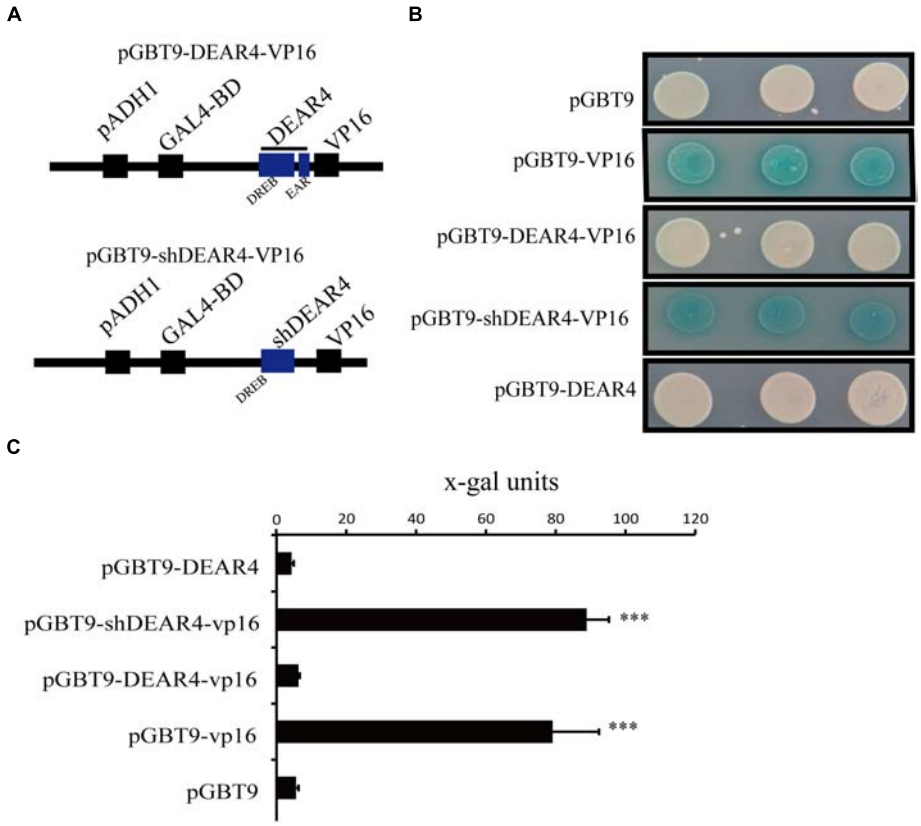

FIGURE 7 | Transcriptional repression activities of DEAR4 in yeast cells. **(A)** Schematic diagram of pGBT9-DEAR4-VP16 and pGBT9-shDEAR4-VP16. **(B)** Comparison results of the Y1H assay using full length *DEAR4* or *shDEAR4* (truncated sequence absenting EAR domain coding region) fused with vp16 and control. **(C)** Liquid assay to measure x-gal activities in yeast containing different construct using CPRG as substrate. The bars are standard deviations (SD) of three biological replicates. The triple asterisk indicates significant difference to control at $P < 0.001$ using student's *t*-test.

that *DEAR4* can be induced by age and dark conditions, as well as multiple abiotic stresses and hormones including ABA, JA, salt, and drought (**Figure 1**). More and more evidence suggested that plants have the capacity of integrating various signaling pathways to provide a greater regulatory potential for enhancing environment adaption. Our data revealed that DEAR4 was involved in age and dark induced leaf senescence based on phenotype and physiological data (**Figures 2–4**). At the molecular level, the precocious leaf senescence phenotype is associated with a gradual increase in the transcript levels of *SAG*s including *SAG12*, *SEN4* and decrease in the expression of the *RBCS* gene (**Supplementary Figure 2**). Previous study has reported that DEAR1, one of the DEAR4 homologs, plays roles in mediating crosstalk between biotic and abiotic stresses. *DEAR1* expression was enhanced by pathogen infection and cold treatment. Over-expression of *DEAR1* caused an activated defense phenotype. Additionally, the induction of DREB1/CBF family genes by cold treatment was suppressed in *DEAR1* over-expression lines, leading to a reduction in freezing tolerance (Tsutsui et al., 2009). In addition, DEAR1 is included in the A-5 subgroup of the DREB/ family that could form a negative feedback regulation of the DREB1/CBF and DREB2 pathway in response to cold and dehydration (Mizoi et al., 2012). There are five DEAR1 homologs including DEAR4 within the Arabidopsis genome that also contain a DREB domain and an EAR motif. The role of DEAR4 in stress response therefore is not surprising. Interestingly, we found that DEAR4 also plays a role in leaf senescence, suggesting that the DEAR genes may play different roles in plant development and response to environmental stimuli. It will be interesting to find out whether the similar negative feedback mechanism exists in DEAR4's function in leaf senescence and stress response.

Jasmonic acid acts as a crucial signal to modulate multiple plant processes including senescence and stress responses. JA content was much higher in senescent leaves than in non-senescent ones (Shan et al., 2011; Seltmann and Berger, 2013). Additionally, exogenous application of JA enhances plants' freezing tolerance with or without cold acclimation. Further study revealed that JA positively regulates *CBF* to up-regulate downstream cold-responsive genes to enhance cold tolerance (Hu et al., 2013, 2017). JAZ proteins were discovered as repressors of JA signaling through the COI1-dependent 26S proteasome pathway for protein degradation. Once JAZ proteins were reduced, various downstream transcription factors including MYC2, MYC3 and MYC4 were activated

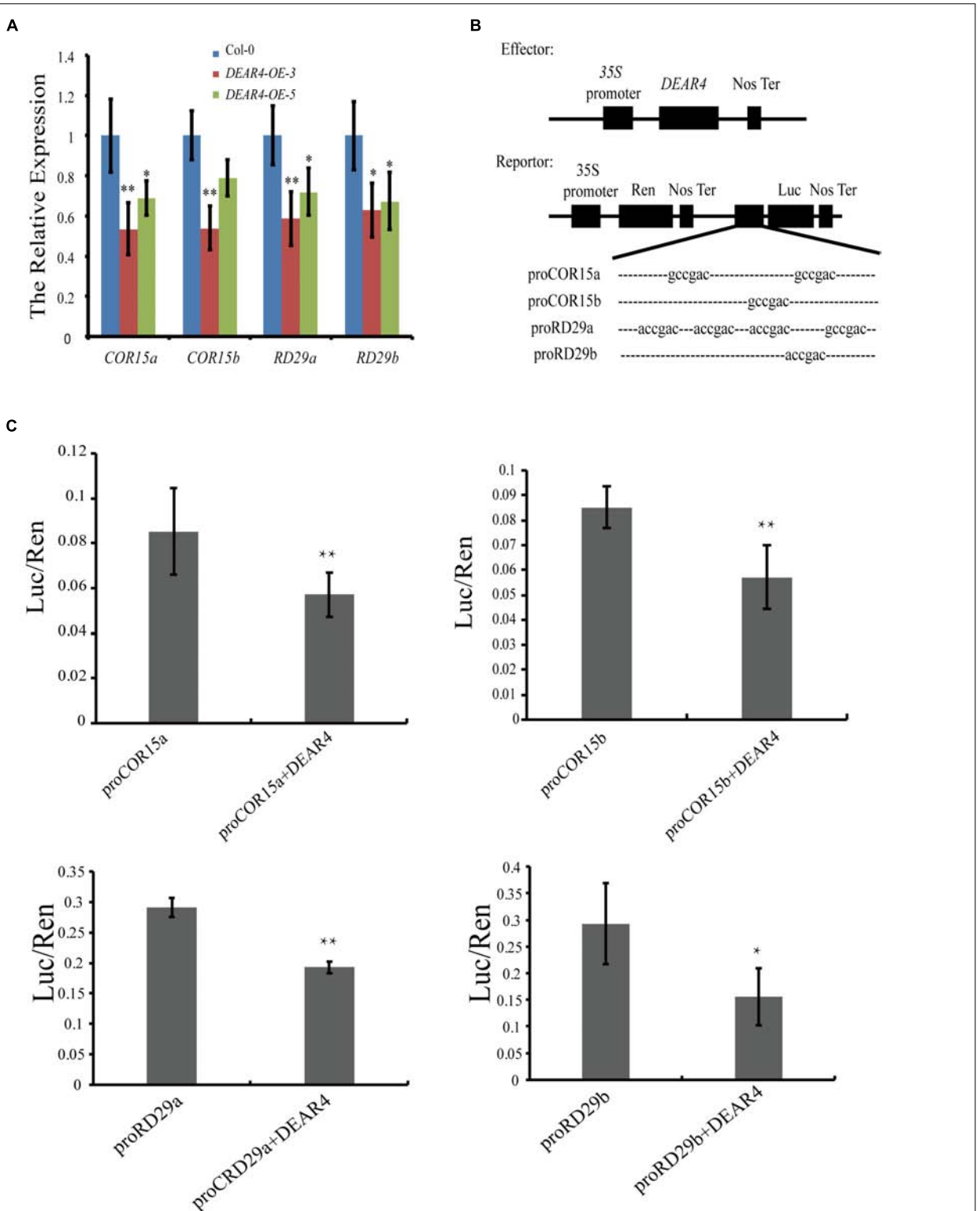

FIGURE 8 | Transcriptional repression of DEAR4 on *COR* and *RD* genes. **(A)** The expression of *COR15a*, *COR15b*, *RD29a*, and *RD29b* in Col-0 and *DEAR4* over-expression lines. **(B)** Dual luciferase (LUC) constructs used in this study. Dual LUC constructs contain the double reporter and effector plasmids. In the double reporter construct, Renilla LUC expression was used to normalize the firefly luciferase activities. The effector construct in this study contains *DEAR4* driven by the *CaMV35S* promoter. **(C)** DEAR4 directly represses the expression of *COR15* and *RD29*. The *firefly LUC* gene was driven by the *COR15* and *RD29* promoters, ratio of firefly and RenLuc indicates the relative activities of promoters. The bars are standard deviations (SD) of three biological replicates. The one and double asterisk indicate significant difference to control at the levels of $0.01 < P < 0.05$ and $P < 0.01$ using student's *t*-test, respectively.

(Fernandez-Calvo et al., 2011; Hu et al., 2013). In darkness, the mutant of *JAZ7* partially liberated *MYC2*/*MYC3*/*MYC4* from suppression, resulting in the up-regulation of the downstream genes related to indole-glucosinolate biosynthesis, sulfate metabolism, callose deposition, and JA-mediated signaling pathways (Yu et al., 2016). In this study, we found that *DEAR4* was induced by exogenous MeJA (**Figure 1E**), meanwhile, DEAR4 can enhance the role of MeJA in promoting senescence (**Figures 4C,D**), which provide clues that *DEAR4* may play roles in JA regulating senescence and stress responses. The DEAR4 protein contains the EAR motif which plays an important role in ethylene-responsive transcriptional regulation. Interestingly, previous studies have reported the mechanism of crosstalk between JA and other plant hormones including ethylene in plant growth and stress responses. JA and ethylene antagonize or coordinately regulate plant stress response (Zhu, 2014; Yang et al., 2019a). JA and ethylene pathways most likely crosstalk at the levels of JAZ–EIN3 and JAZ–EIL1 (Zhu et al., 2011; Kazan and Manners, 2012; Zhang et al., 2014). The EAR domain proteins could be involved in JA signal pathway. For example, the NINJA (Novel Interactor of JAZ, an EAR motif containing protein) mediated JAZ pathway to block the activity of MYC2, repressing the JA-dependent root growth inhibition and defense processes (Li et al., 2019). Both JA and ethylene were involved in leaf senescence. So far, the crosstalk between JA and ethylene's functions in leaf senescence is not clear. Based on our data, DEAR4 could potentially play a role in both JA and ethylene pathways in regulating leaf senescence.

Plant ROS include hydrogen peroxide (H_2O_2), superoxide anion (O^{2-}), hydroxyl radicals (OH) and singlet oxygen ($1O_2$), which can be produced from chloroplast and mitochondrial electron transport chains, and oxidases and peroxidases located in the peroxisomes or in the plasmalemma/apoplast (Wang et al., 2013). ROS are not only as by-products of metabolic pathways but also play signaling roles during normal plant development. Multiple stresses are known to enhance ROS generation (Apel and Hirt, 2004; Mittler et al., 2004). The senescence process also increases accumulation of ROS (Jajic et al., 2015; Li et al., 2016). Thus, ROS production regulation plays key roles in both senescence and stress responses. Given that DEAR4 was involved in age and dark induced senescence, we hypothesized that DEAR4 may be involved in regulating leaf senescence though the proliferation of ROS. Consistent with this hypothesis, over-expression of *DEAR4* can induce the production of ROS. *DEAR4* over-expression lines displayed substantially induced ROS production based on the NBT staining and H_2O_2 content measurement data (**Figure 6**). Leaf senescence is commonly associated with electrolyte leakage which represents loss of membrane integrity. Excessive production of ROS results in membrane lipid peroxidation. Our results demonstrated that DEAR4 was involved in age- and dark induced leaf senescence and multiple stresses responses all of which are associated with membrane damage and accumulation of ROS, suggesting a crucial role of DEAR4 in these processes potentially via ROS regulation.

Leaf senescence is also regulated by environmental stimuli including salinity, drought, low quality light and darkness (Buchanan-Wollaston et al., 2005). Numerous *SAG*s were influenced by diverse abiotic and biotic stresses (Quirino et al., 1999; Weaver and Amasino, 2001). Additionally, some of the genes that regulate stress responses may also have an important role in regulating leaf senescence (Binyamin et al., 2001). For example, among the 43 transcription factor genes up-regulated during senescence, 28 were also induced by various stresses (Lim et al., 2007). The DREB protein family is known to regulate abiotic stress responses in plants. The DEAR4 protein contains a DREB domain. The expression of *DEAR4* is lower in young leaves, but is up-regulated in senescing leaves. Meanwhile, *DEAR4* gene transcript was induced by senescence as well as senescence-stress associated hormones including ABA and JA (**Figure 1**). Detached leaves of *DEAR4* gain-of-function plants accelerated the senescence process induced by age, darkness or MeJA, suggesting that DEAR4 possibly integrates the age-dependent leaf senescence with responses to environmental stimuli including darkness and phytohormones. A large amount of evidence suggested that the *DREB* genes play a major role in cold- and osmotic-stress signal transduction pathways by recognizing the dehydration responsive element (DRE)/C-repeat with a core sequence A/GCCGAC. In this study, we observed that DEAR4 exhibited transcriptional repression activities in yeast cells depending on its EAR motif (**Figure 7**). As expected, DEAR4 was demonstrated to be able to directly repress the expression of DRE element genes *COR* and *RD* genes (**Figure 8**). Interestingly, it has been reported that COR and RD genes were involved in senescence and stress responses (Lee and Seo, 2015; Bremer et al., 2017; Shi et al., 2017b).

DATA AVAILABILITY STATEMENT

All datasets generated for this study are included in the article/**Supplementary Material**.

AUTHOR CONTRIBUTIONS

YG conceived the project. ZZ and YG designed the research, performed the data analysis, and wrote the manuscript. ZZ, WL, MX, and XG performed the experiments.

FUNDING

This work was supported by grants from the National Natural Science Foundation of China (No. 31600991) and the Agricultural Science and Technology Innovation Program, Chinese Academy of Agricultural Sciences (ASTIP-TRI02).

SUPPLEMENTARY MATERIAL

The Supplementary Material for this article can be found online at: https://www.frontiersin.org/articles/10.3389/fpls.2020.00367/full#supplementary-material

REFERENCES

Apel, K., and Hirt, H. (2004). Reactive oxygen species: metabolism, oxidative stress, and signal transduction. *Annu. Rev. Plant Biol.* 55, 373–399. doi: 10.1146/annurev.arplant.55.031903.141701

Asad, M. A. U., Zakari, S. A., Zhao, Q., Zhou, L., Ye, Y., and Cheng, F. (2019). Abiotic stresses intervene with ABA signaling to induce destructive metabolic pathways leading to death: premature leaf senescence in plants. *Int. J. Mol. Sci.* 20:256. doi: 10.3390/ijms20020256

Balbi, V., and Devoto, A. (2008). Jasmonate signalling network in *Arabidopsis thaliana*: crucial regulatory nodes and new physiological scenarios. *New Phytol.* 177, 301–318. doi: 10.1111/j.1469-8137.2007.02292.x

Bengoa, L. S., Astigueta, F. H., Nicosia, S., Moschen, S., Fernandez, P., and Heinz, R. (2019). Transcription factors associated with leaf senescence in crops. *Plants* 8:411. doi: 10.3390/plants8100411

Binyamin, L., Falah, M., Portnoy, V., Soudry, E., and Gepstein, S. (2001). The early light-induced protein is also produced during leaf senescence of *Nicotiana tabacum*. *Planta* 212, 591–597. doi: 10.1007/s004250000423

Bremer, A., Kent, B., Hauss, T., Thalhammer, A., Yepuri, N. R., Darwish, T. A., et al. (2017). Intrinsically disordered stress protein COR15A resides at the membrane surface during dehydration. *Biophys. J.* 113, 572–579. doi: 10.1016/j.bpj.2017.06.027

Buchanan-Wollaston, V., Page, T., Harrison, E., Breeze, E., Lim, P. O., Nam, H. G., et al. (2005). Comparative transcriptome analysis reveals significant differences in gene expression and signalling pathways between developmental and dark/starvation-induced senescence in *Arabidopsis*. *Plant J.* 42, 567–585. doi: 10.1111/j.1365-313x.2005.02399.x

Chen, Y., Wang, Y., Huang, J., Zheng, C., Cai, C., Wang, Q., et al. (2017). Salt and methyl jasmonate aggravate growth inhibition and senescence in *Arabidopsis* seedlings via the JA signaling pathway. *Plant Sci.* 261, 1–9. doi: 10.1016/j.plantsci.2017.05.005

Clough, S. J., and Bent, A. F. (1998). Floral dip: a simplified method for agrobacterium-mediated transformation of *Arabidopsis thaliana*. *Plant J.* 16, 735–743. doi: 10.1046/j.1365-313x.1998.00343.x

Coego, A., Brizuela, E., Castillejo, P., Ruiz, S., Koncz, C., del Pozo, J. C., et al. (2014). The TRANSPLANTA collection of *Arabidopsis* lines: a resource for functional analysis of transcription factors based on their conditional overexpression. *Plant J.* 77, 944–953. doi: 10.1111/tpj.12443

Dubouzet, J. G., Sakuma, Y., Ito, Y., Kasuga, M., Dubouzet, E. G., Miura, S., et al. (2003). *OsDREB* genes in rice, *Oryza sativa* L., encode transcription activators that function in drought-, high-salt- and cold-responsive gene expression. *Plant J.* 33, 751–763. doi: 10.1046/j.1365-313x.2003.01661.x

Earley, K. W., Haag, J. R., Pontes, O., Opper, K., Juehne, T., Song, K., et al. (2006). Gateway-compatible vectors for plant functional genomics and proteomics. *Plant J.* 45, 616–629. doi: 10.1111/j.1365-313x.2005.02617.x

Fernandez-Calvo, P., Chini, A., Fernandez-Barbero, G., Chico, J. M., Gimenez-Ibanez, S., Geerinck, J., et al. (2011). The *Arabidopsis* bHLH transcription factors MYC3 and MYC4 are targets of JAZ repressors and act additively with MYC2 in the activation of jasmonate responses. *Plant Cell* 23, 701–715. doi: 10.1105/tpc.110.080788

Gilmour, S. J., Sebolt, A. M., Salazar, M. P., Everard, J. D., and Thomashow, M. F. (2000). Overexpression of the *Arabidopsis* CBF3 transcriptional activator mimics multiple biochemical changes associated with cold acclimation. *Plant Physiol.* 124, 1854–1865. doi: 10.1104/pp.124.4.1854

Gregersen, P. L., Culetic, A., Boschian, L., and Krupinska, K. (2013). Plant senescence and crop productivity. *Plant Mol. Biol.* 82, 603–622. doi: 10.1007/s11103-013-0013-8

Guo, Y., and Gan, S. S. (2014). Translational researches on leaf senescence for enhancing plant productivity and quality. *J. Exp. Bot.* 65, 3901–3913. doi: 10.1093/jxb/eru248

Hu, Y., Jiang, L., Wang, F., and Yu, D. (2013). Jasmonate regulates the inducer of cbf expression-C-repeat binding factor/DRE binding factor1 cascade and freezing tolerance in *Arabidopsis*. *Plant Cell* 25, 2907–2924. doi: 10.1105/tpc.113.112631

Hu, Y., Jiang, Y., Han, X., Wang, H., Pan, J., and Yu, D. (2017). Jasmonate regulates leaf senescence and tolerance to cold stress: crosstalk with other phytohormones. *J. Exp. Bot.* 68, 1361–1369. doi: 10.1093/jxb/erx004

Huang, B., and Liu, J. Y. (2006). Cloning and functional analysis of the novel gene GhDBP3 encoding a DRE-binding transcription factor from *Gossypium hirsutum*. *Biochim. Biophys. Acta* 1759, 263–269. doi: 10.1016/j.bbaexp.2006.04.006

Jajic, I., Sarna, T., and Strzalka, K. (2015). Senescence, stress, and reactive oxygen species. *Plants* 4, 393–411. doi: 10.3390/plants4030393

Jefferson, R. A., Kavanagh, T. A., and Bevan, M. W. (1987). GUS fusions: beta-glucuronidase as a sensitive and versatile gene fusion marker in higher plants. *EMBO J.* 6, 3901–3907. doi: 10.1002/j.1460-2075.1987.tb02730.x

Jiang, Y., Liang, G., Yang, S., and Yu, D. (2014). *Arabidopsis* WRKY57 functions as a node of convergence for jasmonic acid- and auxin-mediated signaling in jasmonic acid-induced leaf senescence. *Plant Cell* 26, 230–245. doi: 10.1105/tpc.113.117838

Jibran, R., Hunter, A. D., and Dijkwel, P. P. (2013). Hormonal regulation of leaf senescence through integration of developmental and stress signals. *Plant Mol. Biol.* 82, 547–561. doi: 10.1007/s11103-013-0043-2

Kamranfar, I., Xue, G. P., Tohge, T., Sedaghatmehr, M., Fernie, A. R., Balazadeh, S., et al. (2018). Transcription factor RD26 is a key regulator of metabolic reprogramming during dark-induced senescence. *New Phytol.* 218, 1543–1557. doi: 10.1111/nph.15127

Kazan, K., and Manners, J. M. (2012). JAZ repressors and the orchestration of phytohormone crosstalk. *Trends Plant Sci.* 17, 22–31. doi: 10.1016/j.tplants.2011.10.006

Kudo, M., Kidokoro, S., Yoshida, T., Mizoi, J., Todaka, D., Fernie, A. R., et al. (2017). Double overexpression of DREB and PIF transcription factors improves drought stress tolerance and cell elongation in transgenic plants. *Plant Biotechnol. J.* 15, 458–471. doi: 10.1111/pbi.12644

Lee, H. G., and Seo, P. J. (2015). The MYB96-HHP module integrates cold and abscisic acid signaling to activate the CBF-COR pathway in *Arabidopsis*. *Plant J.* 82, 962–977. doi: 10.1111/tpj.12866

Lee, S., Seo, P. J., Lee, H. J., and Park, C. M. (2012). A NAC transcription factor NTL4 promotes reactive oxygen species production during drought-induced leaf senescence in *Arabidopsis*. *Plant J.* 70, 831–844. doi: 10.1111/j.1365-313X.2012.04932.x

Li, C., Shi, L., Wang, Y., Li, W., Chen, B., Zhu, L., et al. (2019). *Arabidopsis* ECAP is a new adaptor protein that connects JAZ repressors with TPR2 co-repressor to suppress jasmonate-responsive anthocyanin accumulation. *Mol. Plant* 13, 246–265. doi: 10.1016/j.molp.2019.10.014

Li, Z., Peng, J., Wen, X., and Guo, H. (2013). Ethylene-insensitive3 is a senescence-associated gene that accelerates age-dependent leaf senescence by directly repressing miR164 transcription in *Arabidopsis*. *Plant Cell* 25, 3311–3328. doi: 10.1105/tpc.113.113340

Li, Z., Wang, X., Chen, J., Gao, J., Zhou, X., and Kuai, B. (2016). CCX1, a putative cation/ca2+ exchanger, participates in regulation of reactive oxygen species homeostasis and leaf senescence. *Plant Cell Physiol.* 57, 2611–2619. doi: 10.1093/pcp/pcw175

Liebsch, D., and Keech, O. (2016). Dark-induced leaf senescence: new insights into a complex light-dependent regulatory pathway. *New Phytol.* 212, 563–570. doi: 10.1111/nph.14217

Lim, P. O., Kim, H. J., and Nam, H. G. (2007). Leaf senescence. *Annu. Rev. Plant Biol.* 58, 115–136.

Lin, R. C., Park, H. J., and Wang, H. Y. (2008). Role of *Arabidopsis* RAP2.4 in regulating light- and ethylene-mediated developmental processes and drought stress tolerance. *Mol. Plant* 1, 42–57. doi: 10.1093/mp/ssm004

Liu, F. X., Tan, Z. B., Zhu, J. Q., and Deng, X. J. (2004). [*Arabidopsis* CBF1 in plant tolerance to low temperature and drought stresses]. *Yi Chuan* 26, 394–398.

Liu, Q., Kasuga, M., Sakuma, Y., Abe, H., Miura, S., Yamaguchi-Shinozaki, K., et al. (1998). Two transcription factors, DREB1 and DREB2, with an EREBP/AP2 DNA binding domain separate two cellular signal transduction pathways in drought- and low-temperature-responsive gene expression, respectively, in *Arabidopsis*. *Plant Cell* 10, 1391–1406. doi: 10.1105/tpc.10.8.1391

Ma, L. F., Zhang, J. M., Huang, G. Q., Li, Y., Li, X. B., and Zheng, Y. (2014). Molecular characterization of cotton C-repeat/dehydration-responsive element binding factor genes that are involved in response to cold stress. *Mol. Biol. Rep.* 41, 4369–4379. doi: 10.1007/s11033-014-3308-1

Mittler, R., Vanderauwera, S., Gollery, M., and Van Breusegem, F. (2004). Reactive oxygen gene network of plants. *Trends Plant Sci.* 9, 490–498. doi: 10.1016/j.tplants.2004.08.009

Mizoi, J., Ohori, T., Moriwaki, T., Kidokoro, S., Todaka, D., Maruyama, K., et al. (2013). GmDREB2A; 2, a canonical DEHYDRATION-RESPONSIVE ELEMENT-BINDING PROTEIN2-type transcription factor in soybean, is posttranslationally regulated and mediates dehydration-responsive element-dependent gene expression. *Plant Physiol.* 161, 346–361. doi: 10.1104/pp.112.204875

Mizoi, J., Shinozaki, K., and Yamaguchi-Shinozaki, K. (2012). AP2/ERF family transcription factors in plant abiotic stress responses. *Biochim. Biophys. Acta* 1819, 86–96. doi: 10.1016/j.bbagrm.2011.08.004

Mostofa, M. G., Li, W., Nguyen, K. H., Fujita, M., and Tran, L. P. (2018). Strigolactones in plant adaptation to abiotic stresses: an emerging avenue of plant research. *Plant Cell Environ.* 41, 2227–2243. doi: 10.1111/pce.13364

Novillo, F., Alonso, J. M., Ecker, J. R., and Salinas, J. (2004). CBF2/DREB1C is a negative regulator of CBF1/DREB1B and CBF3/DREB1A expression and plays a central role in stress tolerance in *Arabidopsis*. *Proc. Natl. Acad. Sci. U.S.A.* 101, 3985–3990. doi: 10.1073/pnas.0303029101

Ono, K., Kimura, M., Matsuura, H., Tanaka, A., and Ito, H. (2019). Jasmonate production through chlorophyll a degradation by stay-green in *Arabidopsis thaliana*. *J. Plant Physiol.* 238, 53–62. doi: 10.1016/j.jplph.2019.05.004

Penfold, C. A., and Buchan-Wollaston, V. (2014). Modelling transcriptional networks in leaf senescence. *J. Exp. Bot.* 65, 3859–3873. doi: 10.1093/jxb/eru054

Qi, T., Wang, J., Huang, H., Liu, B., Gao, H., Liu, Y., Song, S., and Xie, D. (2015). Regulation of jasmonate-induced leaf senescence by antagonism between bHLH subgroup IIIe and IIId factors in *Arabidopsis*. *Plant Cell* 27, 1634–1649. doi: 10.1105/tpc.15.00110

Quirino, B. F., Normanly, J., and Amasino, R. M. (1999). Diverse range of gene activity during *Arabidopsis thaliana* leaf senescence includes pathogen-independent induction of defense-related genes. *Plant Mol. Biol.* 40, 267–278.

Rae, L., Lao, N. T., and Kavanagh, T. A. (2011). Regulation of multiple aquaporin genes in *Arabidopsis* by a pair of recently duplicated DREB transcription factors. *Planta* 234, 429–444. doi: 10.1007/s00425-011-1414-z

Sakuma, Y., Liu, Q., Dubouzet, J. G., Abe, H., Shinozaki, K., and Yamaguchi-Shinozaki, K. (2002). DNA-binding specificity of the ERF/AP2 domain of *Arabidopsis* DREBs, transcription factors involved in dehydration- and cold-inducible gene expression. *Biochem. Biophys. Res. Commun.* 290, 998–1009. doi: 10.1006/bbrc.2001.6299

Sazegari, S., Niazi, A., and Ahmadi, F. S. (2015). A study on the regulatory network with promoter analysis for *Arabidopsis* DREB-genes. *Bioinformation* 11, 101–106. doi: 10.6026/97320630011101

Schramm, F., Larkindale, J., Kiehlmann, E., Ganguli, A., Englich, G., Vierling, E., and von Koskull-Doring, P. (2008). A cascade of transcription factor DREB2A and heat stress transcription factor HsfA3 regulates the heat stress response of *Arabidopsis*. *Plant J.* 53, 264–274. doi: 10.1111/j.1365-313x.2007.03334.x

Seltmann, M. A., and Berger, S. (2013). Phenotyping jasmonate regulation of senescence. *Methods Mol. Biol.* 1011, 3–11. doi: 10.1007/978-1-62703-414-2_1

Shan, X., Li, C., Peng, W., and Gao, B. (2011). New perspective of jasmonate function in leaf senescence. *Plant Signal. Behav.* 6, 575–577. doi: 10.4161/psb.6.4.14899

Sharabi-Schwager, M., Lers, A., Samach, A., Guy, C. L., and Porat, R. (2010a). Overexpression of the CBF2 transcriptional activator in *Arabidopsis* delays leaf senescence and extends plant longevity. *J. Exp. Bot.* 61, 261–273. doi: 10.1093/jxb/erp300

Sharabi-Schwager, M., Samach, A., and Porat, R. (2010b). Overexpression of the CBF2 transcriptional activator in *Arabidopsis* counteracts hormone activation of leaf senescence. *Plant Signal. Behav.* 5, 296–299. doi: 10.4161/psb.5.3.10739

Sharoni, A. M., Nuruzzaman, M., Satoh, K., Shimizu, T., Kondoh, H., Sasaya, T., et al. (2011). Gene structures, classification and expression models of the AP2/EREBP transcription factor family in rice. *Plant Cell Physiol.* 52, 344–360. doi: 10.1093/pcp/pcq196

Shi, Q., Zhang, H., Song, X., Jiang, Y., Liang, R., and Li, G. (2017a). Functional characterization of the maize phytochrome-interacting factors PIF4 and PIF5. *Front. Plant Sci.* 8:2273. doi: 10.3389/fpls.2017.02273

Shi, Y., Huang, J., Sun, T., Wang, X., Zhu, C., Ai, Y., and Gu, H. (2017b). The precise regulation of different COR genes by individual CBF transcription factors in *Arabidopsis thaliana*. *J. Integr. Plant Biol.* 59, 118–133. doi: 10.1111/jipb.12515

Smirnoff, N., and Bryant, J. A. (1999). DREB takes the stress out of growing up. *Nat. Biotechnol.* 17, 229–230. doi: 10.1038/6968

Solanke, A. U., and Sharma, A. K. (2008). Signal transduction during cold stress in plants. *Physiol. Mol. Biol. Plants* 14, 69–79. doi: 10.1007/s12298-008-0006-2

Song, S., Huang, H., Wang, J., Liu, B., Qi, T., and Xie, D. (2017). MYC5 is involved in jasmonate-regulated plant growth, leaf senescence and defense responses. *Plant Cell Physiol.* 58, 1752–1763. doi: 10.1093/pcp/pcx112

Song, Y. (2014). Age-triggered and dark-induced leaf senescence require the bHLH transcription factors PIF3, 4 and 5. *Mol. plant.* 7, 1776–1787. doi: 10.1093/mp/ssu109

Song, Y., Yang, C., Gao, S., Zhang, W., Li, L., and Kuai, B. (2014). Age-triggered and dark-induced leaf senescence require the bHLH transcription factors PIF3, 4, and 5. *Mol. Plant* 7, 1776–1787. doi: 10.1093/mp/ssu109

Sun, S., Yu, J. P., Chen, F., Zhao, T. J., Fang, X. H., Li, Y. Q., et al. (2008). TINY, a dehydration-responsive element (DRE)-binding protein-like transcription factor connecting the DRE- and ethylene-responsive element-mediated signaling pathways in *Arabidopsis*. *J. Biol. Chem.* 283, 6261–6271. doi: 10.1074/jbc.m706800200

Takasaki, H., Maruyama, K., Takahashi, F., Fujita, M., Yoshida, T., Nakashima, K., et al. (2015). SNAC-As, stress-responsive NAC transcription factors, mediate ABA-inducible leaf senescence. *Plant J.* 84, 1114–1123. doi: 10.1111/tpj.13067

Thines, B., Parlan, E. V., and Fulton, E. C. (2019). Circadian network interactions with jasmonate signaling and defense. *Plants* 8:252. doi: 10.3390/plants8080252

Tsutsui, T., Kato, W., Asada, Y., Sako, K., Sato, T., Sonoda, Y., et al. (2009). DEAR1, a transcriptional repressor of DREB protein that mediates plant defense and freezing stress responses in *Arabidopsis*. *J. Plant Res.* 122, 633–643. doi: 10.1007/s10265-009-0252-6

Vainonen, J. P., Jaspers, P., Wrzaczek, M., Lamminmaki, A., Reddy, R. A., Vaahtera, L., et al. (2012). RCD1-DREB2A interaction in leaf senescence and stress responses in *Arabidopsis thaliana*. *Biochem. J.* 442, 573–581. doi: 10.1042/BJ20111739

Wang, Q., Guan, Y., Wu, Y., Chen, H., Chen, F., and Chu, C. (2008). Overexpression of a rice OsDREB1F gene increases salt, drought, and low temperature tolerance in both *Arabidopsis* and rice. *Plant Mol. Biol.* 67, 589–602. doi: 10.1007/s11103-008-9340-6

Wang, Y., Lin, A., Loake, G. J., and Chu, C. (2013). H2O2-induced leaf cell death and the crosstalk of reactive nitric/oxygen species. *J. Integr. Plant Biol.* 55, 202–208. doi: 10.1111/jipb.12032

Wang, Y., Reiter, R. J., and Chan, Z. (2018). Phytomelatonin: a universal abiotic stress regulator. *J. Exp. Bot.* 69, 963–974. doi: 10.1093/jxb/erx473

Wasternack, C. (2007). Jasmonates: an update on biosynthesis, signal transduction and action in plant stress response, growth and development. *Ann. Bot.* 100, 681–697. doi: 10.1093/aob/mcm079

Weaver, L. M., and Amasino, R. M. (2001). Senescence is induced in individually darkened *Arabidopsis* leaves, but inhibited in whole darkened plants. *Plant Physiol.* 127, 876–886. doi: 10.1104/pp.010312

Woo, H. R., Chung, K. M., Park, J.-H., Oh, S. A., Ahn, T., Hong, S. H., et al. (2001). ORE9, an F-box protein that regulates leaf senescence in *Arabidopsis*. *Plant Cell* 13, 1779–1790. doi: 10.1105/tpc.13.8.1779

Woo, H. R., Kim, H. J., Lim, P. O., and Nam, H. G. (2019). Leaf senescence: systems and dynamics aspects. *Annu. Rev. Plant Biol.* 70, 347–376. doi: 10.1146/annurev-arplant-050718-095859

Wu, K., Zhang, L., Zhou, C., Yu, C. W., and Chaikam, V. (2008). HDA6 is required for jasmonate response, senescence and flowering in *Arabidopsis*. *J. Exp. Bot.* 59, 225–234. doi: 10.1093/jxb/erm300

Wu, X. Y., Kuai, B. K., Jia, J. Z., and Jing, H. C. (2012). Regulation of leaf senescence and crop genetic improvement. *J. Integr. Plant Biol.* 54, 936–952. doi: 10.1111/jipb.12005

Xu, H., Wang, X., and Chen, J. (2010). Overexpression of the Rap2.4f transcriptional factor in *Arabidopsis* promotes leaf senescence. *Sci. China Life Sci.* 53, 1221–1226. doi: 10.1007/s11427-010-4068-3

Yang, J., Duan, G., Li, C., Liu, L., Han, G., Zhang, Y., et al. (2019a). The crosstalks between jasmonic acid and other plant hormone signaling highlight the involvement of jasmonic acid as a core component in plant response to biotic and abiotic stresses. *Front. Plant Sci.* 10:1349. doi: 10.3389/fpls.2019.01349

Yang, J., Liu, Y., Yan, H., Tian, T., You, Q., Zhang, L., et al. (2018). PlantEAR: functional analysis platform for plant ear motif-containing proteins. *Front. Genet.* 9:590. doi: 10.3389/fgene.2018.00590

Yang, S. D., Seo, P. J., Yoon, H. K., and Park, C. M. (2011). The *Arabidopsis* NAC transcription factor VNI2 integrates abscisic acid signals into leaf senescence via the COR/RD genes. *Plant Cell* 23, 2155–2168. doi: 10.1105/tpc.111.084913

Yang, Y., Al-Baidhani, H. H. J., Harris, J., Riboni, M., Li, Y., Mazonka, I., et al. (2019b). DREB/CBF expression in wheat and barley using the stress-inducible promoters of HD-Zip I genes: impact on plant development, stress tolerance and yield. *Plant Biotechnol. J.* 18, 829–844. doi: 10.1111/pbi.13252

Yasuhito, S., Jinkil, J., Min-Young, K., Junghyun, K., Nam-Chon, P., and Giltsu C. (2014). Phytochrome-interacting transcription factors PIF4 and PIF5 induce leaf senescence in *Arabidopsis*. *Nat. Commun*. 5:4636. doi: 10.1038/ncomms5636

Yeung, E., van Veen, H., Vashisht, D., Sobral Paiva, A. L., Hummel, M., Rankenberg, T., et al. (2018). A stress recovery signaling network for enhanced flooding tolerance in *Arabidopsis thaliana*. *Proc. Natl. Acad. Sci. U.S.A.* 115, E6085–E6094. doi: 10.1073/pnas.1803841115

Yolcu, S., Li, X., Li, S., and Kim, Y. J. (2017). Beyond the genetic code in leaf senescence. *J. Exp. Bot*. 69, 801–810. doi: 10.1093/jxb/erx401

Yoshida, S. (2003). Molecular regulation of leaf senescence. *Curr. Opin. Plant Biol.* 6, 79–84. doi: 10.1016/s1369526602000092

Yu, J., Zhang, Y., Di, C., Zhang, Q., Zhang, K., Wang, C., et al. (2016). JAZ7 negatively regulates dark-induced leaf senescence in *Arabidopsis*. *J. Exp. Bot.* 67, 751–762. doi: 10.1093/jxb/erv487

Zhang, H., and Zhou, C. (2013). Signal transduction in leaf senescence. *Plant Mol. Biol.* 82, 539–545. doi: 10.1007/s11103-012-9980-4

Zhang, X., Zhu, Z., An, F., Hao, D., Li, P., Song, J., et al. (2014). Jasmonate-activated MYC2 represses ethylene insensitive3 activity to antagonize ethylene-promoted apical hook formation in *Arabidopsis*. *Plant Cell* 26, 1105–1117. doi: 10.1105/tpc.113.122002

Zhang, Y., Wang, Y., Wei, H., Li, N., Tian, W., Chong, K., et al. (2018). Circadian evening complex represses jasmonate-induced leaf senescence in *Arabidopsis*. *Mol. Plant* 11, 326–337. doi: 10.1016/j.molp.2017.12.017

Zhang, Z., and Guo, Y. (2018). Hormone treatments in studying leaf senescence. *Methods Mol. Biol.* 1744, 125–132. doi: 10.1007/978-1-4939-7672-0_11

Zhou, M. Q., Shen, C., Wu, L. H., Tang, K. X., and Lin, J. (2011a). CBF-dependent signaling pathway: a key responder to low temperature stress in plants. *Crit. Rev. Biotechnol.* 31, 186–192. doi: 10.3109/07388551.2010.505910

Zhou, X., Jiang, Y., and Yu, D. (2011b). WRKY22 transcription factor mediates dark-induced leaf senescence in *Arabidopsis*. *Mol. Cells* 31, 303–313. doi: 10.1007/s10059-011-0047-1

Zhu, X., Chen, J., Xie, Z., Gao, J., Ren, G., Gao, S., et al. (2015). Jasmonic acid promotes degreening via MYC2/3/4- and ANAC019/055/072-mediated regulation of major chlorophyll catabolic genes. *Plant J.* 84, 597–610. doi: 10.1111/tpj.13030

Zhu, Z. (2014). Molecular basis for jasmonate and ethylene signal interactions in *Arabidopsis*. *J. Exp. Bot.* 65, 5743–5748. doi: 10.1093/jxb/eru349

Zhu, Z., An, F., Feng, Y., Li, P., Xue, L., Mu, A., Jiang, Z., et al. (2011). Derepression of ethylene-stabilized transcription factors (EIN3/EIL1) mediates jasmonate and ethylene signaling synergy in *Arabidopsis*. *Proc. Natl. Acad. Sci. U.S.A.* 108, 12539–12544. doi: 10.1073/pnas.1103959108

Conflict of Interest: The authors declare that the research was conducted in the absence of any commercial or financial relationships that could be construed as a potential conflict of interest.

frontiers in Plant Science

ORIGINAL RESEARCH
published: 03 April 2020
doi: 10.3389/fpls.2020.00377

Protein Phosphorylation Dynamics Under Carbon/Nitrogen-Nutrient Stress and Identification of a Cell Death-Related Receptor-Like Kinase in Arabidopsis

Xingwen Li[1], Miho Sanagi[1], Yu Lu[1†], Yuko Nomura[2], Sara Christina Stolze[3], Shigetaka Yasuda[4], Yusuke Saijo[4], Waltraud X. Schulze[5], Regina Feil[6], Mark Stitt[6], John E. Lunn[6], Hirofumi Nakagami[2,3], Takeo Sato[1]* and Junji Yamaguchi[1]*

[1] Faculty of Science and Graduate School of Life Sciences, Hokkaido University, Sapporo, Japan, [2] Plant Proteomics Research Unit, RIKEN Center for Sustainable Resource Science, Yokohama, Japan, [3] Max Planck Institute for Plant Breeding Research, Cologne, Germany, [4] Graduate School of Science and Technology, Nara Institute of Science and Technology, Ikoma, Japan, [5] Department of Plant Systems Biology, University of Hohenheim, Stuttgart, Germany, [6] Max Planck Institute of Molecular Plant Physiology, Golm, Germany

Nutrient availability, in particular the availability of sugar [carbon (C)] and nitrogen (N), is important for the regulation of plant metabolism and development. In addition to independent utilization of C and N nutrients, plants sense and respond to the balance of C and N nutrients (C/N-nutrient) available to them. High C/low N-nutrient stress has been shown to arrest early post-germinative growth while promoting progression to senescence in Arabidopsis. Although several signaling components of the C/N-nutrient response have been identified, the inclusive molecular basis of plant C/N-nutrient response remains unclear. This proteome analysis evaluated phosphorylation dynamics in response to high C/low N-nutrient stress. Phosphoproteomics under conditions of C/N-nutrient stress showed a global change in the phosphorylation status of proteins, including plasma membrane H^+-ATPase, carbon and nitrogen metabolic enzymes and signaling proteins such as protein kinases and transcription factors. Further analyses suggested that SNF1-related protein kinase 1 (SnRK1) is involved in primary C/N-nutrient signal mediation via the transcriptional regulation of C/N-regulatory kinases. We also identified a leucine-rich repeat receptor-like kinase with extracellular malectin-like domain, named as LMK1, which was shown to possess cell death induction activity in plant leaves. These results provide important insight into the C/N-nutrient signaling pathways connecting nutrition stress to various cellular and physiological processes in plants.

Keywords: sugar, nitrogen, phosphorylation, kinase, SnRK1, receptor-like kinase, metabolism, cell death

OPEN ACCESS

Edited by:
Yasuhito Sakuraba,
The University of Tokyo, Japan

Reviewed by:
J. C. Jang,
The Ohio State University, United States
Lorenzo Guglielminetti,
University of Pisa, Italy

***Correspondence:**
Hirofumi Nakagami
nakagami@mpipz.mpg.de
Takeo Sato
t-satou@sci.hokudai.ac.jp

†Present address:
Yu Lu,
Graduate School of Life and Environmental Sciences, University of Tsukuba, Tsukuba, Japan

Specialty section:
This article was submitted to Plant Abiotic Stress, a section of the journal Frontiers in Plant Science

Received: *23 December 2019*
Accepted: *16 March 2020*
Published: *03 April 2020*

Citation:
Li X, Sanagi M, Lu Y, Nomura Y, Stolze SC, Yasuda S, Saijo Y, Schulze WX, Feil R, Stitt M, Lunn JE, Nakagami H, Sato T and Yamaguchi J (2020) Protein Phosphorylation Dynamics Under Carbon/Nitrogen-Nutrient Stress and Identification of a Cell Death-Related Receptor-Like Kinase in Arabidopsis. Front. Plant Sci. 11:377. doi: 10.3389/fpls.2020.00377

INTRODUCTION

Plant growth and development are controlled by signaling pathways that are triggered by various environmental conditions and integrated with endogenous cues. Plant growth is dependent on supplies of carbon (C), in the form of sugars, and nitrogen (N) to provide energy and the major components for synthesis of structural components. It is now well-established that C and N nutrients function as signaling molecules in a wide array of cellular processes, enabling plants to coordinate their growth and development with nutrient availability (Rolland et al., 2006; Vidal and Gutiérrez, 2008). Any imbalance between C and N supplies is likely to have a detrimental effect on growth, therefore the C/N ratio in cells is very important, and plants have developed a sophisticated system to sense and respond to the ratio of available C and N nutrients (Coruzzi and Zhou, 2001; Martin et al., 2002; Sato et al., 2009). C/N-nutrient conditions can affect plant phenotypes at all stages in the plant's life cycle. For example, the post-germination growth of Arabidopsis (*Arabidopsis thaliana*) plants is markedly inhibited in medium containing excess sugar and limiting nitrogen supplies (high C/low N-nutrient stress). Growth arrest can be lifted by either lowering the sugar concentration or increasing the nitrogen concentration, or both (Martin et al., 2002). Another example of high C/low N-nutrient stress occurs in Arabidopsis plants grown in elevated CO_2 concentrations with limiting N, which accelerates the progression of plant senescence, including leaf yellowing and anthocyanin accumulation, during the mature developmental stage (Aoyama et al., 2014). Despite the importance of C/N-nutrient responses for proper growth and development, the underlying mechanisms remain unclear.

Previous mutant screening has led to the isolation of the ubiquitin ligase ATL31, which plays a role in the C/N-nutrient response in Arabidopsis (Sato et al., 2009). ATL31 is a member of the plant-specific RING-type ubiquitin ligase ATL family (Serrano et al., 2006; Aguilar-Hernández et al., 2011). ATL31 overexpression resulted in a phenotype insensitive to high C/low N-nutrient stress and an increase in the number of green-colored cotyledons during the early post-germinative growth stage, whereas the *atl31* loss-of-function mutant showed a hypersensitive phenotype. In mature plants, ATL31 negatively regulates the progression of leaf senescence in the presence of elevated atmospheric CO_2 and limited N concentrations (Aoyama et al., 2014). Serine (Ser) and threonine (Thr) residues at the C-terminal region of ATL31 were shown to be phosphorylated by CBL-interacting protein kinases 7, 12, and 14 (CIPK7/12/14) (Yasuda et al., 2014, 2017). Phosphorylation of these residues was found to mediate the direct interaction with and ubiquitylation of 14-3-3 protein, resulting in proteasomal degradation of 14-3-3 under high C/low N-nutrient stress (Yasuda et al., 2014, 2017). 14-3-3 protein generally interacts with phosphorylated target proteins and regulates target functions, which modulates a wide range of physiological pathways (Comparot et al., 2003; Mackintosh, 2004; Chevalier et al., 2009; Jaspert et al., 2011). The target proteins of 14-3-3 involved in plant C/N-nutrient responses, however, remain unidentified. The phosphorylation of ATL31 by CIPK7/12/14 also increases the stability of ATL31 protein under high C/low N-nutrient stress condition (Yasuda et al., 2017). Importantly, CIPK7/12/14 are transcriptionally activated in response to high C/low N-nutrient stress, suggesting the existence of an as yet unknown upstream signaling component that mediates primary C/N-nutrient signaling in Arabidopsis plants.

In this study, we carried out phosphoproteome analysis to investigate the primary and global dynamics of C/N-nutrient related phosphorylation signals in Arabidopsis seedlings. We identified 193 proteins, the phosphorylation levels of which were responsive to short-term high C/low N-nutrient stress. Among the 193 identified phospho-regulated proteins, we found that a plasma membrane H^+-ATPase was a C/N-responsive 14-3-3 target. Besides, we showed that SNF1-related protein kinase 1 (SnRK1), presumably regulates *CIPK7/12/14* gene expressions. We also identified a putative C/N-nutrient responsive receptor-like kinase, which possesses cell death induction activity in plant leaves. In addition, the phosphoproteomics results identified several proteins likely to modulate the progression of senescence in response to C/N-nutrient stress. These results indicate the existence of a comprehensive molecular network involved in primary C/N-nutrient signaling and metabolic adaptation.

MATERIALS AND METHODS

Plant Materials and Growth Condition

Arabidopsis thaliana Columbia ecotype (Col-0) was used as the wild-type (WT) in all experiments. Transgenic Arabidopsis plants constitutively expressing FLAG-tag fused 14-3-3χ (*FLAG-14-3-3χ*) under the control of a 35S promoter in the WT background (Sato et al., 2011) and the double knockdown mutant of *SnRK1α* (*snrk1α1i/1α2*) (Sanagi et al., 2018) have been described. *Nicotiana benthamiana* plants were used for transient protein expression. Arabidopsis and *N. benthamiana* seeds were surface-sterilized and sowed on C/N-modified medium indicated in each experiment. After kept in dark at 4°C for 2–4 days to synchronize germination, the plants were grown at 22°C under short-day (8 h light/16 h dark), long-day (16 h light/8 h dark) or continuous light exposure condition as indicated in each experiment. Glucose was used as sugar and, potassium nitrate and ammonium nitrate were used as nitrogen. In most experiments, we added 100 mM Glc in the control C/N medium. To optimize the growth condition of *snrk1α1i/1α2* mutant plants, we added 10 mM Glucose in the medium for gene expression analysis using *snrk1α1i/1α2* plants.

Phosphoproteome Analysis by LC-MS/MS

Wild-type Arabidopsis seedlings were grown in liquid MS medium containing 100 mM glucose and 30 mM nitrogen (control C/N-nutrient) for 10 days under continuous light exposure. The seedlings were transferred to control C/N-nutrient or MS medium containing 200 mM glucose and 0.3 mM nitrogen (high C/low N-nutrient) for 30 min. Phosphopeptides were enriched as described previously with minor modifications (Nakagami, 2014; Choudhary et al., 2015). LTQ-Orbitrap XL

(Thermo Fisher Scientific) coupled with an EASY-nLC 1000 (Thermo Fisher Scientific) was used for nano-LC-MS/MS analyses. A self-pulled needle (150 mm length × 100 μm i.d., 6-μm opening) packed with ReproSil C18 materials (3 μm; Dr. Maisch GmbH) was used as an analytical column with a "stone-arch" frit (Ishihama et al., 2002). A spray voltage of 2,400 V was applied. The injection volume was 6 μl, and the flow rate was 500 nl min^{-1}. The mobile phases consisted of 0.5% acetic acid and 2% acetonitrile (A) and 0.5% acetic acid and 80% acetonitrile (B). A three-step linear gradient of 5 to 10% B in 10 min, 10 to 40% B in 120 min, 40 to 95% B in 5 min, and 95% B for 10 min was employed. The MS scan range was m/z 300–1,400. The top 10 precursor ions were selected in the MS scan by Orbitrap with resolution = 100,000 and for subsequent MS/MS scans by ion trap in the automated gain control mode, where automated gain control values of 5.00e+05 and 2.00e+05 were set for full MS and MS/MS, respectively. The normalized collision-induced dissociation was set to 35.0. A lock mass function was used for the LTQ-Orbitrap XL to obtain constant mass accuracy during gradient analysis (Olsen et al., 2005). Multi-stage activation was enabled upon detection of a neutral loss of phosphoric acid (98.00, 49.00, or 32.66 amu) (Schroeder et al., 2004) for further ion fragmentation. Selected sequenced ions were dynamically excluded for 60 s after sequencing.

Raw data was processed using MaxQuant software (version 1.6.3.4[1]) (Cox and Mann, 2008) with label-free quantification (LFQ) and iBAQ enabled (Tyanova et al., 2016a). MS/MS spectra were searched by the Andromeda search engine against a combined database containing the sequences from Arabidopsis thaliana (TAIR10_pep_20101214[2]) and sequences of 248 common contaminant proteins and decoy sequences. Trypsin specificity was required and a maximum of two missed cleavages allowed. Minimal peptide length was set to seven amino acids. Carbamidomethylation of cysteine residues was set as a fixed modification, and phosphorylation of serine, threonine, and tyrosine residues; oxidation of methionine residues; and N-terminal acetylation of proteins allowed as variable modifications. Peptide-spectrum-matches and proteins were retained if they were below a false discovery rate of 1%. Statistical analysis of the intensity values obtained for the phosphopeptides ("modificationSpecificPeptides" output file) was carried out using Perseus (version 1.5.8.5[3]) (Tyanova et al., 2016b). Quantified peptides were filtered for reverse hits and contaminants. For further processing, only peptides containing a phospho(STY) modification were kept and the intensity values were log2 transformed. After grouping samples by condition, only those peptides were retained for the subsequent analysis that had 6 valid values in one of the conditions. Data was normalized by subtraction of the median (Matrix access = Columns, Subtract = Median). Missing values were imputed from a normal distribution using the default settings in Perseus (width = 0.3, downshift = 1.8, separately for each column). Two-sample *t*-tests were performed using a *p*-value cut-off of 0.05. The accession numbers for proteomics data generated in this study are PXD016507 for ProteomeXchange and JPST000703 for jPOST (Okuda et al., 2017). To investigate possible interactions between the C/N-responsive phosphoproteins, we used the STRING database[4] for known and predicted protein-protein interactions with the standard setting (von Mering et al., 2005).

Coimmunoprecipitation Analysis

Arabidopsis seedlings constitutively expressing *FLAG-14-3-3χ* were grown in liquid MS medium containing 100 mM glucose and 30 mM nitrogen (control C/N-nutrient) for 10 days under continuous light exposure. The seedlings were transferred to control C/N-nutrient or MS medium containing 200 mM glucose and 0.3 mM nitrogen (high C/low N-nutrient) for 30 min. Proteins were extracted using protein extraction buffer (50 mM Tris, 0.5% Triton X-100, 150 mM NaCl, 10% glycerol, 5 mM $MgCl_2$, 1 mM EDTA, pH 7.5) supplemented with 10 μM MG132, Complete Protease Inhibitor Mixture (Roche Applied Science) and PhosSTOP phosphatase inhibitor cocktail (Roche Applied Science, Germany). Proteins were immunoprecipitated with anti-FLAG M2 magnetic beads (Sigma-Aldrich, M8823) for 1 h at 4°C with shaking. After washing the beads, the bound proteins were eluted with 150 μg/ml 3x FLAG peptide (Sigma-Aldrich, F4799), followed by precipitation in cold acetone and resuspension in SDS sample buffer (62.5 mM Tris, 2% SDS, 10% glycerol, 5% 2-mercaptoethanol, 0.01% bromophenol blue, pH 6.8). The proteins were analyzed by immunoblotting with anti-FLAG (MBL, PM020) and anti-plasma membrane H^+-ATPase (Agrisera, AS07 260) antibodies.

Gene Expression Analysis

WT and inducible RNAi knockdown mutant of *SnRK1α* (*snrk1α1i/1α2*) plants were grown for 11 days on medium containing 10 mM glucose and 30 mM nitrogen in the absence of dexamethasone (DEX) under 16 h light/8 h dark cycles, transferred to medium supplemented with 10 μM DEX, and grown for 5 days. Total RNA was isolated from indicated plant materials using TRIzol reagent (Invitrogen) and treated with RQ1 RNase-free DNase (Promega) according to the manufacturers' protocols. First-strand cDNA was synthesized using oligo(dT) primer (Promega) and ReverTraAce reverse transcriptase (TOYOBO) and subjected to qRT-PCR analysis on a Mx3000P system (Agilent Technologies) using TB Green Premix EX Taq (TaKaRa) and the primers listed in **Supplementary Table S1**, as described by the manufacturer.

Quantification of T6P, G6P, and UDP-Glc

WT plants were grown for 16 days on medium containing 100 mM glucose and 30 mM nitrogen (control) under 16 h light/8 h dark cycles, and transferred to control medium or modified C/N-nutrient medium containing 100 mM glucose and 0.3 mM nitrogen, 300 mM glucose and 30 mM nitrogen or 300 mM glucose and 0.3 mM nitrogen. The seedlings were harvested 1 and 24 h later. T6P, G6P, and UDP-Glc were extracted with chloroform/methanol and measured by anion-exchange

[1] http://www.maxquant.org/

[2] ftp://ftp.arabidopsis.org/home/tair/Proteins/TAIR10_protein_lists/

[3] http://www.maxquant.org/

[4] https://string-db.org/

high performance liquid chromatography coupled to tandem mass spectrometry (LC-MS/MS) as described in Lunn et al. (2006) with modifications as described in Figueroa et al. (2016).

Plasmid Construction

The coding sequence of *LMK1* (*At1g07650.1*) was amplified from Col-0 cDNA. LMK1 with a point mutation (LMK1D805A) and truncated forms of LMK1 (LMK1ΔL, LMK1ΔM, and LMK1ΔLΔM) were generated by PCR-based site-directed mutagenesis using the primers listed in **Supplementary Table S1**. Amplified fragments were cloned into pENTR/D-TOPO vector and transferred to destination vectors using the Gateway system according to the manufacturer's protocol (Invitrogen). The sequences of all amplified fragments and inserts were verified by DNA sequencing.

Transient Expression in *N. benthamiana* Leaves

The surface-sterilized *N. benthamiana* seeds were sowed on 1xMurashige and Skoog (MS) medium supplemented with 1% sucrose, and grown under 16 h light/8 h dark cycles at 22°C on the plates for 2 weeks, then transferred to flowerpot with soil containing compost and vermiculate in the ratio of 1:6 and grown for additional 2 weeks. The various forms of *LMK1* were subcloned into the destination vector pMDC83 (Curtis and Grossniklaus, 2003), with all genes under the control of a CaMV35S promoter and GFP attached to the C-terminal of each encoded protein. These plasmids were introduced into *Agrobacterium tumefaciens* strain GV3101 (pMP90) by electroporation using a MicroPulser electroporator (Bio-Rad), and the subcloned sequences were transiently expressed in *N. benthamiana* as described (Yasuda et al., 2014).

Transient Expression in Arabidopsis Mesophyll Protoplast Cells

The surface-sterilized WT Arabidopsis seeds were sowed on 1xMurashige and Skoog (MS) medium supplemented with 1% sucrose, and grown under 8 h light/16 h dark cycles at 22°C on the plates for 2 weeks, then transferred to flowerpot with soil containing compost and vermiculate in the ratio of 1:6 and grown for additional 3 weeks. Full-length *LMK1* was subcloned into the destination vector pUGW5 (Nakagawa et al., 2007), with the gene under the control of a CaMV35S promoter and GFP attached to the C-terminal of each encoded protein. The plasmids were introduced by polyethylene glycol-mediated transformation (Yoo et al., 2007) into Arabidopsis mesophyll protoplasts prepared from leaf tissues, and images were taken 16 h later.

Confocal Laser-Scanning Microscopy

Fluorescent images were obtained using a Zeiss LSM510 confocal laser scanning microscope equipped with a C-Apochromat (×40/1.2 water immersion) objective 2 days after the inoculation of *Agrobacterium* into *N. benthamiana* leaves. GFP fluorescence was excited by a 488 nm argon laser and detected using a 505–550 nm band-pass emission filter. Images were processed using Image J software.

Preparation of Water-Soluble and Membrane Fractions

Proteins were extracted from *N. benthamiana* leaves expressing GFP or LMK1-GFP using extraction buffer (50 mM Tris, 150 mM NaCl, 10% glycerol, 1 mM EDTA, pH 7.5) supplemented with 10 μM MG132, Complete Protease Inhibitor Mixture (Roche Applied Science) and PhosSTOP phosphatase inhibitor cocktail (Roche Applied Science, Germany). Lysates were centrifuged at 20,000 *g* for 5 min at 4°C to remove cell debris, followed by ultracentrifugation (101,000 *g*, 1 h, 4°C) to separate the soluble and insoluble fractions. Membrane fraction proteins were solubilized by the extraction buffer supplemented with 1% Triton X-100. GFP and LMK1-GFP proteins were enriched by immunoprecipitation using anti-GFP antibody beads (MBL, cat. no. D153-10), followed by SDS-PAGE and western blotting analysis with anti-GFP antibody (MBL, cat. no. 598).

Electrolyte Leakage Analysis

Ion leakage was assayed with infiltrated *N. benthamiana* leaf discs. Forty-eighth after infiltration, 15 leaf discs, each 6 mm in diameter, were generated from four different leaves of each construct. After washing with Milli-Q water, the leaf discs were transferred to tissue culture plates. Each well-contained five leaf discs and 3 ml fresh Milli-Q water. The conductivity of the water was measured at 0, 24, 48, and 72 h using a conductivity meter (HORIBA, LAQUAtwin-EC-33).

RESULTS

Phosphoproteome Analysis Reveals Protein Phosphorylation Dynamics in Response to High C/Low N-Nutrient Stress in Arabidopsis Plants

To assess the effects of high C/low N-nutrient stress on global protein phosphorylation status in Arabidopsis, 10-day-old seedlings were transiently treated with control (100 mM Glc/30 mM N) or high C/low N-nutrient stress (200 mM Glc/0.3 mM N) medium for 30 min and subjected to phosphoproteome analysis with HAMMOC-TiO_2 phosphopeptide enrichment followed by LC-MS/MS analysis. This analysis detected a total of 1785 phosphopeptides, of which 1338 were quantified, with 193 protein groups having significantly changed phosphorylation levels in response to high C/low N-nutrient stress (**Table 1** and **Supplementary Table S2**). The functional networks of the C/N-responsive phosphoproteins were assessed using the STRING (Search Tool for the Analysis of Interacting Genes/Proteins) algorithm (**Figure 1**). Seven groups of proteins with distinct molecular functions were identified. Metabolic enzymes that function in photosynthesis [*rubisco small subunit 1A* (RBCS1A), carbonic anhydrase 2 (CA2), phosphoenolpyruvate carboxylases 1/2 (PPC1/2), phosphoenolpyruvate carboxykinase 1 (PCK1), cytosolic invertase 1 (CINV1), phosphoglucomutase (PGM), β-amylase1] and nitrate reductase 2 (NIA2) formed a highly connected network. Proteins involved in RNA metabolism

TABLE 1 | List of C/N-responsive protein kinases identified by LC-MS/MS analysis.

AGI code[a]	Protein description	Phosphopeptide[b]	Ratio (log2)[c]	*p*-Value[d]
At3g50500	SNF1-related protein kinase 2.2 (SnRK2.2)	S(0.158)S(0.172)VLHS(0.699)QPKS(0.694)T(0.25)VGT(0.026)PAYIAPEILLR	2.34	0.02
		S(0.005)S(0.005)VLHS(0.016)QPK**S**(0.812)T(0.313)VG**T**(0.787)PAY(0.06)IAPEILLR		
At1g07650	Leucine-rich repeat malectin kinase (LMK1)	S(0.002)L**S**(0.997)FSTSGPR	1.27	0.01
At3g58640	Mitogen activated protein kinase kinase kinase-like protein	RS(0.333)IS(0.333)IT(0.333)PEIGDDIVR	1.04	0.01
At3g25840	Spliceosome-associated kinase (PRP4KA)	DIVPET(0.009)GAPVS(0.455)T(0.455)S(0.081)PAVVIAANVGQAK	0.41	0.03
		DIVPET(0.001)GAPVS(0.114)T(0.114)**S**(0.772)PAVVIAANVGQAK		
		DIVPE**T**(0.751)GAPVS(0.122)T(0.122)S(0.005)PAVVIAANVGQAK		
		DIVPET(0.007)GAPVS(0.045)T(0.474)S(0.474)PAVVIAANVGQAK		
At3g17850	Incomplete root hair elongation 1 (IREH1)	VSNSHLTEESDVL**S**(1)PR	−0.46	0.01
At1g18150	Mitogen-activated protein kinase 8 (MPK8)	AAAAVASTLESEEADNGGGY**S**(1)AR	−0.56	0.01
At5g19450	Calcium-dependent protein kinase 19 (CDPK19/CPK8)	SNPFYSEAYTT(0.003)NG**S**(0.991)GT(0.006)GFK	−0.69	0.03
		SNPFYSEAYTT(0.005)NGS(0.092)G**T**(0.903)GFK		
At1g53165	AtMAP4K alpha1	DSYQNDY(0.001)QEEDDS(0.725)S(0.072)GS(0.072)GT(0.072)VVIRS(0.059)PR	−0.76	0.03
		DSYQNDY(0.007)QEEDDS(0.099)S(0.099)GS(0.094)GT(0.071)VVIRS(0.63)PR		
At3g45780	phototropin 1 (phot1/NPH1/RPT1)	AL**S**(1)ESTNLHPFMTK	−1.28	0.00
At3g01090, At3g29160	SNF1-related protein kinase 1α1, 1α2 (SnRK1α1/AKIN10, SnRK1α2/AKIN11)	DGHFLKT(0.212)S(0.212)CGS(0.576)PNYAAPEVISGK	−2.39	0.01

[a]*Accession numbers of Arabidopsis genes.* [b]*Phosphopeptide sequences were detected by LC-MS/MS; phosphorylated amino acids with the localization probability score and are underlined and in bold type when the score is higher than 0.75.* [c]*Average log2 fold difference between high C/low N-nutrient stress and control conditions.* [d]*Calculated by Student's t-tests.*

and translational regulation also formed clusters, including RNA-binding Pumilio proteins (APUM2/4), FHA (forhkead) domain-containing protein involved in miRNA biosynthesis (DDL), pre-18S ribosomal RNA processing factor (PWP2), and 40S and 60S ribosomal subunits. Several transporters and membrane trafficking regulators were identified as being C/N-responsive phosphoproteins, including plasma membrane intrinsic protein (aquaporin) 2E (PIP2E), plasma membrane H^+-ATPase (AHA1/2), clathrin adaptor, clathrin-interacting ENTH/VHS protein (EPSIN1), golgin candidate 5 (GC5), and brefeldin A-inhibited guanine nucleotide-exchange protein 5 (BIG5/MIN7). Besides, transcription factors TCP domain protein (TCP10) and FLOWERING bHLH (FBH4), as well as several signaling proteins, including protein kinases [SNF1-related protein kinase catalytic subunit alpha (SnRK1α), SnRK2.2, calcium-dependent protein kinase (CDPK19/CPK8), phototropin 1 (phot1)], phosphatases [BRI1 suppressor 1-like 2 (BSL2)] and ubiquitin ligase [Non-phototropic Hypocotyl 3 (NPH3), RING domain ligase 2 (RGLG2)] were identified.

Physical Interaction Between H^+-ATPase and 14-3-3 Is Enhanced Under High C/Low N-Nutrient Stress Conditions

Plasma membrane H^+-ATPases act as primary transporters of H^+, which regulates pH homeostasis and membrane potential and drives several nutrient transport processes. High C/low N-nutrient stress increased the phosphorylation levels of Thr residues at the C-terminal regions of plasma membrane H^+-ATPases 1 and 2 (AHA1 and AHA2; **Figure 1** and **Supplementary Table S2**). Phosphorylation of the Thr948 residue in AHA1 and the Thr947 residue in AHA2 has been reported to mediate the binding of 14-3-3 protein, which promotes the activity of H^+-ATPases (Kinoshita and Shimazaki, 1999; Svennelid et al., 1999; Palmgren, 2001; Chevalier et al., 2009). Therefore, we asked if there is any link between high C/low N-nutrient stress response and AHA–14-3-3 interaction. The transgenic Arabidopsis seedlings constitutively expressing FLAG-tag fused 14-3-3χ (*FLAG-14-3-3*χ) were transiently exposed to high C/low N-nutrient stress, and then the interaction was evaluated by co-immunoprecipitation. As shown in **Figure 2**, AHA protein abundance was not affected after the stress exposure but enhanced interaction between AHA and FLAG-14-3-3χ was observed under high C/low N-nutrient stress conditions. These results suggest that C/N conditions modulate H^+-ATPase activity via 14-3-3 binding in Arabidopsis.

SnRK1 Is Involved in the Transcriptional Regulation of C/N-Related Protein Kinases CIPK7/12/14

We previously demonstrated that CIPK7/12/14 kinases directly phosphorylate ATL31 and play important roles in modulating plant growth in response to C/N-nutrient conditions (Yasuda et al., 2017). The expression of *CIPK* genes was increased

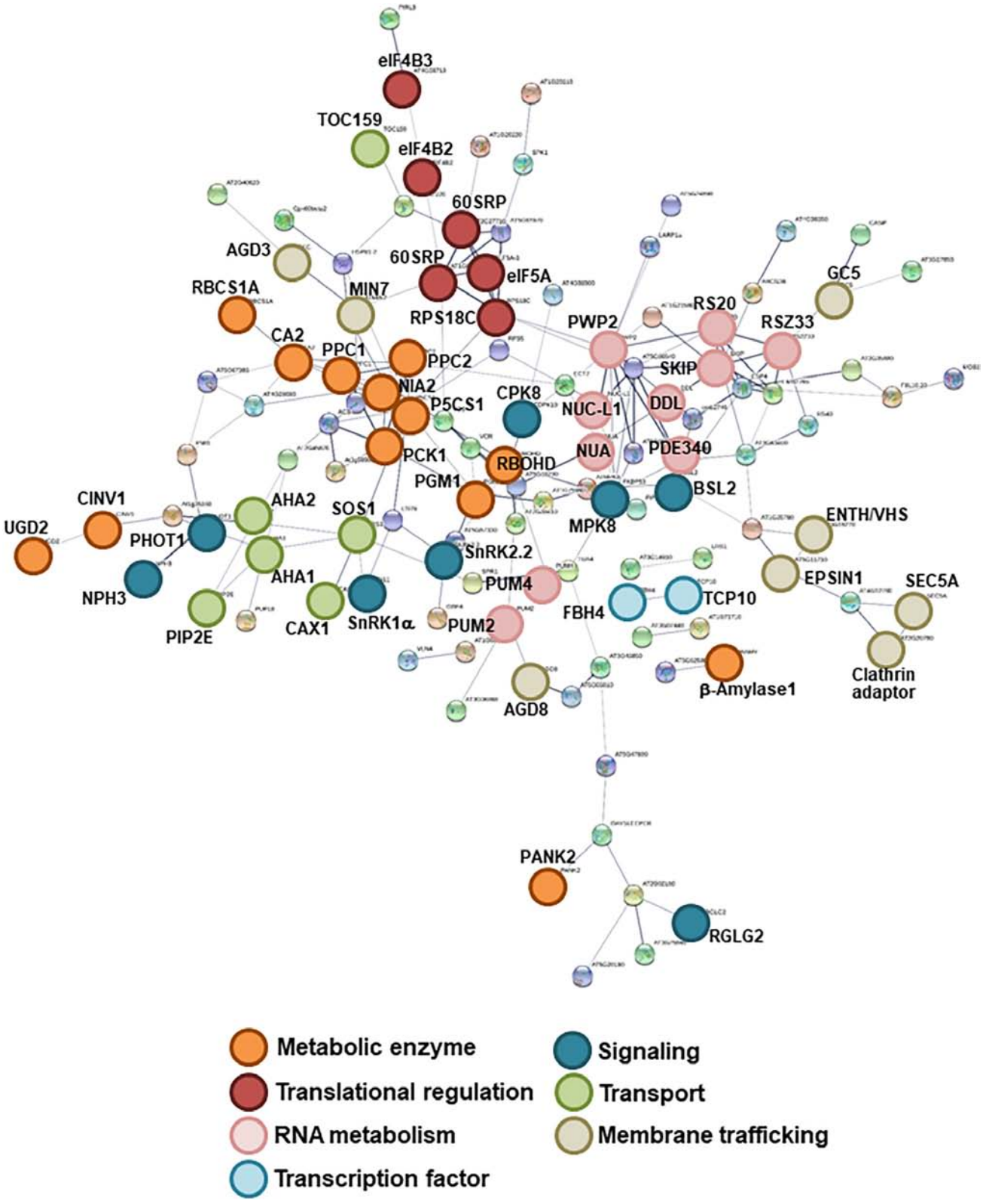

FIGURE 1 | Interaction networks of the identified C/N-nutrient responsive phosphoproteins. Functional network mapping was performed using the STRING protein interaction algorithm (https://string-db.org/). Shown are the associations among C/N-nutrient responsive phosphoproteins identified by LC-MS/MS analysis (**Supplementary Table S2**). Nodes with connections are shown. Line thickness indicates the strength of supporting data.

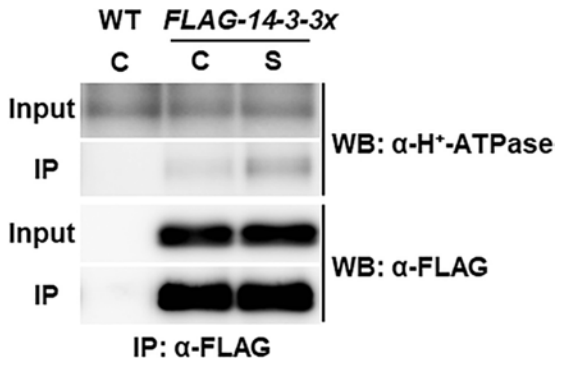

FIGURE 2 | Co-immunoprecipitation analysis of plasma membrane H^+-ATPase and 14-3-3 proteins. WT and transgenic Arabidopsis plants expressing FLAG-14-3-3χ were grown in control liquid medium containing 100 mM Glc/30 mM N, and 10-day-old seedlings were treated with the control (C) or the high C/low N-nutrient stress medium containing 200 mM Glc/0.3 mM N (S) for 30 min. Proteins were extracted and subjected to immunoprecipitation with anti-FLAG antibody beads, followed by immunoblotting with anti-plasma membrane H^+-ATPase and anti-FLAG antibodies. Three independent experiments showed similar results.

under high C/low N-nutrient stress, with these protein products positively regulating the ability of ATL31 to adapt to these conditions, suggesting that upstream components regulate the C/N-responsive expression of *CIPK* genes. Phosphoproteome analysis showed that high C/low N-nutrient stress significantly reduced the phosphorylation level of SNF1-related kinase 1 (SnRK1) (**Table 1**). The putative phosphorylation sites of SnRK1 are found to be located in the activation loop conserved in AMPK-family kinases, suggesting that SnRK1 kinase activity can be affected by high C/low N-nutrient stress. This is in line with our previous reports, showing that high C/low N-nutrient stress reduced the expression of marker genes of the SnRK1 pathway (Lu et al., 2015). Taken together, these findings raised the hypothesis that SnRK1 is involved in primary signal transduction of C/N-nutrient availability. To clarify the function of SnRK1, the *CIPK7/12/14* gene expression levels were measured in *SnRK1α* knockdown plant (*snrk1α1i/1α2*), inducible RNAi knockdown of *SnRK1α1* in the background of a *SnRK1α2* knockout mutant (Sanagi et al., 2018). Induced *SnRK1α1* gene silencing upon DEX treatment resulted in elevated expression of *CIPK7/12/14* genes, suggesting that SnRK1 negatively regulates *CIPK7/12/14* gene expression (**Figure 3**). We also measured expression levels of C/N-nutrient responsive maker genes, *RUBISCO SMALL SUBUNIT 1A* (*RBCS1A*), a photosynthesis-related gene, and *CHALCONE SYNTHASE* (*CHS*), a key enzyme that regulates anthocyanin biosynthesis. *RBCS1A* gene expression was significantly decreased and *CHS* expression was significantly increased in the *snrk1α1i/1α2* mutant compared with WT (**Figure 3**), an expression pattern similar to that observed in WT plants grown under high C/low N-nutrient stress conditions (Martin et al., 2002; Sato et al., 2009; Aoyama et al., 2014). These results suggest that SnRK1 functions as an upstream signaling component in plant C/N-nutrient response.

Trehalose 6-Phosphate Amounts Are Responsive to C/N-Nutrient Availability

Recent studies revealed that SnRK1 could directly bind to trehalose 6-phosphate (T6P), resulting in downregulation of the

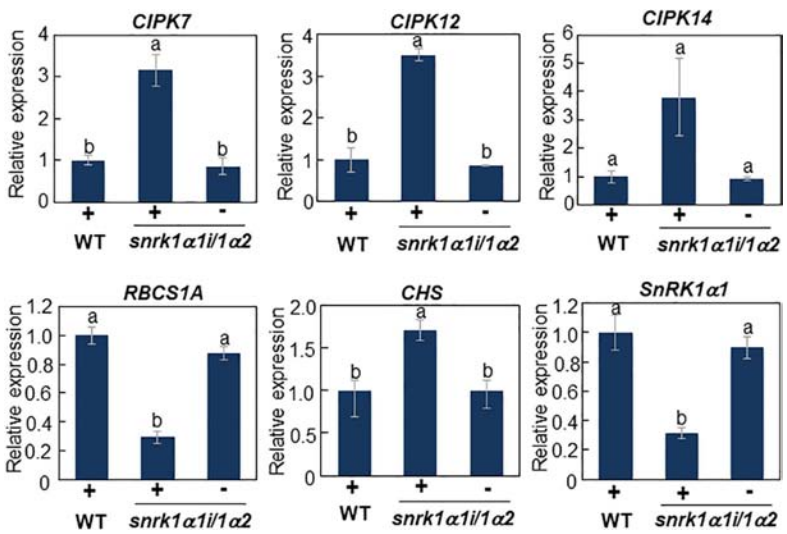

FIGURE 3 | Transcript analysis of *CIPK7*, *CIPK12*, *CIPK14,* and C/N response marker genes in *snrk1α1i/1α2* mutant. WT and inducible RNAi knockdown mutant of SnRK1α (*snrk1α1i/1α2*) plants were grown for 11 days on medium containing 10 mM Glc and 30 mM N in the absence of dexamethasone (DEX) and transferred to medium supplemented with 10 μM DEX. After 5 days, total RNA was purified from each plant. Expression levels of *CIPK7/1/14* and C/N response marker genes were analyzed by qRT-PCR and normalized relative to the level of 18S rRNA in the same samples, and the expression in mutant plants was compared with that in WT plants grown in DEX-treated medium. The results shown are the means ± SD of three biological replicates. Letters above the bars indicate significant differences, as assessed by one-way ANOVA with Turkey's *post hoc* test.

SnRK1 kinase activity in Arabidopsis (Zhang et al., 2009; Zhai et al., 2018). T6P, an intermediate in trehalose biosynthesis, is an essential signal metabolite in plants, modulating not only carbon metabolism but developmental processes such as flowering and senescence (Paul et al., 2008; Wingler et al., 2012; Wahl et al., 2013; Figueroa and Lunn, 2016). These findings prompted us to hypothesize that T6P level is affected by C/N-nutrient availability. Quantification of T6P amounts in Arabidopsis seedlings exposed to various C/N-nutrient conditions showed that cellular T6P level was increased in response to both high C and low N conditions and was synergistically increased by combined high C/low N treatment (**Figure 4**). T6P level was slightly but significantly higher in seedlings exposed to high C/low N (300 mM Glc/0.3 mM N) than to control (100 mM Glc/30 mM N) conditions after 1 h and apparently increased after 24 h, about sixfold at end of day and ninefold at end of night, respectively. Interestingly, the amounts of glucose 6-phosphate (G6P) and UDP-glucose (UDP-Glc), the substrates for T6P biosynthesis, did not correlate with C/N-nutrient availability and were not increased in plants exposed to high C/low N-nutrient stress (**Figure 4**). These results suggest that T6P is involved in the progression of C/N-nutrient responsive senescence via SnRK1.

Identification of a Leucine Rich-Repeat Receptor-Like Kinase LMK1 as a C/N-Responsive Protein

Phosphoproteome analysis also showed that high C/low N-nutrient stress affected phosphorylation levels of several other protein kinases (**Table 1**), including At1g07650, a protein belonging to the leucine-rich repeat receptor-like kinase (LRR-RLK) family (**Figure 5**). LC-MS/MS analysis showed that the Ser989 residue of At1g07650 (At1g07650.1), located in the cytosolic region and close to the predicted kinase domain, was phosphorylated, with high C/low N-nutrient stress inducing a 2.4-fold higher level of phosphorylation than under control conditions (**Table 1**). The LRR-RLK family is one of the largest protein kinase family in plants, with over 200 members present in the Arabidopsis genome (Shiu and Bleecker, 2003). LRR-RLKs, which consist of a ligand-binding extracellular LRR domain and a cytoplasmic serine/threonine kinase domain, play critical roles in various cellular processes, directly modulating growth and development, as well as responding to environmental stress (Diévart and Clark, 2004; Macho and Zipfel, 2014). At1g07650 encodes a protein consisting of 1,014 amino acids, including LRR and Ser/Thr kinase domains, as well as an additional extracellular malectin-like domain and a transmembrane-like hydrophobic domain. This protein, named as leucine-rich repeat malectin kinase 1 (LMK1), along with 11 other proteins, formed the LRR-VIII 2 subfamily (Shiu and Bleecker, 2003) (**Figure 5**). The functions of these proteins remain poorly understood, although one member of this subfamily, At3g14840, also known as LysM RLK1-interacting kinase 1 (LIK1), has been reported to regulate plant innate immunity (Le et al., 2014). Amino acid sequence alignment showed that the kinase domain is highly conserved in this subfamily (**Supplementary Figure S1**).

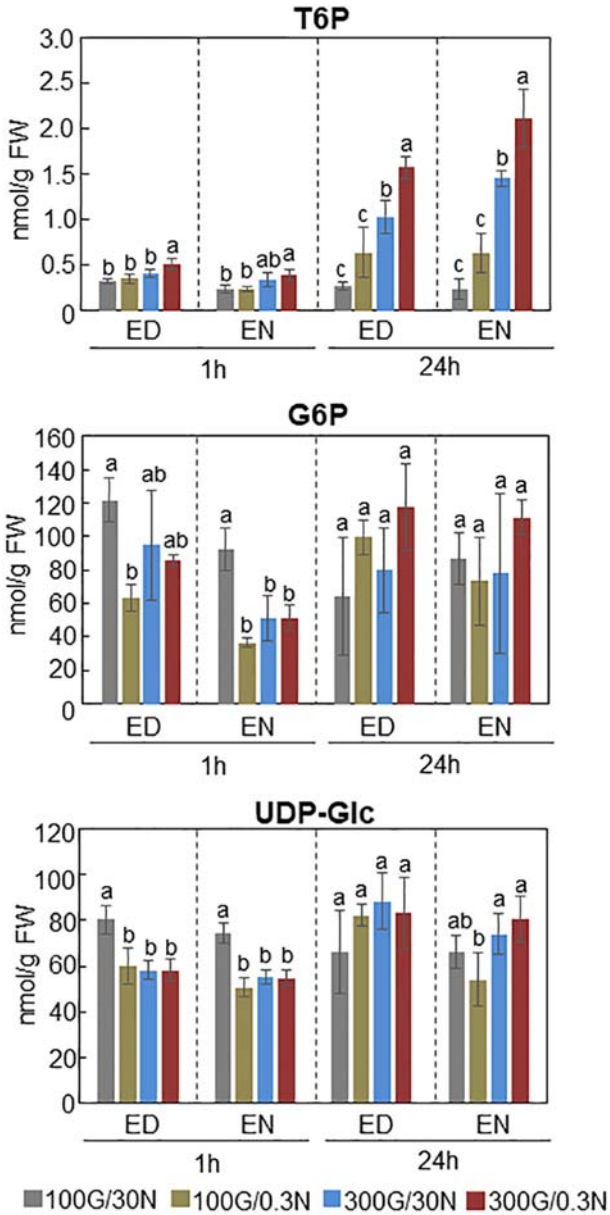

FIGURE 4 | Amounts of T6P, G6P, and UDP-Glc present in WT plants grown under different C/N-nutrient conditions. WT plants were grown for 16 days on medium containing 100 mM Glc and 30 mM N (control), and transferred to control medium or modified C/N-nutrient medium containing 100 mM Glc and 0.3 mM N, 300 mM Glc and 30 mM N or 300 mM Glc and 0.3 mM N. The seedlings were harvested 1 h [end of day (ED) or end of night (EN)] and 24 h (ED or EN) after treatment, followed by metabolite quantification by LC-MS/MS. The results shown are the means ± SD of four biological replicates. Letters above the bars indicate significant differences, as assessed by one-way ANOVA with Turkey's *post hoc* test.

LMK1 Localizes to Membrane Compartments in Plant Cells

To determine the function of LMK1, we first assessed its subcellular location. Hydropathy plot analysis indicated that

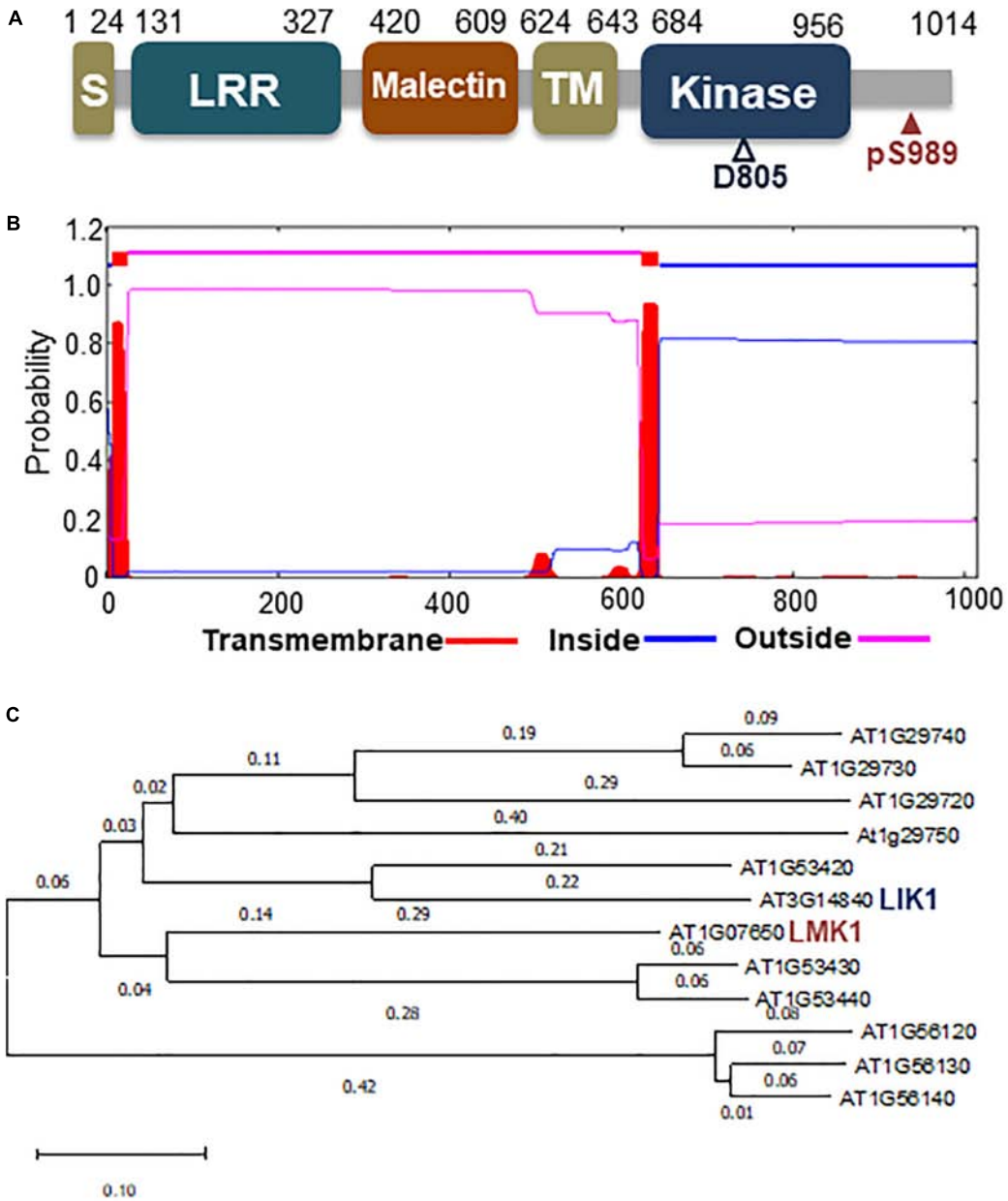

FIGURE 5 | Schematic diagram of LMK1 protein and phylogenetic tree of the LRR-RLK class VIII-2 subfamily**. (A)** Schematic representation of LMK1 protein. S, signal peptide; LRR, leucin-rich repeat domain; malectin, malectin-like domain; TM, transmembrane-like hydrophobic region; kinase, cytosolic Ser/Thr kinase domain. **(B)** Predicted transmembrane region and topology of LMK1, as determined with the TMHMM server v. 2.0 (http://www.cbs.dtu.dk/services/TMHMM/). **(C)** Phylogenetic tree of LRR-RLK class VIII proteins constructed using MEGA X software with the neighbor-joining method.

LMK1 has two hydrophobic regions, amino acids 7–24 and 624–643 (**Figure 5B**). Database search predicted that the first hydrophobic region corresponds to a signal peptide sequence (**Supplementary Figure S1**), suggesting that LMK1 localizes to membrane compartments. To confirm its subcellular location, LMK1 was fused to green fluorescent protein (LMK1-GFP) and transiently expressed in Arabidopsis protoplast cells and *N. benthamiana* leaves under the control of the CaMV35S promoter. Confocal microscope analysis showed that LMK1-GFP fluorescence signals were mainly detected at the periphery of the cells and partly in cytosolic dot-like structures, whereas GFP alone was present throughout cells, including the cytosol and nucleus, in both Arabidopsis protoplast cells and *N. benthamiana* leaves (**Figure 6** and **Supplementary Figure S2**). In addition, fractionation analysis with ultracentrifuge followed by immunoblotting detected LMK-GFP signal in membrane fraction (**Supplementary Figure S2**), together suggesting that LMK1 localizes to the membrane compartments in plant cells.

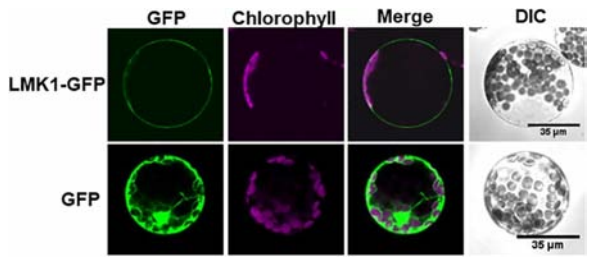

FIGURE 6 | Subcellular localization of LMK1 protein. Confocal laser microscopy showing the subcellular localization of LMK1-GFP transiently expressed in Arabidopsis mesophyll protoplast cells. GFP was the control for fluorescent protein. Confocal microscopic images were taken 16 h after transfection. GFP fluorescence (GFP), chlorophyll autofluorescence (Chlorophyll) and the merged images of these fluorescence signals (Merge) were shown. DIC, differential interference contrast image. We observed more than 100 protoplast cells for each experiment and representative images are shown.

Overexpression of LMK1 Induces Cell Death in *N. benthamiana* Leaves

Transient expression of LMK1-GFP in *N. benthamiana* leaves resulted in macroscopic tissue collapse and electrolyte leakage indicative of programmed cell death (**Figures 7A,B**). In contrast, mock treatment by infection of *Agrobacterium* carrying the p19 vector alone showed no indications of cell death. LIK1, a homolog of LMK1, was shown to have kinase activity which requires conserved aspartate (Asp) residue in the kinase catalytic domain (Le et al., 2014) (**Supplementary Figure S1**). Therefore, we asked if the mutation in the Asp residue of LMK1 (LMK1D805A-GFP) alters the cell death-induction activity. Infiltration of A*grobacterium* carrying a plasmid expressing LMK1D805A-GFP did not induce cell death (**Figures 7A,B** and **Supplementary Figure S3**), implying that the observed cell death in *N. benthamiana* leaves is likely to be associated with LMK1 kinase activity. LMK1 has extracellular LRR and malectin-like domains, which are often responsible for ligand binding and protein-protein interactions. To determine roles of these extracellular domains on the cell death induction activity, the LRR domain (LMK1ΔL), the malectin-like domain (LMK1ΔM), or the both domains (LMK1ΔLΔM) were deleted and expressed in *N. benthamiana* leaves. Deletion of these domains resulted in reduction of the cell death induction activity, and deletion of both the LRR and malectin-like domains showed a synergistic effect (**Figure 7C** and **Supplementary Figure S3**). These findings suggest that the LRR and malectin-like domains of LMK1, along with the cytosolic kinase domain, are involved in the cell death induction.

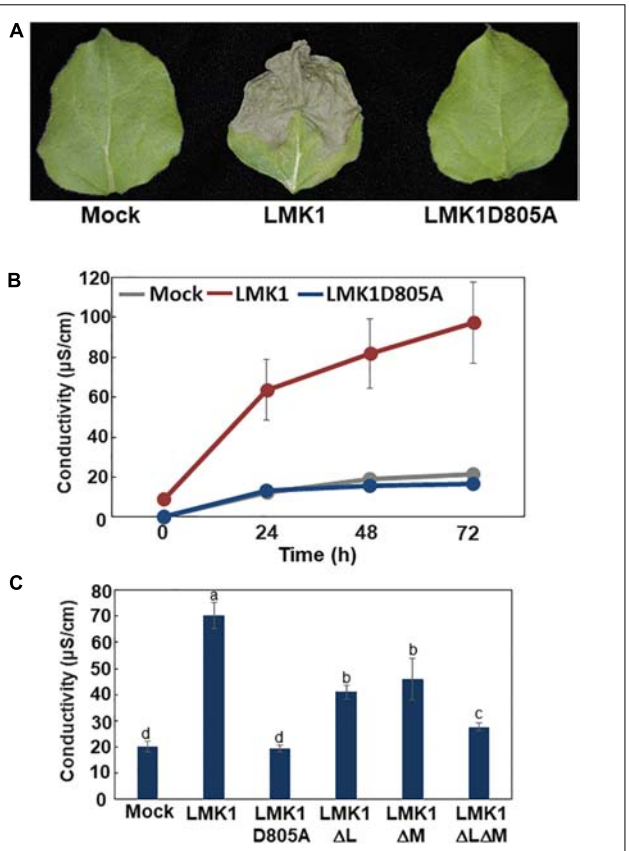

FIGURE 7 | Cell death induction activity of LMK1. **(A,B)** LMK1-GFP and LMK1D805A-GFP were transiently overexpressed in *N. benthamiana* leaves. **(A)** Pictures Staken 6 days after infiltration, **(B)** Ion leakage 0, 24, 48, and 72 h after the leaf discs preparation. The results shown are the means ± SD of three biological replicates. Mock, mock treatment by infection of *Agrobacterium* carrying the p19 vector alone. **(C)** Ion leakage of *N. benthamiana* leaves transiently overexpressing LMK1-GFP and mutated LMK1 proteins fused with GFP. Ion leakage at 72 h after the cut is shown. The results shown are the means ± SD of three biological replicates. Letters above the bars indicate significant differences, as assessed by one-way ANOVA with Turkey's *post hoc* test. Mock, mock treatment by infection of *Agrobacterium* carrying the p19 vector alone.

DISCUSSION

C/N-nutrient availability has a lifelong effect on plant growth, including during early post-germinative growth and progression of senescence. Our previous study showed that high C/low N-nutrient status, resulting from elevated atmospheric CO_2 concentration and limited nitrogen availability, promoted leaf senescence (Aoyama et al., 2014). We also identified several components mediating C/N-nutrient signaling and revealed that altered protein phosphorylation is strongly involved in responses to plant C/N-nutrient imbalance (Maekawa et al., 2012; Yasuda et al., 2014, 2017; Lu et al., 2015; Huarancca Reyes et al., 2015; Huarancca Reyes et al., 2018). However, comprehensive phosphorylation dynamics responsive to C/N-nutrient availability, including proteins targeted by 14-3-3, were unclear. The phosphoproteome analysis in the present study showed that the phosphorylation status of around 200 proteins was altered in response to high C/low N-nutrient stress. Among the proteins altered were key enzymes involved in primary carbon and nitrogen metabolism, several proteins involved in RNA metabolism and translational regulation, transporters and membrane trafficking regulators, and cellular signal transduction

proteins, including protein kinases, phosphatases, ubiquitin ligases, and transcription factors.

Plasma Membrane H^+-ATPase

Using this approach, we found that plasma membrane H^+-ATPases were C/N-responsive 14-3-3 target. Plasma membrane H^+-ATPases are essential for plant life and are required for various physiological processes, including stomatal opening, nutrient uptake in roots, phloem loading, and cell expansion (Kinoshita and Shimazaki, 1999; Svennelid et al., 1999; Palmgren, 2001). Of the 11 plasma membrane H^+-ATPases in Arabidopsis, two, AHA1 and AHA2, are the most highly expressed in seedlings and adult plants (Haruta et al., 2010). Phosphorylation has been shown to modulate plasma membrane H^+-ATPase activities in guard cells. The Thr residues conserved in the C-termini of AHA proteins (Thr948 of AHA1 and Thr947 of AHA2) are phosphorylated in response to light stimuli, with these phosphorylated amino acids mediating direct binding to 14-3-3 and enhancing AHA activity (Kinoshita and Shimazaki, 1999; Svennelid et al., 1999; Palmgren, 2001; Chevalier et al., 2009). Phosphoproteome analysis in the present study showed that high C/low N-nutrient conditions upregulated the levels of phosphorylation of these Thr residues in AHA1 and AHA2 and enhanced the interactions between these plasma membrane H^+-ATPases and 14-3-3 proteins, suggesting that high C/low N-nutrient conditions enhance plasma membrane H^+-ATPase activity, at least in the short term, in Arabidopsis seedlings. Accordingly, the photosynthetic production of sugar was found to induce the phosphorylation of C-terminal Thr residues in plasma membrane H^+-ATPases and to increase the activity of these enzymes in Arabidopsis mesophyll cells (Okumura et al., 2016).

C/N-Related Metabolic Enzymes

Phosphoproteome analysis also revealed the phosphorylation dynamics of several enzymes catalyzing key steps of photosynthesis and primary carbon and nitrogen metabolism, including *rubisco small subunit 1A* (RBCS1A), carbonic anhydrase 2 (CA2), phosphoenolpyruvate carboxylase 1/2 (PPC1/2), phosphoenolpyruvate carboxykinase 1 (PCK1), cytosolic invertase 1 (CINV1), phosphoglucomutase (PGM), β-amylase1), and nitrate reductase (NIA2). Phosphoenolpyruvate carboxylase (PEPC) is crucial in primary metabolism, irreversibly catalyzing the conversion of phosphoenolpyruvate (PEP) to oxaloacetate (OAA) and inorganic phosphate (Chollet et al., 1996). PEPC plays central roles in glycolysis, respiration and photosynthate partitioning, as well as being an important route for carbon dioxide fixation, particularly in C4 plants. PEPC is also involved in interactions between carbon and nitrogen metabolism thorough OAA production. OAA and 2-oxoglutarate are obligate carbon skeletons that bind NH_4^+ and export it to other tissues (O'Leary et al., 2011). The Arabidopsis genome encodes three plant-type PEPCs, AtPPC1, AtPPC2 and AtPPC3, and one bacterial type PEPC, AtPPC4 (Shi et al., 2015). Compared with WT, a double mutant, *ppc1/ppc2*, showed altered amounts of primary carbon and nitrogen metabolites and exhibited growth arrest (Shi et al., 2015). PEPC is also suggested to be involved in carbon metabolism and amino acid remobilization during leaf senescence (Taylor et al., 2010). Due to the irreversible nature of the metabolic reaction catalyzed by PEPC, its activity is strictly regulated at the post-translational level by multiple mechanisms, including allosteric regulation and protein phosphorylation and ubiquitylation (Izui et al., 2004; O'Leary et al., 2011). Plant PEPCs are regulated by phosphorylation of the highly conserved Ser11 residue located near the N termini of PPC1 and PPC2. Phosphorylation of this residue activates PEPC by reducing its sensitivity to allosteric inhibitors while increasing its affinity for PEP (Izui et al., 2004; O'Leary et al., 2011). Our phosphoproteome analysis showed increased phosphorylation of the conserved Ser11 residues in both PPC1 and PPC2, suggesting that PEPC activity is post-translationally promoted in response to high C/low N-nutrient stress.

Senescence-Related Proteins

Phosphoproteome analysis identified several proteins involved in leaf senescence, such as the autophagy related protein ATG13a, the reactive oxygen species (ROS)-producing enzyme RbohD and the transcription factor TCP10. Autophagy is a highly conserved cellular process in all eukaryotes, involving the degradation of intracellular constituents, making autophagy important for recycling essential nutrients under nutrient starvation conditions and during the progression of senescence. The autophagy-related protein ATG13 is involved in regulating the initiation of autophagy. In yeast, ATG13 is an accessory subunit of the ATG1/ATG13 kinase complex and positively regulates ATG1 kinase activity (Mizushima, 2010; Suzuki and Ohsumi, 2010). ATG13 is hyperphosphorylated under nutrient-rich conditions, reducing its affinity for ATG1, but is rapidly dephosphorylated under starvation conditions, resulting in increased ATG1 kinase activity and initiation of autophagy (Mizushima, 2010; Suzuki and Ohsumi, 2010; Alers et al., 2014). In Arabidopsis, ATG13 is encoded by two homologous genes, *ATG13a* and *ATG13b*, with the levels of expression of both being induced during leaf senescence (Suttangkakul et al., 2011). Moreover, double mutant of *ATG13a/b* showed accelerated senescence and was hypersensitive to nutrient limiting conditions (Suttangkakul et al., 2011). Intriguingly, levels of ATG13 phosphorylation were altered in response to sugar and nitrogen availability, although the phosphorylated sites were unknown (Suttangkakul et al., 2011). The phosphoproteome analysis in the present study consistently showed that ATG13 phosphorylation level was reduced in response to high C/low N-nutrient conditions, with Ser248 identified as a C/N-responsive phosphorylation site, suggesting that autophagy is activated via ATG13 dephosphorylation and affects senescence progression under high C/low N-nutrient stress condition.

Respiratory burst oxidase homolog (Rboh) proteins are key enzymes involved in ROS production and function in various physiological processes (Torres and Dangl, 2005). The level of RbohD phosphorylation is upregulated in response to high C/low N-nutrient conditions. Arabidopsis RbohD plays essential roles in ABA-mediated ROS production and stomatal closure (Kwak et al., 2003) and in the ROS burst of plant defense

responses to pathogen attacks (Torres et al., 2002; Kadota et al., 2014). RbohD has also been reported involved in ROS production during the process of leaf senescence (Dai et al., 2018; Yang et al., 2018). Together, these results suggest that RbohD phosphorylation mediates ROS production in response to C/N-nutrient availability and may regulate plant growth pathways, including the progression of senescence and responses to biotic stress.

TCP10 is a member of transcription factor Teosinte branched 1/Cycloidea/PCF (TCP) family. TCP10 and other class II TCPs affect cell division activity and regulate leaf development under control of microRNA miR319 (Palatnik et al., 2003; Koyama et al., 2007; Nicolas and Cubas, 2016). These TCPs have also been reported to regulate the progression of senescence by promoting jasmonate biosynthesis (Schommer et al., 2008). A *jaw-D* mutant, in which levels of TCP2, TCP3, TCP4, TCP10, and TCP24 mRNAs were all strongly reduced, exhibited delayed senescence phenotype, which phenotype was restored by exogenous methyl jasmonate (Schommer et al., 2008). Although expression of these class II TCPs is tightly regulated at the post-transcriptional level by the microRNA, post-translational regulation of the TCP functions remains unclear. We found that the Thr110 residue of Arabidopsis TCP10 is phosphorylated and that its level of phosphorylation was reduced in response to high C/low-N nutrient stress, suggesting an as yet unidentified regulatory mechanism of senescence progression via TCP phosphorylation in response to C/N-nutrient status.

Involvement of T6P-SnRK1 Module in C/N-Nutrient Signal Transduction

SnRK1 kinase, a kinase homologous to yeast sucrose non-fermenting 1 (SNF1) and mammalian AMP-activated kinase (AMPK), is a central regulator of metabolism under conditions of energy limitation and carbon starvation in plants (Baena-González et al., 2007; Smeekens et al., 2010; Emanuelle et al., 2016; Baena-González and Hanson, 2017). In addition, SnRK1 affects plant developmental processes and regulates age-dependent and dark-induced senescence progressions (Baena-González et al., 2007; Cho et al., 2012; Mair et al., 2015; Baena-González and Hanson, 2017; Pedrotti et al., 2018). The proteins SNF1, AMPK, and SnRK1 kinases form heterotrimeric holoenzymes containing a catalytic α-subunit and non-catalytic β- and γ-subunits (the latter being replaced by a hybrid bg subunit in SnRK1) (Emanuelle et al., 2016; Ramon et al., 2019). In Arabidopsis, the *AKIN10* (*SnRK1α1*) and *AKIN11* (*SnRK1α2*) genes encode the catalytic α-subunits, and plants with double knockdown of *AKIN10* and *AKIN11* showed accelerated senescence (Baena-González et al., 2007). Phosphoproteome analysis in the present study found that high C/low N-nutrient stress markedly reduced the levels of phosphorylation of the Ser/Thr residues conserved in the activation loop of AKIN10 and AKIN11. Subsequent qRT-PCR analysis demonstrated that the expression levels of *CIPK7/12/14* genes were increased in the *snrk1α1i/1α2* mutants, even under normal C/N-nutrient conditions, similar to the expression pattern found in WT seedlings grown under high C/low N-nutrient stress conditions and suggesting that SnRK1 mediates C/N-nutrient signaling upstream of CIPK7/12/14. In addition, we found that high C/low N-nutrient stress conditions increase the levels of T6P which has been implicated as a signaling metabolite that regulates progression of senescence and modulates SnRK1 activity in plants (Zhang et al., 2009; Wingler et al., 2012; Figueroa and Lunn, 2016). Recent study has demonstrated that T6P directly binds to the SnRK1 α-subunit AKIN10/11, weakening the affinity of the latter for Geminivirus rep-interacting kinases 1/2 (GRIK1/2) which phosphorylate and activate SnRK1 activity, thereby inhibiting SnRK1 activity in Arabidopsis plants (Zhai et al., 2018). Together, these results suggest that, under high C/low N-nutrient stress conditions, the T6P-SnRK1 module mediates C/N-nutrient signaling and regulates the progression of senescence via *CIPK7/12/14* transcription.

Isolation of Cell Death Related Receptor-Like Kinase LMK1

This study found that the LMK1 protein was a putative C/N-nutrient related protein kinase belonging to the LRR-RLK class VIII-2 subfamily. LRR-RLK proteins have been reported to play essential roles in various types of cellular signaling, including phytohormone perception, pattern triggered immunity (PTI) and fertilization (Diévart and Clark, 2004; Macho and Zipfel, 2014). We found that transient overexpression of *LMK1* induces cell death in *N. benthamiana* leaves. Induction of cell death is an important process in plant defense against pathogens as well as in the progression of senescence (Lim et al., 2007; Coll et al., 2011; Mukhtar et al., 2016). Although little is known about the function of LRR-RLK class VIII-2 proteins, one of these proteins, LIK1, has been reported to interact directly with and be phosphorylated by Chitin elicitor receptor kinase 1 (CERK1) and to negatively regulate ROS production and chitin-induced immunity (Le et al., 2014).

LMK1 contains expected extracellular LRR and malectin-like domains. Transient expression of LMK1 demonstrated that both of these extracellular domains are involved in LMK1-induced cell death. Malectin protein was first identified as a carbohydrate binding protein localizing to the endoplasmic reticulum and being involved in N-glycosylation of membrane proteins in mammals (Schallus et al., 2008). Although proteins homologous to malectin have not yet been identified in plants, malectin-like domains have been detected in the extracellular regions of several receptor-like kinases. Feronia (FER) is a receptor-like kinase with two malectin-like extracellular domains that plays critical roles in controlling Arabidopsis growth, including in fertilization, senescence progression, pathogen resistance, phytohormone signaling, and starch accumulation (Haruta et al., 2014; Du et al., 2016; Liao et al., 2017; Stegmann et al., 2017; Feng et al., 2018). FER has been shown to bind via its extracellular malectin-like domains to the peptide ligand Rapid alkalinization factor (RLAF), to leucine-rich repeat extension (LRX) protein, and to cell wall pectin (Stegmann et al., 2017; Feng et al., 2018; Dünser et al., 2019). Recently, FER was reported to directly phosphorylate ATL6, the closest homolog of ATL31, and to modulate C/N-nutrient responses (Xu et al., 2019), suggesting that the extracellular malectin-like domains of FER can recognize

ligands mediating C/N-nutrient availability. Identification of extracellular ligands and/or interactors is required to further understand LMK1 function in responses to C/N-nutrient stress. Further detailed genetic and physiological analyses of this protein may help to clarify its function and the as yet undetermined physiological processes controlled by C/N-nutrient availability.

DATA AVAILABILITY STATEMENT

The datasets generated for this study can be found in the ProteomeXchange (PXD016507), jPOST (JPST000703).

AUTHOR CONTRIBUTIONS

XL, MSa, HN, and TS designed the experiments. XL, MSa, YL, YN, SS, SY, RF, JL, and TS performed the experiments. XL, MSa, MSt, JL, HN, and TS analyzed the data. XL, MSa, HN, TS, and JY wrote the article. YS, WS, MSt, and JL edited the article. All authors commented on and approved the manuscript.

FUNDING

This work was supported by a Grants in-Aid for Scientific Research to TS (Nos. 15K18819 and 17K08190) from the Japan Society for the Promotion of Science (JSPS), by a grant from the NOASTEC Foundation, Hokkaido University Young Scientist Support Program to TS, by the Max-Planck-Gesellschaft to HN, by Grants in Aid for Scientific Research to JY (Nos. 15H0116705, 2629218885, and 2666004604) and to YS (No. 18H02467) from the JSPS, and by the Max Planck Society to RF, MSt, and JL, XL, MSa, and SY are recipients of JSPS Research Fellowships for Young Scientists, YL was supported by a JSPS postdoctoral fellowship for Research in Japan.

ACKNOWLEDGMENTS

The authors thank Dr. Tsuyoshi Nakagawa (Shimane University, Japan) for kindly providing the Gateway destination vectors used in this study.

SUPPLEMENTARY MATERIAL

The Supplementary Material for this article can be found online at: https://www.frontiersin.org/articles/10.3389/fpls.2020.00377/full#supplementary-material

FIGURE S1 | Signal peptide prediction and alignment of the kinase domains of members of the LRR-RLK class VIII-2 subfamily. **(A)** Predicted signal peptide region of LMK1 protein, as determined by the SignalP-4.1 servers (http://www.cbs.dtu.dk/services/SignalP/). **(B)** Alignment of the kinase domains of members of the LRR-RLK class VIII-2 subfamily. The arrowhead indicates the position of the conserved Asp residue (LMK1D805), which is essential for kinase activity in these proteins.

FIGURE S2 | Subcellular localization of LMK1 protein. **(A)** Confocal laser microscopy showing the subcellular localization of LMK1-GFP transiently expressed in *N. benthamiana* leaves. GFP was the control for fluorescent protein. Confocal microscopic images were taken 48 h after transfection. DIC, differential interference contrast image. **(B)** Immunoblotting analysis using anti-GFP antibody of water-soluble (supernatant: S) and insoluble membrane (pellet: P) fractions of lysate from N. benthamiana leaves expressing GFP or LMK1-GFP protein. Protein extraction buffer contained no detergent. Closed and open arrowheads indicate the position of GFP and LMK1-GFP, respectively.

FIGURE S3 | Expression check of LMK1 proteins in *N. benthamiana* leaves. Intact LMK1 and mutated LMK1 proteins fused with GFP were transiently overexpressed in *N. benthamiana* leaves. Expression of each construct was confirmed by confocal microscopic analysis. Photos were taken 48 h after infiltration. Mock, mock treatment by infection of *Agrobacterium* carrying the p19 vector alone.

TABLE S1 | Primers used in this study.

TABLE S2 | List of C/N-nutrient responsive phosphoproteins identified by LC-MS/MS analysis.

REFERENCES

Aguilar-Hernández, V., Aguilar-Henonin, L., and Guzmán, P. (2011). Diversity in the architecture of ATLs, a family of plant ubiquitin-ligases, leads to recognition and targeting of substrates in different cellular environments. *PLoS One* 6:e23934. doi: 10.1371/journal.pone.0023934

Alers, S., Wesselborg, S., and Stork, B. (2014). ATG13: Just a companion, or an executor of the autophagic program? *Autophagy* 10, 944–956. doi: 10.4161/auto.28987

Aoyama, S., Huarancca Reyes, T., Guglielminetti, L., Lu, Y., Morita, Y., Sato, T., et al. (2014). Ubiquitin ligase ATL31 functions in leaf senescence in response to the balance between atmospheric CO_2 and nitrogen availability in arabidopsis. *Plant Cell Physiol.* 55, 293–305. doi: 10.1093/pcp/pcu002

Baena-González, E., and Hanson, J. (2017). Shaping plant development through the SnRK1-TOR metabolic regulators. *Curr. Opin. Plant Biol.* 35, 152–157. doi: 10.1016/j.pbi.2016.12.004

Baena-González, E., Rolland, F., Thevelein, J. M., and Sheen, J. (2007). A central integrator of transcription networks in plant stress and energy signalling. *Nature* 448, 938–942. doi: 10.1038/nature06069

Chevalier, D., Morris, E. R., and Walker, J. C. (2009). 14-3-3 and FHA Domains Mediate Phosphoprotein Interactions. *Annu. Rev. Plant Biol.* 60, 67–91. doi: 10.1146/annurev.arplant.59.032607.092844

Cho, Y. H., Hong, J. W., Kim, E. C., and Yoo, S. D. (2012). Regulatory functions of SnRK1 in stress-responsive gene expression and in plant growth and development. *Plant Physiol.* 158, 1955–1964. doi: 10.1104/pp.111.189829

Chollet, R., Vidal, J., and O'Leary, M. H. (1996). Phosphoenolpyruvate carboxylase: A ubiquitous, highly regulated enzyme in plants. *Annu. Rev. Plant Physiol. Plant Mol. Biol.* 47, 273–298. doi: 10.1146/annurev.arplant.47.1.273

Choudhary, M. K., Nomura, Y., Wang, L., Nakagami, H., and Somers, D. E. (2015). Quantitative Circadian Phosphoproteomic Analysis of Arabidopsis Reveals Extensive Clock Control of Key Components in Physiological, Metabolic, and Signaling Pathways. *Mol Cell Proteomics.* 14, 2243–2260. doi: 10.1074/mcp.M114.047183

Coll, N. S., Epple, P., and Dangl, J. L. (2011). Programmed cell death in the plant immune system. *Cell Death Differ.* 18, 1247–1256. doi: 10.1038/cdd.2011.37

Comparot, S., Lingiah, G., and Martin, T. (2003). Function and specificity of 14-3-3 proteins in the regulation of carbohydrate and nitrogen metabolism. *J. Exp. Bot.* 54, 595–604. doi: 10.1093/jxb/erg057

Coruzzi, G. M., and Zhou, L. (2001). Carbon and nitrogen sensing and signaling in plants: Emerging "matrix effects." *Curr. Opin. Plant Biol.* 4, 247–253. doi: 10.1016/S1369-5266(00)00168-0

Cox, J., and Mann, M. (2008). MaxQuant enables high peptide identification rates, individualized p.p.b.-range mass accuracies and proteome-wide protein quantification. *Nat. Biotechnol.* 26, 1367–1372. doi: 10.1038/nbt.1511

Curtis, M. D., and Grossniklaus, U. (2003). A Gateway Cloning Vector Set for High-Throughput Functional Analysis of Genes in Planta. *Plant Physiol.* 133, 462–469. doi: 10.1104/pp.103.027979

Dai, C., Lee, Y., Lee, I. C., Nam, H. G., and Kwak, J. M. (2018). Calmodulin 1 regulates senescence and ABA response in Arabidopsis. *Front. Plant Sci.* 9:1–13. doi: 10.3389/fpls.2018.00803

Diévart, A., and Clark, S. E. (2004). LRR-containing receptors regulating plant development and defense. *Development* 131, 251–261. doi: 10.1242/dev.00998

Du, C., Li, X., Chen, J., Chen, W., Li, B., Li, C., et al. (2016). Receptor kinase complex transmits RALF peptide signal to inhibit root growth in Arabidopsis. *Proc. Natl. Acad. Sci. U. S. A.* 113, E8326–E8334. doi: 10.1073/pnas.1609626113

Dünser, K., Gupta, S., Herger, A., Feraru, M. I., Ringli, C., and Kleine−Vehn, J. (2019). Extracellular matrix sensing by FERONIA and Leucine−Rich Repeat Extensins controls vacuolar expansion during cellular elongation in Arabidopsis thaliana. *EMBO J* 38, 1–12. doi: 10.15252/embj.2018100353

Emanuelle, S., Doblin, M. S., Stapleton, D. I., Bacic, A., and Gooley, P. R. (2016). Molecular Insights into the Enigmatic Metabolic Regulator. *SnRK1. Trends Plant Sci.* 21, 341–353. doi: 10.1016/j.tplants.2015.11.001

Feng, W., Kita, D., Peaucelle, A., Cartwright, H. N., Doan, V., Duan, Q., et al. (2018). The FERONIA Receptor Kinase Maintains Cell-Wall Integrity during Salt Stress through Ca^{2+} Signaling. *Curr. Biol.* 28, 666.e–675.e. doi: 10.1016/j.cub.2018.01.023 666–675.e5,

Figueroa, C. M., Feil, R., Ishihara, H., Watanabe, M., Kölling, K., Krause, U., et al. (2016). Trehalose 6-phosphate coordinates organic and amino acid metabolism with carbon availability. *Plant J.* 85, 410–423. doi: 10.1111/tpj.13114

Figueroa, C. M., and Lunn, J. E. (2016). A Tale of Two Sugars: Trehalose 6-Phosphate and Sucrose. *Plant Physiol.* 172, 7–27. doi: 10.1104/pp.16.00417

Haruta, M., Burch, H. L., Nelson, R. B., Barrett-Wilt, G., Kline, K. G., Mohsin, S. B., et al. (2010). Molecular characterization of mutant Arabidopsis plants with reduced plasma membrane proton pump activity. *J. Biol. Chem.* 285, 17918–17929. doi: 10.1074/jbc.M110.101733

Haruta, M., Sabat, G., Stecker, K., Minkoff, B. B., and Sussman, M. R. (2014). A peptide hormone and its receptor protein kinase regulate plant cell expansion. *Science (80-.).* 343, 408–411. doi: 10.1126/science.1244454

Huarancca Reyes, T., Maekawa, S., Sato, T., and Yamaguchi, J. (2015). The Arabidopsis ubiquitin ligase ATL31 is transcriptionally controlled by WRKY33 transcription factor in response to pathogen attack. *Plant Biotechnol.* 32, 11–19. doi: 10.5511/plantbiotechnology.14.1201b

Huarancca Reyes, T., Scartazza, A., Pompeiano, A., Ciurli, A., Lu, Y., Guglielminetti, L., et al. (2018). Nitrate reductase modulation in response to changes in C/N balance and nitrogen source in Arabidopsis. *Plant Cell Physiol.* 59, 1248–1254. doi: 10.1093/pcp/pcy065

Ishihama, Y., Rappsilber, J., Andersen, J. S., and Mann, M. (2002). Microcolumns with self-assembled particle frits for proteomics. *J. Chromatogr.* 6 979, 233–239. doi: 10.1016/s0021-9673(02)01402-4

Izui, K., Matsumura, H., Furumoto, T., and Kai, Y. (2004). PHOSPHO ENOL PYRUVATE CARBOXYLASE: A New Era of Structural Biology. *Annu. Rev. Plant Biol.* 55, 69–84. doi: 10.1146/annurev.arplant.55.031903.141619

Jaspert, N., Throm, C., and Oecking, C. (2011). Arabidopsis 14-3-3 proteins: Fascinating and less fascinating aspects. *Front. Plant Sci.* 2:1–8. doi: 10.3389/fpls.2011.00096

Kadota, Y., Sklenar, J., Derbyshire, P., Stransfeld, L., Asai, S., Ntoukakis, V., et al. (2014). Direct Regulation of the NADPH Oxidase RBOHD by the PRR-Associated Kinase BIK1 during Plant Immunity. *Mol. Cell* 54, 43–55. doi: 10.1016/j.molcel.2014.02.021

Kinoshita, T., and Shimazaki, K. I. (1999). Blue light activates the plasma membrane H^+-ATPase by phosphorylation of the C-terminus in stomatal guard cells. *EMBO J.* 18, 5548–5558. doi: 10.1093/emboj/18.20.5548

Koyama, T., Furutani, M., Tasaka, M., and Ohme-Takagi, M. (2007). TCP transcription factors control the morphology of shoot lateral organs via negative regulation of the expression of boundary-specific genes in Arabidopsis. *Plant Cell* 19, 473–484. doi: 10.1105/tpc.106.044792

Kwak, J. M., Mori, I. C., Pei, Z. M., Leonhard, N., Angel Torres, M., Dangl, J. L., et al. (2003). NADPH oxidase AtrbohD and AtrbohF genes function in ROS-dependent ABA signaling in arabidopsis. *EMBO J.* 22, 2623–2633. doi: 10.1093/emboj/cdg277

Le, M. H., Cao, Y., Zhang, X. C., and Stacey, G. (2014). LIK1, a CERK1-interacting kinase, regulates plant immune responses in arabidopsis. *PLoS One* 9:1–10. doi: 10.1371/journal.pone.0102245

Liao, H., Tang, R., Zhang, X., Luan, S., and Yu, F. (2017). FERONIA Receptor Kinase at the Crossroads of Hormone Signaling and Stress Responses. *Plant Cell Physiol.* 58, 1143–1150. doi: 10.1093/pcp/pcx048

Lim, P. O., Kim, H. J., and Nam, H. G. (2007). Leaf Senescence. *Annu. Rev. Plant Biol.* 58, 115–136. doi: 10.1146/annurev.arplant.57.032905.105316

Lu, Y., Sasaki, Y., Li, X., Mori, I. C., Matsuura, T., Hirayama, T., et al. (2015). ABI1 regulates carbon/nitrogen-nutrient signal transduction independent of ABA biosynthesis and canonical ABA signalling pathways in Arabidopsis. *J. Exp. Bot.* 66, 2763–2771. doi: 10.1093/jxb/erv086

Lunn, J. E., Feil, R., Hendriks, J. H. M., Gibon, Y., Morcuende, R., Osuna, D., et al. (2006). Sugar-induced increases in trehalose 6-phosphate are correlated with redox activation of ADPglucose pyrophosphorylase and higher rates of starch synthesis in Arabidopsis thaliana. *Biochem. J.* 397, 139–148. doi: 10.1042/BJ20060083

Macho, A. P., and Zipfel, C. (2014). Plant PRRs and the activation of innate immune signaling. *Mol. Cell* 54, 263–272. doi: 10.1016/j.molcel.2014.03.028

Mackintosh, C. (2004). Dynamic interactions between 14-3-3 proteins and phosphoproteins regulate diverse cellular processes. *Biochem. J.* 381, 329–342. doi: 10.1042/BJ20031332

Maekawa, S., Sato, T., Asada, Y., Yasuda, S., Yoshida, M., Chiba, Y., et al. (2012). The Arabidopsis ubiquitin ligases ATL31 and ATL6 control the defense response as well as the carbon/nitrogen response. *Plant Mol. Biol.* 79, 217–227. doi: 10.1007/s11103-012-9907-0

Mair, A., Pedrotti, L., Wurzinger, B., Anrather, D., Simeunovic, A., Weiste, C., et al. (2015). SnRK1-triggered switch of bZIP63 dimerization mediates the low-energy response in plants. *Elife* 4, 1–33. doi: 10.7554/eLife.05828

Martin, T., Oswald, O., and Graham, I. (2002). Arabidopsis seedling growth, storage lipid mobilization, and photosynthetic gene expression are regulated by carbon: nitrogen availability. *Plant Physiol.* 128, 472–481. doi: 10.1104/pp.010475

Mizushima, N. (2010). The role of the Atg1/ULK1 complex in autophagy regulation. *Curr. Opin. Cell Biol.* 22, 132–139. doi: 10.1016/j.ceb.2009.12.004

Mukhtar, M. S., McCormack, M. E., Argueso, C. T., and Pajerowska-Mukhtar, K. M. (2016). Pathogen Tactics to Manipulate Plant Cell Death. *Curr. Biol.* 26, R608–R619. doi: 10.1016/j.cub.2016.02.051

Nakagami, H. (2014). StageTip-based HAMMOC, an efficient and inexpensive phosphopeptide enrichment method for plant shotgun phosphoproteomics. *Methods Mol. Biol.* 1072, 595–607. doi: 10.1007/978-1-62703-631-3_40

Nakagawa, T., Kurose, T., Hino, T., Tanaka, K., Kawamukai, M., Niwa, Y., et al. (2007). Development of series of gateway binary vectors, pGWBs, for realizing efficient construction of fusion genes for plant transformation. *J. Biosci. Bioeng.* 104, 34–41. doi: 10.1263/jbb.104.34

Nicolas, M., and Cubas, P. (2016). TCP factors: New kids on the signaling block. *Curr. Opin. Plant Biol.* 33, 33–41. doi: 10.1016/j.pbi.2016.05.006

Okuda, S., Watanabe, Y., Moriya, Y., Kawano, S., Yamamoto, T., Matsumoto, M., et al. (2017). JPOSTrepo: An international standard data repository for proteomes. *Nucleic Acids Res.* 45, D1107–D1111. doi: 10.1093/nar/gkw1080

Okumura, M., Inoue, S. I., Kuwata, K., and Kinoshita, T. (2016). Photosynthesis activates plasma membrane H^+-ATPase via sugar accumulation. *Plant Physiol.* 171, 580–589. doi: 10.1104/pp.16.00355

O'Leary, B., Park, J., and Plaxton, W. C. (2011). The remarkable diversity of plant PEPC (phosphoenolpyruvate carboxylase): recent insights into the physiological functions and post-translational controls of non-photosynthetic PEPCs. *Biochem. J.* 436, 15–34. doi: 10.1042/BJ20110078

Olsen, J. V., de Godoy, L. M., Li, G., Macek, B., Mortensen, P., Pesch, R., et al. (2005). Parts per million mass accuracy on an Orbitrap mass spectrometer via lock mass injection into a C-trap. *Mol. Cell Proteomics.* 4, 2010–2021. doi: 10.1074/mcp.T500030-MCP200

Palatnik, J. F., Allen, E., Wu, X., Schommer, C., Schwab, R., Carrington, J. C., et al. (2003). Control of leaf morphogenesis by microRNAs. *Nature* 425, 257–263. doi: 10.1038/nature01958

Paul, M. J., Primavesi, L. F., Jhurreea, D., and Zhang, Y. (2008). Trehalose metabolism and signaling. *Annu. Rev. Plant Biol.* 59, 417–441. doi: 10.1146/annurev.arplant.59.032607.092945

Palmgren, M. G. (2001). PLANT PLASMA MEMBRANE H^+-ATPases: Powerhouses for Nutrient Uptake. *Annu. Rev. Plant Physiol. Plant Mol. Biol.* 52, 817–845. doi: 10.1146/annurev.arplant.52.1.817

Pedrotti, L., Weiste, C., Nägele, T., Wolf, E., Lorenzin, F., Dietrich, K., et al. (2018). Snf1-RELATED KINASE1-Controlled C/S_1-bZIP Signaling Activates Alternative Mitochondrial Metabolic Pathways to Ensure Plant Survival in Extended Darkness. *Plant Cell* 30, 495–509. doi: 10.1105/tpc.17.00414

Ramon, M., Dang, T. V. T., Broeckx, T., Hulsmans, S., Crepin, N., Sheen, J., et al. (2019). Default activation and nuclear translocation of the plant cellular energy sensor SnRK1 regulate metabolic stress responses and development. *Plant Cell* 31, 1614–1632. doi: 10.1105/tpc.18.00500

Rolland, F., Baena-González, E., and Sheen, J. (2006). SUGAR SENSING AND SIGNALING IN PLANTS: Conserved and Novel Mechanisms. *Annu. Rev. Plant Biol.* 57, 675–709. doi: 10.1146/annurev.arplant.57.032905.105441

Sanagi, M., Lu, Y., Aoyama, S., Morita, Y., Mitsuda, N., Ikeda, M., et al. (2018). Sugar-responsive transcription factor bZIP3 affects leaf shape in Arabidopsis plants. *Plant Biotechnol.* 35, 167–170. doi: 10.5511/plantbiotechnology.18.0410a

Sato, T., Maekawa, S., Yasuda, S., Domeki, Y., Sueyoshi, K., Fujiwara, M., et al. (2011). Identification of 14-3-3 proteins as a target of ATL31 ubiquitin ligase, a regulator of the C/N response in Arabidopsis. *Plant J* 68, 137–146. doi: 10.1111/j.1365-313X.2011.04673.x

Sato, T., Maekawa, S., Yasuda, S., Sonoda, Y., Katoh, E., Ichikawa, T., et al. (2009). CNI1/ATL31, a RING-type ubiquitin ligase that functions in the carbon/nitrogen response for growth phase transition in Arabidopsis seedlings. *Plant J.* 60, 852–864. doi: 10.1111/j.1365-313X.2009.04006.x

Schallus, T., Jaeckh, C., Fehér, K., Palma, A. S., Liu, Y., Simpson, J. C., et al. (2008). Malectin: a novel carbohydrate-binding protein of the endoplasmic reticulum and a candidate player in the early steps of protein *N*-glycosylation. *Mol. Biol. Cell* 19, 3404–3414. doi: 10.1091/mbc.E08-04-0354

Schommer, C., Palatnik, J. F., Aggarwal, P., Chételat, A., Cubas, P., Farmer, E. E., et al. (2008). Control of jasmonate biosynthesis and senescence by miR319 targets. *PLoS Biol.* 6:1991–2001. doi: 10.1371/journal.pbio.0060230

Schroeder, M. J., Shabanowitz, J., Schwartz, J. C., Hunt, D. F., and Coon, J. (2004). A neutral loss activation method for improved phosphopeptide sequence analysis by quadrupole ion trap mass spectrometry. *J. Anal Chem.* 76, 3590–3598. doi: 10.1021/ac0497104

Serrano, M., Parra, S., Alcaraz, L. D., and Guzmán, P. (2006). The ATL gene family from Arabidopsis thaliana and Oryza sativa comprises a large number of putative ubiquitin ligases of the RING-H2 type. *J. Mol. Evol.* 62, 434–445. doi: 10.1007/s00239-005-0038-y

Shi, J., Yi, K., Liu, Y., Xie, L., Zhou, Z., Chen, Y., et al. (2015). Phosphoenolpyruvate Carboxylase in Arabidopsis Leaves Plays a Crucial Role in Carbon and Nitrogen Metabolism. *Plant Physiol.* 167, 671–681. doi: 10.1104/pp.114.254474

Shiu, S. H., and Bleecker, A. B. (2003). Expansion of the receptor-like kinase/Pelle gene family and receptor-like proteins in Arabidopsis. *Plant Physiol.* 132, 530–543. doi: 10.1104/pp.103.021964

Smeekens, S., Ma, J., Hanson, J., and Rolland, F. (2010). Sugar signals and molecular networks controlling plant growth. *Curr. Opin. Plant Biol.* 13, 274–279. doi: 10.1016/j.pbi.2009.12.002

Stegmann, M., Monaghan, J., Smakowska-Luzan, E., Rovenich, H., Lehner, A., Holton, N., et al. (2017). The receptor kinase FER is a RALF-regulated scaffold controlling plant immune signaling. *Science* 355, 287–289. doi: 10.1126/science.aal2541

Suttangkakul, A., Li, F., Chung, T., and Vierstra, R. D. (2011). The ATG1/ATG13 Protein Kinase Complex Is Both a Regulator and a Target of Autophagic Recycling in Arabidopsis. *Plant Cell* 23, 3761–3779. doi: 10.1105/tpc.111.090993

Suzuki, K., and Ohsumi, Y. (2010). Current knowledge of the pre-autophagosomal structure (PAS). *FEBS Lett.* 584, 1280–1286. doi: 10.1016/j.febslet.2010.02.001

Svennelid, F., Olsson, A., Piotrowski, M., Rosenquist, M., Ottman, C., Larsson, C., et al. (1999). Phosphorylation of Thr-948 at the C terminus of the plasma membrane H^+-ATPase creates a binding site for the regulatory 14-3-3 protein. *Plant Cell* 11, 2379–2391. doi: 10.1105/tpc.11.12.2379

Taylor, L., Nunes-Nesi, A., Parsley, K., Leiss, A., Leach, G., Coates, S., et al. (2010). Cytosolic pyruvate,orthophosphate dikinase functions in nitrogen remobilization during leaf senescence and limits individual seed growth and nitrogen content. *Plant J.* 62, 641–652. doi: 10.1111/j.1365-313X.2010.04179.x

Torres, M. A., and Dangl, J. L. (2005). Functions of the respiratory burst oxidase in biotic interactions, abiotic stress and development. *Curr. Opin. Plant Biol.* 8, 397–403. doi: 10.1016/j.pbi.2005.05.014

Torres, M. A., Dangl, J. L., and Jones, J. D. G. (2002). Arabidopsis $gp91^{phox}$ homologues Atrbohd and Atrbohf are required for accumulation of reactive oxygen intermediates in the plant defense response. *Proc. Natl. Acad. Sci. U. S. A.* 99, 517–522. doi: 10.1073/pnas.012452499

Tyanova, S., Temu, T., and Cox, J. (2016a). The MaxQuant computational platform for mass spectrometry-based shotgun proteomics. *Nat. Protoc.* 11, 2301–2319. doi: 10.1038/nprot.2016.136

Tyanova, S., Temu, T., Sinitcyn, P., Carlson, A., Hein, M. Y., Geiger, T., et al. (2016b). The Perseus computational platform for comprehensive analysis of (prote)omics data. *Nat. Methods.* 13, 731–740. doi: 10.1038/nmeth.3901

Vidal, E. A., and Gutiérrez, R. A. (2008). A systems view of nitrogen nutrient and metabolite responses in Arabidopsis. *Curr. Opin. Plant Biol.* 11, 521–529. doi: 10.1016/j.pbi.2008.07.003

von Mering, C., Jensen, L. J., Snel, B., Hooper, S. D., Krupp, M., Foglierini, M., et al. (2005). STRING: Known and predicted protein-protein associations, integrated and transferred across organisms. *Nucleic Acids Res.* 33, 433–437. doi: 10.1093/nar/gki005

Wahl, V., Ponnu, J., Schlereth, A., Arrivault, S., Langenecker, T., Franke, A., et al. (2013). Regulation of flowering by trehalose-6-phosphate signaling in *Arabidopsis thaliana*. *Science* 339, 704–707. doi: 10.1126/science.1230406

Wingler, A., Delatte, T. L., O'Hara, L. E., Primavesi, L. F., Jhurreea, D., Paul, M. J., et al. (2012). Trehalose 6-Phosphate Is Required for the Onset of Leaf Senescence Associated with High Carbon Availability. *Plant Physiol.* 158, 1241–1251. doi: 10.1104/pp.111.191908

Xu, G., Chen, W., Song, L., Chen, Q., Zhang, H., Liao, H., et al. (2019). FERONIA phosphorylates E3 ubiquitin ligase ATL6 to modulate the stability of 14-3-3 proteins in plant C/N responses. *J. Exp. Bot.* 70, 6375–6388. doi: 10.1093/jxb/erz378

Yang, L., Ye, C., Zhao, Y., Cheng, X., Wang, Y., Jiang, Y. Q., et al. (2018). An oilseed rape WRKY-type transcription factor regulates ROS accumulation and leaf senescence in Nicotiana benthamiana and Arabidopsis through modulating transcription of RbohD and RbohF. *Planta* 247, 1323–1338. doi: 10.1007/s00425-018-2868-z

Yasuda, S., Aoyama, S., Hasegawa, Y., Sato, T., and Yamaguchi, J. (2017). Arabidopsis CBL-Interacting Protein Kinases Regulate Carbon/Nitrogen-Nutrient Response by Phosphorylating Ubiquitin Ligase ATL31. *Mol. Plant* 10, 605–618. doi: 10.1016/j.molp.2017.01.005

Yasuda, S., Sato, T., Maekawa, S., Aoyama, S., Fukao, Y., and Yamaguchi, J. (2014). Phosphorylation of arabidopsis ubiquitin ligase ATL31 is critical for plant carbon/nitrogen nutrient balance response and controls the stability of 14-3-3 proteins. *J. Biol. Chem.* 289, 15179–15193. doi: 10.1074/jbc.M113.533133

Yoo, S. D., Cho, Y. H., and Sheen, J. (2007). Arabidopsis mesophyll protoplasts: A versatile cell system for transient gene expression analysis. *Nat. Protoc.* 2, 1565–1572. doi: 10.1038/nprot.2007.199

Zhai, Z., Keereetaweep, J., Liu, H., Feil, R., Lunn, J. E., and Shanklin, J. (2018). Trehalose 6-phosphate positively regulates fatty acid synthesis by stabilizing WRINKLED1. *Plant Cell* 30, 2616–2627. doi: 10.1105/tpc.18.00521

Zhang, Y., Primavesi, L. F., Jhurreea, D., Andralojc, P. J., Mitchell, R. A. C., Powers, S. J., et al. (2009). Inhibition of SNF1-related protein kinasel activity and regulation of metabolic pathways by trehalose-6-phosphate. *Plant Physiol.* 149, 1860–1871. doi: 10.1104/pp.108.133934

Conflict of Interest: The authors declare that the research was conducted in the absence of any commercial or financial relationships that could be construed as a potential conflict of interest.

The reviewer LG declared a past co-authorship with one of the authors JY to the handling Editor.

frontiers in Plant Science

ORIGINAL RESEARCH
published: 21 May 2020
doi: 10.3389/fpls.2020.00564

Genetic Interaction Among Phytochrome, Ethylene and Abscisic Acid Signaling During Dark-Induced Senescence in *Arabidopsis thaliana*

*Hiroaki Ueda†, Takeshi Ito, Ryouhei Inoue, Yu Masuda, Yumi Nagashima, Toshiaki Kozuka and Makoto Kusaba**

Graduate School of Integral Sciences for Life, Hiroshima University, Higashihiroshima, Japan

OPEN ACCESS

Edited by:
Yasuhito Sakuraba, The University of Tokyo, Japan

Reviewed by:
Jinkil Jeong, Salk Institute for Biological Studies, United States
Lin Li, Fudan University, China

***Correspondence:**
Makoto Kusaba
akusaba@hiroshima-u.ac.jp

†Present address:
Hiroaki Ueda, Fruit Tree Research Center, Ehime Research Institute of Agriculture, Forestry and Fisheries, Matsuyama, Japan

Specialty section:
This article was submitted to Plant Abiotic Stress, a section of the journal Frontiers in Plant Science

Received: *18 December 2019*
Accepted: *15 April 2020*
Published: *21 May 2020*

Citation:
Ueda H, Ito T, Inoue R, Masuda Y, Nagashima Y, Kozuka T and Kusaba M (2020) Genetic Interaction Among Phytochrome, Ethylene and Abscisic Acid Signaling During Dark-Induced Senescence in Arabidopsis thaliana. Front. Plant Sci. 11:564. doi: 10.3389/fpls.2020.00564

Leaf senescence is induced by various internal and external stimuli. Dark-induced senescence has been extensively investigated, but the detailed mechanism underlying it is not well understood. The red light/far-red light receptor phytochrome B and its downstream transcription factors, PYHTOCHROME INTERACTING FACTORs (PIFs) 4 and 5, are known to play an important role in dark-induced senescence. Furthermore, the senescence-inducing phytohormones, ethylene and abscisic acid (ABA) are reported to be involved in dark-induced senescence. In this study, we analyzed the relationship between ethylene, ABA and PIFs in dark-induced leaf senescence. A triple mutant of the core ABA signaling components; SNF1-related protein kinases 2D (SRK2D), SRK2E, and SRK2I, displayed an ABA insensitive phenotype in ABA-induced senescence, whilst the ethylene insensitive mutant *ein2* demonstrated low sensitivity to ABA, suggesting that ethylene signaling is involved in ABA-induced senescence. However, the *pif4 pif5* mutant did not display low sensitivity to ABA, suggesting that PIF4 and PIF5 act upstream of ABA signaling. Although PIF4 and PIF5 reportedly regulate ethylene production, the triple mutant *ein2 pif4 pif5* showed a stronger delayed senescence phenotype than *ein2* or *pif4 pif5*, suggesting that EIN2 and PIF4/PIF5 partially regulate leaf senescence independently of each other. While direct target genes for PIF4 and PIF5, such as *LONG HYPOCOTYL IN FAR-RED1* (*HFR1*) and *PHYTOCHROME INTERACTING FACTOR 3-LIKE 1* (*PIL1*), showed transient upregulation under dark conditions (as is seen in the shade avoidance response), expression of *STAY GREEN1* (*SGR1*), *ORESARA1* (*ORE1*) and other direct target genes of PIF5, continued to increase during dark incubation. It is possible that transcription factors other than PIF4 and PIF5 are involved in the upregulation of *SGR1* and *ORE1* at a later stage of dark-induced senescence. Possible candidates are senescence-induced senescence regulators (SIRs), which include the NAC transcription factors ORE1 and AtNAP. In fact, ORE1 is known to bind to the *SGR1* promoter and promotes its expression. It is therefore inferred that the phytochrome-PIF pathway regulates initial activation of senescence and subsequently, induced SIRs reinforce leaf senescence during dark-induced senescence.

Keywords: senescence, ethylene, ABA, strigolactone, phytochrome-interacting factor, ORE1, AtNAP, sugar

INTRODUCTION

Leaf senescence is a system to recover nutrients from unnecessary leaves, which is accompanied by drastic changes in metabolism, gene expression and cell structure. Leaf senescence is induced, not only by internal factors such as aging and flowering, but also by various external stimuli such as prolonged dark incubation, drought, and salinity (Schippers, 2015). However, common phenomena such as yellowing (chlorophyll degradation) and reduction in photosynthetic activity, known as "senescence syndrome" occur irrespective of stimuli that cause leaf senescence (Noodén, 2004).

Leaf senescence is regulated by several phytohormones (Kusaba et al., 2013). For example, ethylene, which is well known to be an important senescence-inducing phytohormone (Grbić and Bleecker, 1995; Oh et al., 1997). Impairment of ethylene signaling components, such as ETHYLENE INSENSITIVE2 (EIN2) and EIN3/EIN3 LIKE1 (EIL1), severely represses leaf senescence in dark-induced senescence. Mutants of strigolactone synthesis genes, such as *MORE AXILLARY GROWTH1* (*MAX1*), *MAX3*, and *MAX4* and the signaling genes *ARABIDOPSIS DOWARF 14* (*AtD14*) and *MAX2,* also exhibit a delayed senescence phenotype, suggesting that strigolactone is a senescence-promoting phytohormone (Woo et al., 2001; Ueda and Kusaba, 2015). Abscisic acid (ABA) also induces leaf senescence, and overexpression of its receptor genes *PYR1-LIKE 8* (*PYL8*) and *PYL9* confers an early senescence phenotype (Lee et al., 2015; Zhao et al., 2016). In addition, the ABA signaling transcription factors ABA INSENSITIVE5 (ABI5) and ENHANCED EM LEVEL (EEL) are reportedly involved in leaf senescence (Sakuraba et al., 2014). Further phytohormones such as jasmonic acid (Zhuo et al., 2020) and salicylic acid (Yoshimoto et al., 2009) are also known to be involved in leaf senescence. These phytohormones are thought to function downstream of senescence-inducing stimuli. The examination of crosstalk between phytohormones is important in order to clarify the complete picture of regulation of leaf senescence in plants. For example, the senescence promoting function of strigolactone is strongly associated with ethylene signaling (Ueda and Kusaba, 2015).

Among several leaf senescence-inducing stimuli, prolonged dark incubation has been the most extensively studied (Liebsch and Keech, 2016). Under dark conditions, limitation of photosynthesis causes sugar starvation in the plant. Reportedly, sugar plays an important role in natural leaf senescence, but its role in dark-induced senescence remains unclear (Moore et al., 2003; Pourtau et al., 2006). On the other hand, it is well established that dark-induced senescence is regulated by the core components of the shade avoidance response, which allows plants to escape from shade in order to acquire light energy (Whitelam and Smith, 1991; Franklin and Whitelam, 2005). The red/far-red light receptor phytochrome degrades its downstream bHLH transcription factors; PHYTOCHROME INTERACTING FACTORs (PIFs) to repress the shade avoidance response (Quail et al., 1995; Legris et al., 2019). *HFR1*, *PIL1*, and *ARABIDOPSIS THALIANA HOMEOBOX PROTEIN2* (*AtHB2*) are known to be the direct targets of PIFs and function in shade avoidance responses. Since mutants of PIF4 and PIF5, which are degraded by Phytochrome B (phyB) (activated by red light), show a strong delayed senescence phenotype in the dark-induced senescence, PIF4 and PIF5 are considered as the central regulators of dark-induced senescence (Sakuraba et al., 2014; Song et al., 2014; Zhang et al., 2015).

During dark-induced senescence, ethylene production is increased, but has been found to be reduced in *pif4*, suggesting that ethylene production is regulated by the phyB-PIF pathway (Song et al., 2014; Ueda and Kusaba, 2015). Consistent with this, the expression of several ACC synthase genes, which are the rate-limiting enzymes in ethylene production, is upregulated during dark incubation, but this upregulation is repressed in *pif* mutants (Song et al., 2014; Qiu et al., 2015). Furthermore, PIF5 directly regulates transcription of the master transcription factor of ethylene signaling, EIN3, suggesting that PIFs regulate ethylene signaling (Sakuraba et al., 2014).

In addition to PIFs and EIN3, NAC and WRKY transcription factors are known to be involved in dark-induced senescence (Kusaba et al., 2013; Kim et al., 2016). Among such NAC transcription factors, ORE1 has been the most intensely analyzed. *ORE1* is induced during leaf senescence and promotes leaf senescence (Kim et al., 2009). EIN3 and PIF4/PIF5 directly regulate expression of *ORE1*, and at the same time, EIN3 represses expression of *miR164* targeting *ORE1* (Li et al., 2013; Sakuraba et al., 2014; Qiu et al., 2015). ORE1 is also involved in a wide spectrum of leaf senescence, including aging (Kim et al., 2009), reactive oxygen species (Woo et al., 2004), ethylene (Kim et al., 2009, 2014), jasmonic acid (Kim et al., 2014), salinity (Balazadeh et al., 2010), the circadian clock (Kim et al., 2018) and nitrogen starvation (Park et al., 2018). Another senescence-induced NAC transcription factor, AtNAP, is also known to be involved in natural senescence (Guo and Gan, 2006) and drought (Zhang and Gan, 2012; Sakuraba et al., 2015) and dark-induced senescence (Yang et al., 2014). In addition, a class of NAC transcription factors, sNACs, are reportedly required for ABA-induced senescence (Takasaki et al., 2015). Furthermore, VND-INTERACTING2 (VNI2) and JUNGBRUNNEN1 (JUB1) are also senescence-induced NAC transcription factors, however, they represse the progression of leaf senescence (Yang et al., 2011; Wu et al., 2012). Since these NAC transcription factor genes are induced during leaf senescence and regulate leaf senescence, they can be referred to as senescence-induced senescence regulators (SIRs). Senescence-regulating WRKY genes such as WRKY53 are also thought to belong to the SIRs group (Hinderhofer and Zentgraf, 2001).

Senescence syndrome is eventually caused by senescence-related enzymes, which is generally induced or activated during leaf senescence. Such enzymes include the chlorophyll-degrading enzymes SGR/ NON-YELLOWING1 (NYE1), NON-YELLOW COLORING1 (NYC1), NYC1 LIKE (NOL) and PHEOPHYTINASE (PPH) /NYC3 (Kusaba et al., 2007; Ren et al., 2007; Sato et al., 2007, 2009; Horie et al., 2009; Morita et al., 2009; Schelbert et al., 2009; Shimoda et al., 2016), the cysteine protease SENESCENCE ASSOCIATED GENE12 (SAG12) (Weaver et al., 1998), and the organelle endonuclease DEFECTIVE IN POLLEN ORGANELLE DNA DEGRADATION1 (DPD1) (Takami et al.,

2018). These enzymes are thought to execute cellular senescence. Such senescence-induced genes can be referred to as senescence-induced senescence executers (SIEs), whose expression may be controlled by senescence-regulating transcription factors.

Thus, leaf senescence progresses through complex interactions between senescence-related factors. The molecular basis of leaf senescence is not yet completely understood. Such processes have been analyzed utilizing delayed/early senescence mutants. However, there are few reports that examine the genetic interaction of these mutants. In this study, we genetically and physiologically dissect the roles of senescence-inducing-pathways in dark-induced leaf senescence using several delayed senescence mutants and their multiple mutants to better understand the complete picture of regulation of dark-induced leaf senescence in plants.

MATERIALS AND METHODS

Plant Material and Growth Conditions

The *Arabidopsis thaliana* ecotype Columbia (Col-0) was used as the wild type plant. The mutant lines *pif4-102* (SALK_140393; Sun et al., 2013), *pif5-3* (SALK_087012; Sun et al., 2013), *ein2-5* (CS16771; Alonso et al., 1999), *ore1-3* (SALK_090154; Kim et al., 2014), and *atnap* (SALK_005010; Guo and Gan, 2006) were obtained from the Arabidopsis Biological Resource Center (ABRC). *pif4 pif 5* double mutant was generated by a cross between *pif4-102* and *pif5-3*. The *srk2d/e/i* triple mutant (Fujita et al., 2009; Umezawa et al., 2009) was kindly provided by Kazuo Shinozaki (RIKEN Center for Sustainable Resource Science). Typically, plants were grown on soil in a growth chamber for a 4-week period under the following conditions: 22°C, 10 h light/14 h dark (short-day) photoperiod, and 80 μmol·photons m^{-2}·s^{-1}. For the natural senescence experiments, plants were grown under long-day conditions (16 h light/8 h dark).

Dark and Phytohormone Treatments

For the dark treatment, the 7th or 8th leaves from the top of 4-week-old plants with 16 leaves were detached and incubated in a box with constant high humidity, in the dark at 22°C. For the light (control) and phytohormone treatments, leaves were incubated under continuous white light conditions (5 μmol m^{-2} s^{-1}) at 22°C. For the physiological treatment, leaves were incubated in 0.5% (w/v) agar media containing 3 mM 2-(*N*-morpholino) ethanesulfonic acid (MES, pH 5.8) supplemented with abscisic acid (Sigma-Aldrich; St. Louis, MO, United States), glucose, or mannitol.

Measurement of Senescence Parameters

Chlorophyll content was measured using a SPAD-502 chlorophyll meter as SPAD value (Konica-Minolta, Japan). Average of SPAD values of three positions in a detached leaf were used. F_v/F_m values were measured using a Junior PAM chlorophyll fluorometer (Walz; Germany) according to Kohzuma et al. (2017). Detached leaves kept in dark for 30 min were subjected to measurement of F_v/F_m.

RNA Extraction and qRT-PCR Analysis

Total RNA was extracted using an Isospin with a spin column (Nippon Gene, Japan). First-strand cDNA was synthesized from 100 ng total RNA using ReverTra Ace qPCR RT Master Mix (Toyobo, Japan). Quantitative, reverse-transcriptase polymerase chain reaction (qRT-PCR) was performed using a KAPA SYBR FAST qPCR kit (Nippon Genetics; Tokyo, Japan) and a Roter-Gene Q 2PLEX (Qiagen; Venlo, Netherlands). qRT-PCR conditions are as follows: initial denaturation at 94°C for 3 min, followed by 40 cycles at 95°C for 5 s, and then 60°C for 10 s. The transcript level of each gene was normalized to that of *ACTIN8* (*ACT8*). Data analysis was performed using the Comparative CT Method, ΔΔCT Method (Livak and Schmittgen, 2001). The sequences of primers used for qRT-PCR are shown in **Supplementary Table S1**.

Accession Numbers

Sequence data from this article can be found in the Arabidopsis Genome Initiative under the following accession numbers: *PIF4*(AT2G43010), *PIF5*(AT3G59060), *HFR1*(AT1G02340), *PIL1*(AT2G46970), *AtHB2*(AT4G16780), *EIN2* (At5g03280), *SRK2D*(AT3G50500), *SRK2E*(AT4G33950), *SRK2I*(AT5G66880), *ORE1* (At5g39610), *MAX4*(AT4G32810), *SGR1*(At4 g22920), *SAG12* (At5g45890), *AtNAP* (At1g69490), and *ACT8*(AT1G49240).

RESULTS

Effect of Sugar on Dark-Induced Senescence

In the majority of plant species, prolonged dark treatment induces leaf senescence. Under dark conditions, photosynthesis is not performed, resulting in sugar starvation. To investigate the role of sugar starvation on dark-induced senescence, we analyzed leaf senescence during dark incubation in the presence of sugar (**Supplementary Figure S1**). Leaves that were the 6th from the top were selected from 4-week-old *A. thaliana* plants and incubated in mock medium or media containing either 50 mM glucose or 50 mM mannitol under dark conditions. Almost no reduction in chlorophyll contents and *Fv/Fm* values, which reflect photosystem II activity, was observed under light conditions but chlorophyll was severely degraded during dark incubation (**Supplementary Figures S1A,B**). Degrees of reduction of chlorophyll contents and *Fv/Fm* values were similar across dark-incubated mock medium, 50 mM glucose, and 50 mM mannitol-treated leaves during dark incubation. However, the chlorophyll content of 50 mM glucose-treated leaves 3 days after the start of treatment (DAT) and the *Fv/Fm* value of 50 mM mannitol-treated leaves at 5 DAT were slightly higher than those of the dark-treated mock condition (**Supplementary Figure S1A,B**). Expression of *DIN6*, a marker gene for sugar starvation (Baena-González et al., 2007), was drastically upregulated in the dark-treated mock condition, but this upregulation was repressed by 50 mM glucose treatment, suggesting that repression of sugar starvation could not fully repress dark-induced leaf senescence.

In addition, the 50 mM mannitol treatment, which does not fully repress sugar starvation, evoked similar responses to simple dark treatment, confirming that sugar starvation is not the major cause of dark-induced senescence.

PIF4/PIF5- Dependent Gene Expression in Dark-Induced Senescence

Reportedly, PIF4 and PIF5 play an important role in dark-induced leaf senescence in *A. thaliana*. To confirm this, we detached and incubated leaves from between the 7th to 12th position from the top of 4-week-old plants in the dark. At 6 DAT, upper (7th to 9th) leaves of Col-0 turned yellow but those of *pif4-102* and *pif5-3* remained green, and in *pif4 pif5* even lower (10th to 12th) leaves remained green (**Figures 1A,B**), confirming that *pif4* and *pif5* are delayed senescence mutants and *pif4 pif5* shows a stronger phenotype.

PIF4 and PIF5 play an important role in shade avoidance and their direct target genes, such as *HFR1*, *PIL1* and *AtHB2* have been identified (Kunihiro et al., 2011; Hornitschek et al., 2012). We examined the expression of these genes in Col-0 leaves during dark incubation and found that expressions of all of them are transiently upregulated at 1 DAT (**Figure 1C**). Such behavior is similar to that observed in high red light /far red light (R/FR) to low R/FR shift in young seedlings, which is thought to reflect a negative feedback regulation of shade avoidance (Sessa et al., 2005; Hornitschek et al., 2012). In *pif4 pif5*, such upregulation of *HFR1*, *PIL1*, and *AtHB2* is not observed, confirming that they are also regulated by PIF4 and PIF5 in dark-treated leaves (**Figure 1C**). Expression of the senescence-induced genes, *SGR1*, *SAG12*, *ORE1*, and MAX4, is severely repressed in *pif4 pif5*, confirming that they are regulated by PIF4 and PIF5 (**Figure 1C**). Among them, *ORE1* and *SGR1* are thought to be direct targets of PIF4/PIF5 (Sakuraba et al., 2014; Song et al., 2014; Zhang et al., 2015). However, *ORE1* and *SGR1* demonstrated a continuous increase in expression rather than the transient upregulation observed in *HFR1*, *PIL1* and *AtHB2*. Meanwhile, the expression of *PIF4* and *PIF5* was not upregulated during dark incubation (**Supplementary Figure S2**).

Roles of ABA in Dark-Induced Senescence

Although ABA is known as a phytohormone that promotes leaf senescence, its genetic contribution to dark-induced senescence has not been examined in detail. To understand its contribution to dark-induced senescence, we analyzed the triple mutant of *SRK2D/E/I*, which encode protein kinases that play a central role in core ABA signaling (Fujii and Zhu, 2009; Fujita et al., 2009). First, we examined the effect of ABA on leaf senescence under light conditions. The 8th leaves from the top of 4-week-old Col-0 and *srk2d/e/i* plants were treated with 100 μM ABA. Col-0 leaves turned yellow but *srk2d/e/i* did not show any yellowing at 3 DAT (**Figure 2A**). Expression of senescence-induced genes was upregulated in Col-0 but not in *srk2d/e/i* at 3 DAT (**Figure 2B**), suggesting that *srk2d/e/i* is insensitive to ABA in leaf senescence.

Next, we incubated *srk2d/e/i* leaves in the dark. *srk2d/e/i* also showed delayed senescence phenotype during dark incubation, but it was much weaker than the ethylene-insensitive mutant *ein2-5*, suggesting that its contribution of ABA to dark-induced senescence is limited (**Figure 2C**).

Crosstalk Between ABA and Ethylene in Leaf Senescence

To investigate the crosstalk between ABA and ethylene, *ein2-5* was treated with 1 μM or 100 μM ABA for 3 days under light conditions. Chlorophyll content was slightly reduced under 1 μM ABA and leaves turned yellow under 100 μM ABA in Col-0 (**Figure 3A**). Unexpectedly, *ein2-5* was resistant to ABA. Almost no reduction in chlorophyll content was observed in the 1 μM ABA treatment, and only a slight reduction in chlorophyll content was observed under the 100 μM ABA treatment (**Figure 3A**). These observations suggest that *ein2-5* is hyposensitive to ABA in leaf senescence, and that activation of ethylene signaling is necessary for efficient induction of leaf senescence by ABA. Consistent with this idea, *ein3-1 eil1-3* was also hyposensitive to ABA in leaf senescence (**Supplementary Figure S3**).

Next, the crosstalk between ABA and PIF4/PIF5 was investigated. Because PIF4 and PIF5 degrade under light conditions, we examined ABA-induced leaf senescence under dark conditions where PIF4 and PIF5 proteins are stable (**Figure 3B**). ABA accelerated chlorophyll degradation in Col-0 under dark conditions, and the acceleration of chlorophyll degradation is significantly inhibited in *ein2-5*, consistent with the observation in **Figure 3A**. Meanwhile, chlorophyll degradation was not delayed in *pif4 pif5* (**Figure 3B** and **Supplementary Figure S4**), suggesting that ABA does not promote leaf senescence through the function of PIF4 and PIF5. In contrast to our observations, Zhao et al. (2016) did not observe a delay of ABA-induced senescence in ethylene insensitive mutants. However, one difference is the lines which were used in the experiments. Zhao et al. (2016) used *ein2-1*, which is a leaky allele of *ein2*, and *ein3-1*, which shows complete ethylene insensitivity only when accompanying a mutation of its paralog *EIL1*, whilst, in this study, we used the null allele *ein2-5* and *ein3-1 eil1-3*. We then treated *ein3-1* with ABA, but found that *ein3-1* also shows a delayed senescence phenotype, although it is slightly weaker than *ein3-1 eil1-3* (**Supplementary Figure S3**). Therefore, the difference of results between our and Zhao et al.'s study could be attributed to the differences in experimental conditions.

Relationship Between PIF4/PIF5 and Ethylene in Dark-Induced Senescence

Next, we investigated the genetic interaction between ethylene signaling and PIF4/PIF5 in dark-induced senescence. *pif4 pif5* shows a delayed senescence phenotype, but the 7th leaf turned completely yellow under dark conditions at 14 DAT (**Figures 4A,B**). *ein2-5* showed a stronger delayed senescence phenotype, with the 7th leaf remaining green at 14 DAT and tuning yellow at 18 DAT. The *ein2-5 pif4 pif5* triple mutant had an even stronger delayed senescence phenotype, retaining a high chlorophyll content even at 18 DAT (**Figure 4B**). The

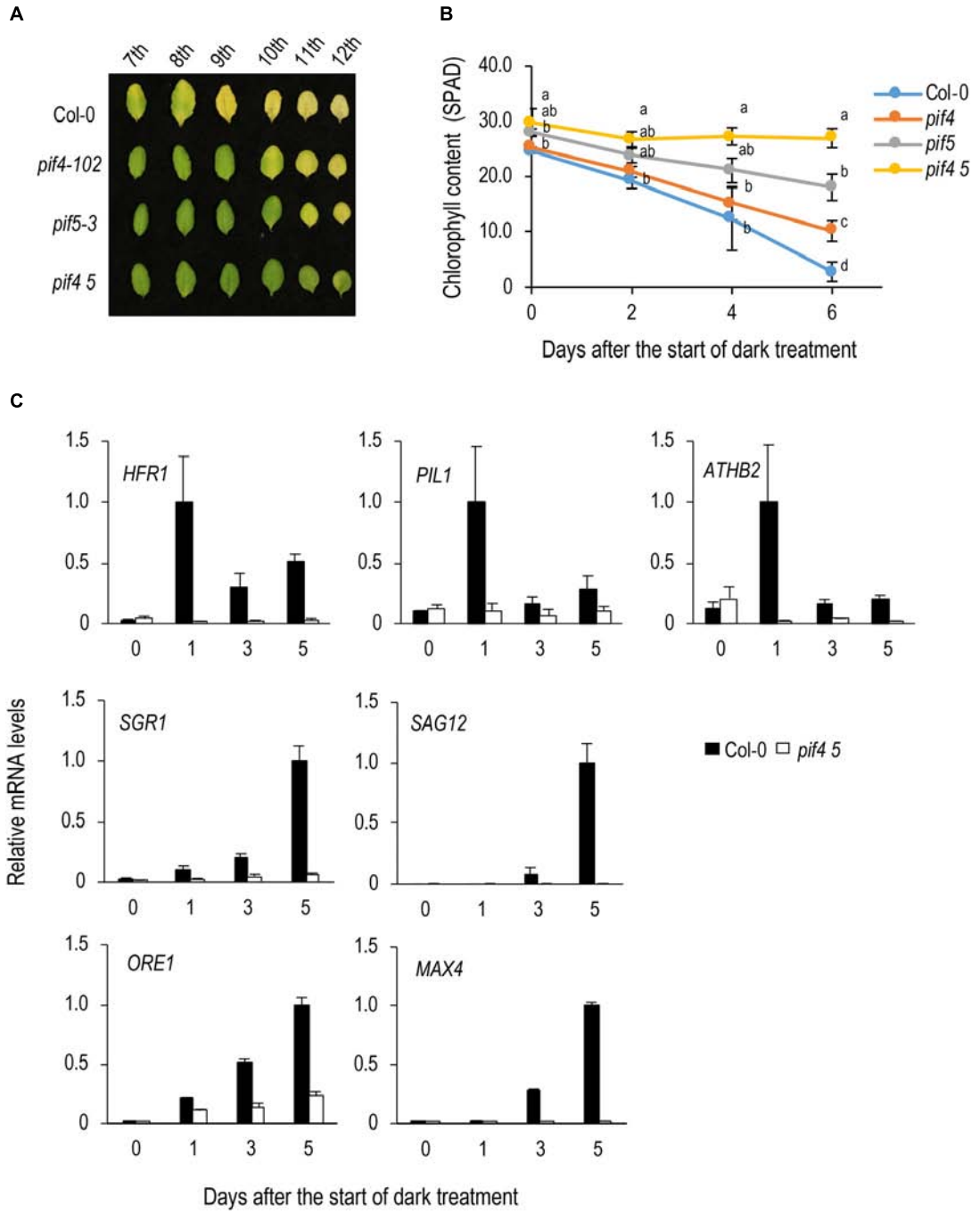

FIGURE 1 | Analysis of the function of PIF4 and PIF5 in dark-induced senescence. **(A)** Dark-induced leaf senescence in *pif4·pif5*. Leaves in the 7th to 12th positions from the top of 4-week-old plants were incubated in the dark for 6 days. **(B)** Changes in chlorophyll content over time in *pif4 pif5* during dark incubation. Detached 8th leaves were used for the analysis. Data for the same day after the start of treatment were statistically compared using Tukey's multiple comparison method ($p < 0.05$). **(C)** qRT-PCR analysis of transcript levels of direct target genes of PIF5 and senescence-induced genes. 8th leaves were used for the analysis. Solid and open bars indicate Col-0 and *pif4 pif5* leaves, respectively. Transcript levels were relative to that in Col-0 leaves at 5 DAT. *ACT8* was used as a reference. Bars indicate standard error ($n = 3$).

ein2-5 pif4 pif5 triple mutant also retained relatively high *Fv/Fm* values and low *SGR1* expression even at the stage that *ein2-5* turned yellow, confirming that *ein2-5 pif4 pif5* is a very strong delayed senescence mutant (**Supplementary Figure S5**). These observations suggest that ethylene has a major role in dark-induced senescence and that PIF4/PIF5 also promotes dark-induced senescence through another pathway in addition to the ethylene signaling pathway.

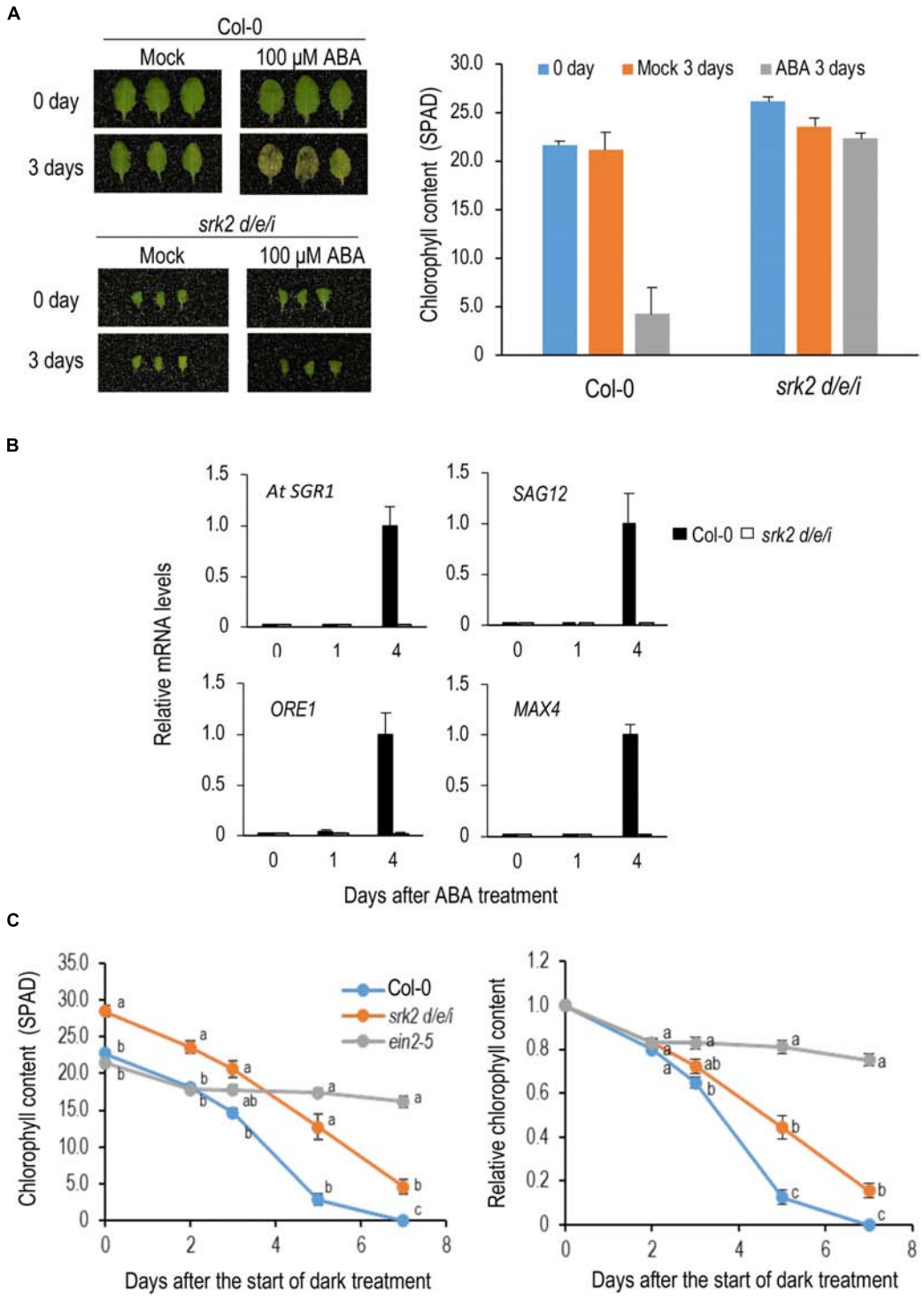

FIGURE 2 | Roles of ABA in dark-induced leaf senescence. **(A)** Sensitivity of *srk2d/e/i* to ABA in leaf senescence. Left, leaves in the 8th position from the top of 4-week-old plants were incubated on the medium containing 100 μM ABA for 3 days under light conditions. Right, Changes in chlorophyll content by ABA treatment. **(B)** qRT-PCR analysis of changes in transcript levels of senescence-induced genes during ABA treatment. Detached 8th position leaves were used for the analysis. *ACT8* was used as a reference. Solid and open bars indicate Col-0 and *srk2d/e/i*, respectively. Transcript levels were relative to that in Col-0 leaves 4 days after ABA treatment. *ACT8* was used as a reference. **(C)** Changes in chlorophyll content over time in *srk2d/e/i* during dark incubation. Detached 8th position leaves were used for the analysis. Chlorophyll content is indicated in SPAD value in the left panel and those relative to day 0 are shown in the right panel. Data for the same day after the start of dark incubation were statistically compared using Tukey's multiple comparison method ($p < 0.05$). Bars indicate standard errors ($n = 6$, 4, and 8 in **A**, **B**, and **C**, respectively).

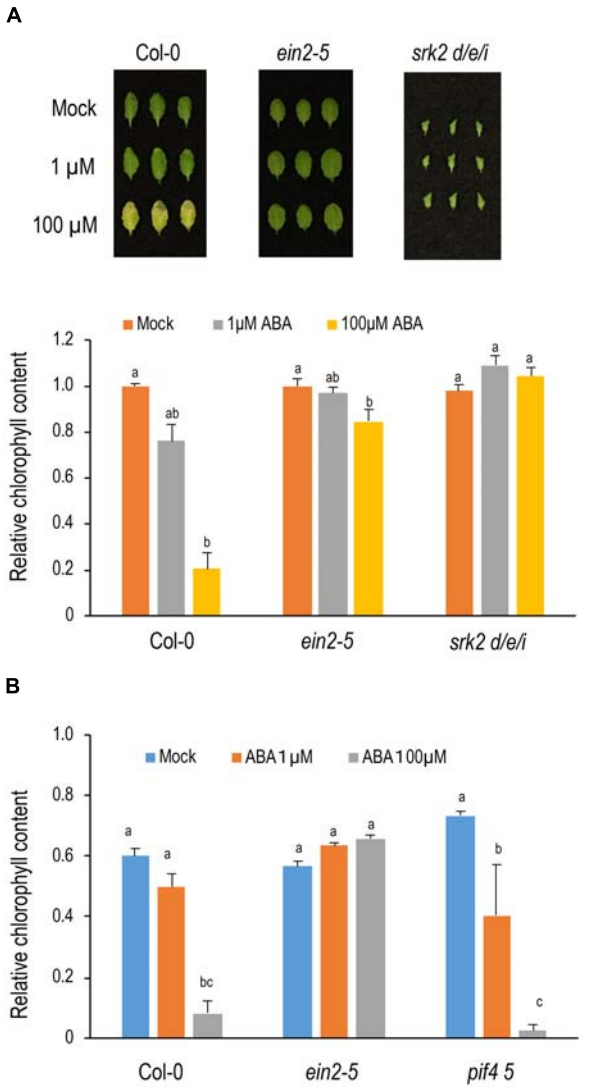

FIGURE 3 | Sensitivity of *ein2*and *pif4 pif5* to ABA in leaf senescence. **(A)** Sensitivity of *ein2-5* and *srk2d/e/i* to ABA in leaf senescence under light conditions. Leaves positioned 8th from the top of 4-week-old plants were incubated on the medium containing 1 or 100 μM ABA for 3 days under light conditions. Lower panel shows chlorophyll content (SPAD value) relative to those of mock condition in each genotype. **(B)** Sensitivity of *ein2-5* and *pif4 pif5* to ABA in leaf senescence under dark conditions. The 8th leaves were incubated on the medium containing 1 or 100 μM ABA for 3 days under dark conditions. Chlorophyll content (SPAD value) were relative to those before ABA treatment in each genotype. Data were statistically compared using Tukey's multiple comparison method in each genotype in A and in all genotypes in B ($p < 0.05$). Bars indicate standard errors ($n = 8$ in **A**, and $n = 4$ in **B**).

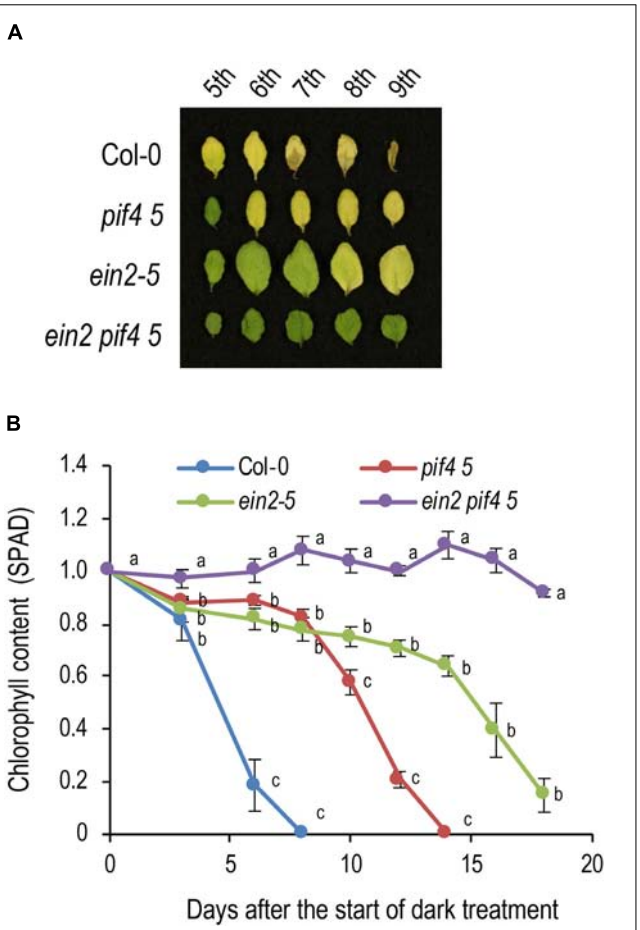

FIGURE 4 | Genetic interaction between *EIN2* and *PIF4/PIF5* in dark-induced senescence. **(A)** Delayed leaf senescence phenotype of the *ein2 pif4 pif5* triple mutant. Leaves in the 5th to 9th positions from the top of 4-week-old plants were incubated in the dark for 14 days. **(B)** Changes in chlorophyll content (SPAD value) over time in the *ein2 pif4 pif5* triple mutant during dark incubation. Detached 7th position leaves were used for the analysis. Data for the same day after the start of dark incubation were statistically compared using Tukey's multiple comparison method ($p < 0.05$). Bars indicate standard errors ($n = 3$).

DISCUSSION

The Phytochrome-PIF-Ethylene Cascade Is the Major Pathway Regulating Dark-Induced Senescence

There could be two main factors that induce dark-induced leaf senescence. The first is the inactivation of photoreceptors by light depletion. Analyses of *phytochrome b* (*phyb*) and *pif* mutants have suggested that it is the major cause of dark-induced leaf senescence (Sakuraba et al., 2014; Song et al., 2014; Zhang et al., 2015). The second is the starvation of energy (sugar) caused by a repression of photosynthesis. This study suggests that this may contribute minimally to the promotion of dark-induced senescence. Meanwhile, in natural leaf senescence, defects in sugar signaling delays, whilst sugar application promotes, leaf senescence during natural senescence (Moore et al., 2003; Pourtau et al., 2006). Taken together, this suggests that sugar starvation does not promote leaf senescence in dark-induced senescence and sugar accumulation promotes leaf senescence in natural senescence.

While a number of phytohormones are known to be involved in the regulation of leaf senescence, the degree of contribution of each phytohormone varies. The observations indicating that

ABA accumulates during dark-induced leaf senescence (Yang et al., 2014), and that the addition of ABA and overexpression of the ABA receptors PYL8 and PYL9 promote leaf senescence (Lee et al., 2015; Takasaki et al., 2015; Zhao et al., 2016) suggest that ABA is involved in dark-induced leaf senescence. In this study, the core ABA-signaling mutant *srk2d/e/i*, which showed ABA insensitivity in ABA-induced senescence, exhibited a delay of dark-induced senescence, confirming that ABA is involved in dark-induced senescence. However, the strength of repression of leaf senescence in *srk2d/e/i* is apparently weaker than that of *ein2-5*. Woo et al. (2001) and Ueda and Kusaba (2015) demonstrated that strigolactone synthesis and signaling mutants exhibit delayed senescence phenotypes, but the degree is also smaller than that of *ein2-5*. These observations suggest that ethylene is the central phytohormone regulating leaf senescence during dark incubation.

In this study, we also analyzed the genetic interaction of PIF4/PIF5 and ethylene signaling. The *ein2 pif4 pif5* triple mutant showed a stronger delayed leaf-senescence phenotype than *ein2*, suggesting that PIF4/PIF5 could promote leaf senescence independent of ethylene signaling although ethylene is the major regulating factor of dark-induced senescence. In fact, it is known that PIF5 directly regulates expression of the senescence regulating transcription factor gene *ORE1* and chlorophyll-degrading enzyme genes such as *SGR* and *NYC1* (Sakuraba et al., 2014; Song et al., 2014; Zhang et al., 2015).

Meanwhile, *ein2 pif4 pif5* showed a stronger delayed senescence phenotype than *pif4 pif5*, suggesting that ethylene signaling could be activated by another signaling pathway instead of PIF4/PIF5 in dark-induced senescence. It is possible that another member of the PIF family or non-red light regulates ethylene signaling in dark-induced senescence. For example, the blue-light receptor cryptochrome (CRY) and its downstream transcription factor cryptochrome-interacting basic-helix-loop-helix (CIB) are reportedly involved in leaf senescence in soybean (Meng et al., 2013). Although the effect of blue light on dark-induced senescence was not directly examined in the study, this could be an interesting potential avenue of research in *A. thaliana*.

Crosstalk Between ABA and Ethylene in Dark-Induced Senescence

ein2-5 and *ein3 eil1* are hyposensitive to ABA in leaf senescence, suggesting that ABA promotes leaf senescence through ethylene signaling. However, leaf senescence induced by ABA progressed in *ein2-5* to some extent, suggesting the presence of an ethylene-independent pathway. *pif4 pif5* did not show hyposensitivity to ABA in leaf senescence, suggesting that ABA does not promote leaf senescence through the function of PIF4 and PIF5. PIF4 and PIF5 may act upstream of ABA in leaf senescence as previously suggested by Sakuraba et al. (2014). Thus, ABA promotes dark-induced senescence in concert with ethylene, though it has less impact on dark-induced senescence than ethylene. Furthermore, the senescence-induced NAC transcription factor AtNAP promotes ABA synthesis via regulation of the expression of *ABSCISIC ALDEHYDE OXIDASE3* (*AAO3*), suggesting a complex regulation of ABA signaling during dark-induced senescence (Yang et al., 2014).

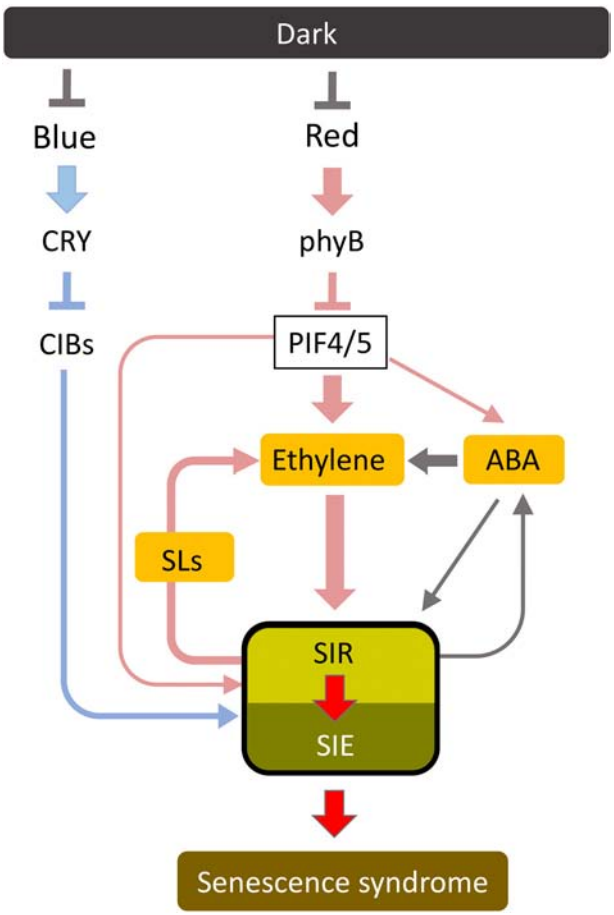

FIGURE 5 | A proposed signal transduction pathway of dark-induced senescence. Dark-induced senescence is mainly regulated by the red light pathway involving phyB and PIF4/PIF5. PIF4 and PIF5 regulate ethylene synthesis and signaling to progress leaf senescence in addition to ABA signaling. ABA mainly promotes leaf senescence via ethylene signaling. PIF4 and PIF5 also directly regulate senescence-induced senescence regulators (SIRs) including the NAC transcription factor ORE1, and senescence-induced senescence executors (SIEs) such as Chl*a*-degrading enzyme SGR1, at the early stage of leaf senescence. At later stages, SIRs enhance their own expression and activity through a positive feedback regulation, which elevates SIE expression and reinforce leaf senescence (senescence syndrome). Furthermore, blue light is thought to repress dark-induced senescence through cryptochrome (CRY) and cryptochrome-interacting basic-helix-loop-helix (CIB).

Roles of Senescence-Induced Senescence Regulators

Genes induced during senescence are called senescence-associated genes (SAGs) (Weaver et al., 1998). SAGs can be classified into two classes, SIEs and SIRs. SIEs include chlorophyll degradation enzymes such as SGR and NYC1 and proteases such as SAG12, which directly cause senescence syndromes. SIRs include NAC transcription factors such as ORE1, AtNAP and

WRKY transcription factors such as WRKY53. SIRs are induced along with the progression of leaf senescence and regulate the progression of leaf senescence. Strigolactone synthesis enzyme genes *MAX3* and *MAX4* (Ueda and Kusaba, 2015), ethylene synthesis genes encoding 1-aminocyclopropane-1-carboxylic acid synthase (ACS) (Qiu et al., 2015), and ABA synthesis genes *AAO3* (Yang et al., 2014) might be included in the SIRs group, in the context that they could regulate leaf senescence.

Among transcription factors that regulate leaf senescence, PIF4 and PIF5 are not included in the SIRs as the stabilization of PIF4 and PIF5 proteins is due to deprivation of light and is not associated with senescence. Genes involved in shade avoidance are known to be under the control of negative feedback regulation to avoid excess signaling (Roig-Villanova et al., 2007; Hornitschek et al., 2009). We revealed that the expression of the shade avoidance genes *HFR1*, *PIL1*, and *AtHB2*, which are directly regulated by PIF5, was upregulated at 1 DAT, but downregulated at 2 DAT and later on during dark incubation. This observation suggests that the expression of these genes is also under the control of negative feedback, which is mediated by hetero-dimerization between PIF5 and HFR1, in the detached leaves during dark incubation. This means that the transcription activation activity of PIF4/PIF5 is limited at 1–2 DAT during dark incubation. In contrast, the expression of senescence-inducible genes *SGR1* and *ORE1*, that are also direct targets of PIF4/PIF5, continues to increase at 2 DAT and later, which appears to inconsistent the expression pattern of *HFR1*, *PIL1* and *AtHB2*.

This contradiction might be explained by the hypothesis that, in addition to PIF4 and PIF5, another factor(s) regulates the expression of *SGR1* and *ORE1*. The stabilized PIF4 and PIF5 enhance the transcription of *PIL1*, *AtHB2*, and *HFR1* and *SGR1* and *ORE1* in the early stage of dark-induced senescence. In the later stage, transcriptional activity of PIF4 and PIF5 are downregulated by the negative feedback regulation and consequently, *PIL1*, *AtHB2*, and *HFR1* are downregulated. On the contrary, expression of *SGR1* and *ORE1* might be further upregulated by other transcription factors, possibly SIR transcription factors. The observation that *SGR1* and *ORE1* were induced, albite slightly, on the first day of dark incubation is consistent with the notion that PIF4 and PIF5 regulate these genes in the early stage.

Liebsch and Keech (2016) present a feedforward loop model of dark-induced senescence. They hypothesize that PIFs play a major role in initial light deprivation, that EIN3 in addition to PIFs enhances the expression of senescence-related genes in "prolonged light deprivation," and that ORE1 further promotes senescence in "persistent darkness." Our observations are largely consistent with their hypothesis. PIF4 and PIF5 stabilized by dark incubation induce the expression of SIR transcription factors and some SIEs in the early stage of dark-induced senescence. In the later stages, SIR transcription factors may mainly function in promotion of leaf senescence.

The majority of SIRs represented by ORE1 and AtNAP are positive regulators of leaf senescence. However, some SIRs such as VNI2 and JUB1 are negative regulators of leaf senescence that are induced during the senescence (Yang et al., 2011; Wu et al., 2012). Although each SIR has a specific function, leaf senescence may be regulated by "total activity" of SIRs to enhance SIE function and cause senescence syndrome. Such total activity of SIRs could be referred to as senescence signaling (Ueda and Kusaba, 2015).

A System Eliminating External Noises That Induce Accidental Leaf Senescence

Leaf senescence can act as a suicide signal, and therefore must be strictly regulated in plants. Plants are exposed daily to external noises that could induce senescence, such as subtle stresses that induce ethylene production and diurnal short-period dark conditions. Such noises must be eliminated to avoid unnecessary premature senescence and plant death. In addition, leaf senescence should progress slowly enough for the plant to salvage nutrients from senescing leaves. Such conditions may be achieved via a multi-step activation system. **Figure 5** shows a model of the signal transduction pathway of dark-induced senescence. Dark-stabilized PIFs may mainly function in the early stage of dark-induced senescence. PIFs upregulate SIRs mainly through the function of several phytohormones. SIRs may promote leaf senescence through the induction of SIEs. The initial input of senescence-inducing stimuli may not work effectively, which eliminates external noises, while continuous input leads to the activation of SIRs and the steady progress of leaf senescence. Inhibitory SIRs such as VNI2 may also play a role in its fine tuning. Thus, the multi-step activation system may provide both a kind of robustness for growth and efficient nutrient salvage when required.

DATA AVAILABILITY STATEMENT

All datasets generated and analyzed for this study are included in the article/**Supplementary Material**.

AUTHOR CONTRIBUTIONS

MK and HU designed the study. HU, RI, YM, TI, and YN conducted the research. MK, HU, and TK wrote the manuscript.

FUNDING

This work was supported by JSPS KAKENHI Grant Numbers JP26292006 (to MK) and JP16J06278 (to HU).

ACKNOWLEDGMENTS

We thank Junro Mogami for his helpful comments.

SUPPLEMENTARY MATERIAL

The Supplementary Material for this article can be found online at: https://www.frontiersin.org/articles/10.3389/fpls.2020.00564/full#supplementary-material

REFERENCES

Alonso, J. M., Hirayama, T., Roman, G., Nourizadeh, S., and Ecker, J. R. (1999). EIN2, a bifunctional transducer of ethylene and stress responses in *Arabidopsis*. *Science* 284, 2148–2152.

Baena-González, E., Rolland, F., Thevelein, J. M., and Sheen, J. (2007). A central integrator of transcription networks in plant stress and energy signaling. *Nature* 448, 938–942.

Balazadeh, S., Siddiqui, H., Allu, A. D., Matallana-Ramirez, L. P., Caldana, C., Mehrnia, M., et al. (2010). A gene regulatory network controlled by the NAC transcription factor ANAC092/AtNAC2/ORE1 during salt-promoted senescence. *Plant J.* 62, 250–264. doi: 10.1111/j.1365-313X.2010.04151.x

Franklin, K. A., and Whitelam, G. C. (2005). Phytochromes and shade-avoidance responses in plants. *Ann. Bot.* 96, 169–175.

Fujii, H., and Zhu, J. K. (2009). Arabidopsis mutant deficient in 3 abscisic acid-activated protein kinases reveals critical roles in growth, reproduction, and stress. *Proc. Natl. Acad. Sci. U.S.A.* 106, 8380–8385. doi: 10.1073/pnas.0903144106

Fujita, Y., Nakashima, K., Yoshida, T., Katagiri, T., Kidokoro, S., Kanamori, N., et al. (2009). Kinases are the main positive regulators of abscisic acid signaling in response to water stress in *Arabidopsis*. *Plant Cell Physiol.* 50, 2123–2132. doi: 10.1093/pcp/pcp147

Grbić, V., and Bleecker, A. B. (1995). Ethylene regulates the timing of leaf senescence in *Arabidopsis*. *Plant J.* 8, 595–602.

Guo, Y., and Gan, S. (2006). AtNAP, a NAC family transcription factor, has an important role in leaf senescence. *Plant J.* 46, 601–612.

Hinderhofer, K., and Zentgraf, U. (2001). Identification of a transcription factor specifically expressed at the onset of leaf senescence. *Planta* 213, 469–473.

Horie, Y., Ito, H., Kusaba, M., Tanaka, R., and Tanaka, A. (2009). Participation of chlorophyll b reductase in the initial step of the degradation of lightharvesting chlorophyll a/b-protein complexes in *Arabidopsis*. *J. Biol. Chem.* 284, 17449–17456. doi: 10.1074/jbc.M109.008912

Hornitschek, P., Kohnen, M. V., Lorrain, S., Rougemont, J., Ljung, K., López-Vidriero, I., et al. (2012). Phytochrome interacting factors 4 and 5 control seedling growth in changing light conditions by directly controlling auxin signaling. *Plant J.* 71, 699–711. doi: 10.1111/j.1365-313X.2012.05033.x

Hornitschek, P., Lorrain, S., Zoete, V., Michielin, O., and Fankhauser, C. (2009). Inhibition of the shade avoidance response by formation of non-DNA binding bHLH heterodimers. *EMBO J.* 28, 3893–3902. doi: 10.1038/emboj.2009.306

Kim, H., Kim, H. J., Vu, Q. T., Jung, S., McClung, C. R., Hong, S., et al. (2018). Circadian control of ORE1 by PRR9 positively regulates leaf senescence in Arabidopsis. *Proc. Natl. Acad. Sci. U.S.A.* 115, 8448–8453. doi: 10.1073/pnas.1722407115

Kim, H. J., Hong, S. H., Kim, Y. W., Lee, I. H., Jun, J. H., Phee, B. K., et al. (2014). Gene regulatory cascade of senescenceassociated NAC transcription factors activated by ETHYLENE-INSENSITIVE2 mediated leaf senescence signalling in *Arabidopsis*. *J. Exp. Bot.* 65, 4023–4036. doi: 10.1093/jxb/eru112

Kim, H. J., Nam, H. G., and Lim, P. O. (2016). Regulatory network of NAC transcription factors in leaf senescence. *Curr. Opin. Plant Biol.* 33, 48–56. doi: 10.1016/j.pbi.2016.06.002

Kim, J. H., Woo, H. R., Kim, J., Lim, P. O., Lee, I. C., Choi, S. H., et al. (2009). Trifurcate feed-forward regulation of age-dependent cell death involving miR164 in *Arabidopsis*. *Science* 323, 1053–1057. doi: 10.1126/science.1166386

Kohzuma, K., Sato, Y., Ito, H., Okuzaki, A., Watanabe, M., Kobayashi, H., et al. (2017). The non-Mendelian green cotyledon gene in soybean encodes a small subunit of photosystem II. *Plant Physiol.* 173, 2138–2147. doi: 10.1104/pp.16.01589

Kunihiro, A., Yamashino, T., Nakamichi, N., Niwa, Y., Nakanishi, H., and Mizuno, T. (2011). Phytochrome-interacting factor 4 and 5 (PIF4 and PIF5) activate the homeobox ATHB2 and auxin-inducible IAA29 genes in the coincidence mechanism underlying photoperiodic control of plant growth of Arabidopsis thaliana. *Plant Cell Physiol.* 52, 1315–1329. doi: 10.1093/pcp/pcr076

Kusaba, M., Ito, H., Morita, R., Iida, S., Sato, Y., Fujimoto, M., et al. (2007). Rice NON-YELLOW COLORING1 is involved in light-harvesting complex II and grana degradation during leaf senescence. *Plant Cell* 19, 1362–1375.

Kusaba, M., Tanaka, A., and Tanaka, R. (2013). Stay-green plants: what do they tell us about the molecular mechanism of leaf senescence. *Photosynth. Res.* 117, 221–234. doi: 10.1007/s11120-013-9862-x

Lee, H. N., Lee, K. H., and Kim, C. S. (2015). Abscisic acid receptor PYRABACTIN RESISTANCE-LIKE 8, PYL8, is involved in glucose response and dark-induced leaf senescence in *Arabidopsis*. *Biochem. Biophys. Res. Commun.* 463, 24–28. doi: 10.1016/j.bbrc.2015.05.010

Legris, M., Ince, Y. C., and Fankhauser, C. (2019). Molecular mechanisms underlying phytochromecontrolled morphogenesis in plants. *Nat. Commun.* 10:5219.

Li, Z., Peng, J., Wen, X., and Guo, H. (2013). Ethylene-insensitive3 is a senescenceassociated gene that accelerates age-dependent leaf senescence by directly repressing miR164 transcription in *Arabidopsis*. *Plant Cell* 25, 3311–3328. doi: 10.1105/tpc.113.113340

Liebsch, D., and Keech, O. (2016). Dark-induced leaf senescence: new insights into a complex light-dependent regulatory pathway. *New Phytol.* 212, 563–570. doi: 10.1111/nph.14217

Livak, K. J., and Schmittgen, T. D. (2001). Analysis of relative gene expression data using real-time quantitative PCR and the 2(-Delta Delta C(T)) Method. *Methods* 25, 402–408.

Meng, Y., Li, H., Wang, Q., Liu, B., and Lin, C. (2013). Blue light-dependent interaction between cryptochrome2 and CIB1 regulates transcription and leaf senescence in soybean. *Plant Cell* 25, 4405–4420. doi: 10.1105/tpc.113.116590

Moore, B., Zhou, L., Rolland, F., Hall, Q., Cheng, W., Liu, Y., et al. (2003). Role of the *Arabidopsis* glucose sensor HXK1 in nutrient, light, and hormonal signaling. *Science* 300, 332–336.

Morita, R., Sato, Y., Masuda, Y., Nishimura, M., and Kusaba, M. (2009). Defect in non-yellow coloring 3, an alpha/beta hydrolase-fold family protein, causes a stay-green phenotype during leaf senescence in rice. *Plant J.* 59, 940–952. doi: 10.1111/j.1365-313X.2009.03919.x

Noodén, L. D. (2004). *Plant Cell Death Processes*. London: Academic Press.

Oh, S. A., Park, J. H., Lee, G. I., Paek, K. H., Park, S. K., and Nam, H. G. (1997). Identification of three genetic loci controlling leaf senescence in *Arabidopsis thaliana*. *Plant J.* 12, 527–535.

Park, B. S., Yao, T., Seo, J. S., Wong, E. C. C., Mitsuda, N., Huang, C. H., et al. (2018). *Arabidopsis* NITROGEN LIMITATION ADAPTATION regulates ORE1 homeostasis during senescence induced by nitrogen deficiency. *Nat. Plants* 4, 898–903. doi: 10.1038/s41477-018-0269-8

Pourtau, N., Jennings, R., Pelzer, E., Pallas, J., and Wingler, A. (2006). Effect of sugar-induced senescence on gene expression and implications for the regulation of senescence in *Arabidopsis*. *Planta* 224, 556–568.

Qiu, K., Li, Z., Yang, Z., Chen, J., Wu, S., Zhu, X., et al. (2015). EIN3 and ORE1 accelerate degreening during ethylene-mediated leaf senescence by directly activating chlorophyll catabolic genes in *Arabidopsis*. *PLoS Genet.* 11:e1005399. doi: 10.1371/journal.pgen.1005399

Quail, P. H., Boylan, M. T., Parks, B. M., Short, T. W., Xu, Y., and Wagner, D. (1995). Phytochromes: photosensory perception and signal transduction. *Science* 268, 675–680.

Ren, G., An, K., Liao, Y., Zhou, X., Cao, Y., Zhao, H., et al. (2007). Identification of a novel chloroplast protein AtNYE1 regulating chlorophyll degradation during leaf senescence in *Arabidopsis*. *Plant Physiol.* 144, 1429–1441.

Roig-Villanova, I., Bou-Torrent, J., Galstyan, A., Carretero-Paulet, L., Portolés, S., Rodríguez-Concepción, M., et al. (2007). Interaction of shade avoidance and auxin responses: a role for two novel atypical bHLH proteins. *EMBO J.* 26, 4756–4767.

Sakuraba, Y., Jeong, J., Kang, M. Y., Kim, J., Paek, N. C., and Choi, G. (2014). Phytochrome-interacting transcription factors PIF4 and PIF5 induce leaf senescence in *Arabidopsis*. *Nat Commun.* 5:4636. doi: 10.1038/ncomms5636

Sakuraba, Y., Kim, Y. S., Han, S. H., Lee, B. D., and Paek, N. C. (2015). The *Arabidopsis* transcription factor NAC016 promotes drought stress responses by repressing AREB1 transcription through a trifurcate feed-forward regulatory loop involving NAP. *Plant Cell* 27, 1771–1787. doi: 10.1105/tpc.15.00222

Sato, Y., Morita, R., Katsuma, S., Nishimura, M., Tanaka, A., and Kusaba, M. (2009). Two short-chain dehydrogenase/reductases, NON-YELLOW COLORING 1 and NYC1-LIKE, are required for chlorophyll b and lightharvesting complex II degradation during senescence in rice. *Plant J.* 57, 120–131.

Sato, Y., Morita, R., Nishimura, M., Yamaguchi, H., and Kusaba, M. (2007). Mendel's green cotyledon gene encodes a positive regulator of the chlorophyll-degrading pathway. *Proc. Natl. Acad. Sci. U.S.A.* 104, 14169–14174.

Schelbert, S., Aubry, S., Burla, B., Agne, B., Kessler, F., Krupinska, K., et al. (2009). Pheophytin pheophorbide hydrolase (pheophytinase) is involved in chlorophyll breakdown during leaf senescence in Arabidopsis. *Plant Cell* 21, 767–785. doi: 10.1105/tpc.108.064089

Schippers, J. H. (2015). Transcriptional networks in leaf senescence. *Curr. Opin. Plant Biol.* 27, 77–83. doi: 10.1016/j.pbi.2015.06.018

Sessa, G., Carabelli, M., Sassi, M., Ciolfi, A., Possenti, M., Mittempergher, F., et al. (2005). A dynamic balance between gene activation and repression regulates the shade avoidance response in Arabidopsis. *Genes Dev.* 19, 2811–2815.

Shimoda, Y., Ito, H., and Tanaka, A. (2016). Arabidopsis STAY-GREEN, Mendel's green cotyledon gene, encodes magnesium-dechelatase. *Plant Cell* 28, 2147–2160. doi: 10.1105/tpc.16.00428

Song, Y., Yang, C., Gao, S., Zhang, W., Li, L., and Kuai, B. (2014). Age-triggered and dark-induced leaf senescence require the bHLH transcription factors PIF3, 4, and 5. *Mol. Plant.* 7, 1776–1787. doi: 10.1093/mp/ssu109

Sun, J., Qi, L., Li, Y., Zhai, Q., and Li, C. (2013). PIF4 and PIF5 transcription factors link blue light and auxin to regulate the phototropic response in *Arabidopsis*. *Plant Cell* 25, 2102–21014. doi: 10.1105/tpc.113.112417

Takami, T., Ohnishi, N., Kurita, Y., Iwamura, S., Ohnishi, M., Kusaba, M., et al. (2018). Organelle DNA degradation contributes to the efficient use of phosphate in seed plants. *Nat. Plants* 4, 1044–1055. doi: 10.1038/s41477-018-0291-x

Takasaki, H., Maruyama, K., Takahashi, F., Fujita, M., Yoshida, T., Nakashima, K., et al. (2015). SNAC-As, stress-responsive NAC transcription factors, mediate ABA-inducible leaf senescence. *Plant J.* 84, 1114–1123. doi: 10.1111/tpj.13067

Ueda, H., and Kusaba, M. (2015). Strigolactone regulates leaf senescence in concert with ethylene in *Arabidopsis*. *Plant Physiol.* 2015. 169, 138–147. doi: 10.1104/pp.15.00325

Umezawa, T., Sugiyama, N., Mizoguchi, M., Hayashi, S., Myouga, F., Yamaguchi-Shinozaki, K., et al. (2009). Type 2C protein phosphatases directly regulate abscisic acid-activated protein kinases in *Arabidopsis*. *Proc. Natl. Acad. Sci. U.S.A.* 106, 17588–17593. doi: 10.1073/pnas.0907095106

Weaver, L. M., Gan, S., Quirino, B., and Amasino, R. M. (1998). A comparison of the expression patterns of several senescence-associated genes in response to stress and hormone treatmentLouis M. *Plant Mol. Biol.* 37, 455–469.

Whitelam, G. C., and Smith, H. (1991). Retention of phytochrome-mediated shade avoidance responses in phytochrome-deficient mutants of *Arabidopsis*, cucumber and tomato. *J. Plant Physiol.* 139, 119–125.

Woo, H. R., Chung, K. M., Park, J. H., Oh, S. A., Ahn, T., Hong, S. H., et al. (2001). ORE9, an F-box protein that regulates leaf senescence in *Arabidopsis*. *Plant Cell* 13, 1779–1790.

Woo, H. R., Kim, J. H., Nam, H. G., and Lim, P. O. (2004). The delayed leaf senescence mutants of *Arabidopsis*, ore1, ore3, and ore9 are tolerant to oxidative stress. *Plant Cell Physiol.* 45, 923–932.

Wu, A., Allu, A. D., Garapati, P., Siddiqui, H., Dortay, H., Zanor, M. I., et al. (2012). JUNGBRUNNEN1, a reactive oxygen species-responsive NAC transcription factor, regulates longevity in *Arabidopsis*. *Plant Cell* 24, 482–506. doi: 10.1105/tpc.111.090894

Yang, J., Worley, E., and Udvardi, M. (2014). A NAP-AAO3 regulatory module promotes chlorophyll degradation via ABA biosynthesis in *Arabidopsis* leaves. *Plant Cell* 26, 4862–4874. doi: 10.1105/tpc.114.133769

Yang, S. D., Seo, P. J., Yoon, H. K., and Park, C. M. (2011). The *Arabidopsis* NAC transcription factor VNI2 integrates abscisic acid signals into leaf senescence via the COR/RD genes. *Plant Cell* 23, 2155–2168. doi: 10.1105/tpc.111.084913

Yoshimoto, K., Jikumaru, Y., Kamiya, Y., Kusano, M., Consonni, C., Panstruga, R., et al. (2009). Autophagy negatively regulates cell death by controlling NPR1-dependent salicylic acid signaling during senescence and the innate immune response in *Arabidopsis*. *Plant Cell* 21, 2914–2927. doi: 10.1105/tpc.109.068635

Zhang, K., and Gan, S. S. (2012). An abscisic acid-AtNAP transcription Factor-SAG113 protein phosphatase 2C regulatory chain for controlling dehydration in senescing *Arabidopsis* Leaves. *Plant Physiol.* 158, 961–969. doi: 10.1104/pp.111.190876

Zhang, Y., Liu, Z., Chen, Y., He, J. X., and Bi, Y. (2015). PHYTOCHROME-INTERACTING FACTOR 5 (PIF5) positively regulates dark-induced senescence and chlorophyll degradation in *Arabidopsis*. *Plant Sci.* 237, 57–68. doi: 10.1016/j.plantsci.2015.05.010

Zhao, Y., Chan, Z., Gao, J., Xing, L., Cao, M., Yu, C., et al. (2016). ABA receptor PYL9 promotes drought resistance and leaf senescence. *Proc. Natl. Acad. Sci. U.S.A.* 113, 1949–1954. doi: 10.1073/pnas.1522840113

Zhuo, M., Sakuraba, Y., and Yanagisawa, S. (2020). A Jasmonate-activated MYC2-Dof2.1-MYC2 transcriptional loop promotes leaf senescence in *Arabidopsis*. *Plant Cell.* 32, 242–262. doi: 10.1105/tpc.19.00297

Conflict of Interest: The authors declare that the research was conducted in the absence of any commercial or financial relationships that could be construed as a potential conflict of interest.

frontiers in Plant Science

ORIGINAL RESEARCH
published: 26 May 2020
doi: 10.3389/fpls.2020.00623

PWR/HDA9/ABI4 Complex Epigenetically Regulates ABA Dependent Drought Stress Tolerance in *Arabidopsis*

*Irfan Ullah Khan[1†], Akhtar Ali[1†], Haris Ali Khan[1], Dongwon Baek[2], Junghoon Park[1], Chae Jin Lim[1], Shah Zareen[1], Masood Jan[1], Sang Yeol Lee[2], Jose M. Pardo[3], Woe Yeon Kim[2] and Dae-Jin Yun[1]**

[1] Department of Biomedical Science and Engineering, Konkuk University, Seoul, South Korea, [2] Division of Applied Life Science, Plant Molecular Biology and Biotechnology Research Center, Gyeongsang National University, Jinju, South Korea, [3] Instituto de Bioquímica Vegetal y Fotosíntesis, cicCartuja, CSIC-Universidad de Sevilla, Seville, Spain

Drought stress adversely affects plant growth and development and significantly reduces crop productivity and yields. The phytohormone abscisic acid (ABA) rapidly accumulates in response to drought stress and mediates the expression of stress-responsive genes that help the plant to survive dehydration. The protein Powerdress (PWR), which interacts with Histone Deacetylase 9 (HDA9), has been identified as a critical component regulating plant growth and development, flowering time, floral determinacy, and leaf senescence. However, the role and function of PWR and HDA9 in abiotic stress response had remained elusive. Here we report that a complex of PWR and HDA9 interacts with ABI4 and epigenetically regulates drought signaling in plants. T-DNA insertion mutants of *PWR* and *HDA9* are insensitive to ABA and hypersensitive to dehydration. Furthermore, the expression of ABA-responsive genes (*RD29A*, *RD29B*, and *COR15A*) is also downregulated in *pwr* and *hda9* mutants. Yeast two-hybrid assays showed that PWR and HDA9 interact with ABI4. Transcript levels of genes that are normally repressed by ABI4, such as *CYP707A1*, *AOX1a* and *ACS4*, are increased in *pwr*. More importantly, during dehydration stress, PWR and HDA9 regulate the acetylation status of the *CYP707A1*, which encodes a major enzyme of ABA catabolism. Taken together, our results indicate that PWR, in association with HDA9 and ABI4, regulates the chromatin modification of genes responsible for regulation of both the ABA-signaling and ABA-catabolism pathways in response to ABA and drought stress.

Keywords: *Arabidopsis thaliana*, epigenetic regulation, powerdress (PWR), HDA9, ABI4, chromatin remodeling, deacetylation, drought stress

OPEN ACCESS

Edited by:
Nam-Chon Paek, Seoul National University, South Korea

Reviewed by:
Gyeong Mee Yoon, Purdue University, United States
Moon-Soo Soh, Sejong University, South Korea

***Correspondence:**
Dae-Jin Yun
djyun@konkuk.ac.kr

† These authors have contributed equally to this work

Specialty section:
This article was submitted to Plant Abiotic Stress, a section of the journal Frontiers in Plant Science

Received: *19 December 2019*
Accepted: *22 April 2020*
Published: *26 May 2020*

Citation:
Khan IU, Ali A, Khan HA, Baek D, Park J, Lim CJ, Zareen S, Jan M, Lee SY, Pardo JM, Kim WY and Yun D-J (2020) PWR/HDA9/ABI4 Complex Epigenetically Regulates ABA Dependent Drought Stress Tolerance in Arabidopsis. Front. Plant Sci. 11:623. doi: 10.3389/fpls.2020.00623

INTRODUCTION

During their life cycles, plants are continuously exposed to environmental challenges including light, heat, cold, flooding, high salinity, and drought stress. Among them, drought stress results in considerable damage to plant growth, and more than 40% of crop production is lost to drought (Guy et al., 1985; May et al., 1998; Hasegawa et al., 2000). Upon exposure to drought stress, plants initiate the expression of resistance genes and subsequent activation of signaling pathways.

Plants have developed complex molecular and signaling mechanisms to adapt to water deficit condition. They respond to drought stress either through osmotic adjustment and regulation of ion homeostasis or by controlling the damage repair system and the detoxification and removal of reactive oxygen species (ROS) (Shinozaki and Yamaguchi-Shinozaki, 2000; Zhu, 2002). The phytohormone abscisic acid (ABA) plays a crucial role in plant physiological processes, regulating many aspects of plant growth and development including seed dormancy, seed maturation, and seedling growth. ABA is also required for drought stress tolerance, which regulates stomatal movement during drought stress and helps plants tolerate extreme water-deficient conditions (Finkelstein and Lynch, 2000; Lopez-Molina et al., 2001). However, the molecular and biochemical mechanism of these signaling pathways are not yet fully understood.

The mechanisms of chromatin modification and the constitution of chromatin complexes regulating gene expression are highly conserved in plants, mammals and yeast (Henderson and Jacobsen, 2007). Chromatin structure and its modification form the basic mechanism of genetic and epigenetic regulation of stress-related gene expression (Horn and Peterson, 2002). Histone acetylation is one of the most important features of chromatin remodeling, which removes positive charges by adding an acetyl group to the lysine residues of histone proteins, thereby reducing the histone–DNA affinity and resulting in chromatin decondensation and active transcription (Bannister and Kouzarides, 2011). Histone acetylation levels are dynamically regulated through the combined actions of histone acetyltransferases (HATs) and histone deacetylases (HDACs). HDACs are enzymes conserved in the eukaryotes that function in biological processes including transcription, genome stability, development and in biotic and abiotic stress responses (Haberland et al., 2009; Seto and Yoshida, 2014; Bosch-Presegué and Vaquero, 2015).

Human NCOR1 is a homolog of the *Arabidopsis* protein powerdress (PWR), which is involved in the floral determinacy network (Yumul et al., 2013). The gene encoding PWR was named *Powerdress* because of the appearance of the single mutant, which has bulged carpel tips reminiscent of excessively padded suit or dress shoulders. PWR has two conserved SWI3/DAD2/N-CoR/TFIII-B (SANT) domains that together function as a histone-interaction module that couples histone tail binding to enzyme catalysis for the remodeling of nucleosomes. PWR interacts with REDUCED Potassium Dependency Protein 3 (RPD3), a class-1-type Histone Deacetylase 9 (HDA9) and mediates Histone 3 (H3) deacetylation. The complex of PWR–HDA9 also regulates flowering time in *Arabidopsis* by repressing *Agamous-Like 19* (*AGL19*) transcription (Kim et al., 2016).

HDA9 requires PWR for its nuclear transport and binding to the promoter region of key negative regulator genes involved in leaf senescence (Yumul et al., 2013; Chen et al., 2016). HDA9 interacts with PWR and WRKY53 to regulate leaf aging, and *hda9* and *pwr* loss-of-function mutants exhibit late senescence phenotype (Chen et al., 2016). Furthermore, ABA promotes leaf senescence and loss of function of its receptors PYL8 and PYL9, resulting in delayed leaf senescence (Zhao et al., 2015). To date, approximately 18 *Arabidopsis* histone deacetylases (HDACs) have been identified. These are divided into three main types. Twelve belong to the reduced Potassium Dependency Protein 3/HDA1 Histone Deacetylase 1 (RPD3) superfamily and are named as HDAs; two are in the histone deacetylase 2 (HD2) family and are named HDTs; and two belong to the silent information regulator protein 2 (SIR2) family and are named SRTs (Pandey et al., 2002; Hollender and Liu, 2008). RPD3-type class 1 HDA6 and HDA19 are involved in the regulation of seed germination, ABA response, salt stress and other abiotic stresses. Unlike *hda6* and *hda19* mutants, mutants of *HDA9* (*hda9-1* and *hda9-2*) are insensitive to ABA and to salt stress during seed germination and root growth (van Zanten et al., 2014; Kang et al., 2015).

Plant endogenous ABA concentration is determined by the rate of ABA metabolism (i.e., biosynthesis, and catabolism). The molecular mechanisms of ABA signaling, biosynthesis, and catabolism have been characterized using genetic and biochemical approaches (Nambara, 2005). *Arabidopsis* contains several *NCED* family genes, including *AtNCED3*, which plays the central role in ABA biosynthesis in response to drought stress (Iuchi et al., 2001). The transcript level of *AtNCED3* rapidly increases in response to drought stress, while a *nced3* mutant carrying a T-DNA insertion is defective in accumulation of endogenous ABA under drought stress and impaired in drought stress tolerance. For ABA catabolism, at least two crucial pathways have been characterized: the oxidative pathway and the sugar-conjugation pathway (Nambara, 2005). The oxidative pathway is stimulated by *CYP707A*-induced hydroxylation of ABA C-80 to phaseic acid (Kushiro et al., 2004; Saito et al., 2004). The four *Arabidopsis CYP707A*-family genes encoding ABA 8′-hydroxylases are induced by exogenous ABA, as well as by dehydration and other abiotic stresses (Kushiro et al., 2004; Saito et al., 2004). By contrast, *CYP707A2* transcripts predominantly accumulate in dry seeds, and the gene is immediately upregulated after seed imbibition. The *cyp707a2* mutant maintains a high level of ABA and exhibits enhanced seed dormancy as compared to the wild type (WT) (Kushiro et al., 2004). These reports indicate that *CYP707A2* is a component in ABA catabolism during seed germination and regulation of seed dormancy. However, the physiological role of other *CYP707A* genes remained unclear.

The interaction and binding of ABA with PYL/PYR1/RCAR receptors results in the deactivation of protein phosphatase type-2C (PP2C) proteins (*ABI1*, *ABI2*, *HAB1* and *HAB2*), thereby releasing SNF1-related protein kinase (SnRK2) kinases. The ABA-mediated disassociation of PP2C from SnRK2s leads to autophosphorylation and subsequently to transphosphorylation, activation of the downstream targets (such as ABI3, ABI4, and ABI5) and ultimately regulation of downstream signaling pathways (Fujii et al., 2009; Umezawa et al., 2009; Antoni et al., 2012). ABI4 is an important transcription factor that was initially identified as a member of the AP2/ERF family and that binds to ABA-responsive *cis*-regulatory elements (CREs), ABRE and regulates the expression of genes in response to abiotic stresses (Mizoi et al., 2012). ABI4 is also a versatile activator and a repressor of several genes. Beside inducing the expression of genes involved in seed dormancy, ABA signaling, salt stress and floral transition (Söderman et al., 2000; Nakabayashi et al., 2005; Koussevitzky et al., 2007; Bossi et al., 2009; Giraud et al., 2009; Reeves et al., 2011; Shu et al., 2018), ABI4 also represses the expression of genes involved in ABA

catabolism (*CYP707A* genes), ethylene biosynthesis (*ACS* genes) and retrograde signaling (*AOX1a*), genes encoding *Arabidopsis* response regulators (*ARRs*) (Huang et al., 2017), as well as genes involved in fatty acid biosynthesis, photosynthesis, pigment and wax metabolic processes (Shu et al., 2013; Dong et al., 2016), by directly binding to their promoters.

PWR also interacts with HOS15 (HIGH EXPRESSION OF OSMOTICALLY RESPONSIVE GENES 15), a homolog of human transducin-β-like protein 1 (TBL1). HOS15 contains a LisH and a WD40-repeat domain and is involved in histone modification and deacetylation during abiotic stresses. Furthermore, HOS15 also interacts with HISTONE DEACETYLASE 9 (HDA9), as determined by affinity purification of HOS15-interacting proteins (Park et al., 2018). Loss-of-function *hos15-2* mutant plants are hypersensitive to ABA during germination and extremely tolerant to drought stress, indicating the importance of HOS15 as a negative regulator (Ali et al., 2019). On the other hand, the function of PWR in abiotic stresses is largely unknown.

Here we report that T-DNA insertion mutants of PWR (*pwr-2* and *pwr-3*) are ABA insensitive and display drought-sensitive phenotypes. Using yeast two-hybrid screening, we observed that both PWR and HDA9 interact with ABI4 along with ABI3. The expression of ABA-responsive genes is downregulated in *pwr* and *hda9* mutants. Transcript levels of genes that are normally repressed by ABI4, such as *CYP707A* genes, *AOX1a* and *ACS4*, are upregulated in the *pwr* and *hda9* mutants. Moreover, in response to drought stress, PWR and HDA9 regulate acetylation at the promoter of *CYP707A1*, which encodes the major enzyme of ABA catabolism. Taking these results together, we conclude that PWR in association with HDA9 and ABI4 regulates the chromatin modification of genes responsible for ABA catabolism in response to drought stress.

MATERIALS AND METHODS

Plant Materials and Growth Conditions

Plants from the *Arabidopsis thaliana* ecotype Columbia-0 (Col-0) background were used in this study. Seeds of the WT and mutants were surface sterilized in a solution containing 3% sodium hypochlorite solution (Yakuri Pure Chemicals, Kyoto, Japan) for 5 min and then rinsed five times with sterilized water. After stratification for 3 day at 4°C in the dark, the plants were grown on half-strength Murashige and Skoog (1/2 MS) medium or soil at 23°C under a 16-h light/8-h dark condition. The T-DNA insertion mutant *pwr-2* (SALK_0718811C) seeds were obtained from ABRC stock center and previously described by Yumul et al. (2013) and the mutant *pwr-3* (SALK_006823), was also obtained from ABRC stock center. The T-DNA insertions in these plants were confirmed by genotyping PCR. The *hda9-1* (Gk_305G03) and *hda9-2* (SALK_007123) mutants were obtained from NASC[1] and ABRC[2], respectively (Alonso et al., 2003; Rosso et al., 2003; Kang et al., 2015). The *pwr-2/hda9-1* double-mutant plants were created by crossing.

RNA Extraction and Quantitative PCR Analysis

Total RNAs (2 μg) from plants (harvested at the time points described in the text for each experiment) were extracted with the RNeasy Plant Mini Kit (Qiagen, Hilden, Germany), treated with DNase I (Sigma, St. Louis, MO, United States) and used to synthesize first-strand cDNA using the Thermoscript^{TM} RT-PCR System (Invitrogen, Carlsbad, CA, United States). Quantitative RT-PCR (qRT-PCR) was performed using SYBR Green PCR Master Mix kit (Bio-Rad SYBR Green Supermix, Hercules, CA, United States) according to the manufacturer's instructions with the CFX96 or CFX384 Realtime PCR detection system (Bio-Rad, CA, United States). The relative expression levels were calculated using the comparative cycle threshold ($2^{-\Delta\Delta CT}$) method. The sequences of the primers used in qRT-PCR are listed in **Supplementary Table S1**.

Physiological and Phenotype Assay

For ABA germination assays, seeds were grown on 1/2 MS medium containing 1.5% sucrose and different concentrations of ABA (Sigma, St. Louis, MO, United States). Successful germination in the presence of ABA was determined by germination rate and the presence of green cotyledons at the indicated concentrations. For drought test, 3-week-old plants were subjected to drought stress by withholding water for 14 day while control plants were watered as before. The drought-stressed plants were then re-watered, and their recovery was monitored. Three experimental repeats were carried out, each involving at least 36 plants from each category.

Plasmid Constructions

The full-length *PWR*, *HDA9* and *ABI4* coding sequences were amplified with the primers listed in **Supplementary Table S1** to generate the entry vector [*PWR*, *HDA9*, *ABI4* with or without stop codons in the *pDONRTM/Zeo* vector (Invitrogen, Carlsbad, CA, United States)]. *pDONRTM/Zeo-HDA9* and *pDONRTM/Zeo-ABI4* were fused into the *pGWB14* destination vectors by *in vitro* recombination using Gateway BP and LR reaction kits (Invitrogen, Carlsbad, CA, United States) to generate *HDA9-3xHA*. *ABI4* was cloned into the *pK7WGF* destination vector to construct *GFP-ABI4*. The specific primer sequences are provided in **Supplementary Table S1**.

Yeast Two-Hybrid Assay

For yeast two-hybrid experiments, *pDONRTM/Zeo-PWR* and *pDONRTM/Zeo*-HDA9 were fused into the yeast two-hybrid destination vector *pDEST22* (harboring the activation domain) and *pDONRTM/Zeo*-ABI4 was fused into the destination vector *pDEST32* (harboring the DNA binding domain) to generate the construct vectors *pDEST22-PWR*, *pDEST22-HDA9, and pDEST32*-ABI4, respectively. These plasmids were transformed into the *Saccharomyces cerevisiae* strain PJ-694-A. Individual colonies of transformants were streaked on agar plates containing

[1]http://www.arabidopsis.info

[2]http://www.arabidopsis.org

synthetic complete (SC) medium lacking tryptophan and leucine, and then grown for 48 h. The interaction of PWR, HDA9, and ABI4 was tested on plates containing medium without histidine and further tested in growth medium containing 3-amino-1,2,4-triazole (3-AT). Empty vector was used as a negative control, while the combination of *pDEST22-SOS2* and *pDEST32-SOS3* was used as positive control.

Nuclear-Cytoplasmic Fractionation Assay

Nuclear proteins were extracted from 2-week-old seedlings treated with dehydration stress for indicated time point by CELLYTPN1 CelLytic PN Isolation/Extraction Kit (Sigma-Aldrich), crude preparation. Anti-H3 (Abcam) and anti-AcH3 (Millipore) antibodies and antigen proteins were visualized by chemiluminescence using ECL detecting reagent (Bio-Rad).

Co-Immunoprecipitation Assay

For co-immunoprecipitation assays, *35S:ABI4-GFP* and *35S:HDA9-HA* expression cassettes were co-infiltrated into leaves of *N. benthamiana*, and after 3 day of incubation, total protein was extracted from the leaves, pulled down with α-GFP, and immunoblotted with α-HA. Each immunoblot was incubated with the appropriate primary antibody (α-HA antibody, 1:2000; α-GFP antibody) for 2 h at room temperature or overnight at 4°C. The membranes were developed using peroxidase-conjugated secondary antibody: 1:2000 for α-rabbit antibody (GE, Little Chalfont, Buckinghamshire, United Kingdom) and 1:1000 for α-rat IgG (Sigma, St. Louis, MO, United States).

Chromatin Immunoprecipitation (ChIP) Assay

ChIP assays were carried out following an established method as previously described (Saleh et al., 2008). Two-week-old control and dehydration-treated *Arabidopsis* plants were treated with 1% formaldehyde for 15 min to fix the chromatin structure and this cross-linking reaction was subsequently stopped by treatment with 0.1 M glycine for 5 min. The DNA-fixed plant tissues were ground with liquid nitrogen and washed with water and then the nuclei were isolated. Nuclear proteins were extracted and sonicated with a Bioruptor (BMS) to fragment the chromosomal DNA. Immunoprecipitation was performed using an antibody to total anti-acetylated H3 (Millipore), with salmon sperm DNA and protein A agarose (upstate Biotechnology).

Measurement of Stomatal Aperture

Leaves of 12-day-old seedlings were floated on stomatal opening buffer (5 mM 2-(N-morpholino) ethanesulfonic acid [MES], 5 mM KCl, 50 mM $CaCl^2$ [pH 5.6]) under light for 3 h. After 5 μM ABA treatment for 2 h, leaves were fragmented in a warning blender. Samples were rinsed with pure water three times for 10 min each. Washed samples were incubated over–night in the secondary fixative solution, 2% OsO^4, in the dark at 4C. After fixation, OsO^4 was removed by washing the samples three times for 10 min each. The samples were then dehydrated chemically for embedding in a series of EtOH solutions: 20, 50, 70, 90%, and finally 100% EtOH sequentially for 40 min each. Epidermal fragments were quickly mounted for scanning electron microscopy (SEM) (JSM-6380LV; JEOL, Eching, Munchen, Germany) assay. At least 10 stomata from three different plants of each genotype were used to measure the stomatal aperture with three biological repeats. Each experiment was replicated three times.

RESULTS

Mutations in PWR Reduces ABA Responsiveness in *Arabidopsis*

Powerdress regulates plant growth and developmental processes (Yumul et al., 2013; Chen et al., 2016; Kim et al., 2016); however, we were interested in assessing its involvement in abiotic stresses. Therefore, to investigate PWR possible involvement in ABA signaling, we tested the physiological response of *pwr-2* and *pwr-3* to exogenously applied ABA. We germinated seeds of WT (Col-0), *pwr-2* and *pwr-3* lines, as well as the loss-of-function *abi2-2* mutant (which is hypersensitive to ABA) as an experimental control, on Murashige and Skoog (MS) medium containing ABA. In the presence of ABA, *pwr-2* and *pwr-3* seedlings exhibited greater germination than WT seedlings, and *abi2-2* seedlings showed even poorer germination and cotyledon greening (**Figures 1A–C**). After exposure to 0.5 μM ABA for 7 days, the percentages of green cotyledons for *pwr-2* and *pwr-3* were 62 and 52–55% respectively, compared with 27–30% for WT and 10–15% for *abi2-2* while, percentages of green cotyledons for *pwr-2* and *pwr-3* were 53 and 49% respectively as compared to 25% of WT on 0.8 μM ABA (**Figure 1B**). Since PWR loss-of-function mutants displayed ABA-insensitive phenotypes, it seemed likely that PWR might play a role in regulating plant response to drought. To test this hypothesis, we exposed 3-week-old WT, *abi2-2*, *pwr-2*, and *pwr-3* plants to 14 days of drought stress. Plants were re-watered after the drought period and their survival rates recorded 2 days after re-watering. The WT and *abi2-2* plants survived the dehydration stress at rates of 80% and 100%, respectively (**Supplementary Figure S1A**). By contrast, *pwr-2* and *pwr-3* mutants were unable to tolerate water-deficient condition and survived at rates of only 10 and 15%, respectively (**Supplementary Figure S1B**). Furthermore, *pwr* mutants showed impaired stomatal closure in leaf epidermal fragments after treatment with exogenous ABA (**Figures 1D,E**), indicating that the drought sensitivity of *pwr* mutants is correlated with reduced stomatal closure. Taken together these results indicating that PWR plays a central role in plant sensitivity to ABA in seed germination and confers tolerance of drought.

PWR and HDA9 Work Together in the Same Pathway

As previously described, HDA9 represses the seedling trait and negatively regulates salt and drought stress tolerance; in addition, HDA9 requires PWR for its nuclear transport and promoter association. Furthermore, PWR and HDA9 also

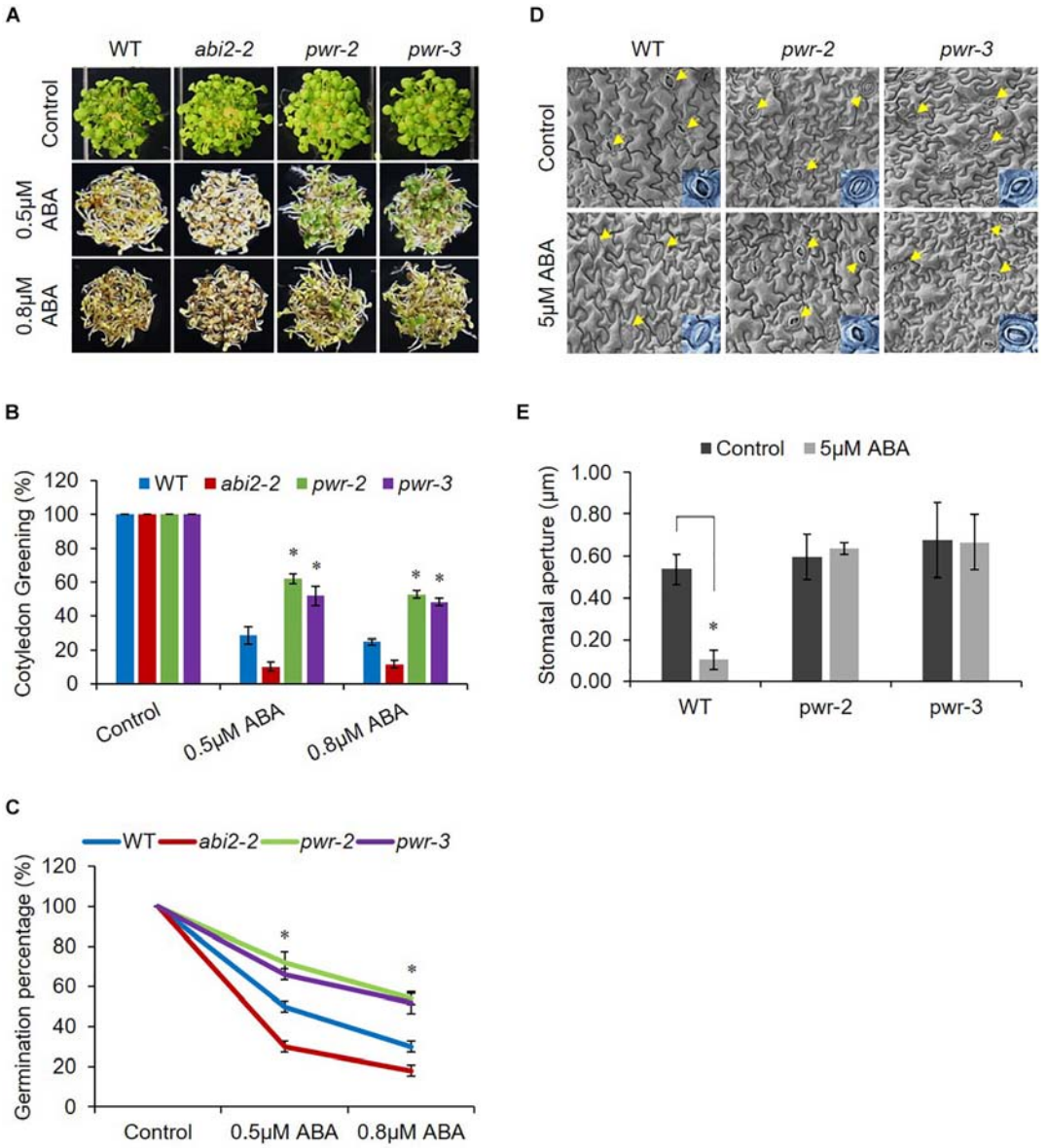

FIGURE 1 | *pwr* mutants are insensitive to ABA. **(A)** WT, *abi2-2*, *pwr-2*, and *pwr-3 Arabidopsis* seeds were germinated on 1/2 MS medium supplemented with 0.5 μM and 0.8 μM ABA (or without ABA for controls). Photographs were taken 7 day after germination. **(B)** The numbers of green cotyledons from each line were counted after 7 day. Mean ±SD values were determined from three replicates (n = 144). Significant difference was determined by Student t-test (*$p < 0.01$). **(C)** Germination rates of indicated genotypes from **(A)**. Mean ±SD values were determined from three replicates (n = 144). Significant difference was determined by Student t-test (*$p < 0.01$). **(D)** *pwr* mutation impairs ABA-induced stomatal closure. Seedlings of WT (Col-0) and *pwr* mutants were exposed to 2-h ABA (5 μM) treatment. Epidermal peels from WT, *pwr-2*, and *pwr-3* were measured for stomatal aperture in control condition and in response to ABA (arrows indicate stomata). **(E)** Quantitative analysis of **(D)** using Image J 1.47V software. At least 10 stomata from three different plants of each genotype were used to measure stomatal aperture. Error bars represent SE. Significant difference was determined by a Student's t-test (*$p < 0.01$).

regulate flowering through repression of *AGL19* (van Zanten et al., 2014; Kang et al., 2015; Kim et al., 2016; Zheng et al., 2016). In this context, we were interested in investigating whether PWR and HDA9 also work together in response to the phytohormone ABA. We therefore tested the physiological response of PWR and HDA9 mutants to exogenous ABA. Compared to WT, *pwr*, *hda9*, and *pwr/hda9* double-mutant seedlings were relatively insensitive to exogenous ABA (**Figure 2A**). In the presence of 0.8 and 0.5 μM ABA (in **Supplementary Figure S2**), the percentages of green cotyledons for *pwr-2*, *pwr-3*, *hda9-1*, *hda9-2*, and *pwr-2/hda9-1* were approximately 83, 85, 82, 84, and 85%, respectively, compared with 55% for WT, 35% for *abi2-2* and 98% for *abi4-1* (**Figure 2B** and **Supplementary Figure S2**). To test root growth phenotypes in the presence of ABA, we transferred 4-days-old seedlings of WT (Col-0), *abi2-2*, *pwr2*, *pwr-3*, *hda9-1*, *hda9-2*, and *pwr-2/hda9-1 Arabidopsis* to MS medium containing 30 μM ABA

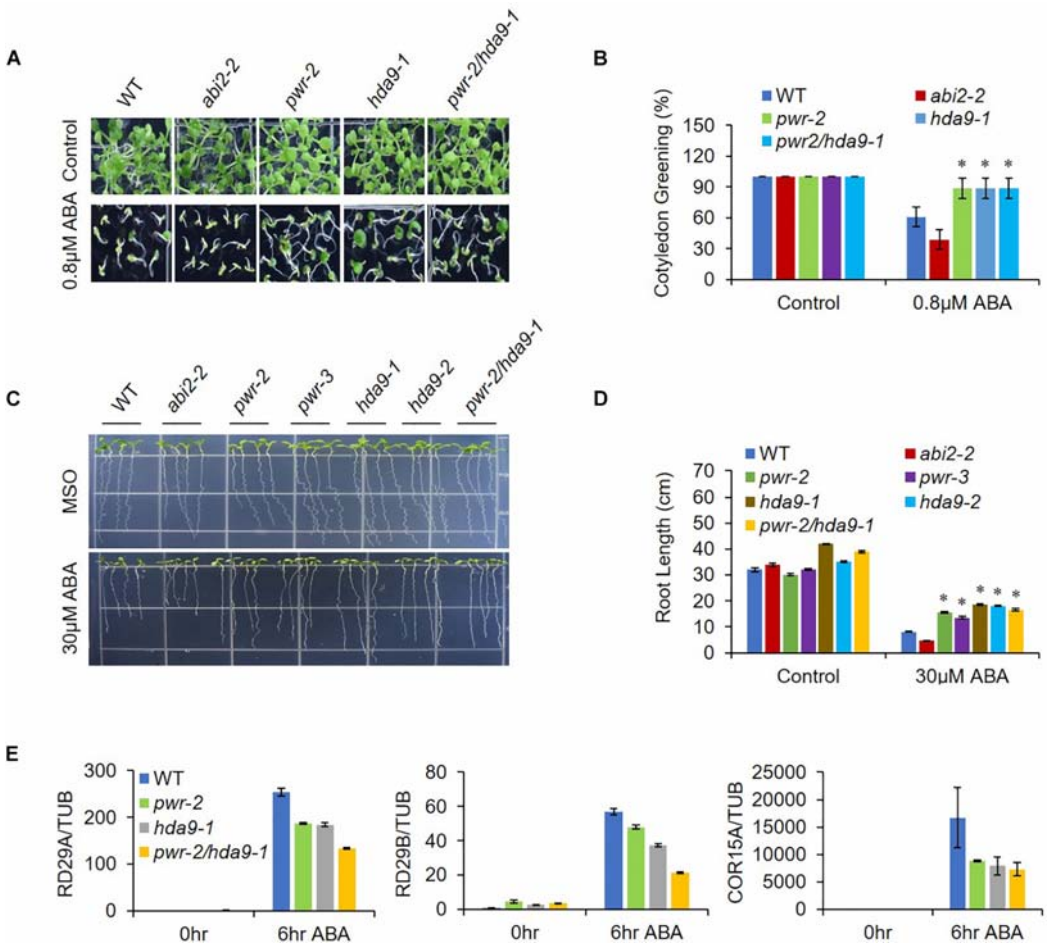

FIGURE 2 | *pwr* and *hda9* mutants are insensitive to ABA. **(A)** Seeds WT, *abi2-2*, *pwr, hda9*, and *pwr/hda9* double mutant were germinated on 1/2 MS medium with 0.8 μM ABA. Photographs were taken 7 day after germination. **(B)** Numbers of green cotyledons were counted after 7 day. Mean ±SD values were determined from three replicates ($n = 45$). Significant difference was determined by Student *t*-test (*$p < 0.01$). **(C)** Root growth phenotypes of WT, *abi2-2*, *pwr-2*, *pwr-3*, *had9-1*, *hda9-2*, and *pwr-2/hda9-1*. Photographs were taken 10 day after transfer of 4-day-old seedlings to MS medium with or without 30 μM ABA. **(D)** Quantification of primary root lengths of the seedling depicted in C. Error bars represent means ± SE of three replicates ($n = 20$ seedlings per replicate). Significant difference was determined by Student *t*-test (*$p < 0.01$). **(E)** Expression of three ABA-responsive stress-related genes (*RD29A*, *RD29B*, and *COR15A*) in WT, *pwr-2*, *hda9-1*, and *pwr-2/hda9-1 Arabidopsis* during ABA stress was analyzed by qRT-PCR. The imbibed seeds were germinated and grown on MS medium for 10 days, and then the seedlings were harvested and treated with 50 μM ABA to obtain cDNA for qRT-PCR. Samples were collected at the indicated time points: 0 h (no treatment) and 6 h. Total RNAs were extracted from those seedlings, and RT-qPCR analysis was performed. *TUB4* was used as internal control. Error bars show SD.

and allowed them to grow for a further 10 days. Compared to that of the WT, the root growth of single and double mutants of PWR and HDA9 was insensitive to ABA (**Figure 2C**). The relative reductions in root length were 37.5–43.3% for *pwr*, 42.8–45.7% for *hda9* and 39.4% for the *pwr-2/hda9-1* double mutant, as compared to 70 and 85%, respectively, for WT and *abi2-2* (**Figure 2D**). Consistent with phenotypes, the induction of ABA-responsive genes, including *RD29A*, *RD29B*, and *COR15A*, upon ABA was lower in *pwr-2*, *hda9-1* and *pwr-2/hda9-1* than in WT plants (**Figure 2E**). Moreover, we also tested the dehydration responses of PWR and HDA9 mutants by exposing 3-week-old plants to 14-days drought stress, re-watering them and then recording the survival rate 2 days later. As expected, like the *pwr-2* and *pwr-3* mutants, *hda9* mutants were extremely sensitive to drought stress (**Figure 3**). Taken together, these results suggested that PWR and HDA9 work together and play a critical role in plant ABA response and drought tolerance.

PWR and HDA9 Physically Interact With ABI4

Arabidopsis HDA9 regulates several aspects of biological processes such as seed dormancy and maturation, flowering time, and stress responses. Moreover, previous reports have shown that developmental and stress-related genes are hyperacetylated and upregulated in *hda9* mutant. The direct interaction between PWR and HDA9 and the similar type of molecular and morphological defects in *pwr* and *hda9* mutants strongly suggest that PWR and HDA9 are working together in same complex (Kim et al., 2013; van Zanten et al., 2014; Kang et al.,

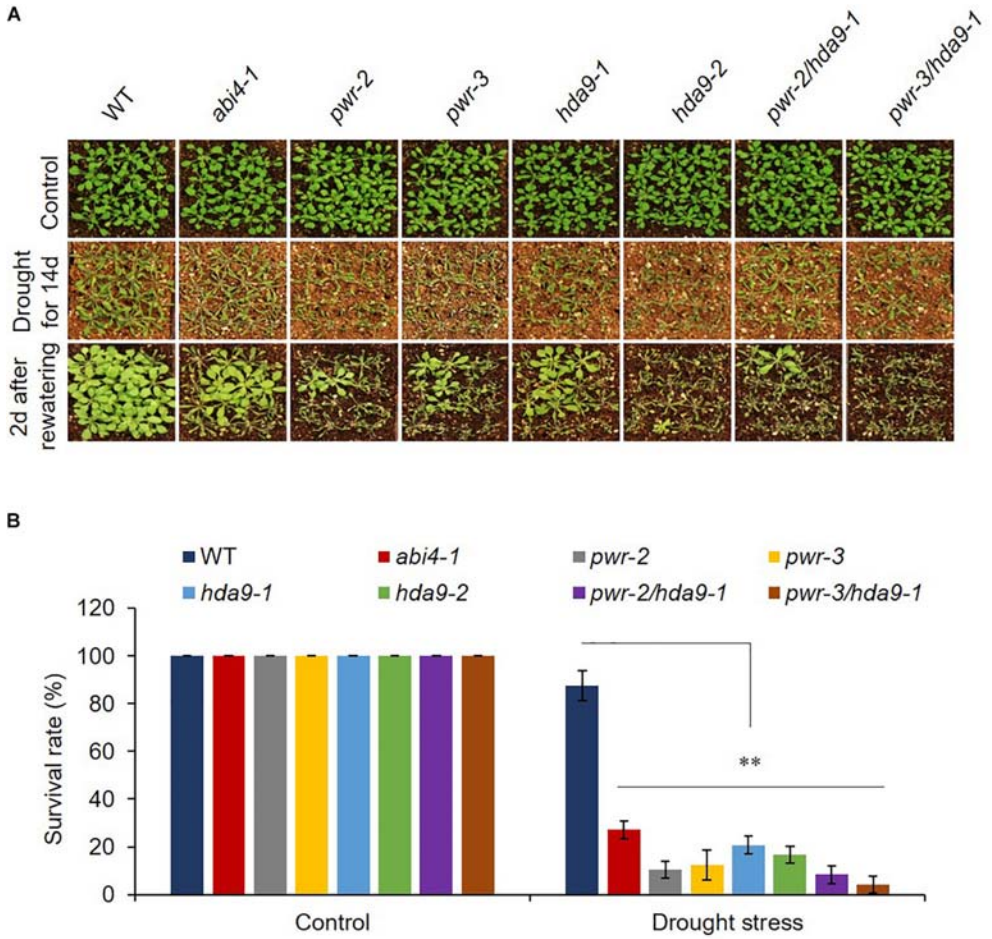

FIGURE 3 | *pwr* and *hda9* mutant plants are drought sensitive. **(A)** 3-week-old plants of genotypes WT, *abi4-1*, *pwr, hda9* single, and *pwr/hda9* double mutants exposed to drought assay by withholding water for 14 days and subsequently rewatered the plants after drought period. Photographs were taken 2 days after rewatering. **(B)** Survival rate (percentage) of genotypes shown in **(A)**. Results are means of three independent biological repeats. Significant difference was determined by Student *t*-test (**$p < 0.001$).

2015; Lee et al., 2016; Zheng et al., 2016). To investigate the interaction of proteins with PWR and HDA9 that are involve in seed germination and response to drought stress, we carried out yeast two-hybrid screening of ABA- and drought-stress-responsive transcription factors, and we observed that PWR and HDA9 specifically interact with ABI3 and ABI4 (**Figure 4A** and **Supplementary Figure S3**). To validate the interaction between ABI4 and the HDA9-PWR complex, we performed a co-immunoprecipitation assay using *Nicotiana benthamiana* leaves transiently expressing 35S:HDA9-HA and 35S:ABI4-GFP. ABI4-GFP successfully pulled down HDA9-HA, indicating that ABI4 forms a complex with HDA9 and PWR (**Figure 4B**).

Genes Repressed by ABI4 Are Upregulated in *pwr* Mutants During Dehydration

ABI4 is identified as a member of the AP2/ERF superfamily that binds specifically to ABRE elements and regulates abiotic-stress-related gene expression (Mizoi et al., 2012). ABI4 plays dual function in regulating gene expression, serving both as an activator and as a repressor (Söderman et al., 2000; Nakabayashi et al., 2005; Koussevitzky et al., 2007; Bossi et al., 2009; Giraud et al., 2009; Reeves et al., 2011; Shu et al., 2018). To identify the transcriptional regulatory function of PWR in drought stress response, we monitored the expression of genes repressed by ABI4 in *pwr* mutants treated with different time point of dehydration stress. Surprisingly, the expression of ABA hydroxylase gene *CYCP707A1* was upregulated in *pwr-2* and *pwr-3* mutants as compared with WT (**Figure 5**), although the expression of other *CYCP707A* genes were unchanged. Similarly, the expression of other ABI4 target genes such *AOX1a* (a retrograde signaling gene) and *ACS4* (an ethylene biosynthesis genes) in *pwr-2* and *pwr-3* in response to dehydration stress was also high (**Figure 5**). These results indicated that ABI4 alone is not enough to suppress these genes and that ABI4 requires the PWR and HDA9 repressor complex to target different genes in regulating plant stress tolerance.

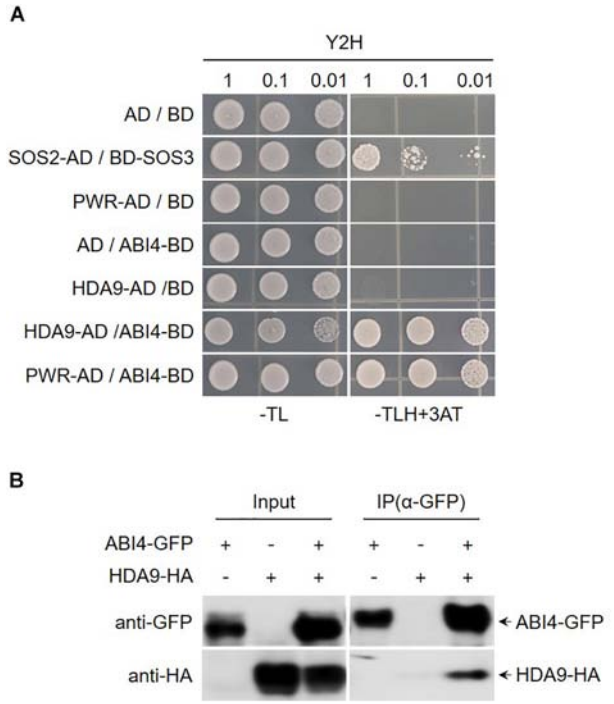

FIGURE 4 | PWR and HDA9 physically interact with ABI4. **(A)** Screening of PWR and HDA9 with ABA transcription factors using yeast two-hybrid assay. BD, *pDEST32* (bait plasmid); AD, *pDEST22* (prey plasmid). The co-transformed yeast strains were plated on the control −TL medium and selective −TLH + 3-AT medium. The combinations with empty plasmid were used as negative controls and SOS2-AD/SOS3-BD was used as positive control. **(B)** Co-immunoprecipitation assay between HDA9 and ABI4. Protein extracts obtained from *N. benthamiana* leaves infiltrated with *Agrobacterium tumefaciens* harboring *35S:HDA9-HA* and *35S:ABI4-GFP* were analyzed using anti-GFP and anti-HA antibodies. Protein extracts (input) were immunoprecipitated (IP) with anti-GFP. Immunoblots were analyzed with anti-GFP and anti-HA to detect interaction between HDA9 and ABI4.

PWR and HDA9 Regulate Acetylation Level at *CYP707A1* Promoter Under Drought Stress

PWR and HDA9 together regulate the acetylation status of numerous genes, specifically at H3K9, H3K14, and H3K27. SANTb-domain proteins such as PWR preferentially bind to acetylated histone H3 but not H4. Moreover, it has been proposed that the SANTb domain of PWR defines the protein's substrate specificity for binding to HDA9 (Kim et al., 2016). Therefore, we were interested to test the acetylation status of histone H3 in response to dehydration stress in *pwr* and *hda9* mutants. Compare to that in WT, the total AcH3 levels in the *pwr* and *hda9* single mutants as well as the *pwr/hda9* double mutant were increased by drought stress (**Figure 6A**). Since the total acetylation level of AcH3 was increased in *pwr* and *hda9* mutant, we assumed that the hyper-induction of *CYP707A1* gene expression in the *pwr* mutant (**Figure 5**) was largely due to hyperacetylation of the CYP707A1 promoter. The transcript levels of all four *CYP707A* genes increase in response to ABA and to abiotic stresses, including dehydration (Kushiro et al., 2004; Saito et al., 2004). To determine whether the increase in *CYP707A1* gene expression in *pwr* and *hda9* upon dehydration is due to chromatin remodeling, we carried out chromatin immunoprecipitation (ChIP) assays to assess the AcH3 level of *CYP707A1*. The level of AcH3 at one region of the *CYP707A1* promoter, P1 (**Figure 6B**), was higher in *pwr* mutant plants than in WT after 90-min dehydration stress, whereas we saw no differences at the P2 and P3 promoter regions (**Supplementary Figures S4A,B**). Interestingly, the level of AcH3 at the P1 region was also high in the *hda9* mutant after dehydration (**Figure 6B**). However, we detected no difference in AcH3 levels in the *CYP707A2* promoter during dehydration stress in the *pwr* mutant compared with the WT (**Supplementary Figure S4C**). Taken together, these results indicated that during drought stress, PWR and HDA9 repress the expression of *CYP707A1* through histone deacetylation to allow ABA accumulation, and that the P1 region is important for the activation or repression of *CYP707A1* during drought stress.

DISCUSSION

Posttranslational protein/histone modifications such as acetylation, methylation, phosphorylation, and ubiquitination play pivotal roles in plant growth and development, genome integrity, and stress responses. Histone acetylation and deacetylation, mediated by histone acetyltransferases (HATs) or histone deacetylases (HDACs), are reversible processes that promote or repress gene expression (Struhl, 1998). The RPD3/HDA1-type class 1 HISTONE DEACETYLASE 9 (HDA9), among the 18 histone deacetylases (HDACs) identified in *Arabidopsis*, interacts directly with PWR, a homolog of the human protein NCOR1 (Pandey et al., 2002; Kim et al., 2016). PWR, which was initially identified as being involved in regulating floral determinacy network, contains two important SANT domains known as SANTa and SANTb, which are required for its interaction with HDA9 and mediation of HISTONE (H3) deacetylation. PWR and HDA9 regulate several processes in *Arabidopsis*, including regulating flowering time by repressing *AGAMOUS-LIKE 19* (*AGL19*). PWR is known for its role in chromatin modification and regulation of developmental processes. Here, we have identified a previously unknown function of PWR regulating abiotic stresses.

Physiological Effect of PWR on ABA and Drought Stress Signaling

PWR regulates plant growth and development, flowering time and the floral determinacy network. Moreover, PWR interacts with HDA9 and regulates flowering time in *Arabidopsis* by repressing *Agamous-Like 19* (*AGL19*) (Yumul et al., 2013; Kim et al., 2016). While HDA9 requires PWR for its nuclear transport and promoter association, and the HDA9-PWR-WRKY53 complex integrates and regulates multiple signaling pathways to mediate global gene expression responsible for leaf senescence (Chen et al., 2016). To explore the relationship between PWR and HDA9 during abiotic stress, we investigated

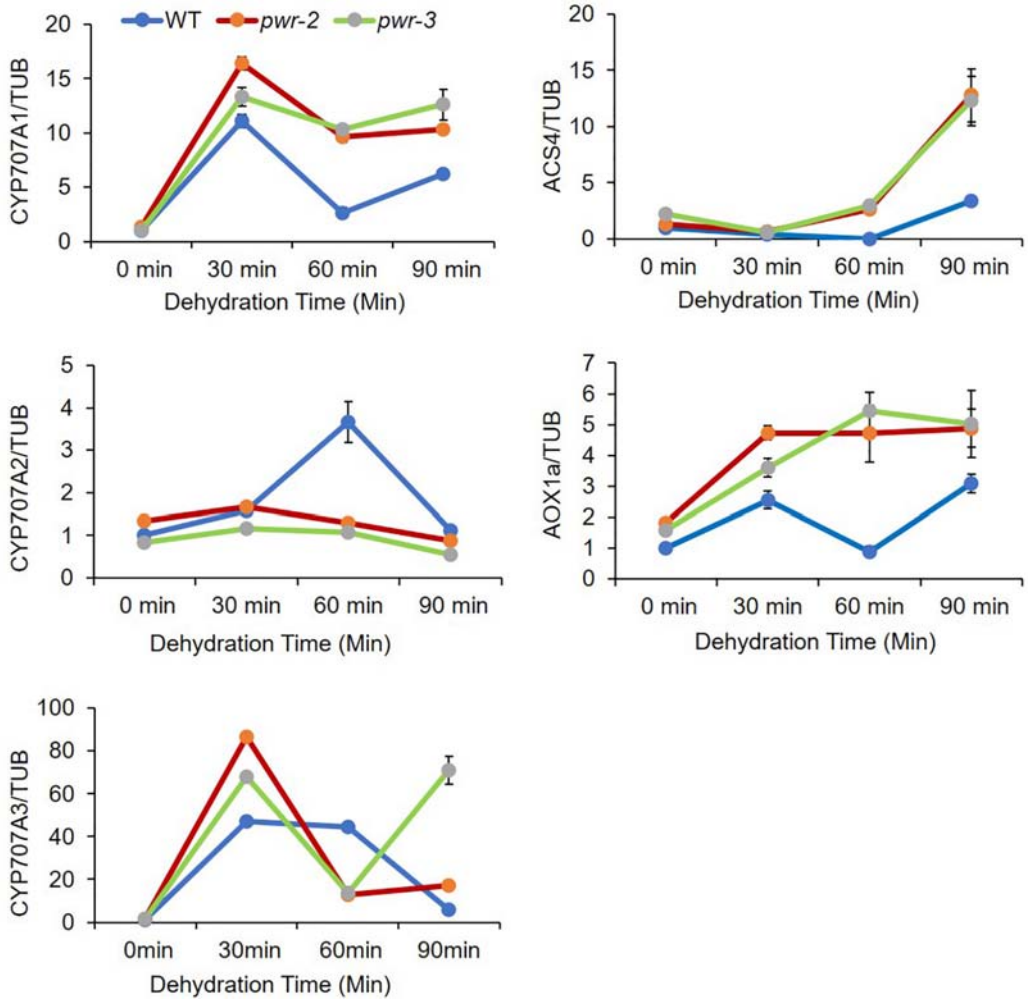

FIGURE 5 | PWR negatively regulates ABI4-responsible genes. The relative expression of ABA hydroxylase genes analyzed by qRT-PCR. 10-day-old seedlings of WT, *pwr-2*, and *pwr-3* were dehydrated at room temperature for indicated time point. Total RNAs were extracted from those seedlings, and RT-qPCR was performed to analyze the abundance of *CYP707A1*, *CYP707A2*, *CYP707A3, ACS4*, and *AOX1a* expression. Expression levels were normalized to that of *TUB4*. Normalized expression is shown as mean ± standard deviation (SD). The experiment was repeated three times.

the phenotypes of loss-of-function mutants of PWR (*pwr-2* and *pwr-3*) in the presence of ABA. Since HDA9 positively regulates plant response to ABA and dehydration (van Zanten et al., 2014; Kang et al., 2015), we expected that PWR might also play a positive role in ABA signaling and dehydration stress. We observed that *pwr-2* and *pwr-3* mutants were less sensitive than WT (Col-0) to ABA and impaired stomatal closure in the presence of exogenous ABA (**Figure 1**). Loss of PWR resulted in ABA-associated phenotypes such as ABA insensitivity in seed germination and post-germinative growth (**Figure 2** and **Supplementary Figure S2**) and enhanced water loss, ultimately leading to drought sensitivity (**Figure 3**). Taken together, these data suggest that unlike HDA9, PWR is a positive regulator of ABA signaling. As previously reported, the phytohormone ABA quickly accumulates in response to stresses and plays a pivotal role in plant survival (Xiong et al., 2002, Xiong and Zhu, 2003). ABA is also a key regulator in stomatal movement that regulates water loss (Luan, 2002; Zhu, 2002). Indeed, ABA-related genes were suppressed in both *pwr* and *hda9* mutants (**Figure 2E**), indicating that PWR is a central regulator of ABA response. Since PWR and HDA9 physically interact and work together in the same complex (Kim et al., 2016), we tested the genetic interaction of PWR and HDA9. As expected, *pwr*, *hda9*, and *pwr*/*hda9* double mutants displayed the same insensitivity toward exogenously applied ABA and hypersensitivity to drought stress (**Figures 2**, **3**). HDA9 binds to the active genes and may either prevent promiscuous cryptic gene expression or compete with other HDACs for binding to the same site. Transcriptome and ChIP-seq analyses have shown that HDA9 also binds the *PYL* gene promoter (Chen et al., 2016). These results indicated that PWR and HDA9 might work with specific transcription factors to repress their target genes during seed germination and drought stress.

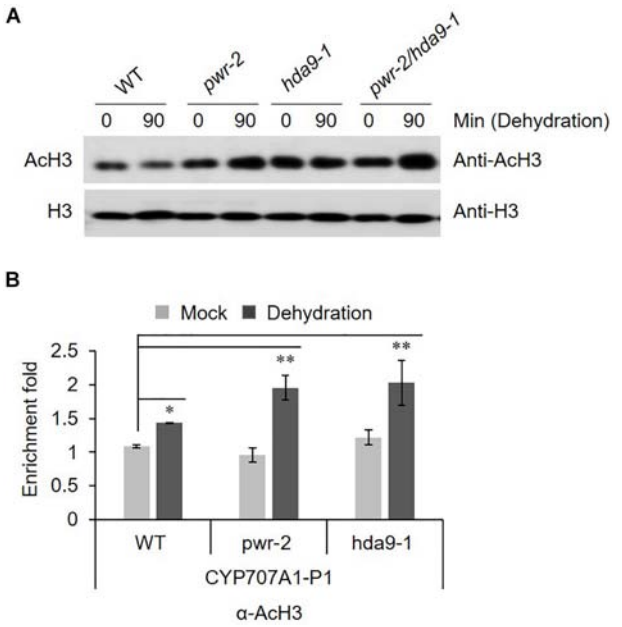

FIGURE 6 | (A) AcH3 level is increased during drought stress. Nuclear protein was isolated from 2 weeks-old *Arabidopsis* WT (Col-0), *pwr-2*, *hda9-1*, and *pwr-2/hda9-1* seedlings after drought stress treatment for 0 or 90 min and then separated by SDS-PAGE. The anti-H3 band from a duplicate gel shows that similar amounts of proteins were loaded. **(B)** ChIP-qPCR assays of the *CYP707A1* promoter using antibody to acetylated histone 3 (AcH3). Chromatin from 2-week-old WT Col-0, *pwr-2* and *hda9-1* mutant plants subjected to drought treatment for 0 or 90 min was immunoprecipitated with anti-AcH3, and the amount of DNA in the immune complex was determined by qRT-PCR. Error bars representing SE ($n = 3$ independent experiments). Significant difference was determined by Student *t*-test (*$p < 0.05$, **$p < 0.01$).

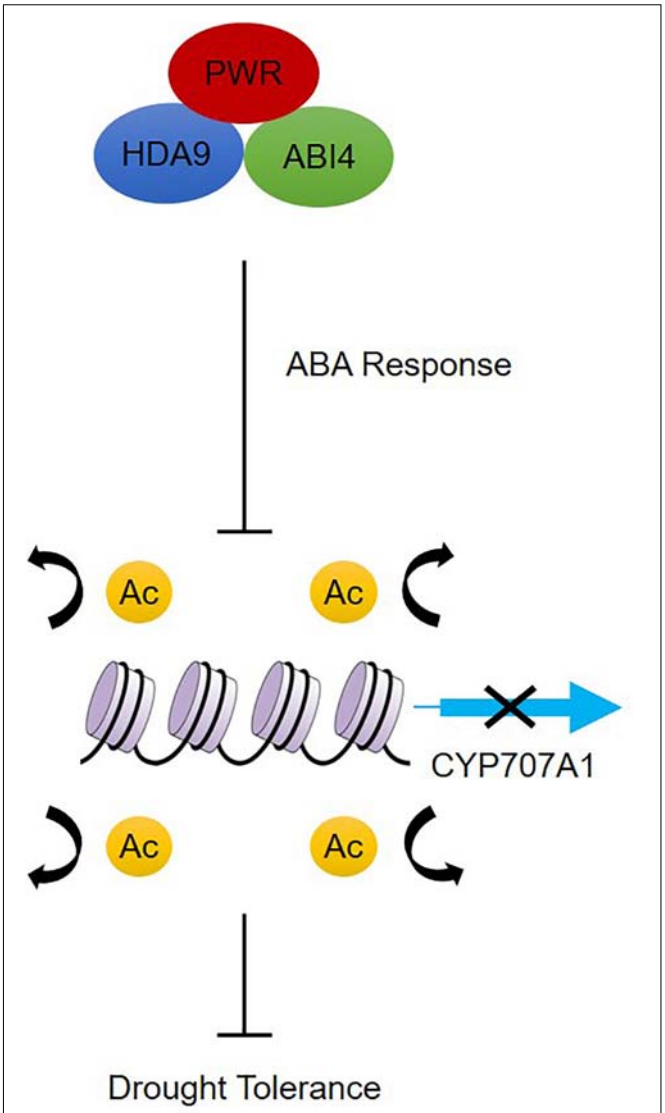

FIGURE 7 | Proposed working model of PWR function in dehydration response. PWR together with HDA9 and ABI4 positively regulate ABA response either by acting at ABA receptors or by repressing negative regulators of the ABA pathway, which results in downstream expression of ABA-responsive genes. In the absence of dehydration stress, *CYP707A1* is expressed and regulates ABA hydroxylation, but dehydration stress triggers *PWR-HDA9-ABI4*-mediated repression of *CYP707A1* expression through the process of deacetylation and activates drought response.

Powerdress and HDA9 Interact With ABI4 and Regulate Histone Acetylation During Drought Stress

HDA9 directly interacts with PWR, and the two proteins work together in the same repressor complex to regulate morphological and developmental processes in plants (Pandey et al., 2002; Kim et al., 2016). Given that the *pwr* and *hda9* mutants were insensitive to ABA and sensitive to drought stress (**Figures 2**, **3**), we assessed the interactions of PWR and HDA9 with the components of the ABA signaling and drought stress pathways. PWR and HDA9 interacted with ABI4 along with ABI3 (**Figure 4** and **Supplementary Figure S3**). ABI4 was initially identified on the basis of the insensitivity of *abi4* mutants to ABA, and later to salt and mannitol (Finkelstein, 1994; Quesada et al., 2000). ABI4 binds specifically to ABRE elements and regulates the expression of several genes in response to abiotic stresses (Mizoi et al., 2012). Notably, ABI4 is a versatile activator and a repressor of gene expression (Söderman et al., 2000; Nakabayashi et al., 2005; Koussevitzky et al., 2007; Bossi et al., 2009; Giraud et al., 2009; Reeves et al., 2011; Shu et al., 2018). ABI4 induces the expression of genes involved in seed dormancy and ABA signaling (Reeves et al., 2011), while repressing genes involved in ABA catabolism (*CYP707A* genes), ethylene biosynthesis (*ACS* genes), retrograde signaling (*AOX1a*), *ARR* genes, which are involved in cytokinin-induced degradation of *ABI5* (Finkelstein and Lynch, 2000; Lopez-Molina et al., 2001; Huang et al., 2017) and genes involved in fatty acid biosynthesis, photosynthesis, pigment and wax metabolic processes (Shu et al., 2013; Dong et al., 2016). These lines of evidence indicate that ABI4 both induces and represses target genes. We therefore tested the genes suppressed by ABI4 in loss-of-function mutants of PWR (*pwr-2* and *pwr-3*). In response to dehydration, the transcript levels of *CYP707A1*,

ACS4 and *AOX1a* in *pwr* mutants were significantly higher than those in WT (**Figure 5**), whereas there were no significant differences in the expression of *CYP707A2* and *CYP707A3* in *pwr* mutants as compared to WT. As PWR and HDA9 regulate the acetylation status of numerous genes specifically at H3K9, H3K14, and H3K27, we measured the total acetyl histone H3 (AcH3) levels in *pwr* and *hda9* mutants (**Figure 6A**). The AcH3 level was significantly increased in *pwr* and *hda9* mutants upon dehydration stress, suggesting that the total AcH3 increases in response to dehydration stress in the mutants. However, effects of the acetylation status at the specific promoter regions of target genes responsible for drought stress responses could not be excluded. Therefore, we analyzed the AcH3 level at the *CYP707A1* promoter and observed that after dehydration, the association of AcH3 was higher at the P1 region, but not the P2 or P3 regions, of the *CYP707A1* promoter in the *pwr-2* mutant compared to WT (**Figure 6B** and **Supplementary Figure S4**). Surprisingly, AcH3 association at the *CYP707A1* P1 region was also increased in the *hda9* mutant upon dehydration (**Figure 6B**). However, there was no difference in the *CYP707A2* promoter AcH3 level during dehydration stress in the *pwr* mutant compared to the WT (**Supplementary Figure S4**), suggesting that PWR and HDA9 are both required for repression of *CYP707A1* in response to drought stress.

Besides its role in regulating plant morphological and developmental processes, little is known about how PWR regulate signal transduction and chromatin modification in response to abiotic stresses. Based on our results, we propose a model for how PWR, together with HDA9 and ABI4, mediates biological functions by negatively regulating the expression of genes through chromatin modification during ABA-dependent drought stress (**Figure 7**). On one hand, PWR and HDA9 mutants displayed the same phenotype with and without exogenous ABA and interact specifically with ABI4, indicating that PWR, HDA9, and ABI4 might regulate the same set of genes in ABA pathway. On the other hand, in the absence of drought stress, ABA-catabolism-related genes such as *CYP707A1* are activated by histone acetylation; the *CYP707A1* gene product, (+)-abscisic acid 8′-hydroxylase, then converts active ABA to the inactive form (8′-hydroxy-ABA) inside guard cells, resulting in loss of turgor pressure and stomatal opening (Xiong et al., 2002, Xiong and Zhu, 2003). ABI4 was previously reported to suppress the *CYP707A* genes by directly binding to their promoters (Shu et al., 2013), and here we report that ABI4 together with PWR and HDA9 may associate with the *CYP707A1* promoter. This possible association with the PWR-HDA9-ABI4 repressor complex represses *CYP707A1* expression through histone deacetylation and results in drought tolerance. In addition to repressing genes, ABI4 is also involved in the activation of several genes. Since HDA9 and PWR regulate a wide range of genes involved in several key physiological processes including autophagy, pathogenesis and senescence, there might be some other unidentified genes through which HDA9 and PWR regulate ABA signaling and drought stress. Further study is required to uncover whether the PWR-HDA9-ABI4 complex is also involved in activating genes responsible for ABA signaling and drought tolerance.

DATA AVAILABILITY STATEMENT

The original contributions presented in the study are included in the article/**Supplementary Material**, further inquiries can be directed to the corresponding author.

AUTHOR CONTRIBUTIONS

IK, AA, and D-JY conceived and designed the experiments. IK, HK, SZ, MJ, DB, JP, and CL performed the experiments. IK, AA, JP, WK and D-JY analyzed the data and wrote the manuscript. All authors reviewed and approved the final manuscript.

FUNDING

This work was supported by the Next Generation Bio-Green21 Program, Rural Development Administration (RDA), Republic of Korea (SSAC, PJ01318201 to D-JY and PJ01318205 to JP); the National Research Foundation of Korea (NRF) funded by the Korean Government (2019R1A2C2084096 to D-JY) and Global Research Lab (2017K1A1A2013146 to D-JY).

SUPPLEMENTARY MATERIAL

The Supplementary Material for this article can be found online at: https://www.frontiersin.org/articles/10.3389/fpls.2020.00623/full#supplementary-material

REFERENCES

Ali, A., Kim, J. K., Jan, M., Khan, H. A., Khan, I. U., Shen, M., et al. (2019). Rheostatic control of ABA signaling through HOS15-mediated OST1 degradation. *Mol. Plant* 12, 1447–1462. doi: 10.1016/j.molp.2019.08.005

Alonso, J. M., Stepanova, A. N., Leisse, T. J., Kim, C. J., Chen, H., Shinn, P., et al. (2003). Genome- wide insertional mutagenesis of *Arabidopsis thaliana*. *Science* 301, 653–657.

Antoni, R., Gonzalez-Guzman, M., Rodriguez, L., Rodrigues, A., Pizzio, G. A., and Rodriguez, P. L. (2012). Selective inhibition of clade A phosphatases type 2C by PYR/PYL/RCAR abscisic acid receptors. *Plant Physiol.* 158, 970–980. doi: 10.1104/pp.111.188623

Bannister, A. J., and Kouzarides, T. (2011). Regulation of chromatin by histone modifications. *Cell Res.* 21, 381–395. doi: 10.1038/cr.2011.22

Bosch-Presegué, L., and Vaquero, A. (2015). Sirtuin-dependent epigenetic regulation in the maintenance of genome integrity. *FEBS J.* 282, 1745–1767. doi: 10.1111/febs.13053

Bossi, F., Cordoba, E., Dupré, P., Mendoza, M. S., Román, C. S., and León, P. (2009). The *Arabidopsis* ABA-INSENSITIVE (ABI) 4 factor acts as a central transcription activator of the expression of its own gene, and for the induction of ABI5 and SBE2.2 genes during sugar signaling. *Plant J.* 59, 359–374. doi: 10.1111/j.1365-313X.2009.03877.x

Chen, X., Lu, L., Mayer, K. S., Scalf, M., Qian, S., Lomax, A., et al. (2016). POWERDRESS interacts with HISTONE DEACETYLASE 9

to promote aging in *Arabidopsis*. *eLife* 5:e17214. doi: 10.7554/eLife.17214

Dong, Z., Yu, Y., Li, S., Wang, J., Tang, S., and Huang, R. (2016). Abscisic acid antagonizes ethylene production through the ABI4-mediated transcriptional repression of ACS4 and ACS8 in *Arabidopsis*. *Mol. Plant* 9, 126–135. doi: 10.1016/j.molp.2015.09.007

Finkelstein, R. R. (1994). Mutations at two new *Arabidopsis* ABA response loci are similar to the abi3 mutations. *Plant J.* 5, 765–771.

Finkelstein, R. R., and Lynch, T. J. (2000). Abscisic acid inhibition of radicle emergence but not seedling growth is suppressed by sugars. *Plant Physiol.* 122, 1179–1186. doi: 10.1104/pp.122.4.1179

Fujii, H., Chinnusamy, V., Rodrigues, A., Rubio, S., Antoni, R., Park, S.-Y., et al. (2009). *In vitro* reconstitution of an abscisic acid signalling pathway. *Nature* 462, 660–664. doi: 10.1038/nature08599

Giraud, E., Van Aken, O., Ho, L. H., and Whelan, J. (2009). The transcription factor ABI4 is a regulator of mitochondrial retrograde expression of ALTERNATIVE OXIDASE1a. *Plant Physiol.* 150, 1286–1296. doi: 10.1104/pp.109.139782

Guy, C. L., Niemi, K. J., and Brambl, R. (1985). Altered gene expression during cold acclimation of spinach. *Proc. Natl. Acad. Sci. U.S.A.* 82, 3673–3677. doi: 10.1073/pnas.82.11.3673

Haberland, M., Montgomery, R. L., and Olson, E. N. (2009). The many roles of histone deacetylases in development and physiology: implications for disease and therapy. *Nat. Rev. Genet.* 10, 32–42. doi: 10.1038/nrg2485

Hasegawa, P. M., Bressan, A. B., Zhu, J. K., and Bohnert, H. J. (2000). Plant cellular and molecular responses to high salinity. *Annu. Rev. Plant Physiol. Plant Mol. Biol.* 51, 463–499. doi: 10.1146/annurev.arplant.51.1.463

Henderson, I. R., and Jacobsen, S. E. (2007). Epigenetic inheritance in plants. *Nature* 447, 418–424.

Hollender, C., and Liu, Z. (2008). Histone deacetylase genes in *Arabidopsis* development. *J. Integr. Plant Biol.* 50, 875–885. doi: 10.1111/j.1744-7909.2008.00704.x

Horn, P. J., and Peterson, C. L. (2002). Molecular biology: chromatin higher order folding–wrapping up transcription. *Science* 297, 1824–1827. doi: 10.1126/science.1074200

Huang, X., Zhang, X., Gong, Z., Yang, S., and Shi, Y. (2017). ABI4 represses the expression of type- ARRs to inhibit seed germination in *Arabidopsis*. *Plant J.* 89, 354–365. doi: 10.1111/tpj.13389

Iuchi, S., Kobayashi, M., Taji, T., Naramoto, M., Seki, M., Kato, T., et al. (2001). Regulation of drought tolerance by gene manipulation of 9-cis-epoxycarotenoid dioxygenase, a key enzyme in abscisic acid biosynthesis in *Arabidopsis*. *Plant J.* 27, 325–333. doi: 10.1046/j.1365-313x.2001.01096.x

Kang, M. J., Jin, H. S., Noh, Y. S., and Noh, B. (2015). Repression of flowering under a noninductive photoperiod by the HDA9- AGL19-FT module in *Arabidopsis*. *New Phytol.* 206, 281–294. doi: 10.1111/nph.13161

Kim, W., Latrasse, D., Servet, C., and Zhou, D. X. (2013). *Arabidopsis* histone deacetylase HDA9 regulates flowering time through repression of AGL19. *Biochem. Biophys. Res. Commun.* 432, 394–398. doi: 10.1016/j.bbrc.2012.11.102

Kim, Y. J., Wang, R., Gao, L., Li, D., Xu, C., Mang, H., et al. (2016). POWERDRESS and HDA9 interact and promote histone H3 deacetylation at specific genomic sites in *Arabidopsis*. *Proc. Natl. Acad. Sci. U.S.A.* 113, 14858–14863. doi: 10.1073/pnas.1618618114

Koussevitzky, S., Nott, A., Mockler, T. C., Hong, F., Sachetto-Martins, G., Surpin, M., et al. (2007). Signals from chloroplasts converge to regulate nuclear gene expression. *Science* 316, 715–719.

Kushiro, T., Okamoto, M., Nakabayashi, K., Yamagishi, K., Kitamura, S., Asami, T., et al. (2004). The *Arabidopsis* cytochrome P450 CYP707A encodes ABA 8#-hydroxylases: key enzymes in ABA catabolism. *EMBO J.* 23, 1647–1656. doi: 10.1038/sj.emboj.7600121

Lee, K., Park, O. S., Jung, S. J., and Seo, P. J. (2016). Histone deacetylation-mediated cellular dedifferentiation in *Arabidopsis*. *J. Plant Physiol.* 191, 95–100. doi: 10.1016/j.jplph.2015.12.006

Lopez-Molina, L., Mongrand, S., and Chua, N. H. (2001). A postgermination developmental arrest checkpoint is mediated by abscisic acid and requires the ABI5 transcription factor in *Arabidopsis*. *Proc. Natl. Acad. Sci. U.S.A.* 98, 4782–4787. doi: 10.1073/pnas.081594298

Luan, S. (2002). Signaling drought in guard cells. *Plant Cell Environ.* 25, 229–237. doi: 10.1046/j.1365-3040.2002.00758.x

May, M. J., Vernoux, T., Leaver, C., Montagu, M. V., and Inzé, D. (1998). Glutathione homeostasis in plants: implications for environmental sensing and plant development. *J. Exp. Bot.* 49, 649–667.

Mizoi, J., Shinozaki, K., and Yamaguchi-Shinozaki, K. (2012). AP2/ERF family transcription factors in plant abiotic stress responses. *Biochim. Biophys. Acta* 1819, 86–96. doi: 10.1016/j.bbagrm.2011.08.004

Nakabayashi, K., Okamoto, M., Koshiba, T., Kamiya, Y., and Nambara, E. (2005). Genome-wide profiling of stored mRNA in *Arabidopsis thaliana* seed germination: epigenetic and genetic regulation of transcription in seed. *Plant J.* 41, 697–709. doi: 10.1111/j.1365-313X.2005.02337.x

Nambara, E. (2005). Marion-poll A: abscisic acid biosynthesis and catabolism. *Annu. Rev. Plant Biol.* 56, 165–185.

Pandey, R., Müller, A., Napoli, C. A., Selinger, D. A., Pikaard, C. S., Richards, E. J., et al. (2002). Analysis of histone acetyltransferase and histone deacetylase families of *Arabidopsis thaliana* suggests functional diversification of chromatin modification among multicellular eukaryotes. *Nucleic Acids Res.* 30, 5036–5055. doi: 10.1093/nar/gkf660

Park, J., Lim, C. J., Khan, I. U., Jan, M., Khan, H. A., Park, H. J., et al. (2018). Identification and molecular characterization of HOS15 interacting proteins in *Arabidopsis thaliana*. *J. Plant Biol.* 61, 336–345. doi: 10.1186/s12870-015-0461-1

Quesada, V., Ponce, M. R., and Micol, J. L. (2000). Genetic analysis of salt-tolerant mutants in *Arabidopsis thaliana*. *Genetics* 154, 421–436.

Reeves, W. M., Lynch, T. J., Mobin, R., and Finkelstein, R. R. (2011). Direct targets of the transcription factors ABA-Insensitive (ABI)4 and ABI5 reveal synergistic action by ABI4 and several bZIP ABA response factors. *Plant Mol. Biol.* 75, 347–363. doi: 10.1007/s11103-011-9733-9

Rosso, M. G., Li, Y., Strizhov, N., Reiss, B., Dekker, K., and Weisshaar, B. (2003). An *Arabidopsis thaliana* T-DNA mutagenized population (GABI-Kat) for flanking sequence tag-based reverse genetics. *Plant Mol. Biol.* 53, 247–259. doi: 10.1023/B:PLAN.0000009297.37235.4a

Saito, S., Hirai, N., Matsumoto, C., Ohigashi, H., Ohta, D., Sakata, K., et al. (2004). *Arabidopsis* CYP707As encode (+)-abscisic acid 8'-hydroxylase, a key enzyme in the oxidative catabolism of abscisic acid. *Plant Physiol.* 134, 1439–1449. doi: 10.1104/pp.103.037614

Saleh, A., Alvarez-Venegas, R., and Avramova, Z. (2008). An efficient chromatin immunoprecipitation (ChIP) protocol for studying histone modifications in *Arabidopsis* plants. *Nat. Protoc.* 3, 1018–1025. doi: 10.1038/nprot.2008.66

Seto, E., and Yoshida, M. (2014). Erasers of histone acetylation: the histone deacetylase enzymes. *Cold Spring Harb. Perspect. Biol.* 6:a018713. doi: 10.1101/cshperspect.a018713

Shinozaki, K., and Yamaguchi-Shinozaki, K. (2000). Molecular responses to dehydration and low temperature: differences and cross-talk between two stress signaling pathways. *Curr. Opin. Plant Biol.* 3, 217–223.

Shu, K., Chen, F., Zhou, W., Luo, X., Dai, Y., and Shuai, H. (2018). ABI4 regulates the floral transition independently of ABI5 and ABI3. *Mol. Biol. Rep.* 45, 2727–2731. doi: 10.1007/s11033-018-4290-9

Shu, K., Zhang, H., Wang, S., Chen, M., Wu, Y., Tang, S., et al. (2013). ABI4 regulates primary seed dormancy by regulating the biogenesis of abscisic acid and gibberellins in *Arabidopsis*. *PLoS Genet.* 9:e1003577. doi: 10.1371/journal.pgen.1003577

Söderman, E. M., Brocard, I. M., Lynch, T. J., and Finkelstein, R. R. (2000). Regulation and function of the *Arabidopsis* ABA-insensitive4 gene in seed and abscisic acid response signaling networks. *Plant Physiol.* 124, 1752–1765. doi: 10.1104/pp.124.4.1752

Struhl, K. (1998). Histone acetylation and transcriptional regulatory mechanisms. *Genes Dev.* 12, 599–606. doi: 10.1101/gad.12.5.599

Umezawa, T., Sugiyama, N., Mizoguchi, M., Hayashi, S., Myouga, F., Yamaguchi-Shinozaki, K., et al. (2009). Type 2C protein phosphatases directly regulate abscisic acid-activated protein kinases in *Arabidopsis*. *Proc. Natl. Acad. Sci. U.S.A.* 106, 17588–17593. doi: 10.1073/pnas.0907095106

van Zanten, M., Zoll, C., Wang, Z., Philipp, C., Carles, A., Li, Y., et al. (2014). HISTONE DEACETYLASE 9 represses seedling traits in *Arabidopsis thaliana* dry seeds. *Plant J.* 80, 475–488. doi: 10.1111/tpj.12646

Xiong, L., Lee, H., Ishitani, M., and Zhu, J. K. (2002). Regulation of osmotic stress responsive gene expression by the LOS6/ABA1 locus in *Arabidopsis*. *J. Biol. Chem.* 277, 8588–8596. doi: 10.1074/jbc.M109275200

Xiong, L., and Zhu, J. K. (2003). Regulation of abscisic acid biosynthesis. *Plant Physiol.* 133, 29–36.

Yumul, R. E., Kim, Y. J., Liu, X., Wang, R., Ding, J., Xiao, L., et al. (2013). *POWERDRESS* and diversified expression of the *MIR172* gene family bolster the floral stem cell network. *PLoS Genet.* 9:e1003218. doi: 10.1371/journal.pgen.1003218

Zhao, T., Rui, L., Li, J., Nishimura, M. T., Vogel, J. P., Liu, N., et al. (2015). A truncated NLR protein, TIR-NBS2, is required for activated defense responses in the exo70B1 mutant. *PLoS Genet.* 11:e1004945. doi: 10.1371/journal.pgen.1004945

Zheng, Y., Ding, Y., Sun, X., Xie, S., Wang, D., Liu, X., et al. (2016). Histone deacetylase HDA9 negatively regulates salt and drought stress responsiveness in *Arabidopsis*. *J. Exp. Bot.* 67, 1703–1713. doi: 10.1093/jxb/erv562

Zhu, J. K. (2002). Salt and drought stress signal transduction in plants. *Annu. Rev. Plant Biol.* 53, 247–273. doi: 10.1146/annurev.arplant.53.091401.143329

Conflict of Interest: The authors declare that the research was conducted in the absence of any commercial or financial relationships that could be construed as a potential conflict of interest.

frontiers in Plant Science

ORIGINAL RESEARCH
published: 02 July 2020
doi: 10.3389/fpls.2020.00879

From Survival to Productivity Mode: Cytokinins Allow Avoiding the Avoidance Strategy Under Stress Conditions

*Avishai Avni[1], Yelena Golan[1], Natali Shirron[1], Yeela Shamai[1], Yaela Golumbic[1], Yael Danin-Poleg[1] and Shimon Gepstein[1,2]**

[1] Faculty of Biology, Technion – Israel Institute of Technology, Haifa, Israel, [2] Kinneret Academic College, Sea of Galilee, Israel

Growth retardation and stress-induced premature plant senescence are accompanied by a severe yield reduction and raise a major agro-economic concern. To improve biomass and yield in agricultural crops under mild stress conditions, the survival must be changed to productivity mode. Our previous successful attempts to delay premature senescence and growth inhibition under abiotic stress conditions by autoregulation of cytokinins (CKs) levels constitute a generic technology toward the development of highly productive plants. Since this technology is based on the induction of CKs synthesis during the age-dependent senescence phase by a senescence-specific promoter (*SARK*), which is not necessarily regulated by abiotic stress conditions, we developed autoregulating transgenic plants expressing the *IPT* gene specifically under abiotic stress conditions. The *Arabidopsis* promoter of the stress-induced metallothionein gene (At*MT*) was isolated, fused to the *IPT* gene and transformed into tobacco plants. The MT:IPT transgenic tobacco plants displayed comparable elevated biomass productivity and maintained growth under drought conditions. To decipher the role and the molecular mechanisms of CKs in reverting the survival transcriptional program to a sustainable plant growth program, we performed gene expression analysis of candidate stress-related genes and found unexpectedly clear downregulation in the CK-overproducing plants. We also investigated kinase activity after applying exogenous CKs to tobacco cell suspensions that were grown in salinity stress. In-gel kinase activity analysis demonstrated CK-dependent deactivation of several stress-related kinases including two of the MAPK components, *SIPK* and *WIPK* and the *NtOSAK*, a member of SnRK2 kinase family, a key component of the ABA signaling cascade. A comprehensive phosphoproteomics analysis of tobacco cells, treated with exogenous CKs under salinity-stress conditions indicated that >50% of the identified phosphoproteins involved in stress responses were dephosphorylated by CKs. We hypothesize that upregulation of CK levels under stress conditions desensitize stress signaling cues through deactivation of kinases that are normally activated under stress conditions. CK-dependent desensitization of environmental stimuli is suggested to attenuate various pathways of the avoidance syndrome including the characteristic growth arrest and the premature senescence while allowing normal growth and metabolic maintenance.

Keywords: abiotic stress, avoidance, cytokinins, stress tolerance, senescence, transgenic plants

OPEN ACCESS

Edited by:
Soyon Park,
Virginia Tech, United States

Reviewed by:
Raquel Lia Chan,
CONICET Santa Fe, Argentina
Guzel Kudoyarova,
Institute of Biology of Karelian Research Centre (RAS), Russia

***Correspondence:**
Shimon Gepstein
gepstein@tx.technion.ac.il;
gepstein@technion.ac.il

Specialty section:
This article was submitted to Plant Abiotic Stress, a section of the journal Frontiers in Plant Science

Received: *05 January 2020*
Accepted: *28 May 2020*
Published: *02 July 2020*

Citation:
Avni A, Golan Y, Shirron N, Shamai Y, Golumbic Y, Danin-Poleg Y and Gepstein S (2020) From Survival to Productivity Mode: Cytokinins Allow Avoiding the Avoidance Strategy Under Stress Conditions. Front. Plant Sci. 11:879. doi: 10.3389/fpls.2020.00879

INTRODUCTION

Abiotic stresses, such as drought and salinity are key challenges for plant growth and agricultural productivity, leading to an annual loss of billions of dollars (Pereira, 2016; Zhu, 2016). The evolution of adaptive mechanisms in plants to particular environmental stresses involved activation of stress avoidance strategy that allows plants to escape the potentially damaging effects of these conditions. Under stress conditions, plants activate the stress-avoidance strategy resulting in reduced vegetative growth, leaf shedding, early flowering, accelerated senescence, and loss of biomass/yield (Cramer et al., 2011; Maggio et al., 2018). The stress-avoidance mechanism balances water uptake and water loss. Water uptake is maintained by solute accumulation to lower the cell water potential and by increasing root growth, whereas water loss is restricted by closing stomata, reducing shoot growth, early flowering, and accelerating leaf senescence (Maggio et al., 2018). As the response of plants to water deficit limits biomass/yield, the development of crop varieties with near-normal growth under moderate water stress is critical (Debbarma et al., 2019). Although many breeding programs and genetic engineering technologies have been applied during the last decade, only a few were deemed successful in overcoming this response as it is polygenic and redundantly programmed (Maggio et al., 2018). Survival mode, as reflected in the stress-avoidance response, is often needed in natural environments, but not in most agricultural environments where stresses are less intense and do not persist long enough to threaten survival.

Salinity and drought stresses affect most aspects of plant biology. The pathways associated with the stress-avoidance response include those associated with osmotic and ionic homeostasis, detoxification response, and growth regulation. Osmotic stress activates several protein kinases including mitogen-activated protein kinases (MAPKs), which mediate osmotic homeostasis and/or detoxification responses. In tobacco, the two most investigated stress-related MAPKs are SIPK (48 kD) and WIPK (44 kD) (Seo et al., 1995; Zhang and Klessig, 1997; Romeis et al., 1999; Zhang et al., 2000). Abscisic acid (ABA) biosynthesis is regulated by osmotic stress at multiple steps. Both ABA-dependent and -independent osmotic stress signaling modify constitutively expressed transcription factors (TFs), leading to the expression of early response transcriptional activators, which then activate downstream stress tolerance effector genes (Wu et al., 2007; Yoshida et al., 2014; Du et al., 2018). Osmotic stress induces ABA accumulation by activating its synthesis as well as by inhibiting its degradation (Dong et al., 2015). ABA regulates inhibition of germination, seed dormancy and dehydration, stomata closure, roots elongation during drought stress, and stress-related gene regulation (Hoth et al., 2002; Seki et al., 2002; Xiong et al., 2006; Finkelstein et al., 2008; Cutler et al., 2010). In addition, ABA induces senescence as part of plant development or as a stress-induced response (Gepstein and Thimann, 1980). Abiotic stress-induced responses are regulated by activation of the expression of many genes via ABA-responsive elements (ABREs) in their promoter regions. ABA triggers cascaded activation of SnRK2 that positively controls the AREB/ABF TFs and the S-type anion channel SLAC1 (Fujita et al., 2013; Zhang et al., 2018). The activated anion channels release anions, which are accompanied by the activated K^+ efflux channels releasing K^+. As both anion and cation are released from the guard cell turgor is reduced leading to stomatal closure (Roelfsema et al., 2012; Misra et al., 2019). The Ca^{2+} signaling pathway is also involved in the regulation of stomatal aperture through Ca^{2+}-dependent protein kinases and CBL (calcineurin B-like protein)-interacting protein kinases. Both kinase systems modulate SLAC1 (Edel and Kudla, 2016).

Drought-responsive genes include effector genes encoding chaperones, enzymes, and ion/water channels, as well as regulatory genes encoding TFs. Several groups of TFs, such as AREB, DREB, NAC, MYB, bZIP, and WRKY, respond to drought stress and act in an ABA-dependent or -independent manner (Joshi et al., 2016). The ABA core signaling pathway largely relies on the activation of SnRK2 kinases to mediate several rapid responses, including gene regulation, stomatal closure, and plant growth modulation. Another kinase, NtOSAK (42 kD), a member of SnRK2 kinase family, is also activated by osmotic stress and ABA in tobacco plants (Kelner et al., 2004; Wawer et al., 2010; Kulik et al., 2011, 2012). Cytokinins (CKs) have a positive role in plant growth and development, but their biosynthesis diminishes during senescence and under water-deficit stress (Chernyad'ev, 2005; Ha et al., 2012). During senescence, applying exogenous CK delays the senescence syndrome (Richmond and Lang, 1957). Since premature senescence negatively impacts yield/biomass, different approaches were used in an attempt to modify the kinetic/severity of the senescence syndrome, especially under stress conditions (Ha et al., 2012; Gepstein and Glick, 2013). Manipulating endogenous CK levels can effectively delay senescence (Gan and Amasino, 1995; Peleg and Blumwald, 2011; Ha et al., 2012; Guo and Gan, 2014). Expression of isopentenyltransferase (*IPT*), the key gene in CK biosynthesis, under different promoters affected plant development, especially on the last phase of the senescence syndrome. Constitutive or inducible expression of the *IPT* gene is associated with arrested senescence phenotype, as well as with loss of apical dominance and altered root growth (Smart et al., 1991; Gan and Amasino, 1995; Peleg and Blumwald, 2011). Inhibition of leaf senescence by autoregulated production of CKs has since been applied to different plants including lettuce, petunia, tobacco, maize, and ryegrass (Jordi et al., 2000; McCabe et al., 2001; Chang et al., 2003; Li et al., 2004; Robson et al., 2004; Peleg and Blumwald, 2011; Golan et al., 2016).

We have previously shown that in transgenic tobacco plants expressing the *IPT* gene under the senescence gene promoter from *Phaseolus vulgaris*, *SARK* (Hajouj et al., 2000), CK is maintained at high levels under water-deficit stress, leading to better survival and increased productivity (Hajouj et al., 2000; Rivero et al., 2007). The molecular mechanisms underlying this have not been fully characterized, although comparative gene-cluster analysis performed in our laboratory suggest that CKs prevent the transcriptional reprograming of known molecular processes associated with stress-tolerance responses (Golan et al., 2016). CKs regulate developmental processes as well as responses to environmental stresses via a complex network of CK signaling

(Ha et al., 2012). The receptor gene, *AHK3* is known to partially mediate delayed senescence by phosphorylation of type B *ARR* (Kim et al., 2006). *CRF6* plants begin to undergo monocarpic senescence sooner than WT plants (Rashotte et al., 2006; Zwack and Rashotte, 2013). *CRF6* is induced by CKs and abiotic stresses suggesting possible interaction between *CRF6* and *ARR2* (Cutcliffe et al., 2011). By an unknown mechanism, stress signals are perceived and transmitted via the His-Asp phosphorelay pathway triggering CK-responsive genes (Ha et al., 2012). Multiple mutually interconnected hormonal signaling cascades act as essential endogenous translators of these exogenous signals in the adaptive responses of plants (Verma et al., 2016). Since CKs and ABA are associated with antagonistic inputs in the context of abiotic stress responses, we considered the possibility of interconnection between the two hormonal signaling cascades. Our technology of improving drought tolerance by *IPT* gene driven by *SARK* promoter has been implemented in various crops, including rice, peanuts, creeping-bentgrass, cassava, and tobacco (Rivero et al., 2007; Peleg et al., 2011; Qin et al., 2011; Merewitz et al., 2012).

It is assumed that the main function of leaf senescence is to recycle cellular material accumulated during leaf growth and maturation into exportable nutrients to supply developing organs such as fruits (Avila-Ospina et al., 2014; Maillard et al., 2015). Thus, leaf senescence, due to its role in nutrient management, is essential for plant productivity (Gregersen et al., 2013). Although the transgenic plants (SARK-IPT) display delayed age-dependent senescence and possess an obvious productivity advantage (Rivero et al., 2007), they may also suffer a delay in the optimal harvest timing and a progressive asynchronous fruit ripening and seed set (Lukac et al., 2012). Notably, the timing of triggering senescence is critical for remobilizing mineral nutrients and carbohydrates and may affect fruit quality. The onset of senescence and the rate of its progression also determine the quality of the yield. If the timing is late or the rate is too slow, grains do not dry-down (ripen) completely before harvest, resulting in moisture and nutrients in the harvested material, and consequently, in post-harvest microbial spoilage (Robson et al., 2012).

Since age-dependent senescence is critical for synchronous crop harvest and delaying the normal senescence (by CKs) may interfere with the optimal harvest timing, we decided to focus on delaying the premature stress-induced senescence and allowing normal senescence and proper harvest. Herein, we describe the development of transgenic tobacco plants carrying the *IPT* gene under a stress-specific promoter of the *Arabidopsis* metallothionein (*AtMT*) gene. The rational for choosing the promoter of the MT gene stems from the known functions related to various abiotic stresses of MT genes. Moreover, our previous study which focused on the expression pattern of various senescence-associated genes identified three MT related genes (Gepstein et al., 2003). The *AtMT2* promoter was selected since it represents a general abiotic stress promoter and over-expression of MTs in various model systems like *Arabidopsis*, tobacco, yeast and *E. coli* established its functional role in homeostasis and tolerance to heavy metal ions, high salinity, drought, low temperature, heavy metal ions, ABA, and ethylene. The *MT2a* overexpressing transgenic *Arabidopsis* seedlings had longer roots, larger leaves, and higher biomass accumulation, compared to WT plants under drought, salinity and oxidative stress conditions plants (Patankar et al., 2019). *SbMT-2* gene from a halophyte confers abiotic stress tolerance and modulates reactive oxygen species (ROS) scavenging in transgenic tobacco (Chaturvedi et al., 2014). Since the accumulated literature points to the involvement of the *MT2a* gene in stress-induced senescence phenomenon, we employed the *AtMT2a* promoter to induce *IPT* gene expression and to increase CK levels, specifically under abiotic stress.

Our current results combined with our previous findings in *Arabidopsis* (Golan et al., 2016), suggest that CKs cause desensitization of plants to environmental stress cues and allow plants to escape stress symptoms of the avoidance syndrome, as reflected by sustainable growth and productivity.

MATERIALS AND METHODS

Plants

Nicotiana tabacum plants ecotype SR-1, were grown on water-soaked peat pellets (Jiffy 7, Kappa Forenade Well) in temperature-controlled growth room at 23°C (± 2°C) under fluorescent lamps (75 $\mu E\ m^{-2}\ s^{-1}$) under long day conditions (18 h light, 8 h dark). The SR-1 plants were used as a genetic background for the development of transgenic plants. WT and transgenic plants were transferred and transplanted into a greenhouse, using 5 l pots and grown for 25 days (1,200 μmol of photons $m^{-2}\ s^{-1}$, 16 h photoperiod, 23–25°C day/night). The *N. tabacum* BY-2 cell line (derived from *N. tabacum* Bright Yellow 2) was generously donated by Dr. S. Yaron from the Technion, Israel and maintained by weekly dilution (1:50) in fresh liquid Murashige and Skoog (MS) media (Sigma, St. Louis, MO, United States) supplemented with 0.2 g L^{-1} KH_2PO_4, 1 mg L^{-1} thiamine, 0.2 mg L^{-1} 2,4-dichlorophenoxyacetic acid (2,4-D), 30 g L^{-1} sucrose, and 0.2 g L^{-1} myoinositol at pH 6.2, as previously described (Shirron and Yaron, 2011).

Construction of Transgenic Plants Expressing pMetallothionein:IPT

The plasmid pJHA212K (Yoo et al., 2005) was used as a template to generate the expression vector in which the 35S promoter was replaced by the AtMT promoter. The AtMT promotor (nucleotides 1–1300 bp) selected form the *Arabidopsis AtMT2a* gene (AT3G09390), was fused to the *IPT* gene (coding sequence, nucleotides 1301–2100) followed by the *NOS* terminator nucleotides 2101–2334 generating *AtMT* promoter-*IPT-NOS* terminator construct (**Supplementary Figure S1**, Gepstein, 2013) and transformed into tobacco SR-1 plants as previously described (Rivero et al., 2007; Golan et al., 2016). The transgenic plants were grown under optimal watering conditions (16 h light, 8 h dark). Five lines of the transgenic plants were characterized, and all displayed similar phenotypes including response to abiotic stresses (data not shown). One representative line (mt7) that showed genetic stability in the transgenic fourth generation (t4) plants was selected for

detailed characterization of its morphological and developmental behavior under stress conditions.

Stress Conditions

Drought Stress

One-month old tobacco plants were transferred into a greenhouse (25°± 2°C, 18 h light, 8 h dark) for three more months until full maturation, Plants were watered with 500 ml every 2 days and excess water drained immediately. For the drought stress treatment, after three months, of watering, plant watering was withheld for 3 weeks. The plants were photographed and leaf samples were collected into liquid nitrogen for RNA analysis. Afterward, the plants were re-watered for 1 week and photographed again. Experiments were conducted in triplicates as independent experiments.

Salinity Stress

Tobacco plants were grown in 250 ml pots for 3 weeks with tap water watering. Plants were subjected to salinity stress by irrigating every other day with 100 ml of 100 mM NaCl solution during the first 10 days, and with 200 mM NaCl for the subsequent 11 days. Following this period, the plants were photographed and samples from mature leaves were collected into liquid nitrogen for RNA analysis. Experiments were conducted in triplicates as independent experiments. To follow the recovery of the plants after salinity stress, plants were watered with tap water for 2 weeks and photographed.

BY-2 Cells

BY-2 cell suspension was grown for 5 days in a shaker incubator at 25°C in dark as described (Shirron and Yaron, 2011). The suspension was divided into four 250 ml flasks (50 ml suspension in each) and for the CKs treatments, 6-benzyloaminopurine (BAP), a synthetic CK, was added into the suspension solution to a final concentration of 10 μM. After 1 h of pre-treatment incubation, NaCl was added to a final concentration of 50 mM. For the phosphoproteomics analysis, the suspension was collected into 50 ml conical tubes half an hour later, centrifuged at 4,500 rpm for 2 min at 4°C, and frozen immediately until protein extraction was performed. For kinase activity assays, samples were collected at 5, 10, 20, 30, 90, and 120 min following salt addition and treated as indicated above. Both experiments were conducted in triplicates as independent experiments.

RNA Extraction

RNA isolation from approximately 150 mg of plant material was performed using the SV Total RNA Isolation kit (Promega #Z3100, Madison, Wisconsin), according to manufacturer's instructions. Following freezing in liquid nitrogen, the samples were grounded with mortar and pestle in 2 ml Eppendorf tubes in the kit suspension solution. RNA was kept at -70°C.

Real-Time PCR Reaction

Total RNA was extracted from the leave samples followed by removal of contaminating DNA with RNase-free DNase I. Primers for amplifying selected genes (**Supplementary Table S1**) were designed using Primer Express software (Applied Biosystems, Foster City, CA, United States). Semi-quantitative expression analyses of RNA were performed by RT-PCR in triplicates under identical conditions using 18S rRNA as an internal control. Concentration, integrity, and extent of contamination by rRNA were monitored using the ND-1000 spectrophotometer (Thermo Fisher Scientific, Waltham, MA, United States). cDNA was prepared from the total RNA with qScript cDNA Synthesis Kit (Quantabio, Beverly, MA, United States) as described by the manufacturer. qRT-PCR was performed using Absolute SYBR Green ROX Mix (ABgene, Portsmouth, NH, United States) or Real Time SYBR Green FastMix ROX (Quantabio, Beverly, MA, United States) kits based on detection of SYBR Green binding to dsDNA. The reaction consisted of 5 μl cDNA, 10 μl SYBR Green mix, 1 μl forward primer (5 pmol), 1 μl reverse primer (5 pmol), and 3 μl double-distilled water (DDW). Reaction conditions were 2 min at 50°C, 15 min at 95°C, and 40 cycles of 15 s at 95°C followed by 1 min at 60°C.

Protein Extraction

Suspensions of BY-2 cells (5 ml) were centrifuged for 2 min at 4500 rpm at 4°C, and the pellet was quickly frozen with liquid nitrogen. The pellets were re-suspended in 1 ml homogenization buffer [100 mM HEPES pH 8.2, 0.05 mM Sodium Deoxycholate Detergent (Thermo Fisher Scientific, Waltham, MA, United States)] and the samples were sonicated in 3 watt (400,000 J) for 15 s × 4 (TPC-40, Telsonic, Switzerland). Then, samples were centrifuged at 4,500 rpm for 2 min at RT and the supernatant was collected. Protein concentration was determined using Bradford protein assay (Bio-Rad, Hercules, CA, United States) with bovine serum albumin (BSA) as a standard.

In-Gel Kinase Activity Assay

Cell suspension was exposed to BAP, a synthetic CK, for 1 h and were then subjected to salinity stress (50 mM NaCl) for one additional hour. Kinase activity assay was performed as previously described (Wu et al., 2007) using myelin basic protein (MBP) as a substrate which enabled measuring the phosphorylation activity of the selected kinases. In brief, equal amounts of proteins were separated on 10% SDS-polyacrylamid gel embedded with specific kinase substrate (0.5 mg/ml MBP for SIPK and WIPK, or 0.5 mg/ml histone for NtOSAK). After electrophoresis, the gels were washed three times for 30 min in washing buffer at RT. Then, the gel was treated with a re-naturing buffer and re-incubated in a reaction buffer containing 0.5 mM ATP (Sigma #A26209, St. Louis, MO, United States), with the addition of 50 mCi g-32P ATP (PerkinElmer, Waltham, MA, United States). Subsequently, the gels were transferred into stop solution for 5 h. After washing, the gels were dried on 3 mm Whatman paper and auto-radiographed on Fujifilm film. Finally, photos were obtained with Typhoon FLA 7000 (GE Healthcare, Chicago, IL, United States) phosphor imager system.

Immunoblotting

Western blot analysis was carried out as previously described (Ben-David et al., 1983), with protein ladder 10–180 kD

(Thermo Fisher Scientific, Waltham, MA, United States). Kinases were identified using specific antibodies reacting with protein extracts of BY-2 cell suspension (Seo et al., 2007; Wu et al., 2007). *WIPK* and *SIPK* (members of the MAPK family), are components of the ABA-independent pathway, and have been reported to be activated under abiotic stress (Mikolajczyk et al., 2000; Zhang et al., 2000; Seo et al., 2007). Antibodies against NtOSAK were generously donated by Prof. Grazyna Dobrowolska (Institute of Biochemistry and Biophysics, Polish Academy of Science, Warsaw, Poland), and antibodies against WIPK and SIPK were generously donated by Prof. Shigemi Seo (National Institute of Agrobiological Sciences, Tsukuba, Japan).

Phosphoproteomics

For phosphoproteomics analysis, proteins were isolated and sent to the Technion's Smoler protein center. The proteins were digested by trypsin and phosphopeptide enrichment was performed using TiO_2. The phosphopeptides were analyzed by LC-MS/MS on Q-exactive mass spectrometer (Thermo Fisher Scientific, Waltham, MA, United States). Data were analyzed with maxQuant 1.4.1.2 against Niben.genome.v0.4.4.proteins.wdesc database of *Nicotiana benthamiana* (Bombarely et al., 2012). Quantitative analysis was performed using Perseus software (Tyanova et al., 2016). Phosphopeptides with $p < 0.05$ were analyzed and their function was identified based on their gi number (Sequence Identifier) using NCBI-nr database.

Proline Quantification

Leaf samples (0.1 g) were frozen in liquid nitrogen and grinded. Thereafter, 1 ml of 3% sulfosalicylic acid was added, samples were centrifuged for 5 min at 14,000 rpm, supernatant was collected, and 0.25 ml from the supernatant were added to 2.75 ml of 3% sulfosalicylic acid, 3 ml acetic acid (glacial), and 3 ml 2.5% ninhydrin solution, mixed gently, and boiled at 100°C for 1 h. After cooling, 3 ml toluene was added to each sample. The samples were vortexed and incubated at RT overnight. The following day, the absorbance of 1 ml from the upper phase was read in spectrophotometer at 520 nm with toluene as reference. For quantification, a standard curve of L-proline (Sigma #P0380, St. Louis, MO, United States) was used.

Na^+ and K^+ Quantification by Optical Emission Spectrometry (ICP) Analysis

Mature, fully expanded, tobacco leaves were dried at 80°C for 2 days. The samples were grounded to fine powder with mortar and pestle. Powder samples (0.1 g each) were heated at 550°C overnight, and 2 ml 67% nitric acid was added. The samples were diluted to a final volume of 25 ml with DDW and were read in ICP, iCAP 6300 (Thermo Fisher Scientific, Waltham, MA, United States) against known standards.

Statistical Analysis

Statistical analysis was performed using GraphPad Prism 6 software (GraphPad Software, La Jolla, CA, United States). Data were analyzed using one tailed *t*-test; $p < 0.05$ was considered statistically significant.

RESULTS

We used two complementary approaches to investigate the effect of elevated CK levels on enhanced plant productivity under stress conditions: (A) developing transgenic tobacco plants carrying the *IPT* gene driven by a stress-induced promoter of the *MT* gene; and (B) applying exogenous CKs to elucidate the role of CKs in signal transduction of stress responses and the phosphoproteome of tobacco cells incubated under salinity stress.

The *MT* Promoter Contains Regulatory Elements Associated With Stress Response

We dissected the *MT* promoter sequence in order to understand the various elements associated with its activation and suppression. Approximately 1.3 Kb genomic sequence upstream of the *Arabidopsis MT* gene was selected as the region of the putative *MT* promoter (**Supplementary Figure S2**). We identified hypothetical stress-response *cis*-elements in the promoter sequence using PLACE software (Higo et al., 1999)[1]. The identified cis-elements included: eight ARR1 binding elements (5′-GATT-3′) corresponding to CK responses; two MYB recognition sites (5′-AACGG-3′, 5′-GGATA-3′) found earlier in the promoter of dehydration-responsive gene rd22; five MYC recognition sites (5′-CATGTG-3′, 5′-CACATG-3′ and 5′-CANNTG-3′) necessary for expression of ERD1 (early responsive to dehydration) (Simpson et al., 2003); two WRKY (5′-TGAC-3′) elements (Eulgem et al., 2000); four cupper response elements (5′-GTAC-3′) (Quinn et al., 2000); seven ACGT elements required for etiolation-induced expression of ERD1 (early responsive to dehydration); three GT-1 motifs (5′-GAAAAA-3′) that play a role in pathogen and salinity-induced gene expression (Park et al., 2004); and two anaerobic condition elements (5′-GTTTAGCAA-3′ and 5′-AAACAAA-3′) (Mohanty et al., 2005). These potential regulatory elements suggest that the *MT* promoter may respond to various stress conditions. The identified functional cis-elements that could be involved in the regulation of *MT* activation support possible roles in signaling via ABA (the presence of MYB elements), and are also associated with the response to CKs (ARR1). Notably, the cis-element response to different hormones suggests cross-talk between signaling pathways.

IPT

Expression of Transgenic Plants Carrying MT:IPT Under Various Stress Conditions

The selected stress-inducible promoter of *Arabidopsis MT* gene was isolated and fused to the *IPT* gene to produce pMT:IPT transgenic tobacco plants (**Supplementary Figure S1**). The transgenic plants were grown under optimal conditions for 3 weeks (16 h light, 8 h dark). During this period, no significant phenotypic differences were observed between WT and the transgenic tobacco plants. Afterward, the plants were

[1]http://www.dna.affrc.go.jp/PLACE

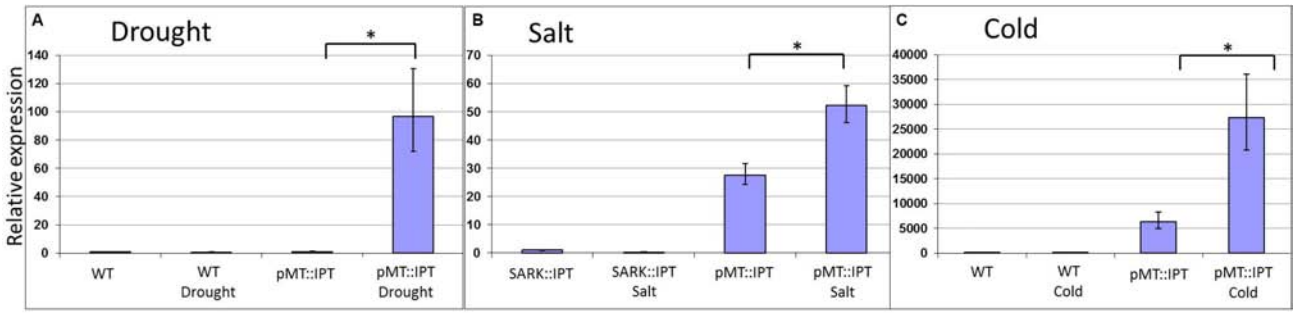

FIGURE 1 | Relative expression of *IPT* in transgenic pMT:IPT and WT in plants under drought **(A)**, salinity **(B)**, and cold **(C)** stress conditions as determined by real-time PCR (RT-PCR). Tobacco plants were grown under optimal conditions for 3 weeks, then they were subjected to cold stress of 4°C for a week. For salinity stress, plants were watered with NaCl solution (100 and then 200 mM) for three more weeks. For the drought-stress treatment, watering of mature tobacco plants was withheld for 3 weeks. Leaf samples were collected simultaneously from all plants (in three independent replicates). Gene expression was determined by RT-PCR. Gene expression in the WT plants under control conditions was used as a reference. Asterisk refers to statistically significant difference between treatments ($p < 0.05$). Values correspond to means ± SE of three independent experiments.

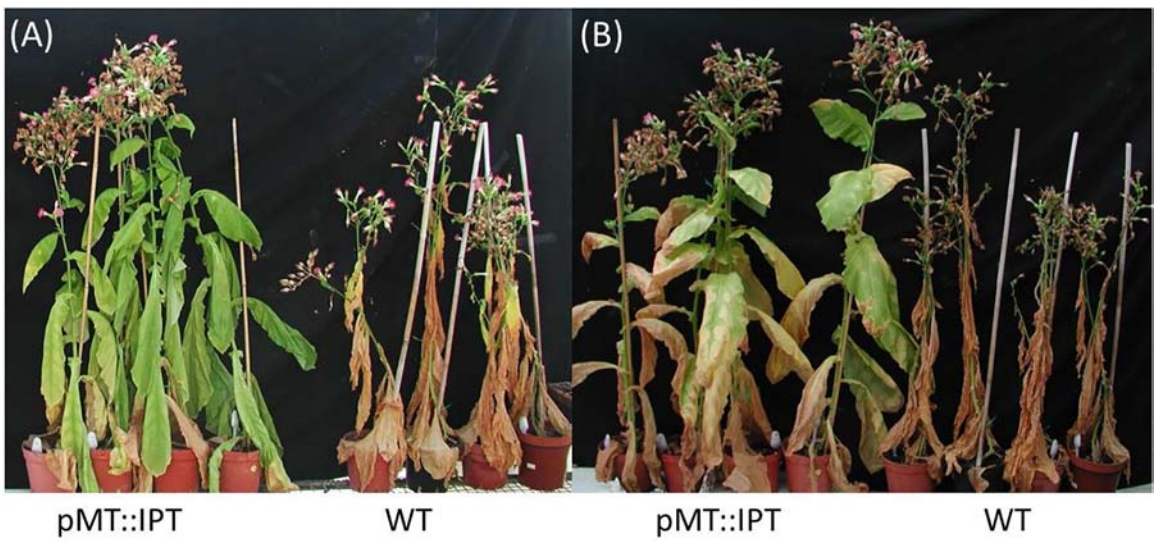

FIGURE 2 | Responses of transgenic pMT:IPT compared to WT plants during drought-stress treatment. Three-month old tobacco plants were subjected to a drought stress of 2 or 3 weeks. **(A)** Withholding watering for 2 weeks. **(B)** Three weeks of withholding watering followed by 1 week of re-watering. Pictures represent one of three independent experiments showing similar results.

subjected to drought and salinity-stress conditions, each in three independent replications. For the drought stress treatment, watering of mature tobacco plants was withheld for 3 weeks. Plants were subjected to salinity stress by irrigating with 300 mM NaCl solution for 3 weeks. The expression levels of the *IPT* gene in pMT:IPT transgenic plants was significantly higher under both abiotic stress conditions compared to non-stressed conditions (**Figure 1**), thereby validating the selective regulatory action of the *MT* promoter under these stress conditions.

pMT:IPT Plants Exhibit Drought Stress Tolerance

Mature transgenic pMT:IPT and WT plants were grown in a greenhouse under optimal conditions (25°C, 16 h light, and 8 h dark) for 3 months, and were then subjected to drought stress. Following 3 weeks of water withholding, WT plants wilted and turned yellow. In contrast, pMT:IPT plants exhibited partial turgor loss, yet, displayed reduced senescence and wilting symptoms (**Figure 2**). These results suggest a survival advantage for the transgenic CK overproducing plants in the field especially after short drought episodes.

The content of proline, known as an osmoprotectant, was determined in leaves of 3-month old plants. Tobacco plants subjected to drought stress conditions were analyzed for proline levels in three independent experiments. The colorimetric assay results indicated, that proline content increased dramatically, as expected, in WT plants under drought stress conditions probably due to enhanced proline biosynthesis (Bates et al., 1973). A minor increase in proline levels was detected in pMT:IPT

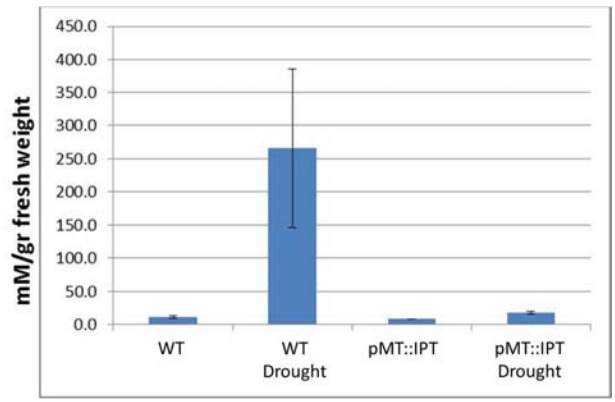

FIGURE 3 | Proline content in pMT:IPT and WT tobacco plants under drought stress. Proline content was determined in leaves taken from mature, 3-month old tobacco plants subjected to drought stress (water withholding for 3 weeks). Proline content was determined by colorimetric assay. Asterisk refers to statistically significant difference between treatments ($p < 0.05$). Values correspond to means ± SE of three independent experiments.

plants under stress conditions compared to non-stressed plants (**Figure 3**), further supporting the stress tolerance of transgenic pMT:IPT plants.

pMT:IPT Transgenic Exhibit High Tolerance to Salinity Stress Conditions

Abiotic stress tolerance of pMT:IPT plants to salinity stress was compared to that of pSARK:IPT and WT plants. Transgenic and WT plants were grown in the temperature- regulated green house for 3 weeks under optimal conditions (16 h light, 8 h dark). The plants were irrigated for three more weeks with salt solution (100 mM NaCl for the first 10 days and 200 mM NaCl for the following 11 days) until yellowing and wilting symptoms appeared in WT plants. Under these conditions, pSARK:IPT transgenic plants displayed mild yellowing, whereas the pMT:IPT plants stayed green (**Figure 4**) in all the three independent experiments. This observation suggests higher degree of salinity-stress tolerance of the pMT:IPT compared to SARK IPT plants.

In addition, pMT:IPT and WT plants were subjected to salinity stress (100 mM NaCl followed by 200 mM NaCl) for 3 weeks and then irrigated with tap water for recovery. The fast recovery of the transgenic pMT:IPT, as can be seen by the improved growth and biomass development already after 1 week (**Figures 5B,C**) whereas, WT plants grew much slower and did not seem to recover. These results emphasize the high salinity-stress tolerance of the pMT:IPT tobacco plants.

Next, Na^+ and K^+ levels were determined under salinity-stress conditions in both WT and pMT:IPT plants as well as under non-stressed conditions. A significant decrease in Na^+ content was detected in the foliage of pMT:IPT compared to WT plants (**Figure 6**), whereas no differences were observed between these plants under non-stressed conditions. A slight increase in K^+ content was found in pMT:IPT plants compared to WT plants under both conditions. Based on the observed reduction in Na^+ accumulation and the increase in the K^+/Na^+ homeostasis, we suggest that pMT:IPT plants maintain plant productivity under salinity stress.

Expression of Candidate Genes Under Stress Conditions

The expression levels of various candidate stress-related genes, in WT and in pMET:IPT plants under normal and salinity-stress conditions were analyzed. The selected candidate genes represent different pathways known to be related to abiotic stress responses: (1) Chaperones: the *NtERD10a* (Early Response to Dehydration) containing DRE/CRT element and belong to Group 2 of the LEA gene family (Kasuga et al., 2004), and *LEA5* that belongs to the same gene family known to maintain the cell membrane integrity under osmotic stress; (2) TFs: The tobacco *WRKY1*, the homolog of *Arabidopsis WRKY33* reported to respond to abiotic stresses in general and to salinity stress in particular (Jiang and Deyholos, 2009), and the *ERF3* (Ethylene responsive factor), an ethylene-related gene, which is known to be upregulated during salinity or drought stresses (Fujimoto et al., 2000; Song and Galbraith, 2006); and (3) Kinases: two MAPK components, *SIPK* and *WIPK* whose expression is known to be upregulated during abiotic stresses (Wu et al., 2007). As expected, all examined genes except *SIPK* were strongly expressed during stress in the WT plants (**Figure 7**), whereas, their expression

FIGURE 4 | Responses of transgenic compared to WT tobacco plants after salinity stress. Three-week old tobacco plants watered with NaCl solution (100 and then 200 mM) for 3 weeks. **(A)** WT plants, **(B)** pSARK:IPT plants, **(C)** pMT:IPT plants. The photo represents one of three independent experiments showing similar results.

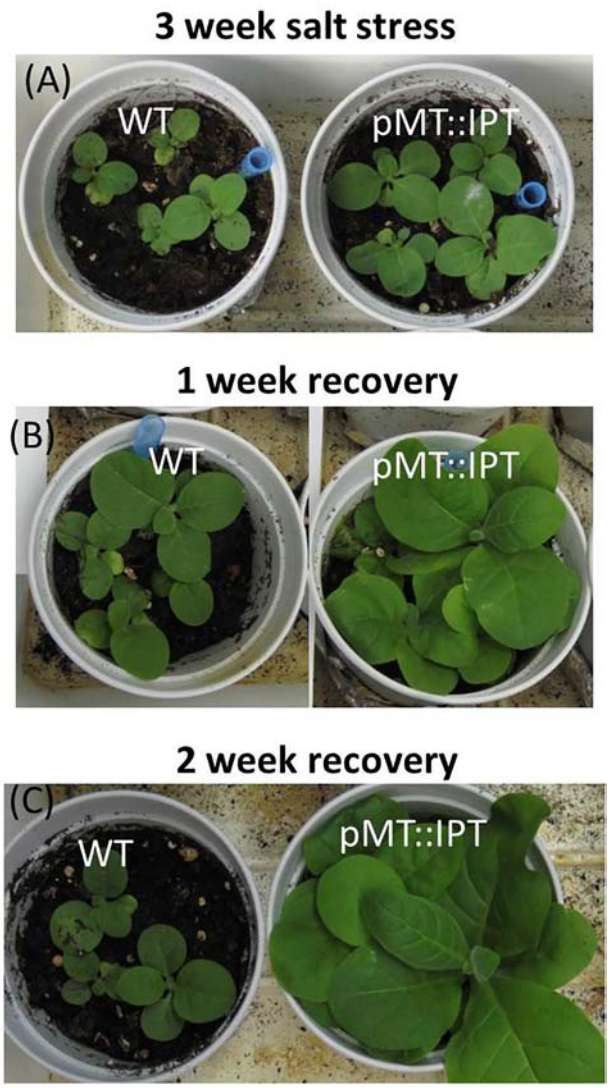

FIGURE 5 | Recovery of pMT:IPT compared to WT tobacco plants after salinity stress. Three week old tobacco plants watered with NaCl solution (100 and then 200 mM) for 3 weeks then transferred to normal watering for two additional weeks. Plants after: **(A)** salinity stress; **(B)** 1 week recovery; **(C)** 2 weeks of recovery. The photo represents one of three independent experiments showing similar results.

levels in the pMT:IPT plants were significantly reduced under the same salinity-stress conditions. *WRKY1* expression was lower in pMT:IPT under stress conditions compared to non-stressed plants. The expression level of *NtERD10a* and *ERF3* genes increased dramatically in WT plants when subjected to salinity stress. However the pMT:IPT plants exhibited lower expression levels under salinity conditions as compared to WT. No significant change in the expression pattern of *SIPK* was observed. These results indicate reversal of the reprograming of the stress responses by CK overproduction as reflected by lowering the expression of *LEA5*, *NtERD10a*, *ERF3*, *WRKY1*, and *WIPK* in pMET:IPT under stress conditions.

CKs Deactivate Components of the ABA-Dependent and Independent Pathways in Tobacco Cell Suspension Under Salinity Stress

Under conditions of osmotic stress, ABA is generally considered a stress hormone, and expression of stress-responsive genes in plants is primarily regulated by ABA-dependent and -independent pathways. Kinases are known to play a major role in transducing extracellular stimuli into intracellular responses and are rapidly activated following stress both through the ABA dependent and independent pathways. BY-2 tobacco cell suspensions enabled direct addition of the NaCl solution, easier penetration into cells, and faster response as compared to mature intact plant. Kinetic assay of the kinase activity was employed to track rapid changes occurring during signal transduction after adding the external stimuli. To assess the influence of CKs on the phosphorylation of the components of the MAPK kinase cascade (WIPK and SIPK), and on the NtOSAK, cells were exposed to BAP, a synthetic CK, for 1 h and were then subjected to salinity stress for one additional hour. Kinase activity was determined by in-gel kinase assay (Zhang and Klessig, 1997; Wu et al., 2007) using myelin basic protein as a substrate which enabled measuring the phosphorylation activity of WIPK, SIPK, or histone as a substrate for NtOSAK, the tobacco homolog of the SnRK2 protein kinases. Kinases were identified using specific antibodies reacting with protein extracts of BY-2 cell suspension (Seo et al., 2007; Wu et al., 2007). *WIPK* and *SIPK* (members of the MAPK family), are components of the ABA-independent pathway and have been reported to be activated under abiotic stress (Mikolajczyk et al., 2000; Zhang et al., 2000; Seo et al., 2007). Our results indeed confirmed their stress-induced activation, but also demonstrated reduced kinase activity during stress in tobacco cell suspension treated with exogenous CKs (**Figure 8**). Similar CKs inhibitory effects were demonstrated on the phosphorylation activity of the NtOSAK under salinity stress in the cell suspension incubated with BAP (**Figure 8**). The in-gel assay showed a clear reduced auto phosphorylation activity of the three identified kinases (WIPK, SIPK, and NtOSAK) as a result of adding BAP to the tobacco cells (**Figure 8**). These results suggest CK-dependent deactivation of the phosphorylation activity of kinases belonging to both ABA-dependent and -independent pathways acting under abiotic conditions.

Modifications in the Phosphoproteome of Stress Response by CKs

A range of post-translational modifications (PTMs) have been linked to plant stress responses. Of these modification, perhaps the most studied is protein phosphorylation, which influences development, metabolism, transcription, translation, proteolysis, homeostasis, and signaling (Hu et al., 2015). We analyzed the phosphoproteome of BY-2 tobacco cells under salinity stress to test the post-translational modifications and to further investigate the effect of CKs on the wide response of protein phosphorylation to the stimuli. Approximately 1547

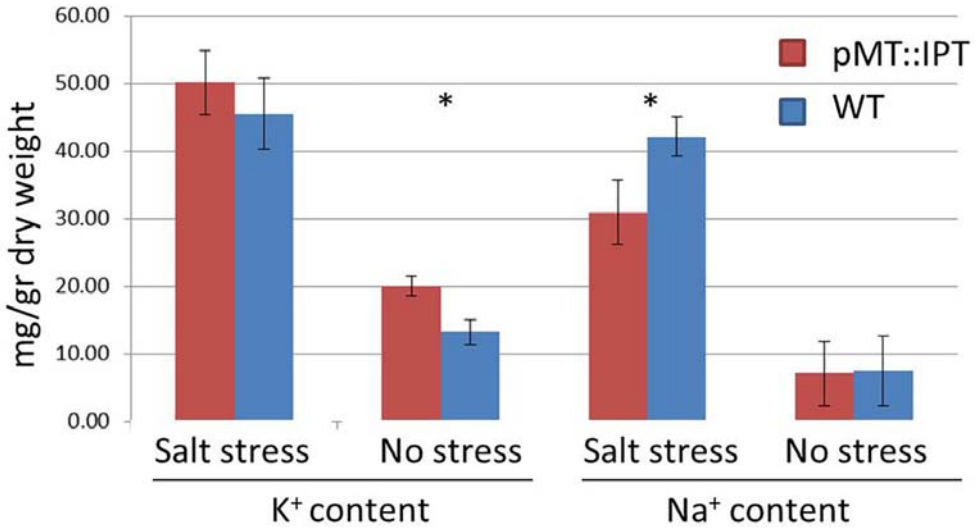

FIGURE 6 | Na^+ and K^+ content in pMT:IPT and WT tobacco plants under salinity stress and non-stressed conditions. Three-week old tobacco plants were watered with NaCl solution (100 and then 200 mM) for 3 weeks. Asterisk refers to statistically significant difference between treatments ($p < 0.05$). Values correspond to means ± SE of three independent experiments.

phosphopeptides were identified, collectively containing 1667 non-redundant phosphorylation sites. Of these sites, 83.8% were phosphorylated at serine residue, 13.5% at threonine, and 2.6% at tyrosine. The distribution of phosphor-Ser (pS), phosphor-Thr (pT), and phosphor-Tyr (pY) was consistent with that of *Arabidopsis* (Nakagami et al., 2010). Of the unique phosphopeptides, 1430 were singly phosphorylated, 105 were doubly phosphorylated, and 9 were phosphorylated at three sites. To identify the corresponding proteins of these phosphopeptides, we analyzed the data using MaxQuant versous database combined from *Nicotiana tabacum*, *Arabidopis thaliana, Solanum lycopersicum*, and *Solanum tuberosum*. The fold-change was calculated for each phosphopeptide. The total number of differentially changed phosphoproteins was 61 (>4-fold change, $p < 0.05$). Next, we analyzed their biological function. We were able to predict the identity and function of 26 proteins (**Table 1**). The remaining proteins were either unidentified proteins (23) or with unknown functions (13).

The identified phosphoproteins were classified by the biological processes of each gene product according to annotations in the NCBI databases. Among the proteins whose activity was reduced due to BAP addition during salinity stress, four are related to stress signal transduction, seven to stress response, and five to replication and translation. Thus, for 11 stress-related phosphoproteins, CKs lead to clearly reduced activation. Among the proteins whose activity was increased due to BAP addition during salinity stress, four are associated with defense of the photosynthetic system and antioxidant activity, two are related to stress responses, three are related to replication and translation, and two are related to cell division (**Table 1**). These results reinforce the preceding results that CKs reduce the response to stress conditions.

DISCUSSION

Stress-Inducible Promoter

Applying exogenous CKs as well as enhanced endogenous CK biosynthesis delay the process of plant aging (Gan and Amasino, 1995; Ha et al., 2012). The development of transgenic plants overexpressing CKs by inducible promoters linked to key genes of CK biosynthesis (such as *IPT*) offer a promising strategy to increase biomass and crop yield by delaying the natural senescence process. While we were studying the delayed aging behavior of the CK-overproducing transgenic tobacco plants (SARK-IPT), we forgot to water the transgenic plants unintentionally and to our surprise, they exhibited dramatic survival under these drought conditions (Rivero et al., 2007). This observation suggested that the phenomenon of CK-induced delayed senescence is also accompanied by an additional advantage of enhanced drought resistance and allowed us to suggest a novel technology for the development of drought-resistant plants (Gepstein et al., 2017). Since then, major crops, including rice, wheat, peanut, cotton etc, have been developed to overexpress CKs under stress conditions (see Hai et al., 2020).

In this study, we designed and developed auto-regulatory CK-overproducing transgenic tobacco plants by expressing the *IPT* gene under the control of a stress-inducible promoter of the *Arabidopsis MT2a* gene. It has been reported that although different signals such as biotic and abiotic environmental stress lead to initiation of stress-induced senescence due to distinct signal transduction pathways, they may share common execution events (Guo and Gan, 2012). We presume that a stress-inducible promoter would have an advantage over age-dependent promoter in the context of conferring synchronous seed set and appropriate harvest timing, which are crucial for best yields and post-harvest storage (Lukac et al., 2012). Choosing

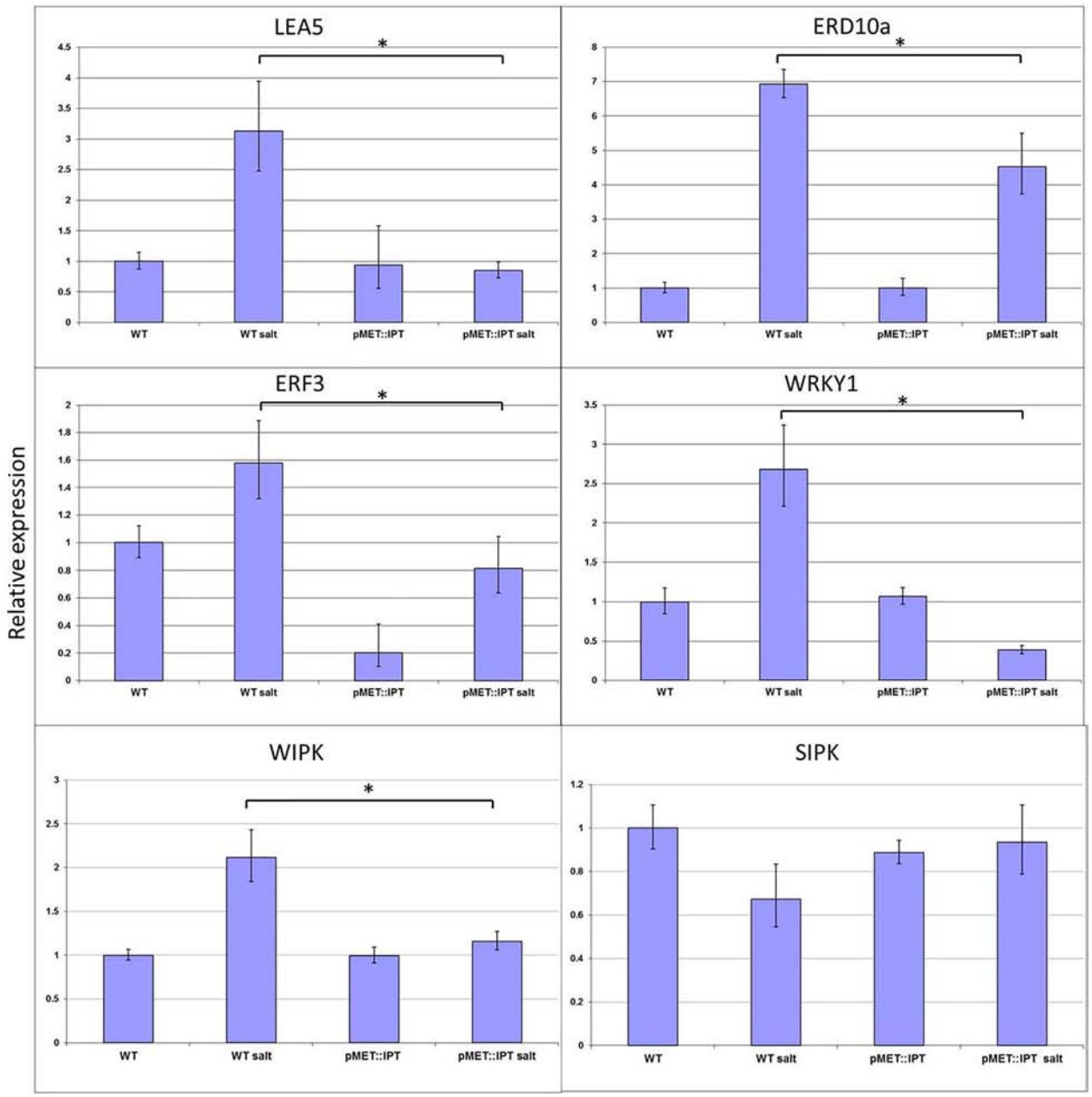

FIGURE 7 | Relative expression of *LEA5*, *ERD10a,* ERF3, *WRKY1*, *WIPK,* and *SIPK* genes in WT and pMT:IPT tobacco plants during salinity stress. Tobacco plants were grown under optimal conditions for 3 weeks and then were watered with NaCl solution (100 and then 200 mM) for three more weeks. Leaf samples were collected simultaneously from WT and pMT:IPT plants (in three independent replicates). Gene expression was determined by real-time PCR. Gene expression in the WT plants under control conditions serves as the reference. Asterisk refers to statistically significant difference between treatments ($p < 0.05$). Values correspond to means ± SE of three independent experiments.

the suitable promoter for auto-regulated CKs biosynthesis is critical for normal development of plants prior to the senescence stage (Ma, 2008). Constitutive overexpression of *IPT* under the transcriptional control of CaMV35S promoter showed developmental abnormality probably due to CK supraoptimal levels (Smart et al., 1991; Ma, 2008; Guo and Gan, 2012). pMT:IPT transgenic tobacco plants produced in the present study displayed normal development, but as expected, exhibited enhanced biomass under abiotic stress conditions. Since CK levels are known to decrease under abiotic stress conditions, and optimal CK levels are required for normal plant development, we assume that the *MT* promoter (in contrast to CaMV35S constitutive promoter) is a suitable promoter for driving the expression of *IPT* gene under stress conditions, as it resulted in enhancing CK biosynthesis up to the optimal levels for normal development.

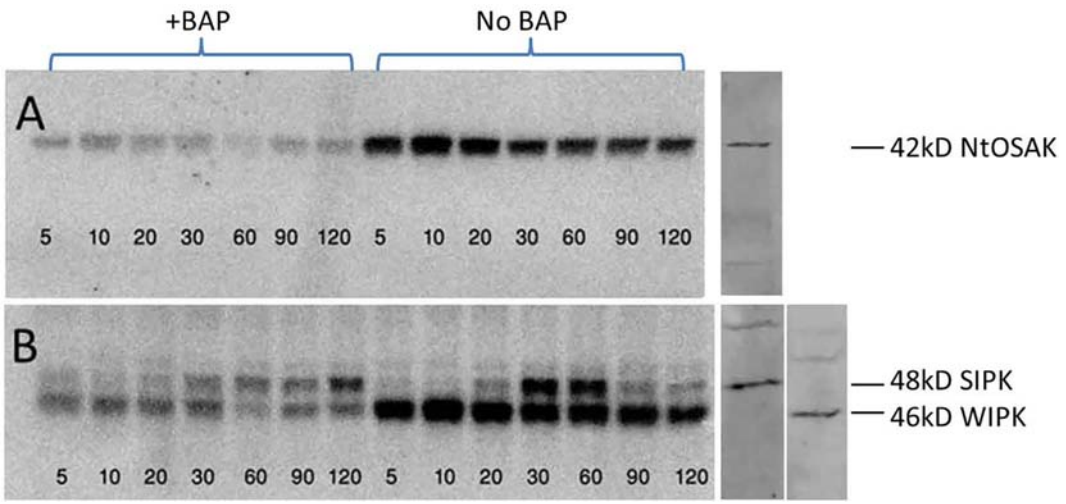

FIGURE 8 | SIPK, WIPK, and NtOSAK kinases activity during salinity stress. Tobacco BY-2 cells were grown for 5 days (at dark, 25°C). The suspension was divided into 250 ml flasks (50 ml suspension in each). After 1 h of pre-treatment incubation, NaCl was added to a final concentration of 50 mM and for the CKs treatments, 6-benzyloaminopurine (BAP), a synthetic CK, was added to final concentration of 10 μM. Samples were collected at indicated times (min). **(A)** In-gel phosphorylation activity of the histone substrate OSAK, and **(B)** phosphorylation of MBP by SIPK and WIPK. Protein ladder 10–180 kDa (Thermo Fisher Scientific, Waltham, MA, United States) was employed for MW estimation as described in "Materials and Methods" section. Kinases were identified by western blot analysis using specific antibodies (right panel) as described in "Materials and Methods" section.

Bioinformatics analysis of the *Arabidopsis MT* promoter suggests the presence of multiple cis-acting elements (**Supplementary Figure S2**). Among the identified cis-acting elements is the ACTG. Plant genome studies revealed that the sequence motif ACGT is functionally important in a variety of promoters that respond to different stimuli such as light, anaerobiosis, jasmonic acid, and hormones including salicylic acid (SA), ABA, and auxin. This core element is present at different relative positions in multiple copies upstream of the transcription start site (Rushton et al., 2010; Mehrotra et al., 2013).

Reprograming of Gene Expression in the CKs Overproducing Plants Under Stress Conditions

The role of CKs in the regulation of abiotic stress responses has been elucidated mainly during the last decade (Zwack and Rashotte, 2015; Hai et al., 2020). However, since, surprisingly, plants with exogenous CKs or biotechnological manipulation of CK endogenous levels demonstrated both positive and negative effects on the tolerance to abiotic stresses, generalizations about the effect of manipulating CK levels on overall stress tolerance are currently difficult to make (Zwack and Rashotte, 2015; Hai et al., 2020). Our studies based on employing the SARK or the MT promoter fused to the *IPT* gene clearly demonstrated positive effect on growth and biomass production under abiotic stresses in model plants such as *Arabidopsis* and tobacco as well in major crops such as rice, wheat, cotton, etc. (see Gujjar and Supaibulwatana, 2019; Hai et al., 2020). Similar positive regulation of drought stress by CKs has been reported also for transgenic plants containing the SAG12 promoter fused to the *IPT* gene (Merewitz et al., 2010; Zhang et al., 2010). In apparent contrast to these findings, *Arabidopsis IPT* mutants, which have rather reduced CK levels, are also more drought resistant compared to WT (Nishiyama et al., 2011). Decreased CK levels achieved by overproduction of the CK-degrading enzyme CK oxidase (CKX) in either a constitutive or root-specific manner, also have a positive effect on drought-stress tolerance (Werner et al., 2010; Nishiyama et al., 2011; Mackova et al., 2013). Plants lacking two CK receptors have enhanced tolerance to drought treatment as well as increased sensitivity to ABA (Tran et al., 2007), suggesting that these receptors and presumably also the downstream output of the CK signal negatively impact drought tolerance. Thus, CK-mediated plant tolerance to drought could be achieved through two seemingly contradictory approaches. This is probably due to the choice of promoter and type of tissue modulated for transgene expression, which led to the regulation of different pathways. Our findings, which led us to the present hypothesis of desensitization of environmental cues followed by CK-dependent reprograming of gene expression under stress is aligned with the positive regulation approach of stress tolerance.

Our data indicate that the stress-induced CK overproduction in the pMT-IPT transgenic plants altered the regular pattern of stress-induced growth inhibition to a more moderated mode of inhibition. To elucidate the molecular events associated with CK influence on plant stress responses, we examined some candidate genes known to be involved in different stress-responsive pathways. Expression levels of selected candidate genes reported to be upregulated under stress conditions (Ingram and Bartels, 1996; Kasuga et al., 2004; Hundertmark and Hincha, 2008), displayed opposite results. The general expression pattern of most of the examined stress-related candidate genes in the present study is characterized by lower expression in the transgenic plants

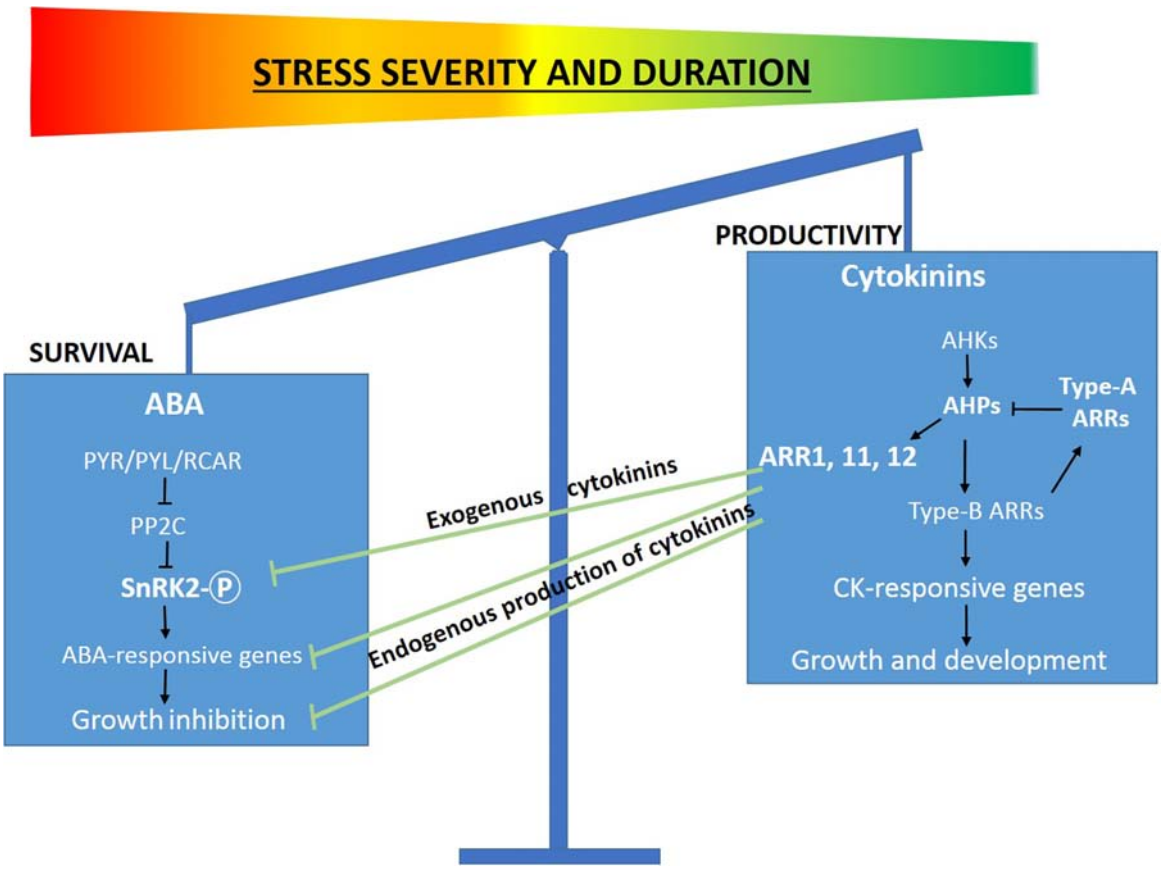

FIGURE 9 | The balance between stress tolerance and productivity modes is reflected by the antagonistic action of ABA and CK signaling. Schematic representation of the working model demonstrating the regulatory role of CKs in promoting productivity under abiotic stress by inactivating SnRK2 the key component of ABA signaling pathway. Under stress conditions, CKs inactivate SnRK2 and inhibit ABA signaling pathway and the downstream upregulation of stress related genes and growth promotion via CK-responsive genes. The model suggests a molecular mechanism underlying the behavior of CK over-expressing transgenic plants under mild abiotic stress conditions for short periods. This model has been partially adapted from Claeys and Inze (2013).

as compared to WT plants exposed to identical environmental stress conditions (**Figure 7**). *LEA5* and *ERD10a* both belong to group 2 of the LEA family. *LEA5* maintains the cell membrane under osmotic stress (Ingram and Bartels, 1996; Hundertmark and Hincha, 2008). *ERD10a* is induced by DREB1 and it is upregulated during stress (Kasuga et al., 2004). It is thought to be a chaperone that defends the cell from aggregation or inactivation of different elements (Kovacs et al., 2008). The expression of these genes was lower in transgenic plants compare to WT under stress conditions. The results of the present study are consistent with our previous experiments describing the transcriptomic analysis of CK-overexpressing *Arabidopsis* plants (Golan et al., 2016). It has been shown that under salinity stress CK triggered transcriptional reprograming that resulted in attenuation of gene clusters related to stress-dependent inhibition of growth and delayed premature plant senescence. In contrast, elevated CK levels led to stress tolerance by retaining the expression of gene clusters associated with plant growth and metabolism whose expression typically decreases under stress conditions (Golan et al., 2016). Since several known pathways related to abiotic stress plant responses are regulated by various plant hormones, it would not be surprising to reveal contradicting results related to expression patterns of specific genes. Gupta et al. showed that genes associated with abiotic environmental stresses were differentially induced by CKs which is not consistent with previous reports (Gupta et al., 2013). The peroxidases, several of which were found to be repressed while others were found to be induced by CKs indicate a complex role for CKs in the regulation of abiotic stress related responses (Passardi et al., 2005).

Signal Transduction of Environmental Stress Stimuli

Plants as non-mobile organisms constantly integrate varying environmental signals to flexibly adapt their growth and development. Local fluctuations in water, sudden changes in other abiotic factors, and stresses can trigger changes in the growth of plant organs. The molecular backbones of signaling cascades of individual hormones have been established; however, it is well accepted now that multiple mutually interconnected hormonal signaling cascades act as essential endogenous translators of these exogenous signals in the adaptive responses

TABLE 1 | Identified phosphoproteins of the BY-2 cells under salinity stress[a].

Protein name	Function	Biological process	Sequence identifier[b]
De-activated stress-related phosphoproteins are due to CK			
MAPK16	MAP kinase cascade	Stress signals	gi565404224
PBL	Disease immune response	Stress signals	gi565396124
MKP1	MAP kinase phosphatase	Stress signals	gi37951311
ERS	Suppress ethylene response	Stress signals	gi7652766
eIF4A	RNA helicase	Replication and translation	gi485943
SR	Pre-RNA splicing	Replication and translation	gi440135805
Histone H3	Mitosis and meiosis	Replication and translation	gi218744593
DNA topoisomerase II	dsDNA replication	Replication and translation	gi26984168
Nucleolin	Cell division	Replication and translation	gi21700195
Histone H1	Mitosis and meiosis	Replication and translation	gi90654966
extracellular cationic peroxidase	Response to ROS and stress	Stress response	gi575603
A/N-InvD	Cytoplasmic neutral invertase	Stress response	gi671775156
NF-Yb-10	Nuclear factor Y Transcription Factors Respond to Abiotic Stress	Stress response	gi565392153
Chl-PGK	Chloroplastic Phosphoglycerate kinase – photorespiration	Stress response	gi298541491
AHA	H^+ ATPase – regulate cytosolic pH under stress	Stress response	gi9789539
GST	Glutathionine S-transferase, oxidative stress responses	Stress response	gi676880
NDPK2	Nucleotide diphosphate kinase 2, reduces accumulation of H_2O_2	Stress response	gi565361307
PEPC	Participate in plants responses to limited water supply	Stress response	gi565363147
PBS1-like	Plant immune response	Stress response	gi460387273
Activated stress-related phosphoproteins are due to CK			
cycD3-1	Cell divisions	Cell divisions	gi568214824
Histone deacetylase	Histone deacetylase, gene repression	Replication and translation	gi269969916
Ribosomal protein s6	Regulating cellular metabolism and protein synthesis	Replication and translation	gi82623405
Trehalose-6-P Synthase	Regulator of Glucose, Abscisic Acid, and Stress Signaling	Stress response	gi565396921
CPL	Repress stress-response genes	Stress response	gi460401650
MCM	DNA replication	Replication and translation	gi311819860
Centrin	Cell divisions	Cell divisions	gi6358511

[a]*BY-2 cells were pre-incubated with 10 μM BAP for 1 h, followed by 30 min of 50 mM NaCl treatment.* [b]*NCBI GenInfo identifier (gi).*

of plants (Verma et al., 2016). Hormonal pathways connected via multiple levels of interactions form powerful regulatory networks that sensitively react to changes in the environment and drive the relevant adaptive responses (Verma et al., 2016). Upon sensing environmental stresses, plants sacrifice growth and activate protective stress responses such as the avoidance syndrome. These include transcriptional changes, phytohormone synthesis and degradation, and finally the direct/indirect molecular defense mechanisms that are translated into developmental and morphological changes. Kinase (including MAPK) cascade is a conserved signaling pathway involved in modulating many cellular responses in all eukaryotes and plays a major role in transducing the extracellular stimuli into intracellular responses. Accumulated evidence indicates that in plants, MAPKs also regulate TFs at both transcription and protein activity levels. The SA-induced protein kinase (SIPK) of tobacco, which is a MAPK, is activated by various biotic and abiotic treatments and has been found to phosphorylate the transcription factor WRKY1 (Menke et al., 2005). In Addition, the involvement of *SIPK*/*WIPK* has been demonstrated in the cell death signaling pathway mediated by phosphorylation of WRKY1 in tobacco plants (Ogata et al., 2015). In general, plant hormones affect similar processes but their signaling pathways act non-redundantly and their signals are integrated at the gene network level (Jaillais and Chory, 2010). Since the interplay between hormone levels and signaling networks plays a crucial role in the trade-off between plant growth and stress adaptation, the antagonistic relationship between ABA and CK signaling should be considered in the context of stress responses. Recent studies provides several lines of evidence showing crosstalk between ABA and CK signaling under abiotic stresses (Huang et al., 2018). Our results emphasizing the inhibitory effect of CKs on the phosphorylation of NtOASK, a homolog of the SNF1-related protein kinases (SnRK2) the key kinase of the ABA signaling pathway. These results are consistent with the study demonstrating that SnRK2 directly interacts with and phosphorylates type-A response regulator 5 (ARR5), a negative regulator of CK signaling (Huang et al., 2018). The results of the kinetic experiments of kinase activities as viewed in the in-gel kinase activity system, suggest a dramatic negative influence of CKs on the rate of phosphorylation of several components of the kinase cascade that are known to be activated under stress conditions. Similar in-gel kinase activity was performed in *Nicotiana attenuata* and the identity of each of the kinases was validated by specific antibodies in a Western blot analysis (Wu et al., 2007). Activity of NtOASK, SIPK, and WIPK was dramatically reduced

by adding exogenous CKs under salinity stress (**Figure 8**), which may indicate suppression of at least several components of the signal transduction of environmental stress cues. In addition, our previous gene expression study suggested that the major regulatory ABA signaling component *SnRK2.3* was among the genes whose expression increased under salinity stress and was attenuated by CK (Golan et al., 2016). The present results confirm previous studies that demonstrated that NtOSAK (*Nicotiana tabacum* osmotic stress-activated protein kinase), a member of the SnRK2 subfamily, is being activated rapidly in response to hyperosmotic stress (Burza et al., 2006). The elevated phosphorylation activity of NtOSAK due to salinity- stress conditions was reduced upon the addition of CKs (**Figure 8**). Taken together, not only the NtOSAK phosphorylase activity is dramatically reduced by CKs, the transcription of its *Arabidopsis* homolog gene *SnRK2* is reduced as well (Golan et al., 2016).

We hypothesize that the antagonistic inputs of ABA and CKs balance the survival mode of growth inhibitory responses and allow the productivity mode required for biomass production (**Figure 9**). Several molecular components of the ABA and CK signaling pathways have been shown to mediate drought stress response and suggest possible regulatory mechanisms responsible for coordinating growth and stress responses. A suggested model depicts how ABA and CKs antagonistically regulate growth processes and environmentally stress responses (Claeys and Inze, 2013). Our assumption that CKs reduce the stress-induced growth and productivity inhibition by desensitization of environmental cues is partially based on the reduced phosphorylation activity of MAPK signaling components (WIPK, SIPK) and of the major component of the core ABA signaling pathway (SnRK2).

Phosphoproteome of the CK-Overproducing Plants Under Abiotic Stress

Protein phosphorylation is a widely used mechanism of post-translational modification that controls the protein activity, stability, turnover, subcellular localization, and interaction with partner proteins including signal transduction of external stimuli. Plant growth adjustment during water deficit is a crucial adaptive response. The rapid fine-tuned control achieved at the post-translational level is believed to be of considerable importance for regulating early changes in plant growth reprogramming. ABA-dependent and -independent pathways are responsible for activating many of plant responses to abiotic stresses including post- translational modifications (Zhu, 2016). In the core ABA signaling pathway, ABA binding to the PYL family of receptors causes the receptor to interact with and inhibit the PP2Cs, leading to release of suppression and activation of the SnRK2s. SnRK2 phosphorylates at least several dozens of downstream effector proteins of ABA action. These phosphorylated effector proteins function in regulating gene expression at various steps, including epigenetic and transcription factor regulation, RNA splicing, and mRNA cleavage or translational repression by miRNAs (Zhu, 2016). Aiming at a better understanding of the CKs influence on the responses to salinity stress in tobacco cells, we carried out a survey of protein phosphorylation events following the addition of exogenous CKs. Adding CKs during salinity stress caused extensive changes in phosphorylation status in critical regulators that are either directly or indirectly involved in plant growth and development (**Table 1**). Among the identified proteins whose activity was reduced due to BAP addition during salinity stress, were those related to major pathways of stress signal transduction, stress responses, and replication and translation. Among the proteins whose phosphorylation status was increased due to BAP addition during salinity stress, were those associated with defense of the photosynthetic system, antioxidant activity, stress responses, replication and translation, and cell division. The systematic phosphoproteomic study related to plant defense mechanisms under abiotic stress could complement the molecular genetic studies and provide novel insights into mechanisms related to post-translational modifications. Our study indicates that alterations in protein phosphorylation may be the result of the elevation in CKs levels and support our notion related to CK role in sustaining growth under abiotic stress as demonstrated in our present and previous study at the level of gene transcription (Golan et al., 2016).

Desensitization of Stress Cues Prevents the Avoidance Syndrome Under Stress Conditions

Plants have evolved the stress avoidance strategy to cope with harsh environmental conditions and to avoid fatal damage of plants. Avoiding extinction is driving the evolution of genes that control growth in threatening stress environments. The stress avoidance strategy is translated in annual plants into reduced vegetative growth, early flowering, accelerated senescence, and fast seed set. The obvious advantage is the survival of plants under environmental stress but it is also accompanied by an enormous reduction in plant productivity. Growth inhibition as a dominant response feature results from being exposed to stress due to the genetic programs that have been adjusted to the external circumstances and are geared toward a survival rather than productivity. While altering the expression of regulators of drought responses has often succeeded in enhancing drought tolerance, at least under laboratory conditions, this usually comes at the cost of growth inhibition, resulting in a significant yield penalty (Yang et al., 2010). Similarly, breeding for enhanced water use efficiency leads to impaired plant productivity (Blum, 2009). Hormones mediate the trade-off between plant growth and stress tolerance throughout the life of the plant (Bohnert et al., 1995). Of special interest is the balance between maintained growth on one hand and ensured survival on the other hand. However, most of the breeding programs and genetic engineering have not succeeded to genetically remove these stress responses because they are polygenic and redundantly programmed (Claeys and Inze, 2013; Maggio et al., 2018). Understanding the molecular basis of these trade-offs would provide novel breeding strategies to optimize crop yield (Claeys and Inze, 2013; Huang et al., 2018). Despite these shortcomings, evidence of drought-tolerant crops are being accumulated reviewed in Huang et al. (2018).

Our results demonstrated the striking phenomenon that CKs allow plants to sustain growth even under unfavorable stress conditions. CKs reprogram plants from the survival mode which is fundamentally based on deactivation of the growth mode to a productive mode. The CK-induced inactivation of the kinase cascade components of the stress signal transduction (**Figure 8**) might explain the prevention of the expression of stress-related genes (**Figure 7**) and possibly the reduction in the level of the stress-induced phosphoproteomics (**Table 1**). Our study suggests that CKs cause desensitization of the environmental cues and as a result prevent the activation of the known avoidance mechanisms and consequently allow sustainable growth and productivity under stress conditions. Plants including high-yield crops react over-cautiously to stress conditions and as a result over-reduce growth to be able to survive stresses for a period of time much longer than a cropping season (Maggio et al., 2018). We hypothesize that we improved yield under stress conditions by removing the premature alarms (stress stimuli) that trigger growth reduction and other unproductive responses. Our results demonstrate that under abiotic stress, CKs antagonize ABA signaling pathway by inactivating NtOASK, a family member of the SnRK2, a key component of the ABA signaling pathway and as a result prevent the ABA-dependent growth arrest (**Figures 8**, **9**). However, under the same conditions, CKs activate the known CK signaling pathway and promote plant growth and productivity. These results are consistent with our *Arabidopsis* transgenic plants demonstrating growth maintenance even under stress conditions (Golan et al., 2016). This may be true for most crops grown under mild stress conditions for a short cropping season (**Figure 9**). Although our experiments were performed not under mild stress, they exhibit this phenomenon probably due to the short period experimentation. However, this manipulation will not solve the problem of growing crops under severe stresses for long periods where the avoidance is required for survival (Claeys and Inze, 2013; Maggio et al., 2018). Our present study performed with tobacco plants supports and supplements our previous conclusions in a study carried out in *Arabidopsis* (Golan et al., 2016), where we showed that CK-dependent desensitization of the stress environmental stimuli might reduce the over sensitivity of plants and allow plants to avoid the evolutionary based avoidance syndrome.

CONCLUSION

We have shown that cytokinins-overexpressing plants regulated by senescence or stress-specific promoter, maintain growth and productivity under abiotic stresses due to desensitization of stress environmental stimuli. We hypothesize that CKs allow sustainable plant growth under unfavorable environmental conditions by deactivating key kinases belonging to the signal transduction of the environmental cues and downstream processes leading to prevention of gene expression related to premature senescence and growth inhibition under stress conditions. Manipulated plants seem to avoid the evolutionary-based avoidance plant strategy and change their survival mode of growth inhibition into productivity mode under stress conditions. This approach, based on the autoregulation of CK biosynthesis, may serve as a generic technology for developing various crops for improved productivity and yield under mild environmental stresses.

Nucleotide Accession Numbers

Nucleotide sequence of MET:IPT_NOS promoter was submitted to the GenBank database under accession number MN862698.

DATA AVAILABILITY STATEMENT

The mass spectrometry proteomics data have been deposited to the ProteomeXchange Consortium via the PRIDE partner repository with the dataset identifier PXD019418.

AUTHOR CONTRIBUTIONS

All authors contributed extensively to the work presented in this paper. AA performed most of the experiments. YeG collected the data and did the bioinformatics analysis. NS established the system of the BY-2 suspension cells. YS carried out promoter isolation and prepared the construct. YaG performed the salinity stress experiments. YD-P assisted with the plant growth experiments and writing the manuscript. SG provided direction and guidance for this project and did the critical revision of the article.

FUNDING

This work was supported by the Nancy and Stephen Grand Technion Energy Program (GTEP), and comprises part of the Leona M. and Harry B. Helmsley Charitable Trust reports on Alternative Energy series of the Technion, Israel Institute of Technology, and the Weizmann Institute of Science. This research was also supported by the I-CORE (Israeli Centers for Research Excellence) Program of the Planning and Budgeting Committee and The Israel Science Foundation.

ACKNOWLEDGMENTS

We thank Dr. Avital Bareket-Samish for editing and critically reading the manuscript, the Smoler Proteomics Center, the Technion, for phosphoproteomics analysis and for assistance in uploading the data.

SUPPLEMENTARY MATERIAL

The Supplementary Material for this article can be found online at: https://www.frontiersin.org/articles/10.3389/fpls.2020.00879/full#supplementary-material

FIGURE S1 | Nucleotide sequence of the metallothionein (Metallo) promoter-IPT-NOS terminator construct. MET::IPT NOS 2334 bp:

The metallothionein promoter nucleotides 1–1300 (blue letters); the IPT coding sequence nucleotides 1301–2100 (black letters); and the NOS terminator nucleotide 2101–2334 (red letters)(Gepstein, 2013). GenBank accession number MN862698.

FIGURE S2 | Nucleotide sequence of metallothionein (MT) promoter. Highlight regions correspond to (1) MYC recognition sites (green); (2) ARR1 binding elements (yellow); (3) cupper response elements (double underlined); (4) WRKY elements (blue); (5) ACGT elements (red); (6) GT-1 motifs (grey); (7) MYB recognition sites (violet); and (8) anaerobic condition elements (teal).

TABLE S1 | Real-time PCR primers used for quantification of stress related gene expression.

REFERENCES

Avila-Ospina, L., Moison, M., Yoshimoto, K., and Masclaux-Daubresse, C. (2014). Autophagy, plant senescence, and nutrient recycling. *J. Exp. Bot.* 65, 3799–3811. doi: 10.1093/jxb/eru039

Bates, L. S., Waldren, R. P., and Teare, I. D. (1973). Rapid determination of free proline for water-stress studies. *Plant Soil* 39, 205–207. doi: 10.1007/Bf00018060

Ben-David, H., Nelson, N., and Gepstein, S. (1983). Differential changes in the amount of protein complexes in the chloroplast membrane during senescence of oat and bean leaves. *Plant Physiol.* 73, 507–510. doi: 10.1104/pp.73.2.507

Blum, A. (2009). Effective use of water (EUW) and not water-use efficiency (WUE) is the target of crop yield improvement under drought stress. *Field Crops Res.* 112, 119–123. doi: 10.1016/j.fcr.2009.03.009

Bohnert, H. J., Nelson, D. E., and Jensen, R. G. (1995). Adaptations to environmental stresses. *Plant Cell* 7, 1099–1111. doi: 10.1105/tpc.7.7.1099

Bombarely, A., Rosli, H. G., Vrebalov, J., Moffett, P., Mueller, L. A., and Martin, G. B. (2012). A draft genome sequence of *Nicotiana benthamiana* to enhance molecular plant-microbe biology research. *Mol. Plant Microbe Interact.* 25, 1523–1530. doi: 10.1094/MPMI-06-12-0148-TA

Burza, A. M., Pekala, I., Sikora, J., Siedlecki, P., Malagocki, P., Bucholc, M., et al. (2006). *Nicotiana tabacum* osmotic stress-activated kinase is regulated by phosphorylation on Ser-154 and Ser-158 in the kinase activation loop. *J. Biol. Chem.* 281, 34299–34311. doi: 10.1074/jbc.M601977200

Chang, H., Jones, M. L., Banowetz, G. M., and Clark, D. G. (2003). Overproduction of cytokinins in petunia flowers transformed with PSAG12-IPT delays corolla senescence and decreases sensitivity to ethylene. *Plant Physiol.* 132, 2174–2183. doi: 10.1104/pp.103.023945

Chaturvedi, A. K., Patel, M. K., Mishra, A., Tiwari, V., and Jha, B. (2014). The SbMT-2 gene from a halophyte confers abiotic stress tolerance and modulates ROS scavenging in transgenic tobacco. *PLoS One* 9:e111379. doi: 10.1371/journal.pone.0111379

Chernyad'ev, I. I. (2005). Effect of water stress on the photosynthetic apparatus of plants and the protective role of cytokinins: a review. *Appl. Biochem. Microbiol.* 41, 115–128. doi: 10.1007/s10438-005-0021-9

Claeys, H., and Inze, D. (2013). The agony of choice: how plants balance growth and survival under water-limiting conditions. *Plant Physiol.* 162, 1768–1779. doi: 10.1104/pp.113.220921

Cramer, G. R., Urano, K., Delrot, S., Pezzotti, M., and Shinozaki, K. (2011). Effects of abiotic stress on plants: a systems biology perspective. *BMC Plant Biol.* 11:163. doi: 10.1186/1471-2229-11-163

Cutcliffe, J. W., Hellmann, E., Heyl, A., and Rashotte, A. M. (2011). CRFs form protein-protein interactions with each other and with members of the cytokinin signalling pathway in Arabidopsis via the CRF domain. *J. Exp. Bot.* 62, 4995–5002. doi: 10.1093/jxb/err199

Cutler, S. R., Rodriguez, P. L., Finkelstein, R. R., and Abrams, S. R. (2010). Abscisic acid: emergence of a core signaling network. *Annu. Rev. Plant Biol.* 61, 651–679. doi: 10.1146/annurev-arplant-042809-112122

Debbarma, J., Sarki, Y. N., Saikia, B., Boruah, H. P. D., Singha, D. L., and Chikkaputtaiah, C. (2019). Ethylene response factor (ERF) family proteins in abiotic stresses and CRISPR-Cas9 genome editing of ERFs for multiple abiotic stress tolerance in crop plants: a review. *Mol. Biotechnol.* 61, 153–172. doi: 10.1007/s12033-018-0144-x

Dong, T., Park, Y., and Hwang, I. (2015). Abscisic acid: biosynthesis, inactivation, homoeostasis and signalling. *Essays Biochem.* 58, 29–48. doi: 10.1042/bse0580029

Du, H., Huang, F., Wu, N., Li, X., Hu, H., and Xiong, L. (2018). Integrative regulation of drought escape through ABA-dependent and -independent pathways in rice. *Mol. Plant* 11, 584–597. doi: 10.1016/j.molp.2018.01.004

Edel, K. H., and Kudla, J. (2016). Integration of calcium and ABA signaling. *Curr. Opin. Plant Biol.* 33, 83–91. doi: 10.1016/j.pbi.2016.06.010

Eulgem, T., Rushton, P. J., Robatzek, S., and Somssich, I. E. (2000). The WRKY superfamily of plant transcription factors. *Trends Plant Sci.* 5, 199–206. doi: 10.1016/s1360-1385(00)01600-9

Finkelstein, R., Reeves, W., Ariizumi, T., and Steber, C. (2008). Molecular aspects of seed dormancy. *Annu. Rev. Plant Biol.* 59, 387–415. doi: 10.1146/annurev.arplant.59.032607.092740

Fujimoto, S. Y., Ohta, M., Usui, A., Shinshi, H., and Ohme-Takagi, M. (2000). Arabidopsis ethylene-responsive element binding factors act as transcriptional activators or repressors of GCC box-mediated gene expression. *Plant Cell* 12, 393–404. doi: 10.1105/Tpc.12.3.393

Fujita, Y., Yoshida, T., and Yamaguchi-Shinozaki, K. (2013). Pivotal role of the AREB/ABF-SnRK2 pathway in ABRE-mediated transcription in response to osmotic stress in plants. *Physiol. Plant.* 147, 15–27. doi: 10.1111/j.1399-3054.2012.01635.x

Gan, S., and Amasino, R. M. (1995). Inhibition of leaf senescence by autoregulated production of cytokinin. *Science* 270, 1986–1988. doi: 10.1126/science.270.5244.1986

Gepstein, S. (2013). *Nucleic Acid Construct for Increasing Abiotic Stress Tolerance in Plants*. U.S. Patent No. 13/810246. Washington, DC: U.S. Patent and Trademark Office.

Gepstein, S., Gepstein, A., and Blumwald, E. (2017). *Drought-Resistant Plants*. U.S. Patent No. US-9624503. Washington, DC: U.S. Patent and Trademark Office.

Gepstein, S., and Glick, B. R. (2013). Strategies to ameliorate abiotic stress-induced plant senescence. *Plant Mol. Biol.* 82, 623–633. doi: 10.1007/s11103-013-0038-z

Gepstein, S., Sabehi, G., Carp, M. J., Hajouj, T., Nesher, M. F. O., Yariv, I., et al. (2003). Large-scale identification of leaf senescence-associated genes. *Plant J.* 36, 629–642. doi: 10.1046/j.1365-313X.2003.01908.x

Gepstein, S., and Thimann, K. V. (1980). Changes in the abscisic acid content of oat leaves during senescence. *Proc. Natl. Acad. Sci. U.S.A.* 77, 2050–2053. doi: 10.1073/pnas.77.4.2050

Golan, Y., Shirron, N., Avni, A., Shmoish, M., and Gepstein, S. (2016). Cytokinins induce transcriptional reprograming and improve Arabidopsis plant performance under drought and salt stress conditions. *Front. Environ. Sci.* 4:63. doi: 10.3389/fenvs.2016.00063

Gregersen, P. L., Culetic, A., Boschian, L., and Krupinska, K. (2013). Plant senescence and crop productivity. *Plant Mol. Biol.* 82, 603–622. doi: 10.1007/s11103-013-0013-8

Gujjar, R. S., and Supaibulwatana, K. (2019). The mode of cytokinin functions assisting plant adaptations to osmotic stresses. *Plants* 8:542. doi: 10.3390/plants8120542

Guo, Y., and Gan, S. S. (2012). Convergence and divergence in gene expression profiles induced by leaf senescence and 27 senescence-promoting hormonal, pathological and environmental stress treatments. *Plant Cell Environ.* 35, 644–655. doi: 10.1111/j.1365-3040.2011.02442.x

Guo, Y., and Gan, S. S. (2014). Translational researches on leaf senescence for enhancing plant productivity and quality. *J. Exp. Bot.* 65, 3901–3913. doi: 10.1093/jxb/eru248

Gupta, S., Shi, X., Lindquist, I. E., Devitt, N., Mudge, J., and Rashotte, A. M. (2013). Transcriptome profiling of cytokinin and auxin regulation in tomato root. *J. Exp. Bot.* 64, 695–704. doi: 10.1093/jxb/ers365

Ha, S., Vankova, R., Yamaguchi-Shinozaki, K., Shinozaki, K., and Tran, L. S. (2012). Cytokinins: metabolism and function in plant adaptation to environmental stresses. *Trends Plant Sci.* 17, 172–179. doi: 10.1016/j.tplants.2011.12.005

Hai, N. N., Chuong, N. N., Tu, N. H. C., Kisiala, A., Hoang, X. L. T., and Thao, N. P. (2020). Role and regulation of cytokinins in plant response to drought stress. *Plants* 9:E422. doi: 10.3390/plants9040422

Hajouj, T., Michelis, R., and Gepstein, S. (2000). Cloning and characterization of a receptor-like protein kinase gene associated with senescence. *Plant Physiol.* 124, 1305–1314. doi: 10.1104/pp.124.3.1305

Higo, K., Ugawa, Y., Iwamoto, M., and Korenaga, T. (1999). Plant cis-acting regulatory DNA elements (PLACE) database: 1999. *Nucleic Acids Res.* 27, 297–300. doi: 10.1093/nar/27.1.297

Hoth, S., Morgante, M., Sanchez, J. P., Hanafey, M. K., Tingey, S. V., and Chua, N. H. (2002). Genome-wide gene expression profiling in *Arabidopsis thaliana* reveals new targets of abscisic acid and largely impaired gene regulation in the abi1-1 mutant. *J. Cell Sci.* 115, 4891–4900. doi: 10.1242/jcs.00175

Hu, X., Wu, L., Zhao, F., Zhang, D., Li, N., Zhu, G., et al. (2015). Phosphoproteomic analysis of the response of maize leaves to drought, heat and their combination stress. *Front. Plant Sci.* 6:298. doi: 10.3389/fpls.2015.00298

Huang, X., Hou, L., Meng, J., You, H., Li, Z., Gong, Z., et al. (2018). The antagonistic action of abscisic acid and cytokinin signaling mediates drought stress response in Arabidopsis. *Mol. Plant* 11, 970–982. doi: 10.1016/j.molp.2018.05.001

Hundertmark, M., and Hincha, D. K. (2008). LEA (late embryogenesis abundant) proteins and their encoding genes in *Arabidopsis thaliana*. *BMC Genomics* 9:118. doi: 10.1186/1471-2164-9-118

Ingram, J., and Bartels, D. (1996). The molecular basis of dehydration tolerance in plants. *Annu. Rev. Plant Physiol. Plant Mol. Biol.* 47, 377–403. doi: 10.1146/annurev.arplant.47.1.377

Jaillais, Y., and Chory, J. (2010). Unraveling the paradoxes of plant hormone signaling integration. *Nat. Struct. Mol. Biol.* 17, 642–645. doi: 10.1038/nsmb0610-642

Jiang, Y., and Deyholos, M. K. (2009). Functional characterization of Arabidopsis NaCl-inducible WRKY25 and WRKY33 transcription factors in abiotic stresses. *Plant Mol. Biol.* 69, 91–105. doi: 10.1007/s11103-008-9408-3

Jordi, W., Schapendonk, A., Davelaar, E., Stoopen, G., Pot, C., De Visser, R., et al. (2000). Increased cytokinin levels in transgenic PSAG12-IPT tobacco plants have large direct and indirect effects on leaf senescence, photosynthesis and N partitioning. *Plant Cell Environ.* 23, 279–289. doi: 10.1046/j.1365-3040.2000.00544.x

Joshi, R., Wani, S. H., Singh, B., Bohra, A., Dar, Z. A., Lone, A. A., et al. (2016). Transcription factors and plants response to drought stress: current understanding and future directions. *Front. Plant. Sci.* 7:1029. doi: 10.3389/fpls.2016.01029

Kasuga, M., Miura, S., Shinozaki, K., and Yamaguchi-Shinozaki, K. (2004). A combination of the Arabidopsis DREB1A gene and stress-inducible rd29A promoter improved drought- and low-temperature stress tolerance in tobacco by gene transfer. *Plant Cell Physiol.* 45, 346–350. doi: 10.1093/Pcp/Pch037

Kelner, A., Pekala, I., Kaczanowski, S., Muszynska, G., Hardie, D. G., and Dobrowolska, G. (2004). Biochemical characterization of the tobacco 42-kD protein kinase activated by osmotic stress. *Plant Physiol.* 136, 3255–3265. doi: 10.1104/pp.104.046151

Kim, H. J., Ryu, H., Hong, S. H., Woo, H. R., Lim, P. O., Lee, I. C., et al. (2006). Cytokinin-mediated control of leaf longevity by AHK3 through phosphorylation of ARR2 in *Arabidopsis*. *Proc. Natl. Acad. Sci. U.S.A.* 103, 814–819. doi: 10.1073/pnas.0505150103

Kovacs, D., Kalmar, E., Torok, Z., and Tompa, P. (2008). Chaperone activity of ERD10 and ERD14, two disordered stress-related plant proteins. *Plant Physiol.* 147, 381–390. doi: 10.1104/pp.108.118208

Kulik, A., Anielska-Mazur, A., Bucholc, M., Koen, E., Szymanska, K., Zmienko, A., et al. (2012). SNF1-related protein kinases type 2 are involved in plant responses to cadmium stress. *Plant Physiol.* 160, 868–883. doi: 10.1104/pp.112.194472

Kulik, A., Wawer, I., Krzywinska, E., Bucholc, M., and Dobrowolska, G. (2011). SnRK2 protein kinases-key regulators of plant response to abiotic stresses. *Omics J. Integr. Biol.* 15, 859–872. doi: 10.1089/omi.2011.0091

Li, Q., Robson, P. R., Bettany, A. J., Donnison, I. S., Thomas, H., and Scott, I. M. (2004). Modification of senescence in ryegrass transformed with IPT under the control of a monocot senescence-enhanced promoter. *Plant Cell Rep.* 22, 816–821. doi: 10.1007/s00299-004-0762-6

Lukac, M., Gooding, M. J., Griffiths, S., and Jones, H. E. (2012). Asynchronous flowering and within-plant flowering diversity in wheat and the implications for crop resilience to heat. *Ann. Bot.* 109, 843–850. doi: 10.1093/aob/mcr308

Ma, Q. H. (2008). Genetic engineering of cytokinins and their application to agriculture. *Crit. Rev. Biotechnol.* 28, 213–232. doi: 10.1080/07388550802262205

Mackova, H., Hronkova, M., Dobra, J., Tureckova, V., Novak, O., Lubovska, Z., et al. (2013). Enhanced drought and heat stress tolerance of tobacco plants with ectopically enhanced cytokinin oxidase/dehydrogenase gene expression. *J. Exp. Bot.* 64, 2805–2815. doi: 10.1093/jxb/ert131

Maggio, A., Bressan, R. A., Zhao, Y., Park, J., and Yun, D. J. (2018). It's hard to avoid avoidance: uncoupling the evolutionary connection between plant growth, productivity and stress "tolerance". *Int. J. Mol. Sci.* 19:3671. doi: 10.3390/ijms19113671

Maillard, A., Diquelou, S., Billard, V., Laine, P., Garnica, M., Prudent, M., et al. (2015). Leaf mineral nutrient remobilization during leaf senescence and modulation by nutrient deficiency. *Front. Plant. Sci.* 6:317. doi: 10.3389/fpls.2015.00317

McCabe, M. S., Garratt, L. C., Schepers, F., Jordi, W. J., Stoopen, G. M., Davelaar, E., et al. (2001). Effects of PSAG12-IPT gene expression on development and senescence in transgenic lettuce. *Plant Physiol.* 127, 505–516. doi: 10.1104/pp.010244

Mehrotra, R., Sethi, S., Zutshi, I., Bhalothia, P., and Mehrotra, S. (2013). Patterns and evolution of ACGT repeat cis-element landscape across four plant genomes. *BMC Genomics* 14:203. doi: 10.1186/1471-2164-14-203

Menke, F. L., Kang, H. G., Chen, Z., Park, J. M., Kumar, D., and Klessig, D. F. (2005). Tobacco transcription factor WRKY1 is phosphorylated by the MAP kinase SIPK and mediates HR-like cell death in tobacco. *Mol. Plant Microbe Interact.* 18, 1027–1034. doi: 10.1094/MPMI-18-1027

Merewitz, E., Gianfagna, T., and Huang, B. (2010). Effects of SAG12-ipt and HSP18.2-ipt expression on cytokinin production, root growth and leaf senescence in creeping bentgrass exposed to drought stress. *J. Am. Soc. Hortic. Sci.* 135, 230–239. doi: 10.21273/jashs.135.3.230

Merewitz, E. B., Du, H., Yu, W., Liu, Y., Gianfagna, T., and Huang, B. (2012). Elevated cytokinin content in ipt transgenic creeping bentgrass promotes drought tolerance through regulating metabolite accumulation. *J. Exp. Bot.* 63, 1315–1328. doi: 10.1093/jxb/err372

Mikolajczyk, M., Awotunde, O. S., Muszynska, G., Klessig, D. F., and Dobrowolska, G. (2000). Osmotic stress induces rapid activation of a salicylic acid-induced protein kinase and a homolog of protein kinase ASK1 in tobacco cells. *Plant Cell* 12, 165–178. doi: 10.1105/tpc.12.1.165

Misra, B. B., Reichman, S. M., and Chen, S. (2019). The guard cell ionome: understanding the role of ions in guard cell functions. *Prog. Biophys. Mol. Biol.* 146, 50–62. doi: 10.1016/j.pbiomolbio.2018.11.007

Mohanty, B., Krishnan, S. P. T., Swarup, S., and Bajic, V. B. (2005). Detection and preliminary analysis of motifs in promoters of anaerobically induced genes of different plant species. *Ann. Bot.* 96, 669–681. doi: 10.1093/aob/mci219

Nakagami, H., Sugiyama, N., Mochida, K., Daudi, A., Yoshida, Y., Toyoda, T., et al. (2010). Large-scale comparative phosphoproteomics identifies conserved phosphorylation sites in plants. *Plant Physiol.* 153, 1161–1174. doi: 10.1104/pp.110.157347

Nishiyama, R., Watanabe, Y., Fujita, Y., Le, D. T., Kojima, M., Werner, T., et al. (2011). Analysis of cytokinin mutants and regulation of cytokinin metabolic genes reveals important regulatory roles of cytokinins in drought, salt and abscisic acid responses, and abscisic acid biosynthesis. *Plant Cell* 23, 2169–2183. doi: 10.1105/tpc.111.087395

Ogata, T., Kida, Y., Arai, T., Kishi, Y., Manago, Y., Murai, M., et al. (2012). Overexpression of tobacco ethylene response factor NtERF3 gene and its homologues from tobacco and rice induces hypersensitive response-like cell death in tobacco. *J. Gen. Plant Pathol.* 78, 8–17. doi: 10.1007/s10327-011-0355-5

Ogata, T., Okada, H., Kawaide, H., Takahashi, H., Seo, S., Mitsuhara, I., et al. (2015). Involvement of NtERF3 in the cell death signalling pathway mediated by SIPK/WIPK and WRKY1 in tobacco plants. *Plant Biol.* 17, 962–972. doi: 10.1111/plb.12349

Park, H. C., Kim, M. L., Kang, Y. H., Jeon, J. M., Yoo, J. H., Kim, M. C., et al. (2004). Pathogen- and NaCl-induced expression of the SCaM-4 promoter is mediated in part by a GT-1 box that interacts with a GT-1-like transcription factor. *Plant Physiol.* 135, 2150–2161. doi: 10.1104/pp.104.041442

Passardi, F., Cosio, C., Penel, C., and Dunand, C. (2005). Peroxidases have more functions than a Swiss army knife. *Plant Cell Rep.* 24, 255–265. doi: 10.1007/s00299-005-0972-6

Patankar, H. V., Al-Harrasi, I., Al Kharusi, L., Jana, G. A., Al-Yahyai, R., Sunkar, R., et al. (2019). Overexpression of a metallothionein 2A gene from date palm confers abiotic stress tolerance to yeast and *Arabidopsis thaliana*. *Int. J. Mol. Sci.* 20:2871. doi: 10.3390/ijms20122871

Peleg, Z., and Blumwald, E. (2011). Hormone balance and abiotic stress tolerance in crop plants. *Curr. Opin. Plant Biol.* 14, 290–295. doi: 10.1016/j.pbi.2011.02.001

Peleg, Z., Reguera, M., Tumimbang, E., Walia, H., and Blumwald, E. (2011). Cytokinin-mediated source/sink modifications improve drought tolerance and increase grain yield in rice under water-stress. *Plant Biotechnol. J.* 9, 747–758. doi: 10.1111/j.1467-7652.2010.00584.x

Pereira, A. (2016). Plant abiotic stress challenges from the changing environment. *Front. Plant Sci.* 7:1123. doi: 10.3389/fpls.2016.01123

Qin, H., Gu, Q., Zhang, J., Sun, L., Kuppu, S., Zhang, Y., et al. (2011). Regulated expression of an isopentenyltransferase gene (IPT) in peanut significantly improves drought tolerance and increases yield under field conditions. *Plant Cell Physiol.* 52, 1904–1914. doi: 10.1093/pcp/pcr125

Quinn, J. M., Barraco, P., Eriksson, M., and Merchant, S. (2000). Coordinate copper- and oxygen-responsive Cyc6 and Cpx1 expression in Chlamydomonas is mediated by the same element. *J. Biol. Chem.* 275, 6080–6089. doi: 10.1074/jbc.275.9.6080

Rashotte, A. M., Mason, M. G., Hutchison, C. E., Ferreira, F. J., Schaller, G. E., and Kieber, J. J. (2006). A subset of Arabidopsis AP2 transcription factors mediates cytokinin responses in concert with a two-component pathway. *Proc. Natl. Acad. Sci. U.S.A.* 103, 11081–11085. doi: 10.1073/pnas.0602038103

Richmond, A. E., and Lang, A. (1957). Effect of kinetin on protein content and survival of detached xanthium leaves. *Science* 125, 650–651. doi: 10.1126/science.125.3249.650-a

Rivero, R. M., Kojima, M., Gepstein, A., Sakakibara, H., Mittler, R., Gepstein, S., et al. (2007). Delayed leaf senescence induces extreme drought tolerance in a flowering plant. *Proc. Natl. Acad. Sci. U.S.A.* 104, 19631–19636. doi: 10.1073/pnas.0709453104

Robson, P., Mos, M., Clifton-Brown, J., and Donnison, I. (2012). Phenotypic variation in senescence in miscanthus: towards optimising biomass quality and quantity. *Bioenergy Res.* 5, 95–105. doi: 10.1007/s12155-011-9118-6

Robson, P. R. H., Donnison, I. S., Wang, K., Frame, B., Pegg, S. E., Thomas, A., et al. (2004). Leaf senescence is delayed in maize expressing the Agrobacterium IPT gene under the control of a novel maize senescence-enhanced promoter. *Plant Biotechnol. J.* 2, 101–112. doi: 10.1046/j.1467-7652.2004.00054.x

Roelfsema, M. R., Hedrich, R., and Geiger, D. (2012). Anion channels: master switches of stress responses. *Trends Plant Sci.* 17, 221–229. doi: 10.1016/j.tplants.2012.01.009

Romeis, T., Piedras, P., Zhang, S., Klessig, D. F., Hirt, H., and Jones, J. D. G. (1999). Rapid Avr 9-and Cf-9-dependent activation of MAP kinases in tobacco cell cultures and leaves: convergence of resistance gene, elicitor, wound, and salicylate responses. *Plant Cell* 11, 273–288.

Rushton, P. J., Somssich, I. E., Ringler, P., and Shen, Q. J. (2010). WRKY transcription factors. *Trends Plant Sci.* 15, 247–258. doi: 10.1016/j.tplants.2010.02.006

Seki, M., Narusaka, M., Ishida, J., Nanjo, T., Fujita, M., Oono, Y., et al. (2002). Monitoring the expression profiles of 7000 *Arabidopsis* genes under drought, cold and high-salinity stresses using a full-length cDNA microarray. *Plant J.* 31, 279–292. doi: 10.1046/j.1365-313x.2002.01359.x

Seo, S., Katou, S., Seto, H., Gomi, K., and Ohashi, Y. (2007). The mitogen-activated protein kinases WIPK and SIPK regulate the levels of jasmonic and salicylic acids in wounded tobacco plants. *Plant J.* 49, 899–909. doi: 10.1111/j.1365-313X.2006.03003.x

Seo, S., Okamoto, M., Seto, H., Ishizuka, K., Sano, H., and Ohashi, Y. (1995). Tobacco MAP kinase: a possible mediator in wound signal transduction pathways. *Science* 270, 1988–1992. doi: 10.1126/science.270.5244.1988

Shirron, N., and Yaron, S. (2011). Active suppression of early immune response in tobacco by the human pathogen *Salmonella Typhimurium*. *PLoS One* 6:e18855. doi: 10.1371/journal.pone.0018855

Simpson, S. D., Nakashima, K., Narusaka, Y., Seki, M., Shinozaki, K., and Yamaguchi-Shinozaki, K. (2003). Two different novel *cis*-acting elements of *erd1*, a *clpA* homologous *Arabidopsis* gene function in induction by dehydration stress and dark-induced senescence. *Plant J.* 33, 259–270. doi: 10.1046/j.1365-313x.2003.01624.x

Smart, C. M., Scofield, S. R., Bevan, M. W., and Dyer, T. A. (1991). Delayed leaf senescence in tobacco plants transformed with tmr, a gene for cytokinin production in agrobacterium. *Plant Cell* 3, 647–656. doi: 10.1105/tpc.3.7.647

Song, C. P., and Galbraith, D. W. (2006). AtSAP18, an orthologue of human SAP18, is involved in the regulation of salt stress and mediates transcriptional repression in *Arabidopsis*. *Plant Mol. Biol.* 60, 241–257. doi: 10.1007/s11103-005-3880-9

Tran, L. S., Urao, T., Qin, F., Maruyama, K., Kakimoto, T., Shinozaki, K., et al. (2007). Functional analysis of AHK1/ATHK1 and cytokinin receptor histidine kinases in response to abscisic acid, drought, and salt stress in *Arabidopsis*. *Proc. Natl. Acad. Sci. U.S.A.* 104, 20623–20628. doi: 10.1073/pnas.0706547105

Tyanova, S., Temu, T., Sinitcyn, P., Carlson, A., Hein, M. Y., Geiger, T., et al. (2016). The Perseus computational platform for comprehensive analysis of (prote)omics data. *Nat. Methods* 13, 731–740. doi: 10.1038/nmeth.3901

Verma, V., Ravindran, P., and Kumar, P. P. (2016). Plant hormone-mediated regulation of stress responses. *BMC Plant Biol.* 16:86. doi: 10.1186/s12870-016-0771-y

Wawer, I., Bucholc, M., Astier, J., Anielska-Mazur, A., Dahan, J., Kulik, A., et al. (2010). Regulation of *Nicotiana tabacum* osmotic stress-activated protein kinase and its cellular partner GAPDH by nitric oxide in response to salinity. *Biochem. J.* 429, 73–83. doi: 10.1042/BJ20100492

Werner, T., Nehnevajova, E., Kollmer, I., Novak, O., Strnad, M., Kramer, U., et al. (2010). Root-specific reduction of cytokinin causes enhanced root growth, drought tolerance, and leaf mineral enrichment in *Arabidopsis* and Tobacco. *Plant Cell* 22, 3905–3920. doi: 10.1105/tpc.109.072694

Wu, J., Hettenhausen, C., Meldau, S., and Baldwin, I. T. (2007). Herbivory rapidly activates MAPK signaling in attacked and unattacked leaf regions but not between leaves of *Nicotiana attenuata*. *Plant Cell* 19, 1096–1122. doi: 10.1105/tpc.106.049353

Xing, Y., Jia, W., and Zhang, J. (2008). AtMKK1 mediates ABA-induced *CAT1* expression and H_2O_2 production via AtMPK6-coupled signaling in Arabidopsis. *Plant J.* 54, 440–451. doi: 10.1111/j.1365-313X.2008.03433.x

Xiong, L., Wang, R. G., Mao, G., and Koczan, J. M. (2006). Identification of drought tolerance determinants by genetic analysis of root response to drought stress and abscisic Acid. *Plant Physiol.* 142, 1065–1074. doi: 10.1104/pp.106.084632

Yang, S., Vanderbeld, B., Wan, J., and Huang, Y. (2010). Narrowing down the targets: towards successful genetic engineering of drought-tolerant crops. *Mol. Plant* 3, 469–490. doi: 10.1093/mp/ssq016

Yoo, S. Y., Bomblies, K., Yoo, S. K., Yang, J. W., Choi, M. S., Lee, J. S., et al. (2005). The 35S promoter used in a selectable marker gene of a plant transformation vector affects the expression of the transgene. *Planta* 221, 523–530. doi: 10.1007/s00425-004-1466-4

Yoshida, T., Mogami, J., and Yamaguchi-Shinozaki, K. (2014). ABA-dependent and ABA-independent signaling in response to osmotic stress in plants. *Curr. Opin. Plant Biol.* 21, 133–139. doi: 10.1016/j.pbi.2014.07.009

Zhang, J., Wang, N., Miao, Y., Hauser, F., Mccammon, J. A., Rappel, W. J., et al. (2018). Identification of SLAC1 anion channel residues required for CO2/bicarbonate sensing and regulation of stomatal movements. *Proc. Natl. Acad. Sci. U.S.A.* 115, 11129–11137. doi: 10.1073/pnas.1807624115

Zhang, P., Wang, W. Q., Zhang, G. L., Kaminek, M., Dobrev, P., Xu, J., et al. (2010). Senescence-inducible expression of isopentenyl transferase extends leaf life, increases drought stress resistance and alters cytokinin metabolism in cassava. *J. Integr. Plant Biol.* 52, 653–669. doi: 10.1111/j.1744-7909.2010.00956.x

Zhang, S., and Klessig, D. F. (1997). Salicylic acid activates a 48-kD MAP kinase in tobacco. *Plant Cell* 9, 809–824. doi: 10.1105/tpc.9.5.809

Zhang, S., Liu, Y., and Klessig, D. F. (2000). Multiple levels of tobacco WIPK activation during the induction of cell death by fungal elicitins. *Plant J.* 23, 339–347. doi: 10.1046/j.1365-313x.2000.00780.x

Zhu, J. K. (2016). Abiotic stress signaling and responses in plants. *Cell* 167, 313–324. doi: 10.1016/j.cell.2016.08.029

Zwack, P. J., and Rashotte, A. M. (2013). Cytokinin inhibition of leaf senescence. *Plant Signal. Behav.* 8:e24737. doi: 10.4161/psb.24737

Zwack, P. J., and Rashotte, A. M. (2015). Interactions between cytokinin signalling and abiotic stress responses. *J. Exp. Bot.* 66, 4863–4871. doi: 10.1093/jxb/erv172

Conflict of Interest: The authors declare that the research was conducted in the absence of any commercial or financial relationships that could be construed as a potential conflict of interest.

frontiers in Plant Science

ORIGINAL RESEARCH
published: 16 July 2020
doi: 10.3389/fpls.2020.01096

Rice ETHYLENE RESPONSE FACTOR 101 Promotes Leaf Senescence Through Jasmonic Acid-Mediated Regulation of *OsNAP* and *OsMYC2*

Chaemyeong Lim[1‡], *Kiyoon Kang*[2‡], *Yejin Shim*[1*], *Yasuhito Sakuraba*[3], *Gynheung An*[4] *and Nam-Chon Paek*[1*†]

[1] Department of Plant Science, Plant Genomics and Breeding Institute, Research Institute of Agriculture and Life Sciences, Seoul National University, Seoul, South Korea, [2] Division of Life Sciences, Incheon National University, Incheon, South Korea, [3] Graduate School of Agricultural and Life Sciences, Biotechnology Research Center, The University of Tokyo, Tokyo, Japan, [4] Department of Plant Molecular Systems Biotechnology, Crop Biotech Institute, Kyung Hee University, Yongin, South Korea

OPEN ACCESS

Edited by:
Randy D. Allen,
Oklahoma State University,
United States

Reviewed by:
Seonghee Lee,
University of Florida, United States
Kenji Gomi,
Kagawa University, Japan

***Correspondence:**
Nam-Chon Paek
ncpaek@snu.ac.kr

†ORCID:
Nam-Chon Paek
orcid.org/0000-0002-9827-2287

‡These authors have contributed equally to this work

Specialty section:
This article was submitted to Plant Abiotic Stress, a section of the journal Frontiers in Plant Science

Received: 05 May 2020
Accepted: 03 July 2020
Published: 16 July 2020

Citation:
Lim C, Kang K, Shim Y, Sakuraba Y, An G and Paek N-C (2020) Rice ETHYLENE RESPONSE FACTOR 101 Promotes Leaf Senescence Through Jasmonic Acid-Mediated Regulation of OsNAP and OsMYC2. Front. Plant Sci. 11:1096. doi: 10.3389/fpls.2020.01096

Leaf senescence is the final stage of leaf development and an important step that relocates nutrients for grain filling in cereal crops. Senescence occurs in an age-dependent manner and under unfavorable environmental conditions such as deep shade, water deficit, and high salinity stresses. Although many transcription factors that modulate leaf senescence have been identified, the mechanisms that regulate leaf senescence in response to environmental conditions remain elusive. Here, we show that rice (*Oryza sativa*) *ETHYLENE RESPONSE FACTOR 101* (*OsERF101*) promotes the onset and progression of leaf senescence. *OsERF101* encodes a predicted transcription factor and *OsERF101* transcript levels rapidly increased in rice leaves during dark-induced senescence (DIS), indicating that OsERF101 is a senescence-associated transcription factor. Compared with wild type, the *oserf101* T-DNA knockout mutant showed delayed leaf yellowing and higher chlorophyll contents during DIS and natural senescence. Consistent with its delayed-yellowing phenotype, the *oserf101* mutant exhibited downregulation of genes involved in chlorophyll degradation, including rice *NAM*, *ATAF1/2*, and *CUC2* (*OsNAP*), *STAY-GREEN* (*SGR*), *NON-YELLOW COLORING 1* (*NYC1*), and *NYC3* during DIS. After methyl jasmonate treatment to induce rapid leaf de-greening, the *oserf101* leaves retained more chlorophyll compared with wild type, indicating that *OsERF101* is involved in promoting jasmonic acid (JA)-induced leaf senescence. Consistent with the involvement of JA, the expression of the JA signaling genes *OsMYC2/JA INSENSITIVE 1* (*OsJAI1*) and *CORONATINE INSENSITIVE 1a* (*OsCOI1a*), was downregulated in the *oserf101* leaves during DIS. Transient transactivation and chromatin immunoprecipitation assays revealed that OsERF101 directly binds to the promoter regions of *OsNAP* and *OsMYC2*, which activate genes involved in chlorophyll degradation and JA signaling-mediated leaf senescence. These

results demonstrate that *OsERF101* promotes the onset and progression of leaf senescence through a JA-mediated signaling pathway.

Keywords: rice, leaf senescence, chlorophyll degradation, jasmonic acid signaling, *OsERF101*, *OsNAP*, *OsMYC2*

INTRODUCTION

Leaf senescence is the final stage of leaf development and involves many molecular and physiological events, including chlorophyll degradation, the breakdown of other cellular components, and cell death, thus allowing plants to recycle nutrients from leaf tissues into seeds (Masclaux-Daubresse et al., 2008; Distelfeld et al., 2014; Yang et al., 2019). Environmental stresses, such as deep shade, water deficit, extreme temperatures, and high salinity, accelerate leaf senescence (Munné-Bosch and Alegre, 2004; Mickelbart et al., 2015). Premature leaf senescence shortens the vegetative growth period, inducing the precocious transition from the vegetative to the reproductive stage and reducing the plant's nutritional capacity, thus negatively affecting crop productivity.

Age-dependent and stress-induced senescence share many regulatory networks and physiological, biochemical, and molecular mechanisms (Gepstein and Glick, 2013; Zhuang et al., 2019). Transcription factors (TFs) participate in the regulatory pathways for leaf senescence and abiotic stress tolerance. For instance, RNA interference (RNAi)-mediated suppression of rice (*Oryza sativa*) *NAC2* (*OsNAC2*), a member of the NAC family, reduces the expression of chlorophyll-degradation and senescence-associated genes, leading to delayed leaf yellowing during dark-induced senescence (DIS) (Mao et al., 2017). Moreover, *OsNAC2*-RNAi transgenic plants display enhanced tolerance against drought and high salt stresses due to upregulation of stress-related and abscisic acid (ABA)-signaling genes (Shen et al., 2017). Overexpression of *ONAC106* causes delayed leaf yellowing in rice, resulting in extended photosynthetic capacity at the reproductive stage in paddy fields and increased grain production. In addition to the biological function of *ONAC106* in leaf senescence, transgenic rice overexpressing *ONAC106* exhibit improved tolerance to salt stress (Sakuraba et al., 2015). The gain-of-function mutant *prematurely senile 1-D* (*ps1-D*) exhibits upregulated expression of *OsNAP*, leading to accelerated leaf yellowing during both natural senescence and DIS (Liang et al., 2014). In addition, overexpression of *OsNAP* confers tolerance to salt and drought stresses (Chen et al., 2014). These distinct phenomena reveal the role of *OsNAP* in regulating diverse genes involved in chlorophyll degradation and abiotic stress responses.

Plant hormones serve as signal molecules and are involved in the regulation of a variety of cellular processes, including leaf senescence and abiotic stress responses. Among them, jasmonic acid (JA) accumulates to high levels in plant cells when plants enter the senescence phase or in unfavorable conditions (He et al., 2002; Wasternack and Hause, 2013; Hou et al., 2016), JA biosynthesis is catalyzed by enzymes including lipoxygenase (LOX), allene oxide synthase (AOS), allene oxide cyclase (AOC), and 12-oxo-PDA reductase (OPR) (He et al., 2002). Increased JA levels activate the downstream signal transduction pathways that are involved in senescence and abiotic stress tolerance. For instance, elevated JA levels are perceived by the F-box protein CORONATINE INSENSITIVE 1 (COI1), followed by ubiquitination and degradation of JA ZIM-domain (JAZ) proteins (Niu et al., 2011; Song et al., 2011; Qi et al., 2014). JAZ degradation causes the release of downstream TFs such as the basic helix-loop-helix (bHLH) TF family members MYC2, MYC3, and MYC4 (Fernández-Calvo et al., 2011). The *oscoi1b* mutant leaves retain their green color during DIS (Lee et al., 2015). Transgenic plants overexpressing a truncated OsJAZ8 protein that which lacks the ubiquitin-binding Jas domain also exhibit a delayed senescence phenotype (Uji et al., 2017). OsMYC2/OsJAI1 directly binds to the promoter of senescence-associated genes, and thus its overexpression leads to leaf yellowing during DIS (Uji et al., 2017). In Arabidopsis, MYC2/JAI1 and its homologous proteins MYC3 and MYC4 regulate the expression of the chlorophyll degradation genes *NON-YELLOWING 1* (*NYE1*), *NON-YELLOW COLORING 1* (*NYC1*), and *PHEOPHYTINASE* (*PPH*) by binding to their promoters (Zhu et al., 2015).

The APETALA2/Ethylene Response Factor (AP2/ERF) family can be divided into four subfamilies depending on the number of AP2/ERF domains and their amino acid similarity, such as APETALA2 (AP2), Related to ABI3/VP1 (RAV), Dehydration Responsive Element Binding protein (DREB), and Ethylene Response Factor (ERF) subfamilies (Sakuma et al., 2002; Nakano et al., 2006). DREB and ERF subfamilies have a single AP2/ERF domain that can bind to both the C-Repeat/Dehydration Responsive Element (CRT/DRE) and the Ethylene Response Element (ERE) in the promoter regions of their target genes. ERFs regulate the expression of abiotic stress-related genes in various plant species including rice (Fukao et al., 2011), Arabidopsis (Phukan et al., 2017), wheat (*Triticum aestivum*) (Gao et al., 2018), maize (*Zea mays*) (Liu et al., 2013), soybean (*Glycine max*) (Zhang et al., 2009), and tobacco (*Nicotiana tabacum*) (Park et al., 2001).

A recent study showed that the rice *ETHYLENE RESPONSE FACTOR 101* (*OsERF101*) plays an important role in enhancing tolerance to drought stress in reproductive tissues (Jin et al., 2018). However, the regulatory functions of *OsERF101* in leaf senescence have not been understood. In this study, our results substantially showed that OsERF101 positively regulates leaf senescence in rice, and directly activates the expression of *OsNAP* and *OsMYC2* that play a central role in mediating chlorophyll degradation and JA-mediated leaf senescence. Thus, our findings provide a new molecular insight of *OsERF101* function in leaf senescence.

MATERIALS AND METHODS

Plant Materials, Growth Conditions, and Dark, Phytohormone, and Stress Treatments

The T-DNA insertion mutant *oserf101* (PFG_2D-00368) was obtained from Crop Biotech Institute at Kyung Hee University, Republic of Korea (Jeong et al., 2002). The *Oryza sativa japonica* cultivar 'Dongjin' (parental line) and the *oserf101* mutant were cultivated in a paddy field under natural long day (NLD) conditions (>14 h sunlight/day, 37°N latitude) in Suwon, Republic of Korea. The germinated rice seedlings were transplanted in a paddy soil and grown in a growth chamber under long day (LD) conditions (14 h light/10 h dark, 37°N latitude) in Seoul, Republic of Korea. For the dark treatment, the detached leaves of rice plants grown in a growth chamber under LD conditions for 3 weeks were incubated on 3 mM MES (pH 5.8) buffer at 28°C in complete darkness. For phytohormone and stress treatments, the sterilized seeds were germinated on half-strength Murashige and Skoog (1/2 MS) solid medium under continuous light (90 μmol m^{-2} s^{-1}) at 30°C. The 10-day-old seedlings were transferred to 1/2 MS liquid medium containing 100 μM 1-aminocyclo-propane-1-carboxylic acid (ACC), 100 μM MeJA, 100 μM ABA, 100 mM NaCl, and 20% polyethylene glycol (PEG) or were dehydrated by air drying. Rice seedlings incubated in 1/2 MS liquid medium without additional phytohormones were used as a mock control.

Determination of Total Chlorophyll and Photosynthetic Capacity

To measure the total chlorophyll, pigments were extracted from an equal fresh weight of rice leaves grown in a paddy field, incubated in complete darkness, or treated with 100 μM MeJA using 80% ice-cold acetone. The extracts were centrifuged at 10,000 g for 10 min at 10°C and then the absorbance of the supernatants was measured at 647 and 663 nm using an UV/VIS spectrophotometer (BioTek). The concentration of chlorophyll was calculated as previously described (Porra et al., 1989). To determine the photosynthetic activity, the *Fv/Fm* ratio was measured using the OS-30p+ instrument (Opti-Sciences). The middle part of each flag leaf of plants grown in a paddy field under NLD conditions was adapted in the dark for 5 min and then the *Fv/Fm* ratio was determined in the flag leaves.

Determination of Phytohormone Sensitivity

To determine the sensitivity to phytohormones, detached leaves of 3-week-old plants grown in paddy soil were floated on 3 mM MES (pH 5.8) buffer containing 50 μM MeJA and 50 μM ABA and incubated in continuous light conditions (90 μmole·$m^{-2}s^{-1}$) at 30°C for 4 days. Detached leaves floated on 3 mM MES buffer (pH 5.8) without phytohormones were used as a control. To assess the ABA sensitivity of rice seedlings, the 10-day-old rice seedlings grown in 1/2 MS solid medium were transferred to 1/2 MS liquid medium containing 5 and 10 μM ABA. Seedlings incubated in 1/2 MS liquid medium without additional phytohormones were used as a mock control.

Quantitative Reverse Transcription PCR (qRT-PCR) and Semiquantitative RT-PCR

Total RNA was extracted from rice tissues using an RNA Extraction Kit (Macrogen, South Korea) according to manufacturer instructions. First-strand cDNA was synthesized with 2 μg of total RNA in a 25 μl volume using M-MLV reverse transcriptase and oligo$(dT)_{15}$ primer (Promega), and diluted with 75 μl of water. The qPCR amplifications were conducted on the LightCycler 2.0 instrument (Roche Diagnostics). The 20 μl of qPCR mixture included 2 μl of the first-strand cDNA mixture, 10 μl of 2X GoTaq PCR Master Mix (Promega), and 1 μl of 10 pM primer pairs (**Supplementary Table S1**). The qPCR conditions were 95°C for 2 min, followed by 50 cycles at 95°C for 5 s, 59°C for 15 s, and 72°C for 10 s. The rice *UBIQUITIN5* (*OsUBQ5*, AK061988) gene was used as an internal control for normalization. The semi-quantitative PCR was performed in a 20 μl volume containing 2 μl diluted cDNA, 1 unit Ex Taq polymerase (TaKaRa Biotechniques), and 1 μl of 10 pM primers (listed in **Supplementary Table S1**). The PCR program included initial denaturation at 94°C for 3 min, followed by specified cycles at 94°C for 30 sec, 55°C for 1 min, and 72°C for 40 sec, followed by a final extension at 72°C for 5 min. The PCR products were electrophoresed on a 1% agarose gel. *OsUBQ5* was used as an equal loading control.

Plasmid Construction and Rice Transformation

To generate the overexpression construct, a full-length cDNA of *OsERF101* was amplified using the primers listed in **Supplementary Table S1**. The amplified fragments were ligated into the pCR8/GW/TOPO TA cloning vector (Invitrogen) and then inserted into the pMDC32 Gateway-compatible binary vector through the LR recombination reaction. The pMDC32-OsERF101 plasmids were introduced into callus of Dongjin seeds by *Agrobacterium tumefaciens* (strain LBA4404)-mediated transformation (Jeon et al., 2000). Agrobacterium-infected calli were transferred to 1/2 MS solid medium containing cytokinin and auxin. Plantlets regenerated from the callus were grown under continuous light conditions (90 μmole·m^{-2} s^{-1}) at 30°C.

Protoplast Transient Transactivation Assays

Reporter plasmids were constructed by the insertion of *OsMYC2* (-1529 to -1 bp) and *OsNAP* (-1502 to -1 bp) promoters into the pJD301 vector (Luehrsen et al., 1992). To construct effector plasmids, *OsERF101* cDNA from the WT cultivar was cloned upstream of a sequence encoding six copies of a MYC epitope tag in the pGA3697 vector. Protoplasts were isolated from young rice seedlings as previously described (Zhang et al., 2011). A reporter plasmid (4 μg) and an effector plasmid (8 μg) were co-transfected, together with 1 μg of an internal control plasmid (pUBQ10-GUS), into 5×10^4 protoplasts using the polyethylene glycol (PEG)-mediated transfection method (Yoo et al., 2007). Transfected protoplasts were incubated in protoplast culture solution (0.4 M mannitol, 15 mM $MgCl_2$, 4 mM MES-KOH

[pH 5.8]) in the dark at room temperature for 16 h. Luciferase (LUC) activity in each cell lysate was determined using the Luciferase Assay System Kit (Promega). LUC activity was normalized against β-glucuronidase (GUS) activity derived from the internal control plasmid.

Chromatin Immunoprecipitation (ChIP) Assays

For the ChIP assay, the *Ubi : OsERF101-Myc* and *Ubi : Myc* were transfected into rice protoplasts as previously described (Zhang et al., 2011). Protoplasts were then subjected to cross-linking with 1% formaldehyde for 30 min under vacuum. Then, nuclei were isolated and lysed, and chromatin complexes were isolated and sonicated, as described (Saleh et al., 2008). DNA was sonicated using a BIORUPTORII (COSMO BIO). Anti-Myc monoclonal antibody (Abcam, Cambridge, UK) and protein A agarose beads (Merck Millipore) were used for immunoprecipitation. DNA recovered from agarose beads was purified using the DNeasy Plant Mini Kit (Qiagen). Quantitative PCR was performed using the KAPA SYBR FAST qPCR Kit (KAPA Biosystems) and gene-specific primers (**Supplementary Table S1**).

RESULTS

Expression of *OsERF101* in Rice

Rice *OsERF101* (LOC_Os04g32620) consists of 4366 bp of genomic DNA with an 807-bp open reading frame containing two exons and encoding a 268-amino acid protein belonging to the ERF transcription factor subfamily. Amino acid sequence alignments between OsERF101 and its putative orthologs demonstrated that they have a single AP2/ERF domain, which is highly conserved in plants (**Supplementary Figure S1**).

To investigate the expression of *OsERF101*, we measured *OsERF101* transcript levels in various organs (root, leaf sheath,

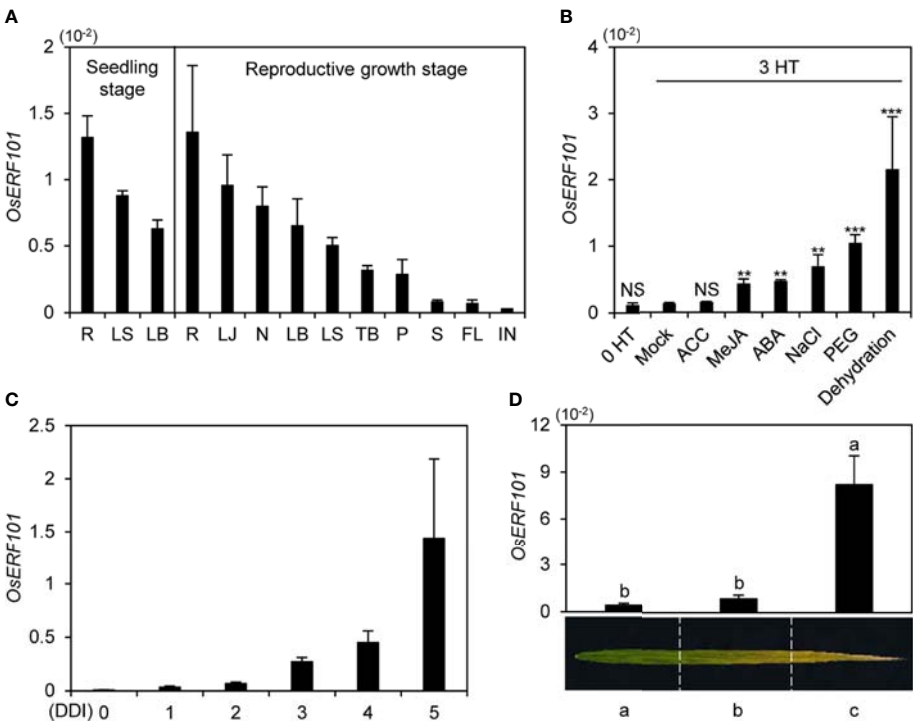

FIGURE 1 | Expression profiles of *OsERF101*. **(A)** *OsERF101* was differentially expressed in various *japonica* cultivar 'Dongjin' (hereafter wild type; WT) tissues: root (R), leaf sheath (LS), leaf blade (LB), lamina joint (LJ), node (N), tiller base (TB), panicle (P), stem (S), flag leaf (FL), and internode (IN). WT seedlings were grown in a growth chamber for 3 weeks under long-day (LD) conditions (14 h light/10 h dark). WT plants were cultivated in a paddy field until the reproductive stage at 120 days after seeding (DAS) under natural long-day (NLD) conditions (>14 h light/day). **(B)** Expression patterns of *OsERF101* in response to abiotic stresses and phytohormones. WT seedlings grown in half-strength Murashige and Skoog (1/2 MS) solid medium for 10 d under continuous light at 28°C were incubated in 1/2 MS liquid medium supplemented with 100 μM ACC, 100 μM MeJA, 100 μM ABA, 100 mM NaCl, or 20% PEG or dehydrated by air drying. Seedlings incubated in 1/2 MS liquid medium without treatment were used as a mock control. Total RNA was isolated from the leaves at 0 and 3 h of treatment (HT). Asterisks indicate statistically significant differences between treated samples and the mock control, as determined by Student's t-test (**$p < 0.01$, ***$p < 0.001$). NS, not significant. **(C)** *OsERF101* expression gradually increased in detached leaves of 3-week-old WT plants grown in a growth chamber under LD conditions. Detached leaves were subjected to complete darkness in 3 mM MES (pH 5.8) at 28°C. **(D)** Expression of *OsERF101* was measured in flag leaves divided into three regions from the green sector (a) to the yellow sector (c) at the ripening stage (130 DAS). *OsERF101* mRNA levels were determined by qRT-PCR analysis and normalized to that of *OsUBQ5* (Os01g22490). Mean and standard deviations were obtained from at least three biological samples. Different letters indicate significantly different values according to a one-way ANOVA and Duncan's least significant range test ($p < 0.05$). Experiments were repeated twice with similar results.

leaf blade, lamina joint, node, tiller base, panicle, stem, flag leaf, and internode). We used wild-type (WT; *japonica* rice cultivar 'Dongjin') plants grown in a growth chamber under long-day (LD) conditions (14.5 h light/9.5 h dark) at 21 days after germination (DAG, seedling stage) or in the paddy field under natural LD (NLD) conditions (≥14 h light/day in Suwon, South Korea, 37°N latitude) at 120 DAG (heading stage). Reverse transcription and quantitative real-time PCR (qRT-PCR) analysis revealed that the *OsERF101* transcripts were most abundant in root, and then (in order of decreasing abundance), in lamina joint, node, leaf blade, and leaf sheath (**Figure 1A**).

To test whether phytohormones and stress treatments affect the expression of *OsERF101*, we examined the *OsERF101* transcript levels in 10-day-old WT seedlings treated with 1-aminocyclopropane-1-carboxylic acid (ACC), MeJA, ABA, NaCl, PEG, or under dehydration stress for 3 h. qRT-PCR analysis showed that *OsERF101* expression increased significantly in response to the MeJA, ABA, NaCl, PEG, and water deficit treatments (**Figure 1B**). In addition, *OsERF101* expression was sharply upregulated in the detached leaves of 2-week-old seedlings during DIS (**Figure 1C**). In the naturally senescing flag leaves, *OsERF101* transcripts accumulated to higher levels in the yellowed tip (**c**) region than in the yellowing middle (**b**) or green bottom (**a**) regions (**Figure 1D**). These results strongly suggested that *OsERF101* is involved in leaf senescence in rice.

OsERF101 Positively Regulates the Onset and Progression of Leaf Senescence

To examine the role of the OsERF101 TF in regulating leaf senescence, we obtained a loss-of-function mutant (PFG_2D-00368) from RiceGE (://signal.salk.edu/cgi-bin/RiceGE), in which a T-DNA fragment was integrated into the second exon of *OsERF101* (**Figure 2A**). To verify the effect of the T-DNA insertion, we performed semi-quantitative RT-PCR analysis and found that in the detached leaves of 3-week-old plants, the *OsERF101* transcript was completely absent in the PFG_2D-00368 line (**Figure 2B**) at 3 days of dark incubation (DDI), indicating that the PFG_2D-00368 line is a knockout mutant (hereafter termed *oserf101*). We next examined the progress of senescence in WT and *oserf101* plants grown in the paddy field under NLD conditions. While there was no significant difference in leaf color between WT and *oserf101* plants at 0 days after heading (DAH) (**Figure 2C**), the *oserf101* leaves retained their green color during grain filling much more than the WT (**Figures 2D, E**). Consistent with the persistence of green leaf color, the chlorophyll levels remained much higher in the flag leaves of the *oserf101* mutant compared to the WT (**Figure 2F**). In addition, the *oserf101* mutant maintained a higher *Fv/Fm* ratio (efficiency of photosystem II) compared to the WT after 20 DAH (**Figure 2G**), indicating that the prolonged greenness of *oserf101* leaves leads to improved photosynthetic activity during grain filling in the autumn fields.

To further examine the effects of *OsERF101* on leaf de-greening in DIS, we monitored the color in sections of leaves detached from 3-week-old WT and *oserf101* plants grown under LD conditions. The *oserf101* leaves retained their green color much longer than the WT leaves (**Figure 3A**), consistent with their relatively higher chlorophyll contents at 3 and 4 DDI (**Figure 3B**). To confirm the positive role of *OsERF101* in leaf senescence, we generated two independent transgenic rice plants overexpressing *OsERF101* (*OsERF101*-OX1 and -OX2) (**Figure 3C**). The detached leaves of 3-week-old *OsERF101*-OX plants exhibited accelerated leaf yellowing compared to those of the WT at 3 DDI (**Figure 3D**). These results indicate that OsERF101 is a positive regulator of the onset and progression of leaf senescence.

Among the rice regulatory genes controlling leaf senescence, *OsNAP* expression is induced by senescence, and OsNAP directly

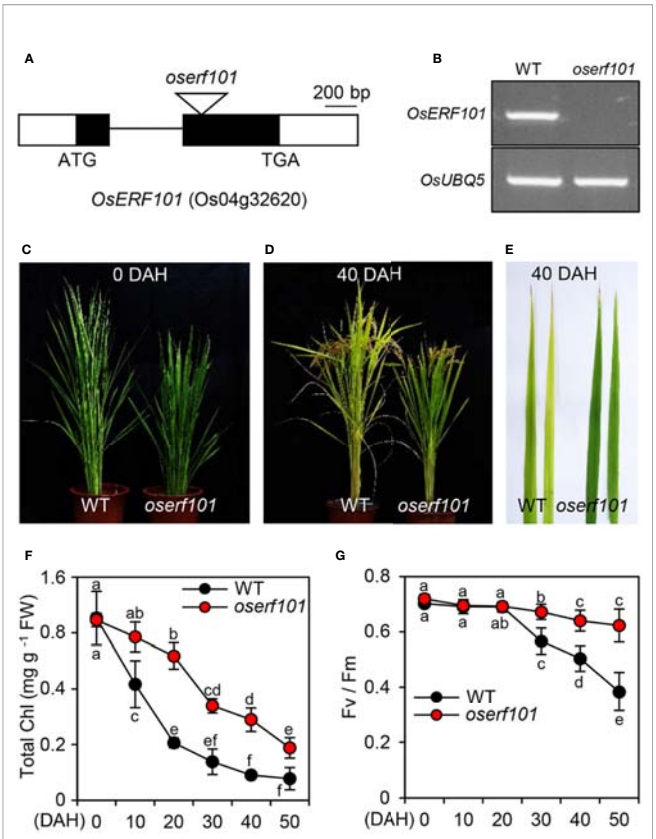

FIGURE 2 | The *oserf101* mutant exhibits delayed natural leaf senescence. **(A)** Position of the T-DNA insertion in the exon region of *OsERF101* (LOC_Os04g32620). Black and white boxes represent exons and untranslated regions, respectively. The black line indicates an intron and the open triangle indicates the location of the T-DNA insertion (*oserf101*, PFG_2D-00368). **(B)** Mutation of *OsERF101* was confirmed by semi-quantitative RT-PCR. Total RNA was isolated from detached second leaves of a 3-week-old WT (the parental *japonica* rice cultivar 'Dongjin') plant and the *oserf101* mutant in which senescence was induced for 3 days of dark incubation as shown in Figure 3A. *OsUBQ5* (Os01g22490) was used as a loading control. **(C, D)** The comparison of senescence phenotypes of WT and *oserf101* plants at 0 and 40 days after heading (DAH) under natural long-day conditions (>14 h light/day). **(E)** Senescing flag leaves of WT and *oserf101* plants at 50 DAH. The images are representative of five independent experiments. **(F, G)** Changes in total chlorophyll (Chl) contents **(F)** and photosynthetic capacity (Fv/Fm) **(G)** of WT and *oserf101* flag leaves after heading. Mean and standard deviations were obtained from more than 10 plants. Different letters indicate significantly different values according to a one-way ANOVA and Duncan's least significant range test ($p < 0.05$).

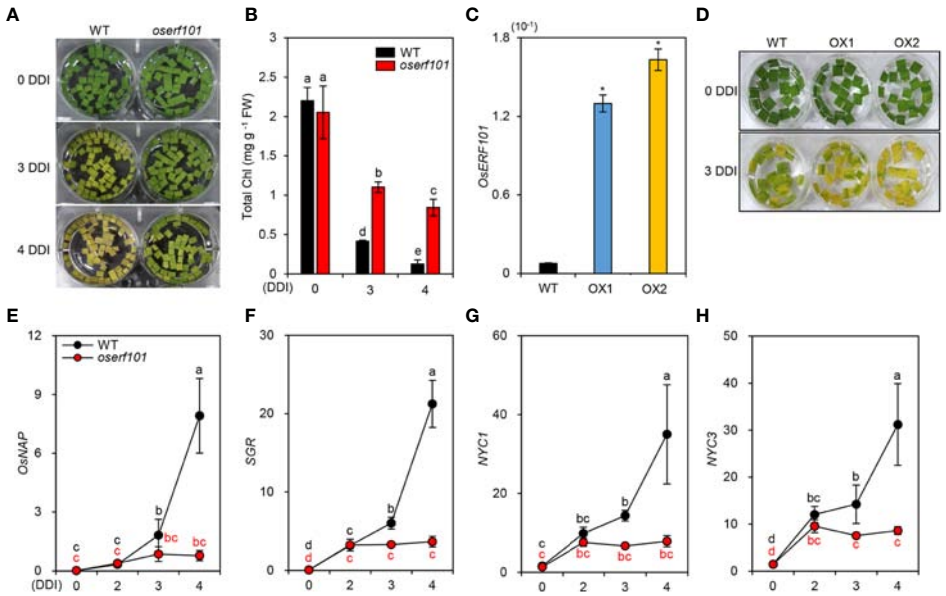

FIGURE 3 | The *oserf101* mutant exhibited delayed leaf yellowing during dark-induced senescence (DIS) conditions. **(A, B)** Detached leaves of 3-week-old WT and *oserf101* plants grown in the greenhouse under natural long-day conditions (>14 h light/day) were incubated in 3 mM MES buffer (pH 5.8) with the abaxial side up at 28°C under complete darkness. The visual phenotypes **(A)** and total chlorophyll (Chl) contents **(B)** were observed after 0, 3, and 4 days of dark incubation (DDI). Different letters indicate significantly different values according to a one-way ANOVA and Duncan's least significant range test ($p < 0.05$). **(C)** Expression of *OsERF101* measured in the leaves of WT and *OsERF101*-overexpressing (*OsERF101*-OX) transgenic plants (OX1, OX2) grown in the greenhouse for one month. **(D)** Detached leaves of 1-month-old *OsERF101*-OX plants exhibited accelerated leaf yellowing at 3 DDI. **(E–H)** Altered expression of *OsNAP* and chlorophyll degradation genes in detached leaves of 3-week-old WT and *oserf101* seedlings during DIS. Total RNA was isolated from detached leaves at 0, 2, 3, and 4 DDI. The transcript levels of *OsERF101* **(C)**, *OsNAP* **(E)**, and chlorophyll degradation genes **(F–H)** were determined by qRT-PCR and normalized to that of *OsUBQ5* (Os01g22490). **(C)** Asterisks indicate statistically significant differences between WT and *OsERF101*-OX plants, as determined by Student's t-test (*$p < 0.05$). **(E–H)** Different letters indicate significantly different values according to a one-way ANOVA and Duncan's least significant range test ($p < 0.05$). Mean and standard deviations were obtained from at least three biological samples. Experiments were repeated twice with similar results. FW, fresh weight.

activates the transcription of chlorophyll degradation genes (Liang et al., 2014) including *STAY-GREEN* (*SGR*, Park et al., 2007), *NYC1* (Kusaba et al., 2007), and *NYC3* (Morita et al., 2009). To investigate whether *OsERF101* affects the expression of *OsNAP* and chlorophyll degradation genes, we measured their transcript levels in the detached leaves of 3-week-old WT and *oserf101* seedlings during DIS. The qRT-PCR results showed that, while the transcript levels of *OsNAP* and chlorophyll degradation genes increased in the WT at 3 DDI, their expression was not altered in the *oserf101* mutant during DIS (**Figures 3E–G**). These results indicate that *OsERF101* acts as a positive regulator of leaf senescence by upregulating the expression of *OsNAP* and chlorophyll degradation genes.

OsERF101 Acts in JA-Mediated Leaf Senescence

In the WT, the expression of *OsERF101* increased in response to treatment with ABA or MeJA (**Figure 1B**), implying that *OsERF101* is positively involved in ABA- or JA-mediated leaf senescence. To assess the function of OsERF101 in JA signaling, we observed the progress of leaf yellowing in the detached leaves of 3-week-old WT and *oserf101* seedlings incubated in 3 mM MES buffer (pH 5.8) containing 50 μM of ABA or MeJA under continuous light conditions. While there was no significant difference in leaf greenness and chlorophyll contents between the WT and *oserf101* seedlings at 4 d of ABA treatment, the *oserf101* leaves retained their green color more than WT leaves at 4 d of MeJA treatment and had higher total chlorophyll contents (**Figures 4A, B**). Consistent with these observations, chlorophyll contents were higher in the whole leaves of 3-week-old *oserf101* seedlings than in those of the WT at 4 d of MeJA treatment (**Supplementary Figure S2**). In addition, we investigated the effects of MeJA on growth of WT and *oserf101* seedlings grown on 1/2 MS solid medium for 10 days. MeJA treatment significantly retarded the growth of shoots and roots in WT and *oserf101* seedlings (**Figure 4C**). However, the shoots and roots of the *oserf101* mutant were much longer than those of the WT under MeJA treatment (**Figures 4D, E**). These results suggested that, compared with WT, the *oserf101* mutant is less sensitive to MeJA.

To identify the effect of *OsERF101* on JA signaling and biosynthesis during DIS, we investigated the transcript levels of JA related genes in the detached leaves of 3-week-old WT and *oserf101* seedlings during DIS (**Figure 3A**). The expression of JA signaling genes (*OsMYC2* and *OsCOI1a*) and JA biosynthesis

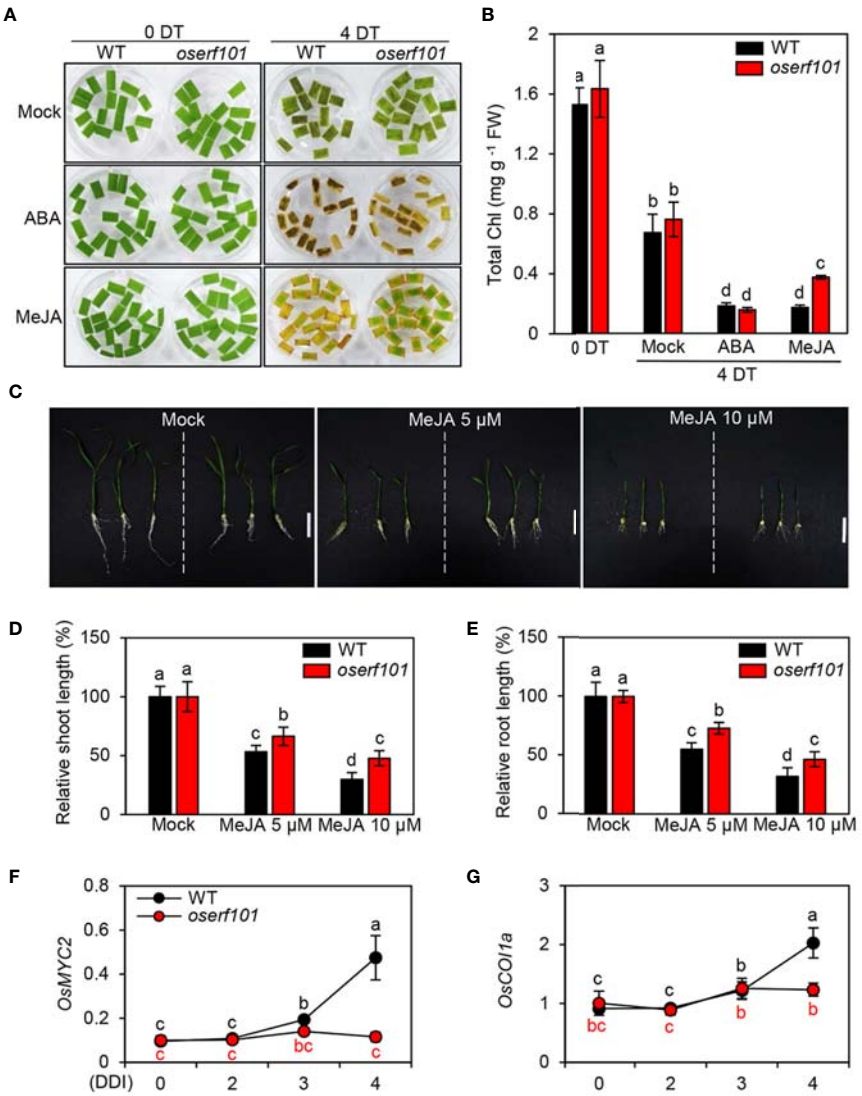

FIGURE 4 | Jasmonic acid (JA) hyposensitivity of the *oserf101* mutants. **(A, B)** Detached leaves of 3-week-old WT and o*serf101* plants grown in the greenhouse under natural long-day conditions (>14 h light/day) were incubated in 3 mM MES buffer (pH 5.8) containing 50 μM abscisic acid (ABA) or 50 μM methyl jasmonate (MeJA) under continuous light at 28°C. Detached leaves floated on 3 mM MES buffer (pH 5.8) without phytohormones were used as a mock control. The MeJA hyposensitive phenotype **(A)** and total chlorophyll (Chl) contents **(B)** were observed at 0 and 4 days after treatment (DT). **(C–E)** The WT and *oserf101* seeds germinated in half-strength Murashige and Skoog (1/2 MS) solid medium for 3 d were grown in 1/2 MS solid medium containing 5 or 10 μM MeJA for 10 d under long-day (LD) conditions (14 h light at 30°C/10 h dark at 25°C). Seedlings grown in 1/2 MS solid medium without MeJA were used as a mock control. The growth phenotype **(C)** and relative shoot **(D)** and root **(E)** length were observed (n = 10). **(F, G)** Altered expression of MeJA signaling genes *OsMYC2* and *OsCOI1a* in detached leaves of 3-week-old WT and *oserf101* seedlings during DIS. Total RNA was isolated from detached leaves at 0, 2, 3, and 4 DDI as shown in **Figure 3A**. The transcript levels of *OsMYC2* **(F)** and *OsCOI1a* **(G)** were determined by qRT-PCR and normalized to that of *OsUBQ5* (Os01g22490). Mean and standard deviations were obtained from at least three biological samples. Different letters indicate significantly different values according to a one-way ANOVA and Duncan's least significant range test ($p < 0.05$). FW, fresh weight.

genes (*OsLOX2* and *OsAOS1*) was significantly upregulated in WT after 3 DDI, while the transcript levels were not altered in *oserf101* mutant during DIS (**Figures 4F, G** and **Supplementary Figure S3**). Taken together, our results suggested that promotes the onset and progression of leaf senescence by upregulating JA signaling and biosynthesis pathways.

OsERF101 Binds to the *OsNAP* and *OsMYC2* Promoter Regions

During DIS, the expression of *OsNAP* and *OsMYC2* was downregulated in the *oserf101* mutant compared to the WT (**Figures 3E** and **4F**). Therefore, we used protoplast transient transactivation assays to determine if OsERF101 activates the

transcription of *OsNAP* and *OsMYC2 in planta*. For the reporter construct, the promoter region of *OsNAP* (-1502 to -1) or *OsMYC2* (-1529 to -1) was fused with the luciferase (LUC) reporter (**Figure 5A**). The LUC activities of the protoplasts transformed with the *proOsNAP : LUC* and *proOsMYC2:LUC* plasmids were significantly enhanced when each of them was co-transfected with the *35S:OsERF101:MYC* effector plasmid (**Figures 5B, C**).

We conducted chromatin immunoprecipitation (ChIP) assays to examine whether OsERF101 directly binds to the promoter regions of *OsNAP* and/or *OsMYC2*. The 1500-bp region upstream of the transcription start site of *OsNAP* or *OsMYC2* was divided into four or five fragments with 50-bp overlap (**Figures 5D, E**). OsERF101 strongly bound to the amplicon-c region of *proOsNAP*, which includes the DRE/CRT motif (GGCCGAC, -447 to -440), and to the amplicon-d region of *proOsMYC2*, which includes a partial ERE motif (ATTTCA, -483 to -477) (**Figures 5F, G**). We further checked the expression levels of *OsNAP* and *OsMYC2* in the developing leaves of WT and *OsERF101*-OX plants grown for one month in the paddy field under NLD conditions. The qRT-PCR analysis revealed that transcripts of *OsNAP* and *OsMYC2* were significantly abundant in two *OsERF101*-OX lines than the transcript levels in the WT (**Supplementary Figure S4**). These results demonstrated that *OsERF101* functions as an upstream activator of *OsNAP* and *OsMYC2* by directly binding to their promoter regions.

Loss of Function of *OsERF101* Negatively Affects Panicle Development and Grain Yield

In addition to exploring the molecular genetic function of *OsERF101* in leaf senescence, we examined several agronomic traits in the *oserf101* mutant plants grown in the paddy field under NLD conditions. We evaluated the number of panicles per plant, panicle length, number of grains per panicle,

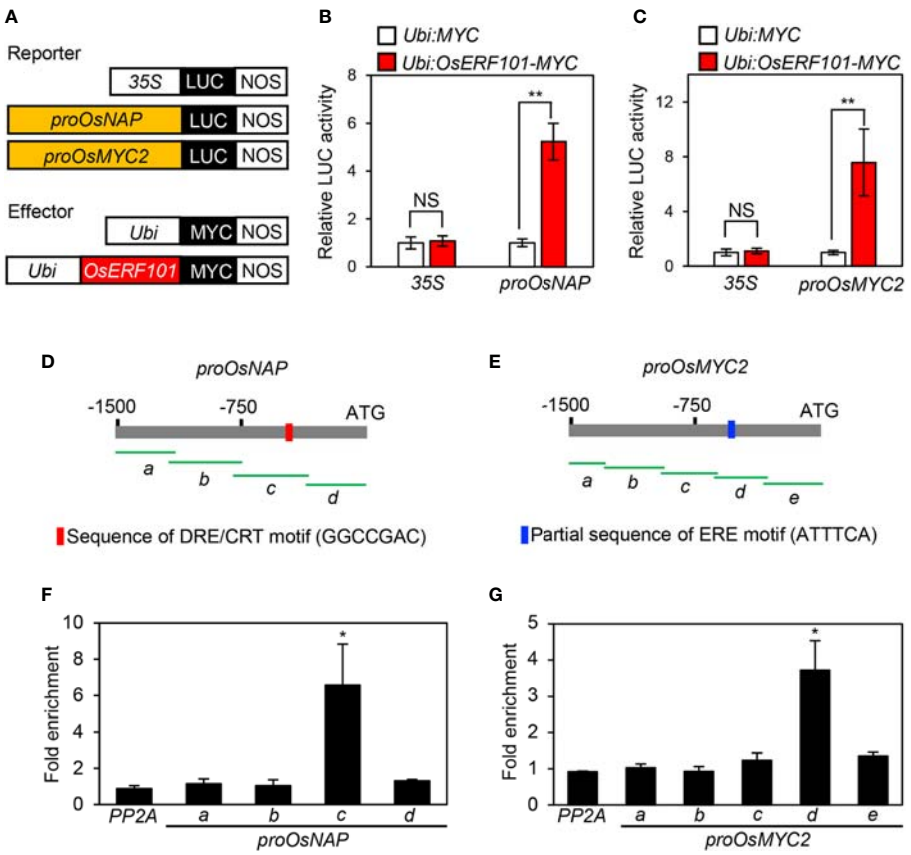

FIGURE 5 | OsERF101 directly activates the transcription of *OsNAP* and *OsMYC2*. **(A)** Reporter and effector constructs used in the transactivation assay. **(B, C)** The activation of the *OsNAP* and *OsMYC2* promoter (*proOsNAP* and *proOsMYC2*) by OsERF101-MYC in the protoplast transient assay. The *35S* promoter was used as a negative control. **(D, E)** Positions of fragments used for the ChIP assay (green horizontal lines) in the promoter regions of *OsNAP* and *OsMYC2*. Red and blue bars indicate the position of the DRE/CRT and partial ERE binding motifs, respectively. **(F, G)** OsERF101 binding affinity assays to the promoter regions of *OsNAP* and *OsMYC2 in planta* examined by ChIP assays. OsERF101-Myc was transiently expressed in protoplasts isolated from 10-day-old WT seedlings. Fold-enrichment of the promoter fragments was measured by immunoprecipitation with an anti-Myc antibody (see *Methods*). The *SERINE/THREONINE PROTEIN PHOSPHATASE 2A* (*PP2A*) gene was used as a negative control. Mean and standard deviations were obtained from more than five biological repeats. Asterisks indicate a significant difference compared with the negative control (Student's *t*-test, $*p < 0.05$, $**p < 0.01$).

fertility, and 500-grain weight. Interestingly, although the panicle length was shorter in the *oserf101* mutant than in the WT (**Figure 6A**), WT and *oserf101* plants produced a similar number of spikelets per panicle (**Figure 6B**), implying that the mutation of *OsERF101* led to higher spikelet density (**Figure 6H**). However, the number of panicles per plant, spikelet fertility, and 500-grain weight were lower in the *oserf101* mutant (**Figures 6C–E**), resulting in reduced grain yield per plant in the mutant (**Figures 6F, G**). Thus, the defect of panicle development and low spikelet fertility in the *oserf101* mutant appear to attenuate the advantage of high spikelet density on improving grain yield.

DISCUSSION

Leaf senescence largely occurs in an age-dependent manner, but can also be triggered by abiotic stresses. The onset and progression of leaf senescence are controlled by multiple regulatory networks in response to environmental cues. Leaf senescence is accompanied by chlorophyll degradation through phytohormone signaling pathways that are driven by many plant-specific TFs (Buchanan-Wollaston, 1997; Lee et al., 2001; Kim et al., 2016). *OsERF101* transcript levels were upregulated by treatment with phytohormones (ABA, MeJA), and by salt (NaCl), osmotic (PEG), and dehydration stresses (**Figures 1B–D**), implying that *OsERF101* is involved in senescence and abiotic stress responses through mediating ABA and MeJA signaling. Overexpression of *OsERF101* confers enhanced tolerance to osmotic and drought stresses at vegetative and reproductive stages, respectively (Jin et al., 2018). The finding that ABA-responsive genes such as *LATE EMBRYOGENESIS ABUNDANT 3* (*LEA3*), *PEROXIDASE 2* (*POD2*), and *RESPONSIVE TO DEHYDRATION 22* (*RD22*) are upregulated in *OsERF101*-overexpressed transgenic rice seedlings in response to osmotic stress treatment (20% PEG)

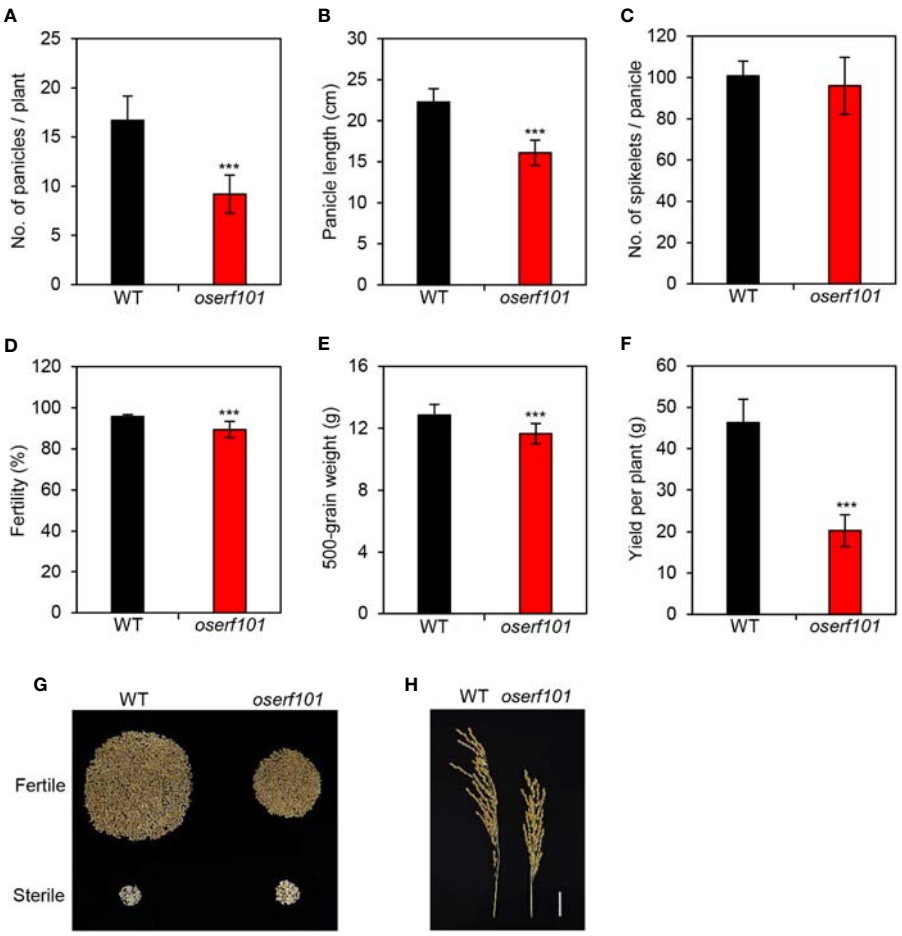

FIGURE 6 | Agronomic traits measured in the *oserf101* mutant. Agronomic traits were compared between the WT and *oserf101* plants after harvest in the autumn. **(A)** Number of panicles per plant. **(B)** Panicle length. **(C)** Number of spikelets per panicle. **(D)** Fertility. **(E)** 500-grain weight. **(F)** Grain yield per plant. **(G)** The relative abundances of fertile and sterile spikelets in the WT and *oserf101* plants. **(H)** Phenotype of panicles. Mean and standard deviations were obtained from 10 rice plants. Asterisks indicate a significant difference between the WT and *oserf101* mutants (Student's *t*-test, ***$p < 0.001$).

suggesting that *OsERF101* participates in the ABA signaling pathway under osmotic stress conditions (Jin et al., 2018). In the present study, we found that overexpression of *OsERF101* led to early leaf yellowing during DIS and natural senescence (**Figure 3**). The detached leaves of the *oserf101* mutant were less sensitive to MeJA, but were sensitive to ABA in continuous light (**Figure 4** and **Supplementary Figure S2**), indicating that OsERF101 mediates leaf senescence *via* the JA signaling pathway, but not the ABA signaling pathway. Indeed, the expression of the JA signaling-associated genes *OsCOI1b* and *OsMYC2* was suppressed in the *oserf101* mutant during DIS (**Figures 4F, G**). Moreover, the ChIP assay showed that OsERF101 directly binds to a partial ERF motif in the promoter region of *OsMYC2* (**Figures 5E, G**). OsMYC2 directly regulates the expression of senescence-associated genes (*SIMILAR TO SAG* and *OsSAG12*), leading to rapid leaf yellowing in *OsMYC2*-OX plants (Uji et al., 2017). Together, these results support the idea that *OsERF101* acts as a positive regulator of leaf senescence in response to JA.

In addition to the involvement of *OsERF101* in regulation of leaf senescence *via* the JA signaling pathway, *OsERF101* is involved in two independent senescence pathways mediated by OsNAP (**Figure 7**). The first is the *OsNAP*-mediated positive feedback loop modulating JA biosynthesis. OsERF101 activates *OsNAP* transcription by directly binding to the DRE/CRT motif of the *OsNAP* promoter region (**Figures 5D, F**). *OsNAP* is involved in various regulatory pathways regulating abiotic stress responses and leaf senescence. Here, we discussed the regulatory function of OsNAP in JA-regulated leaf senescence. Overexpression of *OsNAP* led to an increased level of expression of JA biosynthesis genes including *OsLOX2* and *OsAOC*, thereby upregulating endogenous JA levels in the transgenic plants (Zhou et al., 2013). Thus, the downregulation of JA biosynthesis genes (*OsLOX2* and *OsAOS1*) in the *oserf101* mutant during DIS suggests that *OsERF101* participates in JA biosynthesis (**Supplementary Figure S3**). Finally, increased levels of JA can enhance the transcription of *OsERF101*, and consequently activate the JA–OsERF101–OsNAP positive feedback regulatory loop to promote leaf senescence. The second regulatory function of OsNAP is the *OsNAP*-dependent chlorophyll degradation pathway. In addition, OsNAP is required for the induction of chlorophyll degradation genes including *SGR*, *NYC1*, and *NYC3* (Liang et al., 2014). Our observations indicated that the *oserf101* leaves retained their green color much longer than the WT due to the lower expression of *OsNAP* and chlorophyll degradation genes during DIS, indicating that *OsERF101* upregulates *OsNAP*-induced chlorophyll degradation.

In higher plants, endogenous JA levels and aqrJA signal transduction play important roles in shoot growth, lateral and adventitious root formation, seed germination, and embryo and pollen development (Ueda and Kato, 1980; McConn et al., 1997; Kang et al., 2010; Dave et al., 2011; Valenzuela et al., 2016). For instance, inhibition of JA signaling by knockdown of *OsCOI1a* and *OsCOI1b* expression led to increases in plant height, internode length, and cell length (Yang et al., 2012). Mutation of *OsMADS1* causes a defect in spikelet development due to a lack of glume formation (Chen et al., 2006). OsJAZ1 interacts with the OsMYC2 TF to suppress its activity, which leads to downregulation of the expression of *OsMADS1* (Cai et al., 2014). Genetic studies have indicated that the gain-of-function mutant of *OsJAZ1/EG2*, *eg2-1D*, exhibits downregulated expression of *OsMADS1*, resulting in low spikelet fertility. Thus, the poor spikelet fertility of the *oserf101* mutant appears to be caused by inhibition of JA signaling due to downregulation of *OsCOI1b* and *OsMYC2*, ultimately leading to lower grain yield (**Figures 6D, F**).

Taken together, we concluded that *OsERF101* affects multiple aspects of plant development, including leaf senescence and grain yield through regulating *OsNAP* and JA signaling. These results provide insight into the multiple regulatory mechanisms of *OsERF101* in leaf senescence and spikelet development in rice.

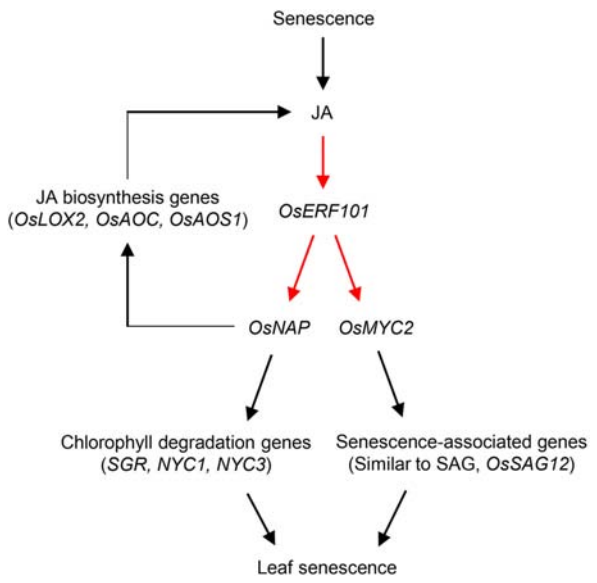

FIGURE 7 | Proposed model of the role of *OsERF101* in the regulation in leaf senescence through JA signaling pathways involving *OsNAP* and *OsMYC2*. Red arrows indicate our findings in this study, and black arrows represent pathways identified in previous studies (Zhou et al., 2013; Liang et al., 2014; Uji et al., 2017).

DATA AVAILABILITY STATEMENT

All datasets presented in this study are included in the article/ **Supplementary Material**.

AUTHOR CONTRIBUTIONS

KK and N-CP designed experiments. CL, YSh, and YSa performed experiments and analyzed data. GA developed plant materials. CL, KK, YSh, and N-CP wrote the article.

FUNDING

This work was carried out with the support of the Basic Science Research Program through the National Research Foundation (NRF) of Korea funded by the Ministry of Education (NRF-2017R1A2B3003310 to N-CP and NRF-2019R1I1A1A01060494 to KK).

SUPPLEMENTARY MATERIAL

The Supplementary Material for this article can be found online at: https://www.frontiersin.org/articles/10.3389/fpls.2020.01096/full#supplementary-material

REFERENCES

Buchanan-Wollaston, V. (1997). The molecular biology of leaf senescence. *J. Exp. Bot.* 48, 181–199. doi: 10.1093/jxb/48.2.181

Cai, Q., Yuan, Z., Chen, M., Yin, C., Luo, Z., Zhao, X., et al. (2014). Jasmonic acid regulates spikelet development in rice. *Nat. Commun.* 5, 3476. doi: 10.1038/ncomms4476

Chen, Z.-X., Wu, J.-G., Ding, W.-N., Chen, H.-M., Wu, P., and Shi, C.-H. (2006). Morphogenesis and molecular basis on naked seed rice, a novel homeotic mutation of OsMADS1 regulating transcript level of AP3 homologue in rice. *Planta* 223, 882–890. doi: 10.1007/s00425-005-0141-8

Chen, X., Wang, Y., Lv, B., Li, J., Luo, L., Lu, S., et al. (2014). The NAC family transcription factor OsNAP confers abiotic stress response through the ABA pathway. *Plant Cell Physiol.* 55, 604–619. doi: 10.1093/pcp/pct204

Dave, A., Hernández, M. L., He, Z., Andriotis, V. M. E., Vaistij, F. E., Larson, T. R., et al. (2011). 12-Oxo-phytodienoic acid accumulation during seed development represses seed germination in Arabidopsis. *Plant Cell* 23, 583–599. doi: 10.1105/tpc.110.081489

Distelfeld, A., Avni, R., and Fischer, A. M. (2014). Senescence, nutrient remobilization, and yield in wheat and barley. *J. Exp. Bot.* 65, 3783–3798. doi: 10.1093/jxb/ert477

Fernández-Calvo, P., Chini, A., Fernández-Barbero, G., Chico, J.-M., Gimenez-Ibanez, S., Geerinck, J., et al. (2011). The Arabidopsis bHLH transcription factors MYC3 and MYC4 are targets of JAZ repressors and act additively with MYC2 in the activation of jasmonate responses. *Plant Cell* 23, 701–715. doi: 10.1105/tpc.110.080788

Fukao, T., Yeung, E., and Bailey-Serres, J. (2011). The submergence tolerance regulator SUB1A mediates crosstalk between submergence and drought tolerance in rice. *Plant Cell* 23, 412–427. doi: 10.1105/tpc.110.080325

Gao, T., Li, G.-Z., Wang, C.-R., Dong, J., Yuan, S.-S., Wang, Y.-H., et al. (2018). Function of the ERFL1a Transcription Factor in Wheat Responses to Water Deficiency. *Int. J. Mol. Sci.* 19:1465. doi: 10.3390/ijms19051465

Gepstein, S., and Glick, B. R. (2013). Strategies to ameliorate abiotic stress-induced plant senescence. *Plant Mol. Biol.* 82, 623–633. doi: 10.1007/s11103-013-0038-z

He, Y., Fukushige, H., Hildebrand, D. F., and Gan, S. (2002). Evidence supporting a role of jasmonic acid in Arabidopsis leaf senescence. *Plant Physiol.* 128, 876–884. doi: 10.1104/pp.010843

Hou, Q., Ufer, G., and Bartels, D. (2016). Lipid signalling in plant responses to abiotic stress: Lipid signalling in plant responses to abiotic stress. *Plant Cell Environ.* 39, 1029–1048. doi: 10.1111/pce.12666

Jeon, J.-S., Lee, S., Jung, K.-H., Jun, S.-H., Jeong, D.-H., Lee, J., et al. (2000). T-DNA insertional mutagenesis for functional genomics in rice. *Plant J.* 22, 561–570. doi: 10.1046/j.1365-313x.2000.00767.x

Jeong, D.-H., An, S., Kang, H.-G., Moon, S., Han, J.-J., Park, S., et al. (2002). T-DNA insertional mutagenesis for activation tagging in rice. *Plant Physiol.* 130, 1636–1644. doi: 10.1104/pp.014357

Jin, Y., Pan, W., Zheng, X., Cheng, X., Liu, M., Ma, H., et al. (2018). OsERF101, an ERF family transcription factor, regulates drought stress response in reproductive tissues. *Plant Mol. Biol.* 98, 51–65. doi: 10.1007/s11103-018-0762-5

Kang, J.-H., Liu, G., Shi, F., Jones, A. D., Beaudry, R. M., and Howe, G. A. (2010). The tomato odorless-2 mutant is defective in trichome-based production of diverse specialized metabolites and broad-spectrum resistance to insect herbivores. *Plant Physiol.* 154, 262–272. doi: 10.1104/pp.110.160192

Kim, H. J., Nam, H. G., and Lim, P. O. (2016). Regulatory network of NAC transcription factors in leaf senescence. *Curr. Opin. Plant Biol.* 33, 48–56. doi: 10.1016/j.pbi.2016.06.002

Kusaba, M., Ito, H., Morita, R., Iida, S., Sato, Y., Fujimoto, M., et al. (2007). Rice NON-YELLOW COLORING1 is involved in light-harvesting complex II and grana degradation during leaf senescence. *Plant Cell* 19, 1362–1375. doi: 10.1105/tpc.106.042911

Lee, R., Wang, C., Huang, L., and Chen, S. G. (2001). Leaf senescence in rice plants: cloning and characterization of senescence up-regulated genes. *J. Exp. Bot.* 52, 1117–1121. doi: 10.1093/jexbot/52.358.1117

Lee, S.-H., Sakuraba, Y., Lee, T., Kim, K.-W., An, G., Lee, H. Y., et al. (2015). Mutation of *Oryza sativa CORONATINE INSENSITIVE 1b* (*OsCOI1b*) delays leaf senescence: OsCOI1b in leaf senescence. *J. Integr. Plant Biol.* 57, 562–576. doi: 10.1111/jipb.12276

Liang, C., Wang, Y., Zhu, Y., Tang, J., Hu, B., Liu, L., et al. (2014). OsNAP connects abscisic acid and leaf senescence by fine-tuning abscisic acid biosynthesis and directly targeting senescence-associated genes in rice. *Proc. Natl. Acad. Sci. U. S. A.* 111, 10013–10018. doi: 10.1073/pnas.1321568111

Liu, S., Wang, X., Wang, H., Xin, H., Yang, X., Yan, J., et al. (2013). Genome-wide analysis of ZmDREB genes and their association with natural variation in drought tolerance at seedling stage of Zea mays L. *PLoS Genet.* 9, e1003790. doi: 10.1371/journal.pgen.1003790

Luehrsen, K. R., de Wet, J. R., and Walbot, V. (1992). Transient expression analysis in plants using firefly luciferase reporter gene. *Methods Enzymol.* 216, 397–414. doi: 10.1016/0076-6879(92)16037-k

Mao, C., Lu, S., Lv, B., Zhang, B., Shen, J., He, J., et al. (2017). A rice NAC transcription factor promotes leaf senescence via ABA biosynthesis. *Plant Physiol.* 174, 1747–1763. doi: 10.1104/pp.17.00542

Masclaux-Daubresse, C., Reisdorf-Cren, M., and Orsel, M. (2008). Leaf nitrogen remobilisation for plant development and grain filling. *Plant Biol.* 10, 23–36. doi: 10.1111/j.1438-8677.2008.00097.x

McConn, M., Creelman, R. A., Bell, E., Mullet, J. E., and Browse, J. (1997). Jasmonate is essential for insect defense in Arabidopsis. *Proc. Natl. Acad. Sci. U. S. A.* 94, 5473–5477. doi: 10.1073/pnas.94.10.5473

Mickelbart, M. V., Hasegawa, P. M., and Bailey-Serres, J. (2015). Genetic mechanisms of abiotic stress tolerance that translate to crop yield stability. *Nat. Rev. Genet.* 16, 237–251. doi: 10.1038/nrg3901

Morita, R., Sato, Y., Masuda, Y., Nishimura, M., and Kusaba, M. (2009). Defect in Non-Yellow Coloring 3, an α/β hydrolase-fold family protein, causes a stay-green phenotype during leaf senescence in rice. *Plant J.* 59, 940–952. doi: 10.1111/j.1365-313X.2009.03919.x

Munné-Bosch, S., and Alegre, L. (2004). Die and let live: leaf senescence contributes to plant survival under drought stress. *Funct. Plant Biol.* 31, 203. doi: 10.1071/FP03236

Nakano, T., Suzuki, K., Fujimura, T., and Shinshi, H. (2006). Genome-wide analysis of the ERF gene family in Arabidopsis and rice. *Plant Physiol.* 140, 411–432. doi: 10.1104/pp.105.073783

Niu, Y., Figueroa, P., and Browse, J. (2011). Characterization of JAZ-interacting bHLH transcription factors that regulate jasmonate responses in Arabidopsis. *J. Exp. Bot.* 62, 2143–2154. doi: 10.1093/jxb/erq408

Park, J. M., Park, C.-J., Lee, S.-B., Ham, B.-K., Shin, R., and Paek, K.-H. (2001). Overexpression of the tobacco *Tsi1* gene encoding an EREBP/AP2-type

transcription factor enhances resistance against pathogen attack and osmotic stress in tobacco. *Plant Cell* 13, 1035–1046. doi: 10.1105/tpc.13.5.1035

Park, S.-Y., Yu, J.-W., Park, J.-S., Li, J., Yoo, S.-C., Lee, N.-Y., et al. (2007). The senescence-induced staygreen protein regulates chlorophyll degradation. *Plant Cell* 19, 1649–1664. doi: 10.1105/tpc.106.044891

Phukan, U. J., Jeena, G. S., Tripathi, V., and Shukla, R. K. (2017). Regulation of Apetala2/Ethylene Response Factors in plants. *Front. Plant Sci.* 8:150. doi: 10.3389/fpls.2017.00150

Porra, R. J., Thompson, W. A., and Kriedemann, P. E. (1989). Determination of accurate extinction coefficients and simultaneous equations for assaying chlorophylls a and b extracted with four different solvents: verification of the concentration of chlorophyll standards by atomic absorption spectroscopy. *Biochim. Biophys. Acta (BBA) - Bioenerg.* 975, 384–394. doi: 10.1016/S0005-2728(89)80347-0

Qi, T., Huang, H., Wu, D., Yan, J., Qi, Y., Song, S., et al. (2014). Arabidopsis DELLA and JAZ proteins bind the WD-Repeat/bHLH/MYB complex to modulate gibberellin and jasmonate signaling synergy. *Plant Cell* 26, 1118–1133. doi: 10.1105/tpc.113.121731

Sakuma, Y., Liu, Q., Dubouzet, J. G., Abe, H., Shinozaki, K., and Yamaguchi-Shinozaki, K. (2002). DNA-binding specificity of the ERF/AP2 domain of Arabidopsis DREBs, transcription factors involved in dehydration- and cold-inducible gene expression. *Biochem. Biophys. Res. Commun.* 290, 998–1009. doi: 10.1006/bbrc.2001.6299

Sakuraba, Y., Piao, W., Lim, J.-H., Han, S.-H., Kim, Y.-S., An, G., et al. (2015). Rice ONAC106 inhibits leaf senescence and increases salt tolerance and tiller angle. *Plant Cell Physiol.* 56, 2325–2339. doi: 10.1093/pcp/pcv144

Saleh, A., Alvarez-Venegas, R., and Avramova, Z. (2008). An efficient chromatin immunoprecipitation (ChIP) protocol for studying histone modifications in Arabidopsis plants. *Nat. Protoc.* 3, 1018–1025. doi: 10.1038/nprot.2008.66

Shen, J., Lv, B., Luo, L., He, J., Mao, C., Xi, D., et al. (2017). The NAC-type transcription factor OsNAC2 regulates ABA-dependent genes and abiotic stress tolerance in rice. *Sci. Rep.* 7:40641. doi: 10.1038/srep40641

Song, S., Qi, T., Huang, H., Ren, Q., Wu, D., Chang, C., et al. (2011). The jasmonate-ZIM domain proteins interact with the R2R3-MYB transcription factors MYB21 and MYB24 to affect jasmonate-regulated stamen development in Arabidopsis. *Plant Cell* 23, 1000–1013. doi: 10.1105/tpc.111.083089

Ueda, J., and Kato, J. (1980). Isolation and identification of a senescence-promoting substance from wormwood (Artemisia absinthium L.). *Plant Physiol.* 66, 246–249. doi: 10.1104/pp.66.2.246

Uji, Y., Akimitsu, K., and Gomi, K. (2017). Identification of OsMYC2-regulated senescence-associated genes in rice. *Planta* 245, 1241–1246. doi: 10.1007/s00425-017-2697-5

Valenzuela, C. E., Acevedo-Acevedo, O., Miranda, G. S., Vergara-Barros, P., Holuigue, L., Figueroa, C. R., et al. (2016). Salt stress response triggers activation of the jasmonate signaling pathway leading to inhibition of cell elongation in Arabidopsis primary root. *J. Exp. Bot.* 67, 4209–4220. doi: 10.1093/jxb/erw202

Wasternack, C., and Hause, B. (2013). Jasmonates: biosynthesis, perception, signal transduction and action in plant stress response, growth and development. An update to the 2007 review in Annals of Botany. *Ann. Bot.* 111, 1021–1058. doi: 10.1093/aob/mct067

Yang, D.-L., Yao, J., Mei, C.-S., Tong, X.-H., Zeng, L.-J., Li, Q., et al. (2012). Plant hormone jasmonate prioritizes defense over growth by interfering with gibberellin signaling cascade. *Proc. Natl. Acad. Sci. U. S. A.* 109, E1192–E1200. doi: 10.1073/pnas.1201616109

Yang, Y. N., Safarova, R. B., Park, S.-Y., Sakuraba, Y., Oh, M.-H., Zulfugarov, I. S., et al. (2019). Chlorophyll Degradation and Light-harvesting Complex II Aggregate Formation During Dark-induced Leaf Senescence in Arabidopsis Pheophytinase Mutants. *J. Plant Biol.* 62, 27–38. doi: 10.1007/s12374-018-0242-0

Yoo, S.-D., Cho, Y.-H., and Sheen, J. (2007). Arabidopsis mesophyll protoplasts: a versatile cell system for transient gene expression analysis. *Nat. Protoc.* 2, 1565–1572. doi: 10.1038/nprot.2007.199

Zhang, G., Chen, M., Li, L., Xu, Z., Chen, X., Guo, J., et al. (2009). Overexpression of the soybean GmERF3 gene, an AP2/ERF type transcription factor for increased tolerances to salt, drought, and diseases in transgenic tobacco. *J. Exp. Bot.* 60, 3781–3796. doi: 10.1093/jxb/erp214

Zhang, Y., Su, J., Duan, S., Ao, Y., Dai, J., Liu, J., et al. (2011). A highly efficient rice green tissue protoplast system for transient gene expression and studying light/chloroplast-related processes. *Plant Methods* 7:30. doi: 10.1186/1746-4811-7-30

Zhou, Y., Huang, W., Liu, L., Chen, T., Zhou, F., and Lin, Y. (2013). Identification and functional characterization of a rice NAC gene involved in the regulation of leaf senescence. *BMC Plant Biol.* 13:132. doi: 10.1186/1471-2229-13-132

Zhu, X., Chen, J., Xie, Z., Gao, J., Ren, G., Gao, S., et al. (2015). Jasmonic acid promotes degreening via MYC2/3/4- and ANAC019/055/072-mediated regulation of major chlorophyll catabolic genes. *Plant J.* 84, 597–610. doi: 10.1111/tpj.13030

Zhuang, Y., Liu, Y., Li, Y., Wei, M., Tang, Y., Li, P., et al. (2019). SALT-INDUCED CHLOROPLAST PROTEIN (SCP) is Involved in Plant Tolerance to Salt Stress in Arabidopsis. *J. Plant Biol.* 62, 429–435. doi: 10.1007/s12374-019-0356-z

Conflict of Interest: The authors declare that the research was conducted in the absence of any commercial or financial relationships that could be construed as a potential conflict of interest.

Advantages of publishing in Frontiers

OPEN ACCESS
Articles are free to read for greatest visibility and readership

FAST PUBLICATION
Around 90 days from submission to decision

HIGH QUALITY PEER-REVIEW
Rigorous, collaborative, and constructive peer-review

TRANSPARENT PEER-REVIEW
Editors and reviewers acknowledged by name on published articles

Frontiers
Avenue du Tribunal-Fédéral 34
1005 Lausanne | Switzerland

Visit us: www.frontiersin.org
Contact us: info@frontiersin.org | +41 21 510 17 00

REPRODUCIBILITY OF RESEARCH
Support open data and methods to enhance research reproducibility

DIGITAL PUBLISHING
Articles designed for optimal readership across devices

FOLLOW US
@frontiersin

IMPACT METRICS
Advanced article metrics track visibility across digital media

EXTENSIVE PROMOTION
Marketing and promotion of impactful research

LOOP RESEARCH NETWORK
Our network increases your article's readership